REMOVAL OF HEAVY METALS AND FLUORIDE BY NANOTECHNOLOGY, PHYTOREMEDIATION AND PLANT MATERIALS

Thesis submitted by

MEGHA T

(Reg No: 4116)

For the award of the degree of

DOCTOR OF PHILOSOPHY *in* ENVIRONMENTAL SCIENCES

Under the faculty of Environmental Studies
COCHIN UNIVERSITY OF SCIENCE AND TECHNOLOGY

CENTRE FOR WATER RESOURCES DEVELOPMENT AND MANAGEMENT
Kunnamangalam, Kozhikode-673 571, Kerala

November 2018

REMOVAL OF HEAVY METALS AND FLUORIDE BY NANOTECHNOLOGY, PHYTOREMEDIATION AND PLANT MATERIALS

Ph.D. Thesis

Author:

Megha T
Research Scholar
Water Quality Division
Centre for Water Resources Development and Management
Kunnamangalam, Kozhikode-673 571
Kerala, India
meg8tee@gmail.com

Supervising Guide:

Dr. P S Harikumar
Supervising guide
Senior Principal Scientist & Head
Water Quality Division
Centre for Water Resources Development and Management
Kozhikode - 673 571
hps@cwrdm.org

November 2018

Date: 19-11-2018

Certificate

Certified that the work presented in this thesis entitled "**REMOVAL OF HEAVY METALS AND FLUORIDE BY NANOTECHNOLOGY, PHYTOREMEDIATION AND PLANT MATERIALS**" submitted to Cochin University of Science and Technology in partial fulfillment of the requirements for the award of Doctor of Philosophy in Environmental Sciences is an authentic record of research work carried out by **Mrs. Megha T** (Reg. No. 4116) under my supervision and guidance at Centre for Water Resources Development and Management, Kozhikode. The results presented in this thesis has not been included in any other thesis submitted previously for the award of any degree. All the relevant corrections and modifications suggested by the audience and recommended by the doctoral committee of the candidate during the pre-synopsis seminar have been incorporated in the thesis.

Dr. P S Harikumar
Supervising Guide
Senior Principal Scientist & Head
Water Quality Division
Centre for Water Resources Development and Management
Kozhikode - 673 571

DECLARATION

I hereby declare that the work presented in the thesis entitled **"REMOVAL OF HEAVY METALS AND FLUORIDE BY NANOTECHNOLOGY, PHYTOREMEDIATION AND PLANT MATERIALS"** *submitted by me to Cochin University of Science and Technology for the award of the degree of Doctor of Philosophy in Environmental Sciences under the Faculty of Environmental Studies is based on the original research work carried out by me under the supervision and guidance of Dr. P S Harikumar, Senior Principal Scientist & Head, Water Quality Division, CWRDM, Kozhikode. I further declare that the contents of this thesis have not been submitted previously for any degree.*

Place: Kozhikode **Megha T**

Date: 19/11/2018

ACKNOWLEDGEMENT

various stages of this research work. I would like to express sincere and deepest gratitude to Mr. Sasidharan Pallikudian, Technical Officer, CWRDM for the unconditional support, technical assistance, constant encouragement and genuine advices provided at all stages of this work. I also express my deep felt gratitude to all my Doctoral Committee & Research Committee members for their valuable suggestions and comments, which greatly improved this thesis.

Timely help offered by Dr. Shiji M, Technical Officer, CWRDM for thesis preparations as well as her constant support also acknowledged. I express my gratitude to all scientists, administrative and technical staff of CWRDM for their kind co-operation and timely help during the tenure of my work. I express my special thanks to Jaseela C and Bindhya Mol K for their help and advices during structuring this thesis. I also express my sincere thanks to all my friends and colleagues, Sameer P.T, Jesiya N.P, Kavya Prabhakar, Silfi Prakash, Moly A, Jesitha K and Indu Das, for their sincere cooperation and support. I thank all the project staff of CWRDM for the help and loving support they extended to me during my research.

I would like to share this moment of happiness with my family. The seamless support, love, affection and caring of my selfless mother Saraswathi K and father Prakasan T, the backbone of my success. I express my deep sense of gratitude to them. No words of gratitude suffice when acknowledging my husband, Mr. Abu Anees P.P, my companion and the wings of my dream, because I cannot conceive the completion of this thesis without his constant support, motivation and encouragement.

This thesis is the fruit of grace, hard work, support and prayers of my family. I thank my sister, in laws and all my family members who encourage and support me to achieve my dreams. I express my sincere love and thanks to all my friends, relatives and well-wishers whose prayers and blessings have enabled me to successfully complete my research work.

I acknowledge with great pleasure and pride, to my sweetheart, my son, Adhiv Anees for being understanding and supporting to enable me to walk to this milestone in my research career.

Dedicated to the Almighty,

my family and dear ones

ABSTRACT

The deterioration of water quality is growing with rapid pace as a consequence of the anthropogenic activities, unskilled utilization of natural water resources, population intensification, unplanned urbanization and swift industrialization. Highly toxic, non-biodegradable, bioaccumulation and persisting nature of heavy metals and the irreversible health threats of fluoride makes them severely hazardous. The prevailing treatment technologies of heavy metals and fluoride have the shortcomings such as high operational and maintenance costs, complicated procedure involved in the treatment and generation of toxic sludge or by-products. The present study deals with the development of effective, efficient and eco-friendly clean up techniques to reduce or remove the toxic heavy metal and fluoride from water.

The study revealed that the *Eichhornia crassipes,* an efficient phyto-remediator exhibited efficient and fast removal of Pb, Cd and Cu in electro assisted phytoremediation system. *Eichhornia crassipes* stimulated by an electric field grown better and assimilated more metal. BCF, an index of hyperaccumulation, indicates that electrically stimulated *Eichhornia crassipes* is a good hyper accumulator of Cd (BCF = 1118.18) and Cu (BCF = 1152.47) and a moderate accumulator of Pb (BCF = 932.26). This method successfully removed 94.27 % of lead and 79.56 % of chromium from wastewater. The phytoremediation ability of *Eichhornia crassipes* and *Salvinia molesta* enhanced by TiO_2 nanoparticles showed better phytoremediation efficiency for the removal

of Pb, Cd and Cu than control, within 3 days. The BCF and TF indicated the increase in uptake potential of metals by plants and translocation of metals from root to its areal part under nano - TiO_2 applied conditions compared to control. The possibility of using ammonium molybdate in phytoremediation of heavy metal (Cd, Pb, Cu, Ni and Zn) contaminated soil by *Amaranthus retroflexus* was studied. The results indicated the phytostabilization of Pb and Zn and the phytoextraction of Cd, Ni, and Cu by ammonium molybdate applied *Amaranthus retroflexus*. Increase in growth was noticed in plants treated with ammonium molybdate than control plant.

Defluoridation ability of some medicinal as well as easily and locally available plant materials were checked and among them, *Vetiveria zizanioides* (80 %), *Tamarindus indica* (75 %) and *Eugenia carryophyllata* (73 %) exhibited better defluoridation efficiency. The batch sorption study of these plant materials revealed that *Vetiveria zizanioides* has the potential to be an efficient defluoridating agent, so activation of *Vetiveria zizanioides* was carried out to improve its efficiency. The batch sorptive defluoridation study of powdered activated *Vetiveria zizanioides* was conducted under variable experimental conditions such as pH, initial concentration, agitation time, interfering co-ions, dose of adsorbent, particle size, agitation speed and temperature. Maximum defluoridation efficiency (92.5 %) was observed at an initial concentration of 10 mg/L. The results showed that 120 min is the time required to reach equilibrium conditions. The influence of co-existing anions on the fluoride removal was observed as in the order: PO_4^{3-} >

$HCO_3^- > SO_4^{2-} > Cl^- \geq NO_3^-$. The adsorption isotherm models fitted the equilibrium data, based on the correlation coefficient, in the order of: Langmuir isotherm > Freundlich isotherm > Temkin isotherm > Dubinin–Radushkevich isotherm. To identify the rate and kinetics of adsorption process pseudo-first-order, pseudo-second-order, intra-particle diffusion model, and Elovich kinetic model were applied. The correlation coefficient and sum of squares of the error were used to evaluate the fitness of the sorption kinetic models and it suggested that the adsorption of fluoride on the activated *Vetiveria zizanioides* follows second order kinetic model. The thermodynamic data confirms the endothermic and spontaneous nature of sorption process. 0.1 M NaOH solution was identified as the suitable eluent to regenerate activated *Vetiveria zizanioides.* A gravity-based household water filter was developed using activated *Vetiveria zizanioides* for the defluoridation and it effectively reduced the fluoride level (below the BIS acceptable limit) in groundwater samples collected from fluoride endemic area of Palakkad district.

In the removal of Pb^{2+}, Cd^{2+} and Cu^{2+} ions from water by *Caesalpinia sappan* (a herbal plant material), the order of metal ions sorption is as follows: 9.14 mg/g for Pb^{2+} > 7.23 mg/g for Cu^{2+} > 6.10 mg/g for Cd^{2+} under varying initial metal concentration from 5 - 45 mg/L. The adsorption data best fitted the Langmuir adsorption isotherm for all three metals. Dubinin - Radushkevich (D-R) isotherm model also fits very well to the experimentally determined data for Pb^{2+}, Cd^{2+} and Cu^{2+}. The kinetic data of adsorption of heavy metal ions on *Caesalpinia*

sappan are best modelled by the pseudo-second-order kinetic equation. Thermodynamic parameters indicated the exothermic behaviour and spontaneous nature of the adsorption process. The batch sorption experiments for the removal of Pb^{2+} and Cd^{2+} from aqueous solutions using algal biomass *Trenteohilia abietina* revealed that the maximum sorption is observed for both metals under a wide range of pH (pH: 4 -12 for Pb^{2+} and pH: 6 - 12 for Cd^{2+}). High (100 %) removal efficiencies were observed for Pb^{2+} and Cd^{2+} at the adsorbent dosage of 2 g/L and 4 g/L, respectively. An increase in adsorption capacity from 20.01 mg/g to 33.83 mg/g for Pb^{2+} and 10.02 mg/g to 16.39 mg/g for Cd^{2+} was observed with the increase in metals concentration from 40 to 70 mg/L. The adsorption data best fitted the Langmuir adsorption isotherm, which indicate favourable adsorption. The maximum adsorption capacity of Pb^{2+} and Cd^{2+} by *T. abietina* was 33.22 mg/g and 16.53 mg/g, respectively. The D-R isotherm model also fits close to the experimentally determined data for both the metals. The experimental data was best fitted the pseudo-second order kinetic model. The good fitting of the kinetics data to Bangham's Model indicate that, in the adsorption of Pb^{2+} and Cd^{2+} on the biosorbent *T. abietina*, pore diffusion plays a vital role in controlling the rate of reaction. The results indicate that both sorbents, *Caesalpinia sappan* and *Trenteohilia abietina* exhibited high metal removal efficiency. The functionalized nanoparticles (iron oxide nanoparticles coated with poly vinyl alcohol and gallic acid) were used for the removal of Pb^{2+} and Cd^{2+}. The functionalized nanoparticles (PG-IONPs) showed better metal removal efficiency compared to the uncoated iron oxide nanoparticles (IONPs). In

the sorption of metals by PG-IONPs, as the initial metal concentration increased from 5 - 25 mg/L, the removal efficiency was varied from 99.98 - 97.93 % for Pb^{2+} and 99.95 - 93.97 % for Cd^{2+}. For IONPs, the removal efficiency was varied from 97.01 - 67.08 % and 98.28 - 82.85 % for Pb^{2+} and Cd^{2+} respectively. The kinetic and thermodynamic investigations were carried out as a part of study. SEM, EDX spectra and FTIR techniques are used to examine structural and morphological characteristics of the adsorbents. The regeneration studies of the sorbents were also conducted. Polyvinyl alcohol and gallic acid coated iron oxide nanoparticles (PG-IONPs) can be considered as fast and efficient, nano-adsorbent for Pb^{2+} and Cd^{2+} removal from contaminated waters. The evaluation of heavy metal contamination in groundwater resources from Madayi panchayath, Kannur district using HPI, HEI and C_d indices indicated the heavy metal pollution. Among the three applied adsorbents (PG-IONPs, *Caesalpinia sappan* and *Tretepohila abietina*), PG-IONPs exhibited high efficiency in the removal of heavy metals in drinking water from Madayi panchayath.

CONTENTS

LIST OF TABLES

LIST OF FIGURES

LIST OF PLATES

LIST OF ACRONYMS

APHA	American Public Health Association
USEPA	U. S. Environmental Protection Agency
UN	United Nations
UNEP	United Nations Environment Programme
UNICEF	United Nations Children's Fund
WHO	World Health Organization
BIS	Bureau of Indian Standards
NIST	National Institute of Standards and Technology
SEM	Scanning Electron Microscope
EDX	Energy-dispersive X-ray spectroscopy
FTIR	Fourier Transform Infra-Red Spectroscopy
XRD	X-ray diffraction
ASTM	American Standard of Testing Material
EC	Electrical conductivity
COD	Chemical Oxygen Demand
BOD	Biochemical Oxygen Demand
EAPR	Electro Assisted-Phytoremediation
MoWR	Ministry of Water Resources
CGWB	Central Ground Water Board
RGNDWM	Rajiv Gandhi National Drinking Water Mission
AAS	Atomic Absorption Spectrophotometer
BCF	Bioconcentration factor

TF	Translocation factor
TA	Translocation ability
NMs	Nano materials
IONPs	Iron oxide nanoparticles
PG-IONPs	Iron oxide coated with polyvinyl alcohol and gallic acid
PVA	Polyvinyl alcohol
HPI	Heavy metal pollution index
HEI	Heavy metal evaluation index
PCA	Principle Component Analysis
CA	Cluster Analysis
CCME	Canadian Council of Ministers of the Environment

Chapter 1

INTRODUCTION

1.1 Introduction

An English Poet W. H Auden said that, *many have lived without love, none without water:* An emotion that stress the half way point of the new decade for action under the simple but impressive theme '*Water is Life'*. The human civilizations were blossomed in the areas where reliable and fresh water was easily available. Safe, clean, and ample freshwater is vital to the existence of all living organisms and for the smooth functioning of ecosystems, economies, and communities, even though it lacks organic nutrients and calories. Number of people lost their life as a consequence of unsafe water in every year, is more than the lives lost from all forms of violence, including war (UNEP, 2010). This emphasis the fact that water is the source of life on earth. Due to the unique chemical composition, the water possesses a special property to attracts other atoms by the asymmetrical electrical charge. Hence, all polar substance gets easily dispersed uniformly within the water molecule as a result of

hydrogen bonding and polar nature, and makes the water, a universal solvent. The affinity of water to dissolve other molecules is very important for the existence of life and when it flows, it harbors dissolved substances which support living organism in the form of minerals and nutrients (Mbugua et al., 2017). But, because of this unique property of water, its quality can be easily altered.

Freshwater scarcity positions a higher rank among the most crucial environmental challenges of this epoch. Water abstraction for practices like domestic use, agricultural and industrial production, mining, forestry practices, and power generation can induce deterioration in quality and quantity of water that influence the aquatic ecosystem as well as the availability of safe water for human consumption (UNEP GEMS/Water Programme, 2008). The access to basic water services are still lack to many people in the world. WHO and UNICEF revealed that, 768 million remain without access to a better-quality source of water and 2.5 billion people remain without access to improved sanitation (WHO/UNICEF, 2013). The safe water is unavailable for 2 billion people as per UN (2013) and the number of people whose right to water is dissatisfied is even greater (Onda et al., 2012).

Globally, the ambient freshwater quality is at peril and freshwater pollution due to toxic substances is prevalent and growing in many regions. Even though, the water quality issues are largely associated with developing nations, they also persist in developed nations. The degradation of the pristine quality conditions of the environment, especially water and soil are amplified because of many factors like the

escalated population density, swift industrialisation and urbanization, etc., and hence, more effective and appropriate approaches for the eradication of toxic contaminants from environment is essential.

1.2 Water quality & water quality challenges

Water quality and quantity are closely allied although not often measured simultaneously. Water quantity is usually measured by means of water level, discharge, and velocity recorded by remote hydrological monitoring stations. For the satisfaction of basic human and environmental needs, the water quality is substantial as water quantity. The quality of water required for each human usage varies, as do the criteria used to assess water quality and the maximum standards of purity are mandatory for drinking water (UNEP GEMS/Water Programme, 2008). A wide range of human activities such as industrial and mining activities, agricultural production, water infrastructure, the direct disposal of untreated or partly treated sewage and human wastes into water systems, urbanization, population growth and climate change directly affect the physico-chemical and biological characteristics of water and magnify the impact on water quality.

Contamination by trace metals, pathogenic organisms, and toxic chemicals and changes in the temperature, salinity, and acidity of water can all destruct aquatic ecosystems and make water unfit for human use. Around 700 new chemicals are introduced into market each year in the United States alone and about 300 - 400 million tons of heavy metals, toxic sludge, solvents, and other waste are released into the world's waters each year as a result of industrial activities. Agricultural practices can

cause nutrient enrichment, pesticide contamination and salinity issues. Mining and drilling generate huge quantities of wastes and by-products and faces many challenges in large-scale waste disposal. Lack of improved sanitation is another issue faced by many people around the world. Growing populations and climate change will also create many water quality challenges (UNEP, 2010).

The industrialization has not only fetched development and prosperity but eventually distressed the ecosystem. Water pollution is one of the visible impacts of rapid industrialization. Several anthropogenic activities have raised the emission of toxic heavy metals to the environment and its tendency to bioaccumulate, non-biodegradable nature, invariably persisting nature in the environment and high toxicity even at low concentration, make it more hazardous. Industrial effluents from electroplating, tannery, leather, textile, paint, pigment & dyes, petroleum refining, wood processing, photographic film production etc., comprises significant quantity of heavy metals in their wastewater (Tripathi & Ranjan, 2015). Fluoride contamination in drinking water has become a critical health hazard of this century as it creates intense effect on human and animals' health including skeletal and dental fluorosis (Alagumuthu et al., 2010). High fluoride ions also cause impaired brain development (Mbugua et al., 2017) and have serious socioeconomic implications. Many of the prevailing remediation methods for theses contaminants are expensive, energy intensive, ineffective at low concentration, time consuming, often associated with generation of toxic by-products and sometimes non-ecofriendly. Consequently, development of efficient,

effective and ecofriendly clean up techniques to reduce or remove the toxic heavy metal and fluoride from water is a necessary.

1.3 Heavy metals pollution

Metals are omnipresent elements in the biosphere, vital to many industrial, infrastructural, and daily life practices. The industrial revolution had increased the redistribution of metals in the environment and accumulation in terrestrial and aquatic habitats, which adversely effects the human health and biota. Those elements with specific gravity greater than 5.0 g/cm^3 and have around five times more density than water is considered as heavy metals and includes mercury (Hg), lead (Pb), cadmium (Cd), arsenic (As), chromium (Cr), nickel (Ni), copper (Cu), zinc (Zn) etc. Heavy metals are the main group of inorganic pollutants, and have the capacity to contaminate an extensive area of land due to use of sludge, smelting industries, pesticides, fertilizers, car exhausts and emissions from municipal waste incinerators.
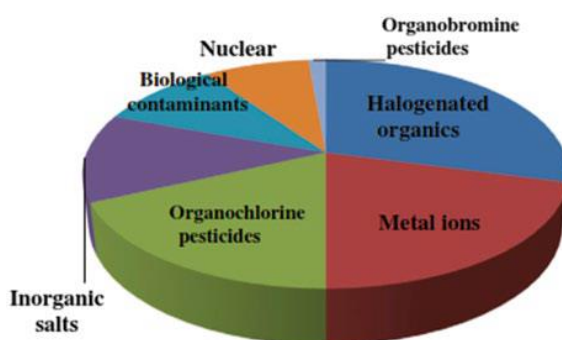
Figure 1.1: Distribution of contaminants regulated by United States Environmental Protection Agency (USEPA) (Reproduced from Thatai et al., 2014)

Heavy metals are ultimately entering into the aquatic ecosystems via direct discharge of industrial effluents and it can also be entered into water during rainfall and leaching from solids. According to the distribution of contaminants, regulated by United States Environmental Protection Agency (USEPA), heavy metals are the most contaminants in industrial effluents (Figure 1.1) (Muhmood & Fawzy, 2016). Volcanic eruptions and weathering have also significantly contributed to heavy metal pollution.

Table 1.1: Anthropogenic sources of heavy metals in the environment (Ali et al., 2013; Sumiahadi & Acar, 2018)

Heavy Metals	Main anthropological sources
Cd	Paints and pigments, plastic stabilizers, electroplating of cadmium containing plastics, phosphate fertilizer
Pb	Aerial emission from combustion of lead petrol, battery manufacture, paints and pigments, herbicides and insecticides
As	Pesticides and wood preservatives
Cu	Pesticides, fertilizers
Cr	Tanneries, Electroplating, steel industries, fly ash
Hg	Release from Au-Ag mining and coal combustion, electronics, medical waste
Ni	Industrial effluents, steel alloys, kitchen appliances, surgical instruments, automobile batteries

Some anthropogenic sources of heavy metals are summarized in Table 1.1. The metal contamination of groundwater can be occurred directly by infiltration of leachate from land disposal of solid wastes, leachate from mine tailings and other mining wastes, liquid sewage or sewage sludge, deep-well disposal of liquid wastes, seepage from industrial waste lagoons or from other spills and leaks from industrial metal processing facilities (e.g., steel plants, plating shops, etc.) (Singh & Prasad, 2015). United States Environmental Protection Agency (UEPA) listed the heavy metals as priority pollutants. Lead, mercury, arsenic and cadmium are ranked first, second, third, and sixth, respectively, by US Agency for Toxic Substances and Disease Registry (ATSDR), on the basis of their prevalence and severity of toxicity. In the present scenario, anthropogenic inputs of metals are more than the natural inputs (Singh & Prasad, 2015).

1.4 The impact of heavy metals in water on human health

The contamination and accumulation of heavy metals is a serious issue around the globe due to the non-biodegradable and persistent nature, toxicity even at low concentration, abundant sources, and its accumulative behaviour. Heavy metals consumption or intake leads to serious destructive effect on human and animal health. Various national and international organization recommended the limits (Table 1.2) of heavy metals in the drinking water, beyond which can lead to many health hazards.

When heavy metals entered into food chains, it accumulates in vital organs, such as the liver, bones, and kidneys, impose a direct threat to

human health and ultimately lead to numerous serious health disorders. Cadmium is toxic even at extremely low levels. The chronic exposure of Cd can lead to harmful health effects, such as lung cancer, kidney dysfunction, prostatic proliferative lesions, hypertension, and bone fractures. Dangerous health conditions like skin cancer, bladder cancer, lung cancer, kidney cancer, and liver cancer can be resulted as a consequence of arsenic exposure. Lead exposure leads to plumbism, nephropathy, inhibition of the synthesis of haemoglobin, gastrointestinal colic, damage to joints, reproductive systems and cardiovascular system and it also severely affect central nervous system (Hu et al., 2017). Lead poisoning also cause acute and chronic harm to the central nervous system and peripheral nervous system (Ogwuebgu & Muhanga, 2005). Psychosis is one of the impacts of chronic lead exposure and high lead exposure also creates some developmental disorders in children like poor IQ (Duruibe et al., 2007), learning disabilities, short-term memory loss, and coordination problems.

Common sources of Cr are leather and tanning industries, electroplating industries, paper and pulp and rubber manufacturing applications. Cr (VI) have more toxicity than Cr (III) in human and animal health. High levels of Cr exposure cause skin ulceration, kidney and liver damage and also affects the central nervous system. Copper is an essential element for human and animal bodies but, a higher dose of it exhibits toxic effects, such as vomiting, diarrhoea, kidney and stomach damage, and loss of strength. The organic form of mercury is highly toxic and found to be associated with physiological stress, abortion and central nervous system disorder in the human.

Table 1.2: Drinking Water Standards (Adapted from: Saha & Paul, 2016).

Heavy Metals	(USEPA, 2008) ($\mu g/L$)	(WHO, 2008) ($\mu g/L$)	(EU, 1998) ($\mu g/L$)	(BIS ISO:10500, 2012) ($\mu g/L$)
Fe	300	NGL*	200	300
Mn	50	400	50	100
Zn	5000	NGL**	NM	5000
Pb	15	10	10	10
Cd	5	3	5	3
Cu	1300	2000	2000	50
Ni	100	70	20	20
Cr	100	50	50	50
Hg	2	6	1	1
As	10	10	10	10

* NGL: No Guideline, because it is not of health concern at concentrations normally observed in drinking water, but may affect the acceptability of water at concentration above 300 μg/L; **NGL: No Guideline, because it occurs in drinking-water at concentrations well below those at which toxic effects may occur and NM: Not Mentioned

Even though, Ni plays an essential role in the synthesis of red blood cells; when it consumed in higher doses for a longer time, it may develop toxic effect like cell damage, liver and heart damage, cancer, nervous system damage and decreased body weight. Iron and manganese

are essential for biological processes, as they play important roles in the synthesis of haemoglobin and functioning of cells. The undesirable amount of iron in water, pose severe toxicity to new-born babies and young children, affect the kidneys, cardiovascular systems, liver and gastrointestinal tract and may also give a rusty taste to drinking water. The toxic impact of manganese in human bodies are neurological disturbances and muscle function damage (Gautam et al., 2015). However, Zn is considered as relatively non-toxic, but its excess level can lead to impairment of growth and reproduction (Duruibe et al., 2007).

The conventional treatment approaches used for heavy metal contaminated water comprises chemical precipitation, ion exchange, chemical oxidation, membrane filtration, reverse osmosis, electro dialysis etc. (Tripathi & Ranjan, 2015). These conventional methods are expensive, energy intensive and often accompanied with generation of toxic by-products. To prevent severe toxic effects and poisoning by heavy metals in water, better and effective remediation techniques for heavy metals in water are required.

1.5 Remediation of heavy metals from water

Several remediation techniques for heavy metals removal from aqueous solutions are available and are mainly based on physical, chemical and biological techniques. These conventional methods include chemical precipitation, filtration, electrochemical treatment, ion exchange, membrane filtration technologies, adsorption, floatation, evaporation and photocatalysis (Gautam et al., 2014). Each method has its own limitations, for example, low selectivity, complex to operate, inefficient in treating

low concentrations of contaminants, difficulty in handling large quantity of sludge, high capital, and energy costs (Muhmood & Fawzy, 2016). However, the treatment of water containing low heavy metal value, using chemical precipitation and electrochemical treatment are ineffective but generates large amount of sludge which need further treatment. Membrane technologies, ion exchange and activated carbon adsorption techniques are extremely costly when treating huge volume of heavy metal contaminated industrial effluent and wastewater containing low concentration, and difficult to use at large industrial scale (Gautam et al., 2014).

Some of the advantages and disadvantages of the existing heavy metals remediation methods are summarized in Table 1.3. Many water and wastewater treatment processes require large amount of energy, which depends upon the factors like the nature of contaminants, quality of the source water, and the types of treatment used. Different stages of treatment are essential for different practices and many of these stages requires extensive energy. Reverse osmosis, a sophisticated technique necessitates larger amount of energy. Among many treatment methods, phytoremediation is a novel clean-up concept in remediation of contaminated water and soil that involves the usage of plants (Singh et al., 2012) and consist of two uptake methods: an initial fast, reversible, metal-binding process (biosorption) and a slow, irreversible, ion sequestration step, bioaccumulation (Fawzy, 2007).

Table 1.3: Heavy metal remediation methods with its advantages and disadvantages

Treatment methods	Advantages	Disadvantages	References
Chemical precipitation	- Simplicity of process - Not metal selective - Inexpensive capital cost	- The demand of a large amount of chemicals - Large amount of sludge containing metals - Sludge disposal cost - High maintenance costs	(Aderhold et al., 1996; Gautam et al., 2014)
Coagulation–flocculation	- Bacterial inactivation capability - Good sludge settling	- Chemical consumption - Increased sludge volume generation - Generally, coagulation flocculation can't treat the heavy metal wastewater completely. Therefore, coagulation flocculation must be followed by other treatment techniques	(Aderhold et al., 1996; Gautam et al., 2014; Muhmood & Fawzy, 2016)
Ion exchange	- Metal selective - Limited pH tolerance - High regeneration - No sludge generation	- Require pre-treatment - Expensive - Suitable ion-exchange resins are not available for all heavy metals - Ion-exchange resins must be regenerated by chemical reagents when they are exhausted and the regeneration can cause serious secondary pollution	(Rengaraj et al., 2003; Gautam et al., 2014; Muhmood & Fawzy, 2016)

(*continued*)

Table 1.3: Heavy metal remediation methods with its advantages and disadvantages

Treatment methods	Advantages	Disadvantages	References
Membrane filtration	• Low solid waste generation • Low chemical consumption • Small space requirement • Possible to be metal selective	• High initial capital cost • High maintenance and operation costs • Membrane fouling • Limited flow-rates	(Madaeni & Mansourpanah, 2003; Qin et al., 2008; Gautam et al., 2014)
Reverse Osmosis	• Purifies water by removing salts such as Ca, Mg, Na, Cl, Cu, as well as bacteria	• Low recovery • Brine disposal • High maintenance	(Muhmood & Fawzy, 2016)
Electrochemical treatment	• No chemical required can be engineered to tolerate suspended solids • Moderately metal selective	• High initial capital cost • Production of hydrogen (with some processes) • Filtration process for flocs	(Gautam et al., 2014)

In spite of its widespread use in the water and wastewater treatment process, activated carbon remains as an expensive material. So, the production of low-cost alternative biosorbents or bio-based adsorbents should be encouraged. Biosorption is a specific term used to describe a process that employs non-living biomass materials of biological origin as biosorbents for the removal of contaminants from aqueous solutions. The prefix "bio" denotes the connection of biological entity, which is dead cells and tissues, living organisms, cellular components or products and

usually, utilised to sequester heavy metals as well as rare earth elements and radionuclides or metalloids (Muhmood & Fawzy, 2016). Magnetic nanoparticles have potential to remove heavy metal ions from aqueous solutions. Surface modification strategy is a good option to improve the heavy metal removal potential of magnetic nanoparticles. To satisfy the demand of safe and clean drinking water, effective, efficient and economical alternative methods for the elimination of heavy metals from water is required.

1.5.1 Phytoremediation technology

Phytoremediation is a novel, integrated multidisciplinary strategy which utilizes the great potential of plants to treat environmental contaminants. Expensiveness, laboriousness and inability to provide the acceptable results are the main drawbacks of many conventional treatment approaches. USEPA (2000) stated that, "Phytoremediation is the name given to a set of technologies that use different plants as a containment, destruction, or an extraction technique. Phytoremediation is an emerging technology that uses various plants to degrade, extract, contain, or immobilize contaminants from soil and water". It can be used to remediate a large variety of contaminants like metals, polyaromatic hydrocarbons, pesticides, solvents, crude oil, explosives, and landfill leachates etc. and can also be utilized for river basin management. Phytoremediation, considered as an emerging, economic and ecological alternative technology for many pollutants, especially for the extraction or removal of inactive metals and metal pollutants from contaminated water and soil. The five major processes involved in phytoremediation are rhizofiltration, phytoextraction, phytostabilization, phytovolatilization, and

phytodegradation and a short outline of all these processes are presented in Figure 1.2. Phytoremediation has also been branded as green remediation, agro remediation, botano-remediation, and vegetative remediation (Andrew, 2007).
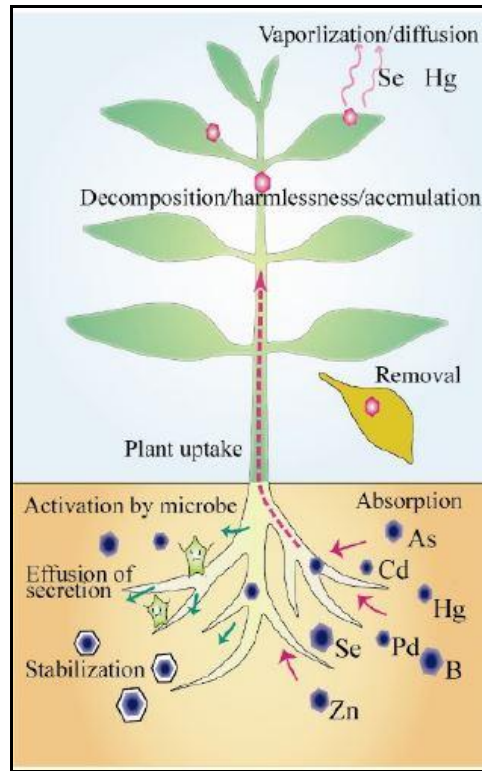
Figure 1.2: Schematic diagram of phytoremediation (Adapted from Sakakibara et al., 2013)

In *Phytoextraction* process, hyperaccumulators or metal-tolerant plants is used to acquire the elevated levels of metals or contaminants in their aboveground tissues with successive harvest, recovery, and disposal or recycling of the metals. The enzymatic breakdown of carbon-containing, or organic compounds to simpler and less toxic chemicals

either alone or combined with soil microbes, comes under *phytodegradation*. *Phytostabilization* denotes the utilization of plants to immobilize contaminants within the soil profile to minimalize biological exposure or pollutant escape (Clayton, 2007). *Phytovolatilization* attributes to the use of plants to uptake of contaminants from soil and water, converting them into volatilized compound and then transpiring into the atmosphere. *Rhizofiltration* refers to the use of both aquatic and terrestrial plants, to absorb, concentrate, and precipitate contaminants from contaminated aqueous media in their root system and can be used for the remediation of metal contaminated groundwater, surface water, and wastewater with low contaminant concentrations.

The phytoremediation potential of numerous plant species has been recognized and considered as hyperaccumulators if they are capable to accumulate potentially phytotoxic elements to concentrations 50-500 times higher than average plants (Lasat, 2000). Many aquatic plants have the ability to bio-accumulate pollutants such as toxic heavy metals and nutrients, in large quantities and effectively remediate wastewater containing various inorganic and organic pollutants including heavy metals, pesticides, nutrients, oils, POPs etc. The macrophytes exhibits absorption of the pollutants at different rates and efficiencies because it depends on the concentration of pollutant, duration of exposure and other factors including environment conditions (pH, temperature etc.), physico-chemical properties of contaminants (solubility, pressure etc.), abundance, biochemical composition, habit and species (Anand et al., 2017).

Macrophytes produces metal-binding cysteine-rich peptides (phytochelatins) to detoxify metals by forming complexes with them, under the pollution stress. The phytoremediation ability of several macrophytes such as water hyacinth (Eichhornia *crassipes)*, duckweed (Lemna spp.), water lettuce (*Pistia stratiotes* L.), vetiver grass (*Chrysopogon zizanioides)*, water spinach (Ipomoea *aquatica)*, bulrush (Typha*)*, common reed (*Phragmites australis*), etc. and microalgae including *Chlorella vulgaris* were utilised for the treatment of different types of wastewater by many researchers. Many macrophytes are excellent tools for phytoremediation approach, because these universally available aquatic plants have the excellent ability to survive in adverse conditions and high colonisation rates (Aisien et al., 2015).

Eichhornia crassipes (water hyacinth) has attained significant attention due to its ability to accumulate pollutants from aquatic environment with rapid proliferation. Its uncontrollable growth in water bodies makes it most problematic plants worldwide and development of some utilisation technique of them is the best management strategy of *Eichhornia crassipes.* Moreover, its application for the wastewater treatment in urban or industrial areas as phytoremediation agent, several beneficial by-products can be developed from it like animal fodder/fish feed, power plant energy (briquette), biogas, bioethanol, biosorbent for the removal of toxic metals, paper manufacturing, composting and fiber board making. Some of the non-degradable and toxic elements like heavy metals can be recovered from *Eichhornia crassipes,* after its application for the removal of metals from wastewater. Even though, it poses serious issues in the field of irrigation, navigation, and power generation, the production

of biofuels can help to overcome both environmental contamination and the depletion of energy sources globally. The briquette manufactured from dried *Eichhornia crassipes* is used for co-firing in coal power plant (Rezania et al., 2015). It has the ability to absorbs and translocate both essentials metals Cu, Zn, and Ni, and nonessentials metals Pb, Cd, and Cr etc. The aquatic fern, *Salvinia molesta* is a native to south-eastern Brazil but it is extensively distributed in tropical and subtropical areas. It possesses potential like fast growing rate, tolerant to pollution and ability to accumulate metals (cadmium, lead, copper, chromium, and zinc etc.). *Salvinia molesta* can translocate and accumulate many toxic metals and have the potential to tolerate the adverse environmental conditions (Cabo et al., 2015).

1.5.1.1 Mechanisms involved in metal phytoremediation

Some heavy metals (Zn, Cu, Fe, Mn, Mo, Co, and Ni) are essential components in metabolism and are required for normal growth but, high concentration of these metals become toxic. The heavy metals, like Cd, Pb, Hg, Se, and As, do not involved in any known physiological function so these metals are not essential for most of the plants. During heavy metal phytoremediation, metal ions that are incorporated to the tissues of living organisms binds to macromolecules like protein. The information about the metal-binding proteins helps to understand the mechanism of metal accumulation. After mobilization, metals first bind to the wall of cell, an ion exchanger with comparatively low selectivity. Then, the transport systems and intracellular high-affinity binding sites, helps and mediates the uptake of metals across the plasma membrane via secondary

transporters like H^+ - coupled carrier proteins and/or channel proteins (Chaney et al., 2007). The root pressure and transpiration pull controls the movement of metal-containing sap from roots to the aerial parts. Afterward, conveyance of the metal to the shoot mainly takes place through the xylem.

High intracellular concentrations of heavy metals are extremely toxic, so plants usually catalyse redox reactions and alter the forms of these metal ions into nontoxic forms in order to permit their accumulation. Examples of these process are the reduction of Cr^{6+} to Cr^{3+} takes place in *Eichhornia crassipes* (Lytle et al., 1998) and reduction of As $^{5+}$ to As $^{3+}$ takes place in *B. juncea* (Pickering et al., 2000). But, the oxidation states of metals such as Cd, Zn, and Pb do not change. On the other hand, detoxification of some intracellular metals is done by binding to low molecular mass organic compounds, by localization in the vacuoles as a metal-organic acid complex, or by binding to histidine (Persans et al., 1999; Kramer et al., 2000; Trivedi & Ansari, 2015). In the case of metals like Zn, there are many mechanisms for regulation of cytoplasmic metal concentration which comprise sequestration in a subcellular organelle to low molecular mass organic ligands, low uptake across the plasma membrane, and precipitation as insoluble salts and active extrusion across the plasma membrane into the apoplast (Brune et al., 1994; Trivedi & Ansari, 2015).

1.5.1.2 Utilization of Phytoremediation by-product

In the establishment of large-scale implementation of phytoremediation process, the management of used macrophytes or

contaminated plant material is the main concern, so the utilization of phytoremediating plants for bioenergy production will be a low cost and effective approach for the optimum utilization and eco-friendly management of the used macrophytes. Because of higher biomass production and high photosynthetic efficiency, macrophytes produces useful amounts of carbohydrate and cellulose; raw material for the production of bio-gas, bioethanol and lipids which are non-polluting and renewable sources of energy. Several aquatic macrophytes can easily be degraded, and produces high bioenergy yield, examples are *Eichhornia crassipes, Typha latifolia, Trapa natans, Pistiastratiotes, Lemna gibba, Phragmites australis, etc.* Besides, macrophytes can be utilized for many other purposes like household, recreational, fertilizers, mulch, fodder, flowers, etc. Macrophytes also have ability to sequester carbon through photosynthesis and accumulation of organic matter (Anand et al., 2017).

In plant biomass, solar energy is stored, is also called as materials having combustible organic matter and it contains carbon, hydrogen and oxygen, so known as oxygenated hydrocarbons. The biomass material contains main constituents such as lignin, cellulose, hemicellulose, mineral matter and ash. It possesses high volatile matter constituents and moisture; low bulk density and calorific value and the proportion of these components differs from species to species (Ghosh & Singh, 2005). After completing the phytoremediation process, the handling or disposal of a huge quantity of metal accumulated biomass is a great challenge. The initial step of post-harvest biomass treatment is its volume reduction. The approaches like compaction and pyrolysis are feasible methods to recycle metals from harvested plant materials. Furthermore, incineration is a

perfect alternative technique for the disposal of harvested biomass, after phytoremediation and the metal residue have to be recycled from the ash. To recycle different metals from ash, further studies are required. Gasification is a novel technology, in this process, harvested biomass can be undergone to a series of chemical reactions to yield clean and combustive gas for producing electrical and thermal energy (Chen et al., 2015).

Leaching tests of the composted material indicates that during composting process, soluble organic compounds formed enhances the solubility of metal (Pb). To prevent further transport of these metals to the environment, the treatment of metal accumulated plant materials would still require prior to its disposal. The volume reduction of biomass by compaction, lowers the cost of its transportation to a hazardous waste disposal facility but, the leachate needed to be collected and treated properly. The phytomining is a promising route to exploit the biomass produced by phytoremediation. If phytoremediation approach is integrated with biomass production and its commercial application as an energy source, turns this approach as profit making operation and the remaining ash can be utilised as valuable bio-ore, this is the basic principle of phytomining technique. This technology involves generation of revenue by extracting saleable metals produced from the plant biomass ash, also termed as bio-ore (Ghosh & Singh, 2005). Although these techniques are considered as theoretically feasible methods for the disposal of harvested biomass but, the analysis of cost/benefit and environmental acceptability should be investigated before proceeding (Chen et al., 2015).

Generally, the biotechnological approaches are utilised to enhance the metal phytoremediation potential of plants. The time-consuming nature of phytoremediation can be tried to overcome with help of different methods. In the present study, the potential of heavy metals phytoremediation of aquatic plants was tried to enhanced with the help of electro - assisted phytoremediation method and nanotechnology. Chelate assisted phytoremediation method was also employed as part of the study, for the remediation of heavy metal contaminated soil.

1.5.1.3 Electro - assisted phytoremediation

An integrated approach of phyto and electro remediation is a novel attempted to effectively remediate heavy metals from water and soil. Electro Assisted-Phytoremediation (EAPR) facilitates, the transportation of metal ions to the roots zone through electro-migration and its deposition at the shoot of plant via adsorption process. Many researchers extensively reported, the utilisation of the combination of phytoremediation and electrochemical, to improvement of aquatic phytoremediation of metals (Rodríguez et al., 2010; Bi et al., 2011; Kubiak et al., 2012). Generally, the electro remediation technique used to influence the movement of ions in porous media but, now a days, it is also applied to aqueous solution to facilitate adsorption of metal like As by the plant, *L. minor* (Kubiak et al., 2012).

Putra et al. (2017) reported that the plants used for EAPR system did not exhibited any phytotoxic symptoms such as yellowing, discoloration, withering, and pigmentation) indicating higher tolerance of plant to high level of heavy metal. Although under that stress, the plants

still able to maintain relatively normal level of photosynthetic pigments. Their results confirm that the EAPR process effectively reduce the level of heavy metal in the chemical laboratory wastewater treatment. Song et al. (2011) studied the performance of laboratory-scale constructed wetlands coupled with micro-electric field (CWMEF) planted cannas (Canna generalis) for heavy metal-contaminating wastewater treatment. The mechanisms like anode oxidation, cathode deoxidation, electro-coagulation, and electro-flotation are involved in electrochemical treatment technology. The stimulation of the suitable voltage and electrical exposure time leads to better growth of plants and so the plants assimilate more metallic ions under electrified conditions. As the applied voltage and electrical exposure time increase, the pH was also increased which is due to the increase in OH^- concentration. Therefore, the high pH leads to the precipitation and flocculation of metallic ions and can be postulated that micro-electric field is supporting heavy metal phytoremediation by precipitation and flocculation of metals (Rajeshwar et al., 1994). In Al electrode used electro assisted phytoremediation system, Al^{3+} could be formed by anodizing of aluminium and its hydrolysis produces $Al(OH)_3$, which improves the flocculation and adsorption of metal ions (Song et al., 2011).

The electric field stimulate the plants to grow better, and assimilated more heavy metal. Knorr (2003) reported that the longer the duration of electrification of the system, the more noticeable stimulating effect occurs. The voltage can stimulate the plants to increase the palisade cells, chloroplast grana and thylakoid lamellas, which enhance the synthesis of chlorophyll. The electric field improves the ability plants to

resist adverse conditions by encouraging CHLab synthesis, preventing MDA synthesis, and catalysing SOD synthesis. Consequently, plants assimilate more metal in EAPR system. EAPR system had more favourable conditions to accumulate metals than the phytoremediation system, for instance the higher pH, and the occurrence of Al ions, which leads to chemical precipitation, physical adsorption and flocculation of metal (Song et al., 2011).

1.5.1.4 Nanotechnology and plant growth

The victory of phytoremediation depends upon plants' capability to accumulate high concentrations of the metals. Researches are in progress to enhance the efficiency of this plant-based technology. Recently, nanoparticles (NP) have attained a lot of consideration because of their increasing ability to synthesize and manipulate such materials. Nowadays nanoscale materials are applied in a variety of different areas such as electronic, biomedical, pharmaceutical, cosmetic, energy, environmental, catalytic and material applications. A worldwide increase in investment in nanotechnology research and development observed because of the potential of this technology (Guzman et al., 2006). Recently, the application of nano particles to solve many of the agriculture-related problems have achieved tremendous improvement compared to conventional agriculture practices and its uses not only promote the plant growth but also control the plant diseases. Nanoparticles can be employed to increase the supply of elements to plant shoots and foliage and to increase seed germination and seedling growth. In addition, it can enhance the ability of water and fertilizer absorption by roots, increase antioxidant

enzyme activity such as superoxide dismutase and catalase thus increase plant resistance against different stresses. Several studies indicate that nano particles have favorable effects on plant growth and development.

Morteza et al. (2013) reported that, TiO_2 nanoparticles significantly influence the chlorophyll content (a and b), total chlorophyll (a + b), chlorophyll a/b, anthocyanins and carotenoids in plants. Accordingly, an application of TiO_2 nanoparticles facilitate the increase in crop yield by promoting the growth of plants. TiO_2 is generally used as photo-catalyst due to its stability in UV light and water. The nano - TiO_2 also influence the germination. It prominently helps aged seeds' vigor and chlorophyll development, stimulates Rubisco activity and improves photosynthesis, thus increase in plant growth and development occur (Yang et al., 2006). TiO_2 nanoparticles promotes light absorbance, accelerate the transport and conversion of the light energy, guard the chloroplasts from aging, and extend the photosynthetic time of the chloroplasts. It improves the plant growth through enhanced nitrogen metabolism, that promotes the absorption of nitrate, thus increases the fresh and dry weights (Yang et al., 2006). Nano anatase TiO_2, effect the antioxidant stress via decreasing the accumulation of superoxide radicles, catalyse, hydrogen peroxide, guaiacol peroxidise, ascorbate peroxidise, and thus increases the evolution oxygen rate, in plants chloroplast under UV-B radiation (Lei et al., 2008). These ability of TiO_2 can be utilised to improve the plants potential for phytoremediation of heavy metals from water. So, in our study we tried to enhance the phytoremediation capacity of *Eichhornia crassipes and Salvinia molesta* using TiO_2 nano particles.

1.5.1.5 Chelate assisted phytoremediation of heavy metals in soil

In soil, heavy metals occur naturally from the pedogenetic processes of weathering of parent materials at levels that are regarded as trace (<1000 mg/Kg) and rarely toxic (Wuana & Okieimen, 2011). The most abundant heavy metals found in soil are As, Hg, Cu, Pb, Zn, Cr and Cd. Numerous anthropogenic activities also induce the serious risk of metals. Both essential and non-essential metal s are toxic to living organisms, above certain concentrations specific to each metal. pH, ionic strength, type of competing cations, functional group and type of clay minerals are the factors which depends the reduction metals in soil. The transport of heavy metals, from soil to water is a threat for many water resources. So, to prevent heavy metal contamination in water, attempt to remediate heavy metals in soil is essential. Traditional treatments method for decontamination of metal in soils are cost prohibitive, when handling large areas of contaminated soil. Major soil remediation techniques for heavy metal removal includes isolation and containment, soil leaching, thermal desorption, electro kinetic remediation, solidification/stabilization (S/S) and vitrification

For remediation of heavy metal-contaminated sites, immobilization, soil washing, and phytoremediation techniques are frequently listed among the best demonstrated available technologies (BDATs). In developing countries, to reduce the associated risks, make the land resource available for agricultural activity, enhance food security, and scale down land tenure problems, low cost and ecologically sustainable remedial choices are required to restore contaminated lands due to the great population density and scarce funds available for

environmental restoration (Wuana & Okieimen, 2011). In soil, chelate assisted phytoremediation of heavy metals is an effective method to detoxify or immobilize metal contaminants. Various chelators such as EDTA, organic acid, citric acid, or nicotianamine may be helps the translocation of metal cations through the xylem. In the shoot cell membrane, metal transporters mediate the uptake of metal ions from the xylem apoplast into the shoot symplast (Khushboo et al., 2016).

EDTA is one of the most applied chelating agents. As EDTA has drawbacks like high toxicity, persistent nature in the environment and expensiveness (Wuana & Okieimen, 2011). The chelating agent also have the following deficiencies: citric acid is a nontoxic acid that forms relatively strong complexes and easily biodegradable, but it presents of lower effectiveness in the removal of metal ions (Palma & Mecozzi, 2007); nitric acid (HNO_3) is lethal to soil micro-flora and destruct the physico-chemical properties of soil; nitrilotriacetic acid (NTA) is a toxicant as a class II carcinogen (Peters, 1999); hydrochloric acid (HCl) can alter soil properties (Neilson et al., 2003); EDGA enhanced metal solubility but plant uptake did not increase accordingly (Römkens et al., 2002). Although, chelators effectively improve the mobility of target heavy metals and its accumulation into aerial parts of the plants but possesses some inhibitory effects on plant growth. So, eco-friendly and effective mobilizing agent is essential to enhance the phytoremediation ability of plants. An immobilizing agent is also required to reduce the risk of bioaccumulation, biomagnification through food chain and to reduce heavy metals contamination of groundwater. The ammonium molybdate act as both mobilizing and immobilize toxic metals, which is fertilizer

(containing nitrogen and molybdenum) to plants, thus can produce more biomass (Qu et al., 2011). Phytoextraction and phytostabilization potential of the *Amaranthus retroflexus* with ammonium molybdate for the remediation metals in soil was investigated as a part of the study.

1.5.2 Heavy metal removal using biosorbents

Several techniques have been established for the removal of heavy metal from wastewater such as chemical precipitation, evaporation, ion exchange, reverse osmosis, solvent extraction, membrane process and electro dialysis etc. but, each method possess its own merits and demerits. They are associated with high operational cost and generation of toxic sludge, disposal of which makes it non eco-friendly and expensive. Adsorption has emerged out to be a better alternative of safe and economical treatment for heavy metal laden wastewater. The main advantage of adsorption technique for heavy metal removal is less initial and operation cost, easy design and less prerequisite to control systems (Tripathi & Ranjan, 2015). The use of activated carbon (AC), traditional adsorbent material is limited because of its high cost and decreased adsorption capacity after regeneration process in comparison with some other sorbents (Grassi et al., 2012). The sorbent may belong to mineral, organic or biological origin. The low-cost materials like wood materials, some aquatic plants, agricultural and industrial by-products, natural zeolite, clay, chitin, peat moss, turba (partially decomposed vegetable matter), microorganisms, polymeric material etc. have high potential to adsorb and accumulate heavy metals (Argun et al., 2007).

Adsorption, a mass transfer process, involves the accumulation of contaminants at the interface of two phases, and the characteristics of adsorbents and adsorbates are quite specific and depend upon their constituents. In the case of physisorption, the attraction interactions involved through weak van der Waals forces and, the process is reversible. On the other hand, chemisorption occurs through strong chemical bonding so, the substances chemisorbed on adsorbent surface are hardly removed. Under favourable conditions, both processes can take place simultaneously or alternatively. Physisorption is escorted by a decline in free energy and entropy of the adsorption system and, thus, it is an exothermic process. If the removal of contaminants from aqueous solution occur through a solid–liquid adsorption system, the contaminants or the solute accumulate at solid surface (Gisi et al., 2016). Many algae, microorganisms, fungi, and plants materials have the potential to take up heavy metal ions. In the metal removal process by biosorption using non-living sorbents like plant materials and dead algal biomass, the extents of sorption dependent on or involve the metabolism-independent metal accumulation occurred at the cell wall by functional groups, polysaccharides, and associated molecules. (Muhmood & Fawzy, 2016). Removal of toxic heavy metals from aqueous solution was attempted using a herbal plant material, *Caesalpinia sappan* (sappan wood) and an algal biomass, *Trenteohilia abietina*, as part of the study.

1.5.3 Removal of heavy metal using iron oxide nanosorbents

Among many detoxification methods of heavy metals in water, nano-based adsorbents are one of the convenient technologies. Iron oxide-based nanomaterial attracted more attention for heavy metals removal due

to their significant characteristics such as small size, high surface area, and magnetic property. Its magnetic property enables easy separation of nanosorbents from aqueous solution and can be reused for more utilization. The reusability of iron oxide based nanosorbents, make it more economic (Dave & Chopda, 2014). Iron oxide nanomaterial also possess photocatalytic property. Iron oxides occur in various forms in nature but magnetite (Fe_3O_4), maghemite (γ-Fe_2O_3), and hematite (α-Fe_2O_3) are the most common forms among them. Its easy synthesis, the ability to control or manipulate matter on an atomic scale, and coating or modification provides unequalled versatility. Moreover, its chemical inertness, low toxicity, and biocompatibility illustrate an excellent potential in combination with biotechnology (Gupta & Gupta, 2005; Xu et al., 2012). Synthesis methods and surface coating mediums show a major role in determining the size distribution, magnetic properties, morphology, and surface chemistry of nanoparticles. The chemical and physical methods was mainly used for its synthesis (Xu et al., 2012).

Among many nano materials, the ability of iron oxide magnetic NMs to treat large volume of contaminated water and being suitable for magnetic separation, no sludge formation, makes it most promising materials for the treatment of heavy metal (Hu et al., 2010). The small size of iron oxide nanosorbents was favourable for the diffusion of metal ions from solution onto the active sites of the adsorbents surface. It suggested that iron oxide nanosorbents were effective and economical sorbents for fast removal and recovery of metal ions from contaminated water (Xu et al., 2012). Aggregation and many other interactions occurred in wastewater disturb the adsorption of heavy metals which may limit the

effectiveness of nanosorbents. Surface modification overcomes such situations by enhancing the efficiency of nanosorbents. Modification of nanosorbent surfaces can be achieved by attaching the inorganic shells and/or organic molecules, which not only stabilizes the nanoparticles and ultimately prevents their oxidation, but also offers specific functionalities that can be ion selective and accordingly, enhance the metal uptake capacity (Xu et al., 2012). Mechanisms involved in the metal adsorption from water by surface modified iron oxide nanosorbent consist of surface sites binding electrostatic interaction, magnetic selective adsorption and modified ligands combination (Zhong et al., 2006; Hao et al., 2010; Hu et al., 2010; Ozmen et al., 2010). As a part of the study, surface modification strategy was utilized to improve heavy removal efficiency of iron oxide nanoparticles by polyvinyl alcohol and gallic acid.

1.6 Fluoride contamination in water

Contamination of water by fluoride is one of the major concerns across the world since few decades. Fluoride related health complications such as dental and skeletal fluorosis in human possess some serious socioeconomic implications. Fluorine is the lightest and most electronegative element in the halogen group, hence it is chemically most energetic element. Due to high lattice energy, the ionic bond formed between fluorine and calcium is very strong when it enters the human body. So, fluoride salts to be very fatal when it is directly ingested to human body (Mbugua et al., 2017). Fluorine is an abundant (625 mg/Kg) element present in the earth's crust and mobile at a higher temperature, is existing in the form of fluorides in many minerals and rocks. Excessive

intake of fluoride through drinking water leads to harmful health effects like dental and skeletal fluorosis. In India, many areas are facing high fluoride levels in drinking water due to fluoride bearing minerals or fluoride rich minerals in the rocks and soils and its impact on human wellbeing amplified the importance of defluoridation studies (Edmunds & Smedley, 2001; Chidambaram et al., 2003).

In water, fluorine exists as negatively charged fluoride ion (F$^-$). Fluorine-bearing minerals such as *fluorite* (CaF_2), *cryolite* (Na_3AlF_6), *apatite* [$Ca_5(Cl,F,OH)(PO_4)_3$], *topaz* [$Al_2SiO_4(F,OH_2)$], *amphiboles* [$A_{0-1}B_2C_5T_8O_{22}(OH,F,Cl)$], *sellaite* ($MgF_2$) and *micas* [$AB_{2-3}(X,Si)_4O_{10}(O,F,OH)_2$] are the main sources of fluoride. Weathering of these fluorine-bearing minerals is the most significant geogenic source of fluoride enrichment in water. Anthropogenic sources also contribute fluoride contamination, which includes many chemical industries (like phosphorous fertilizer plants, aluminum, zinc, steel, smelting industries, etc), glass and ceramic industries, and power plants (Bhat et al., 2015). The fluoride concentration in the groundwater depends upon many factors such as solubility and availability of fluoride minerals, pH, velocity of flowing water, temperature, calcium and bicarbonate ions concentration in water, etc. (Bishnoi & Arora, 2007).

1.6.1 Health hazardous of fluoride

Globally, around 200 million people rely on high fluoride contaminated water source and one of the major environmental problems, moderate to high fluoride contamination in groundwater is reported in countries like India, Algeria, China, Ghana, Brazil, Canada, Ethiopia,

Kenya, Iran, Japan, Italy, Jordan, Malawi, Korea, Mexico, Pakistan, Norway, Sri Lanka, Turkey, Thailand, and the US. Mild fluoride consumption induces dental effects whereas, long-term intake of high fluoride leads to severe skeletal disorders and other adverse disease. The human health risks associated with fluoride contamination broadly categorized as follows: dental effects, skeletal effects, developmental effects, reproductive effects, renal effects, endocrine effects, neurological effects, and carcinogenic effects. Modest level fluoride consumption prevents dental caries. Hence, the most essential step to regulate fluorosis is to ensure permissible fluoride concentration in drinking water. A maximum permissible limit of 1.5 mg/L fluoride concentration in drinking water was recommended by World Health Organization (WHO) (Bhattacharya & Samal, 2018). Above 65 million Indians including 6 million children are at danger due to the presence of fluoride concentration beyond the desirable 1.5 mg/L level in potable water (UNICEF, 1999; Bhattacharya & Samal, 2018). Palakkad and Alappuzha are the two fluoride endemic districts of Kerala where many fluorosis cases were reported. Dental flurosis in children from Palakkad distict are shown in Plate 1.1. Levels of fluoride in drinking water and its effect on human health are presented in Table 1.4.

Table 1.4: Levels of fluoride in drinking water and its effect on human health (Adapted from Saxena & Sewak, 2015)

Concentration of Fluoride in water (mg/L)	Health Effect
Nil	Limited growth and fertility
Below 0.5	Dental carries
0.5 – 1.5	Promote dental health and avoids tooth decay and cavities
1.5 – 4.0	Dental fluorosis, mottling and pitting of teeth
4.0 – 10.0	Dental and skeletal fluorosis, pain in the back and all

Fluoride have both beneficial or detrimental effect on human health, reliant on the level of fluoride in drinking water and if it exceeds 1.5 mg/L, dental fluorosis or skeletal damage may occur (Hu et al., 2003). However, fluoride enters to human body via food, industrial exposure, water, drugs, cosmetics, etc., potable water is the main contributor (75 - 90% of daily intake) (Sarala & Rao, 1993). As a result of its strong electronegativity, fluoride reacted with the positively charged calcium present in teeth and bones which leads to dental fluorosis, skeletal fluorosis, teeth mottling, and deformation of bones in children as well as in adults (Susheela et al., 1993). High fluoride content also affects plants and animals but the severity of damage is depending on the concentration and duration of fluoride exposure (Bishnoi & Arora, 2007). High fluoride exposure in drinking water causes decreased IQ level in children and limit the intellectual and cognitive ability of consumers (Mbugua et al., 2017).

Plate 1.1: Dental flurosis in children from Palakkad distict

1.6.2 Different remediation methods for fluoride in water

The fluoride contamination has caused many health and social related problems in India. Prevention of fluorosis is the only suitable measure as it is irreversible health hazard. Hence, management and mitigation of this serious issue are urgently required. Removal of fluoride from drinking water can be done by Nalgonda process and Activated Alumina process. Aluminum salts as coagulant/regenerate are used in these processes but, small quantities of residual aluminum may remain in the water after treatment. Aluminum have adverse effects of neurotoxicity and bone toxicity, and it is also correlated to Alzheimer disease. (Saxena & Sewak, 2015).

The other remediation methods for fluoride includes: reverse osmosis, ion-exchange, electrodialysis, and adsorption. Among them, the ion-exchange and reverse osmosis are relatively expensive and also require special equipments. Fluoride selective ion-exchange resin is only effective if regeneration is carefully monitored and executed regularly. In the absence of proper regeneration or timely change of resin, the exhausted resin gives false sense of security to the consumers. In ion-

exchange technology, water continuously flows through the bed even when the resin bed is exhausted but no automatic indicator or indication to shut down is possible (Saxena and Sewak, 2015). Because of ease of operation and cost-effectiveness, adsorption is still the viable method for the remediation of fluoride and it is also considered to be an efficient and effective defluoridation method. Adsorption involves physical, ion-exchange or surface chemical reaction of fluoride with adsorbent. The low-cost adsorbents used for defluoridation includes activated alumina, activated carbon, amorphous alumina, zeolite, clay, calcite, charcoal, red mud etc. The materials like kaolinite, charfines, bentonite, lignite and nirmali seeds were also examined for the removal of fluoride from water. Plant materials have the ability to accumulate fluoride from water and hence, can be utilized as defluoridating agents (Harikumar et al., 2012). Kerala is one of the states in southern India, having a rich biodiversity of medicinal plants. The fluoride removal ability of some medicinal plant materials was studied. Defluoridation ability of activated *Vetiveria zizanioides* was investigated in this study.

1.7 Aim and Objectives of the Study

The present study was carried out, to develop efficient, effective and ecofriendly water treatment method for the removal of heavy metals from the contaminated water. The defluoridation study of water using biosorbents and its application on contaminated field water samples was conducted. The assessment of the detoxification of heavy metals from water by nanosorbent and biosorbents and its application on contaminated groundwater samples were also carried out in this study. The transport of heavy metals, from soil to water is a threat for many water resources. So,

an attempt was made to remediate heavy metals in soil using soil phytoremediation technique.

The key objectives of the study are:

- To develop efficient, effective and ecofriendly water treatment method for the removal of heavy metals from the contaminated water.
- To study the defluoridation of water using biosorbents and its application in groundwater samples collected from the contaminated areas.
- To assess the detoxification of heavy metals from water by nanosorbent and biosorbents and its application in polluted samples.
- To use the technology of phytoremediation for the decontamination of soil affected by heavy metal toxicity.

1.8 Scope of the study

The present study deals with development of effective, efficient and ecofriendly clean up techniques to reduce or remove the toxicity of heavy metal and fluoride from water. Globally, heavy metals and fluoride are the growing apprehension due to its adverse health impact on human, animal, plants and eco-system. Treatment of heavy metals from water was conducted using electrically stimulated phytoremediation method. Also, phytoremediation ability of aquatic plants to remove heavy metal from water was tried to enhanced using TiO_2 nanoparticles. The transport of heavy metals, from soil to water is a threat for many water resources. So,

an attempt was made to remediate heavy metals in soil using soil phytoremediation technique. For this purpose, the effect of ammonium molybdate on phytoremediation of toxic heavy metals (Cd, Pb, Cu, Ni and Zn) from soil by *Amaranthus retroflexus* was investigated. the defluoridation of water using cost effective technique. Defluoridation ability of some medicinal as well as easily and locally available plant materials were tested. Defluoridation potential of *Vetiveria zizanioides* was investigated and it was applied on fluoride contaminated groundwater samples from Palakkad district. For the removal of heavy metals from water, two biosorption studies were conducted using a herbal plant material, *Caesalpinia sappan* and an algal biomass, *Trenteohilia abietina*. Surface modification strategy was utilized to improve heavy removal efficiency of iron oxide nanoparticles by poly vinyl alcohol and gallic acid. The assessment of heavy metal contamination in groundwater resources from Madayi panchayath, a clay mining area in northern Kerala, using indexing approach (heavy metal pollution index (HPI), heavy metal evaluation index (HEI) and contamination index (C_d)). The heavy metal in drinking water from Madayi panchayath were tried to remove using functionalized iron oxide nanosorbent (iron oxide nanoparticles coated with poly vinyl alcohol and gallic acid); protonated *Caesalpinia sappan* (herbal plant material) and *Tretepohila abietina* (algal biosorbent). The conclusions and recommendations derived from the study will be useful for the effective and eco-friendly remediation of heavy metals and fluoride from water.

Chapter 2

REVIEW OF LITERATURES

In the last few decades, many precious environmental resources especially water and soil, have loaded with huge amount of pollutants as a result of rapid industrialization, urbanization, population growth and modern agricultural activities. Now a days, a wide variety of contaminants are entering to the aquatic environment, which not only disrupts natural conditions of eco-system but also have toxic impact on living organisms. Heavy metals and fluoride are some of the inorganic contaminants which leads to many health disorders and disfunctions in human and animals. Hence, the remediation of such contaminants is essential for the well-being of the mankind. Expensiveness, ineffectiveness at low concentration, time consumption and sometimes non-eco-friendly nature are the main drawbacks of many of the prevailing remediation techniques available for theses contaminants. Consequently, development of effective, efficient and eco-friendly clean-up methods for the removal or reduction of the toxic contaminants like heavy metal and fluoride from water is necessary, for the protection of human and environmental health.

2.1 Heavy metals related issues and remediation

Among numerous inorganic contaminants in water, contamination and accumulation of heavy metals is a serious problem around the world, because of their persistent, non-biodegradable and bio accumulative nature, abundant sources and high toxicity even at low concentration. Its occurrence in high amount is a potential threat to food safety and have detrimental effects on human and animal health (Hu et al., 2017). Effluents from several industries like electroplating, mining, smelting, tannery, leather, textile, paint, petroleum refining, pigment & dyes, wood processing, photographic film production etc., contains significant quantity of heavy metals. Even though, some heavy metals are extremely essential to living organism, but its concentration beyond the limits suggested by various national and international organization may lead to various physiological disorders (Saha & Paul, 2016).

Verma and Dwivedi (2013) have reported that the metals like zinc (Zn), iron (Fe), copper (Cu) are beneficial for human and animal health in small dosages but beyond the limit it may become toxic. For agriculture purposes, some metals like zinc (Zn), copper (Cu), iron (Fe), manganese (Mn), are applied in prescribed quantities. But, heavy metals like lead (Pb), mercury (Hg), arsenic (As), cadmium (Cd), chromium (Cr) especially hexavalent chromium, nickel (Ni), barium (Ba), cobalt (Co), selenium (Se), vanadium (V), etc. are very toxic, harmful, and poisonous even in at parts per billion level. Tendency of heavy metals to bioaccumulate, i.e., the increase in the heavy metal concentration in a biological organism over time, compared to its concentration in the

environment, makes it more hazardous. In living things, metals are stored sooner than they are broken down or excreted. Its toxicity leads to damaged or reduced mental and central nervous function, damage to blood composition, kidneys, lungs, liver, and other vital organs and lowers the energy levels. While, long-term exposure may have consequences like slowly progressing physical, muscular, and neurological degenerative processes that mimic Parkinson's disease, Alzheimer's disease, muscular dystrophy, and multiple sclerosis. Allergies are also one of its common issues and cancer is the detrimental effect of frequent, long-term contact of some metals or their compounds. Severe mucosal irritation and corrosion, hepatic and renal damage, widespread capillary damage, gastrointestinal irritation, central nervous system disorders followed by depression and possible necrotic changes in the liver and kidney are the impact of excessive intake of Cu in human. The Ni exposure have the effects which vary from skin irritation to damage to the nervous system, lungs, and mucous membranes. Hexavalent chromium, a strong oxidant is highly toxic. The carcinogenicity is a main toxic characteristic of some heavy metals (Argun et al., 2007).

The excessive amounts or imbalances of a metal species exhibits many toxicity symptoms, cellular functioning disorders, long-term devastating disabilities in human beings, and ultimately death. In global context, the pollution by heavy metals is becoming one of the major environment threats. It is a most sever problem in population dense countries particularly like China and India (Dave & Chopda, 2014). The US Environmental Protection Agency (US EPA) and the Agency for Toxic Substances and Disease Registry (ATSDR) enlisted the top 20

hazardous substances which include some heavy metals such as As, Pb, Hg, and Cd (Pandey, 2012). These toxic metals from the environment can be removed by various physicochemical and biological approaches. Majority of the, physicochemical treatment techniques are expensive and not environmentally safe. Chemical precipitation, ion exchange, oxidation/reduction, reverse osmosis, membrane separation, electro dialysis, solvent extraction, sedimentation, filtration, electrochemical techniques, and cation surfactant, etc. are the various treatment methods for heavy metal contaminated water but, some of these approaches are expensive, energy intensive and often linked with generation of toxic by-products (Argun et al., 2007; Tripathi & Ranjan, 2015; Czikkely et al., 2018). So, development of environment friendly, low cost, and effective techniques to remediate toxic heavy metals from water is an obligatory for the wellbeing of mankind and environment. Prevention of transport of toxic metals from soil to water resources can be achieved by proper soil remediation.

Heavy metals can be lethal to human as well as environment even at low concentration. Therefore, effective and efficient remediation strategies are required to reduce or remove the heavy metal contamination. Numerous chemical, physical and biological technical solutions have been utilized and established to remove potential toxic metal from wastewater (Czikkely et al., 2018). Each method has its own merits and demerits. The biological remediation methods are most effective because of its characteristics like natural process, environment friendly nature, inexpensiveness, and high public acceptance. Environmental clean-up using biological agents is termed as bioremediation. Phytoremediation, an

eco-friendly technique has revealed promising results in the decontamination of heavy metals and also been a solution for various emerging environmental issues. The fundamental elements in this technique are plants (terrestrial or aquatic) which plays a vital role for remediation of heavy metal contaminated environments. It is considered as environmentally friendly, efficient, cheap and reliable remediation method for metals (Wani et al., 2017).

Ali et al. (2018) reviewed and stated that phytoremediation involves the usage of plants to remove, transfer, stabilize and/or degrade pollutants in water, soil and sediment. This plant-based technology has increased acceptance in the last ten years as an efficient, cheap and environmentally friendly technology especially for eradicating toxic metals. Currently, in the US alone, 6-8 billion US dollars are expended annually for environmental clean-up and in the worldwide context, it is 25-50 billion US dollars per year. Water hyacinth (*Eichhornia crassipes*), pennywort (*Hydrocotyle umbellata L.*), and duckweed (*Lemna minor L.*) are some important aquatic plants used for the remediation of aquatic ecosystem. More investigations are required in the phytoremediation topic to address technical issues and to find out the geographically appropriate plant species for effective remediation. In phytoremediation process, accumulation of metals by plants is influenced by several factors like variations in plant species, plants growth stage, element characteristics control absorption, accumulation and translocation of heavy metals.

Eichhornia crassipes was utilized for heavy metal removal, world widely. Water hyacinth is although considered to be as one of the most

problematic aquatic plants due to its uncontrollable growth in water bodies but its quest for nutrient has provided way for its usage in phytoremediation process. Besides, its use in solving wastewater treatment problems in urban or industrial areas using this plant, various useful by-products can be developed like animal and fish feed, power plant energy (briquette), biogas, ethanol, composting and fiber board making. For the future aspects, the utilization of invasive plants in contamination abatement phyto-technologies can undoubtedly assist for their sustainable management in wastewater treatment (Rezania et al., 2015).

Taiwo et al. (2015) studied that water hyacinth (*E. crassipes*) can be used for phytoremediation of heavy metals (Zn, Cu and Pb) in water samples for the period of 8 weeks. The study conducted with heavy metals solutions in different concentrations. At the end of 8 weeks of treatment study, it was detected that the amount of the metals in the water were below the detection limit but it was accumulated in the plant. Correspondingly, the results of the Bioconcentration factor (BCF) exhibited that the studied plant (*E. crassipes)* hyperaccumulated Zn than other metals. Hence, heavy metal uptake by *E. crassipes* by phytoremediation technology appears to be a prosperous method for the remediation of heavy metal contaminated environment.

E. crassipes have the ability to remediate different toxic metals (Zn, Cu, Cr, Cd, Ag, Pb, and Ni) from natural water bodies and/or wastewater polluted with low levels. But, a significant reduction in biomass production was reported in metal treated plants compared to the control. More metals were also accumulated in roots than in shoots

(Odjegba & Fasidi, 2007). To overcome the reduction in biomass under metal contaminated media and for better translocation of metals to plants aerial parts, different technique can be used to assist phytoremediation process.

Song et al. (2011) reported that the performance of laboratory-scale constructed wetlands coupled with micro-electric field (CWMEF) using cannas (*Canna generalis*) for heavy metal contaminated wastewater treatment. They observed, a better performance for heavy metal (HM) removal from wastewater by CWMEF than the ordinary constructed wetlands (CWs). Due to the stimulation of the appropriate voltage and electrical exposure time, the plant (cannas) grown better and in fact, assimilated more metal ions in CWMEF than in CWs. The environmental conditions in constructed wetlands coupled with micro-electric field, like the increased pH by electrolysis of water, the occurrence of aluminum ions by anodizing of aluminum, leads to chemical precipitation, physical adsorption and flocculation of metallic ions. This study suggest that the constructed wetland system coupled with micro-electric field (CWMEF) has much better heavy metal removal capacity than do conventional CWs. Putra et al. (2017) also reported about the Electro Assisted-Phytoremediation (EAPR) to reduce the COD, BOD and heavy metal (Pb and Cu) concentration in the wastewater using water hyacinth. Their result displayed that the EAPR method reduced the COD, BOD, Pb and Cu in the 4 h of EAPR process. Titanium electrode and the combined use of stainless steel U316 rod and net wire were used as an anode and cathode in the experiment. The residual concentrations were within the water quality standard of class IV according to government regulation No. 82/2001 of

the water quality management and water pollution regulation of the Republic of Indonesia.

A combination of phyto - and electroremediation was also attempted by Kubiak et al. (2012) for the arsenic removal using *Lemna minor*. This article presents only the preliminary results of electrically enhanced phyto-remediation, using common duckweed, for the arsenic remediation from spiked surface water. The aquatic phytoremediation process improves when combined with electrochemical process (Putra et al., 2017). Under electrified conditions plant can improve ability to resist adverse circumstances by promoting the synthesis of CHLab, inhibiting MDA synthesis, and catalyzing SOD synthesis. Accordingly, the plant assimilates more metal in electrified phytoremediation process (Song et al., 2011).

Various nanomaterials of different sizes and shapes were fabricated and have employed successfully and safely in various fields such as environmental science, medicine, and food processing, etc. However, their use in agriculture purposes, especially for plant production and protection, is an under-explored area by many research communities. Preliminary studies indicated that some nanomaterials have the potential to improve seed germination and growth, plant protection, pathogen detection, and pesticide/herbicide residue detection (Khot et al., 2012). Morteza et al. (2013) studied the effect of titanium dioxide on plant (corn i.e., *Zea mays* L.). The outcome of their study revealed that nano TiO_2 have significant effect on chlorophyll content (a and b), total chlorophyll (a + b), chlorophyll a/b, carotenoids and anthocyanins. The maximum

amount of pigment was recorded in nano TiO_2 sprayed plants compared to control. The application of nanoparticles especially TiO_2 nanoparticles facilitated the increase in crop yield.

Contamination of groundwater resources through the leaching of heavy metals from soil is also a major environmental concern. Most of the existing conventional soil remedial technologies are expensive and inhibit the soil fertility; subsequently, causes negative influences on the ecosystem. Ghosh and Singh, (2005) discussed in detail about mobility, bioavailability and plant response to presence of soil heavy metals. Several practices to enhance phytoextraction and utilization of by-products have been also elaborated. They also mentioned about the needs of proper disposal of biomass produced during process and its viable management by producing renewable energy.

Qu et al. (2011) discussed about the effect of ammonium molybdate on phytoremediation of heavy metal contaminated soil. It has been used to remove the toxic metals in wastewater by forming precipitates (Pb). However, the application of ammonium molybdate in the remediation of the toxic metals contaminated soils is not a widely studied area. The experiment conducted (1) To find the reaction mechanisms of ammonium molybdate with toxic metals; (2) To investigate the effects of ammonium molybdate on (im)mobilization of the toxic metals in soils; and (3) To understand the effects of ammonium molybdate on uptake toxic metals from soils by alfalfa (*Medicago sativa L.*) plants; aforementioned were the main objectives of their study. The amphoteric-immobilization/mobilization effects of ammonium

molybdate on toxic metals were revealed in the study. The ammonium molybdate can be termed as half-extracting agent, half-chemical stabilization agent, or amphoteric agent. Metals like Pb, Hg, Cr, and Zn can be precipitated with ammonium molybdate and could be stabilized by ammonium molybdate, but metals such as Cd, Ni, Cu can be formed more soluble fractions with ammonium molybdate. The heavy metal contents and BCF values in alfalfa plants were increased after treatment with ammonium molybdate. TF < 1 were also observed. The application of ammonium molybdate increases the acid soluble fractions of Cd, Ni, Cu, and residual fractions of Pb, Hg, Cr, and Zn i.e., the toxicities of Cd, Ni, and Cu to plants in soils increases but, the toxicities of Pb, Hg, Cr, and Zn decreases (Qu et al., 2011; Qu et al., 2016). Ogunkunle et al. (2015) reported the heavy metal accumulation by plant from Amaranthaceae family.

The ease of operation, convenience and simplicity of design, makes the adsorption process a better alternative in water and wastewater treatment. Adsorption processes are applied in many wastewater treatment plants, for the removal of dissolved contaminants and that remain from the subsequent biological phases or after chemical oxidation process. Nowadays, the most commonly adopted adsorbent is the activated carbon. Activated carbon is commonly used for the removal of various contaminants from water such as heavy metals and dyes. However, its widespread usage in wastewater treatment is sometimes limited due to its expensiveness, also further issues such as the adsorbent regeneration capacity or the disposal (Gisi et al., 2016). Tripathi and Ranjan, (2015) has reviewed various low-cost adsorbent for the removal of heavy metal

contamination from wastewater. The removal of toxic heavy metals like Pb, Cd, Zn, Cu, Ni, Hg, Cr etc. using effective agent or adsorbent materials like clay, zeolites, chitin and peat moss were reported. Also, various agricultural waste materials such as rice husk, black gram, neem bark, waste tea, walnut shell, Turkish coffee, etc. were recognized as a potent adsorbent for metal removal. Besides, the technical feasibility to remove toxic metals from polluted water using low-cost industrial by - products like blast furnace sludge, fly ash, waste slurry, iron (III) hydroxide and red mud, lignin, coffee husks, tea factory waste, Areca waste and sugar beet pulp were explored.

Some medicinal plants also have potential to remove heavy metals from water. Rao et al. (2010) have confirmed the biosorption potential of Fennel biomass (*Foeniculum vulgari*), a medicinal herb for the effective elimination of Cd (II) ions. Argun et al. (2007) discussed in detail about the adsorption of heavy metal (Cu, Ni, and Cr) ions from aqueous solutions by oak (*Quercus coccifera*) sawdust modified by means of HCl treatment. As a part of the study, the optimum pH, adsorbent mass, contact time, and shaking speed were determined. The adsorption isotherms were studied using concentrations of the metal ions ranging from 0.1 to 100 mg/L. Their results revealed that, the adsorption process follows pseudo-second-order kinetics, as well as Langmuir and D-R adsorption isotherms. And also, discusses about the thermodynamic parameters of the adsorption (the entropy, enthalpy and Gibbs free energy). The spontaneous and endothermic nature of adsorption process was demonstrated by the results. The maximum removal efficiencies obtained were 93% for Cu (II) at pH 4, 84% for Cr (VI) at pH 3 and 82% for Ni (II) at pH 8. The wood-based

materials increase the COD of water, but by acid modification of the adsorbents decreases this issue. The removal study of cadmium and lead from aqueous solutions using red alga *Ceramium virgatum,* exhibited high sorption capacity. The Fourier transform infrared spectra confirms the carboxyl (– C O), hydroxyl (–OH), and amine (–NH) groups which were responsible for the binding of the metal ions (Hannachi, 2012).

Utilization of iron oxide-based nanomaterials for the removal of heavy metals is well recognized adsorbents. Due to its significant physiochemical property, low-priced method and easy regeneration or separation in the presence of external magnetic field makes them more attractive toward water decontamination. Surface modification strategy of iron oxide nanoparticles is an effective method to increase the efficiency of iron oxide nanoparticles for the removal of the heavy metal ions from the aqueous system (Dave & Chopda, 2014). Al-Saad et al. (2012) investigated the sorption behaviour of the iron oxide (α-Fe_2O_3) nanoparticles and its applicability to purify water from the aluminium, arsenic, cadmium, copper, cobalt, and nickel. The adsorption behaviour of iron oxide nanoparticles towards six metallic ions (Al (III), As (III), Cd (II), Cu (II), Co (II), and Ni (II)) has been investigated by batch experiment under different conditions (pH, concentration of metals, contact time, adsorbent dosage, and temperature).

Dorniani et al. (2014) studied the efficacy of two nanocarriers polyethylene glycol and polyvinyl alcohol magnetic nanoparticles coated with gallic acid (GA) in drug delivery. X-ray diffraction and TEM results showed the formation of pure Fe_3O_4 nanoparticles having spherical shape

with the average size of diameter after coating Fe_3O_4 nanoparticles with polyethylene glycol-GA (FPEGG) and polyvinyl alcohol- GA (FPVAG). In the study, thermogravimetric analysis was used to prove the thermal stability after coating and fourier transform infrared (FTIR) revealed the successful coating of two polymers (PEG and PVA) and gallic acid on the superparamagnetic iron oxide nanoparticles. Anticancer activity of the two nanocomposites, FPEGG and FPVAG demonstrated its high anticancer effect.

Water quality management and its assessment in light of heavy metal concentration is of prime importance. For water quality management, the overall water quality status and identification of source of origin of heavy metals are essential. The heavy metal pollution index (HPI) and Factor analysis (FA) are most suitable and effective approaches to evaluate the status of water quality and recognizes the source of contaminants (Saha & Paul, 2016). The most appropriate statistical methods to identify the origin of metals and the correlations between heavy metals at a contaminated site are principal component analysis (PCA) and cluster analysis (CA).

2.2 Fluoride contamination in water and its remediation using plant materials

Contamination of water by fluoride is a serious topic across the globe because of its irreversible health threats. During initial stages, fluoride studies were limited to local or regional scale. Because of its serious socioeconomic implications, this problem demands the need for a global perspective. Bhattacharya and Samal (2018) reviewed that fluoride

contamination severely affected around 200 million people of 29 countries including India. Consumption of fluoride beyond the maximum permissible level of 1.5 mg/L recommended by WHO is related with dental and skeletal fluorosis but, lacking of fluoride intake associated with other health issue, dental caries. Weathering of minerals like fluorite/ fluorspar, apatite, topaz and mica and some industrial activities (mainly phosphorous fertilizer plants; steel, zinc, aluminium, smelting industries; glass and ceramic industries, etc.) contribute fluoride contamination. Fluoride enters into the food chain by its bioaccumulation nature. Moreover, dental fluorosis is highly endangering the most susceptible group, infants and children. The Nalgonda technique and activated alumina processes are the most widely used defluoridation techniques in water. But it has drawback of residual aluminium after treatment.

Babu et al. (2015) reported that issues associated with excess fluoride ion in groundwater is a serious problem in fluoride endemic areas of the developing countries. In India, a plethora of people are facing severe fluorosis problems as a result of high intake fluoride ion (F$^-$) through drinking water and it has been estimated that 62 million people from 19 out of the 32 Indian states are facing dental, skeletal and/or non-skeletal fluorosis. The extent of fluoride contamination in water ranged from 1.0 to 48.0 mg/L.

Fluoride consumption is commonly considered as a double-edged sword. Inadequate amount of fluoride intake in (< 0.5 mg/L), causes health issues like dental caries, deficiency in formation of dental enamel, and lack of mineralization of bones, predominantly among children. While the

excessive fluoride consumption cause health problems in the young and old. If the fluoride consumption exceeds 4 mg/L, it leads to the dental fluorosis in children while the prolonged consumption of fluoride at higher concentrations i.e., more than 10 mg/L causes dental fluorosis, skeletal fluorosis and crippling skeletal fluorosis, perhaps cancer. In India, majority of the population reliant on groundwater source for drinking purpose. High fluoride content in groundwater has been mainly reported from different areas of Indian states such as Andhra Pradesh, Haryana, Assam, Bihar, Gujarat, Chhattisgarh, Karnataka, Maharashtra, Madhya Pradesh, Rajasthan, Odisha, Tamil Nadu, Telangana, West Bengal, Uttar Pradesh, and Punjab (Annadurai et al., 2014). In 2009, RGNDWM & CGWB enumerated that out of 639 Indian districts the fluoride-affected ones were 229 and 218 respectively. But, in 2012, the number was increased to 267 according to MoWR (Saxena & Sewak, 2015).

As per from literatures, the fluoride ingestion from food is roughly in the ratio of 30 to 40 % and from water, it is 60 to 70 % (Saxena & Sewak, 2015). Hence, to regulator the overall fluoride intake, the only controllable aspect was water. The proper defluoridation technique is a necessary for the socio - economic development of man and community. Several defluoridation technologies have been developed over the years to eradicate fluoride ions from water such as electrocoagulation (Drouiche et al., 2009), chemical precipitation (Pinon-Miramontes et al., 2003), ion exchange (Singh et al., 1999), reverse osmosis (Ndiayea et al., 2005), electrodialysis (Amor et al., 2001) and adsorption (Naohito et al., 2009). Also, aluminium salts-based treatment methods have been widely used.

Among the aforementioned methods, most of the methods are quite expensive, generates secondary effluent and sludge.

Various inexpensive materials have been tried for removing fluoride from drinking water, but these materials cannot be applied because their low fluoride adsorption capacities. Many biomaterials have potential to be used as low-cost sorbents and they are widely accessible and environmentally safe. Some low cost and non-conventional adsorbents include agricultural by-products, wood, nut shells, bone, peat, and coconut shells processed into activated carbons (Singanan, 2013).

Alagumuthu et al. (2010) investigated the fluoride adsorption capacity and its kinetics using the sorbent carbonized ground nut shell (GNSC) impregnated with zirconium oxychloride. The equilibrium data were analyzed using the Langmuir, Freundlich and Redlich-Peterson isotherm by linear methods displayed that the data fitted better with Freundlich model than the other two. Thermodynamic studies exhibited the spontaneous nature of fluoride adsorption with increase of entropy and an endothermic process. The kinetic data obeyed the pseudo-second order model. The zirconium impregnated ground nut shell carbon is a cost-effective adsorbent for the defluoridation problem in the developing countries due its great potential application in the fluoride remediation from water. So, development of effective and low-cost, carbon form adsorbent from easily available plant materials is an effective defluoridation method.

MATERIALS AND METHODS

3.1 Methods of water quality assessment

The collection, preservation and analysis of physico-chemical characteristics of water and wastewater samples were carried out as per the standard procedure described in American Public Health Association (APHA, 2012).

3.1.1 Collection and preservation of water samples

The collection and preservation of water samples were done as per APHA methods, mentioned in Section 1060. The equipment and containers used for sample collection were thoroughly cleaned before sampling. Samples for physico-chemical analysis were collected in one litre plastic containers. The containers were of good quality, free of analytes of interest and were rinsed out, two or three times with the sample to be examined. Sterilized containers were used to collect the samples for bacteriological analysis. All the sample containers were labelled properly with information like unique sample code, sample type, date and time of sampling. Accurate sampling location were recorded for further reference,

using global positioning system (GARMIN GPS map model 76CS). Available details of the sampling locations and peculiar characteristics of the samples, if any, were also noted during sample collection. The in-situ parameters such as pH and electrical conductivity, required immediate analysis in the field. The physico-chemical and bacteriological changes of the sample was prevented by appropriate preservation techniques. Samples were kept in cool condition without freezing, to minimize the potential for volatilization or biodegradation between sampling and analysis. For the metal analysis, samples were collected in a separate clean bottle and acidified with HNO_3 to a pH below 2 to minimize precipitation and adsorption on container walls. To get more reliable analytical results, shorter the time that elapses between sampling and analysis.

3.1.2 Analytical methods of water and wastewater

3.1.2.1 pH (APHA, 2012 Section 4500 - H⁺ B)

pH of the water samples was determined by Electrometric method using a multi-parameter PCSTestr35 pH meter. National Institute of Standards and Technology (NIST) buffers having the pH value of 4,7 and 10 were used to calibrate the pH determining instrument.

3.1.2.2 Electrical Conductivity (APHA, 2012 Section 2510 B)

Electrical Conductivity (EC) is directly proportional to its dissolved mineral matter content and is expressed as µS/cm. The electrical conductivity was measured using multi-parameter PCSTestr35 instrument and was calibrated using standard reference solution (0.01M KCl) has a conductivity of 1412 µS/cm at 25°C.

3.1.2.3 Total Dissolved Solids (APHA, 2012 Section 2540 C)

Gravimetric technique was utilized to determine the Total Dissolved Solids. A measured volume of sample was filtered through a standard glass-fiber filter (Whatman grade 934AH) with applied vacuum and the filtrate was transferred to a weighed evaporating dish and evaporated to dryness until a constant weight in an oven at $180 \pm 2°C$. The increased dish weight denotes total dissolved solids.

$$\text{Total Dissolved Soids, mg/L} = \frac{(A - B) \times 1000}{\text{Sample volume (mL)}}$$

where

   A = weight of dried residue and dish, mg

   B = weight of dish, mg

3.1.2.4 Colour (APHA, 2012 Section 2120)

Colour was analysed spectrophotometrically by UV-Visible spectrometer, Thermo Scientific- Evolution 201 at a wavelength between 450 and 465nm using platinum - cobalt standard solutions. Colour of samples as well as platinum - cobalt standards obeys Beer's law.

3.1.2.5 Turbidity (APHA, 2012 Section 2130 B)

The determination of turbidity was done by Nephelometric method using the instrument Systronics Digital Nephelo-Turbidity meter 132. Formazin polymer was considered as the primary standard reference suspension and the instrument was calibrated by using different standard turbidity solutions. Turbidity was measured based on the intensity of scattered light.

To measure turbidity, well mixed samples were taken into measuring cell and the instrument displayed the turbidity value directly.

3.1.2.6 Chloride (APHA, 2012 Section 4500-Cl⁻ B)

Argentometric method was adopted for the determination of chloride in water. $AgNO_3$ reacts with chloride ions in water to form silver chloride. The end point was determined by the formation of silver chromate from excess silver nitrate. 1 mL of potassium chromate indicator was added to the sample and titrated against $0.0141N$ standard silver nitrate solution. The change in colour from yellow to reddish orange was observed at the end of the reaction.

$$\text{Chloride, mg/L} \quad = \quad \frac{\text{Vol. of AgNO}_3 \text{ x N x 35.45 x 1000}}{\text{Sample volume (mL)}}$$

N = Normality of $AgNO_3$.

3.1.2.7 Sulphate (APHA, 2012 Section 4500-SO₄²⁻ E)

Turbidimetric Method was followed to estimate the sulphate concentration in the samples using Systronics Digital Nephelo - Turbidity meter 132. Sulphate ion was precipitated as barium sulphate crystals of uniform size, in an acetic acid medium with $BaCl_2$ and the light absorbance of the $BaSO_4$ suspension was measured by Nephelometer. The instrument was calibrated using 0 to 40 mg/L of standard sulphate solutions and the SO_4^{2-} concentration in samples was determined by comparison of the reading with a calibration curve.

3.1.2.8 Nitrate-N (APHA, 2012 Section 4500-NO₃⁻ E)

Cadmium reduction method was adopted to estimate Nitrate-N. In this method, when the water sample was passed through a column packed with amalgamated cadmium (commercially available Cd granules treated with $CuSO_4$ and packed inside a glass column) nitrate (NO_3^-) was reduced almost quantitatively to nitrite (NO_2^-). The NO_2^- produced thus was determined by diazotizing with sulfanilamide and coupling with N-(1-naphthyl)-ethylenediamine dihydrochloride to form a highly coloured azo dye. The intensity of the azo dye developed was proportional to the concentration of Nitrate – N and was determined at 543 nm using UV - Visible spectrophotometer (Thermo Scientific- Evolution 201). A correction was made for any NO_2^- present in the sample by analysing without the reduction step.

3.1.2.9 Phosphate- P (APHA, 2012 Section 4500-P D)

The estimation of Phosphate-P was carried out by Stannous Chloride method. Phosphate present in samples reacts with ammonium molybdate to form molybdophosphoric acid under acid conditions and reduced by stannous chloride to intensely coloured molybdenum blue. After 10 min, but before 12 min, intensity of colour was measured by UV-Visible spectrophotometer (Thermo Scientific - Evolution 201) at 690nm and compared with a calibration curve.

3.1.2.10 Fluoride (APHA, 2012 Section 4500-F⁻ C)

Ion-Selective Electrode Method was followed to determine fluoride in water samples. The fluoride electrode is an ion-selective

sensor. The main element in the fluoride electrode was the laser-type doped lanthanum fluoride crystal across which a potential was established by fluoride solutions of different concentrations. Ion selective electrode measured the fluoride ion activity in the solution rather than concentration and it depends on the solution total ionic strength and pH, and on fluoride complexing species. An appropriate buffer solution was added to provide a nearly uniform ionic strength background, adjusts pH, and breaks up complexes so that, in effect, the electrode measures concentration. Ion selective electrode (Thermo Scientific Orion 9609BNWP, Made in US) was used to measure fluoride ion concentration and total ionic strength adjustment buffer II (TISAB II) solution was used to maintain pH 5 - 5.5. The manufacturer's instructions were followed to use a selective-ion meter. Ion-selective electrode was frequently recalibrated by checking potential reading of the 1.00 mg F^-/L standard.

3.1.2.11 Total Alkalinity (APHA, 2012 Section 2320 B)

The alkalinity is the measure of water to neutralize acid. Total alkalinity was measured by titrating the water sample against standard sulphuric acid (0.02 N) using methyl orange as indicator. The end point was indicated by a colour change from pale yellow to orange red.

$$\text{Alkalinity, mg/L as CaCO}_3 = \frac{\text{Vol. of H}_2\text{SO}_4 \text{ x N x 50 x 1000}}{\text{Sample volume (mL)}}$$

N = Normality of standard H_2SO_4 solution.

3.1.2.12 Hardness (APHA, 2012 Section 2340 C)

Hardness is expressed in terms of mg/L of calcium carbonate and was determined by the EDTA titrimetric method. To estimate total hardness, water sample was titrated against standard EDTA solution (0.01M) using Eriochrome Black T as indicator in the presence of NH_4Cl-NH_4OH buffer of pH 10. Colour change from wine red to blue was considered as end point.

$$\text{Total Hardness, mg/L as } CaCO_3 = \frac{\text{M of EDTA x Vol. of EDTA x 100 x 1000}}{\text{Sample volume (mL)}}$$

3.1.2.13 Calcium (APHA, 2012 Section 3500-Ca B) & Magnesium (APHA, 2012 Section 3500-Mg B)

Calcium hardness was also determined by EDTA titrimetric method. NaOH solution was added to the sample to attain a pH of 12 to 13. After adding murexide indicator, the sample was titrated against standard EDTA solution (0.01M) with continuous stirring, till the colour of the solution changed from pink to purple. Magnesium was estimated using calculation method. Following equations are used to determine the concentration of calcium and magnesium.

$$\text{Calcium Hardness, mg/L } as \text{ } CaCO_3$$
$$= \frac{\text{M of EDTA x Vol. of EDTA x 40.08 x1000}}{\text{Sample volume (mL)}}$$

$$\text{Calcium, mg/L} = \text{ Calcium hardness x 0.4}$$

$$\text{Magnesium, mg/L}$$
$$= (\text{Total Hardness}$$
$$- \text{ Calcium Hardness}) \text{ x } 0.243$$

3.1.2.14 Sodium (APHA, 2012 Section 3500-Na B) & Potassium (APHA, 2012 Section 3500-K B)

Flame Emission Photometric Method was used to estimate the alkali metals such as sodium and potassium. The determination of sodium and potassium was carried out at a wavelength of 589 nm and 766.5 nm, respectively. Filtered water samples were aspirated to the instrument, Systronics Flame Photometer 128 after calibration using standard solutions. Both the concentrations of sodium and potassium were recorded from display of instrument.

3.1.2.15 Heavy Metals (APHA, 2012 Section 3111 B)

The heavy metals concentration in water was determined by Direct Air-Acetylene Flame Method by Atomic Absorption Spectrophotometer (AAS) (M-series, Thermo). The instrument was operated as per manufacturer's operating manual. Atomic absorption spectrometer, burner, readout, lamps, pressure-reducing valves and vent are the main components of the instrument, involved in the metal analysis. A preliminary treatment of samples was conducted by filtration, followed by acidification of filtrate with conc. HNO_3 and stored until analyses were performed. Stock standard solutions were procured commercially from Merck India Pvt Ltd. All calibration standards and dilution water were

prepared using metal-free water only. The concentration of each metal ion in mg/L was estimated by referring to the appropriate calibration curve.

To assure the quality of analysis, blank analysis was conducted between sample or standard readings to verify baseline stability. Rezero was done when necessary. To check the recovery of metals, a known amount of the metal of interest was added to an analysed sample and reanalysed. Recovery of added metal was found between 85 and 115%. Analysis of an additional standard solution after every ten samples or with each batch of samples were done to confirm that the test is in control.

3.1.2.16 Microbial Analysis

Multiple tube fermentation technique was followed to conduct the standard test for coliform group. Outcomes of examination of replicate tubes and dilutions were described in terms of the Most Probable Number (MPN) of organism present in100 mL of the sample. The MPN value of the analysing samples was obtained from the MPN index chart. The media used for total coliform, faecal coliform and *E. coli* were Mac Conkey broth, Brilliant Green Lactose Broth (BGLB) and Peptone water, respectively. For determining total coliforms, 10, 1, and 0.1 mL of samples were inoculated in to the Mac Conkey broth and incubated at 37.5^0C for 48 hrs. Tubes with gas bubbles and colour change were considered as the positive tubes and count was recorded. The positive tubes were mildly shaken and transferred, three loopful of culture to a fermentation tube containing BGLB broth using a sterile loop. Then, the tubes were incubated at 44.5^0C for 24 hrs. The numbers of positive tubes were recorded and the count was estimated using MPN index chart. Again,

positive tubes were gently shaken and transferred one loopful of culture to a fermentation tube containing peptone water with a sterile loop. The incubation of the inoculated tubes was conducted at 44.5^{0}C for 24 hrs. After incubation, 2-3 drops of Kovac's reagent were added to the tube and the presence of *Escherichia coli* was indicated by the cherry red ring formation.

3.2 Assessment of soil and sediment quality

The physico-chemical characteristics of the soil and sediment samples were determines using the methods reported by Hesse (1971), Black (1965) and Central Soil Analytical Laboratory (2007).

3.2.1 Collection and pre-processing of samples

Soil auger was used to collect the soil samples with minimal disturbance. Soil samples were collected at the depths of 15 - 30 cm, in polythene bottles which were labelled properly from the sampling site itself. The visible objects present on the soil surface like plant materials, roots, undecomposed organic matters were removed from before sample collection. Random samples were collected following the zig-zag movement. Soil samples were pooled to give a composite sample for that site and reduced to 1 to 2 Kg size by quartering method. Sediment samples were collected from the bottom of water bodies. Soil and sediment samples were transported to the laboratory and a portion of the samples were air-dried, sieved and stored in polythene bottles for physico-chemical analysis.

Soil/sediment - water suspension of 1:10 (w/v) was used for the determination of pH and electrical conductivity and the filtrate of the suspension was used to estimate alkalinity, sulphate and chloride. Wet digestion method or Walkley-Black method was followed for the estimation of organic carbon. For the analysis of exchangeable cations like Ca^{2+}, Mg^{2+}, Na^+ and K^+, samples were extracted with 1 M ammonium acetate solution. Extraction of samples using 1 N hydrochloric acid were conducted to determine inorganic phosphorous. Soil and sediment quality characteristics were determined by the following procedures.

3.2.2 Soil and Sediment quality characteristics

3.2.2.1 pH

10 g of the air-dried soil/sediment was taken in a beaker followed by the addition of 100 mL of deionized water to form a 1:10 ratio. The soil/sediment - water mixture was continuously stirred at least 5 times over a 30 min interval, to reach equilibrium. Allow it to stand for an hour to settle out the soil/sediment from the suspension. To measure pH, the glass pH electrode was placed deep into the clear supernatant solution for better electrical contact. The pH meter was calibrated with standard buffer solution, prior to the measurement.

3.2.2.2 Electrical Conductivity (EC)

Soil/sediment - water suspension of 1:10 (w/v) was used to determine the electrical conductivity. 10 g of air-dried soil/sediment sample was mixed with 100 mL of distilled water and the suspension was stirred for 4-5 times over a 30 minutes interval. The mixture was kept overnight to

settle and the EC of the clear supernatant solution was measured with the aid of calibrated conductivity electrode (PCSTestr35 instrument).

3.2.2.3 Alkalinity

10 g of air-dried sample was taken in beaker followed by the addition of 100 mL of distilled water. The suspension was filtered through Whatmann No. 40. The filtrate was titrated against standardized 0.02N sulfuric acid using methyl orange as indicator until the colour changes from golden yellow to orange red.

3.2.2.4 Chloride

The chloride content in the soil/sediment - water suspension was determined by argentometric titration. The suspension was filtered using Whatman No:40 and titrated against 0.0141N silver nitrate solution with potassium chromate indicator. The colour change from yellow to orange red with a curdy precipitate was considered as end point.

3.2.2.5 Sulphate

The same filtrate was used in the estimation of sulphate concentration by turbidimetric method using Systronics Digital Nephelo-Turbidity meter 132. The nephelometer was calibrated using appropriate sulphate standards, prior to analysis and to obtain results the reading were compared with the calibration curve.

3.2.2.6 Organic carbon & Organic matter

The estimation of organic carbon was done by Wet digestion method or Walkley-Black method. 0.5 g of air-dried and sieved soil/sediment

samples was used in this method. During wet combustion, soil/sediment organic matter was digested using the oxidizing agent, potassium dichromate (1N) and to convert all forms of carbon into carbon dioxide, concentrated sulphuric acid (20 mL) was added. The potassium dichromate present in excess after oxidation of carbon was titrated against ferrous ammonium sulphate solution (0.5M). To avoid interference of chloride in oxidation of the organic matter, sulphuric acid containing 1.25 % silver sulphate was used to precipitate chloride as silver chloride. To make the reaction complete, solution was kept to stand for half an hour and then the diluted solution was titrated with 0.5M Ferrous ammonium sulphate solution using diphenyl amine indicator. At the end point, the solution colour changed from yellow to red with an intermediate green colour formation. The blank determination of organic carbon content was analysed without soil/sediment.

$$\text{Organic carbon in the soil (\%)} = \frac{(X - Y) \text{ x } N_1 \text{ x } 0.003 \text{ x } 100 \text{ x } f}{(N_2 \text{ x } S)}$$

where,

X = Volume of FAS used in the blank

Y = Volume of FAS used to oxidize soil/sediment organic carbon (mL)

N_1 = Normality of FAS

N_2 = Normality of potassium dichromate

f = 1.33 Correction factor

S = Weight of soil/sediment taken (g)

The organic matter of soil/sediment sample indicates the whole non-mineral fractions present. Organic matters were contributed to the physical condition of the soil/sediment by holding moisture and affecting the structure. The organic matter of soil/sediment was estimated from its organic carbon content and it was considered as 1.724 times the organic carbon.

3.2.2.7 Exchangeable Sodium & Potassium

To estimate exchangeable sodium and potassium, soil/sediment sample was extracted with ammonium acetate solution (1 M). Soluble sodium and potassium were measured by Flame Emission Photometric Method (Systronics Flame Photometer 128). The standard of sodium and potassium solution were prepared in ammonium acetate. Sodium and potassium were determined at a wavelength of 589 nm and 766.5 nm, respectively.

3.2.2.8 Exchangeable Calcium & Magnesium

To determine exchangeable calcium and magnesium, soil/sediment sample was extracted with neutral ammonium acetate solution (1 M) and both were estimated using complexometric titration with EDTA solution. The extract was titrated with 0.01 M EDTA solution in the presence of NaOH buffer and murexide indicator for the estimation of calcium. The colour change from pink to purple was considered as end point. For the determination of magnesium, ammonium acetate buffer and Eriochrome Black T indicator were added to the filtrate after extraction and titrated with 0.01 M EDTA. The end point was the colour change from wine red to blue.

3.2.2.9 Inorganic Phosphorous

The inorganic phosphorous content in the soil/sediment sample was determined by measuring the orthophosphate using the UV Visible spectrophotometer (Thermo Scientific - Evolution 201). Air dried sample was extracted using 1 N hydrochloric acid and the soil/sediment - acid mixture was shaken in a shaker for a period of 16 hrs for extraction. After centrifugation at 2000 rpm for 5 min, stannous chloride and ammonium molybdate solutions were added to the solution. The intensity of the complex 'molybdenum blue' was measured using UV Visible spectrophotometer at 690 nm.

3.2.2.10 Heavy Metals

The heavy metals present in the soil/sediment sample was extracted using the mixture of acids, HNO_3-$HClO_4$ (USEPA, 1999). Hot, concentrated $HClO_4$ was extremely effective in decomposing organic matter and sulphides, because of its powerful oxidizing and dehydrating properties. Nitric acid dissolves the majority of the metals occurring in nature except gold and platinum Excess amount of nitric acid was added than perchloric acid, so that much of the oxidation was carried out before the action of perchloric acid was initiated. 20 mL of con. HNO_3 and 5 mL of distilled water were added to 0.2 g of air-dried soil/sediment sample. Heated on a hot plate for 2 hrs. 10 mL of $HClO_4$ was added after some time. The heating was continued until the white fumes come and the soil become white. Then, the filtered solution was made up to 50 mL. The analysis of heavy metals like iron, manganese, lead, cadmium, nickel, copper and zinc in the filtrate was

conducted using Atomic Absorption Spectrophotometer (AAS) (M-series, Thermo).

3.2.2.11 Soil texture

Hydrometer method based on Stokes law was followed to analyse the texture of soil/sediment. 40 g of air-dried sample was weighed in to 500 mL beaker and about 30 mL of distilled water and 5 mL of H_2O_2 were added to oxidize the organic matter. The beaker was placed on a sand bath and H_2O_2 was added until the frothing no longer continued. The soil was transferred completely to a beaker containing calgon solution (100 mL) and distilled water (300 mL) and mixed for 5 min with an electric mixer. The entire suspension was transferred to a sedimentation cylinder and made up to the mark using distilled water. The solution was mixed, properly and the readings of hydrometer and thermometer (^{o}C) after 5 and 120 min were noted. The same procedure was also followed to determine the blank value.

3.3 Statistical analysis

The analytical results were subjected to various statistical analyses, for the easy interpretations of data. Maximum, minimum mean and standard deviation values were computed and reported. The statistical software such as SYSTAT 12 was used for the interpretation of water quality results. Pearson correlation analysis of two distinct groups of heavy metals were performed. Chemometric or multivariate analysis techniques such as Principle Component Analysis and Cluster Analysis were used to identify the heavy metal pollution sources affecting water quality. The correlation coefficient and sum of squares of the error were determined in the adsorption study to identify the best fitted kinetic model.

TREATMENT OF HEAVY METALS FROM WATER BY ELECTRO-PHYTOREMEDIATION TECHNIQUE

4.1 Introduction

The increasing levels of heavy metals in the environment, their entry into food chain and their overall consequences is of great concern to scientific community in the field of environmental science. The remediation of toxic heavy metals from wastewaters is recognized as one of the most important fields of water treatments, since the extreme industrial activities creates many dangerous pollution issues to the environment (Li et al., 2009). Cadmium and lead are commonly encountered hazardous heavy metals and are in the EPA's list of priority pollutants (Baziar et al., 2013). The UNEP considers lead and cadmium as the non-essential element for human life but they can compete with the essential trace elements either for the transport systems or in binding to various biomolecules. Both can accumulate in bone and may serve as a source of exposure later in life. Cadmium is a carcinogen by inhalation

and is mainly affects kidneys and the skeleton. Lead is a multi-organ system toxicant and is noxious at very low exposure levels. The duration, level and timing of exposure are the factors which depends the type and severity of effects. Tri-alkyl-lead and tetra-alkyl-lead compounds are the organo - lead compounds which are more toxic than inorganic forms of lead (UNEP, 2010). Hexavalent chromium (Cr [VI]) is recognized to be a strong oxidant and highly toxic (Argun et al., 2007).

Extensive researches have been progressing for the removal of heavy metals by various methods such as ion exchange, filtration, reverse osmosis, biosorption, chemical precipitation, electrochemical treatment, solvent extraction, sedimentation, membrane separation, sensors etc. Many existing treatment techniques are not designed to address today's concerns because of its incomplete metal uptake at low level and expensive operational costs (Shah et al., 2012). For the better availability of good water quality at a lesser cost, it is obligatory to develop some sustainable alternative treatment methods, which are more natural, novel and cost effective. Phytoremediation utilizes the advantages of the unique, selective and naturally occurring uptake capabilities of plant root systems, together with the translocation, bioaccumulation and pollutant storage/degradation abilities of the entire plant body. Also, being aesthetically pleasing, phytoremediation is on average tenfold cheaper than other remediation methods like physical, chemical or thermal. It can also be performed in situ, is solar driven and can required minimal maintenance once established (Hooda, 2007). Phytoremediation has also been known as green remediation, botano-remediation, agro remediation and vegetative remediation (Andrew, 2007). Phytoremediation is a plant

assisted bioremediation technique, utilized to treat contaminated water and soil, including the processes like phytoextraction, phytodegradation, phytovolatilization, phytostabilization, rhizodegradation, phytoreduction, phytostimulation, phytooxidation and phytotransformation (Ullah et al., 2014).

Utilization of AMATS (aquatic macrophytes treatment systems) for the phytoremediation of heavy metals and other pollutants is a well-established and cost effective environmental protective technique (Mahmood et al., 2005). Copper can become extremely toxic to plants due to leaf chlorosis, suppressed root growth and inhibit photosynthesis and reproduction of plants, when present in excess amount, even though it is essential micronutrients for plant metabolism. Lead diminishes chlorophyll production and cadmium toxicity also lead to some extremely sever effects on plants (Ashraf et al., 2011; Hammad, 201; Swain et al., 2014). Heavy metals can create a stressful condition to the plants and its growth becomes limited or impossible and this can influence the phytoremediation. In our study, we tried to enhance the phytoremediation capacity of *Eichhornia crassipes* to treat heavy metals by applying an electric field. The purpose of this study was to investigate the removal of lead, cadmium and copper in a simulated wastewater by a phytoremediation system coupled with electric field. This technique was also applied to lead contaminated wastewater from battery manufacturing industry and chromium contaminated wastewater from an electroplating industry.

4.2 Materials and Methods

4.2.1 Preparation of synthetic heavy metals solution

The simulated wastewater was made by dissolving $Pb(NO_3)_2$, $CuSO_4.5H_2O$ and $(3CdSO_4).8H_2O$ in tap water. All chemicals used were of the highest purity available and of analytical grade procured from Merck. The initial heavy metal concentrations of the simulated wastewater were determined by Atomic Absorption Spectrophotometer, AAS (Thermo Series) with GF 95.

4.2.2 Collection of plant and wastewater for this study

A fast-growing perennial aquatic plant and prolific free-floating aquatic weed, *Eichhornia crassipes* (Water hyacinth) was used for the treatment of heavy metals in this experiment (Plate 4.1). Young plants of *Eichhornia crassipes* were collected from Kottooli wetland in Kozhikode City. This vascular, fast growing aquatic plant with a fibrous root system and large biomass is commonly noticed in tropical and subtropical regions of the world. It can easily adapt to several aquatic conditions and perform an important role in extracting and accumulating many metals from water. Hence, it is utilized as an ideal candidate for the phytoremediation of toxic trace elements from variety of water bodies (Weiliao & Chang, 2004). Collected *Eichhornia crassipes* were put in a hydroponic system containing tap water, for acclimatization period, before being exposed to heavy metal contaminants. Heavy metal contaminated wastewater samples were collected from battery manufacturing industry and electroplating industry located in Kozhikode district, Kerala.

Plate 4.1: *Eichhornia crassipes*

4.2.3 Experimental design and sampling strategy

Three tanks ($45 \times 30 \times 15$cm) were setup with different operating conditions.

Tank 1**: Control A** (with plant and without electric current)

Tank 2: **Control B** (without plant and with electric current)

Tank 3: **Treatment** (with plant and with electric current)

Twelve litres of synthetic heavy metal solution was taken in each tank. The potential of *Eichhornia crassipes* for phytoremediation was utilized in this study because of its large biomass and dense root system. An electric power supply (DC) was used for providing constant voltage between working electrodes (i.e. in control B and treatment).
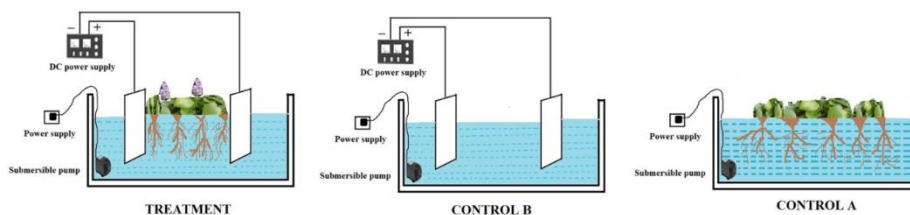
Figure 4.1: Schematic diagram of the electro - assisted phytoremediation system

Initially, aluminum rods (10cm height, 1.9cm breadth and 2.04mm thickness) and sheets (15cm height, 10cm breadth and 0. 2mm thickness) were used as electrodes and both indoor and outdoor experiments were also conducted. Based on the outcome of the initial study, outdoor experiment using aluminum sheets as electrodes were preferred for further study. To remove the oxide and passivation layer from aluminum surface, the electrodes were rubbed with sandpaper and energized by dipping them in 5N HCl for 1 minute. The electrodes in the tanks were positioned vertically. Plants were placed very close to the electrodes. 0.01M KCl was used as supporting electrolyte. Circulation of water was maintained using a submersible pump. The schematic diagram of the experiment is presented in Figure 4.1 and the experimental setup is depicted in Plate: 4.2 and 4.3. Different voltages like 2V, 3V, 4V and 5V were applied to the system 2h/day for 10 days. Due to the formation of bubbles and heat generation, phytoremediation system operated at a voltage of 5V was stopped after 2 days. Based on the optimum results obtained, 4V was selected as an optimum voltage for further experiment. Experiment was

operated 2h/day at voltages of 4V for 25 days continuously. All the units were operated outdoors. Water samples were taken in every 5 days at about 10:30 A.M. In every sampling day, pH, EC, TDS and temperature were measured by using PCS Testr35 instrument. When the experiment was finished, plants from two units (control A and treatment) were sampled and dried in a hot air oven. The residual Pb, Cd and Cu concentrations in water were determined by Atomic Absorption Spectroscopy AAS (Thermo Series) with GF 95. The same experimental condition was applied to treat the heavy metals in the waste water collected from battery recharging industry and electroplating industry from Kozhikode. The effluents were collected in pre-sterilized plastic containers, brought to the laboratory.

Plate 4.2: Experimental setup (outdoor experiment)

Plate 4.3: Experimental setup (indoor experiment)

4.2.4 Analytical procedures

20mL of water samples were taken from each tank in every 5 days at around 10:30 A.M. Plant samples were collected at the end of the experiment and rinsed using tap water twice and deionized water thrice. The *Eichhornia crassipes* samples were divided into leaves, stems and roots. Plant samples were oven-dried for a period of 48 h at 70°C. The oven-dried sample was ground to pass through a 100-mesh sieve and homogenized plant tissues were digested with HNO_3–$HClO_4$ (4:1) mixture and filtered. For quantification of heavy metals, the water samples and digested plant samples were analyzed with Atomic Absorption Spectrophotometer (Thermo Series) with GF 95. Chlorophyll (chl.a + chl.b, CHLab) was determined by optical density values (663 nm and 645 nm using UV-Visible spectrophotometer, Thermo Evolution 201) of

extracting solution, which was made by adding 80% acetone into grinding solution of 0.5 g of fresh leaves (Song et al., 2011).

4.2.5 Data Analysis

The bioconcentration factor (BCF) and translocation ability (TA) are the ratios used to evaluate the mobility of the heavy metals from the polluted substrate into the roots of the plants and their ability to translocate the metals from roots to the harvestable aerial part. The bioconcentration factor (BCF) was calculated as the ratio of the trace element concentration in the plant tissues to the concentration of the element in the external environment (Zayed et al., 1998). BCF is given by,

$$BCF= (P/E) \qquad\qquad (1)$$

where BCF denote the bioconcentration factor and is dimensionless. P represents the trace element concentration in plant tissues (mg kg^{-1} dry wt); E represents the trace element concentration in the water (mg/L) or in the sediment (mg kg^{-1} dry wt). A larger ratio implies better phytoaccumulation capability. The translocation ability indicates the efficiency of the plant in translocating the accumulated metal from its roots to the upper part of the plant. Translocation ability (TA) was calculated by dividing the concentration of a trace element accumulated in the root tissues by that accumulated in shoot/leaf tissues (Wu & Sun, 1998). TA is given by,

$$TA= (A_r/ A_s) \qquad\qquad (2)$$

where TA is the translocation ability and is dimensionless. A_r represents the amount of trace element accumulated in the roots (mg kg^{-1} dry wt), and A_s represents the amount of trace element accumulated in the shoot/leaf (mg kg^{-1} dry wt). A larger TA ratio implies poor translocation capability. All the tests were conducted in triplicates and the data were statistically analyzed.

4.3 Results and Discussion

4.3.1 Removal of lead, cadmium and copper from synthetic solution using electro-phytoremediation system

The initial values of the pH, EC and TDS of the synthetic solution were found to be 6.29 ± 0.01, 274 ± 1.2 μS/cm and 193 ± 0.78 mg/L respectively. The initial heavy metal concentrations of simulated water are summarized in Table 4.1. The metals like Fe, Mn, Ni and Zn were found to be within the permissible limit (BIS ISO:10500, 2012).

Table 4.1: Initial concentration of heavy metals in synthetic solution

Parameters	Initial Concentration
Cd (mg/L)	18.86 ± 0.4
Pb (mg/L)	20.34 ± 0.23
Cu (mg/L)	19.77 ± 0.54
Fe (mg/L)	0.26 ± 0.05
Mn (mg/L)	0.02 ± 0.003
Ni (mg/L)	0.004 ± 0.001
Zn (mg/L)	0.16 ± 0.021

Four different voltages 2V, 3V, 4V and 5V were applied for 2h/day for 10 days. The experiment was stopped in which 5V was applied due to the formation of bubbles and heat generation. Maximum removal of Cd, Pb and Cu was observed in phytoremediation system operated at 4V for 10 days (Figure 4.2). So 4V was applied for further experiments. The plants used in outdoor experiment had grown better than the plants in indoor experiment due to the presence of sunlight. So, after one week, the indoor experiment was discontinued. Treatment of lead, cadmium and copper from synthetic solution using electrically enhanced phytoremediation system was conducted using Al rod and Al sheet as electrodes and the results were compared.
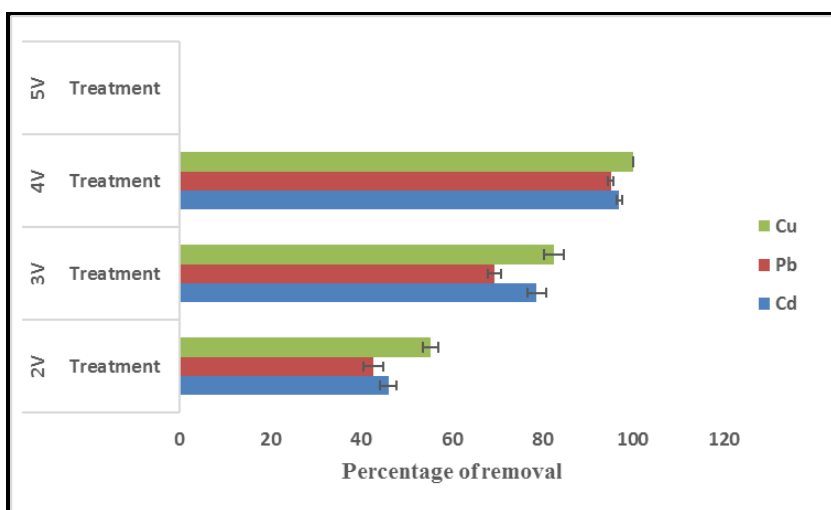
Figure 4.2: Percentage removal of Cd, Pb and Cu at different voltage level

4.3.1.1 Variation of pH

pH changes were recorded during every 5 days and the variations are depicted in Figure 4.3. No significant change in pH was observed in

control A (phytoremediation system) during study. In both experimental sets (i.e., in experiments using Al rod and Al sheet as electrodes), control A presented a lower pH than control B (electro-remediation system) and treatment (electrically stimulated phytoremediation). With electrical exposure, an increase in pH was observed in control B and treatment. The OH$^-$ concentration in solution increases while electrolysis is taking place, which resulted in the increase in pH (Rajeshwar et al., 1994).
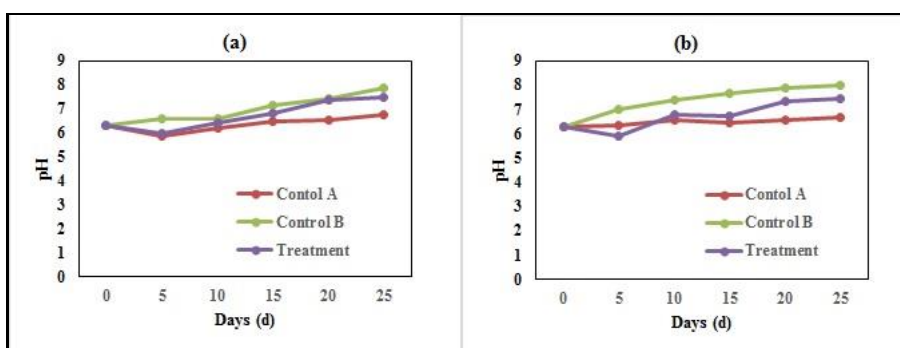
Figure 4.3: Variation of pH during the study (a) Aluminum rods as electrodes (b) Aluminum sheets as electrodes

4.3.1.2 *Removal performance of heavy metal by electrically stimulated phytoremediation system*

For determining the concentration of Cd, Pb and Cu, water samples were collected in every 5 days during study and analyzed using AAS. The residual concentrations of Cd, Pb and Cu in water collected from control A, control B and treatment are summarized in Table 4.2. In the experiment, where aluminum sheet was used as electrode, the electro assisted phytoremediation system (i.e. treatment) reduced 100% of cadmium within 15 days, while in control A and control B, 48.21 ± 1.8

and 84.24 ± 1.7 % of cadmium reduction was observed after 25 days of experiment. The average removal efficiencies of cadmium, lead and copper obtained in the experiment is graphically represented in Figure 4.4. Maximum Cd was removed within a short period in electro assisted phytoremediation system. The order of removal efficiency of Cd is, Electro assisted phytoremediation system (Treatment) > Control B > Control A. Maximum removal of lead was attained by electrically stimulated phytoremediation system within 15 days. After 25 days, it was observed that, 66.67 ± 1.2 and 81.51 ± 0.7 % of lead was removed in control A and control B respectively. The result indicated that, electrically coupled phytoremediation system exhibited better efficiency than phytoremediation system and electrolysis system in lead removal. The electrically stimulated phytoremediation system attained 100% of copper removal within 10 days and took only 5 days to attain a reduction of 99.94 ± 0.004%. The results indicated that, in control A and control B, removal of copper was found to be 89.93 ± 1.6 % and 99.98 ± 0.003 % respectively after 25 days. Phytoremediation experiments in the presence of electrical field was found to have maximum removal efficiency for copper ions

In the experiment where aluminum rod was used as electrode, maximum concentration of heavy metals was removed in electro assisted phytoremediation system compared to control A and control B within 20 days. 96.96 ± 0.22 % of cadmium and 99.97 ± 0.01 % copper was eliminated by electro assisted phytoremediation system from contaminated water within 15 days. The electro assisted phytoremediation experiment where aluminum sheet was used as electrodes exhibited fast and better

removal efficiency compared to the electro assisted phytoremediation system where aluminum rod was used as electrodes.

Table 4.2: Residual Cd, Pb and Cu concentrations in water

Metal	Days	Concentration of metals, mg/L					
		Aluminum sheet used as electrodes			Aluminum rod used as electrodes		
		Control A	Control B	Treatment	Control A	Control B	Treatment
Cd	0	18.86 ± 0.4	18.86 ± 0.4	18.86 ± 0.4	20.41 ± 0.45	20.41 ± 0.45	20.41 ± 0.45
	5	14.57 ± 0.1	11.23 ± 0.21	2.31 ± 0.12	15.34 ± 0.67	14.56 ± 0.21	6.22 ± 0.42
	10	12.56 ± 0.3	8.74 ± 0.15	0.56 ± 0.14	13.42 ± 0.39	11.87 ± 0.71	2.54 ± 0.34
	15	11.98 ± 0.45	6.41 ± 0.34	ND*	12.17 ± 0.47	9.13 ± 0.18	0.62 ± 0.05
	20	10.21 ± 0.23	5.32 ± 0.24	ND*	11 ± 0.19	7.20 ± 0.24	ND*
	25	9.77 ± 0.34	2.97 ± 0.33	ND*	9.36 ± 1.01	4.72 ± 0.37	ND*
Pb	0	20.34 ±0.23	20.34 ± 0.23	20.34 ± 0.23	19.18 ± 0.56	19.18 ± 0.56	19.18 ± 0.56
	5	15.54 ± 0.43	14.98 ± 0.28	7.45 ± 0.23	14.99 ± 0.29	14.35 ± 0.64	13.11 ± 0.74
	10	13.99 ± 0.25	11.97 ± 0.13	0.99 ± 0.12	13.69 ± 0.54	12.97 ± 0.64	9.35 ± 0.36
	15	12.98 ± 0.41	9.87 ± 0.17	ND*	11.52 ± 0.24	8.68 ± 0.35	3.14 ± 0.37
	20	8.01 ± 0.23	6.23 ± 0.53	ND*	9.55 ± 0.06	7.35 ± 0.25	ND*
	25	6.78 ± 0.25	3.76 ± 0.14	ND*	8.18 ± 0.30	4.39 ± 0.28	ND*
Cu	0	19.77 ± 0.54	19.77 ± 0.54	19.77 ± 0.54	19.34 ± 0.42	19.34 ± 0.42	19.34 ± 0.42
	5	11.06 ± 0.24	7.03 ± 0.31	0.01 ± 0.001	12.35 ± 0.81	11.25 ± 0.21	4.93 ± 0.24
	10	8.05 ± 0.32	2.01 ± 0.12	ND*	10.27 ± 0.38	9.08 ± 0.29	0.64 ± 0.34
	15	5.03 ± 0.45	1.62 ± 0.23	ND*	7.27 ± 0.62	5.60 ± 0.28	0.01 ± 0.002
	20	2.90 ± 0.27	0.09 ± 0.09	ND*	4.92 ± 0.38	3.52 ± 0.41	ND*
	25	1.99 ± 0.31	0.004±0.001	ND*	2.94 ± 0.20	1.78 ± 0.24	ND*

* Not detected

In the case of cadmium, within 10 days, 97.05 ± 0.7 % was reduced in electro assisted phytoremediation experiment where aluminum sheet was used as electrodes while only 87.56 ± 1.66 % reduction was noticed in aluminum rod was used as electrodes. Within 10 days, 95.13 ± 0.6% of lead was removed from water in the experiment where aluminum sheet was used, while Al rod removed only 51.25 ± 1.86 % of lead. 99.94

± 0.004 % of copper was reduced by electro assisted phytoremediation experiment where aluminum sheet used as electrodes within 5 days but only a 74.49 ± 1.25 % of reduction in copper was observed in aluminum rod used experiment. In control B also i.e., the system where only electrolysis is taking place, maximum removal of heavy metals was noticed when aluminum sheet was used as the electrode. The results indicate that the treatment of Cd, Pb and Cu using electrically enhanced phytoremediation using aluminum sheet electrodes is more effective than aluminum rod electrode. The treatment system (electrically enhanced phytoremediation using aluminum sheet electrodes) had more favorable conditions to accumulate heavy metals than did control A (phytoremediation system), such as the higher pH, and the presence of aluminum ions, which caused chemical precipitation, physical adsorption and flocculation of metal. So, we had carried our further study using electrically enhanced phytoremediation using aluminum sheet electrodes.

4.3.1.3 *Accumulation of cadmium, lead and copper in Eichhornia crassipes*

For the detailed study, heavy metal accumulation in plants collected from control A and electrically enhanced phytoremediation system using aluminum sheet electrodes was analyzed. The segmentation of *Eichhornia crassipes* into root, stem and leaves was carried out. The accumulation of Cd, Pb and Cu in plant parts is shown in Figure 4.5. The results indicated that maximum concentration of Cd, Pb and Cu were accumulated in *Eichhornia crassipes* collected from treatment (electrically enhanced phytoremediation) than in control A (phytoremediation).
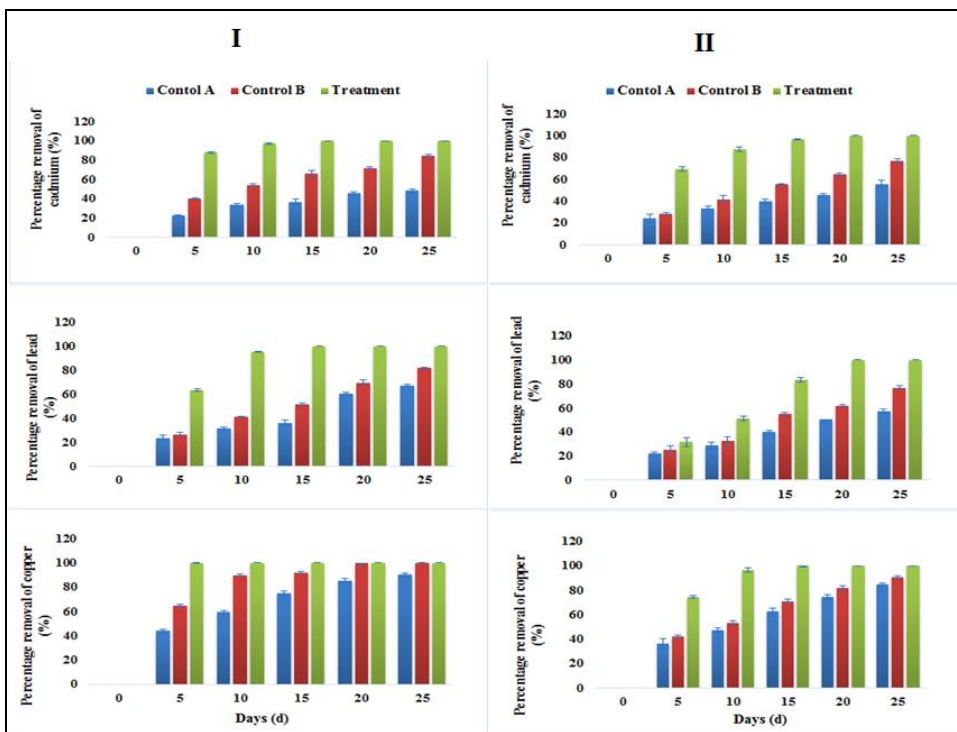
Figure 4.4: Efficiency of cadmium, lead and copper removal at different time intervals in the experiment (I: aluminum sheet used as electrodes and II: aluminum rod used as electrodes)

Cadmium is a toxic non-essential heavy metal and it can cause inhibitory effects on plant growth. Lu et al. 2004 reported that Cd can suppress the development of new roots and reduce the relative growth rates and substantially reduce the growth of *Eichhornia crassipes*. The control plant accumulated maximum level of Cd in its root but in treatment plant maximum accumulation was observed in leaf. This result indicates that *Eichhornia crassipes* can translocate maximum Cd to plants' aerial parts under electrified condition. Maximum concentration of Pb was attained by roots in both control A (5653.51 mg/Kg) and treatment

(7532.4 mg/Kg) plant. Under electrified condition, more Pb content was translocated to its aerial part by the treatment plant compared to control A.

Figure 4.5: Accumulation of Cd, Pb and Cu in plant

Copper (Cu) is one of the micronutrient, essential for plants at very low concentrations. However, excessive concentrations of this metal are highly toxic. In both treatment (9842.76 mg/Kg) and control A (5845.68 mg/Kg), the highest value of Cu concentration was recorded in stem. Compared to control A, treatment plant accumulated more amount of Cu in its aerial part under electrified condition. Many studies revealed that *Eichhornia crassipes* accumulated more amount of heavy metals like Cd, Co, Cr, Cu, Mn, Ni, Pb and Zn in its roots than in the aerial parts (Soltan & Rashed, 2003). But our results indicated that, metals like Pb, Cd and Cu are translocated to its areal parts under electrified condition. Many researchers reported the mechanisms of heavy metal removal in aquatic plants and mentioned that the main way of heavy metal uptake in

emergent and surface-floating plants like *Eichhornia crassipes* was through the roots system. The heavy metal uptake in plants takes place by exchange of cations which occurred in the cell wall. The plants take up metals by absorption and translocation. The accumulation of heavy metals by plant tissue is by absorption to anionic sites in the cell walls. This is the reason why wetland plants can accumulate high magnitude of heavy metals in their pant parts compared to their surrounding environment (Lu et al., 2004).

4.3.1.4 Bioconcentration factor and translocation ability of electrically stimulated Eichhornia crassipes

The potential of plants for accumulating heavy metals was assessed by bioconcentration factor (BCF). The ratio between metal concentration in plant and that of the growth media expresses the bioconcentration factor (BCF), which indicates the affinity of aquatic macrophytes to a specific heavy metal or pollutant (Zhu et al., 1999; Abd-Elmoniem, 2003). Bioconcentration factors of plant for Cd, Pb and Cu in the present study are graphically depicted in Figure 4.6. Higher BCF values reflect the higher phytoaccumulation capacity. Accumulation of metals by macrophytes can be affected by metal concentrations in water and the ambient metal concentration in water was the major factor influencing the metal uptake efficiency. When the metal concentration in water increases, the amount of metal accumulation in plants increases, but the BCF values decrease. Based on the arbitrary criteria by Zayed et al. (1998) and Zhu et al. (1999), maximum BCF values for Cd under

electrified condition was 1118.18, indicating that electrically stimulated *Eichhornia crassipes* is good hyper accumulator of Cd.

If the BCF value is more than or equal to 1000 then that plant species is considered as a hyper accumulator. The plant having the abilities to grow in very high concentration of metal and concentrating high heavy metals in their tissues are known as hyperaccumulators (Wahab et al., 2014). The BCFs of control A for Pb, Cd and Cu were 502.65, 448.12 and 664.90 respectively. The BCFs for all the three metals were lower than 1,000 for control plant, i.e. plant grown under normal condition. The highest level of BCFs observed for Pb and Cu was 932.26 and 1152.47 respectively for treatment. In this study, with the BCF values of treatment plant was a little under 1000 for lead (BCF = 932.26), this suggests that electrically stimulated plant can be considered as a moderate accumulator for Pb. For copper this value exceeds 1000, so electrically stimulated *Eichhornia crassipes* is considered as a good hyper accumulator. From Figure 4.5, Pb accumulated by treatment plants were largely retained in roots. This indicates that *Eichhornia crassipes* used in the electrically stimulated phytoremediation system bioconcentrated more amounts of Pb in its roots than the aerial parts. Accumulation pattern of Cd can be elaborated as follows:

Control A: Root system >Stem system > Leaf system
Treatment: Leaf system >Root system >Stem system
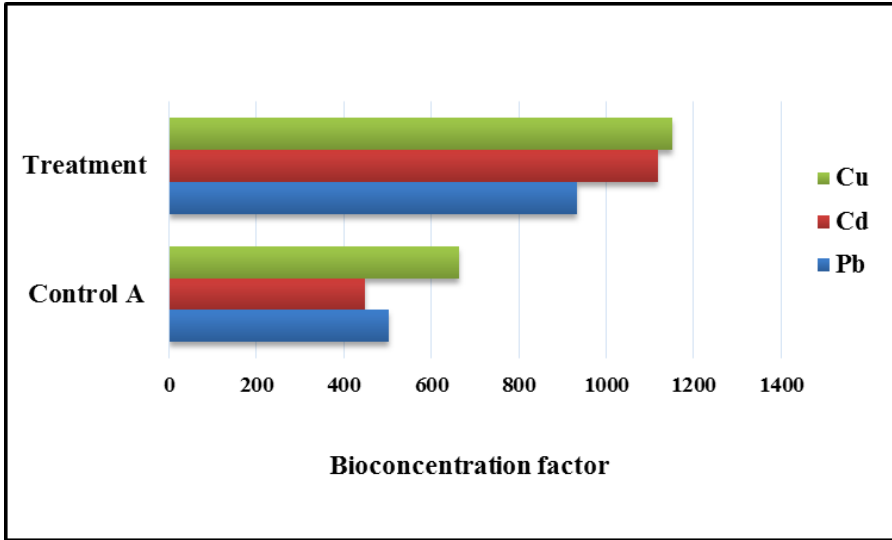
Figure 4.6: Bioaccumulation factors (BCF) of Pb, Cd and Cu in
Eichhornia crassipes

This result indicates that under electrified condition, leaf can effectively bioconcentrate more amount of Cd than roots. Copper, a component of an electron carrier called plastocyanin is active during photosynthesis. It is also a constituent of ascorbic acid oxidase, tyrosinase, and phenoloxidase (Yapoga et al., 2013). For both phytoremediation system and electrically stimulated phytoremediation system, maximum copper was bioconcentrated in stems of *Eichhornia crassipes*. Under electrified condition, more amount of copper accumulation was observed. Accumulation pattern of Cu can be observed as follows:

Control A: Stem system > Root system > Leaf system
Treatment: Stem system > Root system > Leaf system

The root pressure and leaf transpiration are the two processes mainly controlling the translocation of metals from root to shoot/leaf.

Some metals are accumulated in roots, probably due to some physiological barriers against metal transport to the aerial parts, while others are easily transported in plants (Lasat, 2000; Lu et al., 2004). According to Zhu et al. (1999), translocation of trace elements from roots to shoots could be a limiting factor for the bioconcentration of elements in shoots. The translocation ability (TA) is the ratio between the concentrations of a trace element accumulated in the root tissues by that accumulated in stem/leaf tissues; a larger ratio implies poorer translocation capability (Hammad, 2011). For all the three metals, low value of TA was found in treatment system, i.e., in electrically stimulated phytoremediation system (Table 4.3). This result indicates that, *Eichhornia crassipes* has the ability to translocate more amounts of Pb, Cd and Cu under electrified condition. Copper reported minimum value for translocation ability (TA (r/s) = 0.85) compared to other metals. This shows that *Eichhornia crassipes* had translocated more amount of Cu from root to stem under electrified condition.

Table 4.3: Translocation Ability of *Eichhornia crassipes*

Metals	Control A		Treatment	
	TA(r/s)	TA(r/l)	TA(r/s)	TA(r/l)
Pb	1.72	4.40	1.66	1.09
Cd	1.79	3.52	1.61	0.98
Cu	0.88	2.38	0.85	1.81

4.3.1.5 Variation in the production of chlorophyll

The first and most obvious reactions of plants under heavy metal stress are often growth changes (Lu et al., 2004). Chlorophyll content is often measured in plants in order to assess the impact of environmental stress, as changes in pigment content are linked to visual symptoms of plant illness and photosynthetic productivity. Decrease in chlorophyll in several plant species under the impact of heavy metals have reported by many researchers (Zengin & Munzuroglu, 2005). In this study, we emphasized exploring, whether or not an electrical exposure can stimulate *Eichhornia crassipes* growth. In green plants' life activity, chlorophyll plays the role of absorbing, transferring and transforming energy. Leaves were collected from the control plant, treatment plant and plant from fresh water and the chlorophyll content in leaves of *Eichhornia crassipes* was determined using UV-Visible spectrophotometer (Song et al., 2011).
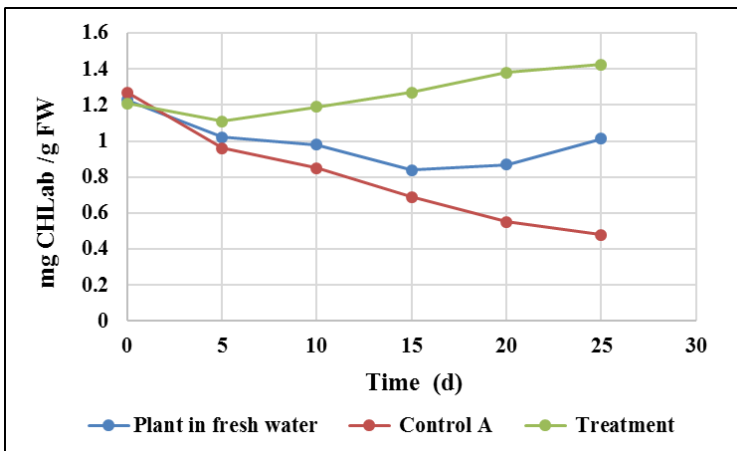
Figure 4.7: Variation in the production of chlorophyll

Chlorophyll content in *Eichhornia crassipes* leaves decreased at the beginning in all the three the plant. From the 10th day of the study, the

chlorophyll content of plant in electrically stimulated phytoremediation system was found to be gradually increasing with electrical exposure (Figure 4.7). The result shows an increase in the production chlorophyll with electrical stimulation. When the heavy metal exposure time increases, the production of chlorophyll content in control A was decreased. Heavy metals hinder metabolic processes by inhibiting the action of enzymes, and this may be the main cause of inhibition. Heavy metal stress can cause inhibition of the enzymes responsible for chlorophyll biosynthesis which associated with decreased chlorophyll content. Cadmium was reported to affect chlorophyll biosynthesis and inhibit protochlorophyll reductase and aminolevulinic acid (ALA) synthesis (Zengin & Munzuroglu, 2005). Cadmium strongly binds to proteins, thereby decreasing the accumulation of pigment–lipoprotein complexes, including photosystem I (PSI) and PSII (Sarvari et al., 1999; Kupper et al., 2007). The Cd induced inhibition of chlorophyll synthesis and interference with photosystems causes chlorosis of leaves of *Eichhornia crassipes* Cd also reduces the contents of large and small subunits of ribulose-1, 5-bisphosphate carboxylase/oxygenase (RuBisCO) along with other enzymes of photosynthesis and chlorophyll biosynthesis. Wilting, which followed chlorosis was reported in the presence of high dose of Cd by researchers (Das et al., 2016). This reduction in chlorophyll of *Eichhornia crassipes* in control A under heavy metal stress can be regarded as a specific response of the plants to metal stress, which resulted in chlorophyll degradation and inhibition of photosynthesis. The chlorophyll content might be reduced due to increased cell or tissue damage or lipid peroxidation (Cho & Park, 1999).

From the experimental results, it can be postulated that 4V voltage is probably suitable to stimulate the *Eichhornia crassipes* to synthesize more chlorophyll. The longer the unit was electrified, the more obvious the stimulating effect was. It was in accordance with Knorr's report (Knorr, 2003). The voltage can stimulate the plants to increase the palisade cells, chloroplast grana and thylakoid lamellas, which enhance the synthesis of chlorophyll. *Eichhornia crassipes* was stimulated by electric field to grow better so it can assimilate more metal.

4.3.2 Application of electro-phytoremediation for the treatment of lead and chromium from wastewater collected from battery manufacturing industry and electroplating industry

The above mentioned experimental condition was applied to remove lead and chromium from wastewater collected from acid lead battery manufacturing industry and electroplating industry. Both the effluents were acidic in nature. The same plant, *Eichhornia crassipes* was used for this study because it can have the ability to reduce the concentration of heavy metals in acidic environment with minor sign of toxicity (Rai & Singh, 2016). Chromium, nickel, iron and zinc are the metals commonly used in electroplating industry. But their level of concentration depends on the type of methods used for plating (Selvakumari et al., 2002). Cr (VI) is an extremely toxic form of chromium, which is generated throughout the world due to many industrial activities such as chromium plating, chemical manufacturing, and chromite mining etc. causing contamination of the water resources within its vicinity (Saha et al., 2017). Storage batteries are manufactured

using lead due to its characteristic properties: corrosion resistance, conductivity and reversibility of the reaction between lead, lead oxide and sulfuric acid (Dermentzis et al., 2012). The toxic metal such as lead in water has to be detoxified before its discharge to environment as per the norms laid down by environment regulatory authorities. Several researchers attempt to find out a suitable technique of treating heavy metals for a long run. The conventional methods are mainly chemical based and residual chemicals can cause a detrimental influence on environment in the long run. In this study, we report an environmentally friendly method for the removal of toxic heavy metals.

4.3.2.1 *Treatment of lead from battery manufacturing industry wastewater by electro - assisted phytoremediation system*

The levels of pollutants in lead acid battery wastewater vary depending upon the process adopted in battery making. The battery manufacturing industrial wastewater collected from Kozhikode was highly acidic probably due to the high concentration of hydrogen ion in the effluent, sourced mainly by sulphuric acid, one of the major raw materials in lead acid battery manufacture (Okareh & Adeolu, 2015). Initial heavy metal concentration of wastewater is presented in Table 4.4. The AAS results indicate that comparatively small quantities of Mn and Cd were present in acid battery wastewater. Fe and Ni were also detected. The other metals Pb, Zn and Cu were present in very high concentrations and are considered to be hazardous for living systems. The treatment technique employed in the industry is not effective, they need to be overhauled and upgraded to improve performance.

Table 4.4: Initial heavy metal concentration of wastewater

Heavy metals	Initial heavy metal concentration of wastewater before treatment	
	Battery manufacturing industry	**Electroplating industry**
Cr	NA*	490 ± 23.7
Cu	78.82 ± 7.42	16.39 ± 1.62
Fe	2.27 ± 0.21	3.95 ± 0.35
Ni	6.84 ± 0.74	134.19 ± 9.38
Zn	324.33 ± 16.81	25.69 ± 2.14
Mn	0.49 ± 0.02	0.51 ± 0.002
Cd	0.28 ± 0.002	0.02 ± 0.001
Pb	18.15 ± 1.15	0.17 ± 0.01

* NA: Not Analyzed

Electrically stimulated phytoremediation was applied for the removal of lead from wastewater. Phytoremediation using *Eichhornia crassipes* was applied in control A and electrolysis using aluminum sheet as electrode was applied in control B. Electrically stimulated phytoremediation system was operated 2h/day from 10:00 A.M to 12:00 P.M at voltages of 4V. All the three units were continued for 25 days. The treatment (electro assisted phytoremediation system) reduced lead by 94.27 ± 0.41 % within 25 days, while control A and control B removed lead by 40.61 ± 2.39 and 74.33 ± 1.87 %, respectively after 25 days. Variations in concentration of lead from acid battery wastewater during the experiment is graphically represented in Figure 4.8 and the removal efficiency of lead is tabulated in Table 4.5. Reduction in concentration of other heavy metals present in the battery industrial effluent was also observed and the percentage of reduction of Cu, Fe, Ni, Zn, Mn and Cd were observed as 50.52 ± 4.27 %, 90.75 ± 1.05 %, 84.65 ± 2.32 %, 11.51

$\pm$ 6.34 %, 100 % and 100 %, respectively. Due to high chemical contents present in the acid battery wastewater, *Eichhornia crassipes* exhibited some toxicity symptoms. It was found that best removal efficiency for lead is achieved by using electrically stimulated phytoremediation.
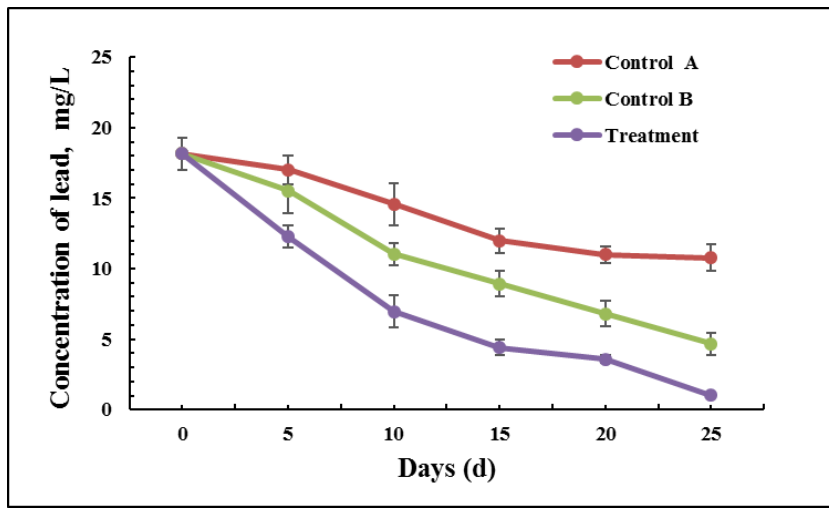
Figure 4.8: Variations in concentration of lead from industrial wastewater during treatment

Table 4.5: Removal efficiency of lead from industrial wastewater by electro assisted phytoremediation system

Days	Percentage of lead removal (%)		
	Control A	Control B	Treatment
0	--	--	--
5	6.17 $\pm$ 1.15	14.55 $\pm$ 1.32	32.34 $\pm$ 1.29
10	19.72 $\pm$ 1.02	39.23 $\pm$ 1.54	61.71 $\pm$ 1.12
15	33.94 $\pm$ 1.51	50.74 $\pm$ 0.86	75.65 $\pm$ 0.89
20	39.28 $\pm$ 1.85	62.42 $\pm$ 1.08	80.22 $\pm$ 1.04
25	40.61 $\pm$ 2.39	74.33 $\pm$ 1.87	94.27 $\pm$ 0.41

4.3.2.2 Application of electro - assisted phytoremediation system for the treatment of chromium from electroplating industrial wastewater

Heavy metal, such as chromium is of considerable concern because it is non-biodegradable, highly toxic and probably carcinogen. The wastewater collected from electroplating industry, Kozhikode was also found to be highly acidic. Since the chromium bath used in electroplating is produced by mixing sulfuric acid, hydrochloric acid and dichromate, resulting in an extremely acidic bath. 490 ± 23.75 mg/L of Cr was observed in the wastewater collected from electroplating industry along with other heavy metals like Cu (16.39 ± 2.62 mg/L), Ni (134.19 ± 9.38 mg/L) and Zn (25.69 ± 3.14 mg/L) (Table 4.4). Comparatively small amount of metals like Pb, Cd and Mn were observed in the wastewater. The same experimental conditions were operated continuously for 25 days, during which water samples were taken once in every 5 days.
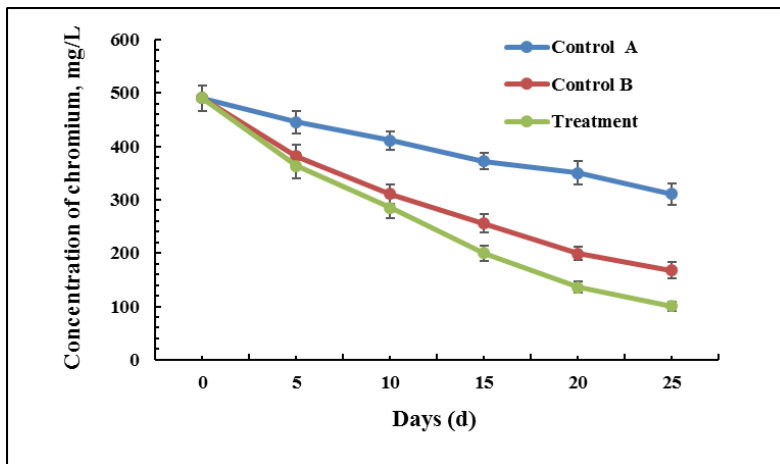
Figure 4.9: Removal of chromium from industrial wastewater by electrically enhanced phytoremediation

On the 25th day of study, 79.56 ± 2.61 % of Cr content in the water was reduced from the initial concentration of 490.6 mg/L by an electric field coupled phytoremediation system. From the graph (Figure 4.9), a steady decrease in the Cr content in the wastewater was noticed in treatment system. The result indicates that maximum removal of chromium was occurred in the electrically stimulated phytoremediation system than control A and control B. The control A and control B showed 36.72 ± 4.23 and 65.83 ± 3.59 % of chromium removal respectively. The order of the removal efficiencies of chromium from electroplating industry are: Electrically stimulated phytoremediation > Electrolysis > Phytoremediation. Along with Cr, the other metals present in electroplating industrial effluent were also reduced. The percentage reduction of Cu, Fe, Ni, Zn, Mn, Cd and Pb were 87.19 ± 0.2 %, 96.71 ± 0.005 %, 27.12 ± 12.35 %, 41.26 ± 3.41 %, 100 %, 100 % and 100 %, respectively.

Plate 4.4: Plant toxicity symptoms

The effluent was highly toxic to plants and it showed visible symptoms of toxicity such as stunted growth, vein chlorosis in younger leaves, yellowing followed by withering of old leaves ultimately death. Cr toxicity symptoms were observed in control A from 15th day of study but the treatment plant showed toxicity symptoms in a much-delayed stage. The electrical stimulation helps *Eichhornia crassipes* to reduce high amount of chromium than control plant.

4.4 Summary

The main goal of present study was the assessment of the performance of electrically stimulated phytoremediation in the removal of heavy metal. Treatment of lead, cadmium and copper from synthetic solution using phytoremediation system coupled with electric field was conducted. In that experiment, the *Eichhornia crassipes,* an efficient phyto-remediator exhibited efficient and fast removal of heavy metals in electro assisted phytoremediation system. Both aluminum rods and sheets were used as electrodes and both indoor and outdoor experiments were also conducted. Based on the results and plants condition, outdoor experiment using aluminum sheets as electrodes were preferred for further study. The results indicate that the treatment of Cd, Pb and Cu using electrically enhanced phytoremediation using aluminum sheet electrodes is more effective than aluminum rod electrode. When the electrical exposure time increases, the pH of the synthetic solution increased in electrolysis system, but a more favorable, moderate increase was shown by the electrically stimulated phytoremediation system. From the results, it can be postulated that 4V voltage is probably suitable to stimulate the

Eichhornia crassipes to synthesize more chlorophyll. *Eichhornia crassipes* stimulated by an electric field grew better and assimilated more metal. Heavy metal accumulation in plants collected from control A and electrically enhanced phytoremediation system using aluminum sheet electrodes indicates that maximum amount of Cd, Pb and Cu were accumulated in *Eichhornia crassipes* collected from treatment. *Eichhornia crassipes* translocated maximum Cd and Cu to plants' aerial parts under electrified condition but more amount of Pb was bioconcentrated in roots. Electrically stimulated plant translocated more amount of Pb content to its aerial part compared to plant in control A. The BCFs of control A for Pb, Cd and Cu were 502.65, 448.12 and 664.90 respectively. BCF an index of hyperaccumulation, indicates that electrically stimulated *Eichhornia crassipes* is a good hyper accumulator of Cd (BCF = 1118.18) and Cu (BCF = 1152.47) and a moderate accumulator of Pb (BCF = 932.26). Translocation ability (TA) ratio indicates that *Eichhornia crassipes* have the ability to translocate more amounts of Pb, Cd and Cu to its upper portion under electrified condition.

The electro-phytoremediation technique was applied to remove lead and chromium from wastewater collected from acid lead battery manufacturing industry and electroplating industry. Both the effluents were acidic in nature. Therefore, aiming the treatment of lead from industrial effluents a pre-treatment should be made to neutralize effluent. Due to high chemical contents present in the acid battery wastewater, *Eichhornia crassipes* exhibited some toxicity symptoms at an earlier stage than the plants used in the treatment of electroplating industry wastewater. The treatment (i.e. electro assisted phytoremediation system) reduced lead

by 94.27 ± 0.41 % within 25 days, while control A and control B removed lead by 40.61 ± 2.39 and 74.33 ± 1.87 %, respectively from battery manufacturing industrial wastewater. A steady decrease in the Cr content in the wastewater collected from electroplating industry was observed in electrically stimulated phytoremediation. The result indicated that maximum removal of chromium was occurred in the electrically stimulated phytoremediation system (79.56 ± 2.61 %) than control A (36.72 ± 4.23 %) and control B (65.83 ± 3.59 %). Cr toxicity symptoms were observed in control A from 15th day of study but the electrically stimulated plant showed toxicity symptoms in a much-delayed stage, indicating that the electrical stimulation helping the plant to resist toxicity and accumulate more metals than control plant. The other heavy metals present in the effluent samples such as Cu, Fe, Ni, Zn, Mn and Cd were also reduced. Hence, the electro - assisted phytoremediation system is also capable for the treatment of Pb, Cd, Cu, Cr, Mn, Fe, Ni, and Zn from water. Considering the overall results, we can state that the electro-phytoremediation technique seems to be promising in the treatment of heavy metals contaminated wastewater.

Chapter **5**

TREATMENT OF CADMIUM, LEAD AND COPPER USING PHYTOREMEDIATION ENHANCED BY TITANIUM DIOXIDE NANOPARTICLES

5.1 Introduction

Heavy metal contamination is a widespread issue that disrupts the environment as a consequence of several anthropogenic activities and their invariably persisting nature in the environment. The ecological balance of the environment and diversity of aquatic organisms have devastatingly affected by heavy metal pollution (Nilantika et al., 2014). Some heavy metals like cadmium, lead and chromium etc. are phytotoxic at both low concentrations as well as very high concentration (Amin, 2012). The prevailing technologies on purification that are used to eradicate these toxic contaminants are costly and sometimes non-ecofriendly also. For the beneficial of community, the research on water purification is focused towards low cost and eco-friendly technologies (Dhote & Dixit, 2009). Phytoremediation is energy efficient, cost-effective, aesthetically pleasing technique of remediation sites with low to moderate levels of contamination.

The excessive concentration of heavy metals in plants can cause oxidative stress and stomatal resistance and can also affect photosynthesis and chlorophyll florescence processes. Copper can inhibit photosynthesis and reproductive processes; lead reduces chlorophyll production; arsenic interferes with metabolic processes, while zinc and tin stimulate the growth of leaves and shoots; ultimately plant growth becomes limited or impossible (Ashraf et al.*,* 2011). The results of some of the experiments indicated that accumulation of some heavy metals such as Cd and Pb may damage chloroplasts in young leaves and the first impact of Cd on plants is the reduction of photosynthetic activity (Ali et al., 2014). Moreover, it has been proved that a decrease in the growth of plants under some stress is due to the restriction of photosynthetic process (Ackerson & Herbert, 1981).

Nanoparticles can be used to increase the supply of elements to plant shoots and foliage and its application can also increase seed germination and seedling growth. Furthermore, nanoparticles can facilitate enhanced ability of water and fertilizer absorption by roots, and increase antioxidant enzyme activity such as superoxide dismutase and catalase. Thus, nanoparticles can increase plant resistance against different stresses. Titanium dioxide nanoparticles are used in agriculture to increase growth and can improve yield; improve the rate of photosynthesis and reduce diseases (Morteza et al., 2013). Titanium dioxide (TiO_2) nanoparticles (NPs) are known for its photocatalytic activity, environmentally friendly nature, high stability and are found to be safe for human. These particles have been used in pathogen treatments as well as decomposition of phytotoxic compounds (Raskar & Laware, 2013).

The effects of nano-TiO_2 on the germination and growth of spinach seeds were studied by many researchers. These nanoparticles improved light absorbance and promote the activity of rubisco activase thus accelerated spinach growth (Remya et al., 2010). Nano- TiO_2 improved the plant growth by enhanced nitrogen metabolism (Yang et al., 2006) that promotes the absorption of nitrate in spinach and accelerating conversion of inorganic nitrogen into organic nitrogen, thereby increasing the fresh weight and dry weight. It has also been found that nano-anatase TiO_2 promoted antioxidant stress by decreasing the accumulation of superoxide radicals, hydrogen peroxide, malonyldialdehyde content and enhance the activities of superoxide dismutase, catalase, ascorbate peroxidase, guaiacol peroxidase and thereby increase the evolution oxygen rate in spinach chloroplasts under UV-B radiation (Lei et al., 2008). In this perspective, we tried to enhance efficiency of phytoremediation capacity of *Eichhornia crassipes* and *Salvinia molesta* using titanium dioxide nanoparticles in this study. The aim of our study was to offer an effective approach to enhance the efficiency of the phytoremediation system for the treatment of heavy metals like Pb, Cd and Cu from water.

5.2 Materials and Methods

5.2.1 Experimental setup

Two free-floating aquatic plants, *Eichhornia crassipes* and *Salvinia molesta* (Plate 5.1) were collected from a natural wetland area, viz. Kottooli wetland in Kozhikode City. In order to simulate the natural environment, plants were placed under natural sun light for one month and the second generations of the plants with similar size were utilized for this

study. Before starting the phytoremediation experiment, the epiphytes and insect larvae grown on plants were removed by rinsing with distilled water. The present study was conducted in two stages. During the Stage I, three different conditions (A, B and C) were applied to *Eichhornia crassipes* and *Salvinia molesta* for 10 days (Plate 5.2 and 5.3). Tanks were setup with different operating conditions and each contained plants and distilled water. Condition A was the control, in which the plants were kept in water under natural conditions. In condition B, TiO_2 nanoparticles entrapped calcium alginate beads (2 g) was applied to the plants and in condition C, TiO_2 powder (2 g) was applied. TiO_2 photocatalyst does not require ultraviolet rays that have an energy level as high as 254 nm and are hazardous to humans. It also allows reaction to be initiated by the near – ultraviolet rays with relatively long wavelength contained in sunlight. So, all the experimental setup was placed in the outdoor for maximum sunlight exposure and was conducted during the summer season. Before and after stage I, the chlorophyll content and fresh weight of *Eichhornia crassipes* and *Salvinia molesta* in A, B and C were determined.

Plate 5.1: (a) *Eichhornia crassipes* and (b) *Salvinia molesta*

In stage II, plants exposed to different conditions were used for the treatment of heavy metals like lead, cadmium and copper from water (Plate 5.4 and 5.5). Before that, plants were washed and rinsed with distilled water. Thirteen liters of mixed heavy metal (Cd, Pb and Cu) solution was taken in each tank ($45 \times 30 \times 15$ cm) and the tanks were named A, B and C for both experiments using *Eichhornia crassipes* and *Salvinia molesta*. Thirteen litres of simulated contaminated water was prepared for each tank by dissolving 0.416 g of Pb $(NO_3)_2$, 1.022 g of $CuSO_4.5H_2O$, and 0.593 g of $(3CdSO_4).8H_2O$ in distilled water. All chemicals used were of the highest purity available and of analytical grade procured from Merck. The heavy metal concentrations were determined by Atomic Absorption Spectrophotometer AAS (Thermo Series) with GF 95.

Plate 5.2: *Eichhornia crassipes* under three different experimental conditions

Plate 5.3: *Salvinia molesta* under three different experimental conditions

The phytoremediation experiments using *Eichhornia crassipes* was conducted with contaminated water having initial concentration of Cd, Pb and Cu, 20.32 ± 0.44 mg/L, 21.45 ± 0.18 mg/L and 21.34 ± 0.22 mg/L respectively. The water with initial concentration of Cd, Pb and Cu were 20.99 ± 0.37 mg/L, 20.78 ± 0.45 mg/L and 20.56 ± 0.46 mg/L respectively, was used in phytoremediation experiments using *Salvinia molesta*. Tank A was the control which comprised of only plants (phytoremediation system). In tank B and tank C, the plants exposed to TiO_2 nanoparticles entrapped calcium alginate beads and TiO_2 nanoparticles powder respectively were used in the treatment of Cd, Pb and Cu.

Experiment was continued for 24 days and water samples were taken in every 3 days. When the experiment was completed, stem, roots and leaves of the plants were separated and dried in a hot air oven. The residual Pb, Cd and Cu concentrations in water and the accumulated metals in different parts of the plants at the conclusion of the experiment

were analyzed using Atomic Absorption Spectrophotometer. The effect of the applied conditions on the growth of *Eichhornia crassipes* and *Salvinia molesta* was examined by using relative growth and chlorophyll content. Phytoremediation potential of these native aquatic macrophytes under different applied conditions was also evaluated by metal accumulation, translocation factor and bioconcentration factor.

Plate 5.4: Treatment of heavy metals using *Eichhornia crassipes*

Plate 5.5: Treatment of heavy metals using *Salvinia molesta*

5.2.2 Synthesis of TiO₂ nanoparticles and the encapsulation method for immobilization of nanoparticles in semipermeable alginates beads

TiO$_2$ nanoparticles were synthesized by simple precipitation method. TiO$_2$ (Fluka 15 %) solution in HCl (10 − 15 %) was stirred in deionized water ([Ti^{3+}] = 0.15 mol L $^{-1}$). A blue-violet solution was obtained at room temperature. The pH was adjusted between 0.5 and 6.5 with sodium hydroxide (NaOH) solution. The solution was then heated at 60^{0}C in an oven for 24 h. The solid obtained was centrifuged, washed with dilute acid (pH = 1) and distilled water in order to remove salts. A solution containing TiO$_2$ nanoparticles (0.5wt %) and sodium alginate (0.5wt %) was prepared with 25 mL distilled water and stirred for 30 min at 85^{0}C. Afterwards, the solution was extruded as small drops by means of syringe into a stirred solution of calcium chloride (4.0wt %), where spherical gel beads were formed (Plate 5.6). The gel beads were retained in the calcium chloride solution for 12 h for hardening and then washed with distilled water. Stability of beads depends on pH values of the aqueous solution and the initial physical states of the beads (Harikumar et al., 2013).

Plate 5.6: TiO$_2$ nanoparticles entrapped calcium alginate beads

5.2.3 Analytical procedures

The plant samples were rinsed with tap water twice and deionized water three times. Rinsed samples were cut into pieces and oven-dried at 70^0 C till constant weight was obtained for the dried samples. The oven-dried samples were ground to pass through a 100-mesh sieve and were digested with $HNO_3 - HClO_4$ (4:1) mixture and filtered. The filtrates were analyzed for heavy metals using AAS with GF 95 (Xinshan et al., 2011). Chlorophyll (chl.a + chl.b, CHLab) was determined by OD (optical density) values (663 nm and 645 nm using UV-Visible spectrophotometer, Thermo Evolution 201) of extracting solution, which was made by adding 80 % acetone into grinding solution of 0.5 g of fresh leaves (Xinshan et al., 2011).

5.2.4 Relative Growth

The relative growth of plants was calculated to assess the effects of applied conditions on the growth of *Eichhornia crassipes* and *Salvinia molesta*.

$$RG = FFW / IFW \qquad (1)$$

Where RG denotes relative growth of plants during experimental period, dimensionless; FFW denotes final fresh weight in grams of plants taken at the end of each experiment, and IFW denotes the initial fresh weight in grams of plants taken before starting experiment (Gakwavu et al., 2012).

5.2.5 Bioconcentration Factor and Translocation factor

The bioconcentration factor (BCF) was calculated as the ratio of the trace element concentration in the plant tissues at harvest to the concentration of the element in the external environment (Zayed et al., 1998). BCF is given by,

$$BCF = (P/E) \qquad\qquad (2)$$

P represents the trace element concentration in plant tissues (mg kg^{-1} dry wt); E represents the trace element concentration in the water (mg/L). BCF is dimensionless. A larger ratio implies better phytoaccumulation capability.

The translocation of heavy metal from roots to aerial part and the internal metal transportation of the plant are generally indicated by Translocation Factor (TF). The translocation factor is determined as a ratio of metal accumulated in the shoot to metal accumulated in the root (Deng et al., 2004)

$$TF = (A_s / A_r) \qquad\qquad (3)$$

Where, TF > 1 indicates that the plant is capable of effectively translocating the accumulated metals from the root to its aerial part. TF is the translocation factor and is dimensionless. A_r represents the amount of trace element accumulated in the roots (mg kg^{-1} dw), and A_s represents the amount of trace element accumulated in the shoot/leaf (mg kg^{-1} dw). All the tests were conducted in triplicates and the data were statistically analyzed.

5.3 Results and Discussion

The *Eichhornia crassipes* and *Salvinia molesta* grown under different conditions were used for the treatment of heavy metals. TiO_2 nanoparticles that applied to plants were synthesized by chemical precipitation method. The materials were characterized by scanning electron microscopy (Figure 5.1) and energy dispersive X-ray spectroscopy (Figure 5.2) spectra. While synthesizing TiO_2 NPs by precipitation method, a mixture of anatase and rutile was precipitated at pH 3. By increasing the pH of the solution, the formation of anatase was favored and at pH 5, only anatase TiO_2 could be formed (Cheng et al., 1995). SEM micrograph indicates the presence of nanoparticles below 50 nm. The energy dispersive X-ray spectra confirm the presence of TiO_2 and showed no significant levels of impurities.
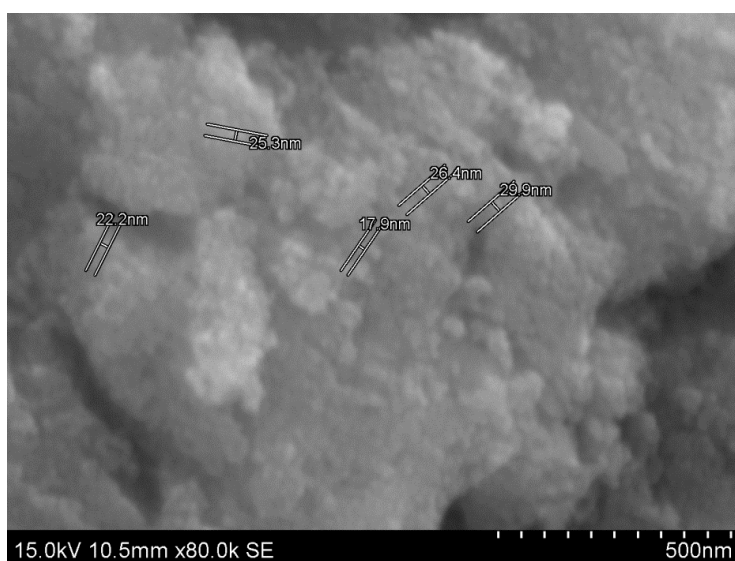
Figure 5.1: SEM micrographs of titanium dioxide nanoparticles

Element	Weight%	Atomic%
O K	40.14	66.75
Ti K	59.86	33.25
Totals	100.00	

Full Scale 1974 cts Cursor: -0.205 (0 cts)   keV
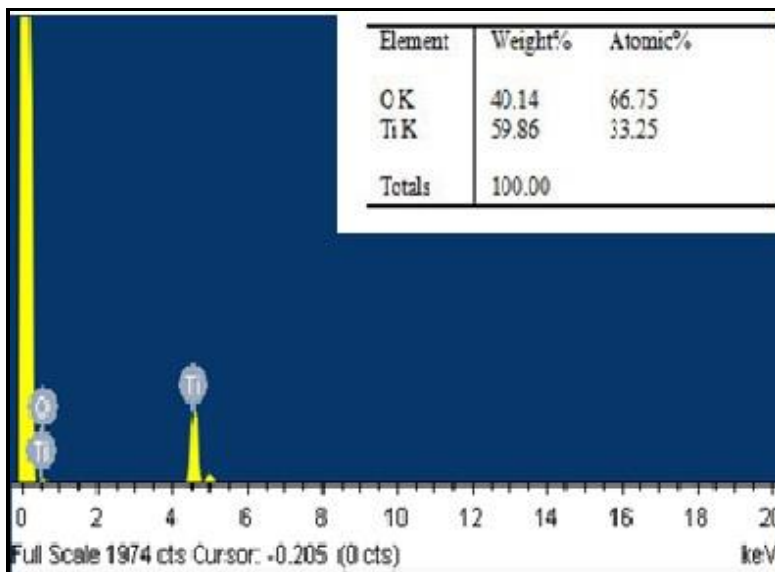
Figure 5.2: EDX spectra of titanium dioxide nanoparticles

5.3.1 Phytoremediation of heavy metals

The ability of *Eichhornia crassipes* and *Salvinia molesta* to uptake more than one metal was analyzed by the phytoremediation of the simulated multi metal contaminated water. The residual concentration of Cd, Pb, and Cu were analyzed for each phytoremediation system (A, B and C) during the study, at an interval of 3 days using AAS and the results are summarized in Table 5.1. The metals other than Cu, Cd and Pb were found to be within the permissible limit.

Table 5.1: Residual concentration of lead, cadmium and copper in water

Metal	DAY	Residual concentration of heavy metals, mg/L					
		Eichhornia crassipes			*Salvinia molesta*		
		A	**B**	**C**	**A**	**B**	**C**
Pb	3	19.14 ± 0.25	10.57 ± 0.07	0.95 ± 0.03	19.64 ± 0.01	12.55 ± 0.11	4.70 ± 0.01
	6	15.48 ± 0.23	7.96 ± 0.03	0.46 ± 0.02	15.89 ± 0.02	9.37 ± 0.06	1.42 ± 0.004
	9	11.57 ± 0.13	5.89 ± 0.12	0.35 ± 0.01	12.41 ± 0.05	7.52 ± 0.02	0.86 ± 0.01
	12	9.75 ± 0.09	3.55 ± 0.05	ND	8.21 ± 0.01	5.72 ± 0.04	0.01 ± 0.0002
	15	6.95 ± 0.04	1.51 ± 0.01	ND	7.04 ± 0.01	3.30 ± 0.04	ND
	18	5.12 ± 0.02	0.82 ± 0.01	ND	5.18 ± 0.23	2.15 ± 0.02	ND
	21	3.01 ± 0.01	0.32 ± 0.01	ND	4.53 ± 0.01	1.48 ± 0.002	ND
	24	2.08 ± 0.01	0.14 ± 0.001	ND	2.99 ± 0.003	0.97 ± 0.001	ND
Cd	3	18.13 ±0.12	14.25 ±0.28	0.19 ± 0.01	18.08 ± 0.05	16.11 ± 0.01	2.19 ± 0.005
	6	14.18 ±0.03	11.24 ±0.05	0.08 ± 0.01	16.13 ± 0.02	14.18 ± 0.08	0.51 ± 0.01
	9	12.11 ±0.11	8.16 ± 0.16	ND	14.16 ± 0.07	10.13 ± 0.01	0.05 ± 0.001
	12	9.88 ± 0.21	4.98 ± 0.21	ND	11.06 ± 0.04	7.96 ± 0.04	ND
	15	5.19 ± 0.11	2.15 ± 0.04	ND	8.11 ± 0.02	5.04 ± 0.05	ND
	18	4.05 ± 0.06	1.01 ± 0.01	ND	6.01 ± 0.05	2.81 ± 0.01	ND
	21	3.59 ± 0.03	0.89 ± 0.04	ND	5.13 ± 0.06	1.02 ± 0.001	ND
	24	2.28 ± 0.03	0.48 ± 0.01	ND	3.78 ± 0.01	0.67 ± 0.03	ND
Cu	3	14.87 ± 0.13	11.59 ± 0.03	4.07 ± 0.02	18.03 ± 0.02	14.45± 0.11	8.05 ± 0.13
	6	11.92 ± 0.06	8.37 ± 0.17	2.67 ± 0.05	14.79 ± 0.04	11.64 ± 0.03	2.51 ± 0.01
	9	8.29 ± 0.02	5.48 ± 0.05	1.41 ± 0.04	11.87 ± 0.03	7.81 ± 0.03	2.51 ± 0.03
	12	7.01 ± 0.09	5.02 ± 0.08	0.36 ± 0.03	7.37 ± 0.13	4.66 ± 0.01	1.21 ± 0.01
	15	4.62 ± 0.05	3.98 ± 0.05	0.26 ± 0.01	5.20 ± 0.03	2.64 ± 0.01	0.90 ± 0.01
	18	3.18 ± 0.05	2.32 ± 0.04	ND	4.91 ± 0.07	1.94 ± 0.02	ND
	21	2.47 ± 0.01	1.14 ± 0.01	ND	3.89 ± 0.04	0.69 ± 0.01	ND
	24	1.64 ± 0.01	0.89 ± 0.001	ND	2.42 ± 0.01	ND	ND

(Values represent Mean ± SD of three replicates) ND - Not detected

5.3.1.1 Removal of lead from synthetic heavy metal solution

In the case of phytoremediation by *Eichhornia crassipes*, the maximum amount of lead reduction was observed in C with minimum time. Within 3 days, it attained 95.53% reduction, whereas control showed only 10.77 % reduction. The TiO_2 nanoparticles applied *Eichhornia crassipes* used phytoremediation system (i.e. C) attained faster removal of Pb compared to control (A) and TiO_2 nanoparticles entrapped calcium alginate beads applied *Eichhornia crassipes* used phytoremediation system (B). Lead was reduced to 50.72 % by TiO_2 nanoparticles entrapped calcium alginate beads applied *Eichhornia crassipes* used phytoremediation experiment (B) within 3 days. *Salvinia molesta* also exhibited a similar trend. All the systems attained a reduction of lead ranged from 85.61 to 100 % within 24 days. But fast reduction in lead concentration was observed in C. It showed 77.37 % of lead reduction on 3rd day and 100 % of reduction on 15th day. The results suggest that the plants exposed to TiO_2 nanoparticles showed efficient phytoremediation ability to remove lead from water.

5.3.1.2 Removal of cadmium from synthetic heavy metal solution

When titanium dioxide nanoparticles applied *Eichhornia crassipes* (C) was used in the phytoremediation of heavy metals, 99.06 % reduction of cadmium was observed within 3 days. Only, 10.78 % of cadmium was removed in the control experiment after 3 days. Cadmium was completely removed in C within 9 days, while in A and B, the efficiency of cadmium removal was found to be 88.78 and 97.64 % respectively after 24 days. Maximum cadmium removal with minimum time period was observed in

C; that is the phytoremediation system enhanced by titanium dioxide nanoparticles. Compared to A, better cadmium removal was exhibited by B. B is phytoremediation system, where TiO_2 nanoparticles entrapped calcium alginate beads were applied *Eichhornia crassipes* was used. Titanium dioxide exposed *Salvinia molesta* (C) attained 89.57 % cadmium removal within 3 days and 100% of cadmium removal within 12 days. The cadmium removal efficiency was found to be 81.99 and 96.81 % after 24 days in A and B respectively. The phytoremediation of cadmium by TiO_2 nanoparticles applied *Eichhornia crassipes* and *Salvinia molesta* showed better performance than control plants. In *Eichhornia crassipes*, 100 % of cadmium was removed in C within 9 days, while in *Salvinia molesta* the same reduction was observed only after 12 days. Results from this experiment indicate that, one of the main limitations of phytoremediation of heavy metals, i.e. the long retention period required for remediation by plants can be overcome by, phytoremediation with TiO_2 nanoparticles.

5.3.1.3 Removal of copper from synthetic heavy metal solution

Maximum removal of copper was observed in C within 18 days of exposure to contaminant water by phytoremediation using *Eichhornia crassipes.* In control (A), compared to other metals, more amount of copper was removed by *Eichhornia crassipes* within 3 days. This may be due to the fact that; copper is one of the micronutrients. In the phytoremediation system using *Salvinia molesta*, 95.62 % reduction was observed in C within 15 days. On 3rd day, the percentage removal of copper was 60.85 % in C and in control (A) it was 12.31 %. The residual concentration of copper observed in control (A) during the final stage was

2.42 ± 0.01 mg/L. The effectiveness of two aquatic macrophytes *Eichhornia crassipes* and *Salvinia molesta* grown under three different conditions were tested for their phytoremediation capacity of three metals (Pb, Cd and Cu) and the results indicated that *Eichhornia crassipes* exposed to nanoparticles reported the maximum and fast removal of these heavy metals.

5.3.2 Heavy metal accumulation in plants

The heavy metal analysis of plant segments of both the aquatic native plants, *Eichhornia crassipes* and *Salvinia molesta* were carried out. Distribution of Cd, Pb and Cu in the organs of *Eichhornia crassipes* and *Salvinia molesta* are presented in Figure 5.3 and 5.4. In A (control), maximum accumulation of metals was observed in root and accumulation of Cd, Pb and Cu in roots of *Eichhornia crassipes* was 6285.04, 5786.30 and 6628.83 mg/Kg respectively. Many studies revealed that *Eichhornia crassipes* accumulated higher concentrations of heavy metals in the roots than that in the aerial parts. But in C, maximum accumulation of Cd was observed in leaf. More amount of metal accumulation was observed in leaf and stem of C compared to A and B. C was the phytoremediation systems in which *Eichhornia crassipes* was directly exposed to titanium dioxide nanoparticles. But the present study showed that in C, Cu accumulation is in the order of leaves > roots > stem, Cd accumulation is in the order of leaves > stem > roots and Pb accumulation is in the order of leaves > stem > roots. The results show that, phytoremediation systems enhanced by titanium dioxide nanoparticles showed more tendency to translocate metals to its areal parts.

Salvinia also exhibited the capacity to accumulate high levels of heavy metals. Compared to all phytoremediation systems, a maximum concentration of 8928.74 mg/Kg of Cd was accumulated in leaves of *Salvinia molesta* grown under condition C. Sune et al., 2007 reported that heavy metal uptake in *Salvinia* occurs through a physical process (fast), which involves adsorption, ionic exchange, chelation, while biological processes such as intracellular uptake (transported through plasmalemma into cells) is slow and help in subsequent translocation of metals (Cd) from roots to leaves. The highest amount of lead and copper accumulated in C was 9192.63 and 9888.82 mg/Kg respectively. In control plant (A), all the three metals were accumulated at highest level in roots. Roots remain in direct contact with the medium and hence this might result in increased metal concentration in the roots. More amount of metal accumulation was observed in leaf of B compared to A. The results indicate that titanium dioxide nanoparticles applied plants were efficient to translocate the metals from root to its aerial parts.

Figure 5.3: Accumulation of cadmium, lead and copper in *Eichhornia crassipes*
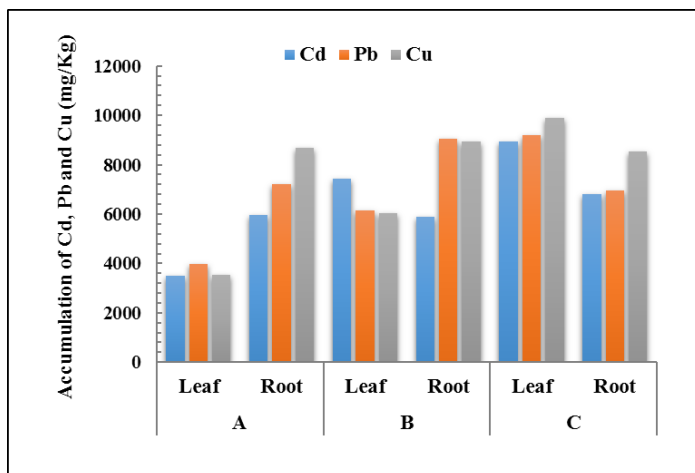
Figure 5.4: Accumulation of cadmium, lead and copper in *Salvinia molesta*

5.3.3 Bioconcentration factor and translocation factor

The mobility of the heavy metals from the polluted medium to the roots of the plants and the ability to translocate the metals from roots to the harvestable aerial part were evaluated respectively by means of the bioconcentration factor (BCF) and the translocation factor (TF). Bioconcentration factor is a useful parameter to evaluate the potential of the plants in accumulating metals. The BCF values for Cd, Pb and Cu in *Eichhornia crassipes* and *Salvinia molesta* at 24 days' exposure to heavy metals are shown in Figure 5.5 and 5.6, respectively. Higher BCF values indicates the higher phytoaccumulation capacity. Maximum bioconcentration factors of Cd, Pb and Cu in *Eichhornia crassipes* was observed in C. In C, the highest BCF values found for Cd, Pb and Cu were

852.49, 848.20 and 1047.99 respectively. If the BCF value is more than or equal to 1000, then that plant species is considered as a hyper accumulator. The plant having the abilities to grow in very high concentration of metal and concentrating high heavy metals in their tissues are known as hyperaccumulators (Wahab et al., 2014). The higher BCF value of *Eichhornia crassipes* for Cu (BCF > 1000) in C indicates that TiO$_2$ nanoparticles applied *Eichhornia crassipes* is considered as a good hyper accumulator. The BCFs of control (A) for Cd, Pb and Cu were 615.67, 516.14 and 698.53 respectively. BCF of B for all the metals were higher than control but less than 1000. Phytoremediation experiments using *Salvinia molesta,* a highest BCF values was observed for Cd, Pb and Cu were 750.12, 777.90 and 896.29 respectively in (C). In experiment B of *Salvinia molesta*, BCFs of all the three metals were found higher than that of A. The results indicated that, plants exposed to TiO$_2$ nanoparticles were accumulated more amount of heavy metals in its upper portions compared to control plants.

The translocation factor for Cd, Pb and Cu in phytoremediation systems using *Eichhornia crassipes* and *Salvinia molesta* are shown in Table 5.2 and 5.3 respectively. The value TF > 1 indicated that there is a transport of metal from root to leaf probably through an efficient metal transporter system and the metals sequestration in the leaf vacuoles and apoplast. TF value more than 1 of plant species indicates their hyperaccumulation potential and is identified as hyperaccumulator plants (Marbaniang & Chaturvedi, 2014). For *Eichhornia crassipes,* maximum TF for cadmium was observed in C (TF(s/r) = 1.22 and TF(l/r) = 1.74) compared to A and B, which indicates the translocation of high Cd content

from roots to its aerial part. Similar trend was observed for Pb also and for Cu, maximum TF observed was TF(l/r) =1.08 in C. These results imply that *Eichhornia crassipes* exposed to nanoparticles accrued an ability to transfer higher metal concentrations from root to its areal part. The lowest translocation factor was observed in the A (control) for Cd and Pb. Similar results were found in phytoremediation systems using *Salvinia molesta* and the translocation factor observed in the C was TF(l/r) = 1.31, TF(l/r) = 1.32 and TF(l/r) = 1.16 for Cd, Pb and Cu respectively. TiO_2 nanoparticles applied plants (C) exhibited better potential to translocate Cd, Pb and Cu to its aerial parts.

Figure 5.5: Bioconcentration factors (BCF) of Pb, Cd and Cu in *Eichhornia crassipes*
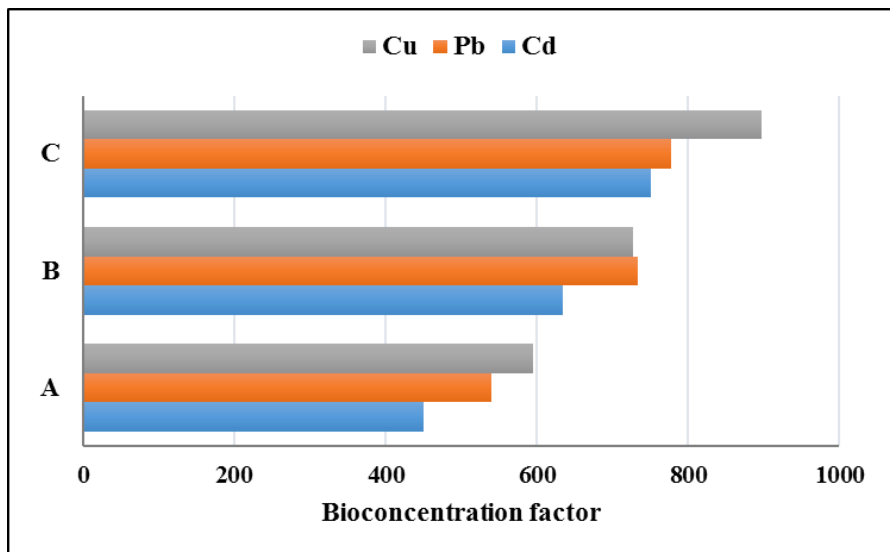
Figure 5.6: Bioconcentration factors (BCF) of Pb, Cd and Cu in *Salvinia molesta*

Table 5.2: Translocation factor of *Eichhornia crassipes*

Metals	TF	A	B	C
Cd	TF(s/r)	0.55	0.91	1.22
	TF(l/r)	0.44	1.57	1.74
Pb	TF(s/r)	0.65	0.76	1.26
	TF(l/r)	0.27	0.83	1.29
Cu	TF(s/r)	0.81	0.50	0.74
	TF(l/r)	0.43	0.56	1.08

Table 5.3: Translocation factor of *Salvinia molesta*

Metals	TF	A	B	C
Cd	TF(l/r)	0.59	1.26	1.31
Pb	TF(l/r)	0.55	0.68	1.32
Cu	TF(l/r)	0.41	0.67	1.16

Translocation is the movement of metal containing sap from the root to the shoot which was primarily controlled by two processes, root pressure and leaf transpiration. Some metals are accumulated in roots, probably due to some physiological barriers against metal transport to the aerial parts, while the others are easily transported in plants. Translocation of trace elements from roots to shoots could be a limiting factor for the bioconcentration of elements in shoots. It can be proposed that there has mechanism in roots that could detoxify heavy metals or transfer them to aerial parts (Gomati et al., 2014).

5.3.4 Physiological response of plants to the applied conditions

5.3.4.1 Variation in the production of chlorophyll

In the life activity of green plants, chlorophyll plays the role of absorbing, transferring and transforming energy. The chlorophyll content of plant after experiment was determined using UV-Visible spectrophotometer. Variation in the production of chlorophyll of both the plants is depicted in Figure 5.7. The result shows that, plants from B and C exhibited an increase in the production of chlorophyll compared to A

(control) for both *Eichhornia crassipes* and *Salvinia molesta*. Maximum chlorophyll production was observed in C for both the plants.

This may be due to the effects of nano-TiO_2 on the content of light harvesting complex II (LHC II) on thylakoid membranes of plants and nano-TiO_2 has ability to increase LHC II content (Hong et al., 2005; Lei et al., 2007). These have the ability to promote energy transfer and oxygen evolution in photosystem II (PS II) of plants (Mingyu, 2007). It has also been reported that nano-anatase TiO_2 promoted antioxidant stress by decreasing the accumulation of superoxide radicals, hydrogen peroxide, malonyldialdehyde content and enhance the activities of superoxide dismutase, catalase, ascorbate peroxidase, guaiacol peroxidase and thereby increase the evolution of oxygen rate in plants chloroplasts (Lei et al., 2008). It helps to increase solar energy trapping that might improve the photo synthetic efficiency of plants.
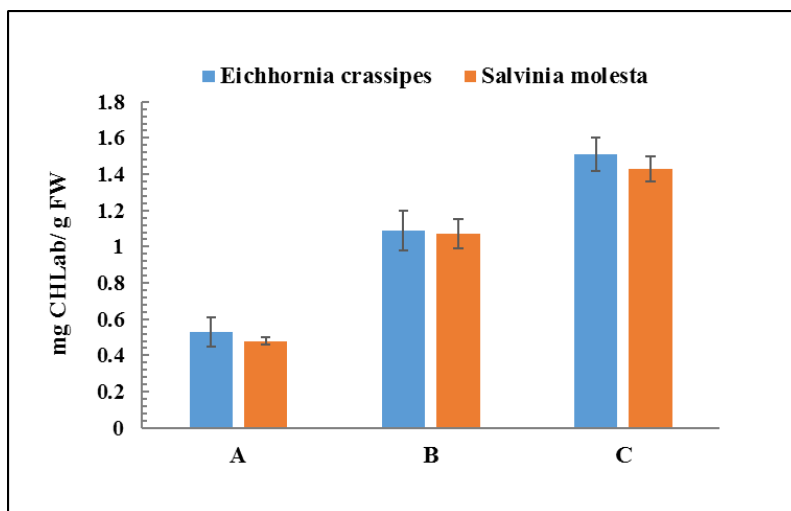
Figure 5.7: Chlorophyll content of plants after treatment

5.3.4.2 *Variations in the relative growth of plants under different conditions*

Variations in the relative growth of *Eichhornia crassipes* and *Salvinia molesta* grown under three different conditions are graphically represented in Figure 5.8. The relative growth of control plants showed a significant decrease for both the plants. The plants exposed to TiO_2 nanoparticles (C) exhibited significant increase in relative growth. The plants in C showed high relative growth compared to plants from A and B. In the case of *Salvinia molesta* an increasing trend was observed in all the conditions but maximum increase in weight after treatment was observed in plant from C. Plant in C was the plant exposed to nano - TiO_2. TiO_2 nanoparticles has the ability to improve light absorbance and promote the activity of rubisco activase thus accelerate the growth of plants (Hong et al., 2005; Zheng et al., 2005).
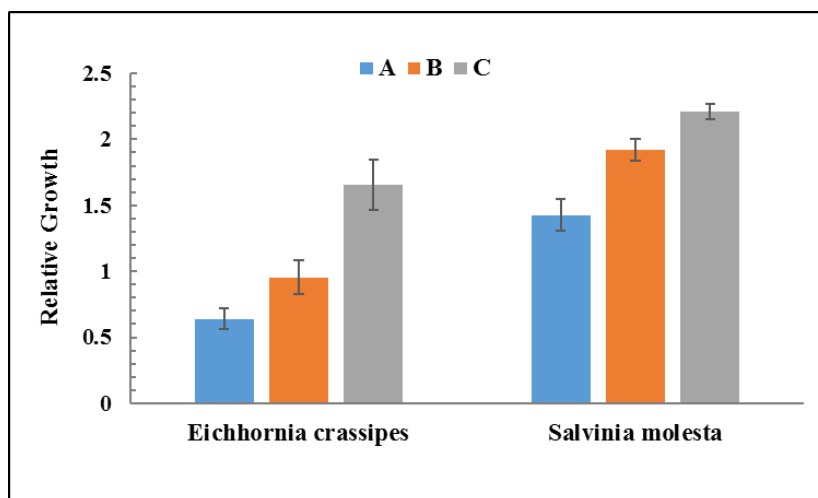
Figure 5.8: Variations in the relative growth of *Eichhornia crassipes* and *Salvinia molesta*

5.4 Summary

A study was carried out to assess the enhancement of phytoremediation capacity of heavy metals (Cd, Pb and Cu) by *Eichhornia crassipes* and *Salvinia molesta* in the presence of titanium dioxide nanoparticles. *Eichhornia crassipes* and *Salvinia molesta,* plants which had been exposed to TiO_2 nanoparticles, showed 99.06 % of phytoremediation efficiency for cadmium removal within 3 days. Maximum phytoremediation efficiency for lead and copper was also observed in plants which are exposed to TiO_2 nanoparticles. It was observed that, in the nano - TiO_2 applied phytoremediation system, more efficient and faster removal of heavy metals was taking place. Results of the study on heavy metal accumulation indicates that titanium dioxide nanoparticles applied plants showed more tendency to translocate metals to its areal parts. Control plant accumulated, more metals in their root portion in both the plants. Nano - TiO_2 applied plants exhibited an increase in the production of chlorophyll compared to A (control) and B.

TiO₂ nanoparticles exposed plants exhibited significant increase in relative growth compared to others. This may be due to the fact that, the plant exposed to nano –TiO_2 has the ability to improve light absorbance and promote the activity of rubisco activase thus accelerating the growth of plants. The determination of bioconcentration factor indicated that, the uptake potential of metals by plants was increased under nano - TiO_2 applied conditions. Plants exposed to TiO_2 nanoparticles achieved ability to transfer higher metal concentrations from root to its areal part. TiO_2 nanoparticles applied plants (C) showed better performance than TiO₂

nanoparticles entrapped calcium alginate beads applied plants (B). Considering the overall results, we can state that TiO_2 nanoparticles applied *Eichhornia crassipes* and *Salvinia molesta* seems to be promising candidate for the phytoremediation of heavy metals from water and exhibited an enhanced phytoremediation ability.

Chapter 6

IMMOBILIZATION AND MOBILIZATION EFFECT OF AMMONIUM MOLYBDATE ON PHYTOREMEDIATION OF TOXIC HEAVY METALS IN SOIL

6.1 Introduction

Industrial revolution, modern agriculture and other anthropogenic activities have intensively augmented the pollution of the biosphere with toxic metals. The burning of fossil fuels, mining and smelting of metalliferous ores, metallurgical industries, municipal wastes, fertilizers, pesticides, sewage sludge etc. are the prime sources of heavy metal contamination (Marques et al., 2009). Leaching of heavy metals and other pollutants from soils generates a significant environmental hazard as it influences the quality of downstream water bodies (Manzoni et al., 2011). The heavy metal insalubrity poses numerous serious health dangers to higher organisms due to their long term tenacity in the environment. They adversely affect plant growth, ground cover and soil microflora. It is well recognized that heavy metals cannot be chemically degraded and want to be physically removed or be transformed into non-hazardous compounds

(Tangahu et al., 2011). Some of the metals would be persistent in soil due to the immobile nature while the other metals would be more mobile, consequently the potential of transfer either through soil profile down to ground water aquifer or via plant - root uptake (bio available) is expected. When heavy metals are mobilized into the soil solution and taken up by plants or transported to the surface/ground water, a critical pollution problem arises. The characteristics of the soil are therefore very important in the attenuation of heavy metals in the environment (Sherene, 2010). To elude such threat of water pollution, severe attention on soil remediation techniques is necessitated.

Soil contamination by heavy metals is a significant problem, which changes the characteristics of water resources and makes it as the source of undesirable substances and dangerous for human health causing various cancers, cardiovascular or neurological diseases etc. Heavy metals in soil leads to changes of soil characteristics and limits productive and environmental functions. Polluted soils are no longer suitable for agricultural production, because they are incapable to produce healthy food. When heavy metals in soils leaches into river water, it diffuses onto farmlands with irrigation, resulting in relatively low levels of heavy metals being spread into wider areas rather than being localized in high concentrations.

In soil, heavy metals originate from anthropogenic sources tend to be more mobile, hence bioavailable than pedogenic, or lithogenic ones (Kaasalainen & Yli-Halla, 2003; Bolan et al., 2010; Wuana & Okieimen, 2011). The chemical form and speciation of a metal are the factors which influence the fate and transport of a heavy metal in soil. But in soil, heavy

metals are adsorbed by initial fast reactions (minutes, hours), followed by slow adsorption reactions (days, years) and are, therefore, redistributed into different chemical forms with varying bioavailability, mobility, and toxicity (Shiowatana et al., 2001). This distribution is supposed to be controlled by different reactions of heavy metals in soils such as (i) mineral precipitation and dissolution, (ii) ion exchange, adsorption, and desorption, (iii) aqueous complexation, (iv) biological immobilization and mobilization, and (v) plant uptake (Levy et al., 1992).
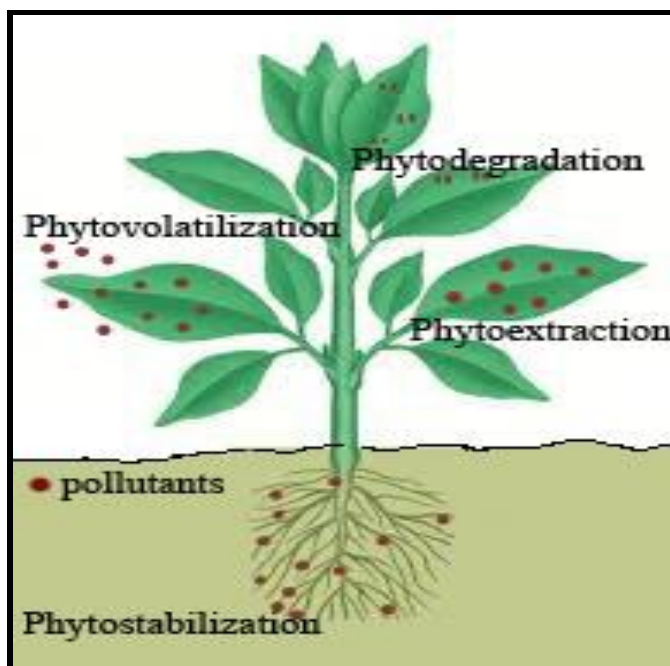
Figure 6.1: Phytoremediation processes

Prevention of heavy metal pollution is critical because remediation of contaminated soils is extremely expensive and challenging. Traditional treatments for metal contamination in soils are cost prohibitive, when large areas of soil are contaminated. Elimination of metals from soil can

be done in situ (on-site), or ex situ (removed and treated off-site) but both are extremely expensive. Methods such as excavation and disposal of heavy metal polluted soils in landfills are not environment friendly and may serve as secondary pollution sources (Garba et al., 2012). Therefore, new environment friendly and less expensive techniques are urgently required. Phytoremediation offers an economical, noninvasive, and safe alternative to conventional cleanup techniques and can be accomplished by phytoextraction, phytodegradation, phytostabilization, phytovolatilization and rhizofiltration (Figure 6.1).

Plants possess highly specific and very effective mechanisms to attain essential micronutrients from the environment, even though it presents at low levels. The plant produced chelating agents, plant induced pH changes and redox reactions helps plant root to solubilize and accumulate micronutrients from soil in very low levels, even from nearly insoluble precipitates. Plants have also exhibited highly specific mechanisms to translocate and accumulate micronutrients. Similar mechanisms are also involved in the uptake, translocation, and accumulation of toxic elements like metals, whose chemical properties simulate those of essential elements (U. S. Department of Energy, 1994; Tangahu et al., 2011).

6.1.1 Chelate-Assisted (Induced) Phytoremediation

Plants extract metals from soil by accumulating the metals (phytoextraction) or, on the other hand, are used in combination with some soil amendments to improve soil conditions (phytostabilization). Chelate-enhanced phytoremediation of metals from contaminated soils is a cost-

effective alternative to conventional techniques of enhanced soil remediation. Metal-chelant complexes are formed during the application of chelating agent to the soil and the plants takes up these complexes mostly through a passive apoplastic pathway. Unless the metal ion is transported as a noncationic chelate, apoplastic transport is further limited by the high cation exchange capacity of cell walls. Chelators have been sequestered from plants that are strongly involved in the uptake and detoxification of heavy metals.

EDTA is one of the common and most tested chelating agents. As EDTA has been accompanying with high toxicity and persistence in the environment and also it is expensive (Wuana & Okieimen, 2011). The most frequently applied chelating agent used for amendments also have deficiencies: nitrilotriacetic acid (NTA) is a toxicant as a class II carcinogen (Peters, 1999); nitric acid (HNO_3) is lethal to soil micro-flora and destruct the physico-chemical properties of soil; hydrochloric acid (HCl) can alter soil properties (Neilson et al., 2003); citric acid is a nontoxic acid that forms relatively strong complexes and easily biodegradable, but it presents of lower effectiveness in the removal of metal ions (Palma & Mecozzi, 2007). EDGA enhanced metal solubility but plant uptake did not increase accordingly (Römkens et al., 2002).

The addition of chelators effectively increased the mobility of target heavy metals in soils, and significantly enhanced the accumulation of these heavy metals in aerial parts of the plants but the application of chelators had inhibitory effects on the growth of the plants (Sun et al., 2009). So, a promising and environmentally friendlier mobilizing agent is required to enhance the phytoremediation ability of plants. In some cases,

an immobilizing agent is also necessary to reduce the risk of bioaccumulation, biomagnification in the food chain and the risk of superficial and groundwater contamination due to toxic metals. The ammonium molybdate (containing nitrogen and molybdenum) is fertilizer to plants, which can produce more biomass (Qu et al., 2011). In this study, we assessed phytoextraction and phytostabilization potential of the *Amaranthus retroflexus* with ammonium molybdate, to evaluate the ability of the *Amaranthus retroflexus* to remediate soils contaminated with multiple heavy metals. Heavy metals selected for study include two essential (copper and zinc) and three toxic (cadmium, lead and nickel) elements.

6.2 Materials and Methods

The effects of application of ammonium molybdate on the growth of *Amaranthus retroflexus* and its heavy metal (Cd, Pb, Cu, Ni and Zn) uptake and accumulation were investigated using the pot-culture experiments.

6.2.1 Cultivars sources and Plant culture

The selection of plant species is critical phase for the success of phytoremediation. Seeds of *Amaranthus retroflexus* were obtained from a nursery situated in Vellimadukunnu, Kozhikode, Kerala. *Amaranthus* (amaranth) plant is native to Asia, Africa and America and is known as a cosmopolitan plant (Khoramnejadian & Saeb, 2015). Amaranth cultivates all year in the tropical region. This plant could grow everywhere, so we considered this plant for our study. The heavy metal

accumulation capacity of plants belonging to the Amaranthaceae family was reported in many studies. *Amaranthus retroflexus* is a good metal accumulator and has been used for the uptake of cadmium, mercury, zinc and copper (Mellem et al., 2012). *Amaranthus retroflexus* seeds were germinated in pots containing soil to a depth of 1cm under normal condition. Soil moisture was maintained carefully by spraying distilled water to ensure the best growth condition. After seedlings grew for 10 days in the potting soil, 18 seedlings with similar biomass were transplanted to pots containing heavy metal contaminated soil at a rate of one seedling per pot.

6.2.2 Experimental design

The experiment consists of 5 treatments and control (phytoremediation of heavy metal contaminated soil by *Amaranthus retroflexus* without adding ammonium molybdate solutions) with replicates for each. Experiments were exposed to natural day and night temperatures. The plants were watered daily with equal amount of distilled water per pot. Plastic pots (45 x 30 x 15 cm) were used for the experiment. Each plastic pot was filled with 5 Kg of soil. In the case of 5 treatments, 50 mL of ammonium molybdate solutions (having Mo contents 0.05, 0.10, 0.30, 0.50, 1.00 g/L respectively) were added to pots containing *Amaranthus retroflexus* (Table 6.1). Ammonium molybdate solution was not applied in control. The pot-culturing experiment is shown in Plate 6.1. After 45 days, the plants were harvested and heavy metal concentrations in plants and soil were determined. Based on the results,

phytoremediation potential of *Amaranthus retroflexus* in the presence of ammonium molybdate for the treatment of heavy metal was evaluated.

Plate 6.1: Pot-culturing experiments

Table 6.1: Concentration of ammonium molybdate applied

Treatment	Concentration of Mo in ammonium molybdate solution, g/L
No.1	0.05
No.2	0.1
No.3	0.3
No.4	0.5
No.5	1

6.2.3 Physicochemical characteristics of soil samples

Soil used for the experiment was contaminated by spiking the heavy metals (Cd, Pb, Cu, Ni and Zn). The contaminated soil received the metals Cd as $CdSO_4$; Pb as $Pb(NO_3)_2$; Cu as $CuSO_4$; Ni as $NiSO_4$ and Zn as $ZnSO_4$. Physicochemical factors of soil such as pH, Electrical conductivity (EC), calcium, magnesium, organic carbon, inorganic phosphorous, sodium, potassium was analyzed and procedures followed were mentioned in chapter 3.

6.2.4 Analysis of heavy metals in soil

Perchloric acid-nitric acid mixture was used to extract heavy metals from soil. Hot, concentrated perchloric acid were extremely effective in decomposing organic matter and sulphides present in soil because of its powerful oxidizing and dehydrating nature. Except gold and platinum, nitric acid dissolves the majority of the metals present in nature. 0.2 g of soil was digested with 20 mL of concentrated HNO_3, 5 mL distilled water and 10 mL of $HClO_4$ and heated on a hot plate for 2 h. The mixture was heated until the white fumes come and the soil become white. Then the solution was filtered and made up to 50 mL. The filtrate was analyzed for heavy metals using Atomic Absorption Spectrophotometer (AAS) (Thermo Series). Replicates were carried out as part of the measurement. Before spiking heavy metals in soil, the concentration of Cd, Pb, Cu, Ni and Zn were determined and necessary blank corrections are done using these values after spiking heavy metals in soil. The initial heavy metals concentrations (after spiking of heavy metals) are shown in Table 6.2.

Table 6.2: Heavy metals concentration in soil before treatment

Heavy metal	Concentration (mg/Kg)
Ni	155.87 ± 1.46
Cd	6.98 ± 1.5
Cu	86.11 ± 2.77
Pb	74.79 ± 2.32
Zn	109.27 ± 1.25

6.2.5 Analysis of heavy metals in plant

The plants were harvested after 45 days. During the harvest, plants were gently removed from soil and washed until free of soil and dust. The lengths of the roots and shoots were measured and roots, leaves, and stems were sectioned carefully. The plant parts were dried in an oven at 70˚C for 72 h, and the dry weight were recorded by electronic balance. Once the plant tissues were dry, they were milled with mortar and pestle and digested. 0.2 g of plant parts were digested at 150˚C for 200 min with 10 mL mixtures of HNO_3/ $HClO_4$ (4:1) (Qu et al., 2008). After complete digestion, the volume of digested samples was adjusted to 50 mL with distilled water. Subsequently, the amount of heavy metals was determined by Atomic Absorption Spectrophotometer (AAS) (Thermo Series). In this experiment, three replicates were carried out.

6.2.6 Data Analysis

All the experiments were performed in triplicate, and bioconcentration factor (Ghosh & Singh, 2005) and translocation factor (Marchiol et al., 2004) were computed. The data collected were analyzed statistically by calculating the mean and standard deviation.

6.2.7 Bioconcentration factor and translocation factor

The bioconcentration factor (BCF) was utilized to estimate the amount of heavy metals absorbed by the plant from the soil. This is an index of the ability of the plant to accumulate a particular metal with respect to its concentration in the soil and was calculated using the formula (Ghosh & Singh, 2005),

$$\text{Bioconcentration factor} = \frac{\text{Metal concentration in the plant tissue}}{\text{Metal concentration in the soil}} \quad (1)$$

The unit of heavy metal concentration of in plant tissue and soil were mg/Kg so the BCF computed was dimensionless. The plants having higher BCF value is more suitable for phytoextraction of heavy metals from soil. BCF Values > 2 were regarded as high values (Mellem et al., 2009).

The translocation factor (TF) was calculated to evaluate the potential of phytoextraction ability of *A. retroflexus*. This ratio is an indication of the ability of the plant to translocate metals from the roots to the aerial parts of the plant (Marchiol et al., 2004).

$$\text{Translocation factor (TF)} = \frac{\text{Metal concentration in aerial parts}}{\text{Metal concentration in roots}} \quad (2)$$

Here also, the dimension of heavy metal concentration of in aerial parts of the plant and root were mg/Kg so the TF calculated was dimensionless. Metals that are accumulated by plants and largely stored in the roots of plants are indicated by TF values < 1, with values greater indicating translocation to the aerial part of the plant (Mellem et al., 2009). Both bioconcentration factor and translocation factor can be utilized to evaluate plant's potential for phytoremediation purpose.

6.3 Results and Discussion

The physico-chemical characteristics of soil used for this experiment is shown in Table 6.3. The results indicate that no major pollutants were observed in the soil collected from Kozhikode district,

Kerala for the study. The initial heavy metals concentrations (after spiking of heavy metals) are depicted in Figure 6.2.

Table 6.3: Physico-chemical characteristics of soil

Parameters	Soil value
pH	6.71± 0.31
EC µS/cm	24.6 ± 3.14
Alkalinity (mg/kg)	644.0 ± 15.6
Chloride (mg/kg)	320.8 ± 11.52
Sulphate (mg/kg)	304.8 ± 17.11
Inorganic phosphorous (mg/kg)	8.0 ± 0.63
Sodium (mg/kg)	250.0 ± 10.35
Potassium (mg/kg)	75.0 ± 8.11
Organic carbon (%)	0.279 ± 0.03
Exchangeable calcium`(mg/kg)	1280 ± 16.52
Exchangeable magnesium (mg/kg)	583.2 ± 11.81
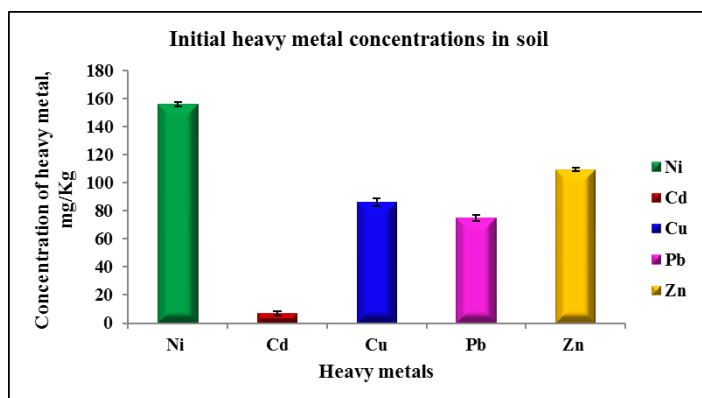
Figure 6.2: Initial heavy metal concentrations in soil

6.3.1 Removal of heavy metals in soil

After 45 days of experiment, the heavy metals concentration remaining in the treated soil was also noted and summarized in Table 6.4. As compared with controls (Figure 6.3), lower concentrations of Ni, Cd and Cu and higher concentrations of Pb and Zn was observed in each of the five treatments after 45 days. These results indicate that *Amaranthus retroflexus* uptakes more amount of Ni, Cd and Cu than Pb and Zn in the presence of ammonium molybdate. The plants in treatment were effectively removed the metals like Ni, Cd and Cu from soil compared to control plants. It may be due to the fact that, Ni, Cd and Cu were chelated and form more soluble fractions with ammonium molybdate and Pb and Zn were precipitated with ammonium molybdate. The mechanism of the reaction of ammonium molybdate with toxic metals can be reported as follows (Qu et al., 2011):

$$Zn/Pb + Mo_2O_7^{2-} \rightarrow (Zn/Pb)\ Mo_2O_7 \qquad \text{(precipitation)}$$
$$Cd/Ni/Cu + NH_4^+ \rightarrow Cd/Ni/Cu\ (NH_3)_4^{2+} \qquad \text{(soluble fractions)}$$
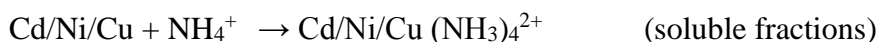
The heavy metal concentration in the root of *Amaranthus retroflexus* are indicated in Table 6.5 and shown in Figure 6.4. Compared to control, the concentrations of Ni, Cd and Cu in root were higher than control, but the concentrations of Pb and Zn were lower than control. A similar trend was also observed in the shoot of *Amaranthus retroflexus* (Table 6.6 and Figure 6.5). Ammonium molybdate has the potential ability to precipitate with Pb and Zn so it stabilizes these metals in soil and decreases the bioavailability of these metals to plant. It also has the ability to chelate and form more soluble fractions with Cd, Cu and Ni, thus it

increases the bio-availability of these metals to plant. Maximum reduction of heavy metal in soil was observed in treatment No.5 (with maximum concentration of ammonium molybdate). After treatment 86.16 % of Ni, 99.64 % of Cd and 92.47 % of Cu was reduced in soil. The result indicated that, *Amaranthus retroflexus* can remove heavy metals (Cd, Cu and Ni) efficiently with ammonium molybdate. The ammonium molybdate has the potential to enhance metal mobility in soil profiles by forming complexes with toxic metals (Qu et al., 2011). It acts as stabilization agent for Pb and Zn and as extracting agent for Cd, Cu and Ni.

Table 6.4: Heavy metal concentration in soil after treatment

Treatment	Ni (mg/Kg)	Cd (mg/Kg)	Cu (mg/Kg)	Pb (mg/Kg)	Zn (mg/Kg)
Control	122.95 ± 2.47	3.73 ± 0.36	45.7 ± 2.18	33.11 ± 1.54	41.81 ± 1.80
No.1	97.37 ± 1.25	2.87 ± 0.73	38.53 ± 2.33	41.09 ± 1.58	46.15 ± 2.12
No.2	83.93 ± 2.89	0.87 ± 0.25	35.52 ± 1.24	47.93 ± 1.82	53.28 ± 1.70
No.3	66.83 ± 4.06	0.075 ± 0.07	33.53 ± 1.32	53.51 ± 2.94	58.45 ± 4.31
No.4	55.79 ± 3.62	0.05 ± 0.02	26.32 ± 1.22	56.02 ± 1.00	65.82 ± 2.23
No.5	21.56 ± 1.74	0.025 ± 0.02	6.48 ± 1.39	63.59 ± 1.75	67.61 ± 1.64

Figure 6.3: Heavy metal concentration in soil after treatment

Table 6.5: Heavy metal concentration in the root of *Amaranthus retroflexus*

Root	Ni (mg/Kg)	Cd (mg/Kg)	Cu (mg/Kg)	Pb (mg/Kg)	Zn (mg/Kg)
Control	16.92 ± 1.6	0.91 ± 0.03	16.6 ± 1.23	26.41 ± 0.68	32.49 ± 1.28
No.1	36.44 ± 3.46	1.53 ± 0.3	21.87 ± 1.7	17.74 ± 0.72	26.74 ± 0.84
No.2	47.14 ± 1.36	2.15 ± 0.26	23.83 ± 0.36	12.56 ± 1.00	22.7 ± 1.38
No.3	57.39 ± 3.27	2.80 ± 0.17	26.81±1.14	9.63 ± 0.61	18.39 ± 2.48
No.4	68.81 ± 1.81	3.07 ± 0.14	31.37 ± 0.78	7.73 ± 0.94	11.75 ± 1.24
No.5	92.66 ± 3.39	3.45 ± 0.11	41.18 ± 1.69	4.51 ± 1.38	7.72 ± 1.03
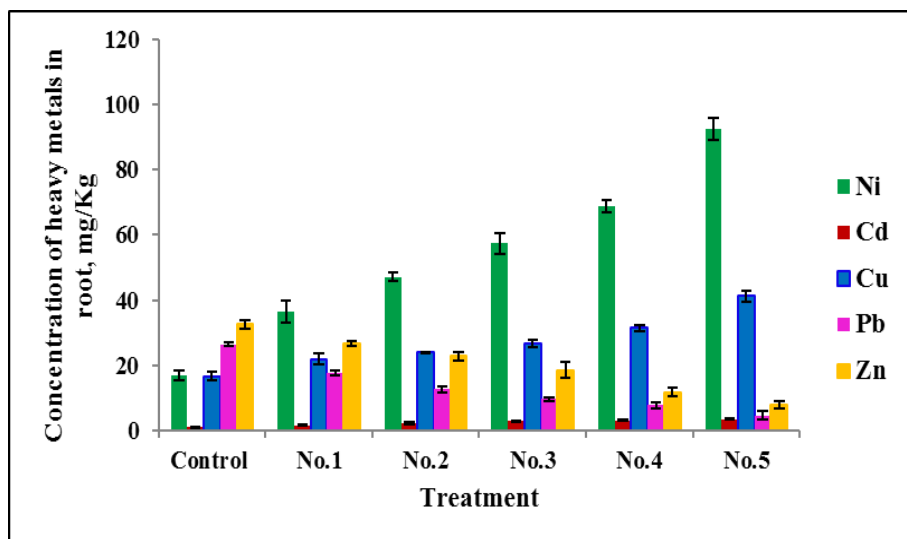
Figure 6.4: Heavy metal concentration in the root of *Amaranthus retroflexus*

Table 6.6: Heavy metal concentration in the shoot of *Amaranthus retroflexus*

Shoot	Ni (mg/Kg)	Cd (mg/Kg)	Cu (mg/Kg)	Pb (mg/Kg)	Zn (mg/Kg)
Control	7.41± 1.28	0.78 ± 0.06	7.86 ± 0.91	11.46 ± 0.80	21.23 ± 0.49
No.1	18.11 ± 2.58	0.89 ± 0.07	8.02 ± 0.09	9.59 ± 0.53	19.73 ± 0.96
No.2	23.58 ± 5.49	1.43 ± 0.08	9.66 ± 0.60	8.73 ± 0.35	15.8 ± 0.65
No.3	24.34 ± 4.39	2.24 ± 0.25	10.58 ± 0.68	6.15 ± 0.28	13.8 ± 0.42
No.4	23.20 ± 3.89	2.28 ± 0.31	11.82 ± 0.34	4.91 ± 0.28	8.6 ± 0.83
No.5	26.91 ± 3.98	2.44 ± 0.12	17.49 ± 2.00	2.06 ± 0.57	5.99 ± 0.87

Figure 6.5: Heavy metal concentration in the shoot of *Amaranthus retroflexus*

6.3.2 Bioaccumulation of heavy metals in *Amaranthus retroflexus*

Accumulation of nickel in the plant parts increased with increasing ammonium molybdate concentration (Figure 6.6). Amount of Ni accumulated ranged from 16.92 mg/Kg to 92.66 mg/Kg with highest concentration being stored in the roots. Much higher Ni levels were found in the roots rather than in the shoots or leaves.
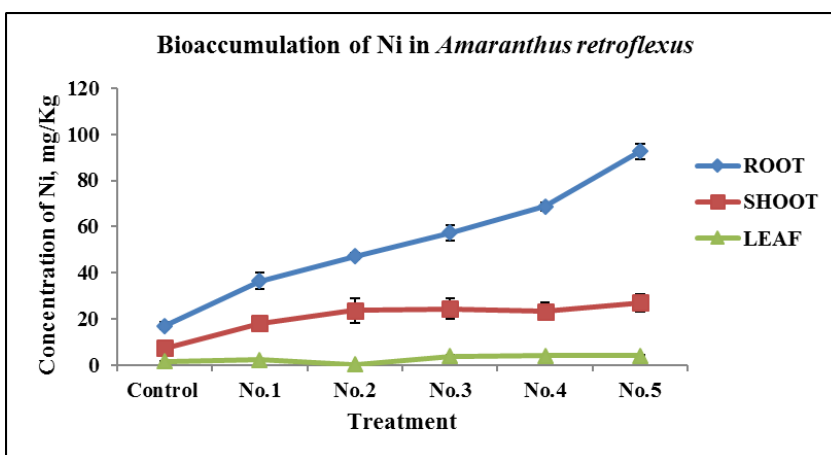
Figure 6.6: Bioaccumulation of Ni in *Amaranthus retroflexus*

Bioaccumulation of cadmium in the roots (0.91 to 3.45 mg/kg) was higher than the shoot (0.78 to 2.44 mg/kg) and leaf (0 to 0.98 mg/kg). The cadmium content in the leaf of control plants was below detectable levels (Figure 6.7). A steady increase was noticed in the accumulation of the cadmium in the plant parts with increasing ammonium molybdate.
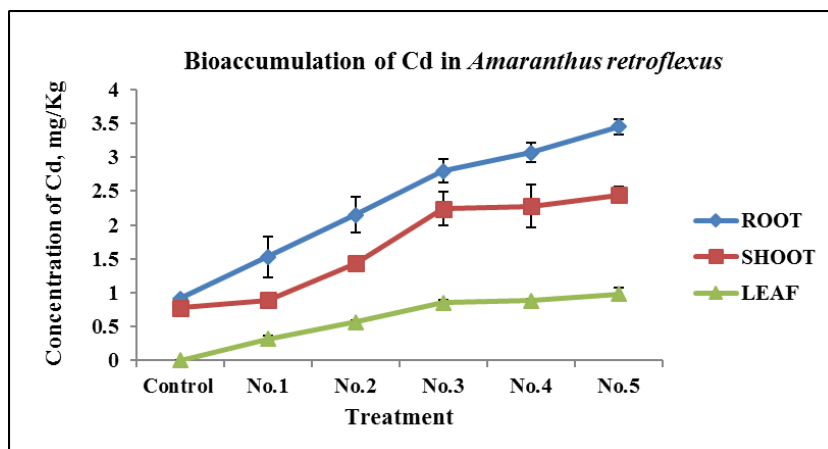
Figure 6.7: Bioaccumulation of Cd in *Amaranthus retroflexus*

The bioaccumulation of copper by *A. retroflexus* (Figure 6.8) exhibited variation among plant parts and bioaccumulation of copper in plant increases with the application of ammonium molybdate. Among the plant parts, the roots accumulated more copper than the shoot and leaf.
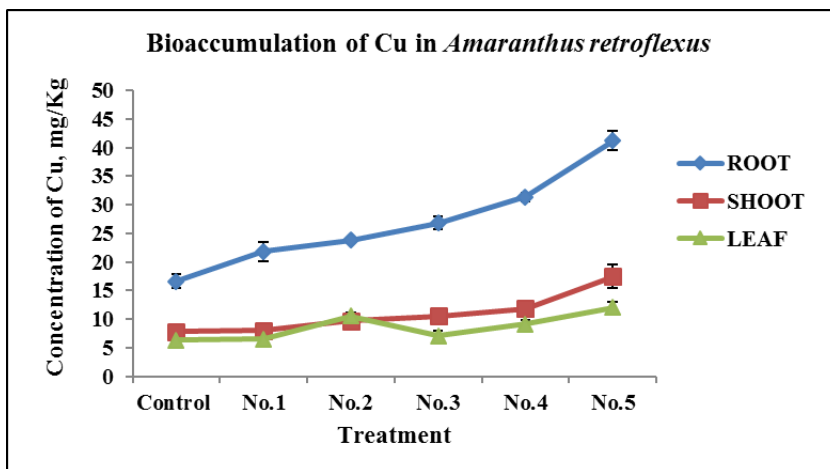
Figure 6.8: Bioaccumulation of Cu in *Amaranthus retroflexus*
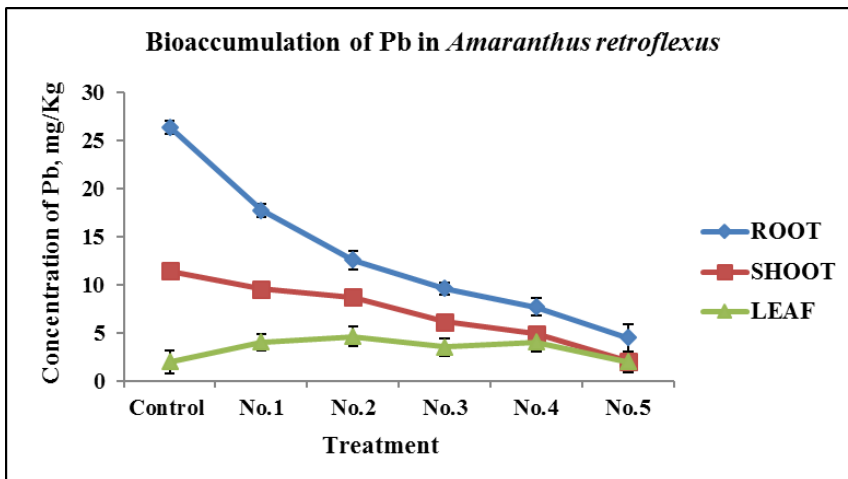
Figure 6.9: Bioaccumulation of Pb in *Amaranthus retroflexus*
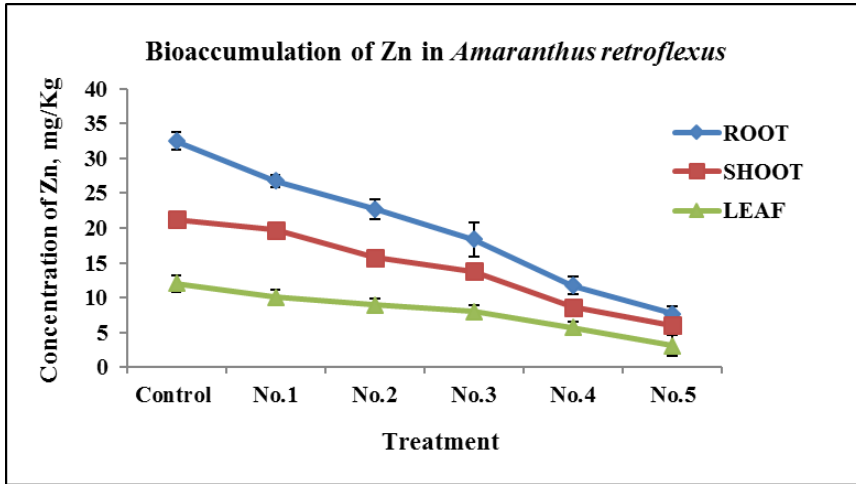
Figure 6.10: Bioaccumulation of Zn in *Amaranthus retroflexus*

The control plant species accumulated more amounts of lead and zinc than the treated plant species (Figure 6.9 and 6.10). With increase in the concentration of ammonium molybdate, the bioaccumulation of Pb and Zn decreases. The metals like Pb and Zn in soil can precipitate with $Mo_2O_7^{2-}$ and the toxicities of these metals to plant will be decreased (Xu et al., 2002). The content of toxic metals in the root were higher than shoots, which may be related to plant uptake of toxic metals and xylem translocation from roots to shoots. Restriction of upward movement from roots into shoots can be considered as one of the tolerance mechanisms (Verkleij & Schat, 1990). The NH_4^+ ion present in ammonium molybdate chelate with toxic metals (such as Cd, Ni and Cu) and form soluble chelating complexes (Rubin et al., 1995). Ammonium molybdate increases the bioavailability of Ni, Cd and Cu in soils and the *A. retroflexus* uptakes more amount of these toxic metals with ammonium molybdate. It also increases the toxicities of these metals to plant.

6.3.3 Effect of ammonium molybdate on plant growth

After 45 days, length of shoot and root of *A. retroflexus* were measured and shoot lengths are shown in Figure 6.11. *A. retroflexus* plant had exhibited high biomass production with the application of ammonium molybdate. The results show that ammonium molybdate could promote *A. retroflexus* plants to produce more biomass, because nitrogen and molybdenum are fertilizer, which can promote *A. retroflexus* plant to improve tillering and biomass gain. Biomass can express the tolerance of plants to toxic metals indirectly (Lasat, 2002).
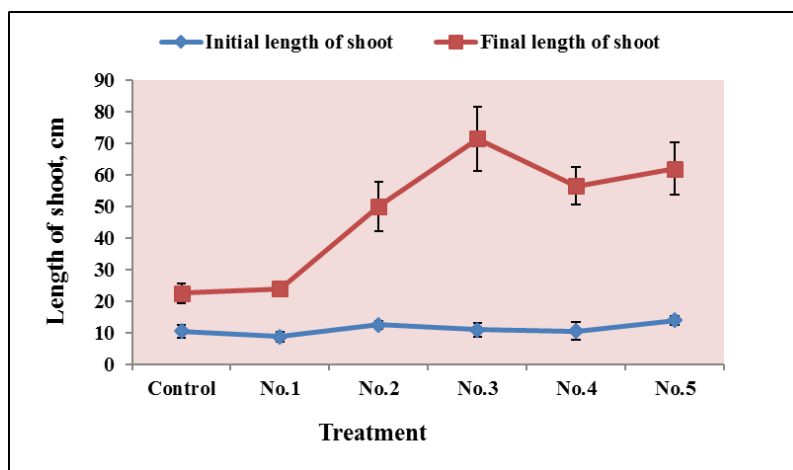
Figure 6.11: Shoot lengths of *A. retroflexus*

The average shoot lengths of treatment plants were longer than the control plants, but the shoot lengths of No.4 and No.5 were shorter than No.3. It may be due to the reason that with addition of ammonium molybdate into soils, Cd, Ni and Cu formed more soluble fractions and the toxicities of Cd, Ni and Cu had reduced the chlorophyll content (Peralta-Videa et al., 2004). Plate 6.2 shows the phytotoxicity symptoms exhibited by *A. retroflexus.*

Plate 6.2: Toxicity symptoms in *Amaranthus retroflexus*

6.3.4 Bioconcentration Factor and Translocation Factor

BCF is the ratio of the metal concentration found within the tissues over the metal concentration found in the soil. The greater is the coefficient, the greater will be the uptake of heavy metal. It was observed that for Cd, Ni and Cu the average BCF values (Table 6.7) of *A. retroflexus* plant treated with ammonium molybdate were higher than control but for Pb and Zn it was lower than control. Maximum BCF value of *A. retroflexus* was found for Cd in treatment No.5. It was 97.6 and 138 for shoots and root respectively. The maximum BCF value of Ni and Cu was also found in treatment No.5. Low BCF value of *A. retroflexus* for Pb and Zn indicates that low amount of metal uptake. This indicates that *A. retroflexus* plant had higher ability to uptake Cd, Ni and Cu with ammonium molybdate. This may be due to the fact that complexation of ammonium molybdate increased the mobility of these metals (Pushenreiter et al., 2001).

Translocation factor is a measure of the ability of plants to transfer accumulated metals from the roots to the shoots. It is given by the ratio of concentration of metal in the shoot to that in the roots (Cui et al., 2007; Li,

2007). A TF value greater than 1 is indicative of metal accumulation and transport into the different plant parts, and less than 1 is suggestive of storage of metal in roots. In this experiment, TF values of *A. retroflexus* were lower than 1, which indicates that maximum amount of heavy metals was stored in roots.

Table 6.7: The average BCF and TF value of *Amaranthus retroflexus*

BCF of shoot					
	Ni	Cd	Cu	Pb	Zn
Control	0.06	0.21	0.17	0.35	0.51
No.1	0.19	0.31	0.21	0.23	0.43
No.2	0.28	1.64	0.27	0.18	0.3
No.3	0.36	29.87	0.32	0.11	0.24
No.4	0.42	45.6	0.45	0.09	0.13
No.5	1.25	97.6	2.7	0.03	0.09
BCF of root					
	Ni	Cd	Cu	Pb	Zn
Control	0.14	0.24	0.36	0.8	0.78
No.1	0.37	0.53	0.57	0.43	0.58
No.2	0.56	2.47	0.67	0.26	0.43
No.3	0.86	37.33	0.8	0.18	0.31
No.4	1.23	61.4	1.19	0.14	0.18
No.5	4.3	138	6.35	0.07	0.11
TF					
	Ni	Cd	Cu	Pb	Zn
Control	0.44	0.86	0.47	0.43	0.65
No.1	0.5	0.58	0.37	0.54	0.74
No.2	0.5	0.67	0.41	0.7	0.7
No.3	0.42	0.80	0.39	0.64	0.75
No.4	0.34	0.74	0.38	0.64	0.73
No.5	0.29	0.71	0.42	0.46	0.78

6.4 Summary

The present study reports the possibility of using ammonium molybdate with phytoremediation for phytostabilization of Pb and Zn and for phytoextraction of Cd, Ni, and Cu by *A. retroflexus*. Ammonium molybdate shows immobilization and mobilization effect on phytoremediation of toxic heavy metals in soil. Ni, Cd and Cu were chelated and form more soluble fractions with ammonium molybdate and Pb and Zn were precipitated with ammonium molybdate. Mobilization effect of ammonium molybdate on Ni, Cd and Cu increases the bioavailability of these metals to plant. Immobilization effect of ammonium molybdate on Pb and Zn decreases the biotoxicity of these metals to plant by decreasing the bioavailability of these metals to plant.

Growth was increased in plants treated with ammonium molybdate than control plant. For Cd, Ni and Cu the average BCF values of *A. retroflexus* plant treated with ammonium molybdate were higher than control. This indicates that *A. retroflexus* plant had higher ability to uptake Cd, Ni and Cu with ammonium molybdate. TF values of *A. retroflexus* were lower than 1, which shows that maximum amount of heavy metals was stored in roots. It was found that application of ammonium molybdate to soil is a promising technology in phytoremediation; it acts as a stabilization agent and as an extracting agent.

DEFLUORIDATION OF WATER USING COST EFFECTIVE TECHNIQUE

7.1 Introduction

Fluoride has been identified as a toxic element for centuries. High level of fluoride in water is a world-wide problem. Fluoride rich rocks through which the water is percolating is the main source of fluoride in aqueous solution. In some areas, industrial activities or mining also contributes to fluoride contamination. The consumption of potable water contaminated by high level of fluoride, adversely affected the human health in many areas of the world (Chen et al., 2010). More than 260 million people are affected by the usage of groundwater having fluoride concentration greater than WHO limit i.e., >1.5 mg/L (Amini et al., 2008; WHO, 2011). Contamination of groundwater by fluoride is a global issue especially in India, China, Africa (Rift valley zone), South America (Andes and western Brazil), Mexico, Pakistan, Sri Lanka, northwest Iran, Nigeria and Kenya (Raj & Shaji, 2017).

Risks associated with consumption of fluoride ions include dental and skeletal fluorosis in man and animals besides impaired brain development. This indicate that, fluoride ions have a capability of restricting the intellectual ability of consumers to make them reliant on throughout their life. Expensiveness, ineffectiveness, and not regeneratable nature are the challenges in some of the previously applied fluoride removal techniques. The development of an affordable, sustainable, and environmentally friendly method for mitigating effects of fluoride in water is necessary for the well-being of human (Mbugua et al., 2017).

7.1.1 Fluoride affected areas in India

Usage of groundwater containing excess fluoride and arsenic as a source of drinking water induced, two major public-health problems in India (Kumar & Kumar, 2015). Shortt et al. (1937) described the first endemic skeletal fluorosis in India. Widespread and alarming contamination of groundwater resources with fluoride has been identified in 19 Indian states (CGWB, 2010). Evapotranspiration of groundwater with residual alkalinity was a reason for high fluoride content in groundwater in many areas of India (Jacks et al., 2005). The main source of fluoride in groundwater from Nalgonda district is the 325- 3200 mg/Kg of fluoride containing granitic rocks present there (Brindha et al., 2011). Andhra Pradesh, Rajasthan, Karnataka, Tamil Nadu, Gujarat, Kerala, Uttar Pradesh, Jammu and Kashmir, Orissa and Punjab are the states where fluoride problem is common. In India, consumption of high amount of fluoride containing water leads to fluorosis in approximately

62 million people including 6 million children (Susheela, 1999; Bishnoi & Arora, 2007). In 2012, the MoWR has enumerated that out of 639 districts, 267 districts were affected by fluoride. 50 to 100 % of districts were affected by fluoride in states such as Rajasthan, Andhra Pradesh and Gujarat, and 30 to 50 % of districts were affected in Haryana, Karnataka, Bihar, Tamil Nadu, Jharkhand, Madhya Pradesh, Uttar Pradesh, Maharashtra, Orissa, and Punjab (Saxena & Sewak, 2015). Palakkad and Alappuzha are the two districts in Kerala, reported high fluoride content in the groundwater (Antu & Harikumar, 2007).

Fluorosis is an irreversible health hazard; its prevention using appropriate remedial measures is an obligatory. For this purpose, elimination of high fluoride from drinking water sources is required. Defluoridation is a term generally used for the process of removal of fluoride. Since 1930, several methods have been described using many materials for the defluoridation process. The defluoridation can be grouped under different categories based on the nature of process: adsorption, ion exchange, chemical treatment, electrolytic defluoridation, membrane separation and electro dialysis etc. One of the cheapest methods to eradicate fluoride ions from wastewater is the addition of excess lime or other calcium salts to form calcium fluoride but this approach decreases the reusability of wastewater by raising the hardness of the water (Hu et al., 2003). Among various processes, adsorption has been reported to be effective based on initial cost, simplicity and flexibility of design and ease of operation and maintenance. Various types of adsorbents have been studied and reported for the defluoridation purpose, including activated carbon, activated alumina, calcite, amberlite

resin, fly ash, minerals, layered double hydroxides, spent bleaching earth, coconut shell carbon and rice husk carbon, etc. with different degrees of success. Activated alumina seems to be a widely used adsorbent for the removal of fluoride but it possesses some disadvantages such as the generation of sludge, residual aluminum, soluble aluminum fluoride complexes, and narrow available pH range (5.0 - 6.0) (Emmanuel et al., 2008; Chen et al., 2010).

The application of plant materials is a traditional technology for purifying potable water that is still in widespread use in rural areas of Latin America. The use of natural products has recently been rediscovered by water-supply technologists and is being further developed with more scientific rigor (Hichour et al., 2000; Harikumar et al., 2012). Adsorption involves the passage of contaminated water through an adsorbent bed, where fluoride removed by physical, ion-exchange or surface chemical reaction with adsorbent. Plant materials are reported to accumulate fluoride and hence application as defluoridating agents has been suggested. The use of medicinal plant materials for the fluoride removal was investigated. Kerala is one of the states in southern India, which has a rich biodiversity of medicinal plants. In the present study, the efficiency of removal of fluoride by using various locally available medicinal plants from Kerala was investigated. The suitability and effectiveness of inexpensive adsorbents to remediate fluoride in contaminated water was assessed in this study. The study investigated defluoridation capacities of the following plant materials: Ramacham (*Vetiveria zizanioides*), Tamarind seed (*Tamarindus indica*), Clove (*Eugenia carryophyllata*), Neem (*Azadirachta indica*), Acacia (*Acacia*

catechu willd), Nutmeg (*Myristica fragarns*), and coffee husk (*Coffea arabica*) which are grown indigenously Kerala (Varier, 1996; Harikumar et al., 2012). The defluoridation ability of the carbonized form of Ramacham (*Vetiveria zizanioides*) was investigated in this study and it was also applied to treat the samples collected from fluoride affected areas of Palakkad district, Kerala.

7.2 Materials and Methods

Locally available raw plant materials were collected from Calicut district, Kerala. The dust and other impurities were removed from each raw plant materials using multiple washing with water and final washing was done with double distilled water. They were open dried in shade and cut into small pieces. Then the materials were oven dried at temperature range of $110^{o}C$ for a period of 5 h. The dried plant materials were grounded with grinder and sieved through standard sieve to obtain particle of sizes 0.1, 0.2 0.3 and 0.5 mm. The powdered materials were stored in clean and air tight plastic containers. All the reagents used for the present study were of AR grade from E. Merck Ltd. India. A standard solution of 1000 mg/L fluoride was prepared by dissolving 2.21 g of anhydrous sodium fluoride in 1000 mL of double distilled water. The fluoride solution of required concentration was prepared by diluting appropriate quantity of standard solution. Ion selective electrode (Thermo Scientific Orion 9609BNWP, Made in US) was used to measure fluoride ion concentration and total ionic strength adjustment buffer II (TISAB II) solution was used to maintain pH 5–5.5. The HCl (0.1 mol/L) and NaOH (0.1 mol/L) solutions were used to adjust pH of the solution to the required level during the study. PCSTestr35 instrument was used to

measure pH of the solutions. The regular calibration of pH meter by pH calibration buffers was carried out.

Plate 7.1: *Vetiveria zizanioides*

The batch adsorption study was carried out in three stages. In the first stage, locally available medicinal plants were selected as the study materials. Medicinal plant materials like pomegranate (*Punica granatum)*, nutmeg *(Myristica fragrans)*, gooseberry *(Phyllanthus emblica*), dried ginger (*Zingiber officinale*), sathavari (*Asparagus racemosus*), kozhinjil (*Tephrosia purpurea*) and karinochi (*Vitex negundo*) were used for the initial defluoridation study. The study also assessed the suitability of some locally available plant materials to effectively remediate fluoride contaminated water. The plant material selected for the defluoridation was ramacham or vetiver root (*Vetiveria zizanioides*), tamarind seed (*Tamarindus indica*), clove (*Eugenia carryophyllata*), neem (*Azadirachta indica*), (*Acacia catechu willd*), coffee husk (*Coffea arabica*) and fern (*Adiantum aethiopicum)*. Based on their defluoridation efficiency, it was found that plants materials like vetiver root, tamarind seed and clove were comparatively more efficient than other adsorbents. During the second stage of this study, batch

adsorption test for the selected adsorbents like vetiver root (*Vetiveria zizanioides*), tamarind seed (*Tamarindus indica*) and clove (*Eugenia carryophyllata*) were conducted by varying contact time, sorbent dosage and particle size. From the results, it was found that vetiver root was an efficient defluoridating material. In the third stage of the study, activated carbon was prepared using vetiver root (*Vetiveria zizanioides*) for better removal of fluoride and its kinetic study was also conducted. Plate 7.1 shows the vetiver root.

7.2.1 Preparation and characterization of activated carbon from *Vetiveria zizanioides*

Either thermal or chemical activation is the process commonly used to produce activated carbon from carbonaceous material. Phosphoric acid was selected as the activating agent in this study in view of its environmental benefits. In phosphoric acid based chemical activation method, increased carbon yield by reduced tar formation was reported many researchers (Lim et al., 2010; Benadjemia et al., 2011). It also provides the opportunity of developing microporous and/or mesoporous carbon having high specific surface area (Jagtoyen & Derbyshire, 1998). Yakout and Sharaf-el-Deen (2012) indicated that H_3PO_4 have the ability to retain carbon and avoid the loss of other volatile materials. It was also reported that H_3PO_4 activation have the ability to promotes dehydration and redistribution of biopolymers and also favors the conversion of aliphatic to aromatic compounds, thus increasing the yield of activated carbon (Olawale et al., 2015).

Among the three-plant materials, vetiver root (*Vetiveria zizanioides*), tamarind seed (*Tamarindus indica*) and clove (*Eugenia carryophyllata*), powdered vetiver root (Plate 7.2) exhibited better defluoridation performance. Acid activation of vetiver root was conducted to increase the porosity and surface area. Activity was controlled by altering the proportion of raw material to activating agent (1:05, 1:1, 1:2 and 1:4). The liquid/solid mixture was stirred well at ambient temperature for 2 h and set aside to soak for 12 h to allow proper penetration of the H_3PO_4 into the vetiver root (Montane and Torne-Fernandez, 2005; Olawale et al., 2015). The materials were carbonized for 1 h, 1½ h and 2 h at 600°C, 700°C and 800°C. After cooling to the ambient temperature, the carbonized vetiver root was washed several times with de-ionized water until it attains pH 6 - 7. It was filtered using Whatman No. 41 filter paper and then dried in the oven at 110°C for 8 h. The dried activated vetiver powder was stored in clean air tight bottles. The amount of fluoride adsorbed at time t, q_t (mg/g) on each activated carbon prepared from vetiver root powder under varying condition were calculated using the following equation.

$$q_t = \frac{(C_0 - C_t)V}{M} \qquad (1)$$

Where C_o and C_t are the fluoride concentrations (mg/L) contained in the original solution and after time t, respectively, m is the adsorbent mass (g) and V is the volume of solution (L). Based on the results, the optimum conditions for the preparation of activated vetiver powder i.e., impregnation ratio of vetiver root powder to activating agent, temperature and carbonizing time were selected for further study. So, in the third

stage of this study, detailed batch sorption experiment using activated *Vetiveria zizanioides* (Plate 7.3) was carried out.

The characterization of the active carbon prepared from *Vetiveria zizanioides* was conducted by the following methods: pH, moisture content and ash content were determined in accordance with American Standard of Testing Material [pH: ASTM D3838-80, moisture: 1999ASTM D3173 and ash: ASTM D3174] (ASTM, 2006). For the information about the surface area of the carbon, iodine number was determined using the method ASTM D4607 – 94 (ASTM, 2011; Joshi et al., 2012). Volatile content and fixed carbon were determined using the method followed by Nwabanne and Igbokwe (2011).

Plate 7.2: Powdered Vetiver root   **Plate 7.3:** Activated Vetiver root

7.2.1.1 Determination of pH:

1 g of activated carbon was taken in a beaker and 100 mL of distilled water was added to it. Stirred for one hour and then the samples were kept to stabilize. pH was measured using a pH meter (PCSTestr35 instrument).

7.2.1.2 Determination of Iodine Number:

To 1 g of activated carbon, 10 mL of 5 % by weight of HCl was added and was allowed to boil. When the solution attained room temperature, 100 mL of 0.1N iodine solution was added to it. After vigorous shaking, the solution was filtered. 25 mL of the filtrate was titrated against 0.1 N sodium thiosulphate solution. Starch was used as indicator.

7.2.1.3 Determination of moisture content and ash content:

Thermal drying method was used to measure moisture content of the samples. 1 g of the dried activated carbon was taken in a crucible. It was dried in an oven at $110^{o}C$ for 4 h for constant weight and then moisture content was calculated. Ash content indicates the amount of inorganic substituent present in the activated carbon. High ash reduces the mechanical strength of carbon and negatively affects adsorptive capacity so it is undesirable for activated carbon. After pre-heating a crucible in a muffler furnace to about $500^{o}C$, it was cooled in a desiccator and weighed. One gram of activated carbon sample was transferred into that crucibles and reweighed. The crucible containing the sample was again heated to $500^{o}C$ in a muffler furnace. It was removed from muffler furnace, allowed to cool in a desiccator to attain room temperature and measured the weight. The ash content was calculated using the following equation:

$$Ash\ (\%) = \frac{wt.of\ ash\ (g)}{dry\ wt.of\ activated\ charcoal\ (g)}\ x\ 100 \quad (2)$$

7.2.1.4 Determination of volatile content and fixed carbon:

The volatile content and fixed carbon of the activated vetiver root powder was determined by the methods followed by Nwabanne and Igbokwe (2011). For determining the volatile content, a pre-weighed sample was placed in a partially closed crucible of known weight. It was then heated at 900ºC in a muffle furnace for 10mins. The percentage of fixed carbon was calculated using the following equation:

Fixed carbon (%) = 100 – Moisture content +

ash content + volatile matter)%   (3)

Surface morphology of activated *Vetiveria zizanioides* root was studied by using Scanning Electron Microscope image of sorbent. Field Emission scanning electron microscope equipment made by Hitachi (SU-6600) was used to take SEM images.

7.2.2   Batch Studies of activated *Vetiveria zizanioides* root

Fluoride batch sorption experiments were conducted to understand the efficiency of adsorbent and the effect of controlling parameters like dosage, contact time, pH, initial concentration, stirring rate and co-ions. The batch experiments were carried out in 250 mL stoppered bottles by agitating a pre-weighed amount (0.5 g) of the adsorbent with 100 mL of the fluoride solutions. The adsorption experiments were conducted by mixing adsorbent and adsorbate using a mechanical shaker. In order to determine the effect of pH on the defluoridation capacity of activated carbon, the adsorption studies were

conducted in the pH range 2 to 12. The effect of adsorbent dosage on defluoridation was studied by varying the dosage from 2.5 up to 35 g/L in test solutions containing initial fluoride concentration, 10 mg/L. The fluoride concentrations were varied from 10 to 40 mg/L to understand the effect of initial fluoride concentration on efficiency of fluoride removal. To obtain the equilibrium adsorption time, fluoride solution (10 mg/L) and optimum adsorbent dose was agitated for periods of 20, 40, 60, 80, 100, 120, 140, 160 and 180 minutes. The effect of co-ions was studied to understand the influence of anions like chloride, sulphate, bicarbonate, phosphate and nitrate and cations like calcium and magnesium on the defluoridation efficiency of the adsorbent. To determine optimum stirring rate, experiment was conducted by changing the stirring rate from 50 to 300 rpm. To attain as close to natural drinking water conditions for fluoride removal, the experiments were performed at room temperature and at pH = 6. To determine the thermodynamic parameters, sorption experiments were conducted at 303K, 313K, 323K and 333K using a temperature-controlled water bath. All analysis was done in triplicate to check the precision and average values only are reported.

The amount of adsorbed at equilibrium, q_e (mg/g) and sorption efficiency (%) were computed as follows:

$$q_e = \frac{(C_0 - C_e)V}{M} \qquad (4)$$

$$\text{Sorption efficiency (\%)} = \frac{(C_0 - C_e) * 100}{C_0} \qquad (5)$$

where C_0 and C_e are the initial and final equilibrium concentrations of fluoride (mg/L), respectively. *V* is the volume of the solution (L), *M is* the mass of dry adsorbent used (g).

7.2.3 Adsorption Isotherms

Adsorption isotherm is the relationship between the amount of substance adsorbed and its concentration in equilibrium solution at constant temperature. Adsorption process was explained using isotherm models such as Langmuir, Freundlich, Temkin and Dubinin-Radushkevich (D-R) while four kinetic models like pseudo-first-order, pseudo-second-order, intra-particle diffusion and Elovich model were used for determination of the behavior of fluoride ions during the adsorption onto activated *Vetiveria zizanioides* root. Freundlich and Langmuir equations were used to find the patterns of adsorption by adsorbent activated Vetiver root for fluoride removal. The sorption isotherm studies were conducted by varying the initial concentration of fluoride from 10 - 40 mg/L and maintaining the adsorbent dosage of 5 g/L.

7.2.4 Column studies

Continuous flow adsorption studies were conducted for defluoridation in a column made of Pyrex glass of 30 cm length and 2 cm internal diameter. The activated *Vetiveria zizanioides* was filled in the column without gap. The glass column was packed with 10 g of adsorbent for bed height of 6.4 cm, 15 g of sorbent with bed height of 9.7 cm and 20 g of sorbent with bed height of 12.7 cm having glass wool

support. The influent synthetic fluoride solution having a concentration of 10 mg/L was allowed to percolate through the packed column, from the top of the column. The influent fluoride solution passed through the column at constant flow rate of 2 mL/min, in down flow manner using a fine metering valve. All the experiments were conducted at room temperature and at neutral pH range. Effluents were collected from the exit point of the column at regular effluent volume and concentration of residual fluoride was determined as described. When the ratio of the effluent to influent fluoride concentrations reached a value close to 1, the column flow was stopped. After column saturation, the fluoride adsorbed activated *Vetiveria zizanioides* was eluted with 0.1 M NaOH for regeneration. Then the bed was washed with distilled water by passing through the column until a neutral pH of the wash effluent was attained. A gravity based defluoridation unit was developed using the carbonized form of Ramacham (*Vetiveria zizanioides*).

7.2.5 Field trial on real groundwater samples collected from fluoride prone area of Palakkad District

Centre for Water Resources Development and Management (CWRDM) conducted a study on "Monitoring, Mapping and Mitigation of Fluoride in Palakkad including Attapady region of Kerala" (CWRDM, 2015). As a part of this study, samples were collected from a total number of 350 stations in 94 Panchayaths of 13 blocks of Palakkad district between May 2014 and December 2014 (Figure 7.1). The collected samples were analyzed for various physico-chemical and bacteriological analysis as per the standard procedure described in APHA

(APHA, 2012). To check the field application of the defluoridation study, five high fluoride detected samples were selected from Muthalamada panchayath of Palakkad district, based on the results reported by CWRDM, for the defluoridation study.
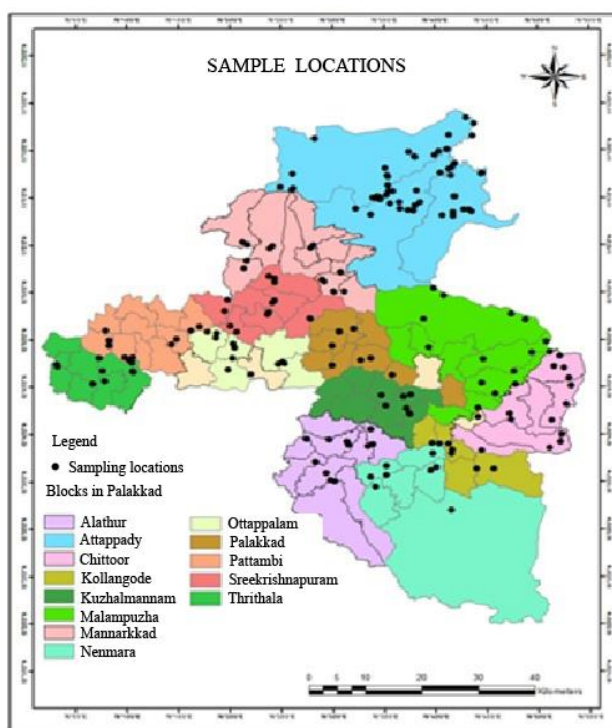
Figure 7.1: Map of Palakkad district showing sample locations

7.3 Results and Discussions

7.3.1 *Stage 1*: Screening test of plant materials based on its defluoridation efficiency

In first stage, medicinal plant materials like pomegranate peel (*Punica granatum)*, nutmeg *(Myristica fragrans*), gooseberry

(Phyllanthus emblica), dried ginger (*Zingiber officinale*), sathavari (*Asparagus racemosus*), kozhinjil (*Tephrosia purpurea*) and karinochi (*Vitex negundo*) were selected for the defluoridation study. Different removal efficiency was exhibited by dried and powdered plant materials. The percentage removal of fluoride was shown in Figure 7.2. Among the selected medicinal plant materials, highest efficiency (70 %) was noted in pomegranate (*Punica granatum)* and Karinochi (*Vitex negundo*) exhibited lowest removal efficiency (30 %) in defluoridation study.
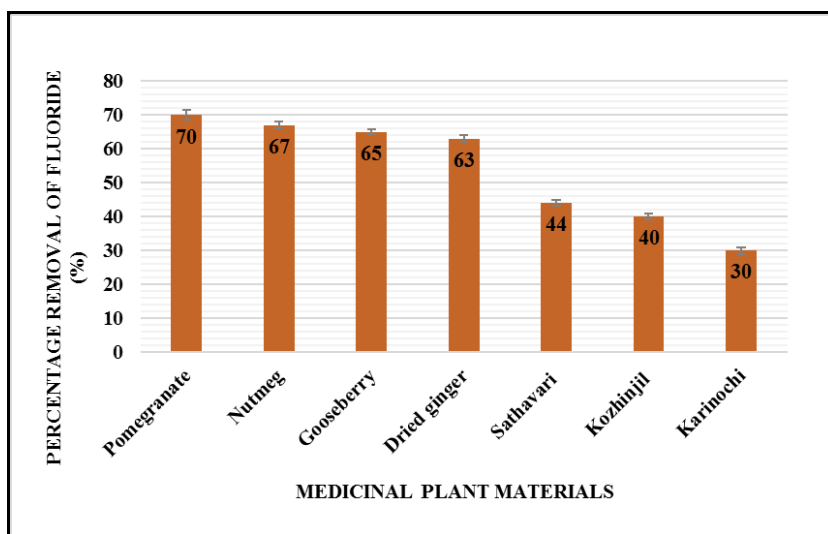
Figure 7.2: Comparison of fluoride removal efficiencies of different medicinal plant materials

The study assesses the suitability of some locally available adsorbents to effectively remediate fluoride contaminated water. The plant material used for the defluoridation was Ramacham (*Vetiveria zizanioides*), Tamarind seed (*Tamarindus indica*), clove (*Eugenia carryophyllata*), neem (*Azadirachta indica*), (*Acacia catechu willd*),

coffee husk (*Coffea arabica*) and fern (*Adiantum aethiopicum)*. The order of removal efficiency of different adsorbents from a solution contaminated with 10 mg/L fluoride is (Figure 7.3): Ramacham (*Vetiveria zizanioides*, 80 %), Tamarind seed (*Tamarindus indica,* 75 %), clove (*Eugenia carryophyllata*, 73 %), neem (*Azadirachta indica* 52 %), *Acacia catechu willd* (47 %), and coffee husk (*Coffea arabica,* 38 %). Based on the screening test, high efficiency in removal of fluoride was exhibited by Ramacham or Vetiver root (*Vetiveria zizanioides*), Tamarind seed (*Tamarindus indica*) and clove (*Eugenia carryophyllata*). So, these plant materials were selected for further defluoridation study. Effect of important controlling factors, viz, dose of adsorbent, contact time and particle size were studied to understand the equilibrium condition for the better fluoride removal.
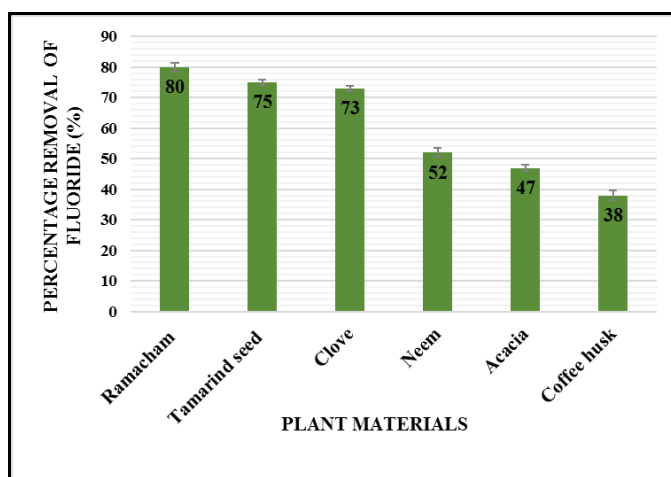
Figure 7.3: Comparison of fluoride removal efficiencies of different plant materials

7.3.2 *Stage 2:* **Batch sorptive defluoridation by tamarind seed, vetiver root and clove**

The results of batch sorptive defluoridation of tamarind seed, vetiver root and clove were conducted under variable experimental conditions are discussed in the following section.

7.3.2.1 Effect of contact time

The contact time or agitation time is an important factor in adsorption dynamics. The effect of contact time on defluoridation by using tamarind seed, vetiver root and clove as adsorbents is depicted in Figure 7.4. To evaluate the defluoridation efficiency, batch sorption study was conducted using 50 mL of 10 mg/L fluoride solution with 0.5 g of the adsorbent at room temperature as a function of time. The effect of contact time was found to be increased up to a certain period of time after which the rate of sorption remains constant until equilibrium was reached. Figure 7.4 reveals that the rate of fluoride removal was higher at the initial stage. This may be due to the availability of larger surface area at the beginning for the adsorption of fluoride ions. It was found that the percentage removal of fluoride for tamarind seed, vetiver root and clove was 51, 59, and 51 respectively. The time to reach equilibrium conditions for the vetiver root (*Vetiveria zizanioides*) was 120 min. So, 120 min was set as minimum agitation time for achieving maximum defluoridation of the sorbent. Maximum removal of fluoride was exhibited by Tamarind seed (*Tamarindus indica,*) and clove (*Eugenia carryophyllata*) at an equilibrium time of 100 min.
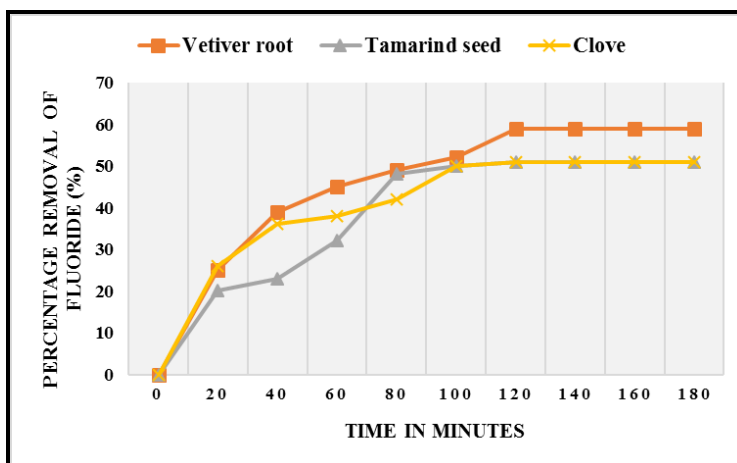
Figure 7.4: Effect of agitation time on defluoridation

7.3.2.2 Effect of sorbent dosage

The response of varying dose of adsorbent on the removal of fluoride at neutral pH is showed in Figure 7.5. As the weight of adsorbent dose increased, the sorption percentage also increased. This might be due to the fact that at higher doses of adsorbent, more sorbent surface and pore volume would be available for the adsorption interaction and this result in higher removal. It was also observed that, initially, the removal of fluoride increases with the dose but beyond certain dose range, there is no significant increase in removal. This perhaps is due to non-adsorbability of fluoride ion as a result of sorbent-sorbate interaction. Results showed that the biosorbents, viz, tamarind seed and clove removed 75 and 70 % of fluoride respectively at a dose of 1 g in 50 mL of 10 mg/L fluoridated water and vetiver root removed 80 % of fluoride at the same dose. Vetiver root showed a maximum removal (85 %) at a dosage of 1.2 g.
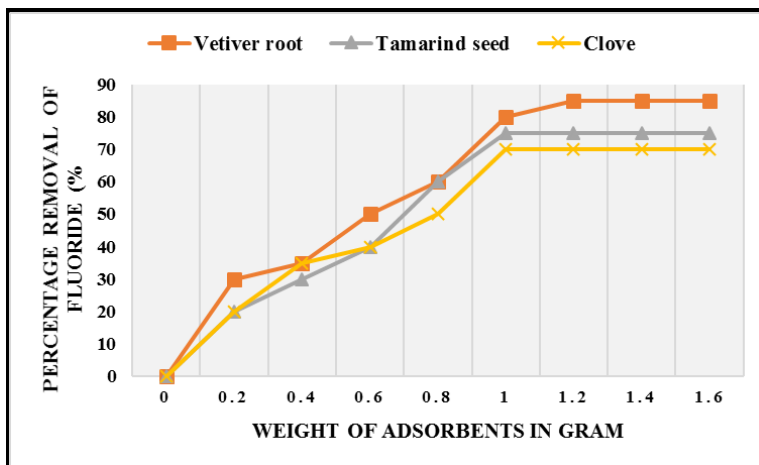
Figure 7.5: Effect of sorbent dosage on defluoridation

7.3.2.3 Effect of particle size

The defluoridation study was conducted using vetiver root, tamarind seed and clove with four different particle sizes viz. 0.1 mm, 0.2 mm, 0.3 mm and 0.5 mm with fluoride solution having initial concentration of 10 mg/L. The effect of particle size on fluoride sorption is given in Figure 7.6. Increase in particle size reduces the sorption rate. Increase in particle size from 0.1 mm to 0.5 mm reduces the sorption level from 85 to 45 per cent for Vetiver root. The breaking of larger particles tends to open tiny cracks and channels on the particle surface of the sorbent. The smaller particle provides more sorption sites and surface area leading to greater sorption. The sorbents with 0.1 mm particle size reported high defluoridation efficiency due to larger surface area, as the adsorption process is a surface phenomenon. Higher percentage of sorption by vetiver root, tamarind seed and clove with smaller particle size was 85 %, 65 % and 60 % respectively and was due to the availability of more specific surface area on the adsorbent surface.
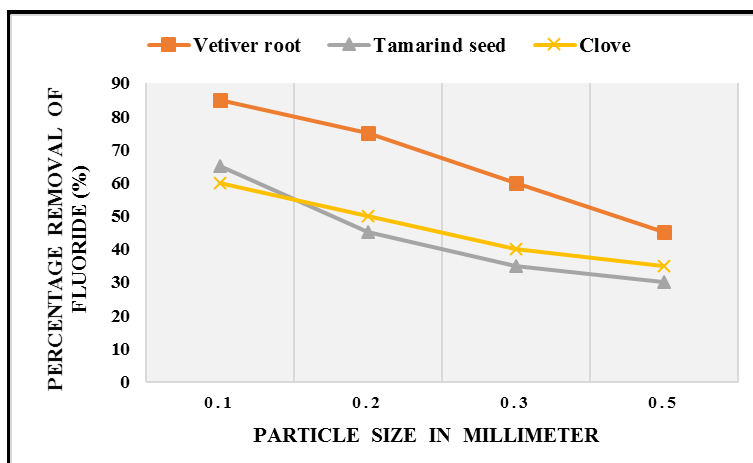
Figure 7.6: Effect of particle size on sorption of fluoride

The present study indicates that the three biosorbent are suitable for the removal of fluoride ions. The percentage of fluoride removal increases with adsorbent dose and time at a given initial solute concentration. Compared to tamarind seed and clove, vetiver root exhibited higher defluoridation capacity. From the adsorption study, it is clear that Vetiver root has the potential to be an efficient defluoridating agent, so in the third stage of this study, activation of powdered vetiver was carried out to improve its efficiency. Phosphoric acid was used to activate vetiver root.

7.3.3 *Stage 3:* Defluoridation using activated *Vetiveria zizanioides*

7.3.3.1 Selection of impregnation ratio, temperature and activation time for the preparation of activated *Vetiveria zizanioides*

Activation of vetiver root or *Vetiveria zizanioides* was carried out by giving heat treatment (at 600˚C - 800˚C) and by altering the impregnation ratio of raw material to activating agent 1:05, 1:1, 1:2 and

1:4. Impregnation ratio is defined as the ratio of the weight of activated vetiver root powder to the weight of H_3PO_4. The carbonization of the material was conducted for 1 h, 1½ h and 2 h at 600^0C, 700^0C and 800^0C. Impregnation ratio, temperature and activation time was selected based on the amount of fluoride adsorbed on the activated vetiver root (adsorption capacity). Batch adsorption tests were carried out using an initial fluoride concentration of 10 mg/L with a dosage of activated *Vetiveria zizanioides* 5 g/L. The amount of fluoride adsorbed on the activated vetiver root or the adsorption capacity was calculated and obtained results are depicted in Figure 7.7.
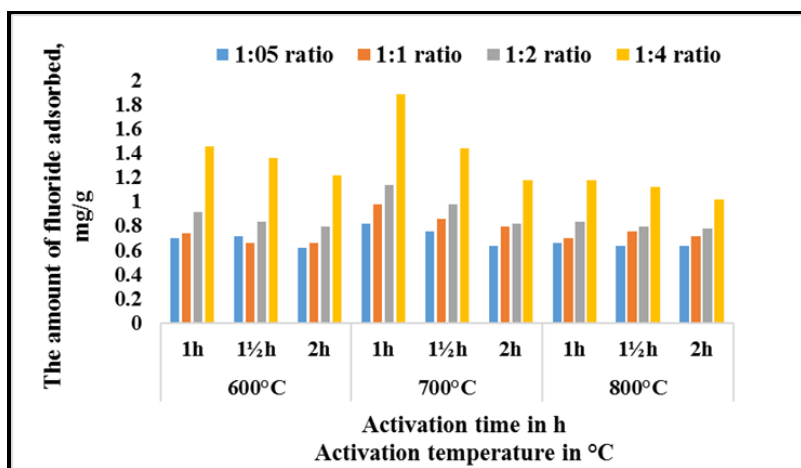
Figure 7.7: The amount of fluoride adsorbed on the activated vetiver root (adsorption capacity) as a function of impregnation ratio, temperature and activation time

The maximum adsorption capacity was observed for activated vetiver root powder prepared by using an impregnation ratio of 1:4 between vetiver root powder and activating agent at an activation time of 1h at 700^0C. This was explained by Olawale et al. (2015), that an increase in concentration of H_3PO_4 was able to unblock and enlarge the pores of the activated carbon produced. Better pore enlargement and unblocking were reported with high concentration of phosphoric acid used for activation. The large pore volume resulted in an increase in the capacity of surface accommodation. A maximum of 1.884 mg/g adsorption capacity was reported by the activated vetiver root prepared with an activation time of 1 h compared to 1½ h (1.44 mg/g) and 2 h (1.18 mg/g). Castro et al. (2000) reported that prolonged carbonization beyond 1h led to reduction in porosity development. Based on the results, the impregnation ratio of 1:4 and an activation time of 1 h at 700^0C was selected as optimum condition for the preparation of activated *Vetiveria zizanioides*. Further defluoridation study was conducted using this activated *Vetiveria zizanioides* powder as adsorbent and its characteristics are tabulated in Table 7.1. The higher value of iodine number indicates that the carbon is highly porous with better effective surface area. Low ash content and moisture content indicates that activated carbon prepared from *Vetiveria zizanioides* root powder is suitable for adsorption process.

From the adsorption study, it is clear that vetiver root (*Vetiveria zizanioides*) has the potential to be an efficient defluoridating agent, so further study was carried out using activated vetiver root (*Vetiveria zizanioides*). Powdered activated Vetiver showed higher efficiency than the other. The batch sorptive defluoridation study of powdered activated

vetiver was conducted under variable experimental conditions such as pH, initial concentration, agitation time, Interfering co-ions, dose of adsorbent, particle size, agitation speed and temperature.

Table 7.1: Characteristics of activated *Vetiveria zizanioides* root

Properties	Values
pH	6.8
Bulk density (g/cm^3)	0.51
Iodine number (mg/g)	817.32
Moisture content (%)	4.1
Volatile matter (%)	26.3
Ash content (%)	3.65
Fixed carbon (%)	65.95

7.3.3.2 Batch sorptive defluoridation study of powdered activated *Vetiveria zizanioides*

7.3.3.2.1 Effect of pH

The pH is an important controlling factor in sorption processes. The adsorption was found to be influenced by the pH of the medium in the present experiment. The effect of pH change on the defluoridation was carried out within a range of pH 2 - 12. Maximum removal was observed around neutral pH (around neutral pH, the surface will be positively charged-columbic interaction between fluoride ion and adsorbent surface will be higher) is shown in Figure 7.8. The highest

removal of fluoride ions by activated *Vetiveria zizanioides* was obtained at pH 6 (94 %), and then a sharp decrease in sorption was observed at pH values higher than 8. In the acidic pH range, the amount of fluoride adsorption slightly decreased and this can be attributed to the formation of weak hydrofluoric acid. In alkaline pH range, there was sharp drop in adsorption which may be due to the competition of the hydroxyl ions with the fluoride for adsorption (Kumar et al., 2008).
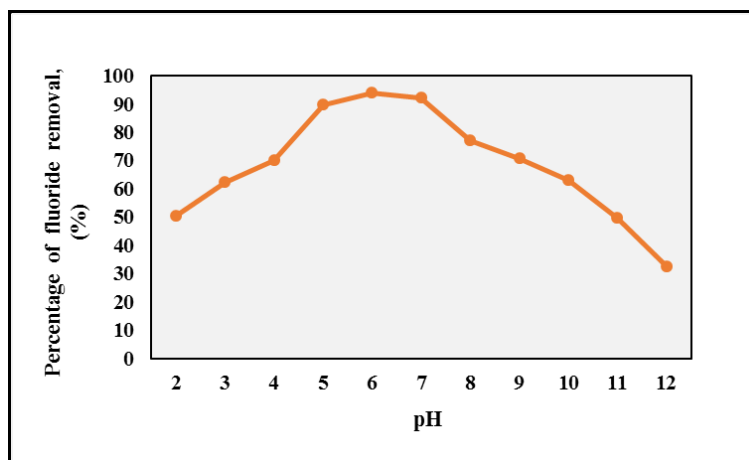
Figure 7.8: Effect of pH on sorption of fluoride

7.3.3.2.2   *Effect of contact time and initial fluoride concentration on defluoridation*

Contact time is a major influencing factor in adsorption dynamics. Batch sorption studies at different initial fluoride concentrations of 10, 20, 30 and 40 mg/L with 5 g/L of adsorbent dosage, at pH 6 and agitating speed of 150 rpm at room temperature were carried out as a function of contact time to assess the defluoridation and adsorption rate constants.

The effect of initial fluoride concentration on adsorption of fluoride onto activated *Vetiveria zizanioides* under varying contact time is shown in Figure 7.9. The effect of agitation time was found to be increasing up to a certain period of time and gradually attains equilibrium after 120 min. The results showed that 120 min is the time required to reach equilibrium conditions i.e., the minimum contact time for attaining the maximum defluoridation, was independent of initial fluoride concentrations. The rate of removal was observed almost insignificant after the reaching the equilibrium time and this may be due to the exhaustion of the adsorption sites (Saeed et al., 2005). The removal of fluoride was found to be 92.5, 77.1, 58.8 and 44.5 % at initial fluoride concentrations of 10, 20, 30 and 40 mg/L respectively. The efficiency of fluoride removal decreases with increase in initial fluoride concentration. Smooth and continuous removal curves were observed, indicating the possibility of monolayer coverage of fluoride ions on the surface of adsorbent (Alagumuthu et al., 2010).
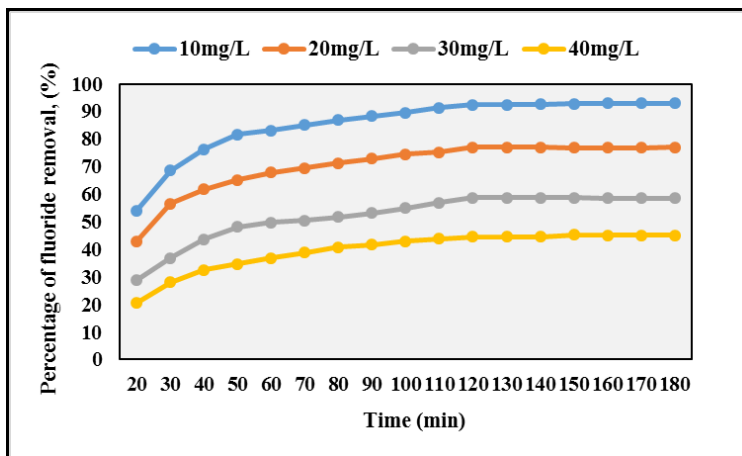
Figure 7.9: Effect of agitation time on defluoridation

7.3.3.2.3 *Effect of interfering co-ions on defluoridation*

The water contaminated with fluoride may contain various other ions also which may compete with fluoride ion in the adsorption process. The influences of coexisting anions such as chloride, sulphate, bicarbonate, nitrate, phosphate and cations like calcium and magnesium on fluoride adsorption by the adsorbent, activated vetiver were examined. Figure 7.10 reveals the inference of anions on fluoride removal efficiency. The defluoridation studies were carried out in the presence of anions like chloride, nitrate, sulphate, carbonate and phosphate in the concentration range 0 - 300 mg/L independently at an initial fluoride concentration of 10 mg/L at neutral pH with contact time of 120 min.

Chloride and nitrate did not show any noticeable interfere with defluoridation efficiency even at a concentration of 300mg/L. A slight increase in fluoride removal was noted in the presence of chloride and nitrate ions. This could be due to an increase in the ionic strength of the solution or a weakening of lateral repulsion between adsorbed fluoride ions (Eskandarpour et al., 2008; Chen et al., 2010). But the fluoride removal exhibited a decreasing trend when sulphate concentration increases. When the concentration of sulphate varied from 0 - 300 mg/L, the fluoride removal efficiency was decreased from 92 % to 78 %. This may be attributed to the high coulombic repulsive forces, which reduce the chance of fluoride interactions with the active sites (Onyango et al., 2004; Tor et al., 2006). A great competitive adsorption with fluoride was observed in the presence of high phosphate and bicarbonate. Under varying concentration of bicarbonate and phosphate from 0 - 300 mg/L, a quick decrease in fluoride removal i.e., from 92 % to 56 % and 92 % to

41 % was observed respectively. This may be attributed to the competition for the same active sites with fluoride and also by the high affinity and capacity for phosphate and carbonate ions on adsorbent. The selective nature of the fluoride by the adsorbent depends on factors like size, charge, electronegativity difference, polarizability etc. The influence of co-existing anions on the fluoride removal by the sorbent, activated vetiver root was observed as in the following order: PO_4^{3-} > HCO_3^- > SO_4^{2-} > $Cl^- \geq NO_3^-$. The results are in good agreement with similar work done by Alagumuthu et al. (2011) and Chen et al. (2010). Interference of cations like calcium and magnesium on the defluoridation ability of activated vetiver was also tested. However, any significant influence on the fluoride adsorption was not observed in the presence of high calcium and magnesium ions.
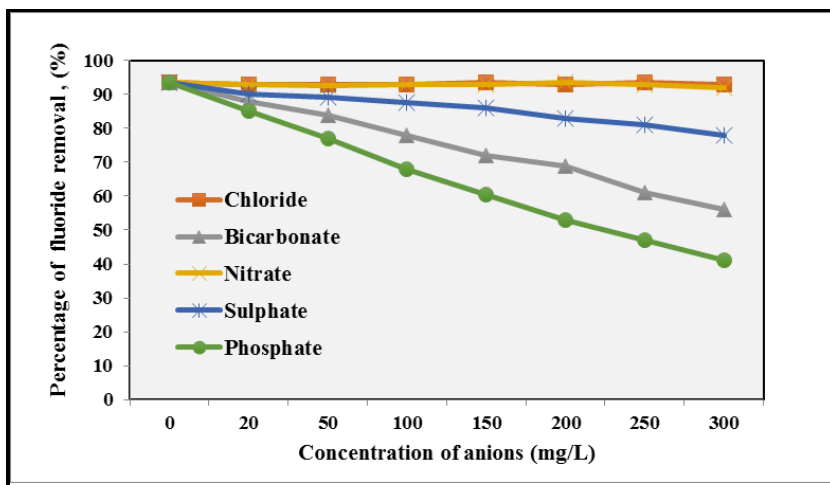
Figure 7.10: Interference of co-ions on defluoridation

7.3.3.2.4   *Effect of sorbent dosage on defluoridation*

The response of adsorbent dose at fixed initial fluoride concentration 10 mg/L, pH 6, shaking speed 150 rpm, and contact time 120 min on the removal of fluoride are presented in Figure 7.11. Initially, the fluoride uptake increases with the corresponding increase in the amount of adsorbent but beyond certain dose range, there was no significant increase observed in the removal of fluoride. No significant improvement was observed in the efficiency of fluoride removal with increase of adsorbent dosage beyond 5 g/L that may be due to low concentration of fluoride available at higher adsorbent dose. 5 g/L was observed as the optimum dose. The initial increasing trend observed in fluoride removal efficiency with increasing adsorbent dosage was due to the increase in surface area and availability of more active sites for adsorption.
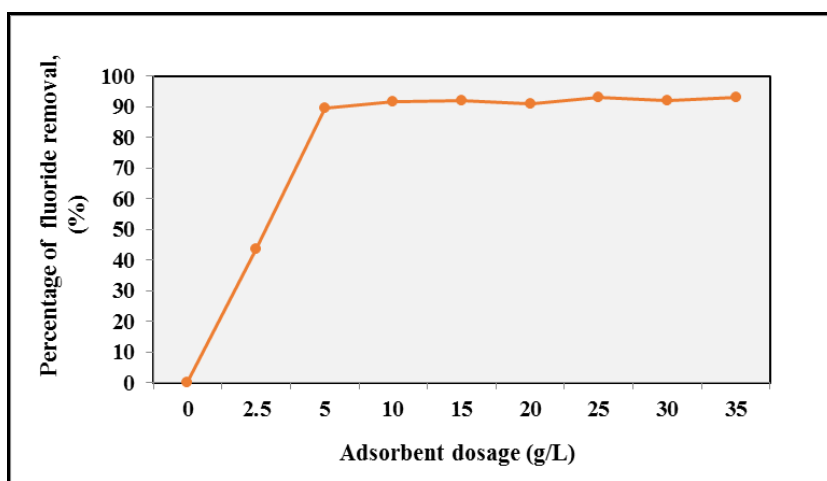
Figure 7.11: Effect of sorbent dosage on defluoridation
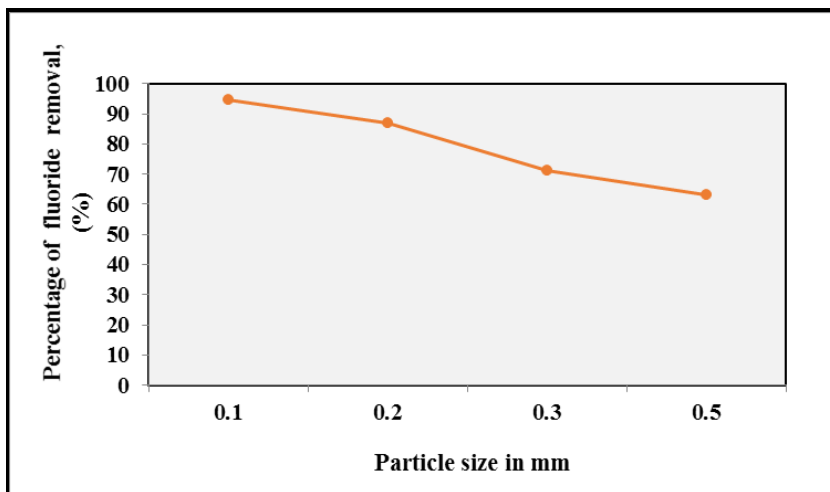
Figure 7.12: Effect of particle size on sorption of fluoride

7.3.3.2.5 Effect of particle size on sorption of fluoride

The adsorption experiment was carried out using activated *Vetiveria zizanioides* with different particle size of 100, 200, 300 and 500 microns at neutral pH. The experiment was conducted at an initial concentration of 10 mg/L, contact time of 120 min, to evaluate the effect of particle size on the fluoride removal efficiency. The effect of particle size on fluoride sorption is given in Figure 7.12. Increase in particle size from 100 to 500 micron reduces the sorption level. The defluoridation efficiency of the activated *Vetiveria zizanioides* with 100 microns (0.1 mm) registered high defluoridation efficiency (94.5 %) due to larger surface area. The smaller particles provide more sorption sites and surface area leading to greater sorption. Hence, the sorbents with particle size of 100 microns has been preferred for further experiments.
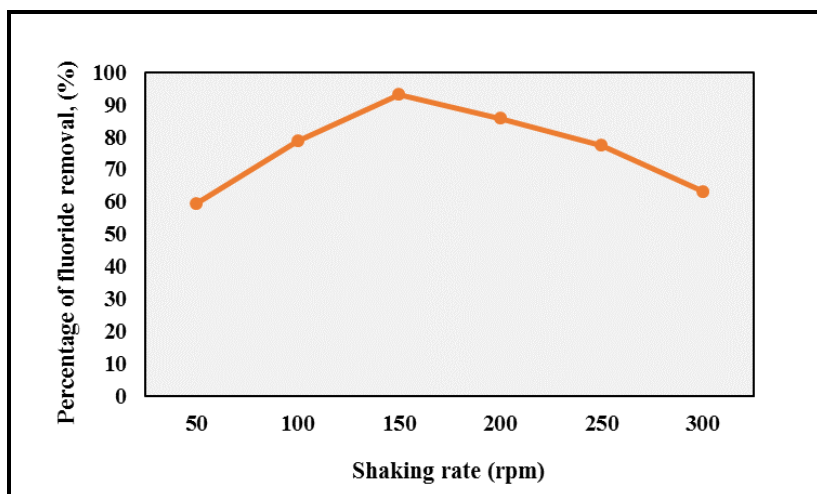
Figure 7.13: Effect of shaking rate on sorption of fluoride

7.3.3.2.6   *Effect of shaking rate on defluoridation*

The influence of varying stirring rate on the removal efficiency of fluoride of activated *Vetiveria zizanioides* is depicted in Figure 7.13. The determination of optimum shaking rate is an important step in water treatment process because shaking consumes energy and it affects the adsorption efficiency. The maximum removal efficiency (93.1 %) was obtained at 150 rpm. From the results, the fluoride removal efficiency recorded lowest at 50 rpm and improved as the shaking rate increases and reached the maximum efficiency at 150 rpm. When shaking of the mixture was taking place, rapid movement of the solid particle in the solution occur and this increases the concentration of fluoride near the surface of the solid adsorbents. This leads to the maximum collision frequency between adsorbent & adsorbate (Kass et al., 2005). Further increase in shaking speed to 300 rpm leads to a declined removal efficiency. Under high shaking rate, sufficient additional energy is

available to break newly formed bonds between the fluoride ions and the adsorbent surface (Argun et al., 2007).

7.3.3.2.7 *Effect of temperature on defluoridation*

As the temperature is a major influencing factor in the sorption process, the sorption of activated *Vetiveria zizanioides* was carried out at different temperatures under the optimized condition. Initially, no significant effect (slight increase) of sorption of fluoride observed with slightly varying temperature (303, 305, 307, 309 and 313K). But an increase in fluoride sorption was observed when sorption study was conducted at four different temperatures 303, 313, 323 and 333K. Results are tabulated in Table 7.2.

Table 7.2: Percentage of fluoride removal under different temperature

C_0 (mg/L)	C_e (mg/L)				q_e (mg/g)				Percentage of fluoride removal (%)			
	303K	313K	323K	333K	303K	313 K	323K	333K	303K	313K	323K	333K
10.45	0.63	0.61	0.47	0.31	1.96	1.97	2.00	2.03	94.00	94.20	95.50	97
15.53	2.73	2.67	2.14	1.79	2.56	2.57	2.68	2.75	82.40	82.80	86.20	88.5
20.06	4.61	4.41	3.75	3.17	3.09	3.13	3.26	3.38	77.00	78.00	81.30	84.2
25.32	8.66	8.56	7.24	6.56	3.33	3.35	3.62	3.75	65.80	66.20	71.40	74.1
30.13	13.50	13.29	12.11	10.70	3.33	3.37	3.60	3.89	55.20	55.90	59.80	64.5

The increase in the amount of fluoride adsorbed with temperature indicates the endothermic nature of the process. The adsorption capacity of fluoride will be enhanced with temperature and is attributed to the possible increase in the number of active sites available for adsorption on the surface. The increase in temperature leads to an increase in kinetic

energy of fluoride ion which increases the collision frequency between the adsorbent and adsorbate. Hence, greater adsorption of fluoride ion on the surface of the adsorbent particles (Oguz, 2005). Similar trend was reported by Karthikeyan and Ilango (2007) while studying fluoride sorption using *Morringa indica* based activated carbon as adsorbent.

7.3.3.3 Adsorption isotherm models

The aim of the sorption isotherms is to reveal the exact relation between the equilibrium concentration of adsorbate in the bulk and the adsorbed amount at the surface. The isotherm results of fluoride on activated *Vetiveria zizanioides* at four different temperatures (303, 313, 323and 333K) were evaluated using four important isotherms including the Langmuir, Freundlich, Temkin, and Dubinin–Redushkevich (D-R) isotherm models.

7.3.3.3.1 *Langmuir Adsorption Isotherm*

The Langmuir adsorption isotherm is the mostly used and considered as the best known of all isotherms (Adane et al., 2015). It is based on the assumption that maximum adsorption corresponds to a saturated monolayer of solute molecules on the adsorbent surface, with no lateral interaction between the adsorbed molecules. The Langmuir adsorption isotherm has been successfully applied in various monolayer adsorption processes to describe process (Eastoe & Dalton, 2000). The non-linear expression of Langmuir model is represented as equation (6).

$$q_e = \frac{q_m\ K_L\ C_e}{1+ K_L\ C_e} \qquad (6)$$

where C_e, is the equilibrium concentration of fluoride ion in solution (mg/L), q_e is the amount of fluoride adsorbed per unit mass of adsorbent at equilibrium (mg/g), q_m (mg/g) is the maximum amount of fluoride per unit mass of adsorbent to form a complete monolayer on the surface bound at high C_e or the adsorption capacity of the adsorbent and K_L is the adsorption equilibrium constant (L/mg). The linearized form Langmuir equation can be illustrated as equation (7).

$$\frac{C_e}{q_e} = \frac{1}{q_m \ K_L} + \frac{C_e}{q_m} \qquad (7)$$

The linear plot of specific sorption (C_e/q_e) against the equilibrium concentration (C_e) (Figure 7.14(a)) indicates that the sorption of fluoride on activated *Vetiveria zizanioides* obeys the Langmuir isotherm model. Parameters for calculating Langmuir isotherm model at temperatures of 303K, 313K, 323K and 333K are tabulated in Table 7.5. The Langmuir constants q_m and K_L were obtained from the slope and intercept of the plot and are given in Table 7.6. The essential characteristics of the Langmuir isotherm i.e., the favourable nature of adsorption can be expressed in terms of a dimensionless constant separation factor R_L that is calculated by equation (8).

$$R_L = \frac{1}{1 + K_L \ C_0} \qquad (8)$$

where K_L is the Langmuir constant and C_0 is the initial concentration of the fluoride ion in the solution. There are four probabilities for the R_L value (Zheng et al., 2009) and are shown in Table 7.3.

Table 7.3: The four probabilities for the R_L value

R_L value	Type of isotherm
$R_L = 0$	Irreversible sorption
$0 < R_L < 1$	Favourable sorption
$R_L > 1$	Unfavourable sorption
$R_L = 1$	Linear sorption
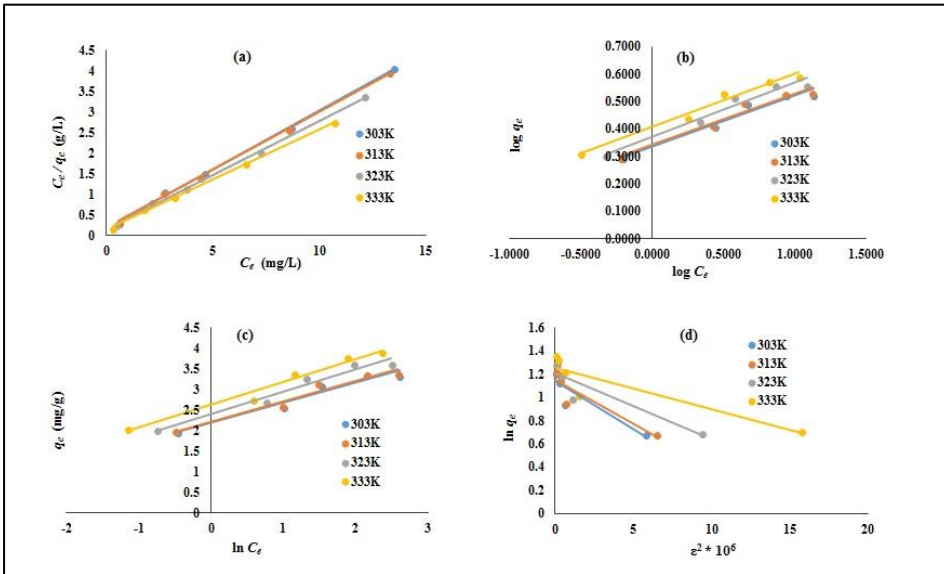
Figure 7.14: Linear plot of adsorption isotherm at 303K, 313K, 323K and 333K. (a) Langmuir, (b) Freundlich, (c) Temkin and (d) D-R isotherm

The variation of separation factor (R_L) was plotted against initial fluoride concentration and shown in Figure 7.15. The R_L values at 303K,

313K, 323K and 333K which were calculated using Langmuir constant are tabulated in Table 7.4. The R_L values for activated *Vetiveria zizanioides* at different temperatures were found in the range of 0.0607 - 0.0194 which indicates that the sorption of fluoride on activated *Vetiveria zizanioides* is favourable. Also, the R_L value does not reached to zero with the increase of C_0 suggests that the sorption of fluoride on activated *Vetiveria zizanioides* is favourable under the conditions used for the experiments.
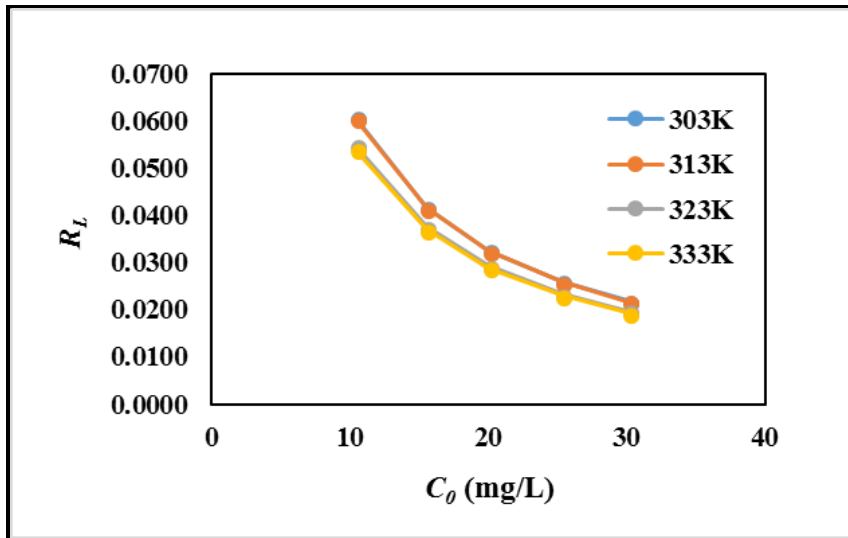
Figure 7.15: The variation of separation factor (R_L) with initial fluoride concentration

Table 7.4: R_L values at different temperatures

C$_0$ (mg/L)	R_L value			
	303K	**313K**	**323K**	**333K**
10.45	0.0607	0.0604	0.0548	0.0540
15.53	0.0417	0.0415	0.0375	0.0370
20.06	0.0326	0.0324	0.0293	0.0289
25.32	0.0260	0.0259	0.0234	0.0230
30.13	0.0219	0.0218	0.0197	0.0194

7.3.3.3.2 Freundlich Adsorption Isotherm

An empirical adsorption isotherm for non-ideal systems was presented by a German physical chemist, Herbert Max Finley Freundlich in 1906. The Freundlich model assumed that the strongest binding sites are occupied first, and the binding strength decreases with the increasing degree of site occupation and has been applied to the adsorbent with heterogeneous surface (Yaacoubi et al., 2015). The non-linear form of Freundlich equation is as follows:

$$q_e = K_f C_e^{1/n} \tag{9}$$

where q_e is the amount of fluoride ion adsorbed on activated *Vetiveria zizanioides* at equilibrium (mg/g) and C_e is the equilibrium concentration of fluoride ion in solution (mg/L). Freundlich constants, K_f indicates the sorption capacity of the adsorbent (mg/g (L/mg)$^{1/n}$), and *n*

gives an indication the favourability of the sorption process or the adsorption intensity. The slope ranges between 0 and 1 is a measure of adsorption intensity or surface heterogeneity, becoming more heterogeneous as its value gets closer to zero. Whereas, a value below unity implies chemisorption process where 1/n above one is an indicative of cooperative adsorption (Foo & Hameed, 2010). To determine the constants K_f and n, equation (9) may be converted to a linearized form by taking logarithms.

$$\log q_e = \log K_f + \frac{1}{n} \log C_e \qquad (10)$$

The plot of log q_e versus log C_e of equation (10) resulted in a straight line. The values for n and K_f can be obtained from the slope and intercept of the plot (Figure 7.14(b)) and are presented in Table 7.6.

7.3.3.3.3 *Temkin isotherm*

The Temkin isotherm considered the effects of some indirect adsorbate/adsorbate interaction on adsorption isotherms (Temkin & Pyzhev, 1940). This isotherm assumes that (1) the heat of adsorption of all molecules in the layer decreases with coverage due to adsorbate-adsorbent interaction, and (2) adsorption is characterized by a uniform distribution of binding energies, up to some maximum binding energy (Mondal et al., 2012). The Temkin model is represented by the equation (11)

$$q_e = \left(\frac{RT}{b}\right) \ln \left(A \, C_e\right) \qquad (11)$$

The Temkin model is linearly represented as equation (12) and generally applied in the form:

$$q_e = B \ln A + B \ln C_e \qquad (12)$$

where q_e is the amount of fluoride adsorbed at equilibrium (mg/g), C_e is concentration of fluoride in solution at equilibrium (mg/L) and A is the Temkin isotherm constant (L/g). B is a constant related to the heat of adsorption and it is defined by the expression B = RT/b. b is the Temkin constant linked to the energy parameter (J/mol), R is the gas constant (8.314 J/mol K) and T is the absolute temperature (K). The constants A and B are calculated from the intercept and slope of the plot of q_e vs. ln C_e and are tabulated in Table 7.6. The linear plots of Temkin isotherm of fluoride sorption on activated *Vetiveria zizanioides* at temperatures of 303K, 313K, 323K and 333K are shown in Figure 7.14(c).

7.3.3.3.4 Dubinin-Radushkevich isotherm or D–R model

D-R model is generally useful to express the adsorption mechanism with a Gaussian energy distribution onto a heterogeneous surface (Foo & Hameed, 2010). The equilibrium data (Table 7.5) were applied to Dubinin-Radushkevich isotherm which was usually applied to distinguish the physical and chemical adsorption of ions (Dubinin, 1960). The Dubinin-Radushkevich isotherm is expressed as the following equation:

$$q_e = q_m \exp\left(-\beta \varepsilon^2\right) \qquad (13)$$

The linear form of equation (13) is given as

$$\ln q_e = \ln q_m - \beta\varepsilon^2 \qquad (14)$$

where q_e is the amount of fluoride adsorbed onto activated *Vetiveria zizanioides* (mg/g) and q_m is the theoretical monolayer sorption capacity or saturation capacity (mg/g). β is the constant of the sorption energy (mol^2/kJ^2), which is related to the average energy of sorption per mole of the adsorbate as it is transferred to the surface of the solid from infinite distance in the solution (Dubinin et al., 1947; Zheng et al., 2009). The intercept and slope of the plot ln q_e versus ε^2 gives the values of q_m and β (Figure 7.14(d)) and are listed in Table 7.6. ε is Polanyi potential, which can be calculated as follows:

$$\varepsilon = RT \ln\left(1 + \frac{1}{C_e}\right) \qquad (15)$$

where R is the gas constant and is equal to 8.314 J/mol K and T is the solution temperature (K). E is the value of mean sorption energy (kJ/mol), can be calculated using D–R parameter β as equation (16)

$$E = \frac{1}{\sqrt{2\beta}} \qquad (16)$$

In addition, the Langmuir and Freundlich, the Dubinin–Radushkevich equation was also used for the determination of adsorption energy (E). The magnitude of E can also provide useful information on adsorption mechanisms, such as ($E < 8$ kJ/mol) for physical adsorption, ($8 < E < 16$ kJ/mol) for chemical adsorption (Dubinin et al., 1947; Zheng et al., 2008).

Table 7.5: Parameters for Langmuir, Freundlich, Temkin and
Dubinin - Radushkevich Adsorption Isotherms

Temperature (K)	C_0 (mg/L)	C_e (mg/L)	log C_e	ln C_e	q_e (mg/g)	log q_e	ln q_e	C_e/q_e (g/L)	ε^2
	10.45	0.63	-0.203	-0.467	1.96	0.293	0.675	0.319	$5.770176 * 10^6$
	15.53	2.73	0.437	1.006	2.56	0.408	0.940	1.068	$0.616900 * 10^6$
303	20.06	4.61	0.664	1.529	3.09	0.490	1.128	1.494	$0.244229 * 10^6$
	25.32	8.66	0.937	2.159	3.33	0.523	1.204	2.599	$0.075793 * 10^6$
	30.13	13.50	1.130	2.603	3.33	0.522	1.202	4.058	$0.032413 * 10^6$
	10.45	0.61	-0.217	-0.501	1.97	0.294	0.677	0.308	$6.431163 * 10^6$
	15.53	2.67	0.427	0.983	2.57	0.410	0.945	1.039	$0.684777 * 10^6$
313	20.06	4.41	0.645	1.485	3.13	0.495	1.141	1.410	$0.282483 * 10^6$
	25.32	8.56	0.932	2.147	3.35	0.525	1.210	2.553	$0.082701 * 10^6$
	30.13	13.29	1.123	2.587	3.37	0.527	1.214	3.945	$0.035656 * 10^6$
	10.45	0.47	-0.328	-0.754	2.00	0.300	0.691	0.236	$9.370792 * 10^6$
	15.53	2.14	0.331	0.762	2.68	0.428	0.985	0.800	$1.057572 * 10^6$
323	20.06	3.75	0.574	1.322	3.26	0.513	1.182	1.150	$0.402742 * 10^6$
	25.32	7.24	0.860	1.980	3.62	0.558	1.285	2.003	$0.120665 * 10^6$
	30.13	12.11	1.083	2.494	3.60	0.557	1.282	3.361	$0.045383 * 10^6$
	10.45	0.31	-0.504	-1.160	2.03	0.307	0.707	0.155	$15.732201 * 10^6$
	15.53	1.79	0.252	0.580	2.75	0.439	1.011	0.650	$1.515383 * 10^6$
333	20.06	3.17	0.501	1.154	3.38	0.529	1.217	0.938	$0.576393 * 10^6$
	25.32	6.56	0.817	1.881	3.75	0.574	1.322	1.748	$0.154389 * 10^6$
	30.13	10.70	1.029	2.370	3.89	0.590	1.358	2.752	$0.061228 * 10^6$

Table 7.6: Langmuir, Freundlich, Temkin and Dubinin–Radushkevich Isotherm constants

Isotherm	Temperature (K)	Linear equation	Correlation coefficient (R^2)	Isotherm parameters
Langmuir	303	y=0.2846x+0.1923	0.9981	q_m = 3.514 (mg/g); K_L=1.4799 (L/mg)
	313	y=0.2813x+0.189	0.9982	q_m = 3.555 (mg/g); K_L =1.488 (L/mg)
	323	y=0.2626x+0.1591	0.9979	q_m = 3.808 (mg/g); K_L =1.651 (L/mg)
	333	y=0.2448x+0.1459	0.9977	q_m = 4.085 (mg/g); K_L =1.678 (L/mg)
Freundlich	303	y=0.1849x+0.3375	0.954	K_f = 2.175 (mg/g) (L/mg)$^{1/n}$; $1/n$ =0.185; n=5.41
	313	y=0.1864x+0.342	0.9507	K_f = 2.198 (mg/g) (L/mg)$^{1/n}$; $1/n$ =0.186; n =5.37
	323	y=0.1962x+0.3723	0.9571	K_f = 2.357 (mg/g) (L/mg)$^{1/n}$; $1/n$ =0.196; n =5.10
	333	y=0.1941x+0.4064	0.9771	K_f = 2.549 (mg/g) (L/mg)$^{1/n}$;$1/n$=0.194; n =5.15
Temkin	303	y=0.4826x+2.1952	0.954	A= 94.509 (L/g); B = 0.4826
	313	y=0.49x+2.2216	0.9513	A= 93.119 (L/g); B = 0.49
	323	y=0.54x+2.4041	0.9574	A= 85.802 (L/g); B = 0.54
	333	y=0.5551x+2.6231	0.9731	A= 112.782 (L/g); B = 0.5551
Dubinin – Radushkevich	303	y= -0.0834x+1.1422	0.8449	β = 0.0834 (mol^2/kJ^2); q_m =3.134 (mg/g); E = 2.449 (kJ/mol)
	313	y= -0.0761x+1.1518	0.8438	β = 0.0761 (mol^2/kJ^2); q_m =3.164 (mg/g); E = 2.563 (kJ/mol)
	323	y=-0.0574x+1.2113	0.8433	β = 0.0574 (mol^2/kJ^2); q_m =3.358 (mg/g); E = 2.951 (kJ/mol)
	333	y=-0.0358x+1.2521	0.8179	β = 0.0358 (mol^2/kJ^2); q_m =3.498 (mg/g); E = 3.737 (kJ/mol)

The equilibrium data of fluoride sorption on activated *Vetiveria zizanioides* at neutral pH and temperatures of 303, 313, 323 and 333K are used to analyse Langmuir isotherm, Freundlich isotherm, Temkin model, and D–R model and the calculated results are tabulated in Table 7.6. The applicability of the isotherm models was analyzed by correlation coefficient (R^2) of respective linear plots. The R^2 values indicate that the adsorption data best fitted the Langmuir adsorption isotherm for all four temperatures (correlation coefficient $R^2 > 0.99$). The correlation coefficient values of the respective linear plots indicate that Freundlich model, Temkin model, and D–R model were found less satisfactory ($R^2 < 0.98$) compared to Langmuir isotherm. R^2 values shows that the Langmuir isotherm model was very appropriate for describing the sorption equilibrium of fluoride on activated *Vetiveria zizanioides*. The adsorption capacity of fluoride on activated *Vetiveria zizanioides* was observed maximum at 333K i.e., $q_m = 4.085$ mg/g. The values of q_m calculated by the Langmuir isotherm equation fits were close to those experimentally determined data at all experimental temperature ranges. This suggest that the fluoride is adsorbed in the form of monolayer coverage on the surface of the activated *Vetiveria zizanioides* or the homogeneous distribution of active sites on adsorbent, since the Langmuir equation assumes that the surface is homogeneous. The results show that the value of adsorption energy K_L of the adsorbent increases on increasing the temperature.

However, the Freundlich model, explains multilayer adsorption, fitted well with the correlation coefficient (R^2) range of 0.954 - 0.9771. The exponent (n) is an index of the diversity of free energies related with

the adsorption of the solute by multiple components of a heterogeneous adsorbent. If $n > 1$, then the isotherm is convex and more adsorbate presence on the adsorbent enhances the free energies of further adsorption, the value of $n = 1$ indicates that the isotherm is linear and, when $n < 1$, the isotherm is concave and adsorbate is bound with weaker and weaker free energies (Hall et al. 1966 and Adane et al. 2015). Under all the four temperatures conditions, the value of Freundlich constant n was found to be larger than 1 (5.41 - 5.15) which suggests the favourable adsorption conditions. The Freundlich adsorption constant (K_f) value for all four temperature conditions (303, 313, 323 and 333K) determined from the intercept of the linear plots (Figure 7.14(a)) were fall between 2.175 and 2.549 (mg/g) (L/mg)$^{1/n}$ and the value is an indication of the adsorption capacity of the adsorbent. The value of K_f increased with increase in temperature. Maximum K_f value was observed at 333K, which confirms that the adsorption reaction was endothermic in nature.

For the Temkin isotherm, R^2 was in the range of 0.954 to 0.9731 with an average value of 0.959 and for the Dubinin-Radushkevich isotherm, it ranged from 0.8449 to 0.8179, with an average value of 0.8375. The E value was found (Table 7.6) in the range of 2.449 – 3.737 kJ/mol, indicating that the type of sorption of fluoride on activated *Vetiveria zizanioides* is essentially physical sorption process. The adsorption isotherm models fitted the equilibrium data, based on the correlation coefficient, in the order of: Langmuir isotherm > Freundlich isotherm > Temkin isotherm > Dubinin–Radushkevich isotherm.

7.3.3.4 Batch kinetic studies

Defluoridation studies were performed in order to investigate the sorption kinetics of fluoride on the adsorbent, activated *Vetiveria zizanioides* using Lagergren's pseudo first-order, pseudo second-order, diffusion models, and Elovich model. The pseudo-first-order (Lagergren's first-order) rate equation can be written as follows (Lagergren, 1898):

$$\log (q_e - q_t) = \log q_e - \frac{k_1 t}{2.303} \qquad (17)$$

where q_e and q_t are the amount of fluoride adsorbed per mass of adsorbent (mg/g) at equilibrium and time t (min), respectively and k_1 is Lagergren's first order rate constant (min^{-1}).

The Lagergren's first-order rate constants k_1 and q_e are determined from the slope and intercept of the plot log $(q_e - q_t)$ versus t and are exhibited in Table 7.7, along with the corresponding correlation coefficients (R^2). Pseudo first-order kinetic plot of different initial concentrations is depicted in Figure 7.16(a).

It was observed that the calculated q_e values of fluoride did not agree with the experimental q_e values for all the experimental conditions. This suggests that the sorption of fluoride on activated *Vetiveria zizanioides* does not follow first-order kinetics at different initial concentrations (10 - 40 mg/L). Also, the correlation coefficient (R^2) values of the pseudo-first-order kinetics were found in the range of 0.9542 - 0.9876 and this indicates that this model did not fit well.

The kinetics of absorption is determined by Pseudo second-order kinetic model based on the absorption capacity of the solution and can be represented as follows (Hussain et al., 2011):

$$\frac{t}{q_t} = \frac{1}{k_2 q_e^2} + \frac{t}{q_e} \tag{18}$$

where q_t is the amount of fluoride adsorbed (mg/g) at time t (min). The equilibrium sorption capacity (q_e) and the second-order constant k_2 (g/mg min) can be determined by plotting changes of t/q_t against t. The k_2 and q_e are calculated from the intercept and slope of the linear plot (Figure 7.16(b)) and are listed in Table 7.7 along with the corresponding correlation coefficients.

It was observed that for all the four different initial concentrations, the values of calculated q_e from the pseudo-second-order were closer to experimental q_e than that calculated from the pseudo-first-order. This indicated the better applicability of the pseudo second-order kinetic model for the defluoridation by sorption using activated *Vetiveria zizanioides*. The linear plots of pseudo second-order model resulted in higher R^2 values than the pseudo first- order. The R^2 values of pseudo second-order ranged between 0.9971 - 0.9991. Similar phenomenon has been observed in the sorption of fluoride on chitin/cellulose composite (Jayapriya et al., 2011)
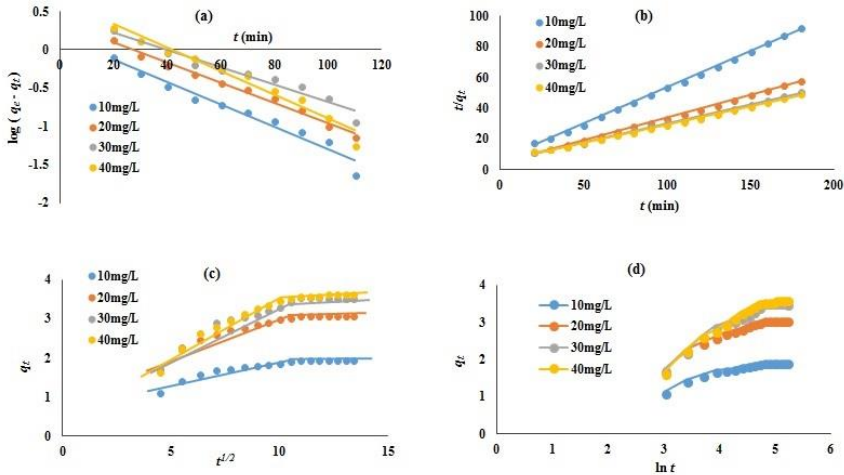
Figure 7.16: Kinetic modeling of adsorption of fluoride (a) Pseudo first-order; (b) Pseudo second-order; (c) Intraparticle diffusion models and (d) Elovich model

The sorption process follows a complex phenomenon accompanied by both the surface and the pore diffusion, but to different extents. Estimation of the extend of a particular diffusion to the total process was done by using the plot following the Weber and Morris equation. Weber-Morris proposed the intra-particle diffusion model (Weber & Morris, 1963; Ho et al., 2000) and is expressed as the following form shown in equation (19)

$$q_t = k_{id} \, t^{1/2} + C \qquad (19)$$

where q_t is the amount of fluoride adsorbed (mg/g) at time t (min) and k_{id} is the intra particle diffusion rate constant (mg/g min$^{1/2}$). The value of the intraparticle diffusion coefficient was estimated from the slope of the plot (Figure 7.16(c)) of q_t against $t^{1/2}$ and listed in Table 7.7. The value of intercept C gives an idea about the boundary layer thickness, i.e. the larger intercept value indicates the greater boundary effect. If a linear plot passing through the origin is obtained then it suggests that the intraparticle diffusion process contributes predominantly in rate determining step. However, if multi-linear plots are resulted, then the sorption process influenced by two or more steps. Multi-linearity in q_t versus $t^{1/2}$ plot (i.e., two or three steps are involved) indicates that the first step involves the external surface adsorption or instantaneous adsorption; the gradual adsorption step is the second step, where intra-particle diffusion is controlling; and the third step is the final equilibrium step, where the solute moves slowly from larger pores to micro pores causing a slow adsorption rate. The variations in the parameters such as solute concentration, temperature, and adsorbent particle size influences the time required for the second step (Gandhi et al., 2016).

It was noticed from Figure 7.16(c) that there are two separate stages involved in the fluoride sorption process i.e., the first linear portion indicates the Stage I and the second curved path followed by a plateau indicates Stage II. Rapid fluoride sorption by adsorbent occurred in Stage I. This is because of that most readily available adsorbing sites on the adsorbent surfaces are immediately utilized by the fluoride ion. Very slow diffusion of adsorbate from surface site into the inner pores is observed in Stage II. Hence, initial portion of fluoride adsorption by

adsorbents may be governed by the initial intra-particle transport of fluoride controlled by surface diffusion process and later part is controlled by pore diffusion. Therefore, the adsorption process of fluoride onto activated *Vetiveria zizanioides* involves surface adsorption as well as intraparticle diffusion. Similar dual nature with initial linear and then plateau was reported by Singh and Majumder (2016) and Liao and Shi (2005). It was observed that the correlation coefficients were not satisfactory. The intraparticle diffusion model gives straight lines with correlation coefficient (R^2) less than 0.98 for all the four different initial concentrations, the intercept of the line fails to pass through the origin in each case. This can be clarified by difference in the rate of mass transfer in the initial and final stages of adsorption process and indicates some degree of boundary layer control which suggests that intra-particle diffusion is not only rate controlling step (Meenakshi & Vishwanathan, 2007; Kumar et al., 2009).

The simplified Elovich kinetic model equation can be expressed as equation 20 (Farahmand, 2016),

$$q_t = \frac{1}{\beta}\ln(\alpha\beta) + \frac{1}{\beta}\ln t \qquad (20)$$

where α and β is the initial desorption rate (mg/ (g min)) and the desorption constant (g/mg) respectively, during any experiments. Both the constant values of Elovich equation can be achieved from the slope and intercepts of plot of q_t versus ln t. The slope i.e., 1/β value reflects the number of sites available for adsorption whereas the intercept i.e., the value of 1/β ln (αβ) indicates the adsorption quantity when ln t equal to

zero (Ahmad et al., 2014). Elovich model plots for fluoride sorption on activated *Vetiveria zizanioides* at various initial fluoride concentrations at 303K is shown in Figure 7.16(d). The α, β and R^2 values were listed in Table 7.7. The correlation coefficient R^2 was found < 0.98 so this model was less satisfactory.

Table 7.7: Kinetics data of Pseudo-first-order, Pseudo-second-order, Intraparticle diffusion model and Elovich kinetic model

Initial fluoride concentration, mg/L	$q_{e,exp}$ (mg/g)	Pseudo-first-order kinetic model			Pseudo-second-order kinetic model			Intraparticle diffusion model			Elovich kinetic model		
		k_1 (min^{-1})	$q_{e,cal}$ (mg/g)	R^2	k_2 (g/mg min)	$q_{e,cal}$ (mg/g)	R^2	k_{id} (mg/g min$^{1/2}$)	C (mg/g)	R^2	α (mg/g min)	β (g /mg)	R^2
10	1.93	0.0336	1.46	0.9609	0.0350	2.12	0.9991	0.0728	1.09	0.7972	0.880	3.03	0.9013
20	3.09	0.0304	2.29	0.9876	0.0193	3.40	0.9987	0.1247	1.62	0.8176	1.006	1.78	0.9157
30	3.54	0.0263	2.87	0.9542	0.0108	4.06	0.9971	0.1777	1.42	0.8595	0.490	1.26	0.9424
40	3.58	0.0355	4.41	0.9631	0.0094	4.23	0.9973	0.1945	1.32	0.864	0.407	1.15	0.9488

7.3.3.4.1 Fitness of the kinetic models

Fitness of the sorption kinetic models were evaluated using correlation coefficient and sum of squares of the error (SSE or ERRSQ). Higher value of correlation coefficient (R^2) indicates a better fitness of the sorption data. Based on R^2 value, it was identified that the pseudo-second-order was a better fit than pseudo-first-order, intraparticle diffusion model and Elovich model. The sum of square of errors (SSE) is the most widely used error function (Mane et al., 2007) and it was used to assess the validity of kinetic models for fitting the sorption data. Lower SSE values suggests better fit to the sorption data and the SSE values are calculated by the following equation (Subramanyam & Das, 2014; Ayawei et al., 2017):

$$\text{SSE} = \sum_{i=1}^{n} \left(q_{e,cal} - q_{e,exp} \right)_i^2 \qquad (21)$$

where $q_{e,\ calc}$ is the theoretical concentration of fluoride on the activated *Vetiveria zizanioides*, which have been calculated from the kinetic models and $q_{e,\ exp}$ is the experimentally measured adsorbed solid phase concentration of the adsorbate adsorbed on the adsorbent. The $q_{e,\ calc}$ obtained from pseudo-first-order and the pseudo-second-order kinetic model was compared with its $q_{e,\ exp}$ value i.e., experimentally measured q_e value and its SSE were calculated using equation (21). The SSE values are listed in Table 7.8, which shows that the lowest SSE values were obtained for Pseudo second-order kinetic model. Pseudo-second-order model has lower SSE values indicating that the adsorption of fluoride on the activated *Vetiveria zizanioides* follows second order kinetic model.

Table 7.8: SSE of pseudo-first-order and the pseudo-second-order kinetic model

Initial fluoride concentration, mg/L	Sum of squares of the error (SSE)	
	Pseudo first-order kinetic model	Pseudo second-order kinetic model
10	0.2216	0.0331
20	0.6441	0.0967
30	0.4594	0.2688
40	0.6749	0.4221

7.3.3.5 Thermodynamic parameters

Thermodynamic parameters such as enthalpy change ($\Delta H°$), free energy change ($\Delta G°$) and entropy change ($\Delta S°$) can be used to determine the spontaneity of a process. The decrease in $\Delta G°$ and $\Delta H°$ values with increasing temperature was exhibited by spontaneous process. The thermodynamic parameters ($\Delta G°$, $\Delta H°$ and $\Delta S°$) can be also used recognize the mechanism (physical and chemical adsorption) involved in adsorption process. As the temperature increased from 303K to 333K, an increase in percentage of fluoride removal was observed, which indicating the process to be endothermic. The thermodynamic parameters ($\Delta G°$, $\Delta H°$ and $\Delta S°$) were calculated using the following equations:

$$\Delta G^0 = -RT \ln K_c \qquad (22)$$

The following equation is used to define the relationship of ΔG° to ΔH° and ΔS°:

$$\Delta G^0 = \Delta H^0 - T\Delta S^0 \qquad (23)$$

The Van't Hoff equation is found by substituting equation (22) into equation (23)

$$\ln K_c = \frac{-\Delta H^0}{R} * \frac{1}{T} + \frac{\Delta S^0}{R} \qquad (24)$$

Where T is the absolute temperature solution in Kelvin (K) and R is the universal gas constant (8.314 J/mol K). ΔG° is directly determined from the equation (22). ΔH° and ΔS° can be obtained from the slope and intercept of the linear Van't Hoff plot of ln K_c versus 1/T. K_c the equilibrium constant, must be dimensionless and is derived from the Langmuir constant (K_L). Here, the unit of K_L is expressed in L/mg. Zhou and Zhou (2014) recommended a relationship between K_L and K_c i.e., K_c can be found as dimensionless by multiplying K_L by the molecular weight of adsorbate (F: 18.9984 g/mol), 1000, and then 55.5 Eq. (25) (Anastopoulos & Kyzas, 2016; Tran et al., 2016).

$$K_c = (18.9984 * 55.5 * 1000 * K_L) \qquad (25)$$

where the term (18.9984 * 55.5 * 1000 * K_L) is dimensionless and the fact 55.5 is the number of moles of pure water per litre.

$$\Delta G^0 = -RT \ln (18.9984 * 55.5 * 1000 * K_L) \qquad (26)$$

$$\ln (18.9984 * 55.5 * 1000 * K_L) = \frac{-\Delta H^0}{R} * \frac{1}{T} + \frac{\Delta S^0}{R} \qquad (27)$$

The thermodynamic parameters of sorption of fluoride using activated *Vetiveria zizanioides* were calculated using equation (25, 26 and 27). The obtained results are exhibited in Table 7.9. The $\Delta G°$ values are found to be negative for all studied temperature conditions (303K-333K), indicates the spontaneous nature of adsorption of fluoride on activated *Vetiveria zizanioides*. The negative quantity of $\Delta G°$ point out that the adsorptive process will occur favourably and spontaneously at a given temperature and the values of $\Delta G°$ vary between -35.924 and -39.829 kJ/mol, which indicates physical adsorption. The positive sign of $\Delta H°$ value indicates the endothermic nature of the sorption process, which was proved by the increase in the adsorption capacity with temperature. An idea about the type of sorption process involved was provided by the magnitude of $\Delta H°$. For physisorption, the heat evolved generally lies in the range of 2.1 - 20.9 kJ/mol, while the heat of chemisorption is in a range of 80 -200 kJ/mol. Hence, the value of $\Delta H°$ (4.017 kJ/mol) confirms that the fluoride adsorption onto activated *Vetiveria zizanioides* is best attributed to a physisorption process (Kannam & Sundaram, 2001; Adane et al., 2015).

The magnitude and sign of $\Delta S°$ show a contributing role in reflecting whether the association of the adsorbate at the solid/solution interface during the adsorption process becomes less random ($\Delta S° < 0$) or more random ($\Delta S° > 0$) (Tran et al., 2016). The positive value of entropy change ($\Delta S°$) 0.1317 kJ/mol indicates a high randomness at the solid/liquid phase with some structural changes in the adsorbate and the adsorbent. This could be because of the increased mobility of adsorbate ions/molecules in the solution with increase in temperature and the higher

affinity of adsorbate on the adsorbent at high temperatures (Saha & Chowdhury, 2011). Moreover, the positive ΔS° value corresponds to the increased degree of freedom of fluoride ions in the solution.

Table 7.9: Thermodynamic parameters for the adsorption of fluoride onto activated *Vetiveria zizanioides* at different temperatures

T	ΔG° (kJ/mol)	ΔH° (kJ/mol)	ΔS° (kJ/mol)
303	-35.924		
313	-37.125		
323	-38.588	4.017	0.1317
333	-39.829		

7.3.3.6 Surface morphology

The surface modification of the fluoride adsorbed material was further confirmed through   Scanning Electron Microscope image. The surface morphology of the adsorbent, activated *Vetiveria zizanioides* particles were observed by using Scanning Electron Microscope image analysis. The morphology of the adsorbent before the adsorption of fluoride is shown in SEM image (Figure 7.17) and the image of fluoride loaded activated *Vetiveria zizanioides* is exhibited in Figure 7.18. It was observed that, SEM micrographs of adsorbent before fluoride sorption was somewhat smooth but after fluoride adsorption the surface became much rockier in appearance.
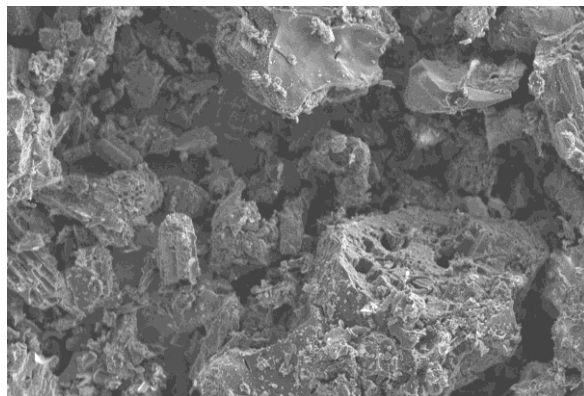
Figure 7.17: SEM images of activated *Vetiveria zizanioides* before fluoride adsorption (x 500 magnification)
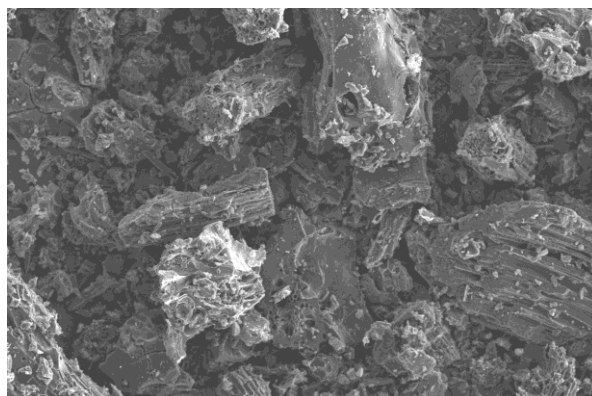
Figure 7.18: SEM images of activated *Vetiveria zizanioides* after fluoride adsorption (x 500 magnification)

7.3.3.7 Sorption - desorption cycle

Water purification based on adsorption technology is economically viable if the adsorbent is regenerable and reusable in many cycles of operation. Besides, reuse of adsorbent helps to reduce

environmental impacts related with disposal of used adsorbents. For analysing the desorption capacity of the activated *Vetiveria zizanioides*, the sorbent was subjected to an adsorption at an initial fluoride concentration of 4 mg/L. The effect of various reagents used for desorption was studied by using different solvents as eluent (Figure 7.19(a)).
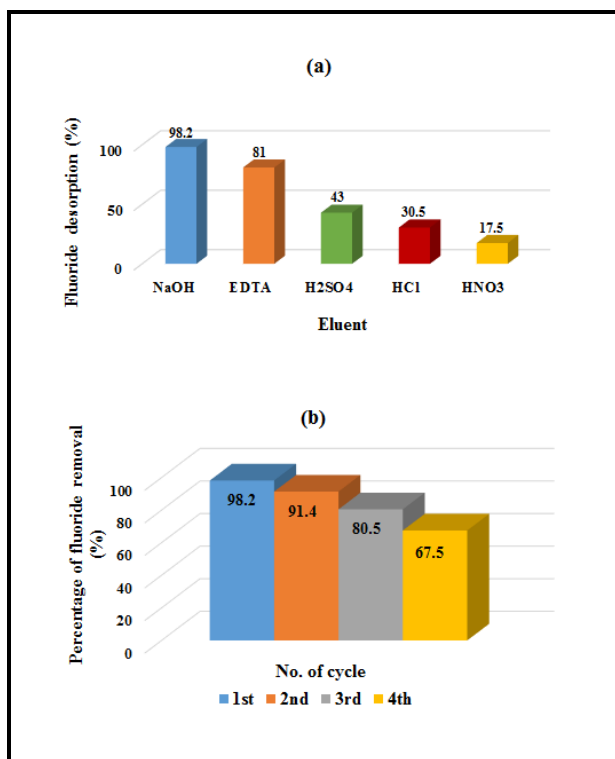
Figure 7.19: (a) Desorption of fluoride by different desorbing agents

(b) Fluoride sorption - desorption cycle

Higher desorption capacity was observed for alkaline solution compared to acidic solutions. From the results, it was identified that 0.1 M NaOH solution was more suitable to be used to regenerate activated *Vetiveria zizanioides,* which desorbed 98.2 % of fluoride ion. A reduction

in sorption efficiency was noticed after each regeneration cycle (Figure 7.19(b)). The vigorous washing of the sorbent causes the gradual dissolution of ion from the adsorbent surface which leads to reduction in sorption efficiency.

7.3.3.8 Column adsorption studies

The batch experiments have shown the better fluoride adsorption capacity of activated *Vetiveria zizanioides*. In this study, continuous flow experiments were also performed to evaluate the column performance for fluoride removal by activated *Vetiveria zizanioides*. Column studies of fluoride on activated *Vetiveria zizanioides* at room temperature are investigated by percolating a 10 mg/L influent concentration at neutral pH value through the column. A column (30 cm length and 2 cm internal diameter) was packed with adsorbent for different bed depth. To study the effect of bed depth or the breakthrough point, bed depths were varied by filling the column with 10 g of adsorbent for bed height of 6.4 cm, 15 g of sorbent with bed height of 9.7 cm and 20 g with bed height of 12.7 cm and a constant flow rate of 2 mL/min was maintained. Effluents fluoride concentrations were determined at regular effluent volume or regular time interval. The breakthrough curve is obtained by plotting a graph between the ratios of effluent concentration to initial concentration against the volume of effluent solution and the S shaped breakthrough curves obtained are shown in Figure 7.20. It was noted that the time required to attain breakthrough increased with an increase in bed depth.
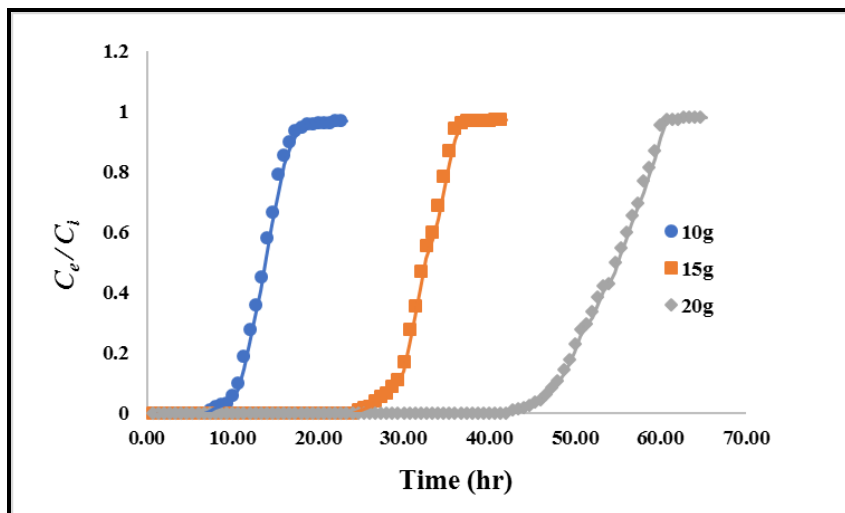
Figure 7.20: Breakthrough curves for different bed depths

The efficiency of fluoride accumulation in a fixed-bed column is dependent on the amount of adsorbent packed inside the column. The breakthrough time was varied with bed height. For the lowest bed depth (6.4 cm), the curve was steeper which indicates the rapid exhaustion of the bed. Steeper breakthrough curves were attained with a reduction in bed depth. Due to the restricted binding sites at low bed depths, a decreased breakthrough time was observed with a decreasing bed depth from 12.7 to 6.4 cm. The fluoride ions do not have enough time to diffuse into the surface of the adsorbent at low bed depth which cause a reduction in breakthrough time. On the contrary, an increase in bed depth causes the diffusion of the fluoride ion deeper into the activated *Vetiveria zizanioides* due to the increased residence time of fluoride solution inside the column. The typical S-shaped breakthrough curves indicates the favourable adsorption in column study. After reaching the column saturation, it was regenerated using 0.1 M NaOH and washed with

distilled water by passing through the column until pH of the wash effluent attained neutral.

7.3.3.9 Gravity based household water filter for removal of fluoride

Based on the adsorption study of activated *Vetiveria zizanioides*, a simple household water treatment unit for defluoridation was developed. The results from sorption study indicates that the sorbent, activated *Vetiveria zizanioides* possess good defluoridating capacity so it was utilized in the construction of water filter for fluoride removal. The household applicability of activated *Vetiveria zizanioides* was investigated using point-of-use domestic gravity-based water filter for removal of fluoride. Domestic water filter has the capacity of 20 L having a top tank of 7 L capacity and a bottom tank of 13L capacity and runs without electricity (Plates 7.4). Transparent tanks made of food grade plastics was selected which helps to detect if any visibly noticeable contaminations are present. The filtration process was taking place inside the cylindrical chamber fixed inside the upper tank and which was attached to an inlet funnel. The raw water was poured in to the filter through the inlet funnel and then percolate through the cylindrical chamber (7.5 cm height and 8 cm diameter). The top cover and top lid were placed at the top, helps to prevents further contamination of water inside the filter. An easily washable and removable plastic disc containing minute holes was placed between the inlet funnel and cylindrical filtering chamber which helps reduce high flow rate due gravity and also eliminates, if any large particles present in the raw water. A sediment filter was also placed in the top of the cylindrical chamber.

The cylindrical column of the household water filter (7.5 cm height and 8 cm diameter) was packed with three materials in four layers in the order: sand, activated *Vetiveria zizanioides* powder, sand and pebbles having glass wool support. Well cleaned sands and pebbles are used in the study. The efficiency of defluoridation was checked by varying bed height of each layer. The bed height of sand, activated *Vetiveria zizanioides* powder, sand layer and pebbles inside the column was arranged in two different ways, i.e., A (1 cm, 4 cm, 1 cm and 1 cm) and B (1 cm, 3 cm, 1 cm and 2 cm) respectively. Another filtering disc was placed at the end of the cylindrical chamber. The sand layer placed above the activated *Vetiveria zizanioides* layer removes the small particles present in the raw water and the layer of pebbles and filtering disc placed at the bottom of the column ensure better filtration and helps to prevents the entering of adsorbent in the filtered water. The defluoridation of the synthetic solution having varying fluoride concentrations of 2 mg/L, 5 mg/L and 10 mg/L by the domestic filtering unit was tested. The filtered solutions were collected and the residual fluoride content was analyzed. The quantity of water filtered effectively until the fluoride concentration in the effluent overshoot 1.5 mg/L (which is the permitted maximum MCL (maximum contaminant level) in India) was estimated and given in Table 7.10.
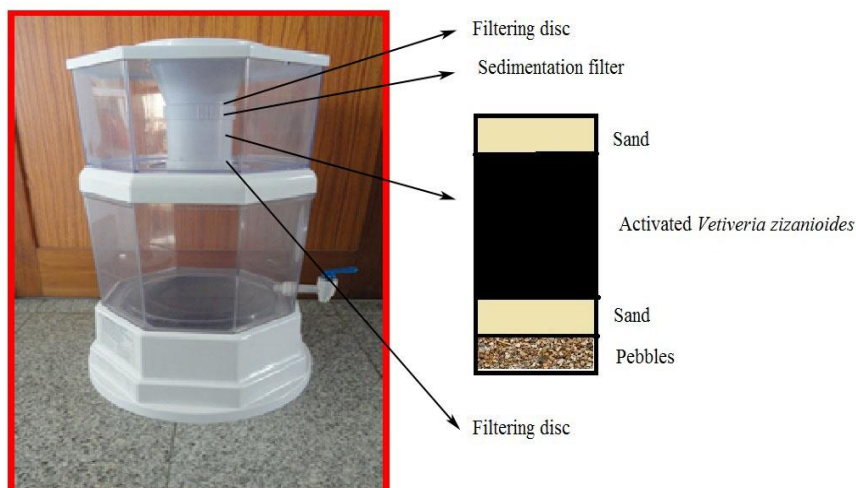
Plate 7.4: Household defluoridation unit

Comparatively, the column of the filter arranged in the order (A) of sand, activated *Vetiveria zizanioides* powder, sand layer and pebbles: (1 cm, 4 cm, 1 cm and 1 cm) was found to be more effective than B (sand, activated *Vetiveria zizanioides* powder, sand layer and pebbles: 1 cm, 3 cm, 1 cm and 2 cm). So, each layer inside column was arranged in the order A for further real water field trial study. From the results, it was observed that point-of-use domestic gravity-based water filter for removal of fluoride was effective for synthetic fluoride solutions having neutral pH at room temperature. After exhaustion, the filter media was regenerated with 0.1 M NaOH solution and washed with ample amount of fresh water or pressure clean it using tap water.

Table 7.10: The quantity of fluoride free water obtained by filtering unit

Initial fluoride concentration, mg/L	Amount of fluoride removed water (< 1.0 mg F/L) obtained, L	
	A	B
2	51.25	36.75
5	23.5	16.5
10	14.75	10.5

7.3.3.10 Application in field level water samples from Palakkad district, Kerala

The defluoridation of the field level samples were performed to check the practical utility of the studied sorbent, activated *Vetiveria zizanioides*. Five water samples from a fluoride-endemic area of Palakkad district, Kerala, India were collected. Five fluoride detected samples were selected from Muthalamada panchayath in Kollangodu block of Palakkad district for testing the practical utility of the household water filter packed with activated *Vetiveria zizanioides*. The details of the selected samples are given in Table 7.11 and the physicochemical parameters determined as per standard methods (APHA, 2012) before and after the treatment are reported in Table 7.12. Fresh plastic bottles

were used to collect ground water samples from bore wells/open wells in the fluoride affected area.

Table 7.11: Details of samples selected for field trial of household water filter for defluoridation

Sl. No.	Sample code	Station	GPS Co-ordinates	Type of source	Panchayath	Block
1	A	Rajappan, Chulliyar medu	N $10^0$36.410' E $76^0$45.568'	Open well	Muthalamada	Kollangodu
2	B	Jailavudeen KSJ Manzil	N $10^0$36.413' E $76^0$45.563'	Open well	Muthalamada	Kollangodu
3	C	Mohanan Nideesh Agro Farm	N $10^0$35.456' E $76^0$47.662'	Bore well	Muthalamada	Kollangodu
4	D	P M Yakoob Govindapuram	N $10^0$36.614' E $76^0$47.270'	Open well	Muthalamada	Kollangodu
5	E	Jailavudeen Manchira	N $10^0$36.593' E $76^0$43.799'	Open well	Muthalamada	Kollangodu

The defluoridation studies of the field level samples were performed at natural pH. pH of the samples ranged between 6.37 - 7.9 and all the selected groundwater samples are observed to be in the neutral pH range except sample E (pH = 7.9). Concentrations of fluoride was detected beyond the BIS limit in all the five samples ranging from 1.8 mg/L to 2.9 mg/L before the treatment using household filter. Among

these five samples, a maximum fluoride concentration of 2.9 mg/L was detected in sample D, which was collected from the area of Govindapuram in Muthalamada panchayath. After the treatment of five groundwater samples, complete elimination of fluoride was observed in sample B and slight fluoride content was detected in remaining four samples but the values observed were well below the acceptable limits of BIS drinking water standards. High alkalinity was observed in all the samples which may increase the interference HCO_3^- ions on the fluoride sorption. Sample E was found to be alkaline in nature and from the batch sorption study of activated *Vetiveria zizanioides* indicated that the sorption process was slow down at alkaline pH range. So, this may be the reason which prevented the complete elimination of fluoride from sample E, collected from Manchira. The results indicate that the household water filter packed with activated *Vetiveria zizanioides* was found to be effective in defluoridation of groundwater samples from the fluoride endemic area, Muthalamada of Palakkad district.

Table 12: Water quality parameters of five field samples before and after treatment

Parameters	Acceptable limit as per BIS	A Before treatment	A After treatment	B Before treatment	B After treatment	C Before treatment	C After treatment	D Before treatment	D After treatment	E Before treatment	E After treatment
pH	6.50-8.50	6.85	6.52	6.88	6.48	7.13	6.89	6.37	6.34	7.90	7.40
EC (micro siemens/cm)		1025.35	660.56	988.73	649.30	890.14	476.06	1049.3	674.65	925.35	508.45
Temperature (^{0} C)		25	27.9	25	27.4	25	26.5	25	26.8	25	27.1
Colour (Hazen)	5	BDL	BDL	BDL	BDL	BDL	BDL	BDL	BDL	BDL	BDL
Turbidity (NTU)	1	BDL	BDL	BDL	BDL	BDL	BDL	BDL	BDL	BDL	BDL
TDS (mg/L)	500	728.00	469.00	702.00	461.00	632.00	338.00	745.00	479.00	657.00	361.00
Fluoride (mg/L)	1	2.00	0.2	2.10	BDL	1.90	0.10	2.90	0.14	1.80	0.34
Total alkalinity (mg/L)	200	326.20	116.00	276.20	74.00	384.60	120.00	280.40	92.00	406.60	140.00
Chloride (mg/L)	250	72.40	70.44	77.21	74.37	22.88	19.17	78.14	75.68	19.07	17.01
Total Hardness (mg/L)	200	520.00	500.00	540.00	508.46	400.00	388.00	538.46	432.00	360.00	336.00
Calcium Hardness (mg/L)		300.00	288.00	400.00	385.00	240.00	228.00	415.00	324.00	340.00	320.00
Calcium (mg/L)	75	120.00	115.20	160.00	154.00	96.00	91.20	166.00	129.60	136.00	128.00
Magnesium (mg/L)	30	53.46	51.52	34.02	30.00	38.88	38.88	30.00	26.24	4.86	3.89
Sodium (mg/L)		62.00	61.00	58.40	55.50	50.50	48.20	79.90	77.20	50.30	50.10
Potassium (mg/L)		10.90	10.40	2.20	2.00	3.10	2.90	12.10	11.50	4.00	3.80
Sulphate (mg/L)	200	56.43	20.52	81.49	46.80	15.28	2.60	77.53	50.60	18.80	3.64
Phosphate-P (mg/L)		0.12	BDL	0.11	BDL	0.25	BDL	0.17	BDL	0.21	BDL
Nitrate - N (mg/L)	45	0.07	0.06	0.12	0.11	0.13	0.11	0.34	0.29	0.21	0.18
Iron (mg/L)	0.3	BDL	BDL	0.02	0.02	0.01	BDL	BDL	BDL	BDL	BDL
Total Coliform, MPN/100ml	Shall not be present in 100 ml sample	$\geq$2400	75	1100	150	93	23	1100	23	$\geq$2400	460
E. coli	Shall not be present in 100 ml sample	Present	Absent	Absent	Absent	Absent	Absent	Present	Absent	Absent	Absent

The parameters other than fluoride was also showed some variations after the treatment. Total alkalinity of the samples before the treatment ranged between 276.2 – 406.6 mg/L. After treatment, the alkalinity was decreased in all the five samples below the acceptable limit as per BIS. Complete removal of phosphate was observed in all the samples and sulphate also showed a decreasing trend after treatment. Chloride, Nitrate, Sodium, Potassium, Calcium and Magnesium exhibited slight variations after treatment of the samples using the household filter. A reduction in total Coliform and *E. coli* was also noticed. The analytical results of the physico-chemical parameters of the field level samples after treatment indicates that gravity-based household water filter was effective for the removal of fluoride.

7.4 Summary

A novel activated carbon adsorbent has been developed for defluoridation of contaminated water samples. Fluoride removal efficiency of some medicinal plant materials like gooseberry (*Phyllanthus emblica*), dried ginger (*Zingiber officinale*), sathavari (*Asparagus racemosus*), pomegranate (*Punica granatum)*, nutmeg (*Myristica fragrans*), kozhinjil (*Tephrosia purpurea*) and karinochi (*Vitex negundo*) were compared during the initial stage of the study and reported an efficiency of 65, 63, 44, 70, 67, 40 and 30 % respectively. The suitability of some easily and locally available plant materials such as ramacham or vetiver root (*Vetiveria zizanioides*), tamarind seed (*Tamarindus indica*), clove (*Eugenia carryophyllata*), neem (*Azadirachta indica*), (*Acacia catechu willd*), coffee husk (*Coffea arabica*) and fern

(*Adiantum aethiopicum* for effectively remediating fluoride contaminated water was also investigated. Ramacham (*Vetiveria zizanioides*) (80 %), Tamarind seed (*Tamarindus indica*) (75 %) and clove (*Eugenia carryophyllata*) (73 %) exhibited better defluoridation efficiency compared to other plant materials. During the second stage of the study, batch adsorption test of vetiver root (*Vetiveria zizanioides*), tamarind seed (*Tamarindus indica*) and clove (*Eugenia carryophyllata*) were conducted by varying contact time, sorbent dosage and particle size. Results indicated that, tamarind seed and clove removed 75 and 70 % of fluoride respectively at adsorbent dosage of 20 g/L of 10 mg/L of fluoride water and vetiver root removes 80 % of fluoride at the same dose. Vetiver root showed a maximum removal (85 %) at a dosage of 24 g/L. The results indicated that the maximum fluoride adsorption takes place at the optimum adsorbent dosage of 24 g/L, equilibration time of 120 min, and a particle size of 0.1 mm for *Vetiveria zizanioides* root powder. For tamarind seed (*Tamarindus indica*) and clove (*Eugenia carryophyllata*), the equilibrium dosage and time found was 20 g/L and 100 min with the particle size 0.1 mm. The results clearly pointed out that, Vetiver root has the potential to be an efficient defluoridating agent, so during the further study, activation of *Vetiveria zizanioides* was carried out to improve its efficiency.

During the third stage of the study, powdered *Vetiveria zizanioides* root was activated using phosphoric acid. The carbonization of the material was conducted for 1 h, 1½ h and 2 h at 600^0C, 700^0C and 800^0C and by altering the impregnation ratio of raw material to activating agent 1:05, 1:1, 1:2 and 1:4. The activated *Vetiveria zizanioides* root

powder prepared by using an impregnation ratio of vetiver root powder to activating agent 1:4 and an activation time of 1 h at 700^0C was selected for further study based on its maximum adsorption capacity. The batch sorptive defluoridation study of powdered activated *Vetiveria zizanioides* was conducted under variable experimental conditions such as pH, initial concentration, agitation time, interfering co-ions, dose of adsorbent, particle size, agitation speed and temperature. The efficiency of fluoride removal was found to be 92.5, 77.1, 58.8 and 44.5 % at initial fluoride concentrations of 10, 20, 30 and 40 mg/L respectively with 5 g/L of adsorbent dosage, at pH 6, shaking speed of 150 rpm at room temperature. The efficiency of fluoride removal was found to be decreased with increase in initial fluoride concentration but the amount of fluoride adsorbed increased. The influence of co-existing anions on the fluoride removal by the sorbent, activated vetiver root, was studied and found to follow the order: PO_4^{3-} > HCO_3^- > SO_4^{2-} > Cl^- ≥ NO_3^-. The minimum contact time for attaining the maximum defluoridation was 120 min and maximum sorption was observed at pH 6, shaking rate 150 rpm and adsorbent dosage of 5 g/L with a particle size of 0.1 mm. The isotherm results indicated that the adsorption process satisfactorily fitted with Langmuir adsorption isotherm which had good correlation coefficient value (R^2 > 0.99) indicating monolayer adsorption. The separation factor (R_L) was found in the range of 0.0607 - 0.0194 indicate the favourable sorption under varying temperature. The maximum adsorption capacity of fluoride on activated *Vetiveria zizanioides* was observed at 333K (q_m = 4.085 mg/g) and the value of adsorption energy K_L of the adsorbent increases on increasing the temperature. The value of

Freundlich constant *n* was found to be larger than 1 (5.41- 5.15) which suggests the favourable adsorption conditions. The value of K_f increased with increase in temperature, which confirms endothermic nature of the adsorption fluoride on activated *Vetiveria zizanioides*. The adsorption isotherm models fitted the equilibrium data, based on the correlation coefficient, in the order of: Langmuir isotherm > Freundlich isotherm > Temkin isotherm > Dubinin–Radushkevich isotherm. The value of Dubinin-Radushkevich mean free energy, *E,* found was < 8 kJ/mol, indicating physisorption.

To identify the rate and kinetics of adsorption process pseudo-first-order, pseudo-second-order, intra-particle diffusion model, and Elovich kinetic model were applied. Pseudo second-order kinetic model was observed better applicable. Weber and Morris intraparticle diffusion model suggests the involvement of surface adsorption as well as intraparticle diffusion. Weber and Morris plots fail to pass through origin which indicated that the process of the mechanism of sorption was complex in nature with the more than one mechanism limiting the rate of adsorption. The evaluation of fitness of the sorption kinetic models were done using correlation coefficient and sum of squares of the error suggest that the adsorption of fluoride on the activated *Vetiveria zizanioides* follows second order kinetic model. SEM micrographs confirmed the adsorption of fluoride ion on the adsorbent surface. The thermodynamic data confirms the endothermic and spontaneous nature of sorption process and also indicates the increased degree of freedom of fluoride ions in the solution. Desorption study identified 0.1 M NaOH solution as the suitable eluent to regenerate activated *Vetiveria zizanioides*. The

typical S-shaped breakthrough curves obtained in the column study indicates the favourable adsorption. Gravity based household water filter for removal of fluoride was developed using activated *Vetiveria zizanioides* and it was applied to the field samples collected from fluoride endemic area of Palakkad district. The active carbon developed from *Vetiveria zizanioides* has been effectively reduce the fluoride level in real groundwater samples below the BIS acceptable limits, and hence, the activated *Vetiveria zizanioides* can be successfully applied to remove fluoride from contaminated water.

DETOXIFICATION OF LEAD, CADMIUM AND COPPER FROM WATER BY USING BIOSORBENTS: EQUILIBRIUM AND THERMODYNAMIC INVESTIGATION

8.1 Introduction

Industrial activities are the major resource of mobilization of many heavy metals in the environment and is of serious concern due to the toxicity of these metals in all forms of life (Al-Garni & Saleh, 2005). As a consequence of unregulated application and inappropriate waste-disposal strategies leads to the release of heavy metals to ecosystem at elevated concentrations. Extremely toxic nature of heavy metals threatens many forms of life by linking the food chain and its nonbiodegradable behaviour is a major apprehension among scientific community. Metals such as mercury, cadmium, copper and silver are markedly more toxic even at very low levels and among the heavy metals, lead, cadmium and mercury have been known as "the big three" due to their potential risks on the bio-environment (Volesky, 1994; Volesky & Holan, 1995; Igwe &

Abia, 2007). When heavy metals are released into the aquatic environment, most of them are strongly retained and their adversative effects can persist for a long time. Thus, it is vital to apply an effective remediation method to wastewaters contaminated with heavy metals.

Treatment of heavy metal contaminated wastewaters are generally done by different methods and among various techniques, adsorption has received much attention and considered as an alternative to conventional precipitation method, especially for water that hold low concentrations of metals and complex forming substances (Patterson, 1975; Erdem & Ozverdi, 2005). In this chapter, the ability of some plant materials and lichens to remove Pb^{2+}, Cd^{2+} and Cu^{2+} from aqueous solution by adsorption has been investigated through batch experiments. Equilibrium sorption isotherm studies, adsorption kinetic and thermodynamic studies of Pb^{2+}, Cd^{2+} and Cu^{2+} ions detoxification from water have been conducted.

8.2 Materials and Methods

8.2.1 Reagents and analytical techniques

All the regents utilised in this study were analytical grade reagents (AR grade), procured from Merck Ltd. India and used without further purification. Stock solutions of Pb^{2+}, Cd^{2+} and Cu^{2+} were prepared by dissolving appropriate quantity of analytical grade chemicals, $Pb(NO_3)_2$, $Cd(NO_3)_2$ and $Cu(NO_3)_2$ in deionised water. Working solutions were prepared by diluting the stock solution with deionised water to desired concentrations. Atomic Absorption Spectrophotometer (AAS)

(Thermo Series) with GF 95 graphite furnace was used to analyse the concentration of heavy metals. The pH adjustments of the solutions were made by using 0.1 mol/L HCl and 0.1 mol/L NaOH and digital pH meter (PCSTestr35 instrument) was used to measure pH of the solutions. The regular calibration of pH meter was carried out by using pH calibration buffers. Morphology and composition of the adsorbents were examined by Scanning Electron Microscopy (SEM) (JEOL Model JSM - 6390LV) and EDS (OXFORD XMX N).

In this chapter we report, two different experiment conducted for heavy metal removal from contaminated water. One is treatment of Pb^{2+}, Cd^{2+} and Cu^{2+} using a herbal plant material of *Caesalpinia sappan* and the second study is biosorption of Pb^{2+} and Cd^{2+} from water by non-living algal biomass of *Tretepohila abietina.*

8.2.2 Removal of lead, cadmium and copper from water using locally available plant *Caesalpinia sappan*

8.2.2.1 Plant material

The medicinal plant, *Caesalpinia sappan* (Family: *Caesalpiniaceae*) is a small thorny tree and is commonly known as Patag. Also, in English known as sappan wood or Brazil wood. Formerly, the sappan wood (Plate 8.1) was utilized in calico printing of cotton, wool and silk but later on, it was largely substituted by synthetic dyes. The wines and meat are being coloured by heart wood and its roots are known as 'yellow wood' are utilised to make yellow dye. The tree was earlier cultivated in south-east Asia for the red dye. The distribution of

Caesalpinia sappan is mainly located in Indian states like Tamilnadu, Kerala, Karnataka, Andra Pradesh and West Bengal (Sarumathy et al., 2011). The nontoxic natural dye, Brazilin is the main component of *Caesalpinia sappan* (sappan wood). Brazilin (6a, 7-dihydro-3, 6a, 10-trihydroxy-benz [b] indeno [1, 2-d] pyran-9 (6H)-one) (Figure 8.1) have an anti-inflammatory action (Kwon et al., 2009) and the pigment is utilised in manufacture of facials which are resistant to light heat and water and are non-irritating. The medicinal plant, sappan wood possess various immunosuppressive activities (Ye et al., 2006), like anti-inflammatory and antibacterial (Nirajan-Reddy et al., 2004), anticancer, and antioxidant etc. Antioxidants are extensively utilized as constituents in dietary supplements in the expectation of maintaining health and preventing disease like coronary heart disease, cancer, and even altitude sickness.

Plate 8.1: *Caesalpinia sappan*

Caesalpinia sappan is also used as a traditional Chinese medicine for activating blood circulation and eliminating stasis. Various biological activities of sappan wood, such as immunomodulation (Choi et al., 1997), protection of the brain, hepato protection (Moon et al., 1992),

anticomplementary, hypoglycemic agent activity, anticonvulsant, xanthin oxidase inhibition and aldose reductase inhibition have been reported. Compounds like phenolics and flavonoids, protosappanin A, protosappanin B, protosappanin E, brazilin, 4-o-methylsappannol have been isolated from sappan wood (Saenjum et al., 2010; Sarumathy et al., 2011). *Caesalpinia sappan* is used in many traditional medicines and Ayurvedic formulations. It is one of the ingredients of drug 'Lukol'™ for the treatment of non-specific leucorrhoea (post IUD) and also, one of the components of famous tooth paste and tooth powder of India, Vicco Vajradanti. The sappan wood is beneficial for stopping bleeding in gums and gives firmness and strength to the gums due to its strong astringent, haemostatic, healing properties. Hence, it is applicable in mobile teeth, aphthous ulcers, stomatitis and gum erosions. Its properties like blood purification, antithirst, antidiabetic, improvement of complexion and several other properties makes the water kept in sappan wood is being widely used as an herbal drink in Kerala.
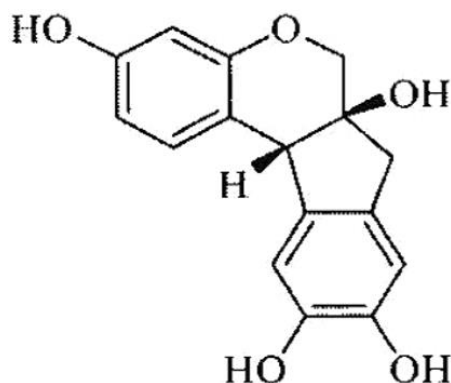
Figure 8.1: The chemical structure of brazilein (Adapted from Lee et al., 2008)

According to Ayurveda, the heartwood is useful in vitiated conditions of pitta, ulcers, wounds, burning sensation, leprosy, skin diseases, dysentery, diarrhoea, epilepsy, diabetes, convulsions, menorrhagia, leucorrhoea, haemoptysis, haemorrhages, stomatopathy and odontopathy (Kirtikar & Basu, 1989; Warriers et al., 1993). Yunani system also utilized the properties of *Caesalpinia sappan* such as healing of wounds and ulcers, stops bleeding from the chest and lungs, beneficial for rheumatism and improvement of complexion. *Caesalpinia sappan* heartwood possess high therapeutic potential and has the ability to protect from UV radiations, can be developed as an effective radio-protective agent. It is used as antimalarial in Malaysia and anti-anaemic in Philippines. The plant is being used worldwide for a large number of medicinal purposes. The heartwood has attained both domestic and international market and being exported from countries like India, Philippines etc. to Europe and USA because of its vast and proven medicinal properties and use as colouring agent (Badami et al., 2004). In the light of *Caesalpinia sappan*'s tremendous health benefits and medicinal values, its ability to eliminate heavy metals such as lead, cadmium and copper from water was investigated in this chapter.

8.2.2.2 Preparation of adsorbent

The barks of sappan wood (*Caesalpinia sappan*) was collected from Kozhikode district in Kerala and were cut down to small pieces. The cut down pieces is washed well using distilled water, open dried in sun light and dried in hot air oven at 110^0 C for five hours. The dried sappan wood is coarsely powdered and sieved. 5 g of sappan wood

powder was boiled with 250 mL of distilled water for 1 h and the powdered heartwood produces a dark red coloured solution in water, when heated. After decanting the solution, again 250 mL of distilled water was added to the same powder and boiled. The process is repeated till the red colour is completely removed. After filtering, the material is kept for drying. The dried powder of sappan wood was then treated with 10 mL of 0.1 M HCl for 1hr under stirring which leads to the loading of H^+ ions on the surface of biosorbent. The excess of H^+ ions on biosorbent was removed by washing with de-ionized water. The filtered sorbent was washed several times with de-ionized water to provide neutral pH. The red colour of the powdered sappan wood was completely removed after this step. It was then dried in an oven at 60^0 C for 1 h. Powdered *Caesalpinia sappan* before and after removing its colour was presented in Plate 8.2.
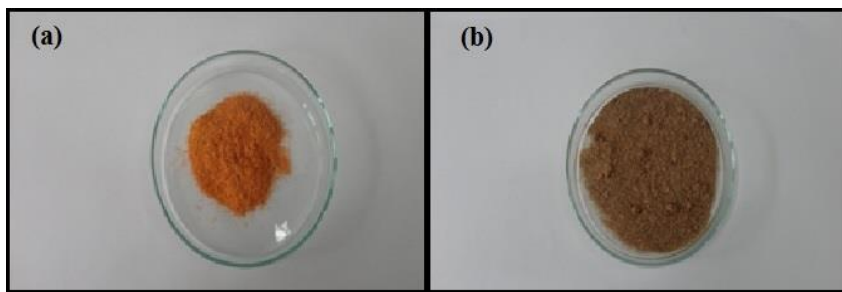
Plate 8.2: (a) Powdered *Caesalpinia sappan* before removing colour (b) Powdered *Caesalpinia sappan* after removing colour (after protonation)

The well dried sappan wood powder was utilized as adsorbent for treatment of lead, cadmium and copper from water. The dried powder of

Caesalpinia sappan was sieved through a range of sieves and only the particles that passed through a 0.3 mm mesh was only used in the study. The separated particles were stored in a clean and air tight containers for further study.

8.2.2.3 Batch sorption experiments

Sorption experiments were conducted in batch conditions to understand the rate and equilibrium data. Single species batch sorption experiments of heavy metals (Pb^{2+}, Cd^{2+} and Cu^{2+}) were conducted. The batch experiments were carried out in 250 mL screw topped flasks by agitating known quantity of the adsorbent, powdered sappan wood with 100 mL of known concentration of heavy metal solutions for a predetermined period in a temperature-controlled shaker. After filtration using Whatmann Filter Paper No. 41, the concentrations of heavy metals (Pb^{2+}, Cd^{2+} and Cu^{2+}) in the filtrate were determined using AAS. All the analysis was done in triplicate to check precision and average values are only reported.

The amount of adsorbate adsorbed at equilibrium, q_e (mg/g) and sorption efficiency (%) was calculated as per equation (1 and 2)

$$q_e = \frac{(C_0 - C_e)V}{m} \qquad (1)$$

$$\text{Sorption efficiency (\%)} = \frac{(C_0 - C_e)*100}{C_0} \qquad (2)$$

where C_0 and C_e are the metal concentrations in the solution before and after treatment, respectively. *V* is the volume of the heavy metal solution (L), *m is* the mass of dry adsorbent used (g).

The influence of important parameters like pH, initial concentration, contact time, temperature, adsorbent dosage and shaking speed were investigated as follows:

8.2.2.3.1 Effect of pH

The effect of solution pH on the sorption of Pb^{2+}, Cd^{2+} and Cu^{2+} on sappan wood (*Caesalpinia sappan*) was examined by varying the initial pH of the solution from pH 2 to 12. pH of the solutions was adjusted using 0.1 mol/L HCl and 0.1 mol/L NaOH and measured by using digital pH meter (PCSTestr35 instrument). The initial concentration of metals was fixed at 10 mg/L.

8.2.2.3.2 Effect of shaking speed

To optimize shaking speed, experiment was conducted by changing the shaking speed from 50 to 300 rpm in speed adjusted shaker. The sorption study was conducted with 10 mg/L of metal solutions having pH 7 at 303K.

8.2.2.3.3 Effect of adsorbent dosage

In 250 mL stoppered bottles, 100 mL of 10 mg/L solutions of Pb^{2+}, Cd^{2+} and Cu^{2+} were agitated with different adsorbent dosage of *Caesalpinia sappan* (1, 2, 3, 4, 5, 10, 15, 20 g/L) to study the effect of adsorbent dosage on sorption of Pb^{2+}, Cd^{2+} and Cu^{2+}. A neutral pH level at a temperature of 303K and shaking speed of 150 rpm for Pb^{2+} and 200 rpm for Cd^{2+} and Cu^{2+} was maintained. The solution from each bottle was

filtered using Whatmann no.41 filter paper and the filtrate was used to analyse residual concentration of Pb^{2+}, Cd^{2+} and Cu^{2+} by AAS.

8.2.2.3.4 *Effect of contact time*

The influence of contact time in sorption of Pb^{2+}, Cd^{2+} and Cu^{2+} on *Caesalpinia sappan* was evaluated for 180 min at regular time intervals of 20 min. An adsorbent dosage of 4 g/L was added to 10 mg/L of metal solutions at 303K. Shaking speed of 150 rpm for Pb^{2+} and 200 rpm for Cd^{2+} and Cu^{2+} was maintained

8.2.2.3.5 *Effect of initial concentration*

The effect of initial concentration on the efficiency of heavy metals adsorption were analysed by varying the initial concentrations of Pb^{2+}, Cd^{2+} and Cu^{2+} from 5 to 45 mg/L at neutral pH range. 4 g/L of adsorbent dosage at a temperature of 303K and shaking speed of 150 rpm for Pb^{2+} and 200 rpm for Cd^{2+} and Cu^{2+} was maintained during the experiment. The contact time for sorption of lead on *Caesalpinia sappan* was 100 min and for cadmium and copper, it was selected as 160 and 120 min respectively, based on equilibrium study. The residual metal concentrations in the solutions were quantified and the amount of heavy metals adsorbed by *Caesalpinia sappan* were calculated.

8.2.2.3.6 *Effect of temperature and thermodynamics*

The temperature is one of the significant factors which influence sorption capacity. The temperature range was varied from 303 to 373 K at pH 7 and 4 g/L adsorbent dosage and the initial concentrations of Pb^{2+}, Cd^{2+} and Cu^{2+} ranged from 25 to 45 mg/L were used to determine the

thermodynamic parameters. A temperature-controlled water bath with shaker was used for this purpose.

8.2.2.3.7 *Effect of light metal ions*

The effect of other cations on the adsorption of Pb^{2+}, Cd^{2+} and Cu^{2+} on *Caesalpinia sappan* was investigated separately, using 10 mg/L of Pb^{2+}, Cd^{2+} and Cu^{2+} solutions containing a known concentration (10 mg/L) of either Na^+, K^+, Ca^{2+} or Mg^{2+} ions at optimum sorption conditions.

8.2.2.3.8 *Desorption study*

The desorption or regeneration of the used sorbent material is essential to make the sorption process more economical. The gently washing with deionized water to remove the unadsorbed metal ions was the initial step in the desorption study of Pb^{2+}, Cd^{2+} and Cu^{2+} adsorbed sorbents. The desorption of the sorbate (Pb^{2+}, Cd^{2+} and Cu^{2+} ions) from sorbent material was done using the desorbing agents 0.1M HCl, 0.1M NaOH, 0.1M HNO_3, and 0.1M EDTA. 50 mL desorbing agents was added to 0.4 g of metal adsorbed sappan wood (*Caesalpinia sappan)* in 250 mL stopped bottle. The bottles were shaken in an electric shaker for 2 hrs at room temperature. The solution from each bottle was filtered through Whatmann no. 41 filter paper, and concentration of metals present in each sample was found using AAS.

8.2.3 Biosorption of lead and cadmium from water by non-living algal biomass of *Tretepohila abietina*

8.2.3.1 *Collection and preparation of biosorbent: Tretepohila abietina*

The algal biosorbent was collected from Chethalayam areas (Near Pulpally-Sultan Bathery Highway) at Wayanad district during February-March 2014. A red or orange colour was observed in the tree trunk of silver oak. The algal samples were carefully collected from the tree trunk of silver oak with the help of long forceps and scalpel. The collected algal samples were freeze-dried and transported to the laboratory. After the identification of *Trentepohlia* species, the collected algal samples were washed with deionized water. The inactivation of the washed alga was done by heating at 80^0 C for 24 h. The dried algal biosorbent was ground to a very fine powder and sieved through a 0.3 mm sieve.

Trentepohlia Martius, a dominant filamentous subaerial green alga and imparts the yellow, red, and orange colours to the tree-bark, leaves, rocks and many artificial substrata (Kharkongor & Ramanujam, 2015; Satpati & Pal, 2015). The representatives of the Trentepohliales are widespread in tropical and temperate regions with humid climates and the occurrence of abundant β-carotene and hematochrome are responsible for imparting colour to the group Trentepohliales (Rindi et al., 2009; Kharkongor & Ramanujam, 2015). *Tretepohila abietina* is the species of *Trentepohlia* on the tree trunk of silver oak and is shown in Plate 8.3 (a and b). *Tretepohila abietina* before washing is presented in Plate 8.3 (c) and Location where *Tretepohila abietina* collected shown in Plate 8.3 (d). This green alga forms bright orange or orange brown patches on the tree

trunk and the orange red pigment protects the algae against intense sunlight. This alga is found more in the areas with humid climate.
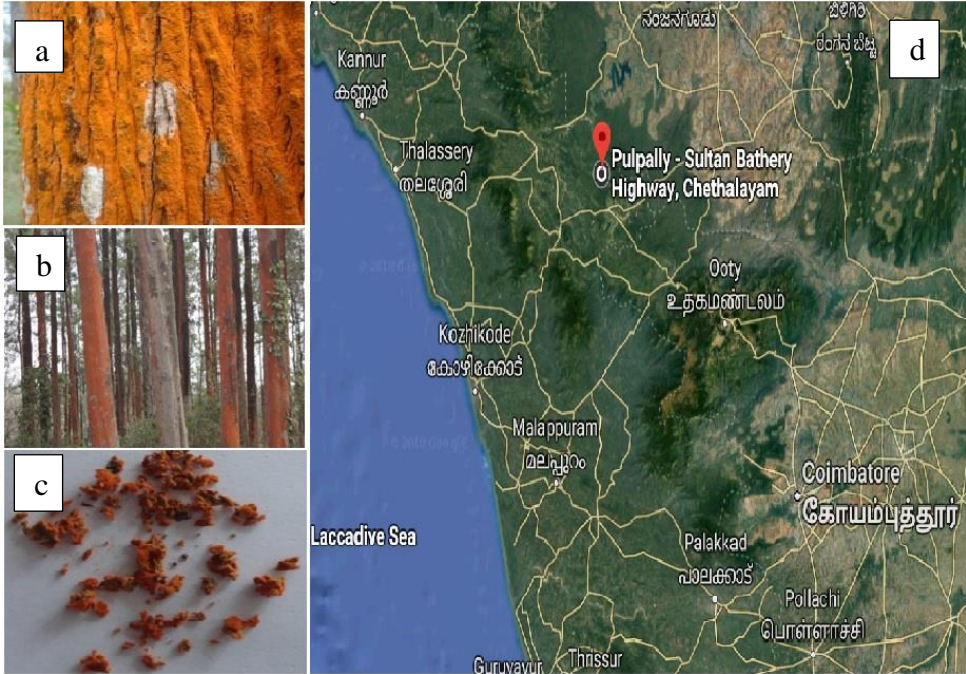
Plate 8.3: (a &b) *Tretepohila abietina* on the tree trunk of silver oak (c) *Tretepohila abietina* before washing (d) Location of *Tretepohila abietina* collected

8.2.3.2 Batch sorption studies

The removal efficiency and adsorption capacity of Pb^{2+} and Cd^{2+} by the biosorbent, *T. abietina* was investigated by batch sorption experiment. Single element adsorption experiments were conducted for both metals and the effect of controlling factors (shaking speed, adsorbent dosage, pH, contact time, initial concentration, light metal ions and temperature) on the metal sorption by biomass, *T. abietina* were

evaluated. The batch experiments were conducted in 250 mL stoppered bottles by shaking a known quantity of biosorbent with 100mL of the metal solutions. To find the optimum pH for biosorption, 0.1 mol/L HCl and 0.1 mol/L NaOH solutions were used to vary pH from 2 to 12. The biosorbent dosage and shaking speed were varied from 0.25-15 g/L and 50-300 rpm, respectively. The initial concentrations of Pb^{2+} and Cd^{2+} were varied from 40-70 mg/L and mixed with optimum dosage biosorbent at optimum pH and room temperature for a predetermined period required for better sorption of Pb^{2+} and Cd^{2+}. The sorption studies were carried out by mixing adsorbent and adsorbate using a mechanical shaker for 120 min using 10 mg/L of metal solutions. To investigate the thermodynamic parameters, sorption experiments were conducted at four different temperature (301K, 333K, 353K and 373K) using a temperature-controlled shaker with water bath. Effect of light metals such as Na^+, K^+, Mg^{2+} and Ca^{2+} on the of Pb^{2+} and Cd^{2+} on *Tretepohila abietina* were also studied. After, each sorption experiment, the sorbent was separated by filtering using Whatmann no. 41 filter paper and metals concentrations in the filtrate were quantified by AAS.

8.2.3.3 Desorption experiments

The Pb^{2+} and Cd^{2+} adsorbed sorbents, *Tretepohila abietina* was gently washed using deionized water to eliminate the unadsorbed ions. 0.1M HCl, 0.1M NaOH, 0.1M HNO_3, and 0.1M EDTA were used to regenerate the metal adsorbed sorbents. 50 mL of desorbing agents was added to known amount of metal adsorbed sorbent, *T. abietina* in 250 mL stopped bottle and agitated using a mechanical shaker for 2 h at room

temperature. The solution was separated using Whatmann no. 41 filter paper and concentration of metals in solution was measured using AAS.

8.2.4 Adsorption isotherms

Langmuir, Freundlich, Temkin and Dubinin-Radushkevich (D-R) isotherm models were used to explained adsorption process. The linearized form of Langmuir, Freundlich, Temkin, and Dubinin - Redushkevich (D-R) isotherm models can be expressed by the following equations (3), (4), (5) and (6) respectively and which are already described in chapter 7.

$$\frac{C_e}{q_e} = \frac{1}{q_m\,K_L} + \frac{C_e}{q_m} \tag{3}$$

$$\log q_e = \log K_f + \frac{1}{n}\log C_e \tag{4}$$

$$q_e = B \ln A + B \ln C_e \tag{5}$$

$$\ln q_e = \ln q_m - \beta \varepsilon^2 \tag{6}$$

where C_e (mg/L), is the equilibrium concentration of heavy metal ions (Pb^{2+}, Cd^{2+} or Cu^{2+}) in solution, q_e (mg/g) is the amount of metal ions adsorbed per unit mass of adsorbent at equilibrium, q_m (mg/g) is the maximum adsorption capacity of the adsorbent, for metal ions. K_L is the adsorption equilibrium constant (L/mg) which related to the energy of adsorption and K_f (mg/g $(L/mg)^{1/n}$) indicates the sorption capacity of the adsorbent. The constant n gives an idea of the adsorption intensity or the favourability of the sorption process. The indication of relatively uniform

surface and a high adsorption at low solution concentrations will be obtained from high and low *n* values (Arshadi et al., 2014). A (L/g) is the Temkin isotherm constant. B = RT/b and is a constant related to the heat of adsorption. b is the Temkin constant linked to the energy parameter (J/mol), R is the gas constant (8.314 J/mol K) and T is the absolute temperature (K). In Dubinin-Radushkevich isotherm model, ε (the Polanyi potential) $= RT \ln\left(1 + \frac{1}{C_e}\right)$ and β (mol²/kJ²) is the constant of the sorption energy. The mean sorption energy, E (kJ/mol), can be calculated using D-R parameter β, i.e., $= \frac{1}{\sqrt{2\beta}}$.

8.2.5 Kinetics and thermodynamic of adsorption

The kinetics and thermodynamic parameters were determined by conducting the experiments at different reaction time and at different temperatures. The pseudo-first order (Lagergren's first-order) model, pseudo-second order model and intraparticle diffusion kinetic model can be expressed by the following equations as equation (7), (8) and (9) respectively and which are also already described in chapter 7.

$$\log (q_e - q_t) = \log q_e - \frac{k_1 t}{2.303} \tag{7}$$

$$\frac{t}{q_t} = \frac{1}{k_2 q_e^2} + \frac{t}{q_e} \tag{8}$$

$$q_t = k_{id} t^{1/2} + C \tag{9}$$

where q_e and q_t are the amount of metal ions adsorbed per mass of adsorbent (mg/g) at equilibrium and time *t* (min), respectively. k_1 (min⁻¹),

k_2 (g/mg min) and k_{id} (mg/g min$^{1/2}$) are the adsorption kinetic constants of Lagergren's first order, second-order and the intra particle diffusion kinetic models, respectively. The value of intercept C in Weber-Morris proposed the intra-particle diffusion model, gives an idea about the boundary layer thickness, i.e. the larger intercept value indicates the greater boundary effect.

The thermodynamic parameters such as Gibbs free energy change ($\Delta G°$), enthalpy change ($\Delta H°$), and entropy change ($\Delta S°$) for the adsorption process were computed using the following equations which are already discussed in chapter 7.

$$\Delta G^0 = -RT \ln K_c \tag{10}$$

$$\Delta G^0 = \Delta H^0 - T\Delta S^0 \tag{11}$$

$$\ln K_c = \frac{-\Delta H^0}{R} * \frac{1}{T} + \frac{\Delta S^0}{R} \tag{12}$$

where R is the universal gas constant (8.314 J/mol K) and T is the absolute temperature of solution in Kelvin (K). The values of K_c, the equilibrium constant, must be dimensionless and is derived from the Langmuir constant (K_L) and were calculated using reported methods (Zhou & Zhou, 2014; Tran et al., 2016; Anastopoulos & Kyzas, 2016).

8.3 Results and Discussion

8.3.1 Removal of lead, cadmium and copper from water using locally available herbal plant *Caesalpinia sappan*

8.3.1.1 Effect of pH

The pH was varied from 2 to 12 to understand the impact of pH variation on the sorption of Pb^{2+}, Cd^{2+} and Cu^{2+} by *Caesalpinia sappan.* The effect of pH on the sorption process is presented in Figure 8.2(a). which indicates that pH of the solution is an important controlling parameter of the biosorption process. The amount of metals adsorbed on *Caesalpinia sappan* increases with increasing pH and at low pH (pH 2) adsorption of metals is negligible. For lead, the maximum removal was found at pH 4-10 and further increase of pH slightly decreased the removal efficiency of lead. Maximum sorption efficiency was observed between pH 6 and 10 in the case Cd^{2+} and Cu^{2+} and further increase in pH leads to a decrease in sorption efficiency.

The protons would compete with metal ions for the active sites responsible for the sorption, at low pH and which leads to a decrease in metal sorption efficiency. At low pH, the protonation of the binding sites resulting from a high concentration of protons leads to reduction in negative charge intensity on the sites, resulting the reduction or even inhibition of the binding of metal ions on the sites. As the pH increases, the hydronium ions are dissociated and the positively charged metal ions are associated with the free binding sites (Farhan & Khadom, 2015). An optimum pH of 7 was maintained for the further sorption study.
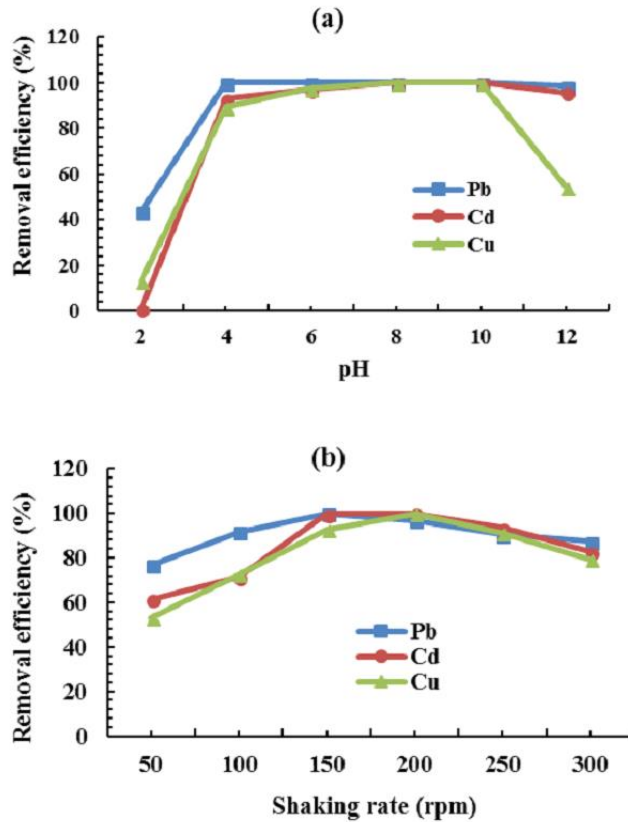
Figure 8.2: Effect of (a) pH (b) Shaking speed on the sorption of Pb^{2+}, Cd^{2+} and Cu^{2+} by *Caesalpinia sappan* (Initial concentration of Pb^{2+}, Cd^{2+} and Cu^{2+} ions:10 mg/L; adsorbent dosage: 4g/L and temperature: 303K)

8.3.1.2 Effect of shaking speed or rate

The chances of interaction between metal ions and biosorbent increases with shaking rate so shaking rate or speed is an important factor effecting sorption process. A low removal efficiency of metals was observed at low shaking rate. The biosorbent settles down and

buries several active sites under its top layers at agitation slow speed. Therefore, only top layer participates in adsorption process because the under buried layers do not have direct contact with metal ions. In the case of all the three metals, adsorption was found to be increases with increase in shaking rate (Raza et al., 2015). Figure 8.2(b) indicates that maximum sorption efficiency or removal efficiency of Pb^{2+} ions by *Caesalpinia sappan* was 100 % at shaking speed of 150 rpm, while for Cd^{2+} and Cu^{2+} attained 100 % and 99.86 % respectively at 200 rpm. So, a shaking speed of 150 rpm was maintained for the sorption of Pb^{2+} ions but for the sorption of Cd^{2+} and Cu^{2+} ions, it was 200 rpm. It was observed that, further increase in shaking speed decreases the adsorption process at high agitation rate, random collisions between particles (adsorbate - adsorbate, adsorbent - adsorbent and adsorbent - adsorbate) do not provide enough time to metal ions to bind with surface of the biosorbent (Feng & Guo, 2012). Shaking speed should be adequate to assure all the binding sites available for metal sorption.

8.3.1.3 Effect of sorbent dosage

The effect of adsorbent dosage on the adsorption of lead, cadmium and copper at fixed initial heavy metal concentration is shown in Figure 8.3. It was observed that the adsorption of metal ions increases as the adsorbent dosage increases from 1 to 4 g/L and thereafter remains almost constant due to the inadequate availability of the number of adsorbing species for a relatively larger number of surface sites on the sorbent at higher dosage of sorbent. Thus, 4 g/L was taken as the adsorbent dosage for further studies.
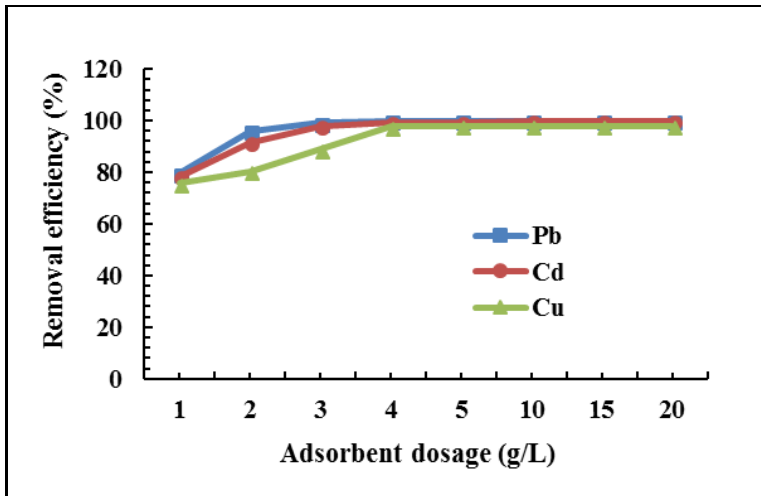
Figure 8.3: Effect of adsorbent dosage on the sorption of Pb^{2+}, Cd^{2+} and Cu^{2+} by *Caesalpinia sappan* (Initial concentration of Pb^{2+}, Cd^{2+} and Cu^{2+} ions:10 mg/L; shaking speed: 150 rpm for Pb^{2+}; 200 rpm for Cd^{2+} and Cu^{2+} ions; pH:7 and temperature: 303K)

8.3.1.4 Effect of contact time

The removal efficiency of Pb^{2+}, Cd^{2+} and Cu^{2+} and the amount adsorbed q_t (mg/g) at different contact times t (min) is plotted in Figure 8.4. A rapid increase in heavy metal removal with increase in the agitation time was observed initially but gradually it attains the equilibrium state. As the contact time increases, the overlapping of active sites with metal species and the decrease in the effective surface area resulting in the conglomeration of exchange particle may occur which leads to the equilibrium state (Das et al., 2013). The percentage of maximum adsorption was 100 % for Pb^{2+} at 100 min. From the figure it is clear that adsorption efficiency of Cd^{2+} and Cu^{2+} by *Caesalpinia sappan* also increases with increasing contact time, reached a maximum

of 100 % and 98.06 % removal at a contact time of 160 and 120 min respectively; afterward removal becomes linearly constant. The result may be due the presence of the more active sites initially and after the accumulation of heavy metal ions and the saturation of the sites leads to an equilibrium state.
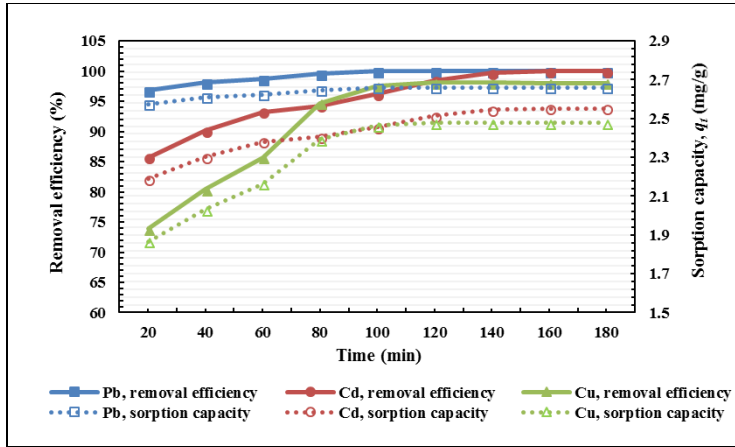
Figure 8.4: Effect of time on biosorption of Pb^{2+}, Cd^{2+} and Cu^{2+} by *Caesalpinia sappan*. (Initial concentration of Pb^{2+}, Cd^{2+} and Cu^{2+}:10 mg/L; sorbent dosage: 4 g/L, pH: 7, shaking speed: 150 rpm for Pb^{2+}; 200 rpm for Cd^{2+} and Cu^{2+} ions, and temperature: 303K)

8.3.1.5 Effect of initial concentration

Based on the batch sorption experiment, to understand the effect of initial metal concentration, a graph of heavy metal removal efficiency and sorption capacity had been plotted against the varying initial metal concentration between 5 - 45 mg/L as illustrated in Figure 8.5. The variations of the initial metal ion, concentration has exhibited a significant effect on the uptake efficiency. From the graph it was found

that the percentage of removal efficiency of Pb^{2+}, Cd^{2+} and Cu^{2+} by *Caesalpinia sappan* decreases and the amount of metals adsorbed, i.e., the sorption capacity increases with increase in initial heavy metal concentration. The required driving force to overcome the resistance to mass transfer between sorbate and sorbent in sorption process is provided by the initial concentration. Subsequently, the sorption capacity attains nearness to saturation of the existing binding sites on sorbents. The maximum metal uptake (Figure 8.5) value corresponds to 9.14 mg/g for Pb^{2+}, 6.10 mg/g for Cd^{2+} and 7.23 mg/g for Cu^{2+}.
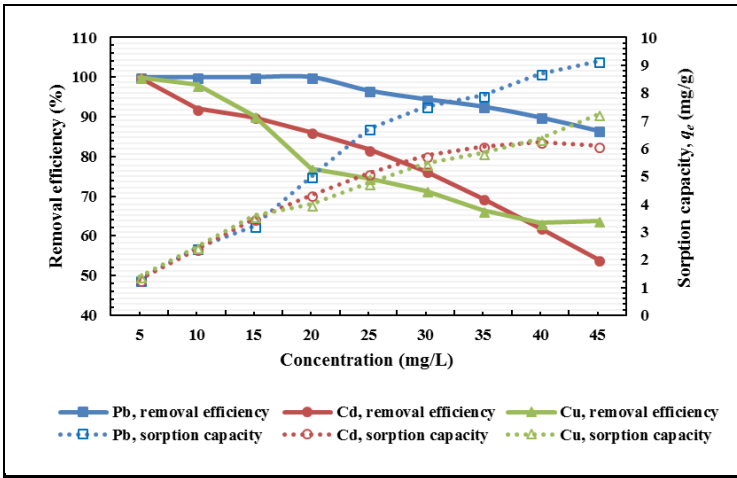
Figure 8.5: Effect of initial concentration of Pb^{2+}, Cd^{2+} and Cu^{2+} on biosorption by *Caesalpinia sappan*. (Sorbent dosage: 4 g/L; pH: 7; temperature: 303K; shaking speed of 150 rpm for Pb^{2+} and 200 rpm for Cd^{2+} and Cu^{2+})

For adsorbent *Caesalpinia sappan,* the observed order of metal ions adsorption is as follows $Pb^{2+} > Cu^{2+} > Cd^{2+}$. The metals with higher electronegativity should adsorb more readily and metals of higher

hydrolysis constants have better adsorptive capacity (Al-Degs et al., 2006; Appel et al., 2008). The difference in the sorption affinity for the studied metals (i.e., Pb^{2+}, Cd^{2+} and Cu^{2+}) are based on those metals physico-chemical properties like hydrated radius, electronegativity, ionic radius, hydrolysis constant among others (Apiratikul & Pavasant 2006; Appel et al. ,2008). This can give a better explanation for the higher removal of Pb^{2+} compared to Cu^{2+} and Cd^{2+}. Pauling's electronegativity of Pb^{2+}, Cu^{2+} and Cd^{2+} are 2.33, 1.90 and 1.69, respectively and the metal sorption affinity of *Caesalpinia sappan* followed the order $Pb^{2+} > Cu^{2+} > Cd^{2+}$, which follows the same order of electronegativity values. Also, the hydrated radius of the metal ions exhibited the sequence $Cd^{2+} = 4.26$ A ° $> Cu^{2+} = 4.19$ A ° $> Pb^{2+} = 4.01$ A °, indicating that smaller radius favoured metal interaction with the adsorbent surface (Sdiri & Higashi, 2013).

8.3.1.6 Effect of other ions

Heavy metal contaminated industrial wastewater also contain several types of impurities such as light metal ions (Na^+, K^+, Mg^{2+} and Ca^{2+}) that influence the process of heavy metal removal (Matheickal &Yu, 1999). The effect of light metal ions, Na^+, K^+, Mg^{2+} and Ca^{2+} on the adsorption of Pb^{2+}, Cd^{2+} and Cu^{2+} by *Caesalpinia sappan* are depicted in Figure 8.6. The presence of Na^+ and K^+ ions reduced the percentage of heavy metal sorption by 0.44 and 2.86 % (for Pb^{2+}), 0.65 and 4.88% (for Cd^{2+}) and 0.32 and 3.86 % (for Cu^{2+}), respectively. But, the percentage of heavy metal uptake in the presence of Ca^{2+} and Mg^{2+} were found to be 62.13 and 61.69 % (for Pb^{2+}), 55.37 and 52.32 % (for Cd^{2+}) and 57.26

and 55.25 % (for Cu^{2+}), respectively. The effect of Na^+ and K^+ on Pb^{2+}, Cd^{2+} and Cu^{2+} uptake was found to be insignificant but the presence of divalent cations, Mg^{2+} and Ca^{2+} had influenced the sorption of Pb^{2+}, Cd^{2+} and Cu^{2+}. The single charged ions have negligible impact on metal sorption than doubly charged ions. Competition for binding sites may reduce the binding capacity of metal in sorption process (Lodeiro et al., 2006).
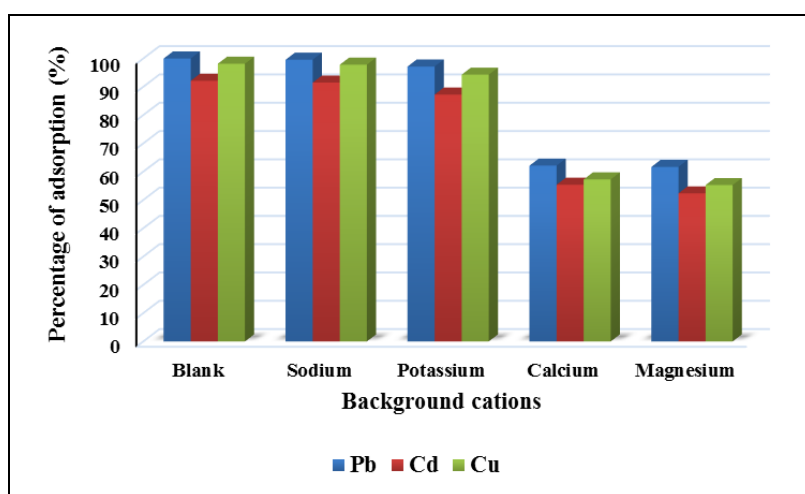
Figure 8.6: Effect of selected light metal ions on the sorption of Pb^{2+}, Cd^{2+} and Cu^{2+} by *Caesalpinia sappan*

8.3.1.7 Determination of adsorption isotherms

The equilibrium adsorption isotherms (capacity studies) are recognized as one of the most fundamental data to comprehend the mechanism of the adsorption and describe the interaction between adsorbate and adsorbent. The experimental equilibrium data obtained from sorption of Pb^{2+}, Cd^{2+} and Cu^{2+} on *Caesalpinia sappan* were

evaluated by applying the Langmuir, Freundlich, Temkin, and Dubinin–Redushkevich (D-R) isotherm models.

The isotherm studies were conducted by varying the initial concentration of Pb^{2+}, Cd^{2+} and Cu^{2+} from 25-45 mg/L and maintaining the adsorbent dosage of 4 g/L at a constant temperature of 303K and neutral pH. Single species sorption experiments were conducted for each heavy metal. The parameters for isotherms models are given in Table 8.1 and the calculated results are tabulated in Table 8.2. The linear plot of C_e/q_e against C_e (Figure 8.7(a)) shows that the sorption of Pb^{2+}, Cd^{2+} and Cu^{2+} on *Caesalpinia sappan* obeys the Langmuir model. The Langmuir constants q_m (Pb^{2+}: 9.94 mg/g; Cd^{2+}: 6.46 mg/g and Cu^{2+}: 10.00 mg/g) and K_L (Pb^{2+}: 1.85 L/mg; Cd^{2+}: 1.10 L/mg and Cu^{2+}: 0.13 L/mg) were obtained from the slope and intercept of the linear plot and are presented in Table 8.2. Maximum adsorption capacity was obtained for Cu^{2+} and Pb^{2+}. The separation factor or equilibrium parameter (R_L) which is a dimensionless constant, can be used to express the essential characteristic of Langmuir isotherm. For all the three metals, the R_L values were $0 < R_L < 1$ which indicates that the sorption of Pb^{2+}, Cd^{2+} and Cu^{2+} on *Caesalpinia sappan* is favourable.

Non-ideal sorption on heterogeneous surfaces and multilayer sorption are explained by Freundlich isotherm model (Freundlich, 1960). By plotting log q_e versus log C_e of equation (10), a straight line was resulted and the values for n (adsorption intensity) and K_f (the sorption capacity) can be obtained from the slope and intercept of the plot (Figure 8.7(b)) and are presented in Table 8.2. The sorption capacities (K_f) of *Caesalpinia sappan* were found as 6.808 (mg/g) (L/mg)$^{1/n}$ for Pb^{2+}; 4.434

(mg/g) (L/mg)$^{1/n}$ for Cd^{2+} and 2.251 (mg/g) (L/mg)$^{1/n}$ for Cu^{2+}. For all the three metals the values of n were found to be greater than1, representing the favourable adsorption condition. The linear form of the Temkin isotherm was plotted as q_e vs. ln C_e (Figure 8.7(c)) and the constants A and B, determined from the intercept and slope of the straight line are exhibited in Table 8.2. Temkin model assumes that heat of adsorption (function of temperature) of all molecules in the layer would decrease linearly rather than logarithmic with coverage, by ignoring the extremely low and large value of concentrations (Tempkin & Pyzhev, 1940; Dada et al., 2012). The sorption data of lead and copper provides a close fit to Temkin isotherm but the experimental data of cadmium are not modelled well. The sorption equilibrium data were also applied to the Dubinin–Radushkevich (D-R) isotherm model to distinguish the type of sorption (physical or chemical) of metal ions with its mean free energy, E. The slope and intercept of the plot ln q_e versus ε^2 gives the values of β and q_m (Figure 8.7(d)) and are presented in Table 8.2. The value of E ranges from 1 to 8 kJ/mol indicates the physical sorption and from 8 to 16 kJ/mol indicates chemical sorption. The results showed that values of E for all the three metals were found in the range 1 to 8 kJ/mol so the sorption of Pb^{2+}, Cd^{2+} and Cu^{2+} on *Caesalpinia sappan* is physical sorption.

Table 8.1: Parameters for Langmuir, Freundlich, Temkin and Dubinin - Radushkevich Adsorption Isotherms

Metal ions	C_0 (mg/L)	C_e (mg/L)	$\log C_e$	$\ln C_e$	q_e (mg/g)	$\log q_e$	$\ln q_e$	C_e / q_e (g/L)	ε^2
	27.83	0.93	-0.032	-0.073	6.73	0.8277	1.906	0.138	$3.382664*10^6$
	31.82	1.75	0.243	0.560	7.52	0.8761	2.017	0.233	$1.296443*10^6$
Pb^{2+}	34.15	2.51	0.400	0.920	7.91	0.8982	2.068	0.317	$0.713606*10^6$
	38.7	3.89	0.590	1.358	8.70	0.9396	2.164	0.447	$0.332165*10^6$
	42.21	5.64	0.751	1.730	9.14	0.9611	2.213	0.617	$0.169081*10^6$
	25.01	4.55	0.658	1.515	5.12	0.7089	1.632	0.889	$0.25075*10^6$
	30.12	7.13	0.853	1.964	5.75	0.7595	1.749	1.240	$0.109381*10^6$
Cd^{2+}	35.08	10.72	1.030	2.372	6.09	0.7846	1.807	1.760	$0.050488*10^6$
	40.32	15.33	1.186	2.730	6.25	0.7957	1.832	2.453	$0.025346*10^6$
	45.11	20.73	1.316	3.031	6.10	0.7851	1.808	3.400	$0.014092*10^6$
	25.54	6.49	0.812	1.870	4.76	0.6778	1.561	1.363	$0.130327*10^6$
	30.56	8.72	0.941	2.166	5.46	0.7372	1.697	1.597	$0.074799*10^6$
Cu^{2+}	35.23	11.86	1.074	2.473	5.84	0.7666	1.765	2.030	$0.041586*10^6$
	40.21	14.78	1.170	2.693	6.36	0.8033	1.850	2.325	$0.0272*10^6$
	45.34	16.41	1.215	2.798	7.23	0.8593	1.979	2.269	$0.022206*10^6$

The correlation coefficients (R^2) presented in Table 8.2 and Figure 8.7 (a-d), indicate that the adsorption data best fitted the Langmuir adsorption isotherm for all three metals. The Langmuir isotherm fits close to the experimental data of the sorption of Pb^{2+} and Cd^{2+} on *Caesalpinia sappan*, this may be due to the homogeneous distribution of active sites on surface of *Caesalpinia sappan*, i.e., the Langmuir equation assumes

that the surface is homogeneous. The values of q_m calculated by the Dubinin - Radushkevich (D-R) isotherm model fits very well to those experimentally determined data for Pb^{2+}, Cd^{2+} and Cu^{2+}. The order of adsorption isotherm models fitted the equilibrium data, based on the correlation coefficient are for Pb^{2+} and Cu^{2+}: Langmuir isotherm > Freundlich isotherm > Temkin isotherm > Dubinin-Radushkevich isotherm and for Cd^{2+}: Langmuir isotherm > Dubinin–Radushkevich isotherm > Temkin isotherm > Freundlich isotherm.
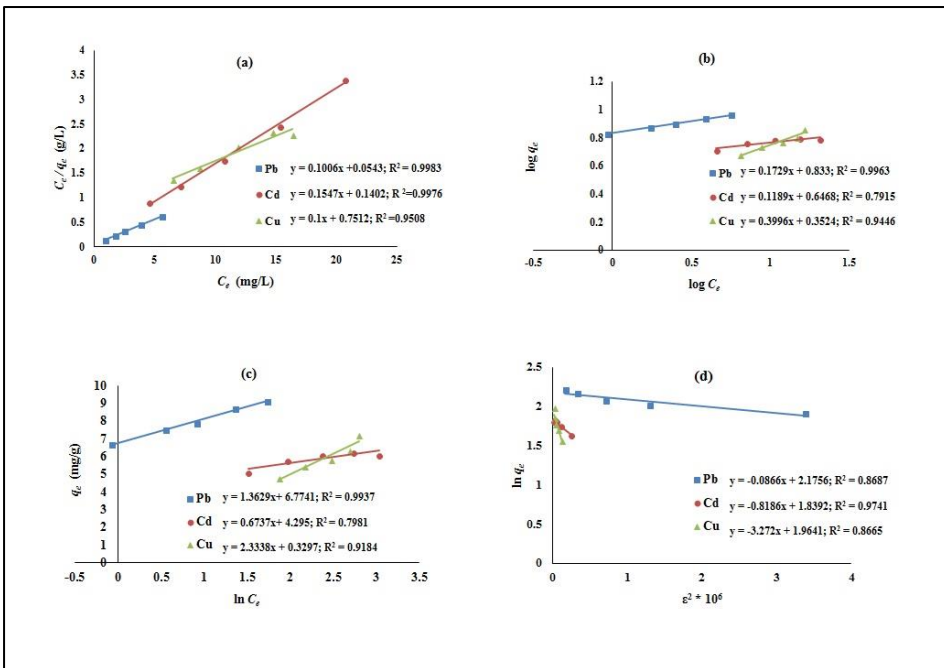
Fig. 8.7. (a) Langmuir, (b) Freundlich, (c) Temkin and (d) Dubinin - Radushkevich Adsorption Isotherms

Table 8.2: Adsorption isotherm parameters for the metal ion biosorption onto *Caesalpinia sappan*

Isotherm models	Parameters	Metal ions		
		Pb^{2+}	Cd^{2+}	Cu^{2+}
	q_m (mg/g)	9.94	6.46	10.00
	K_L(L/mg)	1.85	1.10	0.13
	R_L	0.0126 -0.0190	0.0201-0.0362	0.1657-0.2941
Langmuir	R^2	0.9983	0.9976	0.9508
	K_f (mg/g) (L/mg)$^{1/n}$	6.808	4.434	2.251
	n	5.784	8.410	2.503
Freundlich	R^2	0.9963	0.7915	0.9446
	A (L/g)	144.08	587.13	1.15
	B	1.363	0.674	2.334
	b (kJ/mol)	1.848	3.739	1.079
Temkin	R^2	0.9937	0.7981	0.9184
	q_m (mg/g)	8.807	6.292	7.128
	β (mol^2/kJ^2)	0.0866	0.8186	3.272
	E (kJ/mol)	2.403	0.7815	0.3909
Dubinin – Radushkevich	R^2	0.8687	0.9741	0.8665

8.3.1.8 Sorption kinetic models

In order to investigate the dynamics of adsorption processes or to predict the adsorption kinetics, different kinetic models such as pseudo-first order model or Lagergren rate equation, pseudo-second order model, intraparticle diffusion kinetic model and Elovich kinetic model and were applied to the experimental data obtained from the sorption of metals on *Caesalpinia sappan*. To define the adsorption kinetics of Pb^{2+}, Cd^{2+} and Cu^{2+} ions, the kinetic parameters for the adsorption process of metal ions

(the initial concentration of 10 mg/L) on *Caesalpinia sappan* were studied for contact times of 180 min at regular time intervals of 20 min. A rapid increase in removal of heavy metal with increase in the contact time was noticed initially (especially in the case of Cd^{2+} and Cu^{2+} ions) but gradually it attains the equilibrium state. The adsorption of Pb^{2+}, Cd^{2+} and Cu^{2+} ions on *Caesalpinia sappan,* reaches equilibrium at 100 min, 160 and 120 min respectively.
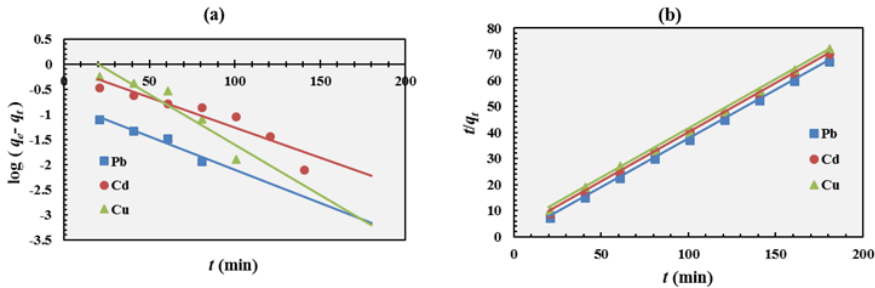
Figure 8.8: Kinetics modelling of adsorption of Pb^{2+}, Cd^{2+} and Cu^{2+} on *Caesalpinia sappan* (a) pseudo first-order; (b) pseudo second-order

Pseudo first-order kinetic plot of Pb^{2+}, Cd^{2+} and Cu^{2+} ions (log (q_e - q_t) against t) and the second-order kinetic plot (t/q_t against t) are depicted in Figure 8.8 (a & b). The Lagergren's first-order rate constants k_1 and q_e determined from the slope and intercept of the plot and correlation coefficients (R^2) are exhibited in Table 8.3. The value of $q_{e,cal}$ calculated from the Lagergren's first-order rate equation was lower than the experimentally determined, $q_{e,exp}$ value for Pb^{2+} and Cd^{2+} but the value of $q_{e,cal}$ was close to $q_{e,exp}$ value for Cu^{2+} ions . The k_2 and q_e of

Pb^{2+}, Cd^{2+} and Cu^{2+} ions are calculated from the intercept and slope of the linear second-order kinetic plot (Figure 8.8 (b)) and the calculated value of $q_{e,cal}$ of all the three metals were found to be close to the experimentally determined, $q_{e,exp}$ values. A much better R^2 values were observed for the linearized pseudo-second order kinetics model ($R^2 = 1$ for Pb^{2+}, $R^2 = 0.9996$ for Cd^{2+} and $R^2 = 0.9985$ for Cu^{2+}) for all the three metals than those for the first-order model ($R^2 = 0.95$ for Pb^{2+}, $R^2 = 0.8726$ for Cd^{2+} and $R^2 = 0.8783$ for Cu^{2+}). The better R^2 values and the closely approximate values of calculated and experimentally measured values of q_e indicates that the sorption process appears to follow pseudo-second order reaction kinetics. The pseudo- first and second-order kinetics rate constants for the adsorption of Pb^{2+}, Cd^{2+} and Cu^{2+} ions on *Caesalpinia sappan* were $k_1 = 0.0306$, 0.0279, and 0.0463 min^{-1}, respectively, and $k_2 = 0.4293$, 0.0647, and 0.0392 g/mg min, respectively.
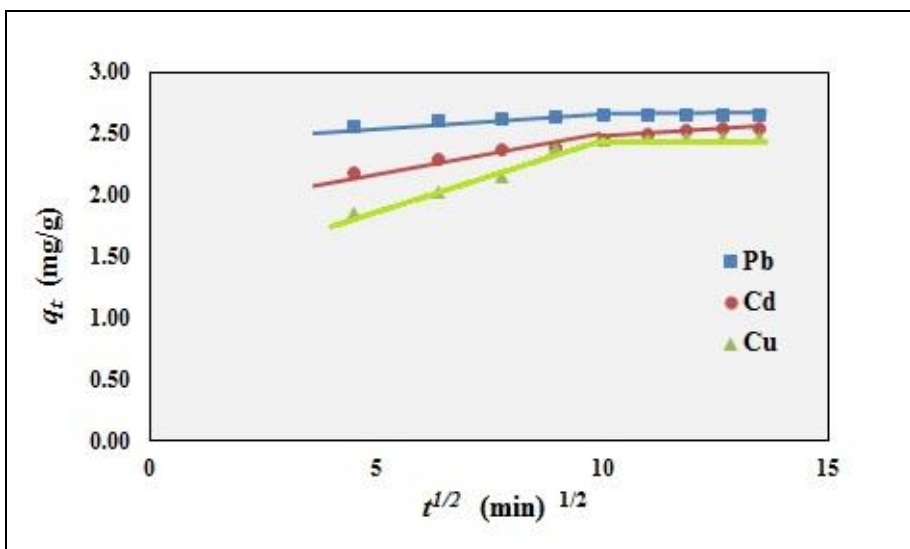
Figure 8.9: Intraparticle diffusion plot

Intraparticle diffusion constant can be achieved from the slope of the plot (Figure 8.9) of q_t against $t^{1/2}$ and listed in Table 8.3. According to Weber and Morris proposed intraparticle diffusion model, if the plot of q_t against $t^{1/2}$ gives a straight line then the adsorption of a solute is controlled by the intra-particle diffusion process. But multi - linearity of the plots (Figure 8.9) indicates the involvement of two or more steps in sorption process. It is apparent from the plots that there are two separate stages; stage I is indicated by the first linear portion and stage II is the second curved path followed by a plateau. A rapid uptake of heavy metals by the adsorbent occurred in stage I, because of the fast utilization of the most readily available adsorbing sites on the surfaces of the sorbent, *Caesalpinia sappan*.

Table 8.3: Kinetics data of pseudo-first-order, pseudo-second-order and intraparticle diffusion model

Kinetic models	Parameters	Values		
		Pb^{2+}	Cd^{2+}	Cu^{2+}
	$q_{e,exp}$ (mg/g)	2.66	2.5528	2.4764
Pseudo-first-order kinetic model	k_1 (min^{-1})	0.0306	0.0279	0.0463
	$q_{e,cal}$ (mg/g)	0.1700	1.1267	2.5386
	R^2	0.95	0.8726	0.8783
Pseudo-second-order kinetic model	k_2 (g/mg min)	0.4293	0.0647	0.0392
	$q_{e,cal}$ (mg/g)	2.6752	2.6344	2.6357
	R^2	1	0.9996	0.9985
Intraparticle diffusion model	k_{id} (mg/g min$^{1/2}$)	0.0094	0.0417	0.0726
	C (mg/g)	2.5499	2.0322	1.6172
	R^2	0.8488	0.9677	0.8659

Very slow diffusion of adsorbate, i.e., Pb^{2+}, Cd^{2+} and Cu^{2+} ions from surface site on *Caesalpinia sappan,* into the inner pores is observed in Stage II. Therefore, early stage of heavy metal adsorption may be administrated by the initial intra-particle transport of metal ions controlled by surface diffusion process and later stage is controlled by pore diffusion process. The adsorption of Pb^{2+}, Cd^{2+} and Cu^{2+} on *Caesalpinia sappan* involves surface adsorption as well as intraparticle diffusion. It was observed that the correlation coefficients of the Weber and Morris plots were not much satisfactory for Pb^{2+} and Cu^{2+}. But, for Cd^{2+}, R^2 value was higher than that of pseudo-first order kinetic model.

8.3.1.9 Effect of temperature and adsorption thermodynamics

To evaluate the effect of temperature or thermodynamics of the adsorption of Pb^{2+}, Cd^{2+} and Cu^{2+} on *Caesalpinia sappan* were performed at four different temperatures (303, 333, 353 and 373K). It was observed that the percentage of reduction of metal ions decreases with increase of temperature. The attractive forces between adsorbent surface and metal ions are weakened and the sorption decreases as the temperature increases. At high temperature, the thickness of the boundary layer decreases, due to the increased tendency of the metal ion to escape from the biomass surface to the solution phase, which results in a decrease in adsorption as temperature increases (Aksu & Kutsal, 1991).

The values of $\Delta G°$, $\Delta H°$ and $\Delta S°$ for initial metal concentrations of 25 - 45 mg/L are presented in the Table 8.4. The $\Delta H°$ and $\Delta S°$ were obtained from the slope and intercept of Vant's Hoff plot (ln K_c versus 1/T) of each metal ions. The Van't Hoff plots are depicted in Figure 8.10

(a-c). The negative value for the Gibbs free energy for all three metals indicates that the spontaneous adsorption process and also the degree of spontaneity of the adsorption of Pb^{2+}, Cd^{2+} and Cu^{2+} on *Caesalpinia sappan* increases with increasing temperature. Negative value of enthalpy change ($\Delta H°$), implies the exothermic behaviour of the adsorption process and also confirms possibility of physical adsorption with the increase in temperature of the system (Mall et al., 2006). The positive value of entropy change ($\Delta S°$) proposes that some structural deviations occur on the adsorbent, *Caesalpinia sappan* and the randomness at the solid/liquid interface in the adsorption system increases during the adsorption process (Gupta, 1998).

Table 8.4: Thermodynamic parameters for the adsorption of Pb^{2+}, Cd^{2+} and Cu^{2+} onto *Caesalpinia sappan* at different temperatures

Metal ions	T (K)	$\Delta G°$ (kJ/mol)	$\Delta H°$ (kJ/mol)	$\Delta S°$ (J/mol K)
Pb	303	-42.51	-19.15	76.91
	333	-44.66		
	353	-46.32		
	373	-47.89		
Cd	303	-39.66	-15.25	80.22
	333	-41.71		
	353	-43.62		
	373	-45.26		
Cu	303	-32.90	-3.53	96.97
	333	-35.81		
	353	-37.81		
	373	-39.65		
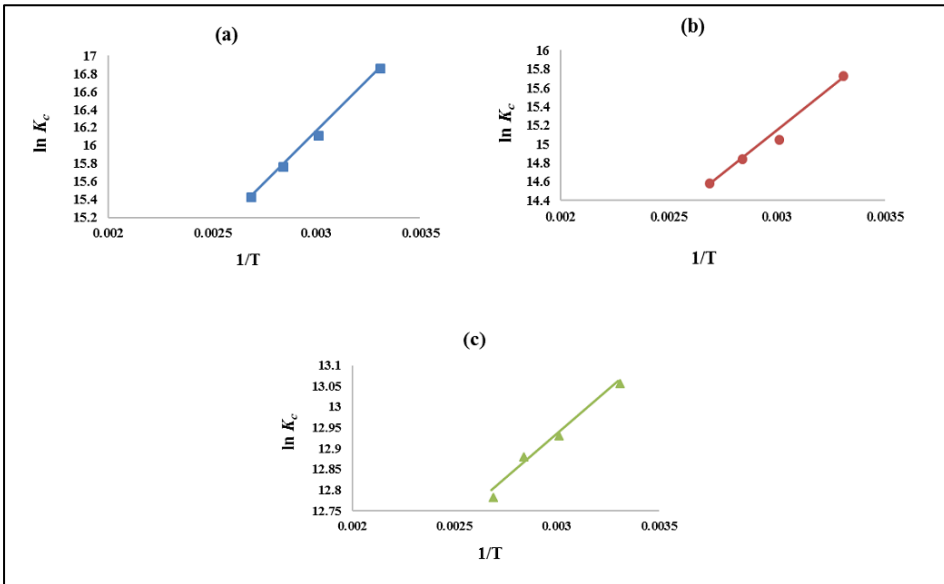
Figure 8.10: Van't Hoff plot for thermodynamic study of (a) lead, (b) cadmium and (c) copper adsorption onto *Caesalpinia sappan*

8.3.1.10 Surface morphology of the adsorbent

The surface morphological characteristics of adsorbent, was examined by Scanning electron micrographs (SEM) and Energy-dispersive X-ray (EDX) spectra. 0.1M HCl treated *Caesalpinia sappan* was used as adsorbent in the present study. Figure 8.11(a) represents SEM image of *Caesalpinia sappan* surface before adsorption and Figure 8.11(b), Figure 8.12(a) and (b) shows the surface of *Caesalpinia sappan* after the adsorption of copper, lead and cadmium respectively. Figure 8.11(a) reveals a sheet like structure with troughs and crests in a synchronised manner. The micrographs clearly depicted the different

surface morphology of metal adsorbed and non-adsorbed *Caesalpinia sappan*.
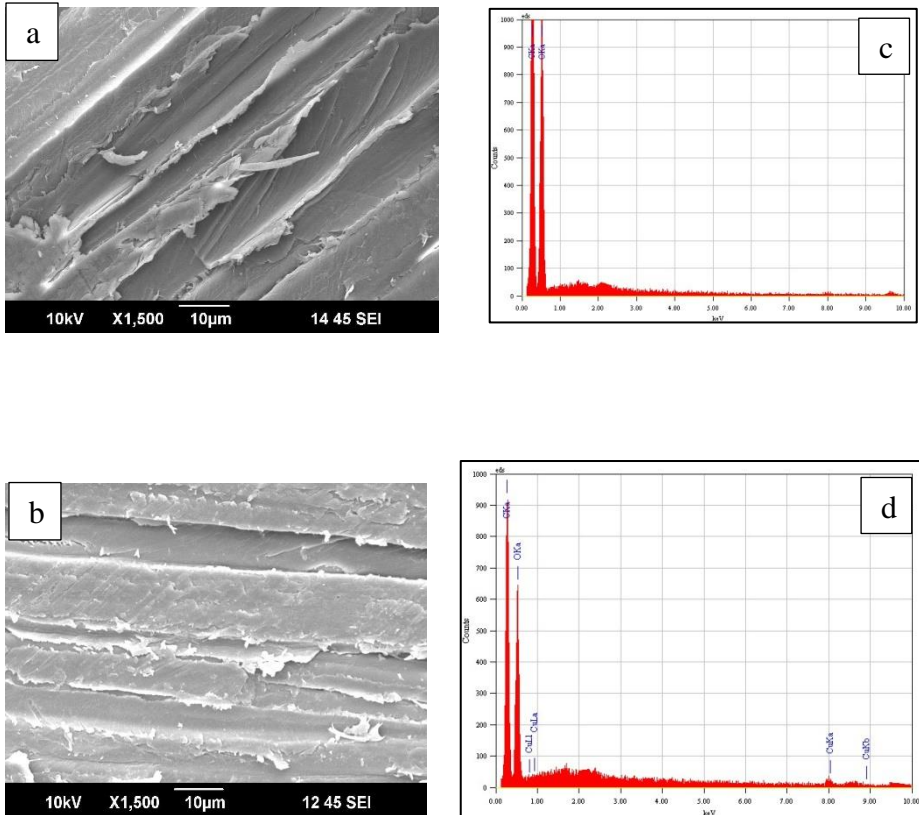
Figure 8.11: (a) and (b) are SEM image of *Caesalpinia sappan* surface before adsorption and after the adsorption of copper and (c) and (d) are the EDX spectra of *Caesalpinia sappan* before adsorption and after the adsorption of copper
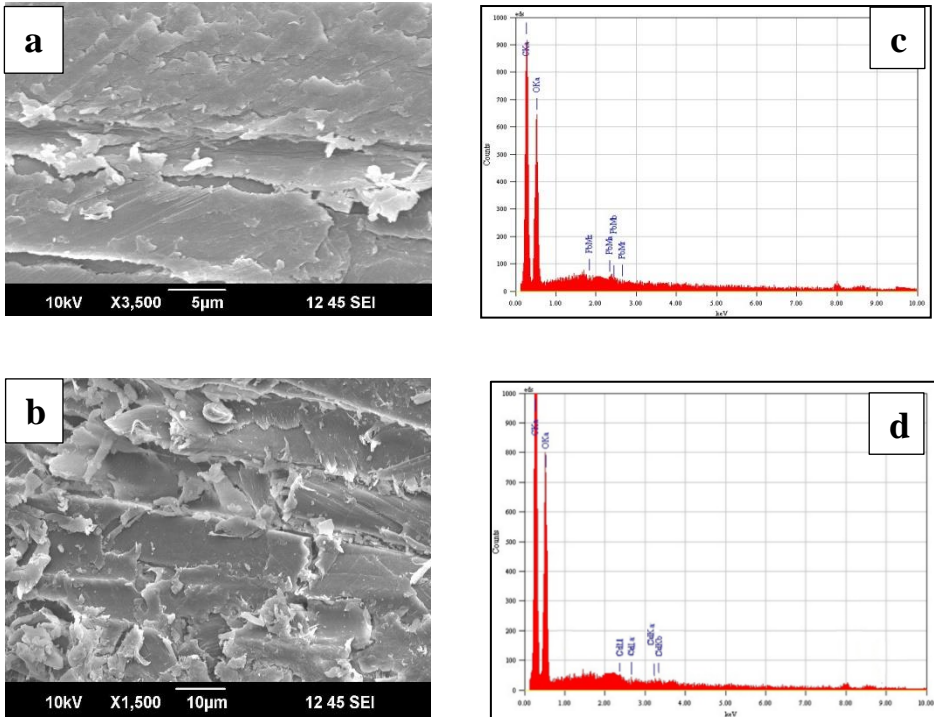
Figure 8.12: (a) and (b) are SEM image of lead and cadmium adsorbed *Caesalpinia sappan* surface respectively and (c) and (d) are the EDX spectra of lead and cadmium adsorbed *Caesalpinia sappan*

Figure 8.11(c) shows the typical EDX patterns for adsorbent, *Caesalpinia sappan* before metal adsorption and Figure 8.11(d), Figure 8.12(c and d) represents EDX spectra of *Caesalpinia sappan* after the adsorption of copper, lead and cadmium respectively. EDX patterns for *Caesalpinia sappan* before metal adsorption (Figure 8.11(c)) did not display the characteristic signal of metals, whereas in the EDX spectra of

metal adsorbed *Caesalpinia sappan*, signals of the presence of Cu^{2+}, Pb^{2+} and Cd^{2+} were observed.

8.3.1.11 Desorption study

Biosorption technology used water purification is economical with respect to the regeneration of biosorbent. Furthermore, regeneration of biosorbent reduces the environmental impacts related with biosorbent disposal. The desorption study was carried out to check the reusability of *C. sappan* as an adsorbent. Among four desorbing agents (0.1 M HCl, 0.1 M NaOH, 0.1 M HNO_3, and 0.1 M EDTA), 0.1 M HCl was found to be suitable for the desorption study, as it desorbed 97.1 % of Pb^{2+}, 93.2 % of Cd^{2+} and 95.8 % of Cu^{2+} ions. Filtered and deionized water washed biosorbent was dried at 60°C for next sorption study. The sorption - desorption cyclic study was conducted for five consecutive cycles. In fifth cycle, the efficiency of metal biosorption was declined from 97.1 % to 68.3 % for Pb^{2+}, 93.2 % to 56.8 % for Cd^{2+} and 95.8 % to 64.1 % for Cu^{2+} ions. Moreover, the biodegradable nature of biosorbent, *Caesalpinia sappan* leads to its easy disposal.

8.3.2 Biosorption of lead and cadmium ions from water by non-living algal biomass of *Tretepohila abietina*

8.3.2.1 Factors influencing the adsorption of Pb^{2+} and Cd^{2+}

The influence of controlling parameters such as shaking rate, adsorbent dosage, pH, initial concentration and contact time on the sorption was investigated by batch sorption experiment. For both Pb^{2+} and Cd^{2+} ions, single species experiments were conducted. The effect of

shaking rate on removal efficiency of Pb^{2+} and Cd^{2+} was determined by varying the agitation rate from 50 to 300 rpm (Figure 8.13(a)). Removal efficiency of both the metals were increases with agitation rate and reaches maximum sorption between 100 - 200 rpm and 150 - 250 rpm for Pb^{2+} and Cd^{2+}, respectively. As the shaking rate increases, a slight decrease in removal efficiency was observed. So, 150 rpm was selected as the optimum shaking rate in all subsequent experiment for both the metals.
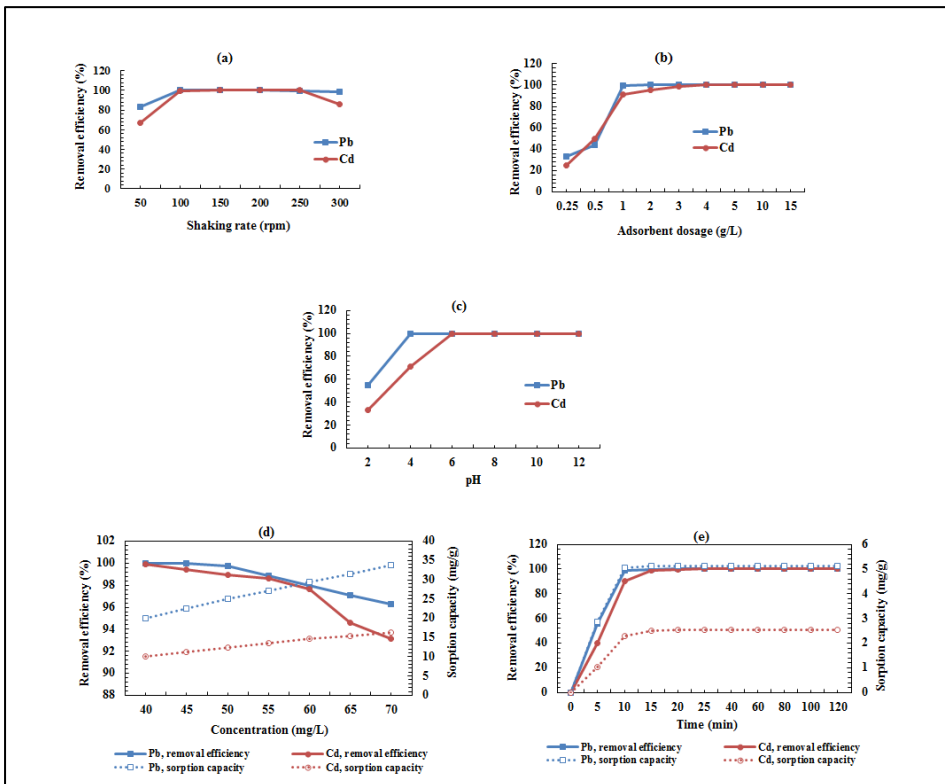
Figure 8.13: Effect of (a) shaking rate; (b) sorbent dose; (c) pH; (d) initial concentration of metals and (e) contact time on the metal removal efficiencies of algal biosorbent, *Tretepohila abietina*

The influence of sorbent dosage on removal of Pb^{2+} and Cd^{2+} was investigated by varying the sorbent dosage from $0.25 - 15$ g/L (Figure 8.13(b)) and the results clearly show that the efficiency of metal removal increases up to the optimum sorbent dosage (For Pb^{2+}: 2 g/L and Cd^{2+}: 4 g/L) beyond which the removal efficiency remained constant. The study was conducted at 301K and 100 mL of 10 mg/L Pb^{2+} and Cd^{2+} solutions were agitated with sorbent at 150 rpm speed. The pH of the solution controls the degree of ionization and extent of surface protonation of the adsorbent so it has a significant role in metal sorption. To evaluate the influence of pH on the adsorption, pH was adjusted in the range 2-12 for both Pb^{2+} and Cd^{2+} solutions and the studies were carried out using 10 mg/L of 100 mL metal solutions. In acidic pH range, lower metal sorption was observed, may be due to the competition between metal and H^+ ions for binding to the sorption sites, partial protonation of the functional groups and particle attrition (Arshadi et al., 2014). With increase in pH, removal efficiency of metals as well as metals uptake was increased. From Figure 8.13(c), 100% removal was observed between pH range of 4 -12 and 6 - 12 for Pb^{2+} and Cd^{2+}, respectively. According to Arshadi et al. (2014), the increased pH (i.e., fewer H_3O^+, the more negatively charged surface - active sites) leads to the deprotonation of adsorbent surface, which will increase the active sites for metal ion binding, so, more active functional groups participate on metal ion uptake by complexation reaction or chelating and amount of metal adsorbed consequently increases. pH 7 was maintained as optimum pH for further experiment.

The influence of initial metal (Pb^{2+} and Cd^{2+}) concentration in the range of 40 to 70 mg/L on sorption was studied and is portraited in Figure 8.13(d). It is evident from the figure that the equilibrium sorption capacity of *Tretepohila abietina* increased with increasing initial Pb^{2+} and Cd^{2+} concentration, while the removal efficiency exhibited an opposite trend. As the initial concentration of Pb^{2+} ions increased from 40 to 70 mg/L, the removal efficiency of Pb^{2+} decreased from 100 % to 96.29 % and the adsorption capacity of *T. abietina* increased from 20.01 mg/g to 33.83 mg/g. In the case of Cd^{2+}, with increased metal concentration, the removal efficiency of Cd^{2+} decreased from 99.9 % to 93.16 % and the adsorption capacity of biosorbent increased from 10.02 mg/g to 16.39 mg/g. The initial metal concentration provides the necessary driving force to overcome the resistance to the mass transfer of metal ions between the aqueous phase and the solid phase, therefore an increase in initial metal ion concentration, enhances the interaction between metal ion and biosorbent, resulting increased adsorption capacity (Kumar et al., 2010(b)).

The effect of contact time (0 - 120min) on the biosorption of Pb^{2+} and Cd^{2+} by biosorbent, *T. abietina* (For Pb^{2+}: 2 g/L and Cd^{2+}: 4 g/L) from aqueous metal solutions having concentration of 10 mg/L with pH 7 at 301K is shown in Figure 8.13(e). The results revealed that the amount adsorbed and percentage of metal removal increases with increasing contact time and 100 % of metal sorption was reached at 20 min and 25 min for Pb^{2+} and Cd^{2+}, respectively. Rapid removal of metals was observed within 15 min i.e., 99.80 % and 98.72 % of Pb^{2+} and Cd^{2+} were removed respectively. The rapid adsorption during the early stages is may

be due to the high concentration gradient between the metal ions in the solution and that on the adsorbent and the occurrence of large number of vacant sites existing during this period. So, 25 min is considered as the optimum time to reach equilibration for Pb^{2+} and Cd^{2+} ions in this study and used for all the further experiments. The influence of light metal ions such as Na^+, K^+, Mg^{2+} and Ca^{2+} on the sorption of Pb^{2+} and Cd^{2+} by the biosorbent *Tretepohila abietina* (For Pb^{2+}: 2 g/L and Cd^{2+}: 4 g/L) was studied using the metal solutions having initial concentration of 10 mg/L. The effect of Na^+ and K^+ on removal of Pb^{2+} and Cd^{2+} was found to be insignificant but the presence of divalent cations such as Mg^{2+} and Ca^{2+} had reduced the efficiency of sorption of Pb^{2+} and Cd^{2+}. The removal efficiency of Pb^{2+} in the presence of Ca^{2+} and Mg^{2+} was reduced by 18.8 and 21.1 %, respectively. For Cd^{2+}, it was reduced by 23.6 and 26.5 % in the presence of Ca^{2+} and Mg^{2+}, respectively. According to Lodeiro et al. (2006), the competition for binding sites may diminish the binding capacity of metal ion in sorption process.

8.3.2.2 Sorption isotherms

The adsorption isotherm specifies how the adsorbed molecules distribute between the liquid phase and the solid phase when the adsorption process reaches an equilibrium state (Kumar et al., 2010(a)). To find the suitable model for the adsorption process, the analysis of the isotherm data by fitting them to different isotherm models was done. The adsorption capacity of the sorption process was investigated using linearized form of Langmuir, Freundlich, Temkin and Dubinin - Radushkevich adsorption isotherms. The isotherm studies were

conducted in single species sorption method by varying the initial concentration of Pb^{2+} and Cd^{2+} from 50 - 70 mg/L at a constant temperature of 301K and neutral pH. The sorbent dosage maintained for sorption of Pb^{2+} and Cd^{2+} were 2 g/L and 4 g/L, respectively. Parameters for plotting Langmuir, Freundlich, Temkin and Dubinin - Radushkevich isotherms are tabulated in Table 8.5. The ability of *Tretepohila abietina* to adsorb Pb^{2+} and Cd^{2+} from water was evaluated from the general nature of the Langmuir isotherm plot (C_e against C_e / q_e,). The lead and cadmium sorption isotherm followed the linearized Langmuir model, as shown in Figure 8.14(a). The constant parameters and correlation coefficient (R^2) are summarized in Table 8.6. The Langmuir constant q_m i.e., adsorption capacity of *Tretepohila abietina* for Pb^{2+} and Cd^{2+} were calculated as 33.22 and 16.53 mg/g respectively. Sorption energy constants, K_L of *T. abietina* for Pb^{2+} and Cd^{2+} were 17.71 and 7.29 L/mg respectively. The dimensionless separation factor or equilibrium parameter, R_L expresses the essential characteristics of Langmuir equation and R_L values for Pb^{2+} and Cd^{2+} obtained in this study were between 0 and 1, which indicate favourable adsorption (Bhatt & Shah, 2013).

Table 8.5: Parameters for plotting Langmuir, Freundlich, Temkin and Dubinin - Radushkevich adsorption isotherms

Metal ions	C_0 (mg/L)	C_e (mg/L)	$\log C_e$	$\ln C_e$	q_e (mg/g)	$\log q_e$	$\ln q_e$	C_e / q_e (g/L)	ε^2
	50.14	0.11	-0.959	-2.207	25.02	1.398	3.219	0.0044	$33.465054*10^6$
	55.05	0.62	-0.208	-0.478	27.22	1.435	3.304	0.0228	$5.777146*10^6$
Pb^{2+}	60.25	1.21	0.083	0.191	29.52	1.470	3.385	0.0410	$2.272390*10^6$
	65.12	1.92	0.283	0.652	31.60	1.500	3.453	0.0608	$1.100821*10^6$
	70.26	2.61	0.417	0.959	33.83	1.529	3.521	0.0772	$0.658872*10^6$
	50.05	0.53	-0.276	-0.635	12.38	1.093	2.516	0.0428	$7.038569*10^6$
	55.13	0.75	-0.125	-0.288	13.60	1.133	2.610	0.0552	$4.495989*10^6$
Cd^{2+}	60.06	1.42	0.152	0.351	14.66	1.166	2.685	0.0969	$1.779868*10^6$
	65.45	3.53	0.548	1.261	15.48	1.190	2.740	0.2280	$0.389610*10^6$
	70.37	4.81	0.682	1.571	16.39	1.215	2.797	0.2935	$0.223430*10^6$

The adsorption intensity (n) and the sorption capacity (K_f) were directly obtained from the slope and intercept of the plot, $\log q_e$ versus $\log C_e$ (Figure 8.14(b)) and are exhibited in Table 8.6. Freundlich constants K_f of *T. abietina* were calculated as 29.74 and 13.72 (mg/g) $(L/mg)^{1/n}$ and n were obtained as 11.06 and 8.93 for Pb^{2+} and Cd^{2+} respectively. For both metals, the values of n were found to be greater than1, indicates the favourable sorption condition. Figure 8.14(c) shows the linear form of the Temkin isotherm was plotted as q_e against $\ln C_e$ and a straight line was observed for both the metals. The values of the

Temkin constant b, indicates that the heat of adsorption is maximum for Cd^{2+} compared to Pb^{2+} (Table 8.6). The values of mean free energy, E obtained from D-R isotherm model (Figure 8.14(d)) were 8.452 and 3.686 kJ/mol for Pb^{2+} and Cd^{2+} respectively. The E value for Pb^{2+} was found in the range of 8 - 16 kJ/mol, indicating that the type of sorption of Pb^{2+} on biosorbent *T. abietina* is essentially chemisorption based on ion-exchange but for the sorption of Cd^{2+}, it was found in the range of 1 to 8 kJ/mol, indicates the physical sorption.
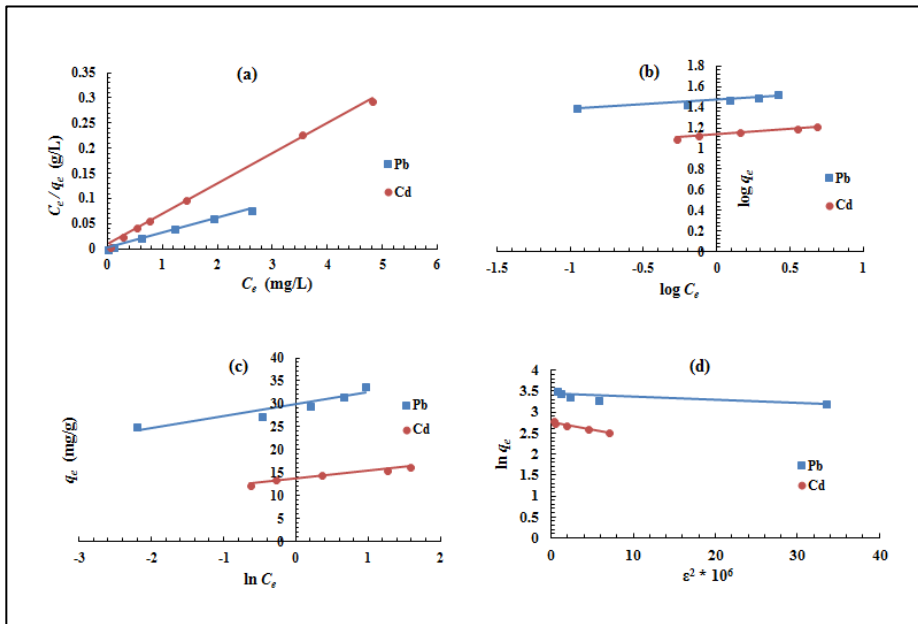
Figure 8.14: (a) Langmuir, (b) Freundlich, (c) Temkin and (d) Dubinin - Radushkevich adsorption isotherms for adsorption of Pb^{2+} and Cd^{2+} by algal biosorbent *T. abietina*

Evaluation of the suitable isotherm model for the sorption of Pb^{2+} and Cd^{2+} by *T. abietina* was conducted using the correlation coefficients value (R^2) and the results indicates that R^2 values of Langmuir isotherm

for Pb^{2+} and Cd^{2+} were 0.9946 and 0.9982 respectively. The Langmuir isotherm fits very close to the experimental data of the sorption of both the metals and the Langmuir equation assumes a homogeneous distribution of active sites on surface of *T. abietina*. The values of q_m determined by the Dubinin-Radushkevich isotherm model also fits close to the experimentally determined data for Pb^{2+} and Cd^{2+}. The order of adsorption isotherm models fitted the equilibrium data are for Pb^{2+}: Langmuir isotherm > Freundlich isotherm > Temkin isotherm > Dubinin-Radushkevich isotherm and for Cd^{2+}: Langmuir isotherm > Dubinin-Radushkevich isotherm > Temkin isotherm > Freundlich isotherm.

Table 8.6: Isotherm models constants and correlation coefficients for adsorption of Pb^{2+} and Cd^{2+} onto biosorbent *T. abietina*

Isotherm models	Parameters	Metal ions	
		Pb^{2+}	Cd^{2+}
Langmuir	q_m (mg/g)	33.22	16.53
	K_L(L/mg)	17.71	7.29
	R_L	0.0008 - 0.0014	0.0019 - 0.0034
	R^2	0.9946	0.9982
Freundlich	K_f (mg/g) $(L/mg)^{1/n}$	29.74	13.72
	n	11.06	8.93
	R^2	0.9094	0.9445
Temkin	A (L/g)	97967.21	5224.57
	b (kJ/mol)	0.9621	1.555
	R^2	0.8839	0.9559
Dubinin – Radushkevich	q_m (mg/g)	31.09	15.99
	β (mol²/kJ²)	0.007	0.0368
	E (kJ/mol)	8.452	3.686
	R^2	0.672	0.961

8.3.2.3 Adsorption kinetics

Kinetic models such as Pseudo-first-order, Pseudo-second-order kinetic model, Intraparticle diffusion model, Elovich kinetic model and Bangham's model were used to fit the experimental data to realize the potential rate-controlling steps involved in the process of sorption of Pb^{2+} and Cd^{2+} onto the biosorbent *Tretepohila abietina*. To evaluate the adsorption kinetics of Pb^{2+} and Cd^{2+} ions sorption by *Tretepohila abietina* were studied for contact period of 120 min using 10 mg/L of metal solutions. A sharp increase in adsorption capacity was noticed initially but gradually it attains the equilibrium state. The adsorption of Pb^{2+} and Cd^{2+} ions onto *T. abietina* attains the equilibrium state at 20 min and 25 min respectively. The calculated kinetics parameters for sorption of heavy metal ions onto the biosorbent *T. abietina* are tabulated in Table 8.7.

The pseudo-first-order rate constants k_1 and q_e determined from the slope and intercept of the Lagergren's plot (Figure 8.15(a) i.e., log (q_e - q_t) against t) and the second-order constants, k_2 and q_e were calculated from the intercept and slope of the linear second-order kinetic plot (Figure 8.15(b) i.e., t/q_t against t). As revealed in Table 8.7, the high correlation coefficient (R^2) of pseudo-second-order equation ($R^2 = 0.9992$ for Pb^{2+} and $R^2 = 0.9971$ for Cd^{2+}) is obviously superior to that of pseudo-first-order equation ($R^2 = 0.9473$ for Pb^{2+} and $R^2 = 0.9557$ for Cd^{2+}). Furthermore, the adsorption capacity $q_{e,cal}$ calculated from pseudo–second-order model is 5.187 and 2.607 mg/g for Pb^{2+} and Cd^{2+} respectively and is very similar to experimentally determined, $q_{e,exp}$ values. Results indicated that the adsorption process of Pb^{2+} and Cd^{2+} by

the biosorbent *Tretepohila abietina* followed the pseudo-second-order kinetics rather than the first-order model.
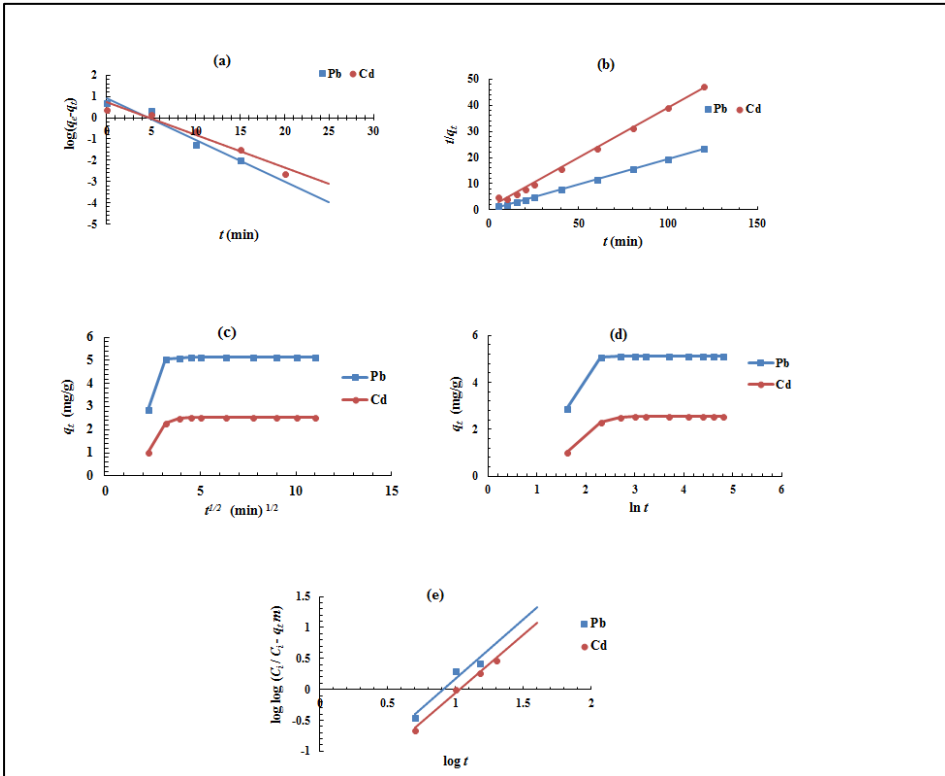
Figure 8.15: (a) pseudo-first-order; (b) pseudo-second-order, (c) Intraparticle diffusion plot, (d) Elovich kinetic model and (e) Bangham's model of the heavy metal adsorption on *T. abietina*

The Weber and Morris equation i.e., equation (9) was used to elucidate whether the sorption process is controlled by bulk diffusion or intraparticle diffusion. Weber and Morris model suggests that if sorption of a solute is controlled by the intraparticle diffusion process then the plot

of q_t against $t^{1/2}$ gives a straight line. The involvement of two or more steps in sorption process was indicated by the multi - linearity of the plots (Figure 8.15(c)). The plots of both the metals possess the similar general features, initial curved portion followed by linear portion and a plateau. The initial portion is attributed to the bulk diffusion and subsequent linear portion is attributed to the intraparticle diffusion. The fitness of particle diffusion model indicates that the removal of Pb^{2+} and Cd^{2+} is a surface process under the studied conditions.

Table 8.7: Kinetic parameters for the adsorption of Pb^{2+} and Cd^{2+} by the biosorbent *Tretepohila abietina*

Kinetic models	Parameters	Values	
		Pb^{2+}	Cd^{2+}
	$q_{e,exp}$ (mg/g)	5.125	2.543
Pseudo-first-order kinetic model	k_1 (min^{-1})	0.4489	0.3540
	$q_{e,cal}$ (mg/g)	8.175	5.226
	R^2	0.9473	0.9557
Pseudo-second-order kinetic model	k_2 (g/mg min)	0.1980	0.1816
	$q_{e,cal}$ (mg/g)	5.187	2.607
	R^2	0.9992	0.9971
Intraparticle diffusion model	k_{id} (mg/g min$^{1/2}$)	0.1140	0.0860
	C (mg/g)	4.178	1.822
	R^2	0.2323	0.2932
Elovich kinetic model	α (mg/g min)	1486.99	19.68
	β (g/mg)	2.372	3.213
	R^2	0.3878	0.4686
Bangham's model	K_0	2.081	0.660
	α	1.915	1.883
	R^2	0.9494	0.993

The simplified Elovich kinetic model equation was already discussed in chapter 7 can be expressed as equation (13)

$$q_t = \frac{1}{\beta}\ln(\alpha\beta) + \frac{1}{\beta}\ln t \qquad (13)$$

where α is the initial desorption rate (mg/ (g min)) and β is the desorption constant (g/mg) during experiments. The slope and intercept of plot of q_t against ln t gives the values of both constants of Elovich equation. The value of slope (1/β) indicates the number of sites available for adsorption whereas the value of intercept (1/β ln (αβ)) reflects the adsorption quantity when ln t equal to zero. Elovich model plots for the sorption of Pb^{2+} and Cd^{2+} on the biosorbent *Tretepohila abietina* at 301K are shown in Figure 8.15(d). The correlation coefficient (R^2) obtained for both metals were < 0.98 so this model was less satisfactory.

The results suggest that the intra particle diffusion process is not the rate controlling step involved in the Pb^{2+} and Cd^{2+} adsorption process thus for confirming whether the pore diffusion is rate controlling step or not we analyse the Bangham's kinetic Model. Kinetic data were tested using Bangham's equation (Singh & Majumder, 2015) expressed as follows:

$$\log\log\left(\frac{C_i}{C_i - q_t\, m}\right) = \log\left(\frac{K_0\, m}{2.303\, V}\right) + \alpha\log(t) \qquad (14)$$

Where C_i and V are the initial concentration (mg/L) and the volume (mL) of the heavy metal solutions respectively. m is the mass of the adsorbent (g/L), q_t is the amount of the metals adsorbed at time t

(mg/g) and K_0 and α are constants. The plot of $\log\log\left(\frac{c_i}{c_i - q_t\,m}\right)$ against log t for the sorption of Pb^{2+} and Cd^{2+} on the biosorbent *T. abietina* are shown in Figure 8.15(e). The plots of both metals were found to be linear having high correlation coefficient (>0.9) close to 1 which indicates that the kinetic data is best fitted with Bangham's model compared to intraparticle diffusion model. Therefore, the adsorption of Pb^{2+} and Cd^{2+} on the biosorbent *T. abietina* was pore diffusion controlled.

8.3.2.4 Effect of temperature and thermodynamic parameters

Temperature plays a major role in biosorption of metal ions so, to understand the effect of temperature or thermodynamics, the sorption of Pb^{2+} and Cd^{2+} on *T. abietina* were performed at four different temperatures (301, 333, 353 and 373K). With increase in temperature, a slight decrease in removal efficiency and adsorption capacity was observed but a significant change was not observed. The increase in temperature, weakens the attractive forces between adsorbent surface and metal ions consequently the sorption decreases. $\Delta H°$ and $\Delta S°$ values were determined from the slope and intercept of Vant's Hoff plot (ln K_c versus 1/T) (Figure 8.16) of each metal ions and the $\Delta G°$, $\Delta H°$ and $\Delta S°$ values are presented in the Table 8.8. The $\Delta H°$ is negative value which implies an exothermic adsorption process and the positive $\Delta S°$ value corresponds to an increase in degree of freedom of the system under study. The negative values of $\Delta G°$ confirms the spontaneity of the adsorption Pb^{2+} and Cd^{2+} onto *T. abietina.*
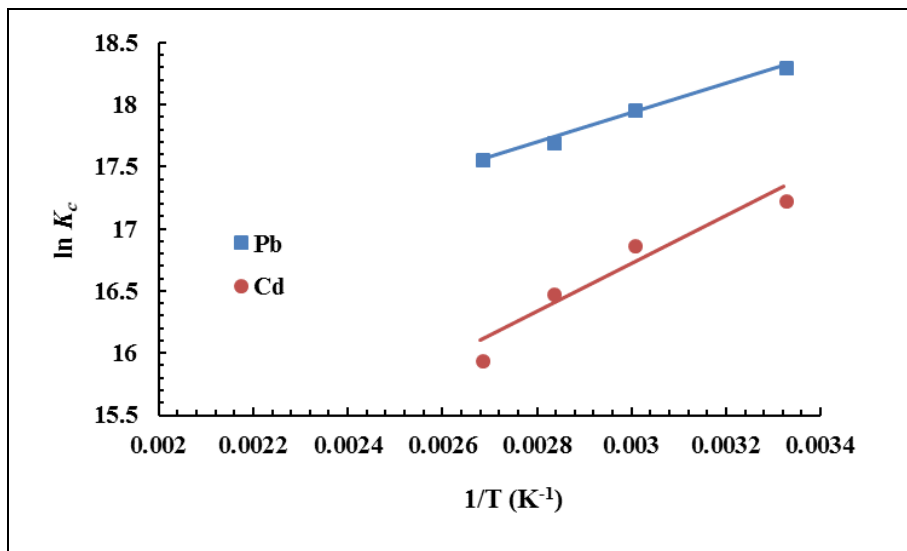
Figure 8.16: Van't Hoff plot

Table 8.8: Thermodynamic parameters for the adsorption of Pb^{2+} and Cd^{2+} onto *T. abietina* at different temperatures

Metal ions	T (K)	ΔG° (kJ/mol)	ΔH° (kJ/mol)	ΔS° (J/mol K)
Pb²⁺	301	-45.84	-9.86	119.58
	333	-49.76		
	353	-51.96		
	373	-54.51		
Cd²⁺	301	-43.14	-16.05	90.81
	333	-46.73		
	353	-48.39		
	373	-49.46		

8.3.2.5 Desorption and reusability studies

The desorption and reusability study of algal biosorbent, *Tretepohila abietina* loaded with metal ions were carried out using different types of desorption agents (0.1 M HCl, 0.1 M NaOH, 0.1 M HNO$_3$, and 0.1 M EDTA) and stirred at 150 rpm for 2 h at room temperature. The results showed that 0.1 M HCl was suitable as a desorption agent due to its highest metal desorption activity (98.4 % for Pb^{2+}and 95.7 % for Cd^{2+}) and used for further adsorption–desorption cycles. Adsorption- desorption cycles were repeated for five times to check the reusability of *T. abietina* in batch experiment mode. To regenerate, the biosorbent was washed thoroughly with deionized water and dried at 60$°$C for subsequent sorption study. The adsorption capacity of *T. abietina* for Pb^{2+} and Cd^{2+} ions were not declined significantly even after the fifth adsorption-desorption cycle. Moreover, the biodegradable nature of algal biosorbent, *T. abietina* make its easy disposal.

8.3.2.6 Surface analysis

The morphology of the biosorbent *Tretepohila abietina* was investigated using scanning electron micrographs (SEM) and Energy-dispersive X-ray (EDX) spectra to understand the surface features. Figure 8.17(a) represents SEM image of biosorbent before adsorption and Figure 8.17(b and c) shows the surface of *T. abietina* after the sorption of Pb^{2+} and Cd^{2+} respectively. The SEM image of *T. abietina* (Figure 8.17(a)) indicates cracks and channels which may increases the sorption ability of biosorbent. As breaking of large particles generates tiny cracks and channels on the particle surface of the adsorbent material

leads to more accessibility to better diffusion (Karthikeyan et al., 2004). It can be observed from SEM images that the surface of the adsorbent material has porous and irregular structure. The EDX spectra (Figure 8.17(d)) of *T. abietina*, before metal adsorption did not exhibit the characteristic signals of Pb^{2+} and Cd^{2+}. But, the signals of the presence of Pb^{2+} and Cd^{2+} were observed in EDX (Figure 8.17(e and f)) pattern of biosorbent after metals adsorption.

8.3.2.7 FTIR analysis of biosorbent

Figure 8.18 shows the FTIR spectra of the biosorbent *Tretepohila abietina.* The peak at 3349.29 cm^{-1} was due to normal OH stretch. The peaks at 2925.37 cm^{-1} indicates the methylene C-H asym/sym stretch. The major peak between 1050 - 990 cm^{-1} with a maximum at 1032.02 cm^{-1} implies the presence of aliphatic phosphates (P-O-C stretch). The band observed between 1750-1725 implies the presence of ester. The peaks at 1661.66 cm^{-1} and 1370.49 cm^{-1} indicates alkenyl C=C stretch and carboxylate, respectively. The spectra also show small intensity peaks at 1159.03 cm^{-1} and 669.33 cm^{-1}, indicating the presence of secondary amine and alcohol (OH out of plane bend) group. The presence of functional groups increases the sorption capacity of the biosorbent, by binding with the metal ions.
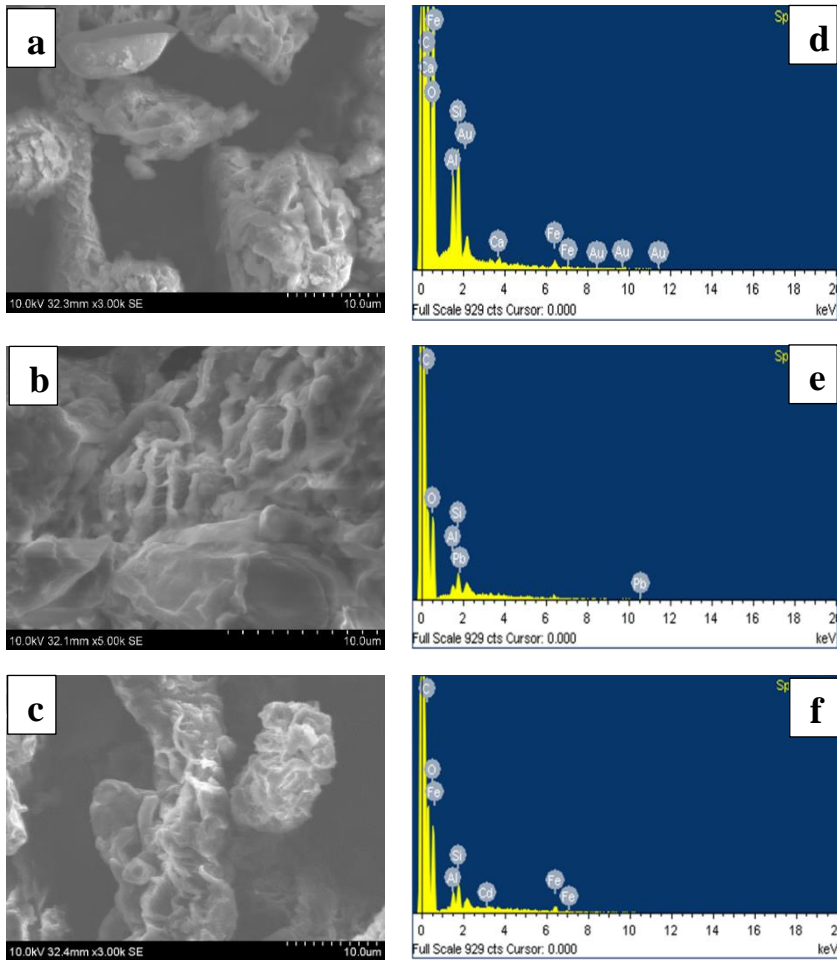
Figure 8.17: (a) (b) and (c) are SEM image of *T. abietina* surface before adsorption and after the adsorption of Pb^{2+} and Cd^{2+} and (d), (e) and (f) are the corresponding EDX spectra
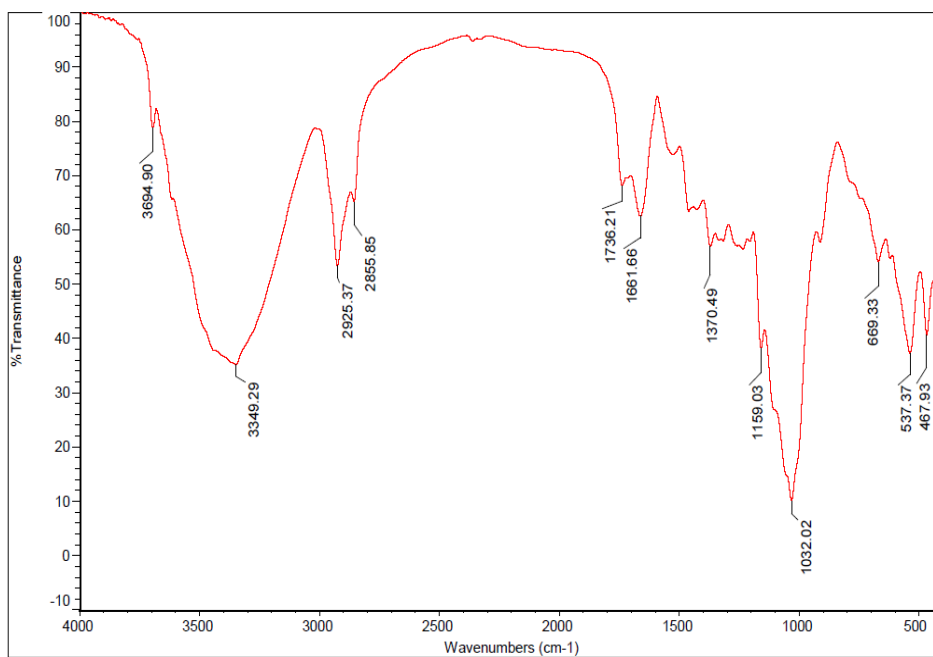
Figure 8.18. FTIR spectra of the biosorbent *Tretepohila abietina*

8.4 Summary

For the removal of heavy metals from water, two biosorption studies were conducted using an herbal plant material, *Caesalpinia sappan* and an algal biomass, *Trenteohilia abietina*. Before the biosorption of Pb^{2+}, Cd^{2+} and Cu^{2+} ions by *Caesalpinia sappan*, the plant material was boiled and washed with deionised water and undergone protonation so that the biosorbent does not impart colour to water. Maximum removal efficiency was observed between pH 4 and 10 for Pb^{2+} and for Cd^{2+} and Cu^{2+}, it was found between pH 6 and 10. An optimum pH of 7 was maintained for the

sorption study by *C. sappan.* The maximum removal efficiencies were observed at shaking speed of 150 rpm for Pb^{2+} ions and at 200 rpm for Cd^{2+} and Cu^{2+} ions. For adsorbent *Caesalpinia sappan,* the order of metal ions sorption is as follows: 9.14 mg/g for Pb^{2+} > 7.23 mg/g for Cu^{2+} > 6.10 mg/g for Cd^{2+} under varying initial metal concentration from 5 - 45 mg/L. The results of batch adsorption experiments, clearly suggest that the operating parameters such as solution pH, initial metal concentration, contact time, temperature, adsorbent dosage, presence of light metal ions and shaking speed were effective on the removal efficiency of metal ions. But the operating conditions required for the better removal efficiency of each heavy metals ions from aqueous solution would be different. The experimentally obtained equilibrium data were analyzed by different isotherm models and the high correlation coefficients (R^2) values indicate that the adsorption data best fitted the Langmuir adsorption isotherm for all three metals. Dubinin - Radushkevich (D-R) isotherm model also fits very well to the experimentally determined data for Pb^{2+}, Cd^{2+} and Cu^{2+} and the kinetic data of adsorption of heavy metal ions on *Caesalpinia sappan* are best modelled by the pseudo-second-order kinetic equation. Thermodynamic parameters indicated the exothermic behaviour and spontaneous nature of the adsorption process. The desorbing agent, 0.1M HCl was found to be suitable for the desorption study. The biosorption properties of *C. sappan* for Pb^{2+}, Cd^{2+} and Cu^{2+} ions indicate that *Caesalpinia sappan* may be used as an inexpensive, effective, herbal and easily cultivable biosorbent that can be useful in water treatment for the adsorption of metal ions.

The removal of Pb^{2+} and Cd^{2+} from aqueous solutions using algal biomass *Trenteohilia abietina* by batch sorption experiments revealed that the maximum sorption is possible for both metals under a wide range of pH (pH: 4 -12 for Pb^{2+} and pH: 6 - 12 for Cd^{2+}). High removal efficiencies were observed for Pb^{2+} and Cd^{2+} at the adsorbent dosage of 2 g/L and 4 g/L respectively. The increase in metals concentration from 40 to 70 mg/L leads to an increase in adsorption capacity from 20.01 mg/g to 33.83 mg/g for Pb^{2+} and from 10.02 mg/g to 16.39 mg/g for Cd^{2+}. Rapid removal was observed for both the metals. The Langmuir isotherm model were better fitted to represent the experimental data, indicate favourable adsorption and the maximum adsorption capacity of Pb^{2+} and Cd^{2+} by *T. abietina* was 33.22 mg/g and 16.53 mg/g, respectively. The q_m determined by the Dubinin-Radushkevich isotherm model also fits close to the experimentally determined data for both the metals. and 3.686 kJ/mol for Pb^{2+} and Cd^{2+}. The mean free energy obtained for the biosorption of Pb^{2+} and Cd^{2+} as 8.452 kJ/mol and 3.686 kJ/mol, indicating the involvement of chemisorption and physical sorption in the removal of Pb^{2+} and Cd^{2+} respectively. The kinetic model that best represented the experimental data was the pseudo-second order. The good fitting of the kinetics data to Bangham's Model indicate that in the adsorption of Pb^{2+} and Cd^{2+} on the biosorbent *T. abietina*, pore diffusion plays a vital role in controlling the rate of reaction. The calculated $\Delta G°$, $\Delta H°$ and $\Delta S°$ values disclosed that the sorption of Pb^{2+} and Cd^{2+} ions onto *T. abietina* was exothermic and spontaneous under examined conditions. The reusability of *T. abietina* as a biosorbent was found good after five consecutive sorption-desorption cycles and 0.1 M HCl was suitable as a desorption

agent. The recovered algal biosorbent, *T. abietina* is biodegradable, inexpensive and environment friendly. The algal biosorbent, *Trenteohilia abietina* has the potential for removal and recovery of metal ions from contaminated water.

TREATMENT OF LEAD AND CADMIUM USING SURFACE MODIFIED IRON OXIDE NANOPARTICLES

9.1 Introduction

Application of iron oxide nanoparticles-based nanomaterials for the remediation of toxic elements like heavy metals from water is a well-recognized technique. Nowadays, the materials such as magnetic NMs, carbon nanotubes, activated carbon, and zero-valent iron have wide application in the field of water and wastewater treatment. Among these, iron oxide magnetic NMs, owing to its significant physiochemical property, convenient for magnetic separation, the capability to treat large volume of wastewater, inexpensive method and easy regeneration in the presence of external magnetic field make them as most promising materials for purification of heavy metals (Hu et al., 2010; Xu et al., 2012; Dave & Chopda, 2014). The iron oxide nanomaterials possess unique properties like high surface-area-to-volume ratio, extremely small size, excellent magnetic properties, surface modifiability and great

biocompatibility. Iron oxide nanomaterials have been applied in wastewater treatment, as nanosorbents and photocatalysts in many environmental clean-up technologies (Xu et al., 2012). In remediation of heavy metals from water, surface modification strategy is utilised to improve the heavy metal removal efficiency of iron oxide nanoparticles. Magnetic property of iron oxide nanoparticles enables its easy separation and reusability for further application. The reusability of iron oxide-based nanosorbent decreases its economic burden (Dave & Chopda, 2014).

Surface modification can be done by the attachment of organic molecules and/or inorganic shells, which not only stabilizes the nanoparticles and ultimately prevents their oxidation, but also offers specific functionalities having selectivity for metal ion and thus improve the capacity for heavy metal uptake in water treatment process. Various types of functionalized materials have been employed for grafting the surface of NMs for the removal of heavy metal (Ambashta & Sillanpää, 2010; Girginova et al., 2010). For example, carbon-encapsulated magnetic nanoparticles were applied for the removal of Cu^{2+} and Cd^{2+} (Bystrzejewski et al., 2009). Surface sites binding (Hu et al., 2010), magnetic selective adsorption (Ozmen et al., 2010), electrostatic interaction (Zhong et al., 2006), and modified ligands combination (Hao et al., 2010) are the main mechanisms involved in the sorption of contaminants from wastewater by surface modified iron oxide. By surface modification strategy iron oxide nanoparticles can achieve high metal removal efficiency.

Adsorption based treatment technology is considered as the most promising technique in the removal of heavy metal from contaminated water due to its high efficiency, low cost-effective, and simple operation. Adsorption mechanism involves surface complexation i.e., the reaction between adsorbate (an ion or molecule) and the functional group present on the adsorbent surface. The adsorption mechanism is based on the surface complex formed during adsorption. Surface complexes are mainly outer- and inner-sphere surface complexes, which formerly were known as physical and chemical adsorption, respectively. In the outer-sphere surface complex formation, surface charge is a crucial factor, since electrostatic interactions and van der Waals forces (both are weak forces) are involved in the process. But in inner-sphere surface complexation, a covalent or ionic bond (strong forces) is involved, and it is irrespective to the surface charge. Removal of lead and cadmium using functionalised iron oxide nanoparticles such as iron oxide nanoparticles coated with polyvinyl alcohol and gallic acid was studied in this chapter. The results of the removal study were also compared with the results of uncoated iron oxide nanoparticles.

9.2 Materials and Methods

9.2.1 Reagents

All the chemicals and regents used were AR grade procured from Merck Ltd. India. Iron (III) nitrate nine hydrate {Fe $(NO_3)_3$.$9H_2O$} and ammonium hydroxide (NH_4OH) were used for the synthesis of iron oxide nanoparticles. For functionalization of iron oxide nanoparticles, polyvinyl alcohol (98 % degree of hydrolysis) and gallic acid were utilized.

Polyvinyl alcohol (PVA) is a hydrophilic polymer with a simple chemical structure having high hydroxyl group and form cross linked network within the water solution, which is applied in biomedical and pharmaceutical fields due to its properties such as biocompatibility, nontoxicity, noncarcinogenicity, nonimmunogenicity, and inertness in body fluids. Gallic acid (3,4,5-trihydroxybenzoic acid), an anticancer drug, can be found from a variety of natural products such as gallnut, black tea, and sumac, and it also possesses the properties like antimutagenic, antiviral, anti-inflammatory, and antimicrobial (Dorniani et al., 2014).

Lead and cadmium, synthetic solutions were used in the adsorption studies were prepared using lead nitrate $\{Pb(NO_3)_2\}$ and cadmium sulphate$\{(3CdSO_4).8H_2O\}$ respectively. Deionized water was used in all experiments. Stock solution (1000 mg/L) of Pb^{2+} was prepared by dissolving 1.5985g of $Pb(NO_3)_2$ in 1000 mL of deionized water and 1000 mg/L Cd^{2+} stock solution was prepared by dissolving 2.2819 g of $(3CdSO_4).8H_2O$ in 1000 mL of deionized water. Experimental solutions of the desired concentrations were obtained by successive dilutions.

9.2.2 Preparation of nanosorbent

9.2.2.1 Preparation of iron oxide nanoparticles

Iron oxide nanoparticles was prepared by using iron (III) nitrate nine hydrate $\{Fe(NO_3)_3.9H_2O\}$ as inorganic salt and ammonium hydroxide (NH_4OH) as precipitating agent. 0.5 M ammonium hydroxide solution was prepared and added drop-wise to 0.1 M iron (III) nitrate

solution under vigorous stirring. The volume ratio of two solutions was 1:1. In this step, instant formation of red precipitate was observed. The supernatant was removed from the red precipitate by decantation. Deionized water was added to the precipitate and the solution was decanted after centrifugation at 3000 rpm. The last procedure was repeated three times to remove the impurities. Dry powder was obtained by filtering and drying under vacuum. Then it was heated at 250^0C for 2 h in air to get Fe_2O_3 particles from $Fe_2(OH)_6$ (Park et al., 2001). In this experiment, when NH_4OH was added as precipitating agent, the iron oxide particles were formed by following chemical reactions.

$$2Fe(NO_3)_3 + 6\ NH_4OH \longrightarrow Fe_2(OH)_6 \downarrow + 6\ NH_4NO_3$$
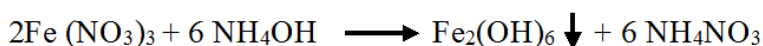
$Fe_2(OH)_6$ particles were flocculated and precipitated in the aqueous solution immediately after its formation. The $Fe_2(OH)_6$ precipitates were transformed into iron oxide by calcination for 2 h at 250 °C by the following reaction (Mahan et al., 1987).

$$Fe_2(OH)_6 \longrightarrow Fe_2O_3 + 3H_2O \downarrow$$
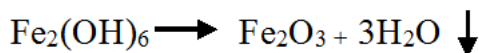
9.2.2.2 Preparation of surface modified iron oxide nanoparticles

The prepared iron oxide nanoparticle was dispersed in 100 mL deionized water and mixed with 1 % polyvinyl alcohol. After stirring the mixture for 24 h, the precipitates were collected by a permanent magnet and washed three times to remove the excess polyvinyl alcohol, which does not participate in the coating process and then dried in an oven. The 2 % of gallic acid (dissolved in deionized water) was added into the iron

oxide nanoparticle - polyvinyl alcohol and the mixture was stirred for 24 h. Finally, the coated iron oxide was washed and dried in an oven to obtain iron oxide nanoparticles coated with polyvinylalcohol and gallic acid (Dorniani et al., 2014).
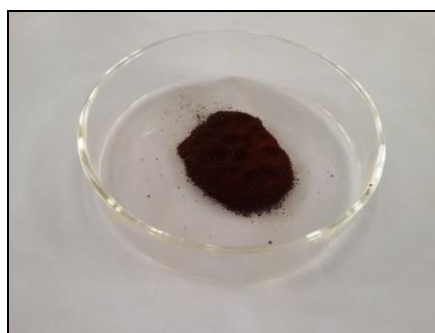
Plate 9.1: Iron oxide nanoparticles coated with polyvinylalcohol and gallic acid
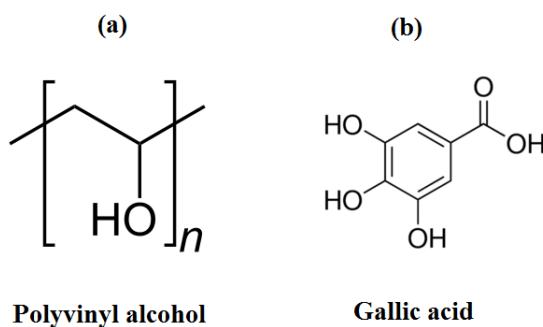
Figure 9.1: (a) Polyvinyl alcohol and (b) Gallic acid

Gallate anion were immobilized on the surface of iron oxide nanoparticles prepared using polyvinyl alcohol (PVA) as a polymer stabilizer, to improve the reducing of the size distribution of the nanoparticles (Dorniani et al., 2014). In this study, iron oxide

nanoparticles were chosen as a core and PVA - gallate anion chosen as shells to be adsorbed on the surface of the core. Removal of lead and cadmium using this surface modified iron oxide nanoparticles were studied in this chapter.

9.2.3 Sorption experiment

Contaminated aqueous solutions were artificially prepared by adding appropriate quantities of metals into the deionized water. Sorption experiments were conducted under different conditions, to understand the rate and equilibrium data in single species batch sorption system. The known quantity of the nanosorbents, nanoparticles were transferred into 250 mL screw topped flasks and agitated with 100 mL of known concentration of heavy metal solutions for a predetermined period in a temperature-controlled shaker. After sorption study, the residual concentrations of heavy metals (Pb^{2+} and $Cd^{2+)}$ in the aqueous solution were determined using AAS. All the analysis was done in triplicate to check precision and average values are only reported. Five different conditions were applied to study the adsorption behavior. The adsorption behavior was studied under five different conditions of: 1) pH, 2) adsorbent dosage, 3) contact time, 4) initial metal concentration, 5) temperature. A comparison of adsorption capacity of iron oxide nanoparticles (IONPs) and iron oxide coated with polyvinyl alcohol and gallic acid (PG-IONPs) were carried out.

To find the optimum pH for adsorption, 0.1 mol/L HCl and 0.1 mol/L NaOH solutions were used to vary pH from 2 to 12 and the sorbent dosage was also varied from 0.5-10 g/L. The initial metal concentrations

were varied from 5-25 mg/L and mixed with optimum dosage of nanosorbent at optimum pH and room temperature for a predetermined period required for better sorption of Pb^{2+} and Cd^{2+}. The sorption studies were carried out by mixing nanosorbent and metal solutions (20 mg/L) using a mechanical shaker for 180 min. To investigate the effect of temperature on adsorption, sorption experiments were conducted at four different temperature (333K, 353K, 373K and 393K) using a temperature-controlled shaker with water bath. 150 rpm agitation speed was maintained for study.

The sorption efficiency (%) and amount of adsorbate adsorbed at equilibrium, q_e (mg/g) were calculated as per equation (1 and 2).

$$\text{Sorption efficiency (\%)} = \frac{(C_0 - C_e) * 100}{C_0} \tag{1}$$

$$q_e = \frac{(C_0 - C_e)V}{m} \tag{2}$$

where C_0 and C_e are the metal concentrations in the solution before and after treatment, respectively. V is the volume of the heavy metal solution (L), *M is* the mass of nanosorbent used (g).

The linearized form of Langmuir, Freundlich, Temkin and Dubinin - Radushkevich adsorption isotherms were used to investigate the adsorption capacity of iron oxide coated with polyvinyl alcohol and gallic acid. Kinetics of the adsorption of Pb^{2+} and Cd^{2+} on functionalized iron oxide nanoparticles were studied using pseudo-first order (Lagergren's first-order) model, pseudo-second order model and intraparticle diffusion kinetic model. The results iron oxide nanoparticles

and iron oxide coated with polyvinyl alcohol and gallic acid were compared. Thermodynamic parameters of PG-IONPs were also studied under different temperatures.

9.2.4 Desorption study of functionalized iron oxide nanoparticles

The Pb^{2+} and Cd^{2+} adsorbed nanosorbents were regenerated using 0.1 M HCl and 0.1 M NaOH. 50 mL of desorbing agents was added to known amount of metal adsorbed, functionalized iron oxide nanoparticles in 250 mL stopped bottle and agitated at 150 rpm for 1 h at room temperature using a mechanical shaker. After separation of nanosorbent, the concentration of metals in solution was measured using AAS.

9.3 Results and Discussions

9.3.1 Characterization of the iron oxide nanoparticles coated with poly vinyl alcohol and gallic acid

Fourier Transform - Infrared Spectrometer was used to identify the functional groups and chemical bonding of the coated materials. FTIR spectrums shows the characteristic peaks of iron oxide nanoparticles, PVA coated iron oxide nanoparticles and the iron oxide nanoparticles coated with poly vinyl alcohol and gallic acid in Figure 9.2, Figure 9.3 and Figure 9.4, respectively. Figure 9.2 shows that the iron oxide nanoparticles (IONPs) have absorption peak at 531.19 cm^{-1} and 448.28 cm^{-1}, which is due to Fe–O stretching in Fe_2O_3. The absorption bands in the range 400 - 750 cm^{-1} indicates Fe–O vibration mode of iron oxide nanoparticles. However, the PG-IONPs nanocomposites show

characteristic peaks of Fe–O at 531.65 cm^{-1} and 449.13 cm^{-1} respectively, which confirm the presence of iron oxide nanoparticles in the nanocomposites. PVA coated iron oxide nanoparticles also have absorption peaks between the range of 400 - 750 cm^{-1}. Figure 9.3 shows the presence of absorption band at 3323.18 cm^{-1}which indicates the hydroxyl (-OH) groups. The absorption bands in the range 3400-3200 cm^{-1} represents the intermolecular hydrogen bonded –OH group having polymeric association.
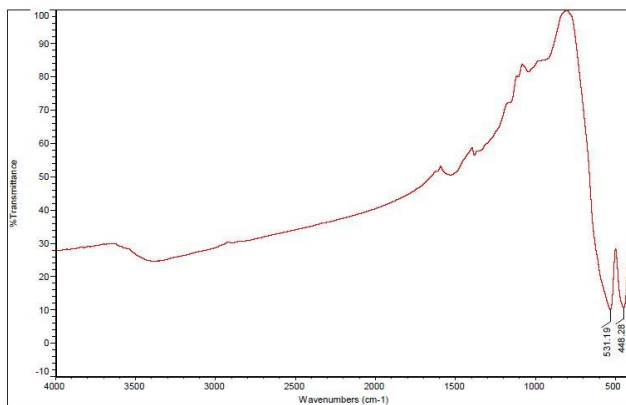
Figure 9.2: FTIR spectrum of iron oxide nanoparticles (IONPs)
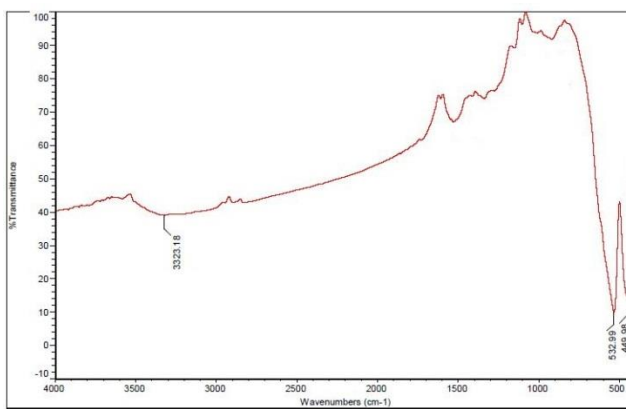
Figure 9.3: FTIR spectrum of PVA coated iron oxide nanoparticles

In PG-IONPs nanocomposite (Figure 9.4), the carboxylic acid O–H stretching band was observed at 2969.05 cm^{-1}. 1158 cm^{-1} is attributable to M–O–C (M=Fe) bond. This evidence confirms the attachment of PVA onto iron oxide nanoparticles via hydrogen bond between hydroxyl group of PVA and protonated surface of the oxide (Kayal & Ramanujan, 2010). FTIR spectrum of the PG-IONPs nanocomposite shows the characteristic peaks for GA, confirming that the surface of PVA is loaded with GA, for example, the peaks observed at 1562.17 and 1372.03 cm^{-1}, which are due to asymmetry and symmetry COO− stretching, respectively (Kayal & Ramanujan, 2010).
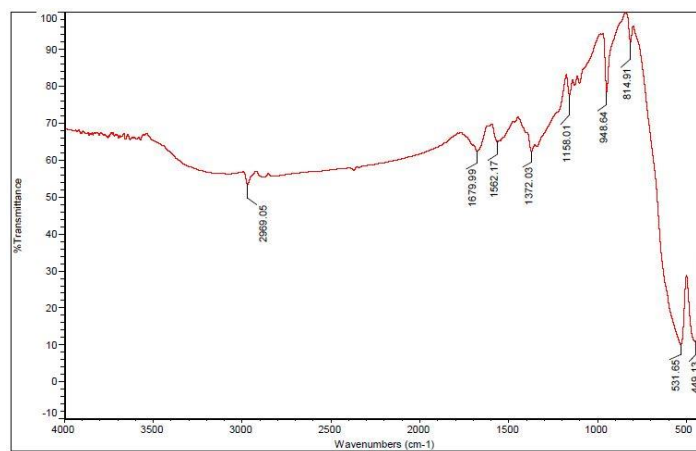
Figure 9.4: FTIR spectrum of iron oxide nanoparticles coated with poly vinyl alcohol and gallic acid (PG-IONPs)

Scanning Electron Microscopy (SEM) was used to study the surface morphology of IONPs and PG-IONPs (Figure 9.5(a-b)). The IONPs were rough and aggregated. The morphological characteristics of PG-IONPs (the iron oxide nanoparticles functionalised with PVA and gallic acid) was different from that of IONPs and which was favourable

for metal adsorption. EDX spectra of IONPs (Figure 9.6) confirmation the presence of iron and oxygen but the EDX spectra of PG-IONPs (Figure 9.7) shows the presence of iron, oxygen and carbon.
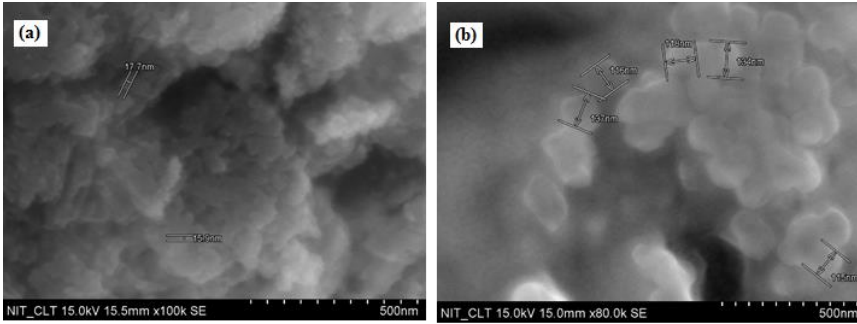
Figure 9.5: SEM images of (a) IONPs and (b) PG-IONPs
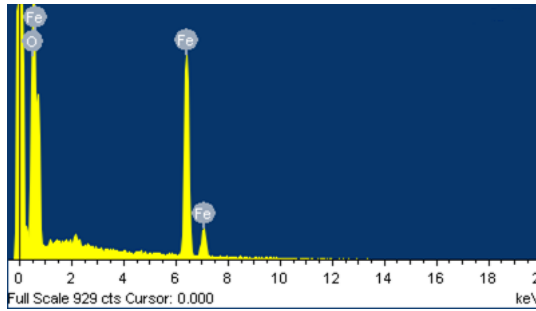
Figure 9.6: EDX spectra of IONPs
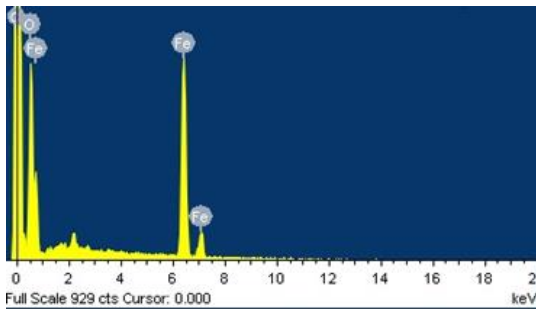
Figure 9.7: EDX spectra of PG-IONPs

The X-ray diffraction patterns of iron oxide nanoparticles and iron oxide nanoparticles coated with polyvinyl alcohol and gallic acid are shown in Figure 9.8(a) and Figure 9.8(b). For IONPs, characteristic peaks observed at 2θ: 24.22^0, 33.22^0, 35.71^0, 40.91^0, 49.56^0, 54.14^0, 62.51^0 and 64.08^0 and for PG-IONPs, peaks observed at 2θ: 23.87^0, 32.90^0, 35.38^0, 40.60^0, 49.21^0, 53.83^0, 62.20^0 and 63.79^0. For both iron oxide nanoparticles and iron oxide nanoparticles coated with polyvinyl alcohol and gallic acid, eight characteristic peaks were observed. The diffraction peaks obtained for iron oxide nanoparticles coated with polyvinyl alcohol and gallic acid were matched with the diffraction peaks of iron oxide nanoparticles which indicates that the coating process for Fe_2O_3 did not affect the phase change of iron oxide.
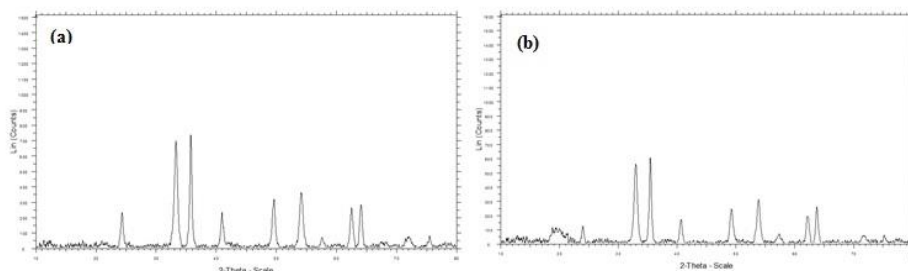
Figure 9.8: X-ray diffraction patterns for (a) IONPs and (b) PG-IONPs

9.3.2 Removal of Pb^{2+} and Cd^{2+} using PG-IONPs and IONPs

9.3.2.1 Effect of pH

The pH of the metal solution played a significant role in the removal of Pb^{2+} and Cd^{2+} and the effect of pH is shown in Figure 9.9(a). Adsorption studies were carried out in the pH range of 2 -12 for both

Pb^{2+} and Cd^{2+} at 303K (equilibrium time: 120 min; adsorbent dose: 1 g/L; adsorbate concentration: 10 mg/L; agitation speed: 150 rpm). The best pH range of Pb^{2+} and Cd^{2+} removal was observed between pH 4 and 12 in PG-IONPs. In the case of IONPs, maximum adsorption of Pb^{2+} and Cd^{2+} was observed from pH 6 and pH 8, respectively. Percentage of sorption and metal uptake increases with increase in pH. The electrostatic repulsion between the cations and surface sites resulted as the pH increases, so less insignificant competitive adsorption of H^+ ions and the positively charged metal ions gets adsorbed on the free binding sites, which leads to an increase in the total metal uptake. pH 7 was maintained during further sorption study.
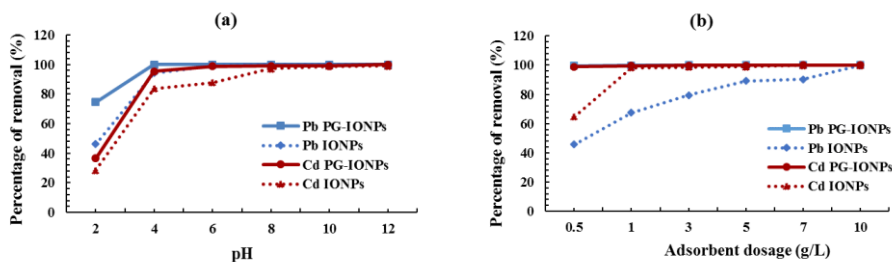
Figure 9.9: Effect of (a) pH and (b) adsorbent dosage on adsorption of Pb^{2+} and Cd^{2+}

9.3.2.2 Effect of adsorbent dosage

Effect of adsorbent dosage on removal of Pb^{2+} and Cd^{2+} from aqueous solution is presented in Figure 9.9(b). Adsorbent dosage was varied from 0.5 to 10 g/L for both Pb^{2+} and Cd^{2+} at 303K (equilibrium time: 120 min; pH: 7; adsorbate concentration: 10 mg/L; agitation speed: 150 rpm). Metal sorption capacity was found to increases with increases

the adsorbent dosage. In the case of PG-IONPs, the percentage removal of Pb^{2+} and Cd^{2+} increased from 99.61 % to 100 % and 98.86 % to 100 %, respectively. The percentage removal of Pb^{2+} and Cd^{2+} increased from 45.69 % to 99.98 % and 64.84 % to 99.83 %, respectively in the case of IONPs. Iron oxide nanoparticles coated with polyvinyl alcohol and gallic acid (PG-IONPs) exhibited maximum removal of Pb^{2+} and Cd^{2+} by using minimum amount of adsorbent dosage than iron oxide nanoparticles (IONPs). The functionalization of iron oxide nanoparticles increases the availability of more binding sites for complexation of metal ion which increases the metal sorption capacity of PG-IONPs. 1 g/L was taken as the adsorbent dosage for further studies.

9.3.2.3 Effect of contact time
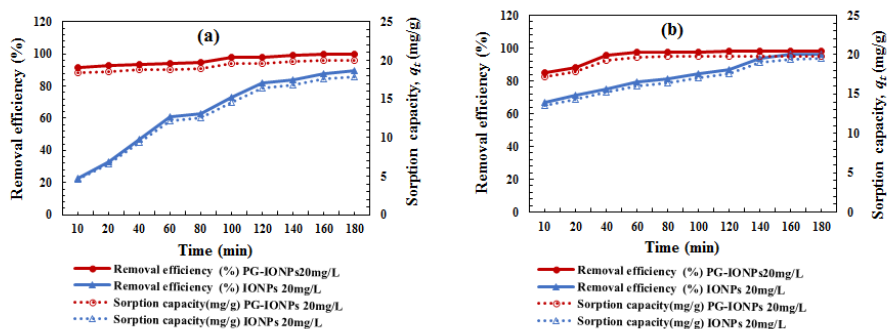
Figure 9.10: Effect of contact time on adsorption of (a) Pb^{2+} and (b) Cd^{2+}

To understand the suitable contact time at which the nanosorbents are saturated and the adsorption is at equilibrium, the effect of contact time was examined from 10 to 180 min at optimal conditions (adsorbent

dose: 1g/L; pH: 7; adsorbate concentration: 20 mg/L; agitation speed: 150 rpm). The influence of contact time on the removal of Pb^{2+} and Cd^{2+} from aqueous solution is depicted in Figure 9.10 (a and b). It was observed that the removal of Pb^{2+} and Cd^{2+} increases with rise in contact time. In the case of PG-IONPs, 91.77 % of Pb^{2+} and 84.89 % of Cd^{2+} was removed within 10 min of contact time and at 180 min, the removal of Pb^{2+} and Cd^{2+} was reached up to 99.85 % and 98.16 %, respectively. After 140 min, the rate of sorption was slow. Only, 22.71 % of Pb^{2+} and 66.72 % of Cd^{2+} was adsorbed by IONPs at 10 min.

Fast removal of metal ions was observed in the case of PG-IONPs compared to IONPs, this may be due to that the functional group present on the PG-IONPs provides more adsorption site for metal ions. The metal removal by PG-IONPs could be due to different sorption processes: adsorption (physisorption/chemisorption), co-ordination, complexion as a result of the ion binding groups such as hydroxyl, carboxylic, phenolic functional groups in PG-IONPs. PG-IONPs exhibited maximum sorption capacity of 19.98 mg/g and 19.86 mg/g for Pb^{2+} and Cd^{2+} at 180 min. Initially, the rate of removal was high and then slowed down as move towards the equilibrium condition.

9.3.2.4 Effect of temperature

Temperature plays a major role in adsorption of metal ions and the influence of temperature is presented in Figure 9.11. The effect of temperature on sorption were studied under four different temperature (333K, 353K, 373K and 393K) using a temperature-controlled shaker with water bath. The percentage of removal of Pb^{2+} and Cd^{2+} showed a

decreasing trend with increase in temperature for both nanosorbents, PG-IONPs and IONPs. As the temperature increases, the attractive forces between adsorbent surface and metal ions are weakened and the sorption decreases. As the temperature varied from 333 - 393 K, the sorption of Pb^{2+} and Cd^{2+} by PG-IONPs varied from 99.28 - 97.48 % and 99.89 - 91.04 %, respectively. But, in the case of IONPs, the sorption of Pb^{2+} and Cd^{2+} was varied from 98.60 - 44.63 % and 98.87 - 79.31 %, respectively. Compared to PG-IONPs, IONPs showed sharp decrease in the removal of metals with increase in temperature. This may be due to that the bonding between PG-IONPs and Pb^{2+} and Cd^{2+} ions were stronger than the bonding between IONPs and metal ions. In the energy dependent mechanisms in metal removal process, the temperature of the adsorption medium played a significant role.
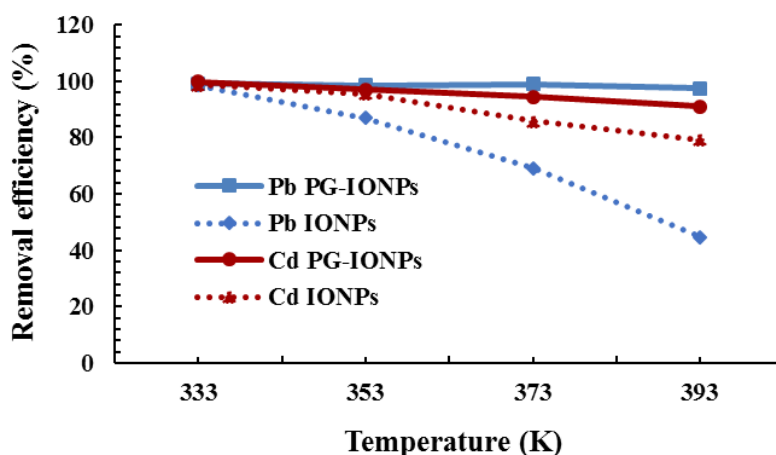
Figure 9.11: Effect of temperature on adsorption of Pb^{2+} and Cd^{2+}

9.3.2.5 Effect of initial metal ion concentration

As the initial metal concentration increased from 5 - 25 mg/L, a slight decrease in Pb^{2+} removal (99.98 - 97.93 %) by PG-IONPs was observed but, its sorption capacity was increased from 5.0 - 24.48 mg/g. The influence of initial metal concentration on the removal efficiency and sorption capacity of Pb^{2+} is depicted in Figure 9.12(a). For IONPs, the removal of Pb^{2+} decreased from 97.01 - 67.08 % and sorption capacity varied from 4.85 - 16.77 mg/g. A decreasing trend of Cd^{2+} removal was also observed with increasing initial metal concentration (Figure 9.12(b)). In the sorption of Cd^{2+} by PG-IONPs, the removal efficiency of Cd^{2+} decreased from 99.95 - 93.97 % with increase in initial concentration from 5 - 25 mg/L but for IONPs it decreased from 98.28 - 82.85 %.
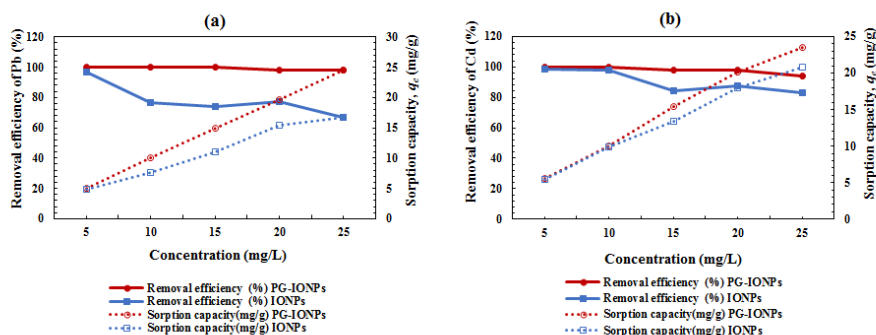
Figure 9.12: Effect of initial concentration of (a) Pb^{2+} and (b) Cd^{2+}

Initial metal concentration acted as a driving force to overcomes mass transfer resistance between solution and nanosorbent, so the sorption capacity of the nanosorbent increases with increase in the metal concentration. But, the increase in metal concentration resulted in relative

reduction of available binding sites which leads to the reduction in metal removal efficiency. PG-IONPs showed better results compared to IONPs, this may be due to the availability of more functional groups or active sites on the PG-IONPs.

9.3.3 Sorption equilibrium studies

The linearized sorption isotherm models such as Langmuir, Freundlich, Temkin and Dubinin - Radushkevich adsorption isotherms were used to investigate the information about the adsorption mechanisms and adsorbate-adsorbent interactions. The isotherm studies were conducted by varying the initial concentration of Pb^{2+} and Cd^{2+} from 5 - 25 mg/L and maintaining the adsorbent dosage of 1g/L at a constant temperature of 303K and neutral pH. Single species sorption experiments were conducted for each heavy metal. The linearized form of Langmuir, Freundlich, Temkin, and Dubinin - Redushkevich (D-R) isotherm models are detailly described in chapter 7 and 8. Isotherm models were applied to investigate the adsorption capacity of both, PG-IONPs (iron oxide coated with polyvinyl alcohol and gallic acid) and IONPs (iron oxide nanoparticle).

The values of Langmuir constants were calculated from the linear plot of C_e/q_e against C_e (Figure 9.13(a)) for the sorption of Pb^{2+} and Cd^{2+} by PG-IONPs and IONPs. For the metal sorption by PG-IONPs, Langmuir constants, q_m (Pb^{2+}: 23.42 mg/g and Cd^{2+}: 24.21 mg/g) and K_L (Pb^{2+}: 71.17 L/mg and Cd^{2+}: 14.75 L/mg) were obtained are presented in Table 9.1. In the case of Pb^{2+} and Cd^{2+} adsorption by IONPs, Langmuir constants obtained were q_m (Pb^{2+}: 19.57 mg/g and Cd^{2+}: 20.45 mg/g) and

K_L (Pb^{2+}: 0.52 L/mg and Cd^{2+}: 2.43 L/mg). Maximum adsorption capacity was found for sorption of Pb^{2+} and Cd^{2+} by PG-IONPs. For the sorption of Pb^{2+} and Cd^{2+} by PG-IONPs and IONPs, the separation factor or equilibrium parameter (R_L) values found were $0 < R_L < 1$, which indicates that the sorption of Pb^{2+} and Cd^{2+} on both PG-IONPs and IONPs is favourable.

By plotting log qe versus log Ce (Freundlich plots) a straight line was resulted and the values for n (adsorption intensity) and K_f (the sorption capacity) can be obtained from the slope and intercept of the plot (Figure 9.13(b)) and are presented in Table 9.1. The values of sorption capacities (K_f) and adsorption intensity (n) of PG-IONPs were found higher than that of IONPs, for both Pb^{2+} and Cd^{2+}. For both the metal sorption by PG-IONPs and IONPs, the values of n were found to be greater than1, representing the favorable adsorption condition.

Figure 9.13(c) shows the linear form of the Temkin isotherm plot (q_e against ln C_e) and a straight line was observed for the sorption of both the metals by PG-IONPs and IONPs. The values of the Temkin constant b, indicates that the heat of adsorption is presented in Table 9.1. In the case of PG-IONPs, the values of mean free energy (E) (Pb$^{2+:}$ 10.10 kJ/mol and Cd$^{2+:}$ 9.21 kJ/mol) was found in the range of 8–16 kJ/mol, indicating that the type of sorption of Pb^{2+} and Cd^{2+} on PG-IONPs (iron oxide coated with polyvinyl alcohol and gallic acid) is essentially chemical. But for the sorption of Pb^{2+} and Cd^{2+} by IONPs, it was found in the range of 1 to 8 kJ/mol, indicates the physical sorption.
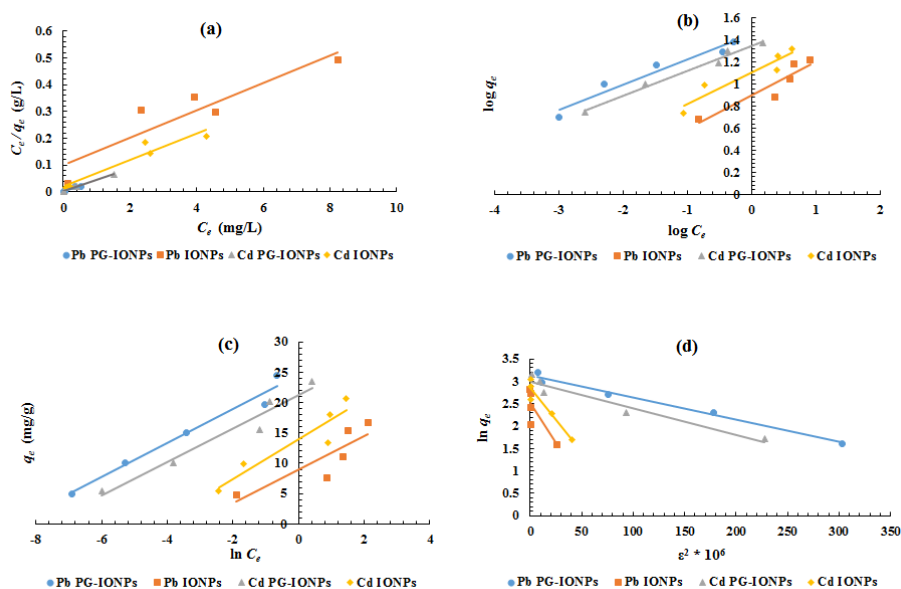
Figure 9.13: (a) Langmuir, (b) Freundlich, (c) Temkin and (d) Dubinin -
Radushkevich Adsorption Isotherms

Evaluation of the suitable isotherm model for the sorption of Pb^{2+}
and Cd^{2+} by PG-IONPs and IONPs was conducted using the correlation
coefficients value (R^2). The Langmuir isotherm fits very close to the
experimental data of the sorption of both the metals by PG-IONPs and
the Langmuir equation assumes a homogeneous distribution of active
sites on surface. The values of q_m determined by the Dubinin-
Radushkevich isotherm model also fits close to the experimentally
determined data for sorption of Pb^{2+} and Cd^{2+} on PG-IONPs. R^2 value of
Pb^{2+} sorption by PG-IONPs indicates that the Dubinin-Radushkevich
isotherm is the best followed by the Langmuir isotherm, Temkin and then

the Freundlich isotherm. The order of adsorption isotherm models fitted the equilibrium data are for Cd^{2+} sorption by PG-IONPs: Langmuir isotherm > Freundlich isotherm > Temkin isotherm > Dubinin-Radushkevich isotherm. For the metal sorption by IONPs, the order of the fitted isotherm model was as follows, Pb^{2+}: Freundlich isotherm > Langmuir isotherm > Temkin isotherm > Dubinin-Radushkevich isotherm and Cd^{2+}: Langmuir isotherm > Dubinin-Radushkevich isotherm > Freundlich isotherm > Temkin isotherm.

Table 9.1: Isotherm parameters for adsorption of Pb^{2+} and Cd^{2+} by PG-IONPs and IONPs

Isotherm models	Parameters	Pb		Cd	
		PG-IONPs	IONPs	PG-IONPs	IONPs
Langmuir	q_m (mg/g)	23.42	19.57	24.21	20.45
	K_L (L/mg)	71.17	0.52	14.75	2.43
	R_L	(0.0006 - 0.0028)	(0.0721 - 0.2797)	(0.0027 - 0.0121)	(0.0162 - 0.0694)
	R^2	0.9808	0.834	0.989	0.9208
Freundlich	K_f (mg/g) (L/mg)$^{1/n}$	28.24	7.97	22.14	12.73
	n	4.43	3.30	4.44	3.51
	R^2	0.9422	0.8548	0.9813	0.8879
Temkin	A (L/g)	6253.1	25.7	2172.9	74.2
	b (kJ/mol)	897.3	911.1	910.7	776.1
	R^2	0.9687	0.739	0.9509	0.87
Dubinin – Radushkevich	q_m (mg/g)	22.84	12.37	19.87	17.47
	β (mol^2/kJ^2)	0.0049	0.0359	0.0059	0.0285
	E (kJ/mol)	10.10	3.73	9.21	4.19
	R^2	0.9834	0.6596	0.9355	0.9134

9.3.4 Sorption kinetics

Lagergren's pseudo-first-order, pseudo-second-order and intraparticle diffusion models were utilized for analysis of sorption kinetics which are discussed in chapter 7 and 8. The pseudo-first-order rate constants k_1 and q_e determined from the slope and intercept of the Lagergren's plot (Figure 9.14 (a and b)) and are listed in Table 9.2 along with the correlation coefficients (R^2). It was observed from R^2 value that the pseudo first-order model did not fit well. The second-order constants, k_2 and q_e were calculated from the intercept and slope of the linear second-order kinetic plot (Figure 9.14 (c and d) and are revealed in Table 9.2. The high correlation coefficient (R^2) value indicates that the adsorption data of Pb^{2+} and Cd^{2+} by PG-IONPs and IONPs were well fitted to pseudo-second order equation. R^2 value obtained from the adsorption data of Pb^{2+} and Cd^{2+} ranged as, 0.9995 - 1 for PG-IONPs and 0.9542 - 0.9999 for IONPs. For the pseudo second-order kinetic model, a good agreement between experimental and calculated q_e values was also observed which indicates that the pseudo-second-order model better represents the reaction mechanism, directing to a chemisorption character. PVA and gallic acid on the iron oxide nanoparticles provide plenty of surface functional groups as active sorption sites.
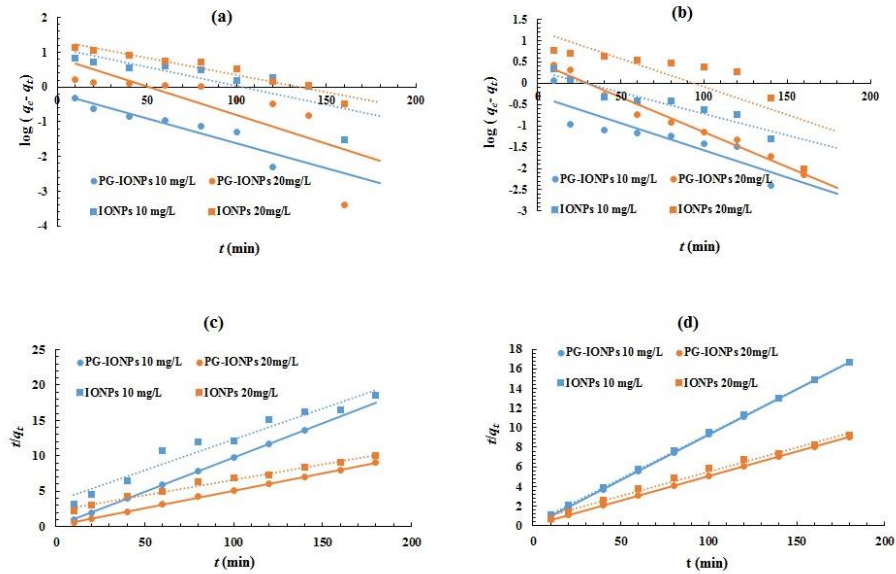
Figure 9.14: Pseudo-first-order plot (a) Pb^{2+} and (b) Cd^{2+} and pseudo-second-order (c) Pb^{2+} and (d) Cd^{2+}

A rate-limiting step is required for the pseudo-second-order kinetic model which may comprise of chemisorption and the diffusion processes (Ho & McKay, 1999). Weber and Morris proposed model was utilized to understand whether the sorption process is controlled by intraparticle diffusion or bulk diffusion. According to intraparticle diffusion models, if sorption of a solute is controlled by the intraparticle diffusion process, the plot of q_t versus $t^{1/2}$ gives a straight line (Pelit et al., 2011). In the case sorption of Pb^{2+} (Figure 9.15(a)) and Cd^{2+} (Figure 9.15(b)) by both PG-IONPs and IONPs, R^2 value of Weber and Morris

plot or intraparticle diffusion model plot was ranged between (0.8376 - 0.9841) and (0.4417 - 0.976), respectively. High R^2 value and better correlation between experimental and calculated values indicates that the pseudo second-order model better represents the reaction mechanism involved in the sorption of Pb^{2+} and Cd^{2+} by PG-IONPs and IONPs.
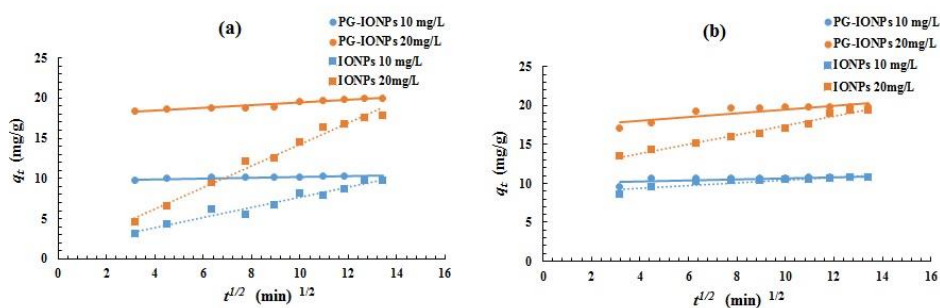
Figure 9.15: Intraparticle diffusion plot (a) Pb^{2+} and (b) Cd^{2+}

Table 9.2: Kinetic parameters for the adsorption of Pb^{2+} and Cd^{2+} by PG-IONPs and IONPs

Kinetic models	Parameters	Pb				Cd			
		PG-IONPs		IONPs		PG-IONPs		IONPs	
		10 mg/L	20 mg/L	10 mg/L	20 mg/L	10 mg/L	20 mg/L	10 mg/L	20 mg/L
	$q_{e,exp}$ (mg/g)	10.25	19.98	9.74	17.88	10.78	19.858	10.78	19.48
Pseudo-first-order kinetic model	k_1(min^{-1})	0.033	0.038	0.025	0.023	0.029	0.038	0.023	0.030
	$q_{e,cal}$ (mg/g)	0.66	6.80	13.11	21.24	0.50	3.06	1.98	17.00
	R^2	0.8585	0.5884	0.6558	0.9335	0.7735	0.9776	0.9075	0.6375
Pseudo-second-order kinetic model	k_2 (g/mg min)	0.141	0.017	0.002	0.001	0.131	0.029	0.029	0.004
	$q_{e,cal}$ (mg/g)	10.29	20.20	11.40	22.78	10.82	20.08	10.94	20.37
	R^2	1	0.9995	0.9542	0.9869	1	1	0.9999	0.9915
Intraparticle diffusion model	k_{id} (mg/g min$^{1/2}$)	0.049	0.171	0.625	1.341	0.068	0.240	0.173	0.600
	C (mg/g)	9.72	17.71	1.43	0.85	10.02	17.14	8.73	11.45
	R^2	0.8376	0.9324	0.9535	0.9841	0.4417	0.7363	0.7934	0.976

Adsorption of Pb^{2+} and Cd^{2+} on PG-IONPs was confirmed by the EDX spectra of Pb^{2+} and Cd^{2+} loaded PG-IONPs. EDX peaks of lead (Figure 9.16) and cadmium (Figure 9.17) observed were clearly confirmed the adsorption of Pb^{2+} and Cd^{2+} on PG-IONPs surfaces
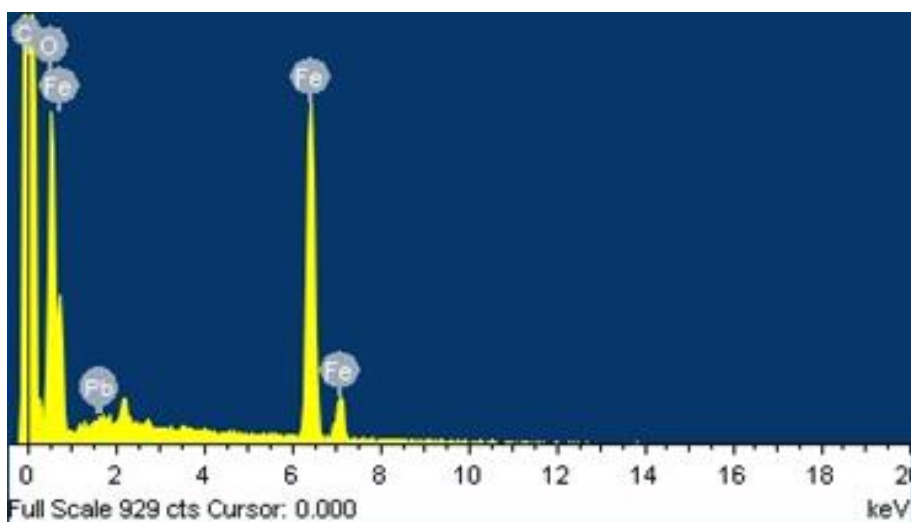
Figure 9.16: EDX spectra of Pb^{2+} loaded PG-IONPs.
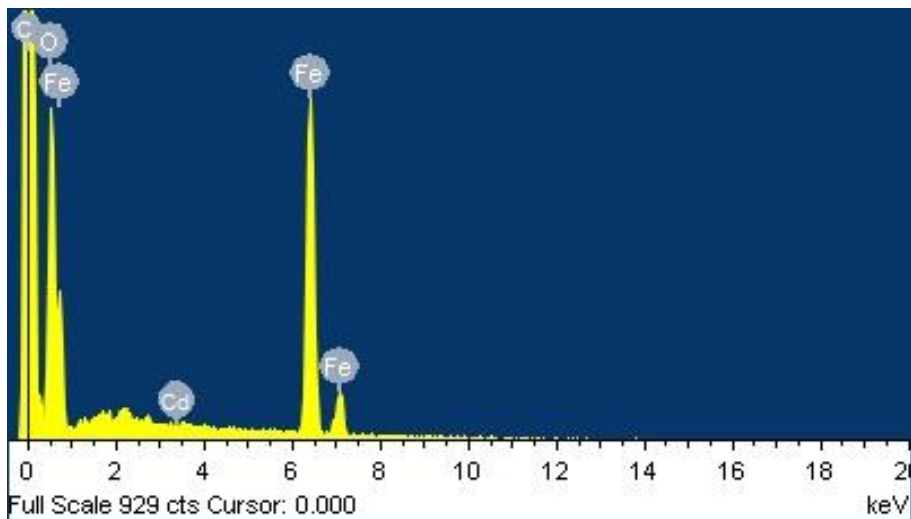
Figure 9.17: EDX spectra of Cd^{2+} loaded PG-IONPs.

9.3.5 Adsorption thermodynamics of metal ions on functionalized iron oxide nanosorbent

The thermodynamic studies were carried out by varying temperature from 303 to 373 K and the values of $\Delta G°$, $\Delta H°$ and $\Delta S°$ are presented in the Table 9.3. The negative value for the Gibbs free energy for Cd^{2+} indicates the spontaneous adsorption of Cd^{2+} on PG-IONPs with increasing temperature. The calculation of thermodynamic parameters was discussed in chapter 7. Negative value of enthalpy change ($\Delta H°$) for Pb^{2+} and Cd^{2+}, implies the exothermic behaviour of the adsorption process. The magnitude and sign of $\Delta S°$ show a contributing role in reflecting whether the association of the adsorbate at the solid/solution

interface during the adsorption process becomes less random ($\Delta S° < 0$) or more random ($\Delta S° > 0$) (Tran et al. 2016). The positive value of entropy change ($\Delta S°$) reflect an increased degree of disorderliness at the solid/liquid interface during the adsorption of Cd^{2+} on the nanosorbent, PG-IONPs.

Table 9.3: Thermodynamic parameters for the adsorption of Pb^{2+} and Cd^{2+} on PG-IONPs

Metal ions	T (K)	PG-IONPs		
		$\Delta G°$ (kJ/mol)	$\Delta H°$ (kJ/mol)	$\Delta S°$ (J/mol K)
Pb	303	14.39	-2.78	-56.66
	333	16.08		
	353	17.22		
	373	18.36		
Cd	303	-46.19	-43.13	10.46
	333	-46.48		
	353	-47.63		
	373	-46.46		

9.3.6 Regeneration and stability of functionalized iron oxide nanosorbent

The efficiency of functionalized NPs was investigated for multiple adsorptions-desorption cycles. The Pb^{2+} and Cd^{2+} adsorbed nanosorbents were regenerated using 0.1 M HCl and 0.1 M NaOH. 50 mL of desorbing agents was added to 2 g of metal adsorbed, functionalized iron oxide nanoparticles in 250 mL stopped bottle and agitated at 150 rpm for 1h at room temperature using a mechanical shaker. The dried desorbed nanosorbent were reused for another adsorption cycle and the adsorption-desorption process was repeated five

times, separately for Pb^{2+} and Cd^{2+}. Adsorption was conducted using 10 mg/L metal solution. A decrease in adsorption yield was observed in every cycle. 0.1 M HCl was found as suitable desorbing agent than 0.1 M NaOH. Both, Pb^{2+} and Cd^{2+} desorption was favourable using an acidic desorbing agent because at low pH, the competition between H^+ ions and metal ions occurs. In the first cycle Pb^{2+} adsorption yield was 99.95 % but on fifth cycle it reduced to 56 %. Cd^{2+} removal yield was 99.77 % in the first cycle and reduced to 52.1 % in the fifth cycle. Thus, functionalized iron oxide nanoparticles using PVA and gallic acid can be regenerated and reused for Pb^{2+} and Cd^{2+} removal and recovery

9.4 Summary

The iron oxide nanoparticles (Fe_2O_3) were synthesized by co-precipitation and its surface was coated by polyvinyl alcohol and gallic acid. The removal of toxic metals such as lead and cadmium from aqueous solution was studied using functionalized nanoparticles (PG-IONPs) and its metal removal efficiency was compared with the uncoated iron oxide nanoparticles (IONPs). The functionalized iron oxide nanoparticles were characterized using FTIR, SEM EDX and XRD. The presence of functional groups on PG-IONPs were confirmed by FTIR. Batch sorption experiments under different conditions such as pH, adsorbent dosage, contact time, temperature and initial metal concentration were carried out and the results revealed that the maximum sorption of metals by PG-IONPs is possible under a wide range of pH (pH: 4 -12 for Pb^{2+} and pH: 6 - 12 for Cd^{2+}). Better sorption of metals was exhibited by PG-IONPs than IONPs. Compared to IONPs, PG-IONPs

exhibited high removal efficiencies for both Pb^{2+} and Cd^{2+} at minimal adsorbent dosage. The increase in metals concentration from 5 to 25 mg/L leads to an increase in adsorption capacity and observed a maximum adsorption capacity of 24.48 mg/g and 23.52 mg/g for Pb^{2+} and Cd^{2+}, respectively by PG-IONPs which was better than that of IONPs. As the temperature increases, both nanosorbents exhibited a decreasing trend in the removal of lead and cadmium. Compared to IONPs, PG-IONPs exhibited only a slight decrease in metal sorption. The results indicate that the bonding between PG-IONPs and metal ions were stronger than the bonding between IONPs and metal ions at higher temperature. In the case of PG-IONPs, 91.77 % of Pb^{2+} and 84.89 % Cd^{2+} removal was attained within 10 min of contact time. Initially, the rate of removal was high and then slowed down as move towards the equilibrium condition. After 140 min, the rate of sorption was slow and reaches equilibrium by PG-IONPs. PG-IONPs showed fast removal of metals than IONPs this may be due to that the functional group present on the PG-IONPs provides more active adsorption site for metal ions.

The sorption equilibrium data was best described by Langmuir equation. The values of q_m determined by the Dubinin-Radushkevich isotherm model also fits close to the experimentally determined data for sorption of Pb^{2+} and Cd^{2+} on PG-IONPs. For the sorption of both Pb^{2+} and Cd^{2+}, the values of mean free energy (E) was found in the range of 8 - 16 kJ/mol for PG-IONPs, indicating the chemical sorption but the value of E was found in the range of 1 to 8 kJ/mol, indicates involvement of physical sorption in the sorption of Pb^{2+} and Cd^{2+} by IONPs. Sorption dynamics data were best described using pseudo-second-order rate

equation. High R^2 value and better correlation between experimental and calculated values indicates that the sorption dynamics data were best described by using pseudo-second-order kinetic model, in the case of both nanosorbents. Thermodynamic studies illustrated that Pb^{2+} and Cd^{2+} adsorption by the functionalised nanosorbent was exothermic in nature. Sorption of Pb^{2+} and Cd^{2+} on the PG-IONPs was confirmed using EDX spectra. The better regeneration of exhausted PG-IONPs was done using desorbing agent, 0.1 M HCl and its reusability were also investigated. Polyvinyl alcohol and gallic acid coated iron oxide nanoparticles (PG-IONPs) can be considered as fast and efficient, nano-adsorbent for Pb^{2+} and Cd^{2+} removal from contaminated waters.

ASSESSMENT OF HEAVY METAL CONTAMINANTS IN GROUNDWATER USING INDEXING APPROACH AND APPLICATION OF THREE TYPE OF ADSORBENTS FOR HEAVY METAL REMOVAL

10.1   Introduction

The impacts of many anthropological activities on environment, especially in the aquatic system have been reported globally. Several lands and water-based activities, industrial activities, high population density and over exploitation are instigating the pollution of aquifers which leads to unsafe and vulnerable ground water. When groundwater becomes contaminated by pollutants, it directly affects the human health. WHO (World Health Organisation) had indicated this issue earlier and had issued standards for safe ground water since 1958 (Mohankumar et al., 2016). Heavy metals in water denotes to the dense, heavy, metallic elements that may occur in trace amounts, but are very toxic and tend to accumulate, hence are generally mentioned as trace metals. Heavy metals

such as Hg, As, Pb, Cd, Cr, Co, Fe, Mn, etc., have been acknowledged as deleterious to human health and aquatic ecosystem (Jameel et al., 2012). The problems related to the contamination of toxic metals as a consequence of mining activities started in the Middle Age (Vink et al., 1999). The issues associated to water quality is more severe in the areas where mining and mineral processes industries are located. Several classes of wastes are produced from mining processes, which may lead to many types of pollution (Howladar et al., 2014; Khan et al., 2017).

Even though Kaolin is an important raw material in many industrial sectors, its mining and processing produces large quantities of waste (Bhimani & Vyas, 2013). China Clay (Kaolin) comprising dominantly of kaolinite, which is one of the most sophisticated industrial minerals with a host of applications, viz., in ceramics, refractories, filler for rubber, paper coating, cement, paint, textiles, insecticides, fertilizers and others including abrasives, asbestos products, chemicals, cosmetics, fibreglass, pharmaceuticals, electrical ware, foundry and glass (Department of Economics & Statistics, 2015). During the processing of primary kaolin in kaolin industry, two types of wastes are produces. The first type of waste derives from the first processing step i.e., the separation of sand from ore and the second type is the outcomes of the second processing step, in which wet sieving for the separation of finer fraction and purification of the kaolin occur. For the production a 1 ton of pure kaolin, kaolin industry generates a 9 ton of waste products. Traditionally, the mining and mineral processing wastes have been dumped in landfills and often discarded directly into ecosystems without any adequate treatment (Bhimani & Vyas, 2013). For the mining and

refining of China Clay, water is essential, hence the waste water from kaolin industry without adequate treatment can contaminate the groundwater resources near the mining and refining area.

The Department of Mining and Geology identified two major china clay zones in Kerala. One is the southern china clay zone, located between Kundara and Thiruvananthapuram (Thiruvananthapuram and Kollam districts) and other is the northern china clay zone, identified between Kannapuram, Madayi - Cheruthazham (Kannur district) to Nileswarm - Manjeshwaram (Kasargod district). World class clay with finest quality is obtained from Kerala (Department of Economics & Statistics, 2015). Active clay mining is taking place in Madayi panchyath, Kannur district. Some water quality issues like high Fe content and acidic nature were reported by the local residents. Hence, the quality of the groundwater resources and heavy metal contaminations in groundwater near the mining area were assessed in this study. We have attempted, adsorbents such as nanosorbents, algal species and herbal plant material for the removal of heavy metals from contaminated groundwater.

10.2 Materials and Methods

10.2.1 Study area and collection of samples

The study area is located in the Madayi panchayath, Pazhayangadi in Kannur district, the northern part of an Indian state, Kerala. It is located between latitudes $12^o0'0''$ to $12^o2'0''$ N and longitudes $75^o14'0''$ to $75^o16'0''$ E, with an area of 1674.597 Ha. Madayi is situated between the northern bank of Kuppam river to the southern bank of Perumba river and a canal known as Sultan Canal is passing

through the area by connecting Kuppam and Perumba rivers. Several small streams (thodu) like Kavilevallapil thodu and Kakki thodu are flowing through the study area. Madayipara is a famous flat-topped hillock situated in Madayi panchayath having rich biodiversity.

As the groundwater resource is the main source of water for drinking, cooking and irrigation purposes in this area. Hence, to assess the contamination of groundwater resources near the mining area, 35 water samples (34 groundwater samples and 1 water sample from a water supply point) were collected from different areas of Madayi panchayath during March 2014. 7 soil and 4 sediment samples were also collected from there. The coordinates of the sampling sites were obtained using the GPS device, GARMIN GPS map model 76CS and the sampling sites are illustrated in Figure 10.1. ArcGIS version 10.0 was used to map the sampling locations of groundwater, soil and sediment samples. The collection, preservation and analysis of groundwater samples were carried out as per the standard methods mentioned in APHA (2012). The in-situ parameters like pH and electrical conductivity were analysed immediately from the sampling locations. For the physico-chemical and bacteriological analysis, the samples were transported to laboratory after proper preservation. To determine the concentration of heavy metals, Atomic Absorption Spectrophotometer (AAS) with graphite furnace, (M-series, Thermo) was used after filtration (Whatman no. 41) and preservation (concentrated HNO_3) of the samples.
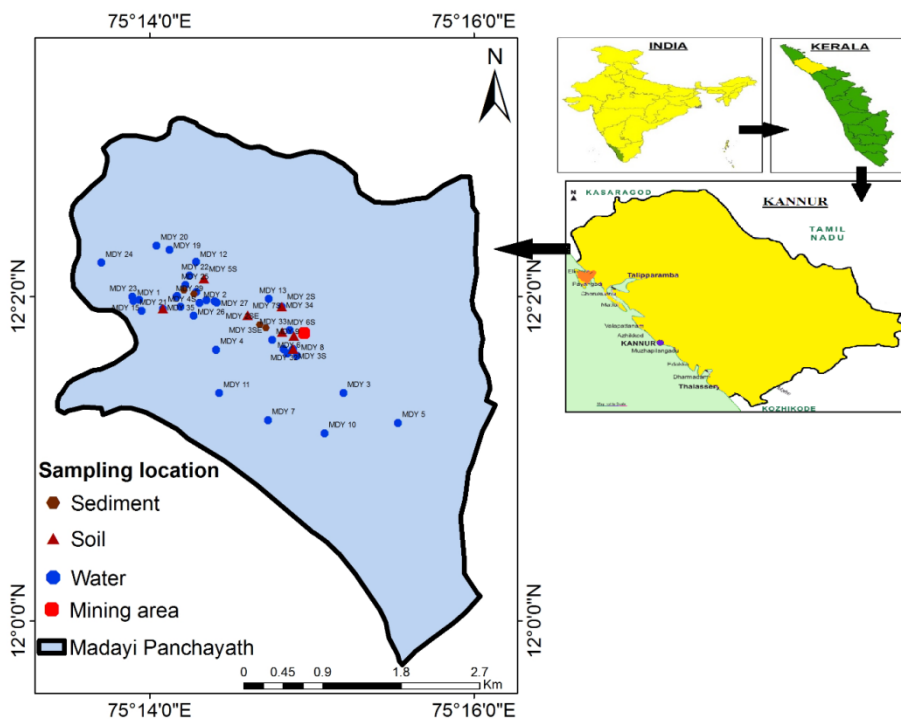
Figure 10.1: Map showing locations of sampling stations in Madayi panchayath

Seven soil samples were collected from Madayi area using a soil auger and pooled to give a composite sample for that location. Soil samples were collected at depths of 15 – 30 cm, in polythene bottles which were labelled properly at site of collection. Four sediment samples were collected from the Kavilevalappil thodu (Plate 10.1), through which the wastewater pipe line of mining industry is passing. The air-dried and sieved portion of the collected sediment samples was kept in polythene bottles and used for analysis. The physico-chemical characteristics of the

soil and sediment samples were analysed and the procedures used for analysis were discussed in chapter 3 (Material and Methods). Analytical grade chemicals and reagents were used for the study.

Plate 10.1: (a) China clay mining area; (b) Groundwater sampling; (c) Open well from Madayi and (d) Sediment sample site

10.2.2 Data evaluation

The pollution indices such as heavy metal pollution index (HPI), heavy metal evaluation index (HEI) and contamination index (C_d) were used to evaluate the heavy metal contamination level in groundwater samples from Madayi panchayath. 35 water samples were analysed for seven metals (Fe, Mn, Pb, Cd, Cu, Ni and Zn).

10.2.2.1 Heavy metal pollution index (HPI)

Heavy metal pollution index (HPI) is a powerful technique used to assess the aggregate influence of individual heavy metal on the overall quality of water and has been developed and formulated by Mohan et al. (1996). The HPI was determined in two steps. First step is a rating approach, a weightage (W_i) is assigns to every parameter which reflects the relative importance of individual quality considerations in a composite way (Bhardwaj et al., 2017) and second is the selection of the pollution parameter on which the index is to be based (Prasad & Bose, 2001; Sobhanardakani et al., 2017). The value of W_i lies between zero and one and can be calculated by making values inversely proportional to the recommended standard (S_i) for the corresponding parameter (Horton, 1965; Mohan et al., 1996; Prasad & Bose, 2001). S_i is the highest tolerant value for drinking water denotes to the maximum admissible concentration (MAC) in drinking water in the absence of any alternate water source and I_i is the maximum desirable value refers to the standard limits for the same parameters in drinking water. For determining heavy metal pollution index in this study, the standard of each heavy metal in µg/L for drinking water suggested by Bureau of Indian Standards (BIS) IS:10500 (2012) was considered. The HPI model helps to assess the water quality and its suitability for the purpose of drinking (Mohan et al., 1996; Bhardwaj et al., 2017).

The HPI model is presented in equation (1) (Mohan et al., 1996) as follows:

$$\text{HPI} = \frac{\sum_{i=1}^{n} W_i Q_i}{\sum_{i=1}^{n} W_i} \qquad (1)$$

where, Q_i is the sub-index of ith parameter and W_i is the unit weightage for the ith parameter. n is the number of parameters considered.

The sub-index (Q_i) of the parameter is determined by equation (2):

$$Q_i = \sum_{i=1}^{n} \frac{|M_i - I_I|}{S_i - I_i} \qquad (2)$$

where M_i is the measured value of heavy metal of ith parameter, I_i indicates the desirable value of the ith parameter and S_i is the standard value of the ith parameter or the standard maximum admissible value of the ith parameter. The quantity $|M_i - I_i|$ means the numerical difference of the two values, ignoring the algebraic sign (Bhardwaj et al., 2017). The value of heavy metal pollution index (HPI) indicates, low heavy metal pollution (HPI < 100), heavy metal pollution on the threshold risk (HPI = 100) and high heavy metal pollution (critical pollution index) (HPI > 100) (Sobhanardakani et al., 2017). If the water samples have HPI > 100, water is not potable (Mohan et al., 1996; Prasad & Bose, 2001). HPI was determined to assess the heavy metal contamination level in groundwater samples from Madayi.

10.2.2.2 Heavy metal evaluation index (HEI)

HEI focuses on estimating the overall water quality with respect to heavy metals (Edet & Offiong, 2002). The water quality is classified into three categories based on this index which include: low heavy metals

(HEI < 400), moderate to heavy metals (400 < HEI < 800) and high heavy metals (HEI > 800) (Sobhanardakani et al., 2017).

The heavy metal evaluation index is computed using equation (3):

$$\text{HEI} = \sum_{i=1}^{n} \frac{H_C}{H_{mac}} \qquad (3)$$

where H_c is the monitored value of the ith parameter and H_{mac} denotes the maximum admissible concentration (MAC) of the ith parameter. HEI was applied for easy interpretation of the pollution index and level of pollution (Edet & Offiong, 2002; Prasanna et al. 2012) in this study.

10.2.2.3 Contamination index (C_d)

In this technique, the quality of water is evaluated on the basis of the degree of contamination. The C_d is computed as a sum of the contamination factors of individual components exceeding the upper permissible value (Sobhanardakani et al., 2017) and the index summarizes the collective effects or degree of contamination of several parameters considered potentially harmful to household water (Herojeet et al., 2015). The contamination index is calculated from the following equations:

$$C_d = \sum_{i=1}^{n} C_{fi} \qquad (4)$$

where

$$C_{fi} = \frac{C_{Ai}}{C_{Ni}} - 1 \qquad (5)$$

where C_{fi}, C_{Ai}, and C_{Ni} indicates the contamination factor, analytical value, and upper permissible concentration, respectively, of the ith component. N represents the 'normative value' and C_{Ni} (upper permissible concentration) was taken as the maximum admissible concentration (MAC). Backman et al. (1997) and Edet and Offiong (2002), classified the C_d into three categories as follows: low ($C_d < 1$), medium ($C_d = 1 - 3$) and high ($C_d > 3$).

To identify the relationship between the trace metals, Pearson correlation matrix was performed. Based on the correlation coefficient value "r," the association between two metals were determined. Chemometric or multivariate analysis techniques such as PCA and CA were used to identify the heavy metal pollution sources affecting water quality. Statistical analyses were conducted using SYSTAT software.

10.3 Results and Discussion

10.3.1 Water quality characteristics groundwater samples from Madayi panchayath

The quality of groundwater resources is associated with chemical and biological processes involved due to the physical transportation and spreading of contaminants and its levels. Hence, the physico-chemical characteristics of groundwater related to the distribution of contaminants. Among 35 water samples collected from Madayi panchayath during March 2014, 34 samples were groundwater (open well) and one (MDY 32, Pazhayangadi) was collected from water supply point near mining area. The physico-chemical parameters obtained from the analysis of water samples are exhibited in Table 10.1. The pH value, a good

indicator of groundwater quality, exhibited some dissimilarities with spatial variations (Figure 10.2(a)). The pH values of samples ranged between 2.79 and 8.09. Among 35 samples, pH values of 26 samples were within the range of 6.5 to 8.5 (IS 10500: 2012). But acidic pH was observed in 7 samples collected from near the china clay mining area in Madayi panchayath. The abnormal value of pH, signifies some pollution and was probably due to the percolation of contaminants from the mining area.

Electrical conductivity and total dissolved solids of water samples from Madayi panchayath ranged from 191.5 - 53676 µS/cm and 136.0 - 38110.0 mg/L respectively. A high TDS value of 38110.0 mg/L was obtained in sample MDY- 21 (Figure 10.2(b)), collected from a site near to Perumba river and Sultan canal. Similarly, high values are also reported in samples MDY-1 and MDY-23, collected from open wells near Vellachal road and both sites are also near to Perumba river. The salinity intrusion can contribute to high TDS value. The TDS of 46 % of the collected samples are beyond the drinking water standard prescribed by BIS (IS 10500: 2012). TDS value was not found to be within the limit in samples collected from the sites near the mining area such as MDY-6, MDY- 8, MDY-9, MDY-30, MDY-31 and MDY-27. The TDS is an indicator of the overall suitability of water for many types of uses and high TDS value can influence the taste, hardness and corrosive property of the water (Akhtar et al., 2014).
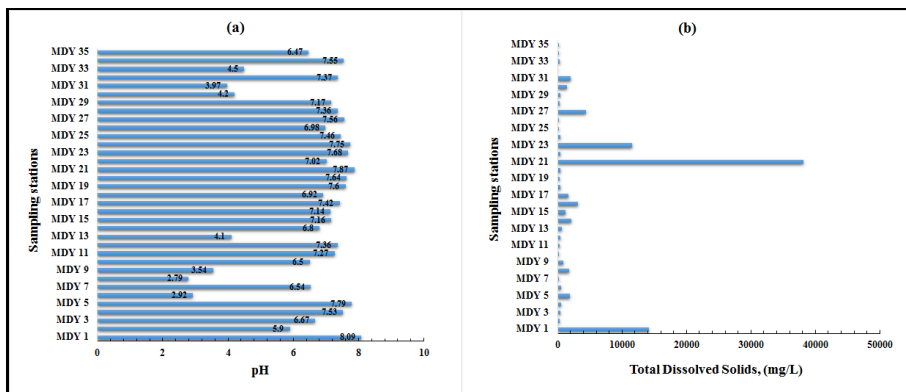
Figure 10.2: Spatial variation of (a) pH and (b) Total dissolved solids

The alkalinity of the samples ranged between 0 to 410 mg/L, and the highest value was reported in sample collected from bank of Perumba river. In five samples alkalinity value was found to be exceeding the BIS limit of 200 mg/L. But in seven groundwater sample collected from near the china clay mining area, alkalinity was found to be zero and all these samples were highly acidic in nature. The hardness of the samples ranged from a minimum of 80 mg/L to a maximum of 4204 mg/L and was expressed in terms of equivalent quantity of $CaCO_3$. The hardness of natural waters is contributed by the combinations of calcium and magnesium with bicarbonate, carbonate, sulphate and other species. The hardness of 21 groundwater samples were found to be exceeding the BIS standard (IS 10500: 2012) and among them, in 13 samples hardness was >300 mg/L, so it comes under the classification of very hard water. Very hard water samples were also noticed in locations near mining area. Hardness lower than 300 mg/L is considered as potable but, beyond this limit causes kidney problems and gastrointestinal irritation (Nirmala et al., 2012) and high hardness also impart scaling effect when such waters

are heated. The results of analysis revealed that calcium and magnesium in the groundwater samples from Madayi panchayath were in a range of 16 to 1121.6 mg/L and 4.86 to 340.2 mg/L, respectively and both cations are the major cause of hardness in water. Maximum value of calcium and magnesium was reported in sample collected from a site near to Perumba river and Sultan canal (MDY- 21) and maximum sodium and potassium were reported in same sample. High sodium and potassium content were also observed in groundwater samples collected from the bank of Perumba river (MDY-1 and MDY-23) may be due to saline intrusion. The value of sodium and potassium varied from 6.75 to 13876 mg/L and 0.04 to 174.00 mg/L, respectively.

The natural sources, sewage and industrial effluents and saline intrusion may originate chloride in drinking-water. Chloride concentration was observed between 15.42 – 21778 mg/L. Chloride in 29% of samples were higher than the limit of BIS (IS 10500: 2012) and the samples collected from the banks of Perumba river and Sultan canal, very high chloride content was observed. Water having high chloride concentration usually give rise to an unpleasant taste and may be objectionable for some agricultural activities. In the samples from the locations near the mining area, no high chloride value was noted but high sulphate values were observed in many samples. Sulphate value varies from 1.68 to 1268 mg/L. Maximum sulphate concentration was found in groundwater sample near mining area, MDY-31. Nitrate and phosphate ranged between 0 - 8.71 mg/L and 0.01 - 3.10 mg/L, respectively. The maximum value for both anions was observed in a sample near

Kavilevallapil thodu (MDY-18) and eutrophication was also observed there.

10.3.2 Bacteriological status of groundwater samples from Madayi panchayath

Microbiological parameters such as total coliform and *Escherichia coli* (*E. coli*) gives an indication of unsafe and unsatisfactory drinking water. Hence the bacteriological contamination of 35 samples were analysed. Figure 10.3 explains the percentage of samples having the total coliform bacteria and *E. coli.* Of the total sample collected, total coliform bacteria were detected in 89 % of the water samples. The presence of *E. coli* was detected in only 5 groundwater samples (MDY-1, MDY-11, MDY-29, MDY-30 and MDY-35). But the presence of *E. coli* was detected in comparatively less samples (14 %), this may be due to the fact that majority of the sample collected wells are well distanced from the septic tanks.
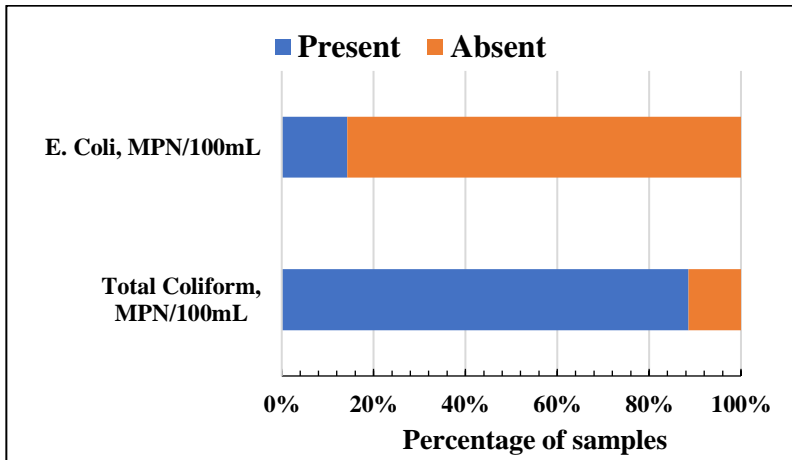
Figure 10.3: Percentage of samples tested positive for the presence of total coliform and *E. coli* in Madayi

10.3.3 Heavy metal concentration and its spatial distribution in groundwater samples from Madayi

In the present study, the levels of Fe, Mn, Pb, Cd, Cu, Ni and Zn in groundwater samples of Madayi panchayath during March 2014 were determined. The analytical results of heavy metal concentrations are summarised in Table 10.2 and spatial variation of heavy metal concentrations are shown in Figure 10.5. High iron concentration was observed in samples from near the locations where china clay mining activities are taking place. Fe values ranged between 0.001- 200.1 mg/L. Maximum value of 200.1 mg/L was observed in MDY-18, sample near Kavilevallapil thodu through which the wastewater drainage from mining is passing. In sample MDY-8 (near china clay mining area), 192.3 mg/L of Fe was detected. High heavy metal content in drinking water lead to a variety of health concerns and demonstrates adverse health effect.

The other heavy metals such as Mn (BDL - 16.93 mg/L); Pb (BDL - 0.63 mg/L); Cd (BDL - 0.5836 mg/L); Cu (BDL - 4.74 mg/L); Ni (BDL - 0.5816 mg/L) and Zn (BDL - 9.1 mg/L) were also detected in many samples. In many groundwater samples, metals like Fe, Mn, Pb, Cd, Cu Ni and Zn were found higher than acceptable limit of BIS (IS 10500: 2012). Measured concentration of heavy metal were found in the order Fe > Mn > Zn > Cu > Ni > Pb > Cd. The results revealed that cadmium concentration was found above the acceptable limit of BIS in 71 % of water sample collected from the study area.

Table 10.1: Water quality characteristics of groundwater samples from Madayi panchayath

Sl No.	Parameters	BIS Standard	MDY 1	MDY 2	MDY 3	MDY 4	MDY 5	MDY 6	MDY 7	MDY 8	MDY 9
1	pH	6.5 - 8.5	8.09	5.90	6.67	7.53	7.79	2.92	6.54	2.79	3.54
2	Colour, (Hazen)	5	27.20	BDL	6.10	6.20	BDL	93.30	BDL	150.63	BDL
3	Turbidity, (NTU)	1	8.12	BDL	1.80	4.10	BDL	48.38	BDL	72.13	BDL
4	Electrical Conductivity, (μS/cm)	-	19887	401.41	577.46	746.48	2647.89	833.80	338.03	2518.3	1162.0
5	Total Dissolved Solids, (mg/L)	500	14120	285.0	410.0	530.0	1880.0	592.0	240.0	1788.0	825.0
6	Total alkalinity as CaCO3, (mg/L)	200	410.0	137.0	168.0	147.0	252.0	BDL	105.0	BDL	BDL
7	Total Hardness as CaCO3, (mg/L)	200	3240.0	168.0	272.0	224.0	520.0	400.0	124.0	1704.0	748.0
8	Chloride, (mg/L)	250	6867.0	54.94	39.24	192.28	824.04	58.86	44.94	313.92	137.34
9	Sulphate, (mg/L)	200	1168.0	13.20	61.20	3.16	54.80	330.0	19.36	708.0	352.0
10	Nitrate - N, (mg/L)	10	4.20	0.32	0.49	0.35	0.86	0.56	1.32	1.34	BDL
11	Phosphate - P, (mg/L)	-	0.09	BDL	0.03	0.02	BDL	0.08	0.05	0.05	BDL
12	Calcium, (mg/L)	75	920.0	57.60	89.60	51.20	102.40	110.40	35.20	396.80	182.40
13	Magnesium, (mg/L)	30	228.42	5.83	11.66	23.33	64.15	30.13	8.75	173.02	70.96
14	Sodium, (mg/L)	-	4471.0	33.48	18.13	124.0	530.0	9.61	20.10	20.49	37.90
15	Potassium, (mg/L)	-	126.0	6.59	6.73	15.0	7.0	2.88	12.30	5.35	7.98

BDL: Below Detection Limit

(***Continued***)

Table 10.1: Water quality characteristics of groundwater samples from Madayi panchayath

Sl No.	Parameters	BIS Standard	MDY 10	MDY 11	MDY 12	MDY 13	MDY 14	MDY 15	MDY 16	MDY 17	MDY 18
1	pH	6.5 - 8.5	6.50	7.27	7.36	4.10	6.80	7.16	7.14	7.42	6.92
2	Colour, (Hazen)	5	BDL	6.20	5.90	42.50	7.30	0.20	0.90	BDL	81.32
3	Turbidity, (NTU)	1	BDL	1.20	2.88	2.33	5.38	0.50	1.10	BDL	22.38
4	Electrical Conductivity, (μS/cm)	-	346.5	442.3	528.2	912.7	3035.2	1662.0	4478.9	2302.8	546.5
5	Total Dissolved Solids, (mg/L)	500	246.0	314.0	375.0	648.0	2155.0	1180.0	3180.0	1635.0	388.0
6	Total alkalinity as $CaCO_3$, (mg/L)	200	116.0	168.0	179.0	0.0	105.0	116.0	105.0	84.0	96.0
7	Total Hardness as $CaCO_3$, (mg/L)	200	144.0	216.0	240.0	584.0	416.0	240.0	696.0	100.0	120.0
8	Chloride, (mg/L)	250	43.16	47.09	70.63	47.09	1221.0	518.40	1455.0	824.04	125.57
9	Sulphate, (mg/L)	200	13.20	18.80	23.20	326.0	40.0	37.60	251.20	19.0	41.20
10	Nitrate - N, (mg/L)	10	2.86	1.56	3.01	0.93	0.43	0.63	0.85	0.10	8.71
11	Phosphate - P, (mg/L)	-	0.07	0.09	0.25	0.90	1.75	2.00	0.03	0.06	3.10
12	Calcium, (mg/L)	75	43.20	40.0	68.80	174.40	94.40	86.40	208.0	20.80	28.80
13	Magnesium, (mg/L)	30	8.75	28.19	16.52	35.96	43.74	5.83	42.77	11.66	11.66
14	Sodium, (mg/L)	-	24.21	27.29	33.13	32.53	710.0	265.0	861.0	557.0	79.50
15	Potassium, (mg/L)	-	6.29	10.27	6.59	8.45	28.0	26.0	29.50	40.0	10.0

BDL: Below Detection Limit

(***Continued***)

Table 10.1: Water quality characteristics of groundwater samples from Madayi panchayath

Sl No.	Parameters	BIS Standard	MDY 19	MDY 20	MDY 21	MDY 22	MDY 23	MDY 24	MDY 25	MDY 26	MDY 27
1	pH	6.5 - 8.5	7.60	7.64	7.87	7.02	7.68	7.75	7.46	6.98	7.56
2	Colour, (Hazen)	5	7.50	BDL	5.10	BDL	8.12	BDL	BDL	5.50	1.00
3	Turbidity, (NTU)	1	8.78	12.00	1.80	BDL	1.20	BDL	BDL	1.80	1.40
4	Electrical Conductivity, (μS/cm)	-	416.9	664.8	53676	605.6	16268	528.2	316.9	231.0	6267.6
5	Total Dissolved Solids, (mg/L)	500	296.0	472.0	38110	430.0	11550	375.0	225.0	164.0	4450.0
6	Total alkalinity as $CaCO_3$, (mg/L)	200	74.0	96.0	290.0	210.0	230.0	136.0	105.0	96.0	138.0
7	Total Hardness as $CaCO_3$, (mg/L)	200	80.0	84.0	4204.0	292.0	1892.0	184.0	140.0	104.0	1020.0
8	Chloride, (mg/L)	250	129.5	153.0	21778	51.01	5886.0	109.9	39.24	15.70	2524.0
9	Sulphate, (mg/L)	200	4.52	52.40	132.0	21.20	520.0	20.24	12.92	8.92	246.0
10	Nitrate - N, (mg/L)	10	0.42	0.25	0.50	0.32	6.89	1.03	0.30	0.05	0.27
11	Phosphate - P, (mg/L)	-	1.30	0.08	0.05	BDL	0.06	1.56	0.02	BDL	0.03
12	Calcium, (mg/L)	75	22.40	24.0	1121.6	68.80	416.0	60.80	44.80	33.60	160.0
13	Magnesium, (mg/L)	30	5.83	5.83	340.20	29.16	207.04	7.78	6.80	4.86	150.66
14	Sodium, (mg/L)	-	73.40	116.0	13876	27.95	3527	50.0	18.15	8.69	1573
15	Potassium, (mg/L)	-	0.04	45.0	174.0	9.94	117.0	10.0	9.02	1.91	55.0

BDL: Below Detection Limit

(***Continued***)

Table 10.1: Water quality characteristics of groundwater samples from Madayi panchayath

Sl No.	Parameters	BIS Standard	MDY 28	MDY 29	MDY 30	MDY 31	MDY 32	MDY 33	MDY 34	MDY 35
1	pH	6.5 - 8.5	7.36	7.17	4.20	3.97	7.37	4.50	7.55	6.47
2	Colour, (Hazen)	5	0.40	0.10	0.20	0.30	BDL	14.91	2.30	16.42
3	Turbidity, (NTU)	1	0.60	0.30	0.70	0.80	0.20	9.21	1.50	8.44
4	Electrical Conductivity, (μS/cm)	-	425.4	642.3	2073.2	2901.4	191.5	447.9	321.1	295.8
5	Total Dissolved Solids, (mg/L)	500	302.0	456.0	1472.0	2060.0	136.0	318.0	228.0	210.0
6	Total alkalinity as $CaCO_3$, (mg/L)	200	130.2	189.0	BDL	BDL	84.00	BDL	52.00	95.00
7	Total Hardness as $CaCO_3$, (mg/L)	200	212.0	324.0	988.0	1260.0	96.0	104.0	92.0	112.0
8	Chloride, (mg/L)	250	56.27	87.84	134.96	67.68	15.42	50.13	34.70	42.42
9	Sulphate, (mg/L)	200	29.20	36.80	729.20	1268.0	7.04	53.96	27.68	1.68
10	Nitrate - N, (mg/L)	10	3.65	1.44	0.39	0.64	1.05	1.63	1.02	0.13
11	Phosphate - P, (mg/L)	-	1.0	2.0	0.32	0.06	0.05	0.09	0.05	0.06
12	Calcium, (mg/L)	75	48.0	75.20	360.0	464.0	30.40	30.40	16.0	22.40
13	Magnesium, (mg/L)	30	22.36	33.05	21.38	24.30	4.86	6.80	12.64	13.61
14	Sodium, (mg/L)	-	26.95	39.80	34.0	44.67	6.75	21.50	22.0	22.80
15	Potassium, (mg/L)	-	8.81	11.77	7.04	6.46	0.80	1.80	4.50	9.60

BDL: Below Detection Limit

Percentage of groundwater samples above/below BIS limit of heavy metals were illustrated in Figure 10.4. Cd values observed beyond the BIS standard were ranged from 0.004 - 0.5836 mg/L. High Cd values were obtained in samples such as MDY-18, MDY-8, MDY-6 and MDY-33 i.e., samples from near mining area and area through wastewater after mining is passing. 0.12 mg/L of Cd was also noticed in a sample collected from the bank of Perumba river.
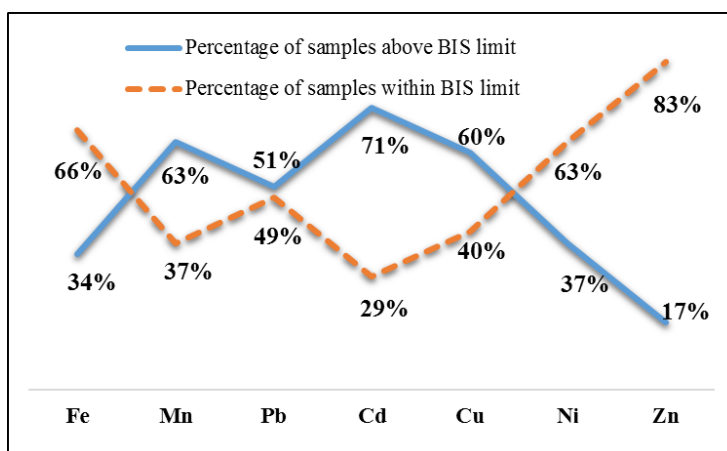
Figure 10.4: Percentage of groundwater samples above/below BIS limit

For Pb, 51 % of samples exceeds the BIS acceptable limit of 0.01 mg/L and in those samples, it was ranged from 0.016 - 0.63 mg/L. Maximum value of Pb was observed in sample collected from Pazhayangadi, near mining area. In majority of the samples collected from near mining area, concentration of Pb was observed beyond the limit and Pb was also detected in samples from Vengara Muttom through where the wastewater from mining industry flows.

Table 10.2: Heavy metals concentration in groundwater samples from Madayi panchayath

Sample Code	Fe (mg/L)	Mn (mg/L)	Pb (mg/L)	Cd (mg/L)	Cu (mg/L)	Ni (mg/L)	Zn (mg/L)
MDY 1	0.22	0.04	0.02	0.04	0.1	0.1766	0.379
MDY 2	0.01	0.1	BDL	0.012	0.02	BDL	0.672
MDY 3	0.63	0.15	0.03	0.006	BDL	0.0072	BDL
MDY 4	0.83	0.17	BDL	BDL	0.04	0.0052	BDL
MDY 5	0.11	0.01	0.021	0.004	0.058	BDL	0.481
MDY 6	14.1	1.43	0.078	0.21	0.153	0.2433	5.961
MDY 7	0.01	BDL	BDL	BDL	BDL	BDL	BDL
MDY 8	192.3	12.47	0.63	0.5684	4.74	0.5202	8.03
MDY 9	27.95	16.93	0.006	0.001	BDL	0.0168	BDL
MDY 10	0.095	0.02	BDL	BDL	BDL	BDL	0.681
MDY 11	0.11	0.57	BDL	0.004	0.023	0.0012	BDL
MDY 12	0.39	0.16	BDL	BDL	BDL	BDL	0.59
MDY 13	3.6	1.85	0.016	0.005	0.23	0.0368	0.16
MDY 14	0.88	0.28	0.008	0.004	0.08	0.1042	BDL
MDY 15	4.13	0.45	0.024	0.002	1.205	BDL	BDL
MDY 16	0.95	0.36	0.02	0.007	0.0225	BDL	0.57
MDY 17	0.001	BDL	BDL	0.003	BDL	BDL	0.014
MDY 18	200.1	12.34	0.07	0.5836	2.9	0.4865	9.1
MDY 19	0.76	0.04	0.0086	0.004	BDL	0.0528	0.098
MDY 20	0.05	0.11	BDL	BDL	BDL	0.008	0.561
MDY 21	0.72	0.64	0.37	0.12	0.3	0.5816	4.21
MDY 22	0.08	0.04	BDL	0.002	BDL	BDL	BDL
MDY 23	0.83	0.21	BDL	0.005	0.06	BDL	0.349
MDY 24	0.01	0.062	0.05	0.011	0.11	0.0469	BDL
MDY 25	2.74	0.46	BDL	0.006	1.31	BDL	BDL
MDY 26	0.02	0.04	BDL	0.015	BDL	BDL	BDL
MDY 27	0.5845	0.21	0.0277	BDL	0.16	0.0364	0.0081
MDY 28	0.4808	0.04	0.0578	0.0583	0.177	BDL	0.279
MDY 29	0.5306	0.034	BDL	0.0361	0.171	0.005	0.0037
MDY 30	9.9	3.17	0.0232	0.007	0.146	BDL	0.0019
MDY 31	15.0701	5.14	0.0753	0.0148	0.229	0.1337	5.145
MDY 32	0.0416	BDL	BDL	BDL	0.077	BDL	BDL
MDY 33	4.2761	0.9905	0.172	0.1985	0.0961	0.18	7.0073
MDY 34	3.46	0.85	0.006	0.007	0.41	0.0618	0.76
MDY 35	1.283	0.07	0.0243	0.089	0.1031	BDL	5.185

BDL: Below Detection Limit

The concentrations of Mn, Cu and Ni were found high than BIS limit in 63 %, 60 % and 37 % of samples respectively with spatial variations. High concentration of Mn (16.93 mg/L) and Cu (4.74 mg/L) was observed near china clay mining area but maximum value of Ni was observed in sample MDY- 21, near to Perumba river and Sultan canal. In 17 % of the collected samples, the concentrations of Zn exceeded BIS limit (IS 10500: 2012). A maximum value of 9.1 mg/L was observed in sample near Kavilevallapil thodu from Vengara Muttom area.
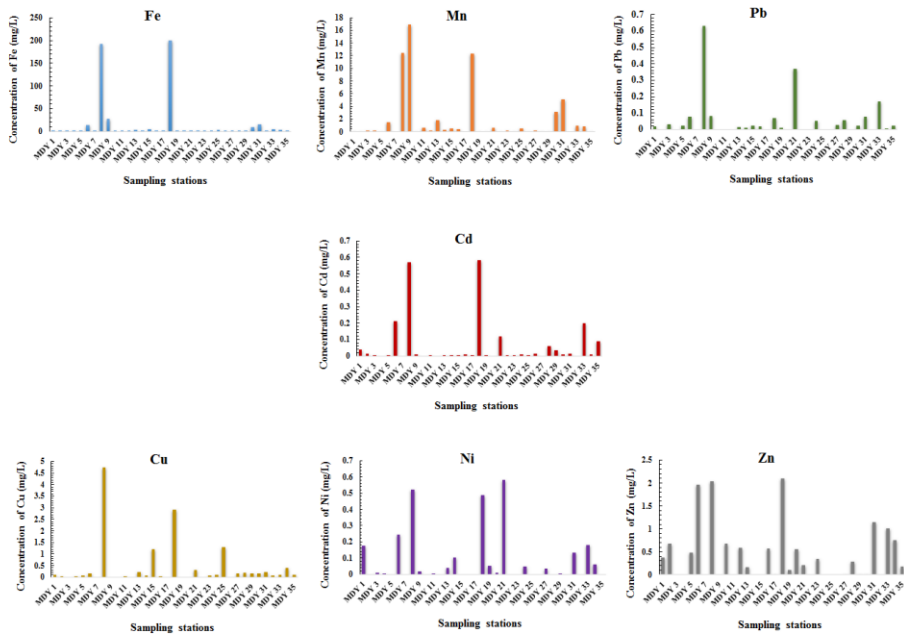
Figure 10.5: Spatial variations of heavy metals

10.3.4 Integrated pollution indices

For the evaluation of heavy metal pollution in groundwater samples from Madayi area, pollution indices such as HPI, HEI, and C_d

were computed individually. For calculating HPI, HEI and C_d, the BIS (10500: 2012) water standard for each heavy metal parameter in µg/L was considered. In order to calculate the overall heavy metal pollution index (HPI) of the groundwater samples from Madayi area, the mean concentration value of the selected heavy metals (Fe, Mn, Pb, Cd, Cu, Ni and Zn) have been considered. The details of unit weightage (W_i) and standard permissible value (S_i) for the computation of HPI is shown in Table 10.3.

Though, the iron has reported maximum concentration value in the groundwater samples, the weightage (W_i) of Fe is very less, therefore, in evaluation of HPI of overall groundwater quality, this parameter does not contribute much on this index value. Heavy metals like Cd, Pb and Ni have been given no relaxation in drinking water standard hence, they have been given high weightage (W_i) value in calculation of HPI. So, even though these metals present in small concentration level in water, it makes the quality of water poor and contribute high values in HPI calculations. Concentration of Zn has been found higher than the desirable limit of drinking water standard in only six groundwater samples. The overall heavy metal pollution index value of groundwater samples from Madayi area was found to be 1474.49 and that was higher the critical pollution index value of 100. The HPI value higher than 100 is considered as unacceptable and indicates that the water is critically polluted with respect to heavy metals (Prasad & Kumari, 2008; Prasad & Mondal, 2008; Bhardwaj et al., 2017).

Table 10.3: Mean HPI of groundwater from Madayi

Heavy metals	Mean value (µg/L) M_i	Standard permissible value (µg/L) S_i	Highest desirable value (µg/L) I_i	Unit weightage (W_i)	Sub index (Q_i)	$W_i Q_i$
Fe	13921.51	1000	0	0.001	1392.15	1.39
Mn	1698.19	300	100	0.0033	799.09	2.66
Pb	51.77	10	0	0.1	517.69	51.77
Cd	58.05	3	0	0.3333	1934.95	644.98
Cu	369.16	1500	50	0.00067	22.01	0.015
Ni	77.26	20	0	0.05	386.31	19.32
Zn	1435.6	15000	5000	0.000067	35.64	0.0024

$\sum W_i Q_i = 720.14$; $\sum W_i = 0.4884$ and HPI= 1474.49

The heavy metal pollution index (HPI) was calculated individually for each sample and the index values are summarised in Table 10.4. Seven heavy metals namely Fe, Mn, Pb, Cd, Cu, Ni and Zn were used to calculate HPI. The minimum HPI value obtained was 0.64 (MDY-12), sample from Moolakkeel and this sampling location is away from mining area. Out of 35 samples, in 11 groundwater samples, the HPI value was found below the critical value (HPI < 100). In sample MDY-32, a water sample from a water supply point also obtained a low HPI value. This indicates that these 11 samples were not critically polluted with respect to heavy metals. But for the remaining groundwater samples, HPI value was found above the critical index value of 100. Very high HPI value was reported particularly in sampling points like MDY-8, MDY-18, MDY-6, MDY-33, MDY-35, MDY-21, MDY-28, MDY-29 and MDY-1. At sampling sites MDY-8 and MDY-18, the index value obtained was much higher when compared to other sampling locations. The sampling sites MDY-8 is near the mining area. The sample MDY-18

is from Vengara Muttom area, a sampling location near Kavilevallapil thodu where the drainage of wastewater from mining industry flows. Very high Fe value was reported in both these sites along with other heavy metals and the metals like Cd, Pb and Fe contribute mainly to the very high HPI index value in both the sites. High HPI value was also observed in majority of the sampling sites near the mining area. The samples collected from the bank of Perumba river also reported high index value. The mean value of HPI index (1433.7) indicates the heavy metal pollution in the study area.

Table 10.4: Results of different indices evaluation

Sample Code	HPI	HEI	Cd	Sample Code	HPI	HEI	Cd
MDY 1	952.7	24.61	17.61	MDY 19	109.9	5.73	-1.27
MDY 2	273.7	4.40	-2.60	MDY 20	0.72	0.85	-6.15
MDY 3	198.7	6.49	-0.51	MDY 21	3491.3	109.4	102.4
MDY 4	0.728	1.68	-5.32	MDY 22	46.35	0.88	-6.12
MDY 5	134.9	3.65	-3.35	MDY 23	114.4	3.26	-3.74
MDY 6	4943.7	109.3	102.3	MDY 24	353.6	11.30	4.30
MDY 7	0.92	0.01	-6.99	MDY 25	137.3	7.15	0.15
MDY 8	14291	516.04	509.0	MDY 26	342.1	5.15	-1.8
MDY 9	412.0	96.22	89.22	MDY 27	57.47	5.98	-1.02
MDY 10	0.89	0.21	-6.79	MDY 28	1445.6	25.96	18.96
MDY 11	91.42	3.42	-3.58	MDY 29	822.3	13.04	6.04
MDY 12	0.64	0.96	-6.04	MDY 30	215.1	25.22	18.22
MDY 13	150.8	15.04	8.04	MDY 31	505.4	51.85	44.85
MDY 14	108.4	9.21	2.21	MDY 32	0.93	0.09	-6.91
MDY 15	95.72	9.50	2.50	MDY 33	4871.2	100.5	93.48
MDY 16	200.5	6.54	-0.46	MDY 34	173.6	12.64	5.64
MDY 17	69.17	1.00	-6.00	MDY 35	2075.5	34.03	27.03
MDY 18	13491.1	469.6	462.6	Mean	1433.7	48.31	41.31

The computed HEI and C_d values for each location are also shown in Table 10.4. Edet and Offiong, (2002) used HEI for easy interpretation of

the pollution index. The mean HEI value obtained for groundwater samples from Madayi panchayath was 48.31. This index values ranged from 0.01 to 516.04. In majority of the groundwater samples from Madayi, the HEI index values obtained were less than 400 so these samples come under the category of 'low heavy metals'. But in samples MDY- 8 and MDY-18, HEI value was 516.04 and 469.6 respectively so both these samples come under the category of 'moderate to heavy metals'. High Fe content and other metals like Mn, Pb, Cd, Cu, Ni and Zn were also reported in these two sites. Similarly, highest C_d values were also reported in the same sites. Based on three categories of contamination index (C_d) value (low: $C_d < 1$; medium: Cd = 1- 3 and high: $C_d > 3$) (Edet & Offiong, 2002; Sobhanardakani et al., 2017), the 43 % of groundwater samples come under the category of 'high'. Majority of samples reported high C_d are from the locations near to mining area and samples collected from the bank of Perumba river also reported high value of contamination index. The results of HPI, HEI and C_d indicates the heavy metal pollution in some samples from Madayi area.

The heavy metal pollution may be due to leaching of heavy metals from the mining wastes and may be due to the application of fertilizers in nearby agricultural areas. The drainage of wastewater from mining industry containing very acidic water passes through Kavilevallapil thodu (Vengara Muttom area) and Kakki thodu in the study area. The highly acidic nature of the effluent, increases the chance of corrosion of the drainage pipelines. So, the percolation of acidic wastewater to the neighbouring groundwater resources can increases and

also solubilise the heavy metals present in those area, which increase the transport of heavy metals to the groundwater resources. The local residents from this study area also reported that the mining waste from mining area overflows to the neighbouring areas during the rainy season and so the agricultural lands were converted to barren lands. Sultan canal, a canal which connects Perumba river and Kuppam river is also passing through the study area, which can also increase the distribution and transportation of many contaminants in this area. All these activities may increase the contamination of the groundwater resources in Madayi area. The sampling was conducted during the summer season and the high values of metals concentration reported in many sampling sites, may also be due to reduced aquifer recharge and reduced dilution of contaminants, as a result of increase in temperature during the summer season. The indexing approach for the evaluation of groundwater samples from Madayi panchayath indicates the heavy metals contamination in groundwater samples so, the treatment of the heavy metal contaminated drinking water is necessary.

10.3.5 Correlation analyses

The association or interrelationship among all the seven heavy metals (Fe, Mn, Pb, Cd, Cu, Ni and Zn) was assessed by Pearson correlation analysis. Pearson's correlation coefficients among heavy metals in groundwater samples from Madayi panchayath have been summarized in Table 10.5. In the present study, only the positive and strong ($r > 0.7$) correlation among heavy metals were considered. The results of Pearson correlation analysis showed very strong correlation

between Fe - Cd (r = 0.938), Fe - Cu (r = 0.918), Cd – Cu (r = 0.851), Pb - Ni (r = 0.806), Cd - Ni (r = 0.813) and Cd - Zn (r = 0.808) in water samples during the study. This result indicate that these heavy metals are the main contributory parameters. Heavy metals displaying very high correlation indicates same source of contamination (Bhardwaj et al., 2017). Fe also showed a positive correlation with metal ions such as Mn (r = 0.684), Pb (r = 0.611), Ni (r = 0.706) and Zn (r = 0.729) in groundwater samples from Madayi area indicating that the metal ions are from the same source. The main source of Fe in groundwater is from the china clay mining industry. Pb also showed a positive correlation with Cu (r = 0.714). Among the metals, Mn was the only metal not strongly correlated with other metal but was positively correlated with other metals, indicating that Mn level in groundwater increases with an increase in level of other metal ions and vice versa.

Table 10.5: Pearson Correlation of heavy metals in groundwater samples

Pearson Correlation Matrix							
Heavy metals	**Fe**	**Mn**	**Pb**	**Cd**	**Cu**	**Ni**	**Zn**
Fe	1						
Mn	0.684	1					
Pb	0.611	0.420	1				
Cd	0.938	0.614	0.697	1			
Cu	0.918	0.609	0.714	0.851	1		
Ni	0.706	0.479	0.806	0.813	0.657	1	
Zn	0.729	0.476	0.513	0.808	0.617	0.657	1

10.3.6 Principle Component Analysis and Cluster Analysis

The multivariate statistical techniques such as Principle Component Analysis (PCA) and Cluster Analysis (CA) was used in the

interpretation of data to understand the water quality with respect to heavy metals. PCA was applied to the all the seven heavy metals (Fe, Mn, Pb, Cd, Cu, Ni and Zn) in 35 water samples from Madayi area to identify metal contamination and confirm the sources of contamination and described in Table 10.6. The principal components that have eigen values higher than one were considered for the interpretation. The results show that there was only one eigen value higher than one so, only the first principal component (PC1) include a large portion of the total variance. The Principle component analysis help us to find the causes of the trace metals whether it is of natural or / and anthropogenic source. The first principal component (PC1) explained 73.40% of the variation in the data and represented strong contributions (> 0.75) by the variables Fe, Mn, Pb, Cd, Cu, Ni and Zn. PC1 was loaded mainly by variable in the order of Cd, Fe, Cu, Ni, Zn, Pb and Mn indicating a significant water quality impact from industrial effluent and agricultural runoff (Wu et al., 2008; Herojeet et al., 2015)

Table 10.6: Principle component analysis of different heavy metals in groundwater from Madayi

	Component
	1
Fe	0.941
Mn	0.704
Pb	0.795
Cd	0.963
Cu	0.903
Ni	0.857
Zn	0.804
Eigen value	5.14
Percent of Total Variance Explained	73.40

Cluster analysis (CA) incorporates a number of dissimilar methods which organize objects (observations) into groups termed clusters without unexplanation or interpretation. Objects inside the clusters are similar whereas objects in different clusters are dissimilar. This exploratory method is utilised to determine the data structure not only among observations, but also among variables, arranged into a tree diagram, generally known as a dendrogram. The similarity was measured using Euclidean distance (Praus, 2007). The cluster analysis generated a dendrogram as revealed in Figure 10.6, grouping 35 water samples into three clusters. Cluster 1 (C1) comprised sampling stations such as MDY-8 and MDY-18 with the highest levels of Fe, Pb, Cd, Cu, Ni, and Zn. C1 contains the locations near the china clay mining area and Vengara Muttom area where the drainage of wastewater from mining industry flows with the most significant pollution by anthropogenic activities. The indexing approach (HPI, HEI and C_d) also indicated the moderate to high heavy metal pollution in these sampling locations.

The sampling locations in cluster 2 (C2) were MDY-9, MDY-31, MDY-6 and MDY-30. All these sampling sites were near the china clay mining area, Pazhayangadi. So, there is possibility of similar contamination. The value of Fe exceeds the acceptable and permissible limit prescribed by BIS (IS 10500: 2012) in all these four sites along with other toxic metals. The three indices used in this study, also suggested metal pollution in these sites, but less polluted compared to MDY-8 and MDY-18. The remaining samples were in Cluster 3 (C3) and many of the sampling locations in C3 were significantly affected by saline intrusion.

These sites were comparatively less polluted with respect to heavy metals.

Cluster Tree
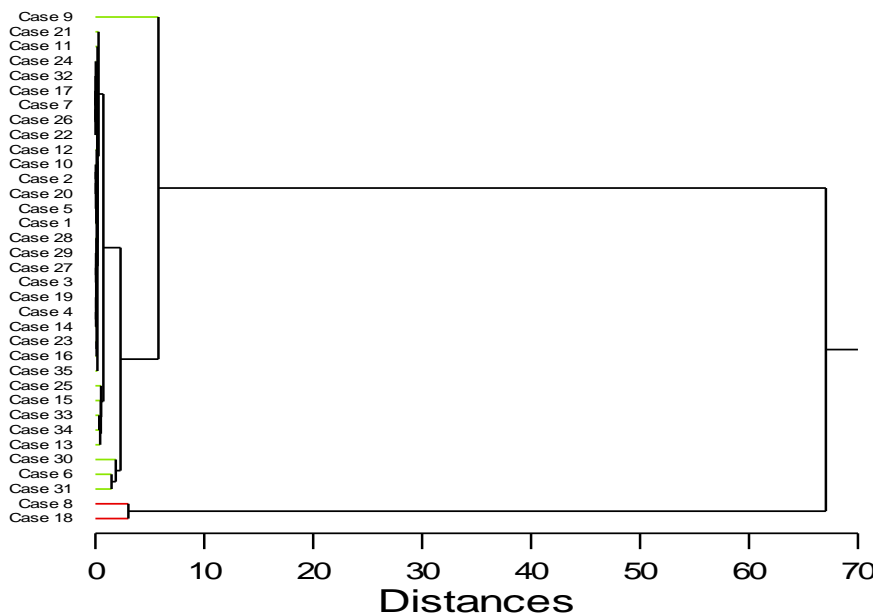
Figure 10.6: Dendrogram generated from heavy metal values of different sampling sites

10.3.7 Heavy metals in soil and sediment samples from Madayi

The concentrations of heavy metals and physico chemical characteristic of the soil samples from Madayi area is given in Table 10.7. and showed wide variations among the sampling sites. Seven soil samples were collected from the study area and its spatial distribution is shown in Figure 10.1. The heavy metals concentration in the soil samples ranged from: Fe - 18602 to 301486 mg/Kg, Mn - 73.43 to 765.88 mg/Kg, Cd - 1.68 to 11.53 mg/Kg, Pb - 0 to 162.98 mg/Kg, Ni - 9.58 to 44.68

mg/Kg, Cu - 14.63 to 103.40 mg/Kg, Zn - 42.43 to 207.90 mg/Kg. Very high iron value was observed in the soil samples such as MDY- 1S, MDY-3S and MDY-6S. These sampling points were very close to the china clay mining area, Pazhayangadi. Here waste containing high iron from mining area, were flows to the neighbouring residential area during rainy season. So, the soils collected from near the clay mining area were yellowish in colour (Plate 10.2) and detected high Fe values. High Mn values were also reported in the above-mentioned sites compared to other soil sampling sites from Madayi area.

Plate 10.2: Yellowish colour soil from the residential area near the clay mining area

The value of Cd was found higher than limit (10 mg/Kg) prescribed for residential land use by Canadian Soil Quality Guidelines

for the Protection of Environmental and Human Health (CCME, 2007) in samples, MDY- 1S (11.53 mg/Kg) and MDY-6S (10.08 mg/Kg). The concentration of Pb, above Canadian Soil Quality Guidelines value (140 mg/Kg) was observed in samples MDY-3S (near mining site) and MDY-4S (near Sultan canal). Cu was found above the guidelines value (63 mg/Kg) in samples MDY- 1S, MDY- 3S and MDY- 6S but Ni was observed below the guidelines value (50 mg/Kg) in all the soil samples. The Canadian Soil Quality Guidelines value of Zn was 200 mg/Kg, was found above this value in sample MDY- 1S.

Soil pH is the most commonly recognized influencing parameter on the availability and mobility of heavy metals in the soil. Acidic nature of soil controls availability, mobility and toxicity of heavy metal ions and most metals tend to be less mobile in soil with high pH as they tend to form insoluble complexes (Anegbe et al., 2018). Highly acidic pH was observed in samples near the mining site (MDY-1S, MDY- 3S and MDY- 6S), which may influence the mobility of heavy metals to the nearby groundwater resources but comparatively high pH was reported in soil samples away from mining site (MDY- 4S and MDY- 5S).

Table 10.7: Physico-chemical parameters of soil samples

Parameters	MDY 1S	MDY 2S	MDY 3S	MDY 4S	MDY 5S	MDY 6S	MDY 7S
pH	2.86	4.98	3.37	6.00	6.75	3.45	5.14
Electrical Conductivity (µs/cm)	1750.0	270.0	1390.0	132.0	128.0	1560.0	328.0
Alkalinity (mg/Kg)	40.0	240.0	160.0	560.0	498.0	80.0	244.8
Sulphate (mg/Kg)	537.2	429.2	445.2	195.2	160.4	512.6	303.5
Calcium (mg/Kg)	1200.0	1680.0	1680.0	1760.0	1530.0	1200.0	1088.0
Magnesium (mg/Kg)	48.6	97.2	291.6	48.6	123.8	68.4	103.8
Chloride (mg/Kg)	1720.0	160.0	1600.0	560.0	280.0	920.0	720.0
Inorganic Phosphorous (mg/Kg)	460.0	140.0	320.0	95.0	90.0	375.0	85.0
Sodium (mg/Kg)	185.0	246.5	357.0	265.3	161.5	132.0	105.0
Potassium (mg/Kg)	18.0	167.0	63.0	68.0	87.5	68.0	13.5
Organic Carbon (%)	3.39	1.56	2.47	0.68	0.82	3.06	1.12
Organic matter (%)	5.85	2.68	4.26	1.17	1.41	5.28	1.93
Sand (%)	74.25	91.25	78.00	95.25	94.10	79.4	86.70
Clay (%)	19.50	4.75	15.50	4.50	5.30	13.90	7.90
Silt (%)	6.25	4.00	6.50	0.25	0.60	6.70	5.40
Iron (mg/Kg)	301486	23134	187526	18602	21320	251385	87593
Manganese (mg/Kg)	765.88	125.80	511.23	73.43	80.0	668.75	300.0
Cadmium (mg/Kg)	11.53	4.08	9.73	9.95	1.68	10.08	5.10
Lead (mg/Kg)	132.10	110.30	144.53	162.98	BDL	112.98	64.03
Nickel (mg/Kg)	44.68	22.08	39.68	12.90	9.58	25.15	20.25
Copper (mg/Kg)	103.40	15.73	72.00	14.63	28.25	80.00	50.03
Zinc (mg/Kg)	207.90	42.43	163.63	127.50	65.00	185.25	95.75

BDL: Below Detection Limit

Other soil characteristics were also summarised in Table 10.7 and the results revealed that comparatively high organic carbon and organic matter content were also observed in MDY-1S, MDY-3S and MDY-6S which influences the metals concentrations. The texture analysis revealed that relatively, high contents of clay and silt was observed in sites near the china clay mining area. The mobilisation of heavy metals in the soil is depends on the pH, clay content, organic matter content and other soil properties so these factors influences the heavy metal pollution (Mapanda et al., 2005). The heavy metals accumulated in the soil at toxic levels can

be transferred from soil to the other ecosystem, such as underground water or crops, and can disturb human health through the water supply and food. Soils, act as filters of many toxic chemicals, may adsorb and hold heavy metals from wastewater. The contaminated soils release heavy metals into groundwater, when the capacity of soils to retain toxic metals is reduced, due to continuous overloading of contaminants or changes in pH (Taghipour et al., 2012).

Table 10.8: Physico-chemical parameters of sediment samples

Parameters	MDY 1SE	MDY 2SE	MDY 3SE	MDY 4SE
pH	5.0	5.3	4.5	5.7
Electrical Conductivity(μs/cm)	68000	253	462	74000
Alkalinity (mg/Kg)	240	200	139	360
Sulphate (mg/Kg)	20100	428.8	546.7	22400
Calcium (mg/Kg)	13900	1360.0	1223.0	14800
Magnesium (mg/Kg)	20842	145.8	382.5	25515
Chloride (mg/Kg)	171300	240.0	485.8	176000
Inorganic Phosphorous (mg/Kg)	960	385.0	420.0	982.0
Sodium (mg/Kg)	104650	226.5	124.0	115950
Potassium (mg/Kg)	3361	128.0	62.0	3875
Organic carbon (%)	5.31	5.91	5.62	5.03
Organic matter (%)	9.15	10.18	9.7	8.7
Sand (%)	85.00	75.00	77.40	93.50
Clay (%)	11.00	21.00	18.71	5.70
Silt (%)	4.00	4.00	3.89	0.80
Iron (mg/Kg)	121792	297733	210060	124320
Manganese (mg/Kg)	670.0	509.4	262.5	252.0
Cadmium (mg/Kg)	26.08	50.15	52.53	31.18
Lead (mg/Kg)	154.3	144.9	151.7	142.7
Nickel (mg/Kg)	33.68	42.25	20.0	30.80
Copper (mg/Kg)	40.3	108.7	77.5	65.0
Zinc (mg/Kg)	166.5	240.5	229.1	155.0

Four sediment samples were collected from the Kavilevalappil thodu (Plate 10.1) through which the wastewater pipe line of mining industry is passing. The discharges from mining industries can destruct

the natural sediment characteristics. The physico chemical characteristics of sediment samples were tabulated in Table 10.8. pH of all the samples were in acidic range. The results indicated that the high Cl^-, Na^+ and K^+ contents in MDY-1SE and MDY-4SE sediment sample. Both these points were near the Perumba river so the results give an indication of saline intrusion. High organic matter and clay content were observed in sediment sample near mining area (MDY- 2SE and MDY-3SE). The organic content has a high relationship with heavy metal concentrations in sediment (Ahmad et al., 2009) and high OC was reported in the above-mentioned sites.

The heavy metal concentrations in the sediment samples from Madayi panchayath were evaluated by comparing with the sediment quality guideline proposed by USEPA. These guideline values are shown in Table 10.9. In sediment samples also, very high Fe contents were detected and according to USEPA guideline, all the samples were heavily polluted with respect to Fe value. Other metal concentrations were ranging over following intervals: Cd: 26.08 -52.53 mg/Kg; Pb: 142.7 - 154.3 mg/Kg; Ni: 20.0 - 42.25 mg/Kg; Zn: 155.0 - 240.5 mg/Kg; Cu: 40.3 - 108.7 mg/Kg. All the four sediment samples were heavily polluted by Cd and Pb with respect to the guideline value. Ni was moderately polluted in all the sites. Cu pollution was high in MDY-2SE, MDY-3SE and MDY-4SE but moderate in MDY-1SE. Zn was heavily polluted in samples near the china clay mining area. Mn pollution was detected in two samples. The mean value of the metals follows the order: Fe > Mn > Zn > Pb > Cu > Cd > Ni. The changes in environmental conditions such

as pH and redox potentials leads to the remobilisation of heavy metals from the sediment to water.

Table 10.9: USEPA guideline for sediment[*]

Heavy metal	Not polluted	Moderately polluted	Heavily polluted
Cd	-	-	> 6
Cu	< 25	25 - 50	> 50
Ni	< 20	20 - 50	> 50
Pb	< 40	40 - 60	> 60
Zn	< 90	90 - 200	> 200
Mn	< 300	-	> 500
Fe	< 17000	17000 - 25000	> 25000

*All concentrations in mg/Kg dry weight

The overall results of soil and sediment analysis indicate the heavy metal pollution. However, the high concentration of toxic heavy metals in the soil and sediment may adversely affect the environmental quality and human health if they enter into water and food chain. In order to reduce such risk, the consumption of contaminated water and plant should be strictly discouraged. Proper treatment of heavy metal contaminated drinking water is essential.

10.3.8 Removal of heavy metals using selected adsorbents

Water quality and heavy metal analysis of 35 groundwater samples from Madayi panchayath revealed the heavy metal contamination in several samples. So, removal of heavy metals from drinking water is a necessary in these samples. Three heavy metal contaminated water samples (MDY-6, MDY-8 and MDY-18) were selected from the study area and treatment of heavy metals from these

samples were conducted using three different sorbents (A, B and C). A was functionalised iron oxide nanosorbent (iron oxide nanoparticles coated with polyvinyl alcohol and gallic acid); B was protonated *Caesalpinia sappan* (herbal plant material) and C was *Tretepohila abietina* (algal biosorbent). The synthesis or preparation and characterisation of those materials are discussed in chapter 9 (for A) and chapter 8 (for B and C). From the previous studies, it was observed that these three sorbents work well at a variety of pH levels. 100mL of water samples were treated using 0.5g of sorbents using batch sorption techniques. The results of the treatment of three samples are shown in Table 10.10.

Table 10.10: Removal of heavy metals from groundwater samples

	Treatment	**Fe**	**Mn**	**Pb**	**Cd**	**Cu**	**Ni**	**Zn**
MDY 6	Initial concentration (mg/L)	14.1	1.43	0.078	0.21	0.153	0.2433	5.961
Percentage of removal (%)	A	97.43	100.00	100.00	100.00	100.00	100.00	99.95
	B	93.96	100.00	100.00	100.00	100.00	100.00	99.16
	C	96.20	100.00	100.00	100.00	100.00	100.00	99.88
MDY 8	Initial concentration (mg/L)	192.3	12.47	0.63	0.5684	4.74	0.5202	8.03
Percentage of removal (%)	A	56.68	98.36	100.00	100.00	87.32	100.00	89.91
	B	46.85	71.05	100.00	100.00	79.32	98.46	78.46
	C	43.01	79.95	100.00	100.00	78.06	89.43	56.29
MDY 18	Initial concentration (mg/L)	200.1	12.34	0.07	0.5836	2.9	0.4865	9.1
Percentage of removal (%)	A	51.57	70.50	100.00	100.00	99.83	100.00	86.48
	B	42.18	56.97	100.00	100.00	98.93	100.00	78.68
	C	38.23	51.54	100.00	99.66	97.17	100.00	70.44

In sample MDY-6 (pH = 2.92), metals like Mn, Pb, Cd, Cu and Ni were completely removed by all the three adsorbents. More than 99 % of Zn was removed by A, B and C methods. More amount of Fe was

removed (97.43 %) by A, functionalised iron oxide nanosorbent. The sorbents, B and C removed 93.96 % and 96.20 % of Fe respectively. In the case sample MDY- 8 (pH = 2.79), complete removal of Pb and Cd was exhibited by all the three sorbents under highly acidic condition also. Ni was also removed completely by iron oxide nanoparticles coated with poly vinyl alcohol and gallic acid and the other biosorbents were removed 98.46 % (B) and 89.43 % (C) of Ni from water. In sample MDY-8, maximum Mn removal was showed by A (98.36 %). In this sample, 56.68, 46.85 and 43.01 % of Fe was removed by A, B and C. In the case sample MDY-18, the removal efficiency of Fe, Mn, Pb, Cd, Cu, Ni and Zn by sorbent A i.e., iron oxide nanoparticles coated with poly vinyl alcohol and gallic acid were 51.57, 70.50, 100.0, 100.0, 99.83, 100.0 and 86.48 %, respectively. The biosorbent such as *Caesalpinia sappan* and *Tretepohila abietina* also showed better reduction in concentration of metals like Pb, Cd, Cu and Ni. The results suggest that, all the three sorbents were effective in the treatment of heavy metals from heavy metals contaminated real water samples. The nanosorbent (iron oxide nanoparticles coated with poly vinyl alcohol and gallic acid) exhibited comparatively better performance in the removal of heavy metals from field samples from Madayi area.

10.4   Summary

Madayi, near Pazhayangadi in Kannur district, is a clay mining area in northern Kerala, with rich biodiversity. The active mining is generating some drinking water issues there. So, the groundwater quality near the mining area was evaluated in this study. In order to assesses the

quality of drinking water resources of Madayi area, 35 water samples were collected. High iron problems are observed near the china clay mining area during sampling. Hence, the quality of drinking water resources in the study area were evaluated on the basis on heavy metal concentration in water samples. The physico-chemical characteristics of groundwater samples revealed highly acidic nature of samples collected from near the china clay mining area, indicating the percolation of contaminants from the mining area. High TDS, alkalinity, chloride, calcium, magnesium, sodium and potassium reported in the samples collected from near Perumba river, indicating salinity intrusion. TDS values were found to be exceeds the BIS limit in samples collected from the sites near the mining area. No alkalinity was detected in samples near mining area because of the highly acidic nature. Very hard water and high sulphate concentration were also noticed in locations near mining area. High nitrate and phosphate were found in sample near Kavilevallapil thodu, through which the wastewater drainage from mining is passing and eutrophication was also observed there. Of the 35-water sample collected, total coliform bacteria were detected in 89 % of samples and the presence of *E. coli* was detected in only 14 %.

Concentration of seven heavy metals in water namely Fe, Mn, Pb, Cd, Cu, Ni and Zn were analysed. The analytical results indicate high Fe concentration in samples near mining area and Vengara Muttom compared to other sites. Maximum value of 200.1 mg/L was reported in sample near Kavilevallapil thodu (Vengara Muttom) through which the wastewater drainage from mining is passing. The order of concentration of heavy metals found were as follows: Fe > Mn > Zn > Cu > Ni > Pb >

Cd. The results revealed that high concentration of Cd, Pb, Mn, Zn, above the acceptable limit of BIS were also found in water samples collected from near the mining area. High heavy metals contents were also detected in samples from Vengara Muttom through where the wastewater from mining industry flows. Results indicates that groundwater samples from near china clay mining area and near Kavilevallapil thodu, Vengara Muttom contains high metal concentrations. The heavy metal analytical results were evaluated using the HPI, HEI and C_d indices. The overall HPI value of groundwater samples from Madayi area was found to be 1474.49 and that was higher the critical pollution index value of 100. The heavy metal pollution index was calculated individually for each sample, high HPI values were found in groundwater samples from Pazhayangadi, Vengara Muttom and near Perumba river. The similarity in heavy metal contamination in Pazhayangadi and Vengara Muttom areas were observed by Cluster Analysis (CA) and Principle Component Analysis (PCA). The correlation analysis of heavy metal concentrations exhibited strong positive correlations among Fe, Cd, Cu, Ni, Pb, Zn ions suggesting that these metals are from common sources. High Fe contents were recorded in soil samples from Pazhayangadi, Madayi. Compared to Canadian Soil Quality Guidelines, high Cd, Pb and Cu were also detected from this location. Heavy metals in four sediment samples from the study area were compared with the sediment quality guideline proposed by USEPA and the results indicates metal pollution in this area. The values of the calculated indices (HPI, HEI and C_d) in groundwater collected from Madayi area indicates heavy metal pollution, so severe precautions such

as treatment of contaminated drinking water resources; effective treatment of wastewater from china clay mining industry; establishment of sustainable mining activities and management of the use of agricultural inputs (chemical fertilizers and metal-containing pesticides) must be taken into consideration in this area.

Some treatment methods were applied on heavy metal contaminated drinking water from Madayi panchayath. Three metal contaminated water samples were treated using three different sorbents such as functionalised iron oxide nanosorbent (iron oxide nanoparticles coated with polyvinyl alcohol and gallic acid); protonated *Caesalpinia sappan* (herbal plant material) and *Tretepohila abietina* (algal biosorbent). The results suggest that, all the three sorbents were effectively removed heavy metals from heavy metals contaminated real water samples. The nanosorbent (iron oxide nanoparticles coated with polyvinyl alcohol and gallic acid) exhibited comparatively better performance in the removal of heavy metals from field samples from Madayi area.

SUMMARY, CONCLUSIONS AND RECOMMENDATIONS

In the present scenario, the deterioration of water quality as a consequence of the anthropogenic activities, unskilled utilization of natural water resources, population intensification, unplanned urbanization and swift industrialization, is growing with rapid pace. Furthermore, impacts of the current environmental strategies has increased the awareness to develop environmentally friendly, robust and economically feasible processes proficient to remove contaminants from water and at same time, to safeguard the health of mankind. Highly toxic, non-biodegradable, bioaccumulation and invariably persisting nature of heavy metals and the irreversible health threat of fluoride, makes them severely hazardous. The prevailing treatment technologies of heavy metals and fluoride, with different degree of success to control and minimize contamination, have the shortcomings such as high operational and maintenance costs, complicated procedure involved in the treatment and generation of toxic sludge or by-products. The present study deals with the development of effective, efficient and eco-friendly clean up techniques to reduce or remove the toxicity of heavy metal and fluoride from water.

The study was under taken to (1) to develop efficient, effective and ecofriendly water treatment method for the removal of heavy metals from the contaminated water (2) to study the defluoridation of water using biosorbents and its application in groundwater samples collected from the contaminated areas (3) to assess the detoxification of heavy metals from water by nanosorbent and biosorbents and its application in polluted samples and (4) to use the technology of phytoremediation for the decontamination of soil affected by heavy metal toxicity.

The assessment of the performance of electrically stimulated phytoremediation for the removal of heavy metal was conducted. Treatment of lead, cadmium and copper from synthetic solution using phytoremediation system coupled with electric field was carried out. In that experiment, the *Eichhornia crassipes,* an efficient phyto-remediator exhibited efficient and fast removal of heavy metals in electro assisted phytoremediation system. Both aluminium rods and sheets were used as electrodes and both indoor and outdoor experiments were also conducted. Based on the results and plants condition, outdoor experiment using aluminium sheets as electrodes were preferred for further study. The results indicate that the treatment of Cd, Pb and Cu ions using electrically enhanced phytoremediation using aluminium sheet electrodes is more effective than aluminium rod electrode. When the electrical exposure time increases, the pH of the synthetic solution increased in electrolysis system, but a more favourable, moderate increase was exhibited by the electrically stimulated phytoremediation system. From the results, it can be postulated that 4V voltage is probably suitable to stimulate the *Eichhornia crassipes* to synthesize more chlorophyll. *Eichhornia crassipes* stimulated by an

electric field grown better and assimilated more metal. Heavy metal accumulation in plants collected from control and electrically enhanced phytoremediation system using aluminium sheet electrodes indicates that maximum amount of Cd, Pb and Cu were accumulated in *Eichhornia crassipes* collected from treatment (i.e., electrically enhanced phytoremediation system). *Eichhornia crassipes* translocated maximum Cd and Cu to plants' aerial parts under electrified condition but more amount of Pb was bioconcentrated in roots. Electrically stimulated plant translocated more amount of Pb content to its aerial part compared to plant in control. The BCFs of control for Pb, Cd and Cu were 502.65, 448.12 and 664.90 respectively. BCF, an index of hyperaccumulation, indicates that electrically stimulated *Eichhornia crassipes* is a good hyper accumulator of Cd (BCF = 1118.18) and Cu (BCF = 1152.47) and a moderate accumulator of Pb (BCF = 932.26). Translocation ability (TA) ratio indicates that *Eichhornia crassipes* have the ability to translocate more amounts of Pb, Cd and Cu to its upper portion under electrified condition.

The electro-phytoremediation technique was also applied to remove lead and chromium from wastewater collected from acid lead battery manufacturing industry and electroplating industry, respectively. Both the effluents were acidic in nature. Therefore, a pre-treatment of industrial effluents should be made to minimize the acidity. Due to high chemical contents present in the acid battery wastewater, *Eichhornia crassipes* exhibited some toxicity symptoms at an earlier stage than the plants used in the treatment of electroplating industry wastewater. The electro assisted phytoremediation system reduced 94.27 ± 0.41 % of lead

within 25 days, while control and electro-remediation system removed lead by 40.61 ± 2.39 and 74.33 ± 1.87 %, respectively from battery manufacturing industrial wastewater. A steady decrease in the Cr content in the wastewater collected from electroplating industry was observed in electrically stimulated phytoremediation. The result indicates that maximum removal of chromium was occurred in the electrically stimulated phytoremediation system (79.56 ± 2.61 %) than control (36.72 ± 4.23 %) and electro-remediation system (65.83 ± 3.59 %). Cr toxicity symptoms were observed in control plant from 15th day of study but the electrically stimulated plant showed toxicity symptoms in a much-delayed stage, indicating that the electrical stimulation helps the plant to resist toxicity and accumulate more metals than control plant. The other heavy metals present in the effluent samples such as Cu, Fe, Ni, Zn, Mn and Cd were also reduced. Hence, the electro - assisted phytoremediation system is also capable for the treatment of Pb, Cd, Cu, Cr, Mn, Fe, Ni, and Zn from water. Considering the overall results, we can state that the electro-phytoremediation technique seems to be promising in the treatment of heavy metals contaminated wastewater.

The enhancement of phytoremediation capacity of heavy metals (Cd, Pb and Cu) by *Eichhornia crassipes* and *Salvinia molesta* in the presence of titanium dioxide nanoparticles was assessed. TiO_2 nanoparticles exposed *Eichhornia crassipes* and *Salvinia molesta* showed better phytoremediation efficiency for the removal of lead, cadmium and copper within 3 days. It was observed that, in the nano - TiO_2 applied phytoremediation system, more efficient and faster removal of heavy metals was taking place. Results of the study on heavy metal accumulation

indicates that titanium dioxide nanoparticles applied plants showed more tendency to translocate metals to its areal parts. Control plant accumulated more metals in their root portion in both the plants. Nano-TiO_2 applied plants exhibited an increase in the production of chlorophyll compared to A (control) and B (calcium alginate -TiO_2 nanoparticles applied plants). TiO_2 nanoparticles exposed plants exhibited significant increase in relative growth compared to others. This may be due to the fact that, the plant exposed to nano -TiO_2 has the ability to improve light absorbance and promote the activity of rubisco activase thus accelerating the growth of plants. The determination of bioconcentration factor indicated that, the uptake potential of metals by plants was increased under nano - TiO_2 applied conditions. Plants exposed to TiO_2 nanoparticles achieved ability to transfer higher metal concentrations from root to its areal part. TiO_2 nanoparticles applied plants (C) showed better performance than TiO_2 nanoparticles entrapped calcium alginate beads applied plants (B). Considering the overall results, we can state that TiO_2 nanoparticles applied *Eichhornia crassipes* and *Salvinia molesta* seems to be promising candidate for the phytoremediation of heavy metals from water and exhibited an enhanced phytoremediation ability.

The possibility of using ammonium molybdate with phytoremediation for phytostabilization of Pb and Zn and for phytoextraction of Cd, Ni, and Cu by *Amaranthus retroflexus* was studied. Ammonium molybdate shows immobilization and mobilization effect on phytoremediation of toxic heavy metals in soil. Ni, Cd and Cu were chelated and form more soluble fractions with ammonium molybdate and Pb and Zn were precipitated with ammonium molybdate. Mobilization

effect of ammonium molybdate on Ni, Cd and Cu increases the bioavailability of these metals to plant. Immobilization effect of ammonium molybdate on Pb and Zn decreases the biotoxicity of these metals to plant by decreasing the bioavailability of these metals to plant. Growth was increased in plants treated with ammonium molybdate than control plant. For Cd, Ni and Cu the average BCF values of *Amaranthus retroflexus* plant treated with ammonium molybdate were higher than control. This indicates that *Amaranthus retroflexus* plant had higher ability to uptake Cd, Ni and Cu with ammonium molybdate. TF values of *A. retroflexus* were lower than 1, which shows that maximum amount of heavy metals was stored in roots. It was found that ammonium molybdate acts as a stabilization agent and as an extracting agent in the phytoremediation of heavy metal contaminated soil.

A novel activated carbon adsorbent has been developed for defluoridation of contaminated water samples. Fluoride removal efficiency of some medicinal plant materials like gooseberry *(Phyllanthus emblica)*, dried ginger (*Zingiber officinale*), sathavari (*Asparagus racemosus*), pomegranate (*Punica granatum)*, nutmeg *(Myristica fragrans*), kozhinjil (*Tephrosia purpurea*) and karinochi (*Vitex negundo*) were compared during the initial stage of the study and reported an efficiency of 65, 63, 44, 70, 67, 40 and 30 % respectively. The suitability of some easily and locally available plant materials such as ramacham or vetiver root (*Vetiveria zizanioides*), tamarind seed (*Tamarindus indica*), clove (*Eugenia carryophyllata*), neem (*Azadirachta indica*), (*Acacia catechu willd*), coffee husk (*Coffea arabica*) and fern (*Adiantum aethiopicum)* for effectively remediating fluoride contaminated water was also investigated.

Ramacham (*Vetiveria zizanioides*) (80 %), Tamarind seed (*Tamarindus indica*) (75 %) and clove (*Eugenia carryophyllata*) (73 %) exhibited better defluoridation efficiency compared to other plant materials. During the second stage of the study, batch adsorption test of vetiver root (*Vetiveria zizanioides*), tamarind seed (*Tamarindus indica*) and clove (*Eugenia carryophyllata*) were conducted by varying contact time, sorbent dosage and particle size. Results indicated that, tamarind seed and clove removed 75 and 70 % of fluoride respectively at adsorbent dosage of 20 g/L of 10 mg/L of fluoride water and vetiver root removes 80 % of fluoride at the same dose. Vetiver root showed a maximum removal (85 %) at a dosage of 24 g/L. The results indicated that the maximum fluoride adsorption takes place at the optimum adsorbent dosage of 24 g/L, equilibration time of 120 min, and a particle size of 0.1 mm for *Vetiveria zizanioides* root powder. The results clearly pointed out that, Vetiver root has the potential to be an efficient defluoridating agent, so during the further study, activation of *Vetiveria zizanioides* was carried out to improve its efficiency.

During the third stage of the study, powdered *Vetiveria zizanioides* root was activated using phosphoric acid. The carbonization of the material was conducted for 1 h, 1½ h and 2 h at 600^0C, 700^0C and 800^0C and by altering the impregnation ratio of raw material to activating agent 1:05, 1:1, 1:2 and 1:4. The activated *Vetiveria zizanioides* root powder prepared by using an impregnation ratio of vetiver root powder to activating agent 1:4 and an activation time of 1 h at 700^0C was selected for further study based on its maximum adsorption capacity. The batch sorptive defluoridation study of powdered activated *Vetiveria zizanioides*

was conducted under variable experimental conditions such as pH, initial concentration, agitation time, interfering co-ions, dose of adsorbent, particle size, agitation speed and temperature. The efficiency of fluoride removal was found to be 92.5, 77.1, 58.8 and 44.5 % at initial fluoride concentrations of 10, 20, 30 and 40 mg/L respectively with 5 g/L of adsorbent dosage, at pH 6, shaking speed of 150 rpm at room temperature. The efficiency of fluoride removal was found to be decreased with increase in initial fluoride concentration but the amount of fluoride adsorbed increased. The influence of co-existing anions on the fluoride removal by the sorbent, activated vetiver root, was studied and found to follow the order: $PO_4^{3-} > HCO_3^- > SO_4^{2-} > Cl^- \geq NO_3^-$. The minimum contact time for attaining the maximum defluoridation was 120 min and maximum sorption was observed at pH 6, shaking rate 150 rpm and adsorbent dosage of 5 g/L with a particle size of 0.1 mm. The isotherm results indicated that the adsorption process satisfactorily fitted with Langmuir adsorption isotherm which had good correlation coefficient value ($R^2 > 0.99$) indicating monolayer adsorption. The separation factor (R_L) was found in the range of 0.0607 - 0.0194 indicate the favourable sorption under varying temperature. The maximum adsorption capacity of fluoride on activated *Vetiveria zizanioides* was observed at 333K ($q_m =$ 4.085 mg/g) and the value of adsorption energy K_L of the adsorbent increases on increasing the temperature. The value of Freundlich constant *n* was found to be larger than 1 (5.41 - 5.15) which suggests the favourable adsorption conditions. The value of K_f increased with increase in temperature, which confirms endothermic nature of the adsorption fluoride on activated *Vetiveria zizanioides*. The adsorption isotherm models fitted the equilibrium data, based on the correlation coefficient, in the order of:

Langmuir isotherm > Freundlich isotherm > Temkin isotherm > Dubinin–Radushkevich isotherm. The value of Dubinin-Radushkevich mean free energy (E) found was < 8 kJ/mol, indicating physisorption.

To identify the rate and kinetics of adsorption process pseudo-first-order, pseudo-second-order, intra-particle diffusion model, and Elovich kinetic model were applied. Pseudo second-order kinetic model was observed better applicable. Weber and Morris intraparticle diffusion model suggests the involvement of surface adsorption as well as intraparticle diffusion. Weber and Morris plots fail to pass through origin which indicated that the process of the mechanism of sorption was complex in nature with the more than one mechanism limiting the rate of adsorption. The evaluation of fitness of the sorption kinetic models were done using correlation coefficient and sum of squares of the error suggest that the adsorption of fluoride on the activated *Vetiveria zizanioides* follows second order kinetic model. SEM micrographs confirmed the adsorption of fluoride ion on the adsorbent surface. The thermodynamic data confirms the endothermic and spontaneous nature of sorption process and also indicates the increased degree of freedom of fluoride ions in the solution. Desorption study identified 0.1 M NaOH solution as the suitable eluent to regenerate activated *Vetiveria zizanioides*. The typical S-shaped breakthrough curves obtained in the column study indicates the favourable adsorption. Gravity based household water filter for removal of fluoride was developed using activated *Vetiveria zizanioides* and it was applied to the groundwater samples collected from fluoride endemic area of Palakkad district. The active carbon developed from *Vetiveria zizanioides* has been effectively reduce the fluoride level in groundwater samples

below the BIS acceptable limits, and hence, the activated *Vetiveria zizanioides* can be successfully applied to remove fluoride from contaminated water.

For the removal of heavy metals from water, two biosorption studies were conducted using a herbal plant material, *Caesalpinia sappan* and an algal biomass, *Trenteohilia abietina*. Before the biosorption of Pb^{2+}, Cd^{2+} and Cu^{2+} ions by *Caesalpinia sappan*, the plant material was boiled and washed with deionised water and undergone protonation so that the biosorbent does not impart colour to water. Maximum removal efficiency was observed between pH 4 and 10 for Pb^{2+} and for Cd^{2+} and Cu^{2+}, it was found between pH 6 and 10. An optimum pH of 7 was maintained for the sorption study by *C. sappan.* The maximum removal efficiencies were observed at shaking speed of 150 rpm for Pb^{2+} ions and at 200 rpm for Cd^{2+} and Cu^{2+} ions. For adsorbent *Caesalpinia sappan,* the order of metal ions sorption is as follows: 9.14 mg/g for Pb^{2+} > 7.23 mg/g for Cu^{2+} > 6.10 mg/g for Cd^{2+} under varying initial metal concentration from 5 - 45 mg/L. The results of batch adsorption experiments, clearly suggest that the operating parameters such as solution pH, initial metal concentration, contact time, temperature, adsorbent dosage, presence of light metal ions and shaking speed were effective on the removal efficiency of metal ions. But the operating conditions required for the better removal efficiency of each heavy metals ions from aqueous solution would be different. The experimentally obtained equilibrium data were analyzed by different isotherm models and the high correlation coefficients (R^2) values indicate that the adsorption data best fitted the Langmuir adsorption isotherm for all three metals. Dubinin - Radushkevich (D-R) isotherm model also fits

very well to the experimentally determined data for Pb^{2+}, Cd^{2+} and Cu^{2+} and the kinetic data of adsorption of heavy metal ions on *Caesalpinia sappan* are best modelled by the pseudo-second-order kinetic equation. Thermodynamic parameters indicated the exothermic behaviour and spontaneous nature of the adsorption process. The desorbing agent, 0.1 M HCl was found to be suitable for the desorption study. The biosorption properties of *C. sappan* for Pb^{2+}, Cd^{2+} and Cu^{2+} ions indicate that *Caesalpinia sappan* may be used as an inexpensive, effective, herbal and easily cultivable biosorbent that can be useful in water treatment for the adsorption of metal ions.

The removal of Pb^{2+} and Cd^{2+} from aqueous solutions using algal biomass *Trenteohilia abietina* by batch sorption experiments revealed that the maximum sorption is possible for both metals under a wide range of pH (pH: 4 -12 for Pb^{2+} and pH: 6 - 12 for Cd^{2+}). High removal efficiencies were observed for Pb^{2+} and Cd^{2+} at the adsorbent dosage of 2 g/L and 4 g/L respectively. The increase in metals concentration from 40 to 70 mg/L leads to an increase in adsorption capacity from 20.01 mg/g to 33.83 mg/g for Pb^{2+} and from 10.02 mg/g to 16.39 mg/g for Cd^{2+}. Rapid removal was observed for both the metals. The Langmuir isotherm model were better fitted to represent the experimental data, indicate favourable adsorption and the maximum adsorption capacity of Pb^{2+} and Cd^{2+} by *T. abietina* was 33.22 mg/g and 16.53 mg/g, respectively. The q_m determined by the Dubinin-Radushkevich isotherm model also fits close to the experimentally determined data for both the metals. The mean free energy obtained for the biosorption of Pb^{2+} and Cd^{2+} as 8.452 kJ/mol and 3.686 kJ/mol, indicating the involvement of chemisorption and physical sorption

in the removal of Pb^{2+} and Cd^{2+} respectively. The kinetic model that best represented the experimental data was the pseudo-second order. The good fitting of the kinetics data to Bangham's Model indicate that in the adsorption of Pb^{2+} and Cd^{2+} on the biosorbent *T. abietina*, pore diffusion plays a vital role in controlling the rate of reaction. The calculated $\Delta G°$, $\Delta H°$ and $\Delta S°$ values disclosed that the sorption of Pb^{2+} and Cd^{2+} ions onto *T. abietina* was exothermic and spontaneous under examined conditions. The reusability of *T. abietina* as a biosorbent was found good after five consecutive sorption-desorption cycles and 0.1 M HCl was suitable as a desorption agent. The recovered algal biosorbent, *T. abietina* is biodegradable, inexpensive and environment friendly. The algal biosorbent, *Trenteohilia abietina* has the potential for removal and recovery of metal ions from contaminated water.

The iron oxide nanoparticles (Fe_2O_3) were synthesized by co-precipitation method and its surface was coated by polyvinyl alcohol and gallic acid. The removal of toxic metals such as lead and cadmium from aqueous solution was studied using functionalized nanoparticles (PG-IONPs) and its metal removal efficiency was compared with the uncoated iron oxide nanoparticles (IONPs). The functionalized iron oxide nanoparticles were characterized using FTIR, SEM EDX and XRD. The presence of functional groups on PG-IONPs were confirmed by FTIR. Batch sorption experiments under different conditions such as pH, adsorbent dosage, contact time, temperature and initial metal concentration were carried out and the results revealed that the maximum sorption of metals by PG-IONPs is possible under a wide range of pH (pH: 4 -12 for Pb^{2+} and pH: 6 - 12 for Cd^{2+}). Better sorption of metals was exhibited by

PG-IONPs than IONPs. Compared to IONPs, PG-IONPs exhibited high removal efficiencies for both Pb^{2+} and Cd^{2+} at minimal adsorbent dosage. The increase in metals concentration from 5 to 25 mg/L leads to an increase in adsorption capacity and observed a maximum adsorption capacity of 24.48 mg/g and 23.52 mg/g for Pb^{2+} and Cd^{2+}, respectively by PG-IONPs which was better than that of IONPs. As the temperature increases, both nanosorbents exhibited a decreasing trend in the removal of lead and cadmium. PG-IONPs exhibited only a slight decrease in metal sorption under high temperature, compared to IONPs. The results indicate that the bonding between PG-IONPs and metal ions were stronger than the bonding between IONPs and metal ions at higher temperature. In the case of PG-IONPs, 91.77 % of Pb^{2+} and 84.89 % Cd^{2+} removal was attained within 10 min of contact time. Initially, the rate of removal was high and then slowed down as move towards the equilibrium condition. After 140 min, the rate of sorption was slow and reaches equilibrium by PG-IONPs. PG-IONPs showed fast removal of metals than IONPs this may be due to that the functional group present on the PG-IONPs provides more active adsorption site for metal ions.

The sorption equilibrium data was best described by Langmuir equation. The values of q_m determined by the Dubinin-Radushkevich isotherm model also fits close to the experimentally determined data for sorption of Pb^{2+} and Cd^{2+} on PG-IONPs. For the sorption of both Pb^{2+} and Cd^{2+}, the values of mean free energy (E) was found in the range of 8 - 16 kJ/mol for PG-IONPs, indicating the chemical sorption but the value of E was found in the range of 1 to 8 kJ/mol, indicates involvement of physical sorption in the sorption of Pb^{2+} and Cd^{2+} by IONPs. High R^2 value and

better correlation between experimental and calculated values indicates that the sorption dynamics data were best described using pseudo-second-order kinetic model, in the case of both nanosorbents. Thermodynamic studies illustrated that Pb^{2+} and Cd^{2+} adsorption by the nanosorbents was exothermic in nature. Sorption of Pb^{2+} and Cd^{2+} on the PG-IONPs was confirmed using EDX spectra. The better regeneration of exhausted PG-IONPs was done using desorbing agent, 0.1 M HCl and its reusability were also investigated. Polyvinyl alcohol and gallic acid coated iron oxide nanoparticles (PG-IONPs) can be considered as fast and efficient, nano-adsorbent for Pb^{2+} and Cd^{2+} removal from contaminated waters.

Madayi, near Pazhayangadi in Kannur district, is a clay mining area in northern Kerala, with rich biodiversity. The active mining is generating some drinking water issues there. So, the groundwater quality near the mining area was evaluated in this study. In order to assesses the quality of drinking water resources of Madayi area, 35 water samples were collected. High iron problems are observed near the china clay mining area during sampling. Hence, the quality of drinking water resources in the study area were evaluated on the basis on heavy metal concentration in water samples. The physico-chemical characteristics of groundwater samples revealed highly acidic nature of samples collected from near the china clay mining area, indicating the percolation of contaminants from the mining area. High TDS, alkalinity, chloride, calcium, magnesium, sodium and potassium reported in the samples collected from near Perumba river, indicating salinity intrusion. TDS values were found to be exceeds the BIS limit in samples collected from the sites near the mining area. No alkalinity was detected in samples near mining area because of

the highly acidic nature. Very hard water and high sulphate concentration were also noticed in locations near mining area. High nitrate and phosphate were found in sample near Kavilevallapil thodu, through which the wastewater drainage from mining is passing and eutrophication was also observed there. Of the 35-water sample collected, total coliform bacteria were detected in 89 % of samples and the presence of *E. coli* was detected in only 14 %.

Concentration of seven heavy metals in water namely Fe, Mn, Pb, Cd, Cu, Ni and Zn were analysed. The analytical results indicate high Fe concentration in samples near mining area and Vengara Muttom compared to other sites. Maximum value of 200.1 mg/L was reported in sample near Kavilevallapil thodu (Vengara Muttom) through which the wastewater drainage from mining is passing. The order of concentration of heavy metals found were as follows: Fe > Mn > Zn > Cu > Ni > Pb > Cd. The results revealed that high concentration of Cd, Pb, Mn, Zn, above the acceptable limit of BIS were also found in water samples collected from near the mining area. High heavy metals contents were also detected in samples from Vengara Muttom through where the wastewater from mining industry flows. Results indicates that groundwater samples from near china clay mining area and near Kavilevallapil thodu, Vengara Muttom contains high metal concentrations. The heavy metal analytical results were evaluated using the HPI, HEI and C_d indices. The overall HPI value of groundwater samples from Madayi area was found to be 1474.49 and that was higher the critical pollution index value of 100. The heavy metal pollution index was calculated individually for each sample, high HPI values were found in groundwater samples from Pazhayangadi,

Vengara Muttom and near Perumba river. The similarity in heavy metal contamination in Pazhayangadi and Vengara Muttom areas were observed by Cluster Analysis (CA) and Principle Component Analysis (PCA). The correlation analysis of heavy metal concentrations exhibited strong positive correlations among Fe, Cd, Cu, Ni, Pb, Zn ions suggesting that these metals are from common sources. High Fe contents were recorded in soil samples from Pazhayangadi, Madayi. Compared to Canadian Soil Quality Guidelines, high Cd, Pb and Cu were also detected from this location. Heavy metals in four sediment samples from the study area were compared with the sediment quality guideline proposed by USEPA and the results indicates metal pollution in this area. The values of the calculated indices (HPI, HEI and C_d) in groundwater collected from Madayi area indicates heavy metal pollution, so severe precautions such as treatment of contaminated drinking water resources; effective treatment of wastewater from china clay mining industry; establishment of sustainable mining activities and management of the use of agricultural inputs (chemical fertilizers and metal-containing pesticides) must be taken into consideration in this area.

Some treatment methods were applied on heavy metal contaminated drinking water from Madayi panchayath. Three metal contaminated water samples were treated using three different sorbents such as functionalized iron oxide nanosorbent (iron oxide nanoparticles coated with poly vinyl alcohol and gallic acid); protonated *Caesalpinia sappan* (herbal plant material) and *Tretepohila abietina* (algal biosorbent). The results suggest that, all the three sorbents were effectively removed heavy metals from heavy metals contaminated groundwater samples. The

nanosorbent (iron oxide nanoparticles coated with polyvinyl alcohol and gallic acid) exhibited comparatively better performance in the removal of heavy metals from field samples from Madayi area.

The following are some of the suggestions / recommendations drawn from the study:

- The electro-phytoremediation technique is an effective treatment method for heavy metals contaminated wastewater. The electro-assisted phytoremediation system is capable to treat metals like Pb, Cd, Cu, Cr, Mn, Fe, Ni, and Zn from water. While, treating chemically rich metal containing effluents, the electro-assisted phytoremediation technique can be very effective, if it is combinedly applied with other remediation method. Before designing the large-scale implementation of this technique, a cost efficiency analysis needs to be conducted. Further studies are required to produce the electrical energy required for electro-assisted phytoremediation technique from the used biomasses itself.

- TiO_2 nanoparticles applied *Eichhornia crassipes* and *Salvinia molesta* exhibited an enhanced phytoremediation ability for heavy metal removal. Application study of this technique in effluents is recommended.

- Application of ammonium molybdate in phytoremediation of heavy metal contaminated soil using *Amaranthus retroflexus* is effective in laboratory scale experiment. Its field application and utilization of this method with different plant species is encouraged.

- The ultimate utilization of phytoremediation by-products by bioenergy production, conversion of metal accumulated biomass to valuable bio-ore, recovery of metals using phytomining technique will be an economic and effective approach for the optimum utilization and eco-friendly management of the plants used in phytoremediation. Economic viability of the technology and proper disposal of biomass produced need to be studied.

- The activated *Vetiveria zizanioides* can be successfully applied for the defluoridation of fluoride contaminated water. Fabrication of low-cost defluoridating units with biosorbents and its activated forms should be encouraged and its optimization study need to be carried out.

- Polyvinyl alcohol and gallic acid coated iron oxide nanoparticles (PG-IONPs) can be considered as fast and efficient, nano-adsorbent for Pb^{2+} and Cd^{2+} removal from contaminated waters. So, this nanosorbent can be tried for other toxic metals also. A heavy metal treatment unit can be developed using polyvinyl alcohol and gallic acid coated iron oxide nanoparticles followed by its optimization study.

- More functionalized nanosorbents and low-cost biosorbents can be developed to control and minimize heavy metals in water. They should be efficient to remove different contaminants, which possess greater adsorption capacity and high selectivity for different concentrations.

BIBLIOGRAPHY

Abd-Elmoniem, E. M. (2003). Response of hyper and non-hyper accumulator plants to nickel element. *Annals of Agricultural Science, Moshtohor*, 41, 1701-1710.

Ackerson, R. C., & Herbert, R. R., (1981). Osmoregulation in cotton in response to water stress. I. Alterations in photosynthesis, leaf conductance, translocation, and ultra-structure. *American Society of Plant Physiology*, 67, 484-488.

Adane, B., Siraj, K., & Meka, N. (2015). Kinetic, equilibrium and thermodynamic study of 2-chlorophenol adsorption onto *Ricinus communis* pericarp activated carbon from aqueous solutions. *Green Chemistry Letters and Reviews*, 8(3-4), 1-12.

Aderhold, D., Williams, C. J., & Edyvean, R. G. J. (1996). The removal of heavy-metal ions by seaweeds and their derivatives, *Bioresource Technology*, 58, 1-6.

Ahmad, A.K., Mushrifah, I., & Shuhaimi-Othman, M. (2009) Water Quality and Heavy Metal Concentrations in Sediment of Sungai Kelantan, Kelantan, Malaysia: A Baseline Study. *Sains Malaysiana* 38(4), 435–442.

Ahmad, M. A., Puad, N. A. A., & Bello, O. S. (2014). Kinetic, equilibrium and thermodynamic studies of synthetic dye removal

using pomegranate peel activated carbon prepared by microwave-induced KOH activation. *Water Resources and Industry*, 6, 18-35.

Aisien, E. T., Aisien, F. A., & Gabriel, O.I. (2015). Improved Quality of Abattoir Wastewater Through Phytoremediation. In A.A. Ansari et al. (Eds.), *Phytoremediation: Management of Environmental Contaminants* (Vol. 2, pp. 3-10). Switzerland: Springer International Publishing Switzerland.

Akhtar, M. M., Tang, Z., & Mohamadi, B. (2014). Contamination Potential Assessment of Potable Groundwater in Lahore, Pakistan. *Polish Journal of Environmental Studies.* 23(6), 1905-1916.

Aksu, Z., & Kutsal, T. A. (1991). A bioseparation process for removing Pb (II) ions from wastewater by using C. vulgaris. *Journal Chemical Technology and Biotechnology*, 52(1), 108-118.

Alagumuthu, G., & Rajan, M. (2010). Kinetic and equilibrium studies on Fluoride removal by zirconium (IV)-impregnated groundnut Shell carbon. *Hemijska industrija.* 64 (4), 295-304.

Alagumuthu, G., Veeraputhiran, V., & Venkataraman, R. (2010) Adsorption Isotherms on Fluoride Removal: Batch Techniques. *Archives of Applied Science Research*, 2 (4), 170-185.

Alagumuthu, G., Veeraputhiran, V., & Venkataraman, R. (2011). Fluoride Sorption Using *Cynodon dactylon* - Based Activated Carbon. *Hemijska industrija* 65(1), 23-35. doi:10.2298/HEMIND100712052A

Al-Degs, Y. S., El-Barghouthi, M. I, Issa, A. A., Khraisheh, M. A., & Walker, G. M. (2006). Sorption of Zn(II), Pb(II), and Co(II) using

natural sorbents: equilibrium and kinetic studies. *Water Research*. 40, 2645–2658.

Al-Garni, & Saleh, M. (2005). Biosorption of lead by Gram -ve capsulated and non-capsulated bacteria. *Water Science Technology*, 31(3), 345-349.

Ali, A. K. S., Matinizadeh, M., Shirvany, A., Madani, M. E., Talebi, K. T., Monemian, S. M., & Abdi, E. (2014). Evaluation of Pollution Intensity in Different Districts of Tehran Based on Measuring Chlorophyll, Plumb and Cadmium Heavy Metal Contents in Trees. *International Journal of Environmental Research*, 8(4), 1105-1114.

Ali, H., Khan, E., & Sajad, M. A. (2013). Phytoremediation of heavy metals – concepts and applications. *Chemosphere*, 91, 869-81.

Ali, M., Bhat, A. K., Dolkar, T., & Malik. M. A. (2018). Phytoremediation: A Plant - Based Technology. *International Journal of Current Microbiology and Applied Sciences,* 7(3), 766-777.

Al-Saad, K. A., Amr, M. A., Hadi, D. T., Arar, R. S., AL-Sulaiti, M. M., Abdulmalik, T. A., Alsahamary, N. M., & Kwak, J. C. (2012). Iron oxide nanoparticles: applicability for heavy metal removal from contaminated water. *Arab Journal of Nuclear Sciences and Applications,* 45(2), 335-346.

Ambashta, R.D., & Sillanpää, M. (2010). Water purification using magnetic assistance: a review. *Journal of hazardous materials,* 180(1–3), 38-49. doi: 10.1016/j.jhazmat.2010.04.105

Amin, M. (2012). Phytoremediation of heavy metals from municipal wastewater by *Typhadomingensis. African Journal of Microbiology Research*, 6(3), 643-647.

Amini, M., Mueller, K., Abbaspour, K. C., Rosenberg, T., Afyuni, M., Moller, K. N., Sarr, M., & Johnson, C. A., (2008). Statistical modelling of global geogenic fluoride contamination in groundwaters. *Environmental Science and Technology,* 42(10),3662-3668.

Amor, Z., Bariou, B., Mameri, N., Taky, M., Nicolas, S., & Elmidaoui, A. (2001). Fluoride removal from brackish water by electrodialysis. *Desalination*, 133(3), 215-223.

Anand S., Bharti S. K., Dviwedi N., Barman S. C., & Kumar N. (2017). Macrophytes for the Reclamation of Degraded Waterbodies with Potential for Bioenergy Production. In K., Bauddh et al. (Eds.) *Phytoremediation Potential of Bioenergy Plants* (pp. 333-351). Singapore: Springer.

Anastopoulos, I., & Kyzas, G. Z. (2016). Are the thermodynamic parameters correctly estimated in liquid-phase adsorption phenomena. *Journal of Molecular Liquids*, 218, 174–185.

Andrew, E. A. (2007). Phytoremediation: an environmentally sound technology for pollution prevention, control and remediation in developing countries. *Educational Research and Review 2* (7), 151-156.

Anegbe, B., Okuo, J. M., Atenaga, M., Ighodaro, A., Emina., A., & Oladejo N. A. (2018). Distribution and Speciation of Heavy Metals in Soils around Some Selected Auto Repair Workshops in Oghara, Delta

State, Nigeria. *International Journal of Environment, Agriculture and Biotechnology*. 3(2), 574-584.

Annadurai, S. T., Rengasamy, J. K., Sundaram, R., & Munusamy, A. P. (2014). Incidence and effects of fluoride in Indian natural ecosystem: A review. *Advances in Applied Science Research*, 5(2), 173-185.

Antu, C. D., & Harikumar, P. S. (2007, January). Genesis of fluoride in the shallow unconfined aquifer of muthalmada area in Bharatapuzha Basin. *Proceedings of XIX Kerala Science Congress*, 29-31. Kannur

APHA. (2012) Standard methods for the examination of water and wastewater (22nd ed.). American Public Health Association, Washington DC.

Apiratikul, R., & Pavasant, P. (2006). Sorption isotherm model for binary component sorption of copper, cadmium, and lead ions using dried green macroalga, *Caulerpa lentillifera*. *Chemical Engineering Journal*, 119, 135-145.

Appel, C, Ma, L.Q., Rhue R. D., & Reve, W. (2008). Sequential sorption of lead and cadmium in three tropical soils. *Environmental pollution*. 155, 132-140.

Argun, M. E., Dursun, S., Ozdemir, C., & Karatas, M. (2007). Heavy metal adsorption by modified oak sawdust: Thermodynamics and kinetics. *Journal of Hazardous Materials,* 141(1), 77-85.

Arshadi, M., Amiri, M.J., & Mousavi, S. (2014). Kinetic, equilibrium and thermodynamic investigations of Ni(II), Cd(II), Cu(II) and Co(II) adsorption on barley straw ash, *Water Resources and Industry*,6, 1-17. http://dx.doi.org/10.1016/j.wri.2014.06.001

Ashraf, M. A., Maah, M. J., & Yusoff, I. (2011). Heavy metals accumulation in plants growing in ex tin mining catchment. *International Journal of Environmental Science and Technology*, 8(2), 401-416.

ASTM (2006) American Society for Testing and Materials. Annual Book of Standards, 2006

ASTM (2011) Standard Test Method for Determination of Iodine Number of Activated Carbon

Ayawei, N., Ebelegi, A. N., & Wankasi, D. (2017). Modelling and Interpretation of Adsorption Isotherms. *Journal of Chemistry*, 11. https://doi.org/10.1155/2017/3039817

Babu, S. S., Kumar, S., Roychowdhury, T., Vidyadharan, V., Roychowdhury, N., Samanta, J., & Bhowmick, S. (2015). Occurrence and impacts of fluoride in drinking water - A Review. *Indian Groundwater,* 5, 40-54.

Backman, B., Bodis, D., Lahermo, P., Rapant, S., & Tarvainen, T. (1997). Application of a groundwater contamination index in Finland and Slovakia. *Environmental Geology,* 36, 55-64. doi:10.1007/s002540050320

Badami, S., Moorkoth, S., & Suresh, B. (2004). *Caesaplinia sappan* − A medicinal and dye yielding plant. *Natural Product Radiance,* 3(2), 75-82.

Baziar, M., Mehrasebi, M. R., Assadi, A., Fazil, M. M., Maroosi, M., & Rahimi, F. (2013). Efficiency of non-ionic surfactants - EDTA for treating TPH and heavy metals from contaminated soil. *Journal of Environmental Health Science and Engineering,* 11, 41

Benadjemia, M., Milliere, L., Reinert, L., Douche, N. B., & Duclaux, L. (2011). "Preparation, characteristics and methylene blue absorption of phosphoric acid activated carbon from globe artichoke leaves". *Journal of Fuel Processing Technology*. 92(6), 1203-1212.

Bhardwaj, R., Gupta, A., & Garg, J. K. (2017). Evaluation of heavy metal contamination using environmetrics and indexing approach for River Yamuna, Delhi stretch, India. *Water Science* 31, 52-66.

Bhat, N., Jain, S., Asawa, K., Tak, M., Shinde, K., Singh, A. & Gupta, V. V. (2015). Assessment of fluoride concentration of soil and vegetables in vicinity of zinc smelter, Debari, Udaipur, Rajasthan. *Journal of clinical and diagnostic research,* 9(10), 63-69.

Bhatt, R. R., & Shah, B. A. (2013). Sorption studies of heavy metal ions by salicylic acid–formaldehyde–catechol terpolymeric resin: Isotherm, kinetic and thermodynamics. *Arabian Journal of Chemistry*. Retrieved from http://dx.doi.o rg/10.1016/j.a rabjc.2013.0 3.012

Bhattacharya, P., & Samal, A. C. (2018). Fluoride contamination in groundwater, soil and cultivated foodstuffs of India and its associated health risks: A review. *Research Journal of Recent Sciences,* 7(4), 36-47.

Bhimani, P., & Vyas, C. M. (2013) Performance of Concrete with China Clay (Kaolin) Waste. *International Journal of Latest Trend s in Engineering and Technology (IJLTET)*, 2(3), 49 - 54.

Bi, R., Schlaak, M., Siefert, E., Lord, R., & Connolly, H. (2011). Influence of electric fields (AC and DC) on phytoremediation with

metal polluted soils with rapeseed (*Brassica napus*). *Chemosphere,* 83, 318-326.

BIS. (2010). *Indian Standard Drinking Water Specification -Second Revision* (IS 10500: 2012). Bureau of Indian Standards, New Delhi

Bishnoi, M., & Arora, S. (2007). Potable groundwater quality in some villages of Haryana, India: Focus on fluoride. *Journal of Environmental Biology*, 28(2), 291-294.

Black, C. A. (1965). *Methods of soil analysis*. Madison: American Society of Agronomy Inc.

Bolan, N., Naidu, R., Choppala, G., Park, J., Mora, M. L., Budianta, D., & Panneerselvam, P. (2010). Solute Interactions in Soils in Relation to the Bioavailability and Environmental Remediation of Heavy Metals and Metalloids. *Pedologist,* 53(3), 1-18.

Brindha, K., Rajesh, R., Murugan, R., & Elango, L. (2011). Fluoride contamination in groundwater in parts of Nalgonda district, Andhra Pradesh, India. *Environ-mental Monitoring and Assessment,* 172 (1-4), 481-492.

Brune, A., Urbach, W., & Dietz, K. J. (1994). Compartmentation and transport of Zn in barley primary leaves as basic mechanisms involved in Zn tolerance. *Plant, Cell & Environment*, 17, 153-162.

Bystrzejewski, M., Pyrzyńska, K., Huczko, A., & Lange H. (2009). Carbon-encapsulated magnetic nanoparticles as separable and mobile sorbents of heavy metal ions from aqueous solutions. *Carbon*, 47(4),1201- 4.

Cabo, L. D., Serafini, R., Arreghini, S., & Iorio, A. F. (2015). On-Site and Full-Scale Applications of Phytoremediation to Repair Aquatic

Ecosystems with Metal Excess. In A.A. Ansari et al. (Eds.), *Phytoremediation: Management of Environmental Contaminants* (Vol. 2, pp. 27-40). Switzerland: Springer International Publishing Switzerland.

Castro, J.B., Bonelli, P.R., Cerrella, E. G., & Cukierman, A. L. (2000). Phosphoric Acid Activation of Agricultural Residues and Bagasse from Sugar Cane: Influence of the Experimental conditions on Adsorption Characteristics of Activated Carbons. *Industrial and Engineering Chemistry Research, 39* (11), 4166-4172. doi**:**10.1021/ie000267

CCME (2007). Canadian Environmental Quality Guidelines, Canadian Council of Ministers of the Environment. Winnipeg.

Central Soil Analytical Laboratory. (2007). Manual on soil analysis. A compilation of soil analytical works followed at Central Soil Analytical Laboratory, Thiruvananthapuram.

CGWB, 2010. Groundwater Quality in Shallow Aquifers of India. CGWB, Faridabad, p 64

Chaney, R. L, Angle, J. S., Broadhurst, C. L., Peters, C. A., Tappero, R. V., & Sparks, D. L. (2007). Improved understanding of hyperaccumulation yields commercial phytoextraction and phytomining technologies. *Journal of Environmental Quality*, 36, 1429 -1443.

Chen, J., Chen, Y., Shi, Z. Q., Su, Y., & Han, F. X. (2015). Phytoremediation to Remove Metals/Metalloids from Soils. In A.A. Ansari et al. (Eds.), *Phytoremediation: Management of*

Environmental Contaminants (Vol. 2, pp. 297-304). Switzerland: Springer International Publishing Switzerland.

Chen, N., Zhang, Z., Feng, C., Li, M., Zhu, D., Chen, R., & Sugiura, N. (2010). An excellent fluoride sorption behavior of ceramic adsorbent. *Journal of Hazardous Materials*, 183, 460-465.

Cheng, H., Ma, J., Zhao, Z & Qi, L. (1995). Hydrothermal preparation of uniform nano size rutile and anatase particles. *Chemistry of Materials,* 7, 663-671.

Chidambaram, S., Ramanathan, A. L., & Vasudevan, S. (2003). Fluoride removal studies in water using natural materials. *Water SA*, 29 (3), 339-343.

Cho, U. H., & Park, J. O. (1999). Distribution and phytotoxicity of cadmium in tomato seedlings. *Journal of Plant Biology*, 42, 49-56.

Choi S Y., Yang, K. M., Jeon, S. D., Kim J. H, Khil, L. Y., & Chang, T. S. (1997). Brazilin modulates immune function mainly by augmenting T cell activity in halothane administered mice. *Planta Medica,* 63, 405-408.

Clayton, L.R. (2007). Phytoremediation. *Encyclopaedia of plant and crop science*. London, UK: Taylor & Francis.

Cui, S., Zhou, Q., & Chao, L. (2007). Potential hyperaccumulation of Pb, Zn, Cu and Cd in endurant plants distributed in an old smeltery, north-east China. *Environment Geology*, 51(6), 1043-1048.

CWRDM (2015) *Monitoring, Mapping and Mitigation of Fluoride in Palakkad including Attapady region of Kerala.* Centre for Water Resources Development and Management, Kozhikode.

Czikkely, M., Neubauer, E., Fekete, I., Ymeri, P., & Fogarassy, C. (2018). Review of heavy metal adsorption processes by several organic matters from wastewaters. *Water*, 10, 1377. doi:10.3390/w10101377

Dada, A. O., Olalekan, A. P., Olatunya, A. M., & DADA, O. (2012). Langmuir, Freundlich, Temkin and Dubinin–Radushkevich Isotherms Studies of Equilibrium Sorption of Zn^{2+} Unto Phosphoric Acid Modified Rice Husk. *IOSR Journal of Applied Chemistry*, 3(1), 38-45. ISSN: 2278-5736. www.iosrjournals.org

Das, B., Devi, R. R., Umlong, I. M., Borah, K., Banerjee, S., & Talukdar, A. K. (2013). Arsenic (III) adsorption on iron acetate coated activated alumina: thermodynamic, kinetics and equilibrium approach. *Journal of Environmental Health Sciences & Engineering*, 11, 42. doi:10.1186/2052-336X-11-42

Das, S., Goswami, S., & Talukdar, A, D. (2016). Physiological responses of water hyacinth, *Eichhornia crassipes* (Mart.) Solms, to cadmium and its phytoremediation potential. *Turkish Journal of Biology,* 40, 84-94.

Dave, P. N., & Chopda, L. V. (2014). Application of Iron Oxide Nanomaterials for the Removal of Heavy Metals. *Journal of Nanotechnology,* 14. http://dx.doi.org/10.1155/2014/398569

Deng, H., Ye, Z. H., & Wong, M. H. (2004). Accumulation of lead, zinc, copper and cadmium by 12 wetland plant species thriving in metal-contaminated sites in China. *Environmental Pollution*, 132, 29-40.

Department of economics & statistics. *Compendium of Environment Statistics Kerala* (2014-2015), Govt of Kerala.

Dermentzis, K., Valsamidou, E., & Marmanis, D. (2012). Simultaneous removal of acidity and lead from acid lead battery wastewater by aluminum and iron electrocoagulation. *Journal of Engineering Science and Technology Review*, 5(2), 1-5.

Dhote, S., & Dixit, S. (2009). Water quality improvement through macrophytes - a review. *Environmental Monitoring and Assessment*, 152, 149-153.

Dorniani, D., Kura, A. U., Hussein-Al-Ali, S. H., Hussein, M. Z. B., Fakurazi, S., Shaari, A. H., & Ahmad, Z. (2014). *In Vitro* Sustained Release Study of Gallic Acid Coated with Magnetite-PEG and Magnetite-PVA for Drug Delivery System. *The Scientific World Journal,* 11 pages. http://dx.doi.org/10.1155/2014/416354

Drouiche, N., Lounici, H., Drouiche, M., Mameri, N., & Ghaffour, N. (2009). Removal of fluoride from photovoltaic wastewater by electrocoagulation and products characteristics, Desalination *and Water Treatment*, 7(1-3), 236-241.

Dubinin, M. M. (1960). The potential theory of adsorption of gases and vapors for adsorbents with energetically non-uniform surface, *Chemical Reviews*. 60, 235-266.

Dubinin, M. M., Zaverina, E. D., & Radushkevich, L. V. (1947). Sorption and structure of active carbons. I. Adsorption of organic vapors. *Zhurnal Fizicheskoi Khimii*, 21, 1351-1362.

Duruibe, J. O., Ogwuegbu, M. O. C., & Egwurugwu, J. N. (2007). Heavy metal pollution and human biotoxic effects. *International Journal of Physical Sciences*, 2(5), 112-118.

Eastoe, J., & Dalton, J. S. (2000). Dynamic surface tension and adsorption mechanisms of surfactants at the air water interface, *Advances in Colloid and Interface Science*, 85, 103-144.

Edet, A. E., & Offiong, O. E. (2002). Evaluation of water quality pollution indices for heavy metal contamination monitoring. A study case from Akpabuyo-Odukpani area, Lower Cross River Basin (southeastern Nigeria). *Geo Journal*, 57(4), 295-304. doi: 10.1023/B: GEJO.0000007250.92458.de

Edmunds, W. M., & Smedley, P. L. (2001). Fluoride in natural waters. In: O. Selinus (Ed.), *Essentials of medical geology* (pp 311-33). Netherlands: Springer.

Emmanuel, K. A., Ramaraju, K. A., Rambabu, G., & Rao, A. V. (2008). Removal of Fluoride from drinking water with Activated Carbons prepared from HNO_3 activation - A comparative study. *Rasayan Journal of Chemistry*. 1 (4), 802-818.

Erdem, M., & Ozverdi, A. (2005). Lead adsorption from aqueous solution onto siderite. *Separation and Purification Technology,* 42, 259-264.

Eskandarpour, A., Onyango, M. S., & Ochieng, A. (2008). Removal of fluoride ions from aqueous solution at low pH using schwertmannite. *Journal of Hazardous Materials,* 152, 571-579.

Farahmand, E. (2016). Adsorption of Cerium (IV) from Aqueous Solutions Using Activated Carbon Developed from Rice Straw. *Open Journal of Geology*, 6, 189-200.

Farhan, S. N. & Khadom, A. A (2015). Biosorption of heavy metals from aqueous solutions by *Saccharomyces Cerevisiae. International*

Journal of Industrial Chemistry, 6(2), 119–130. DOI 10.1007/s40090-015-0038-8.

Fawzy, M. (2007). Biosorption of cadmium and lead by *Phragmites australis* L. biomass using factorial experimental design. *Global Journal of Biotechnology and Biochemistry,* 2, 10-20.

Feng, N. C. & Guo, X. Y. (2012). Characterization of adsorptive capacity and mechanisms on adsorption of copper, lead and zinc by modified orange peel. *Transactions of Nonferrous Metals Society of China*, 22(5), 1224–1231.

Foo, K. Y., & Hameed, B. H. (2010). Insights into the modeling of adsorption isotherm system. *Chemical Engineering Journal*, 156, 2–10.

Freundlich, H. (1906). Uber die adsorption in losungen (adsorption in solution), *Zeitschrift für physikalische Chemie* 57, 384–470.

Gakwavu, R. J., Sekomo, B. C., & Nhapi, I., (2012). Zinc and Chromium removal mechanisms from industrial wastewater by Water hyacinth, *Eichhornia crassipes. Applied Ecology and Environmental Science*, 10(4), 493-502.

Gandhi, N., Sirisha, D., & Chandra Sekhar, K. B. (2016). Adsorption of Fluoride (F$^-$) from aqueous solution by using Ragi seed (*Eleusine coracana*) powder. *Journal of Chemical and Pharmaceutical Research*, 8(7), 127-141.

Garba, S. T., Osemeahon, A. S., Maina, H. M., & Barminas, J. T. (2012). Ethylenediaminetetraacetate (EDTA) - Assisted phytoremediation of heavy metal contaminated soil by *Eleusine indica L.* Gearth. *Journal of Environmental Chemistry and Ecotoxicology* 4(5), 103-109.

Gautam, R. K., Mudhoo, A., Lofrano, G., & Chattopadhyaya, M. C. (2014). Biomass-derived biosorbents for metal ions sequestration: Adsorbent modification and activation methods and adsorbent regeneration. *Journal of Environmental Chemical Engineering*, 2, 239-259.

Gautam, R. K., Sharma, S. K., Mahiya, S., & Chattopadhyaya, M. C. (2015). Contamination of Heavy Metals in Aquatic Media: Transport, Toxicity and Technologies for Remediation. In S. K. Sharma (Ed.), *Heavy Metals in Water Presence, Removal and Safety* (pp. 1-24). UK: The Royal Society of Chemistry.

Ghosh, M., & Singh, S. P. (2005). A review on phytoremediation of heavy metals and utilization of its byproducts. *Applied Ecology and Environmental Research,* 3(1), 1-18.

Girginova, P. I., Daniel-da-Silva, A. L., Lopes, C. B., Figueira, P., Otero, M., & Amaral, V.S. (2010). Silica coated magnetite particles for magnetic removal of Hg^{2+} from water. *J Colloid Interface Sci,* 345(2), 234-40.

Gisi, S. D., Lofrano, G., Grassi, M., & Notarnicola, M. (2016). Characteristics and adsorption capacities of low-cost sorbents for wastewater treatment: A review. *Sustainable Materials and Technologies,* 9, 10-40.

Gomati, S., Adhikari, S., and Mohanty, P. (2014). Phytoremediation of Copper and Cadmium from Water Using Water Hyacinth, *Eichhornia Crassipes*. *International Journal of Agricultural Science and Technology*, 2(1), 1-7.

Grassi, M., Kaykioglu, G., Belgiorno, V., & Lofrano, G. (2012). Removal of emerging contaminants from water and wastewater by adsorption process. In: G. Lofrano (Ed.), *Emerging compounds removal from wastewater* (pp 15-37). Netherlands: Springer.

Gupta, A.K., & Gupta, M. (2005). Synthesis and surface engineering of iron oxide nanoparticles for biomedical applications. *Biomaterials*, 26(18), 3995-4021.

Gupta, V. K. (1998). Equilibrium uptake, sorption dynamics, process development, and column operations for the removal of copper and nickel from aqueous solution and wastewater using activated slag, a low-cost adsorbent. *Industrial and Engineering Chemistry Research*. 37, 192-202.

Guzman, K. A. D, Taylor, M. R., & Banfield, J. F. (2006). Environmental risks of nanotechnology: national nanotechnology initiative funding, 2000-2004. *Environmental Science Technology*, 40(5), 1401-1407.

Hammad, D, M. (2011). Cu, Ni and Zn Phytoremediation and Translocation by Water Hyacinth Plant at Different Aquatic Environments. *Australian Journal of Basic and Applied Sciences*, 5(11), 11-22.

Hannachi, Y. (2012). Characterization of the biosorption of lead and cadmium with the red alga (*Ceramium virgatum*). *The Holistic Approach to Environment*, 2(3), 93-109.

Hao, Y. M., Man, C., & Hu, Z. B. (2010) Effective removal of Cu(II) ions from aqueous solution by amino functionalized magnetic nanoparticles. *J Hazard Mater*, 184(1-3), 392-9.

Hao, Y. M., Man, C., & Hu, Z. B. (2010). Effective removal of Cu(II) ions from aqueous solution by amino functionalized magnetic nanoparticles. *Journal of Hazardous Materials,*

Harikumar, P.S., Jaseela, C., Megha, T. (2012). Defluoridation of water using biosorbents. *Natural Science*, 4(4), 245-251. doi:10.4236/ns.2012.44035

Harikumar, P.S., Joseph, L., & Dhanya, A., (2013). Photocatalytic degradation of textile dyes by hydrogel supported titanium dioxide nanoparticles. *Journal of Environmental Engineering and Ecological Science*, 2(2), 1-9.

Herojeet, R., Rishi, M. S., & Kishore, N. (2015). Integrated approach of heavy metal pollution indices and complexity quantification using chemometric models in the Sirsa Basin, Nalagarh valley, Himachal Pradesh, India. *Chinese Journal of Geochemistry*, 34(4), 620–633. doi:10.1007/s11631-015-0075-1

Hesse, P. R. (1971). *Textbook of soil chemical analysis*, New Delhi: CBS Publishers.

Hichour, M., Persin, F., Sandeaux, J., & Gavach, C. (2000). Fluoride removal from waters by Donnan dialysis. *Separation and Purification Technology*, 18(1), 1-11.

Ho, Y. S., Ng, J. C., & McKay, G. (2000). Kinetics of pollutant sorption by biosorbents: Review. *Separation and Purification Technology*, 29, 189-232.

Ho, Y.S., & McKay, G. (1999). Pseudo-second order model for sorption processes. *Process biochemistry,* 34(5), 451-465.

Hong, F., Zhou, J., Liu, C., Yang, F., Wu, C., Zheng, L & Yang, P. (2005). Effect of nano −TiO$_2$ on photochemical reaction of chloroplasts of spinach. *Biological Trace Element Research*, 105, 269-280.

Hooda, V. (2007). Phytoremediation of toxic metals from soil and waste water. *Journal of Environmental Biology*, 28(2), 367-376.

Horton, R. K., (1965). An index-number system for rating water quality. *Journal of the Water Pollution Control Federation*, 37, 300–306.

Howladar, M. F., Deb P. K., Muzemder A. T. M. S. H. & Ahmed M. (2014). Evaluation of water resources around Barapukuria coal mine industrial area, Dinajpur, Bangladesh. *Applied Water Science, 4*, 203–222. doi:10.1007/s13201-014-0207-5

Hu, B., Jia, X., Hu, J., Xu, D., Xia, F., & Li, Y. (2017). Assessment of Heavy Metal Pollution and Health Risks in the Soil-Plant-Human System in the Yangtze River Delta, China. *International Journal of Environmental Research Public Health*, 14(9), 1042. doi:10.3390/ijerph14091042

Hu, C.Y., Lo, S.L., & Kuan, W.H. (2003). Effects of co-existing anions on fluoride removal in electrocoagulation (EC) process using aluminum electrodes. *Water Research,* 37, 4513-4523.

Hu, H. B., Wang, Z. H., & Pan, L. (2010). Synthesis of monodisperse Fe$_3$O$_4$–silica core–shell microspheres and their application for removal of heavy metal ions from water. *Journal of Alloys and Compounds*, 492(1-2), 656-61.

Hussain, S., Aziz, H. A., Isa, M. H., Ahmad, A., Leeuwen, J. V., Zou, l., Beecham, S., & Umar, M. (2011). Orthophosphate removal from

domestic wastewater using limestone and granular activated carbon. *Desalination,* 271(1-3), 265–272.

Igwe, J. C. & Abia, A. A. (2007). Equilibrium sorption isotherm studies of Cd(II), Pb(II) and Zn(II) ions detoxification from waste water using unmodified and EDTA-modified maize husk. *Electronic Journal of Biotechnology*, 10(4), 536-548. doi:10.2225/vol10-issue4-fulltext-15

Jacks, G., Bhattacharya, P., Chaudhary, V., & Singh, K. P. (2005). Controls on the genesis of some high-fluoride groundwaters in India. *Applied Geochemistry,* 20 (2), 221-228.

Jagtoyen, M., & Derbyshire, F. (1998). "Activated carbons from yellow poplar and white oak by Hydrogen tetraoxophosphate activation". *Carbon,* 36, 1085-1097.

Jameel, A. A., Sirajudeen, J. & Vahith, R. A. (2012). Studies on heavy metal pollution of groundwater sources between Tamilnadu and Pondicherry, India. *Advances in Applied Science Research*, 3(1), 424-429.

Jayapriya, G., Ramya, R., Rathinam, X. R., & Sudha, P. N. (2011). Equilibrium and kinetic studies of fluoride adsorption by chitin/cellulose composite. *Archives of Applied Science Research*, 3 (3), 415-423.

Joshi, S., Pradhananga, M. A., & Pradhananga, R. R. (2012). Adsorption of Fluoride Ion onto Zirconyl–Impregnated Activated Carbon Prepared from Lapsi Seed Stone. *Journal of Nepal Chemical Society*, 30, 13-23.

Kaasalainen, M., & Yli-Halla, M. (2003). Use of Sequential Extraction to Assess Metal Partitioning in Soils. *Environmental Pollution,* 126, 225-233.

Kannam, N., & Sundaram, S. (2001). Kinetics and mechanism of removal of methylene blue by adsorption on various carbons-a comparative study. *Dyes and Pigments*, 51(1), 25-40.

Karthikeyan, G., & Ilango, S. S. (2007). Fluoride sorption using *Morringa indica*-based activated carbon, *Iranian Journal of Environmental Health Science & Engineering*, 4(1), 21-28.

Karthikeyan, G., Anbalagan, K., & Andal, N. M. (2004). Adsorption dynamics and equilibrium studies of Zn (II) onto chitosan. *Journal of Chemical Sciences*. 116(2), 119-127.

Kass, A., Yechieli, G. Y., Vengosh, A., & Starinsky, A. (2005). The impact of freshwater and wastewater irrigation on the chemistry of shallow groundwater: a case study from the Israeli Coastal aquifer. *Journal of Hydrology*, 300(1-4), 314-331.

Kayal, S., & Ramanujan, R.V. (2010). Doxorubicin loaded PVA coated iron oxide nanoparticles for targeted drug delivery. *Materials Science and Engineering C*, 30(3), 484-490.

Khan, M. H. R., Seddique, A. A., Rahman, A & Shimizu, Y. (2017). Heavy Metals Contamination Assessment of Water and Soils in and Around Barapukuria Coal Mine Area, Bangladesh. *American Journal of Environmental Protection*. 6(4), 80-86.doi: 10.11648/j.ajep.20170604.11

Kharkongor, D. & Ramanujam, P. (2015). Spatial and Temporal Variation of Carotenoids in Four Species of *Trentepohlia*

(Trentepohliales, Chlorophyta). *Journal of Botany,* 8. http://dx.doi.org/10.1155/2015/201641

Khoramnejadian, S., & Saeb, K. (2015). Accumulation and Translocation of Heavy Metals by Amaranthus Retroflexus. *Journal of Earth Environment & Health Science*, 1(2), 58-60. doi: 10.4103/2423-7752.170581

Khot, L. R., Sankaran, S., Maja, J. M., Ehsani, R., & Schuster, E. W. (2012). Applications of nanomaterials in agricultural production and crop protection: A review. *Crop Protection*, 35, 64-70.

Khushboo, C., Sumira, J., & Suphiya, K. (2016). Heavy metal ATPase (HMA2, HMA3, AND HMA4) genes in hyperaccumulation mechanism of heavy metals. In: Plant metal interaction Emerging remediation techniques (pp. 545-556). Elsevier.

Kirtikar, K. R & Basu, B. D. (1989). In E. Blatter et al. (Eds.), Indian Medicinal Plants (pp. 847-848). Lalit Mohan Basu, Allahabad.

Knorr, D. (2003) Impact of non-thermal processing on plant metabolite. *Journal of Food Engineering*, 56(2-3), 131-134.

Kramer, U., Pickering, I. J., Prince, R. C., Raskin, I., & Salt, D. E. (2000). Subcellular localization and speciation of Ni in hyperaccumulator and nonaccumulator *Thlaspi* species. *Plant Physiology*, 122, 1343-1353.

Kubiak, J. J., Khankhane, P. J., Kleingeld, P. J., & Ana T. Lima, A. T. (2012). An attempt to electrically enhance phytoremediation of arsenic contaminated water. *Chemosphere*, 87, 259-264.

Kumar, A., & Kumar, V. (2015). Fluoride Contamination in Drinking Water and its Impact on Human Health of Kishanganj, Bihar, India. *Research Journal of Chemical Sciences*, 5(2), 76-84.

Kumar, E., Bhatnagar, A., Ji, M., Jung, W., Lee, S. H., & Kim, S. J. (2009) Defluoridation from aqueous solutions by granular ferric hydroxide (GFH). *Water Research*; 43(2), 490-498.

(a) Kumar, S. P., Ramakrishnan, K., Kirupha, D. S & Sivanesan, S. (2010). Thermodynamic and kinetic studies of cadmium adsorption from aqueous solution onto rice husk. *Brazilian Journal of Chemical Engineering*, 27(02), 347 - 355.

(b) Kumar, S., Gupta, A. & Yadav, J. P. (2008). Removal of fluoride by thermally activated carbon prepared from neem (*Azadirachta indica*) and kikar (*Acacia arabica*) leaves. *Journal of Environmental Biology*, 29, 227-232.

Kupper, H., Parameswaran, A., Leitenmaier, B., Trtilek, M., & Setlik, I. (2007). Cadmium induced inhibition of photosynthesis and long-term acclimation of cadmium stress in the hyperaccumulator *Thlapsicaerulescens*. *New Phytologist,* 175, 655 - 674.

Kwon, H. J., Paek, J. Y., Yong Hyun Kim, Y.H., & Man, D. H. (2009). Structural Analysis of Brazilin from *Caesalpinia sappan* L. 2009 International Symposium & Annual Meeting. The Korean Society for Microbiology and Biotechnology, 323-336.

Lagergren, S. (1898). Zur theorie der sogenannten adsorption geloester stoffe, Kungliga Svenska Vetenskapsakad. *Handlingar*, 24, 1-39.

Lasat, M, M. (2000). Phytoextraction of metals from contaminated soil: a review of plant/soil/metal interaction and assessment of pertinent

agronomic issues. *Journal of Hazardous Substance Research*, 2(5), 1-25.

Lasat, M. M. (2002). Phytoextraction of toxic metals: a review of biological mechanisms. *Journal Environmental Quality,* 31(1), 109-120. doi: 10.2134/jeq2002.1090

Lasat, M. M., Pence, N. S., Garvin, D. F., Abbs, S. D., & Kochian, L. V. (2000). Molecular physiology of zinc transport in the Zn hyperaccumulator *Thlaspi caerulescens*. *Journal of Experimental Botany*, 51(342), 71-79.

Lee, D. K., Cho, D. H., Lee, J. H., & Shin, H.Y. (2008). Fabrication of nontoxic natural dye from sappan wood. *Korean Journal of Chemical Engineering*., 25(2), 354-358.

Lei, Z., Mingyu, S., Xiao, W., Chao, L., Chaunxiang, Q., Liang, C., Hao, H., Xiao, L., & Fashui, H. (2008). Antioxidant stress is promoted by nano-anatase in spinach chloroplasts under UV-Beta radiation, *Biological Trace Element Research*, 121, 69-79.

Lei, Z., Zheng, L., & Su, M. (2007). Effects of nano-anatase on spectral characteristics and distribution of LHCII on the thylakoid membranes of spinach. *Biological Trace Element Research*, 120, 273-283.

Levy, D. B., Barbarick, K. A., Siemer, E. G., & Sommers, L. E. (1992). Distribution and partitioning of trace metals in contaminated soils near Leadville, Colorado. *Journal of Environmental Quality,* 21(2), 185-195.

Li, M. S., Luo, Y. P., & Su, Z. Y. (2007). Heavy metal concentration in soil and plant accumulation in a restored manganese mine land in Guangxi, South China. *Environmental Pollution,* 147, 168-175.

Li, S., Liu, W., Gu, S., Cheng, X., Xu, Z., & Zhang, Q. (2009). Spatio-temporal dynamics of nutrients in the upper Han River basin, China. *Journal of Hazardous Materials*, 162(2-3), 1340-1346.

Liao, X. P., & Shi, B. (2005). Adsorption of fluoride on zirconium(IV)-impregnated collagen fiber. *Enviornmental Science & Technology*. 39, 4628-4632.

Lim, W.C., Srinivasakanan, C., & Balasubramanian, N. (2010). "Activation of palm shells by phosphoric acid impregnation for high yielding activated carbon". *Journal of Analytical and Applied Pyrolysis,* 88, 181-186.

Lodeiro, P., Barriada, J. L., Herrero, R., & Sastre de Vicente, M. E. (2006). The marine macroalga *Cystoseira baccata* as biosorbent for cadmium (II) and lead (II) removal: Kinetic and equilibrium studies, *Environmental Pollution (Barking, Essex: 1987)* 142(2), 264-273.

Lu, X., Kruatrachue, M., Pokethitiyookb, P., & Homyokb, K. (2004). Removal of Cadmium and Zinc by Water Hyacinth, *Eichhornia crassipes*. *ScienceAsia*, 30, 93-103.

Lytle, C. M., Lytle, F. W., Yang, N., Qian, J. H., Hansen, D., Zayed, A., & Terry, N. (1998). Reduction of Cr (VI) to Cr (III) by wetland plants: potential for in situ heavy metal detoxification. *Environmental Science & Technology*, 32, 3087-3093.

Madaeni, S.S., & Mansourpanah, Y. (2003). COD removal from concentrated wastewater using membranes. *Filtrration & Separation,* 40, 40-46.

Mahan, M. & Mayers, J. (1987). University Chemistry, Benjamin/Cummings, California.

Mahmood, Q., Zheng, P., Islam, E., Hayat, Y., Hassan, M, J., Jilani, G., & Jin, R, C. (2005). Lab scale studies on Water hyacinth (*Eichhornia crassipes* marts solms) for biotreatment of textile wastewater. *Caspian Journal of Environmental Sciences*, 3(2), 83-88.

Mahmoud, A. E. D., & Fawzy, M. (2016). Bio-based Methods for Wastewater Treatment: Green Sorbents. In A.A. Ansari et al. (Eds.), *Phytoremediation* (pp. 209-238). Switzerland: Springer International Publishing Switzerland.

Mall, I. D., Srivastava, W. C., & Argawal N. K. (2006). Removal of orange G and Methyl Violet Dyes by Adsorption onto Bagasse Fly Ash-Kinetic Study and Equilibrium Isotherm Analyses. *Dyes and Pigments*, 69, 2006, 210-223.

Mane, V. S., Mall, I. D., & Srivastava, V. C. (2007). Kinetic and equilibrium isotherm studies for the adsorptive removal of Brilliant Green dye from aqueous solution by rice husk ash. *Journal of Environmental Management*, 84(4), 390-400.

Manzoni, S., Molini, A., & Porporato, A. (2011) Stochastic modelling of phytoremediation. Proceedings of the Royal Society A. 467: 3188–3205. doi:10.1098/rspa.2011.0209

Mapanda, F, Mangwayana, E. N, Nyamangara, J., Giller, K. E. (2005). The effect of long-term irrigation using wastewater on heavy metal contents of soils under vegetables in Harare, Zimbabwe. *Agriculture, Ecosystems and Environment,* 107, 151- 65.

Marbaniang, D., & Chaturvedi, S. S. (2014). Assessment of Cr^{+6} Accumulation and Phytoremediation Potential of Three Aquatic

Macrophytes of Meghalaya, India. *International Journal of Science and Research*, 3(6), 36-42.

Marchiol, L., Assolari, S., Sacco, P., & Zerbi, G. (2004). Phytoextraction of heavy metals by canola (*Brassica napus*) and radish (*Raphanus sativus*) grown on multicontaminated soil. *Environmental Pollution,* 132, 21-27.

Marques, A. P. G. C., Rangel, A. O. S. S., & Castro, P. M. L. (2009). Remediation of Heavy Metal Contaminated Soils: Phytoremediation as a Potentially Promising Clean-Up Technology. *Critical Reviews in Environmental Science and Technology,* 39,622-654.

Matheickal, J. T. & Yu, Q. (1999). Biosorption of lead (II) and copper (II) from aqueous solutions by pre-treated biomass of Australian marine algae. Biores. Technol., 69:223-229.

Mbugua, G., Mwangi, I. W., Swaleh, S., Wanjau, R. N., Ram, M., & Ngila, J.C. (2017). Remediation of Fluoride Laden Water by Complexation with Triethylamine Modified Waste Polythene Material. *Material Science: An Indian Journal*, 15(01), 1-19.

Meenakshi, S., & Vishwanathan, N. (2007). Identification of selective ion-exchange resin for fluoride sorption. *Journal of colloid and interface science*, 308(2), 438-450.

Mellem, J. J., Baijanth, H., & Odhav, B. (2009). Translocation and accumulation of Cr, Hg, As, Pb, Cu and Ni by *Amaranthus dubius* (Amaranthaceae) from contaminatedsites. *Journal of Environment Science and Health*, 44(9), 568-575.

Mellem, J. J., Baijanth, H., & Odhav, B. (2012). Bioaccumulation of Cr, Hg, As, Pb, Cu and Ni with the ability for hyperaccumulation by

Amaranthus dubius. *African Journal of Agricultural Research,* 7(4), 591-596.

Mingyu, S. (2007). Effects of nano-anatase TiO2 on absorption, distribution of light and photoreduction activities of chloroplast membrane of spinach. *Biological Trace Element Research,* 118, 120-130.

Mohan, S.V., Nithila, P., & Reddy, S. J. (1996). Estimation of heavy metal in drinking water and development of heavy metal pollution index. *Journal of Environmental Science and Health*, A31(2), 283–289.

Mohankumar, K., Hariharan, V., & Rao P. N. (2016). Heavy Metal Contamination in Groundwater around Industrial Estate vs Residential Areas in Coimbatore, India. *Journal of Clinical Diagnostic Research*, 10(4), BC05-BC07 doi: 10.7860/JCDR/2016/15943.7527

Mondal, N. K., Bhaumik, R., Banerjee, A., Datta, J. K., & Baur, T. (2012). A comparative study on the batch performance of fluoride adsorption by activated silica gel and activated rice husk ash. *International Journal of Environmental Sciences,* 2(3), 1643-1661. ISSN 0976 – 4402

Montane, D., & Torne-Fernandez, V. F. (2005). Activated carbons from lignin: kinetic modeling of the pyrolysis of Kraft lignin activated with phosphoric acid. *Chemical Engineering Journal*, 106(1), 1-12.

Moon, C. K., Park K. S., Kim S. G., Won, H. S., & Chung, J. H. (1992). Brazilin protects cultured rat hepatocytes from trichlorobromethane-induced toxicity. *Drug and Chemical Toxicology*. 15, 81-91.

Morteza, E., Moaveni, P., Aliabadi, F. H., & Kiyani, M. (2013). Study of photosynthetic pigments changes of maize (Zea mays L.) under nano TiO$_2$ spraying at various growth stages. *SpringerPlus,* 2, 247.

Naohito, K., Fumihiko, O., Hisato, T., & Isao, Y. (2009). Removal of fluoride ion by bone char produced from animal biomass. *Journal of Oleo Science*, 58(10), 529-533.

Ndiayea, P. I., Moulin, P., Dominguez, L., Millet, J. C., & Charbit, F. (2005). Removal of fluoride from electronic industrial effluent by RO membrane separation. *Desalination*, 173(1) 25-32.

Neilson, J. W., Artiola, J. F., & Maier, R. M. (2003). Characterization of lead removal from contaminated soils by nontoxic soil-washing agents. *Journal of Environmental Quality,* 32(3), 899-908.

Nilantika, P., Samujjwal, C., & Mahuya, S. (2014). Lead toxicity on non-specific immune mechanisms of freshwater fish Channa punctatus. *Aquatic Toxicology*, 152, 105-112.

Nirajan-Reddy V. L., Ravikanth, V., Jansi-Lakshmi V. V. N. S., Suryannarayan-Murty, U., & Venkateswarlu, Y. (2004). Inhibitory activity of homoisoflavonoids from *Caesalpinia sappan* against *Beauveria bassiana*. *Fitoterapia*. 74, 600-602.

Nirmala, B., Kumar, S. B. V., Suchetan, P. A. & Prakash S. M. (2012). Seasonal Variations of Physico Chemical Characteristics of Ground Water Samples of Mysore City, Karnataka, India. *International Research Journal of Environment Sciences,* 1(4), 43-49.

Nwabanne, J. T., & Igbokwe, P. K. (2011). Preparation of Activated Carbon from Nipa Palm Nut: Influence of Preparation Conditions.

Research Journal of Chemical Sciences, 1(6), 53-58. ISSN 2231-606X

Odjegba, V. J., & Fasidi, I. O. (2007). Phytoremediation of heavy metals by *Eichhornia crassipes. Environmentalist,* 27(3), 349-355.

Ogunkunle, C. O., Ziyath, A. M., Adewumi, F. E., & Fatoba, P.O (2015). Bioaccumulation and associated dietary risks of Pb, Cd, and Zn in amaranth (*Amaranthus cruentus*) and jute mallow (*Corchorus olitorius*) grown on soil irrigated using polluted water from Asa River, Nigeria. *Environmental Monitoring and Assessment*, 187(5), 281. doi:10.1007/s10661-015-4441-6

Oguz, E. (2005). Adsorption of fluoride on gas concrete materials. *Journal of Hazardous Materials*. 117, 227-233.

Ogwuegbu, M. O. C., & Muhanga, W. (2005). Investigation of Lead Concentration in the Blood of People in the Copperbelt Province of Zambia, *Journal of Environment* (1), 66 -75.

Okareh, O, T., & Adeolu, A, T. (2015). Removal of Lead Ion from Industrial Effluent Using Plantain (*Musa paradisiaca*) Wastes. *British Journal of Applied Science & Technology*, 8(3), 267-276.

Olawale, A. S., Ajayi, O. A., Olakunle, M. S., Ityokumbul, M. T., & Adefila, S. S. (2015). Preparation of phosphoric acid activated carbons from Canarium Schweinfurthii Nutshell and its role in methylene blue adsorption. *Journal of Chemical Engineering and Materials Science*. 6(2), 9-14. doi: 10.5897/JCEMS2015.0219 ISSN 2141-6605

Onda, K., LoBuglio, J., & Bartram, J. (2012). Global access to safe water: Accounting for water quality and the resulting impact on MDG

progress. *International Journal of Environmental Research and Public Health,* 9(3), 880-894. doi:10.3390/ijerph9030880

Onyango, M. S., Kojima, Y., Aoyi, O., Bernardo, E. C., & Matsuda, H. (2004). Adsorption equilibrium modeling and solution chemistry dependence of fluoride removal from water by trivalent-cation-exchanged zeolite F-9. *Journal of colloid and interface science,* 279(2), 341-350.

Ozmen, M., Can, K., Arslan, G., Tor, A., Cengeloglu, Y., & Ersoz, M. (2010). Adsorption of Cu(II) from aqueous solution by using modified Fe3O4 magnetic nanoparticles. *Desalination,* 254(1-3), 162-9.

Palma, L. D, & Mecozzi, R. (2007). Heavy metals mobilization from harbor sediments using EDTA and citric acid as chelating agents. *Journal of Hazardous Materials,* 147(3), 768-775.

Pandey, V. C. (2012). Phytoremediation of heavy metals from fly ash pond by *Azolla caroliniana*. *Ecotoxicology and Environmental Safety*, 82, 8-12.

Park, J. Y., Oh, S. G., & Ha, B. H. (2001). Characterization of Iron (III) oxide nanoparticles prepared using ammonium acetate as precipitating agent. *Korean Journal of Chemical Engineering*, 18(2), 215-219.

Patterson, J. J. (1975). *Wastewater Treatment Technology,* New York, Ann Arbor Inc.

Pelit, L., Ertas, F. N., Eroglu, A.E., Shahwan, T., & H. Tural, H. (2011). Biosorption of Cu(II) and Pb(II) ions from aqueous solution by natural spider silk. *Bioresource Technology,* 102, 8807-8813.

Peralta-Videa, J. R., Gardea-Torresdey, J.L., De-la- Rosa, G., Gonzales, J. H., & Herrera, I. (2004). Effect of heavy metals on alfalfa plants at different growth stages. *Advances in Environmental Research,* 8, 679-685.

Persans, M. W., Yan, X., Patnoe J-M. M. L., Kramer, U., Salt, D. E. (1999). Molecular dissection of the role of histidine in Ni hyperaccumulation in *Thlaspi goesingense* (Halacsy). *Plant Physiology,* 121, 1117-1126.

Peters, R. W. (1999). Chelant extraction of heavy metals from contaminated soil. *Journal of Hazardous Materials,* 66 (1-2), 151-210.

Pickering, I. J., Prince, R. C., George, M. J., Smith, R. D., George, G. N., & Salt, D. E. (2000). Reduction and coordination of arsenic in Indian mustard. *Plant Physiology*, 122,1171-1177.

Pinon-Miramontes, M., Bautista-Margulis, R.G., & Perez-Hernandez, A. (2003). Removal of arsenic and fluoride from drinking water with cake alum and a polymeric anionic flocculent, *Fluoride*, 36(2), 122-128.

Prasad, B., & Bose, J. M. (2001). Evaluation of the heavy metal pollution index for surface and spring water near a Limestone mining area of the lower Himalayas. *Environ Geology*, 41(1-2), 183-188. doi:10.1007/s002540100380

Prasad, B., & Kumari, S., (2008). Heavy metal pollution index of ground water of an abandoned open cast mine filled with fly ash: a case study. *Mine Water and the Environment*. 27 (4), 265–267.

Prasad, B., & Mondal, K. K., (2008). The impact of filling an abandoned opencast mine with fly ash on ground water quality: a case study. *Mine Water and the Environment*, 27(1), 40–45.

Praus, P. (2007). Urban water quality evaluation using multivariate analysis. *Acta Montanistica Slovaca* 12 (2), 150-158.

Pushenreiter, M., Stőger, G., Lombi, E., Horak, O., & Wenzel, W. (2001). Phytoextraction of heavy metal contaminated soils with *Thlaspi goesingense* and *Amaranthus hybridus*: Rhizosphere manipulation using EDTA and ammonium sulphate. *Journal of Plant Nutrition and Soil Science*, 164(6), 615-621.

Putra, R. S., Trahadinata, G. A., Latif, A., & Solehudin, M. (2017). Wastewater Treatment of Chemical Laboratory Using Electro Assisted-Phytoremediation (EAPR). *AIP Conference Proceedings,* 1823. doi: 10.1063/1.4978150

Qin, J.J., Wai, M.N., Oo, M.H., & Wong, F.S. (2008). A feasibility study on the treatment and recycling of a wastewater from metal plating. *Journal of Membrane Science,* 208, 213-221.

Qu, J., Song, X., Feng, Y., Cong, Q., Yuan, X., & Quan, X. (2016). Stabilization of Pb, Hg, Cr, Zn in Soil with Ammonium Molybdate and Uptake by Alfalfa Plants. *Academia Journal of Biotechnology*, 4(4), 145-152. doi:10.15413/ajb.2015.0130

Qu, J., Wang, L., Yuan, X., Cong, Q., & Guan, S. S. (2011). Effect of ammonium molybdate on phytoremediation by alfalfa plants and (im)mobilization of toxic metals in soil. *Environmental Earth Sciences,* 64, 2175-2182.

Qu, J., Yuan, X., Cong, Q., & Wang, S. (2008). Determination of total mass and morphology analysis of heavy metal in soil with potassium biphthalate-sodium hydroxide by ICP-AES. *Spectroscopy and Spectral Analysis*, 28, 2674-2678.

Rai, P, K., & Singh, M, M. (2016). *Eichhornia crassipes* as a potential phytoremediation agent and an important bioresource for Asia Pacific region. *Environmental Skeptics and Critics*, 5(1), 12-19.

Raj, D., & Shaji, E. (2017). Fluoride contamination in groundwater resources of Alleppey, southern India. *Geoscience Frontiers,* 8, 117-124.

Rajeshwar, K., Ibanez, J., & Swain, G. (1994). Electrochemistry and environment. *Journal of Applied Electrochemistry,* 24, 1077-1091.

Rao, R. A. K., Khan, M. A., & Rehman, F. (2010). Utilization of Fennel biomass (*Foeniculum vulgari*) a medicinal herb for the biosorption of Cd (II) from aqueous phase. *The Chemical Engineering Journal,* 156, 106 -113.Raskar, S., & Laware, S. L. (2013). Effect of titanium dioxide nano particles on seed germination and germination indices in onion. *Plant sciences feed*, 3 (9), 103-107.

Raza, M. H., Sadiq, A., Farooq, U., Athar, M., Hussain, T., Mujahid, A., & Salman, M. (2015). *Phragmites karka* as a Biosorbent for the Removal of Mercury Metal Ions from Aqueous Solution: Effect of Modification. *Journal of Chemistry,* 12. http://dx.doi.org/10.1155/2015/293054

Remya, N., Saino, H. V., Baiju, G. N., Maekawa, T., Yoshida, Y., & Sakthi, K. D. (2010). Nanoparticulate material delivery to plants. *Plant Science*, 179, 154-163.

Rengaraj, S., Joo, C. K., Kim, Y., & Yi, J. (2003). Kinetics of removal of chromium from water and electronic process wastewater by ion exchange resins: 1200H, 1500H and IRN97H. *Journal of Hazardous Materials,* 102, 257-275.

Rezania, S., Ponraj, M., Talaiekhozani, A., Mohamad, S. E., Din, M. F. M., Taib, S. M., Sabbagh, F., & Sairan, F. M. (2015). Perspectives of phytoremediation using water hyacinth for removal of heavy metals, organic and inorganic pollutants in wastewater. *Journal of Environmental Management,* 163, 125-133.

Rindi, F., Lam, D. W., & L´opez-Bautista, J. M. (2009). Phylogenetic relationships and species circumscription in *Trentepohli*a and *Printzina* (Trentepohliales, Chlorophyta). *Molecular Phylogenetics and Evolution*, 52(2), 329-339.

Rodríguez, C. T. C., Amaya-Chávez, A., Roa-Morales, G., Barrera-Díaz, C. E. & Ureña-Núñez, F. (2010). An integrated electrocoagulationphytoremediation process for the treatment of mixed industrial wastewater, *International Journal of Phytoremediation,* 12(8), 772-784.

Römkens, P., Bouwman, L., Japenga, J., & Draaisma, C. (2002). Potentials and drawbacks of chelate- enhanced phytoremediation of soil. *Environmental Pollution,* 116, 109-121.

Rubin, J., Bartolome, J., & Tomkinson, J. (1995). The dynamics of NH_4^+ in the NH_4MF_3 perovskites. II. Inelastic neutron scattering study. *Journal of Physics: Condensed Matter,* 7(46), 8723-8740.

Saeed, A., Akhter, M. W., Iqbal, M. (2005). Removal and recovery of heavy metals from aqueous solution using papaya wood as a new biosorbent. *Separation and Purification Technology*, 45(1), 25–31.

Saenjum, C., Chaiyasut, C., Kadchumsang, S., Chansakaow, S., & Suttajit, M. (2010). Antioxidant activity and protective effects on DNA damage of *Caesalpinia sappan* L. extract, *Journal of Medicinal Plants Research,* 4(15), 1594-1600.

Shah, B., Mistry, C., & Shah, A. (2012). Seizure modelling of Pb(II) and Cd(II) from aqueous solution by chemically modified sugarcane bagasse fly ash: isotherms, kinetics, and column study. *Environment Science and Pollution Research,* 20(4), 2193-2209.

Saha, P., & Chowdhury, S. (2011). *Insight into Adsorption Thermodynamics,* Vienna, Austria, InTech.

Saha, P., & Paul, B. (2016). Assessment of Heavy Metal Pollution in Water Resources and their Impacts: A Review. *Journal of Basic and Applied Engineering Research*, 3(8), 671-675.

Saha, P., Shinde, O., & Sarkar, S. (2017). Phytoremediation of industrial mines wastewater using water hyacinth. *International Journal of Phytoremediation*, 19(1), 87-96.

Sakakibara, M., Sugawara, M., Sano, S., & Sera, K. (2013). Phytoremediation of heavy metal-contaminated river water by aquatic macrophyte *Eleocharis acicularis* in a mine site, southwestern Japan. *NMCC Annual Report*, 20, 226-233.

Sarala, K., & Rao P.R. (1993). Endemic fluorosis in the village Ralla Anantapuram in Andhra Pradesh: An epidemiological study. *Fluoride*, 26, 177-180.

Sarumathy, K., Dhana Rajan, M. S., Vijay, T., & Dharani, A. (2011). In Vitro Study on Antioxidant Activity and Phytochemical Analysis of *Caesalpinia Sappan. International Journal of Institutional Pharmacy and Life Sciences,* 1(1), 31-39.

Sarvari, E., Fodor, F., Czech, E., Varga, A., Zaray, G., & Zolla, L. (1999). Relationship between changes in ion content of leaves and chlorophyll-protein composition in cucumber under Cd and Pb stress. *Zeitschrift für Naturforschung C,* 54, 746-753.

Satpati, G. G., & Pal, R. (2015). *Trentepohlia sundarbanensis* sp. nov. (Trentepohliaceae, Ulvophyceae, Chlorophyta), a new chlorophyte species from Indian Sundarbans. *Phykos,* 45 (1), 1-4.

Saxena, K. L., & Sewak, R. (2015). Fluoride Consumption in Endemic Villages of India and Its Remedial Measures. *International Journal of Engineering Science Invention*, 4(1), 58-73.

Sdiri, A., & Higashi, T. (2013) Simultaneous removal of heavy metals from aqueous solution by natural limestones. Applied Water Science. 3:29-39. doi:10.1007/s13201-012-0054-1

Selvakumari, G., Murugesan, M., Pattabi, S., & Sathishkumar, M. (2002). Treatment of electroplating industry effluent using maize cob carbon. *Bulletin of Environmental Contamination Toxicology*, 69,195-202.

Sherene, T. (2010). Mobility and transport of heavy metals in polluted soil environment. *Biological Forum - An International Journal,* 2(2), 112-121.

Shiowatana, J., McLaren, R. G., Chanmekha, N., & Samphao, A. (2001). Fractionation of arsenic in soil by a continuous flows sequential

extraction method. *Journal of Environmental Quality,* 30(6), 1940-1949.

Shortt, H. E., Pandit, C. G., & Raghavachari T. N. S. (1937). Endemic fluorosis in the Nellore District of South India. *Indian Medical Gazette*, 72, 396-98.

Singanan, M. (2013). Defluoridation of drinking water using metal embedded biocarbon technology. *International Journal of Environmental Engineering*, 5(2), 150-160.

Singh, A., & Prasad, S. M. (2015). Remediation of heavy metal contaminated ecosystem: an overview on technology advancement. *International Journal of Environmental Science and Technology,* 12, 353-366. doi 10.1007/s13762-014-0542-y

Singh, D., Tiwari, A., & Gupta, R. (2012). Phytoremediation of lead from wastewater using aquatic plants. *Journal of Agriculture, Science and Technology,* 8, 1-11.

Singh, G., Kumar, B., Sen, P. K., & Majumdar, J. (1999). Removal of fluoride from spent pot liner leachate using ion exchange. *Water Environment Research*, 71(1), 36-42.

Singh, T. P., & Majumder, C. B., (2015). Kinetics for removal of fluoride from aqueous solution through adsorption from Mousambi peel, Ground nut shell and Neem leaves. *International Journal of Science, Engineering and Technology*. 3(4), 879-883.

Singh, T.P., & Majumder, C. B. (2016). Comparing Fluoride Removal Kinetics of Adsorption Process from Aqueous Solution by Biosorbents. *Journal Asian Journal of Pharmaceutical and Clinical Research*, 9(4), 108-112.

Sobhanardakani, S., Taghavi, L., Behzad Shahmoradi, B. & Jahangard, A. (2017). Groundwater quality assessment using the water quality pollution indices in Toyserkan Plain. *Environmental Health Engineering and Management Journal*, 4(1), 21–27. doi:10.15171/EHEM.2017.04

Soltan, M, E., & Rashed, M, N. (2003). Laboratory study on the survival of water hyacinth under several conditions of heavy metal concentrations. *Advances in Environmental Research*, 7, 321-334.

Song, X., Yan, D., Liu, Z., Chen, Y., Lu, S., & Wang, D. (2011). Performance of laboratory-scale constructed wetlands coupled with micro-electric field for heavy metal-contaminating wastewater treatment. *Ecological Engineering,* 37, 2061-2065.

Song, X., Yan, D., Liu, Z., Chen, Y., Lu, S., & Wang, D. (2011). Performance of laboratory-scale constructed wetlands coupled with micro-electric field for heavy metal-contaminating wastewater treatment. *Ecological Engineering*, 37, 2061- 2065.

Subramanyam, B., & Das, A. (2014). Linearised and non-linearised isotherm model's optimization analysis by error functions and statistical means. *Journal of Environmental Health Science & Engineering*, 12, 92. doi:10.1186/2052-336X-12-92

Sumiahadi, A., & Acar, R. (2018). A review of phytoremediation technology: heavy metals uptake by plants. *IOP Conference Series: Earth and Environmental Science,* 142. doi :10.1088/1755-1315/142/1/012023

Sun, Y., Zhou, Q., An, J., Liu, W., & Liu, R. (2009). Chelator-enhanced phytoextraction of heavy metals from contaminated soil irrigated by

industrial wastewater with the hyperaccumulator plant (*Sedum alfredii Hance). Geoderma,* 150(1-2), 106-112.

Sune, N., Sanchez, G., Caffaratti, S., & Maine, M. A. (2007). Cadmium and chromium removal kinetics from solution by two aquatic macrophytes. *Environmental Pollution*, 145, 467-473.

Susheela, A. K., (1999). Fluorosis Management Programme in India. *Current Science*, 77 (10), 1250-1256.

Susheela, A. K., Kumar, A., Bhatnagar, M., & Bahadur, M. (1993). Prevalence of endemic fluorosis with gastro intestinal manifestations in people living in some north Indian villages. *Fluoride,* 26, 97-104.

Swain, G., Adhikari, S., & Mohanty, P. (2014). Phytoremediation of Copper and Cadmium from Water Using Water Hyacinth, *Eichhornia crassipes*. *International Journal of Agricultural Science and Technology,* 2 (1), 1-7.

Taghipour, H., Mosaferi, M., Pourakbar, M., & Armanfar, F. (2012). Heavy Metals Concentrations in Groundwater Used for Irrigation. *Health Promotion Perspectives*. 2(2): 205–210. doi:10.5681/hpp.2012.024

Taiwo O. I., Babajide, S. O., Taiwo A. A., Osunkiyesi, A. A., Akindele, O. I., & Sojobi O. A. (2015). Phytoremediation of Heavy Metals (Cu, Zn, and Pb) Contaminated Water Using Water Hyacinth (*Eichornia Crassipes*). *IOSR Journal of Applied Chemistry*, 8(5), 65-72.

Tangahu, B. V., Abdullah, S. R. S., Basri, H, Idris, M., Anuar, N., & Mukhlisin, M. (2011). A Review on Heavy Metals (As, Pb, and Hg) Uptake by Plants through Phytoremediation. *International Journal of Chemical Engineering,* 31. doi:10.1155/2011/939161.

Temkin, M. J., & Pyzhev, V. (1940). Recent modifications to Langmuir isotherms, *Acta Physicochimica URSS,* 12, 217–222.

Tempkin, M. I., & Pyzhev, V. (1940). Kinetics of ammonia synthesis on promoted iron catalyst, Acta Physicochimica U.R.S.S, 12, 327–356.

Thatai, S., Khurana, P., Boken, J., Prasad, S., & Kumar, D. (2014). Nanoparticles and core–shell nanocomposite based new generation water remediation materials and analytical techniques: a review. *Microchemical* Journal, 116, 62-76.

Tor, A., Cengeloglu, Y., Aydin, M. E., & Ersoz, M. (2006). Removal of phenol from aqueous phase by using neutralized red mud. *Journal of Colloid and Interface Science*. 300, 498-503.

Tran, H. N., You, S. J., & Chao, H. P. (2016). Thermodynamic parameters of cadmium adsorption onto orange peel calculated from various methods: A comparison study. *Journal of Environmental Chemical Engineering,* 4, 2671–2682.

Tripathi, A., & Ranjan, M. R. (2015). Heavy Metal Removal from Wastewater Using Low Cost Adsorbents. *Journal of Bioremediation and Biodegradation,* 6(6), 315. doi:10.4172/2155-6199.1000315

Trivedi, S., & Ansari, A.A. (2015). Molecular Mechanisms in the Phytoremediation of Heavy Metals from Coastal Waters. In A.A. Ansari et al. (Eds.), *Phytoremediation Management of Environmental Contaminants* (Vol. 2, pp. 219-231), Switzerland: Springer International Publishing Switzerland.

U. S. Department of Energy. (1994). Summary report of a workshop on phytoremediation research needs (Report no. DOE/E M-0224). U. S. Department of energy, Santa Rosa, California.

Ullah, A., Mushtaq, H., Ali, H., Munis, M, F, H., Javed, M, T, & Chaudhary, H, J. (2014). Diazotrophs-assisted phytoremediation of heavy metals: a novel approach. *Environment Science and Pollution Research*, 22, 2505-2514.

UN. (2013). *The Report of the High-Level Panel of Eminent Persons on the Post-2015 Development Agenda.* United Nations, New York.

UNEP GEMS/Water Programme. (2008). *Water Quality for Ecosystem and Human Health*. 2nd Edition, United Nations Environment Programme Global Environment Monitoring System (GEMS)/Water Programme, Canada.

UNEP. (2010). *Clearing the Waters: A focus on water quality solutions.* United Nations Environment Programme, Nairobi, Keniya.

UNEP. (2010). *Final review of scientific information on lead*. United Nations Environment Programme, Chemicals Branch, DTIE.

UNICEF. (1999). *States of the art report on the extent of fluoride in drinking water and the resulting endemicity in India.* Report by fluorosis and rural development foundation for UNICEF, New Delhi.

USEPA. (1999). SW-846, Reference Methodology. Standard opening procedure for the digestion of soil/ sediment sample using a hot plate/beaker digestion technique, Chicago

USEPA. (2000). *Introduction to Phytoremediation* (Report No. EPA/600/R-99/107). National Risk Management Research Laboratory, U. S. Environmental Protection Agency, Washington DC. http://www.clu-in.org/download/remed/introphyto.pdf.

Varier, P. S. (1996). *Indian medicinal plants: A compendium of 500 species*, (pp. 1-5). Madras, Orient Longman Ltd.

Verkleij, J. A. C., & Schat, H. (1990). Mechanisms of metal tolerance in higher plants. In: Shaw AJ (Ed.), *Heavy metal tolerance in plants: evolutionary aspects* (pp. 179-193). Boca Raton: CRC Press.

Verma, R., & Dwivedi, P. (2013). Heavy metal water pollution- A case study. *Recent Research in Science and Technology,* 5(5), 98-99.

Vink, R., Behrebdlt, H. & Salmons, W. (1999). Development of the heavy metal pollution trends in several European Rivers: an analysis of point and diffuse sources. *Water Science and Technology*, 39(12), 215-223. Retrieved from http://dx.doi.org/10.1016/S0273-1223(99)00338-8

Volesky, B. & Holan, Z. R. (1995). Biosorption of heavy metals. *Biotechnology Progress*, 11(3), 235-250.

Volesky, B. (1994). Advances in biosorption of metals: selection of biomass types. *FEMS Microbiology Reviews*, 14(4), 291-302.

Wahab, A, S, A., Ismail, S, N, S., Praveena, S, M., & Awang, S. (2014). Heavy metals uptake of Water mimosa (*Neptuniaoleracea*) and its safety for human consumption. *Iranian Journal of Public Health*, 43(3), 103-111.

Wani, R. A., Ganai, B. A., Shah, M. A., & Uqab, B. (2017). Heavy Metal Uptake Potential of Aquatic Plants through Phytoremediation Technique - A Review. *Journal of Bioremediation and Biodegradation,* 8, 4. doi: 10.4172/2155-6199.1000404

Warriers, P. K, Nambiar, V. P. K., & Ramankutty, C, (1993). In P. S. Vaidhyarathnam Varriers (Ed). *Indian Medicinal Plants, A compendium of 500 species* (Vol. 1, pp. 291-294). Chennai, Tamil Nadu, Orient Longman LTD.

Weber, W. J., & Morris, J. C. (1963). Kinetics of adsorption of carbon from solution. *Journal of the Sanitary Engineering Division*, 33, 317.

Weiliao, S., & Chang, W, L. (2004). Heavy metal phytoremediation by water hyacinth at constructed wetlands in Taiwan. *Journal of Aquatic Plant Management Society*, 42, 60-68.

WHO. (2011). Guidelines for Drinking-water Quality, fourth ed. World Health Organization

WHO/UNICEF. (2013). *Progress on Sanitation and Drinking-Water: 2013 Update.* World Health Organization/United Nations Children's Fund, New York.

Wu, F. Y. & Sun, E. J. (1998). Effects of Copper, Zinc, Nickel, Chromium and Lead on the growth of water convolvulus in water culture. *Journal of Environmental Protection*, 21(1), 63-72.

Wu, Y. F., Liu, C. Q., & Tu, C. L. (2008). Atmospheric deposition of metals in TSP of Guiyang, PR China. *Bulletin of environmental contamination and Toxicology,* 80(5), 465–468.

Wuana, R. A., & Okieimen, F. E. (2011). Heavy Metals in Contaminated Soils: A Review of Sources, Chemistry, Risks and Best Available Strategies for Remediation. *ISRN Ecology,* 20. doi:10.5402/2011/402647

Xinshan, S., Denghua, Y., Zhenhong, L., Yan, C., Shoubo, L & Daoyuan, W. (2011). Performance of laboratory-scale constructed wetlands coupled with micro-electric field for heavy metal-contaminating wastewater treatment. *Ecological Engineering*, 37, 2061- 2065.

Xu, L., Xiao, L. S., & Zhang, Q. X. (2002) Overall treatment of process effluent from ammonium molybdate. *Rare Metals and Cemened Carbides*, 38, 6-8.

Xu, P., Zeng, G. M., Huang, D. L., Feng, C. L., Hu, S., Zhao, M. H., Cui Lai, C., Wei, Z., Huang, C., Xie, G. X., & Liu, Z. F. (2012). Use of iron oxide nanomaterials in wastewater treatment: A review. *Science of the Total Environment*, 424, 1-10.

Yaacoubi, H., Songlin, Z., Mouflih, M., Gourai, M., & Said Sebti, S. (2015). Adsorption isotherm, kinetic and mechanism studies of 2-nitrophenol on sedimentary phosphate. *Mediterranean Journal of Chemistry,* 4(4), 289-296.

Yang, F., Hong, F., You, W., Liu, C., Gao, F., Wu, C & Yang, P. (2006). Influences of nano-anatase TiO_2 on the nitrogen metabolism of growing spinach. *Biological Trace Element Research*, 110 (2), 179-190.

Yapoga, S., Ossey, Y, B., & Kouame, V. (2003). Phytoremediation of zinc, cadmium, copper and chrome from industrial wastewater by *Eichhornia crassipes*. *International Journal of Conservation Science*, 4(1), 81-86.

Ye, M., Xie, W., Lei, F., Meng, Z., Zhao, Y., Su, H., & Du, L. (2006). Brazilein, an important immunosuppressive component from Caesalpinia sappan L. *International Immunopharmacology*, 6, 426-432.

Zayed, A., Gowthaman, S., & Terry, N. (1998). Phytoaccumulation of trace elements by wetland plants: I. Duckweed. *Journal of Environmental Quality*, 27, 715-721.

Zengin, F, K., & Munzuroglu, O. (2005). Effects of some heavy metals on content of chlorophyll, proline and some antioxidant chemicals in bean (*Phaseolus vulgaris L.*) Seedlings. *Acta Biologica Cracoviensia Series Botanica*. 47(2), 157-164.

Zheng, H., Liu, D., Zheng, Y., Liang S., & Liu, Z. (2009). Sorption isotherm and kinetic modeling of aniline on Cr-bentonite. *Journal of Hazardous Materials,* 167, 141-147.

Zheng, H., Wang, Y., Zheng, Y., Zhang, H., Liang, S., & Long, M. (2008). Equilibrium, kinetic and thermodynamic studies on the sorption of 4-hydroxyphenol on Cr-bentonite. *Chemical Engineering Journal,* 143, 117-123.

Zheng, L., Hong, F., Lu, S & Liu, C. (2005). Effect of nano-TiO_2 on strength of naturally aged seeds and growth of spinach. *Biological Trace Element Research*, 104, 83-91.

Zhong, L. S., Hu, J. S., Liang, H. P., Cao, A. M., Song, W. G., & Wan, L. J. (2006). Self-assembled 3D flower like iron oxide nano structures and their application in water treatment. *Advanced Materials,* 18(18), 2426-2431.

Zhou, X., & Zhou, X. (2014). The unit problem in the thermodynamic calculation of adsorption using the Langmuir equation. *Chemical Engineering Communications*, 201 (11), 1459-1467.

Zhu, Y, l., Zayed A, M., Qian, J, H., Souza, M., & Terry, N. (1999). Phytoaccumulation of trace elements by wetland plants: II. Water hyacinth. *Journal of Environmental Quality*, 28, 339-344.

ANNEXURE I

LIST OF PUBLICATIONS

Publications related to the topic of research:

- Harikumar, P. S., & Megha, T. (2017). Treatment of heavy metals from water by electro-phytoremediation technique. *Journal of Ecological Engineering*, 18(5), 8-17. doi: 10.12911/22998993/76208

- Harikumar, P. S., & Megha, T. (2017). Treatment of cadmium, lead and copper using phytoremediation enhanced by Titanium dioxide nanoparticles. *Eco-chronicle*, 12(2), 25-34.

- Megha, T., & Harikumar, P. S. (2013). Immobilization and mobilization effect of ammonium molybdate on phytoremediation of toxic heavy metals in soil. *Acta Biologica Indica*, 2(1), 353-360.

- Harikumar, P.S., Jaseela, C., & Megha, T. (2012). Defluoridation of water using biosorbents. *Natural Science*. 4(4), 245-251. doi:10.4236/ns.2012.44035

Other publication in the field of Environmental Science:

- Harikumar, P. S., Jesitha, K., Megha, T., & Kamalakshan, K. (2014). Persistence of Endosulfan in selected areas of Kasaragod district, Kerala. *Current Science*, 106(10), 1421-1429.

ANNEXURE II

LIST OF PAPER PRESENTATIONS

(*National / International Conferences*)

- Megha, T., & Harikumar, P. S. (2014). *Electrically enhanced phytoremediation of heavy metals.* Proceedings of the International Symposium on Integrated Water Resources Management, 19-21 February 2014, Centre for Water Resources Development and Management, Kozhikode, Kerala.

- Megha, T., & Harikumar, P. S. (2012). *Immobilization and Mobilization Effect of Ammonium Molybdate on Phytoremediation of Toxic Heavy Metals in Soil*. Proceedings of the Second National Symposium on Innovative Approaches and Modern Technologies for Crop Productivity, Food Safety and Environmental Sustainability, 19-20 November 2012, Thrissur, Kerala

TREATMENT OF HEAVY METALS FROM WATER BY ELECTRO-PHYTOREMEDIATION TECHNIQUE

Harikumar Puthenveedu Sadasivan Pillai[1*], Megha Tharayil[1]

[1] Water Quality Division, Centre for Water Resources Development and Management, Kozhikode – 673571, Kerala, India

*[1]Corresponding author's e-mail: hps@cwrdm.org

ABSTRACT

The performance of electrically stimulated phytoremediation in the removal of lead, cadmium and copper was assessed in this study. A combination of phyto and electro remediation was attempted in this study for the remediation of the metals from water. Three tanks were set up with different operating conditions for this experiment: control A (only phytoremediation system), control B (only electro remediation) and treatment (combination of phyto and electro remediation). The electrically enhanced phytoremediation system and electro remediation system were operated 2h/day at voltages of 4V for 25 days continuously. In this experiment, the *Eichhornia crassipes,* an able phyto-remediator exhibited efficient and fast removal of heavy metals from synthetic solution in electro assisted phytoremediation system. The electrically enhanced phytoremediation using aluminum sheet electrodes showed better and effective removal of Cd, Pb and Cu than aluminum rod electrodes. A more favorable and moderate increase of pH was noticed in electrically stimulated phytoremediation system. *Eichhornia crassipes* has a tremendous potential to reduce the maximum amount of cadmium (within 15 days), lead (within 15 days) and copper (within 10 days) under electrically stimulated condition. Under electrified condition, maximum amount of Cd and Cu was accumulated in the aerial parts of *Eichhornia crassipes* but maximum concentration of Pb was attained by roots. This indicates the high heavy metal accumulation capacity of *Eichhornia crassipes* under electrified conditions. The results showed that 4V voltage is probably suitable to stimulate the *Eichhornia crassipes* to synthesize more chlorophyll and voltage can improve the growth and ability to resist adverse circumstances by promoting chlorophyll synthesis. *Eichhornia crassipes* stimulated by an electric field has grown better and assimilated more metal. Bioconcentration factor (BCF) an index of hyperaccumulation, indicates that electrically stimulated *Eichhornia crassipes* is a good hyper accumulator of Cd (BCF = 1118.18) and Cu (BCF = 1152.47) and a moderate accumulator of Pb (BCF = 932.26). Translocation ability (TA) ratio indicates that *Eichhornia crassipes* have the ability to translocate more amounts of Pb, Cd and Cu to its upper portion under electrified condition. The results imply that the electro-phytoremediation technique seems to be promising in the treatment of wastewater contaminated with heavy metals.

Keywords: phytoremediation, *Eichhornia crassipes,* bioconcentration factor, translocation ability

INTRODUCTION

Rising levels of heavy metals in the environment, their entry into food chain and their overall consequences are of great concern to scientific community in the field of environmental science. The remediation of toxic heavy metals from wastewaters is recognized as one of the most important fields of water treatments, since the extreme industrial activities creates many

dangerous pollution issues to the environment [Li et al. 2009]. Cadmium and lead are commonly encountered hazardous heavy metals and are in the EPA's list of priority pollutants [Baziar et al. 2013]. The UNEP considers lead and cadmium as the non-essential element for human life but they can compete with the essential trace elements either for the transport systems or in binding to various biomolecules. Both can accumulate in bone and may serve as a source of exposure later in life. Cadmium is a carcinogen by inhalation and is mainly affects kidneys and the skeleton. Lead is a multi-organ system toxicant and is noxious at very low exposure levels. The duration, level and timing of exposure are the factors which depends the type and severity of effects. Tri-alkyl-lead and tetra-alkyl-lead compounds are the organo-lead compounds which are more toxic than inorganic forms of lead [UNEP, 2010].

Extensive researches have been progressing for the removal of heavy metals by various methods such as ion exchange, filtration, reverse osmosis, biosorption, chemical precipitation, electrochemical treatment, solvent extraction, sedimentation, membrane separation, sensors etc. Many existing treatment techniques are not designed to address today's concerns because of its incomplete metal uptake at low level and expensive operational costs [Shah et al. 2012]. For the better availability of good water quality at a lesser cost, it is obligatory to develop some sustainable alternative treatment methods, which are more natural, novel and cost effective. Phytoremediation utilizes the advantages of the unique, selective and naturally occurring uptake capabilities of plant root systems, together with the translocation, bioaccumulation and pollutant storage/degradation abilities of the entire plant body. Also, being aesthetically pleasing, phytoremediation is on average tenfold cheaper than other remediation methods like physical, chemical or thermal. It can also be performed in situ, is solar driven and can required minimal maintenance once established [Hooda, 2007]. Phytoremediation has also been known as green remediation, botano-remediation, agro remediation and vegetative remediation [Andrew, 2007]. Phytoremediation is a plant assisted bioremediation technique, utilized to treat contaminated water and soil, including the processes like phytoextraction, phytodegradation, phytovolatilization, phytostabilization, rhizodegradation, phy-

toreducation, phytostimulation, phytooxidation and phytotransformation [Ullah et al. 2014].

Utilization of AMATS (aquatic macrophytes treatment systems) for the phytoremediation of heavy metals and other pollutants is a well-established and cost effective environmental protective technique [Mahmood et al. 2005]. Copper can become extremely toxic due to leaf chlorosis, suppressed root growth and inhibit photosynthesis and reproduction of plants, when present in excessive amount, even though it is an essential micronutrient for plant metabolism. Lead diminishes chlorophyll production and cadmium toxicity also lead to some extremely sever effects on plants [Swain et al. 2014; Hammad, 2011 and Ashraf et al. 2011]. Heavy metals can create stressful conditions to the plants and their growth becomes limited or impossible and this can influence the phytoremediation. So, in our study we tried to enhance the phytoremediation capacity of *Eichhornia crassipes* to treat heavy metals by using electric current. The purpose of this study was to investigate the removal of lead, cadmium and copper in simulated wastewater by a phytoremediation system coupled with electric field.

MATERIALS AND METHODS

Preparation of synthetic heavy metals solution

The simulated wastewater was made by dissolving $Pb(NO_3)_2$, $CuSO_4 \cdot 5H_2O$, and $(3CdSO_4) \cdot 8H_2O$ in tap water. All chemicals used were of the highest purity available and of analytical grade procured from Merck. The initial heavy metal concentrations of the simulated wastewater were determined by Atomic Absorption Spectrophotometer.

Collection of plant for this study

A fast-growing perennial aquatic plant and prolific free-floating aquatic weed, *Eichhornia crassipes* (Water hyacinth) was used for the treatment of heavy metals in this experiment. Young plants of *Eichhornia crassipes* were collected from Kottooli wetland in Kozhikode City. *Eichhornia crassipes* can easily adapt to several aquatic conditions and perform an important role in extracting and accumulating many metals from water. Hence, it is utilized as an ideal

candidate for the phytoremediation of toxic trace elements from variety of water bodies [Weiliao and Chang, 2004]. Collected plants were put in a hydroponic system containing tap water, for acclimatization period, before being exposed to heavy metal contaminants.

Experimental design and sampling strategy

Three tanks (45×30×15 cm) were setup with different operating conditions.

Tank 1**: Control A** (with plant and without electric current)

Tank 2: **Control B** (without plant and with electric current)

Tank 3: **Treatment** (with plant and with electric current)

Twelve liters of synthetic heavy metal solution was taken in each tank. An electric power supply (DC) was used for providing constant voltage between working electrodes (i.e. in control B and treatment). Initially, aluminum rods (0.10 m height,0.019 m breadth and 2.04 mm thickness) and sheets (0.15 m height, 0.10 m breadth and 0.2 mm thickness) were used as electrodes and both indoor and outdoor experiments were also conducted. Based on the results and condition of the plant, outdoor experiment using aluminum sheets as electrodes were preferred for further study. To remove the oxide and passivation layer from aluminum surface, the electrodes were rubbed with sandpaper and energized by dipping them in 5N HCl for 1 minute. The electrodes in the tanks were positioned vertically. Plants were placed very close to the electrodes. 0.01M KCl was used as supporting electrolyte. Circulation of water was maintained using a submersible pump. The experimental setup is depicted in Figure 1. Different voltages: 2V, 3V, 4V and 5V were operated 2 h/day for 10 days. Due to the formation of bubbles and heat generation, phytoremediation system operated at a voltage of 5V was stopped after 2 days. From the results obtained, 4V was selected as an optimum voltage for further experiment. The experiment was operated 2h/day at voltages of 4V for 25 days continuously. All the units were operated outdoors. Water samples were taken in every 5 days at about 10:30 A.M. On every sampling day, pH, EC, TDS and temperature were measured by using PCS Testr35 instrument. When the experiment was finished, plants from two units (control A and treatment) were sampled and dried in a hot air oven. The residual Pb, Cd and Cu concentrations in water were determined by Atomic Absorption Spectroscopy AAS (Thermo Series) with GF 95.

ANALYTICAL PROCEDURES

20mL of water samples were taken from each tank in every 5 days at around 10:30 A.M. Plant samples were collected at the end of the experiment and rinsed using tap water twice and deionized water thrice. The *Eichhornia crassipes* samples were divided into leaves, stems and roots. Plant samples were oven-dried for 48 h at 70ºC. The oven-dried sample was ground to pass through a 100-mesh sieve and homogenized plant tissues were digested with HNO_3–$HClO_4$ (4:1) mixture and filtered. For quantification of heavy metals, the water samples and digested plant samples were analyzed with Atomic Absorption Spectrophotometer (Thermo Series) with GF 95. Chlorophyll (chl.a + chl.b, CHLab) was determined by optical density values (663 nm and 645 nm using UV-Visible spectrophotometer, Thermo Evolution 201) of extracting solution, which was made by adding 80% acetone into grinding solution of 0.5 g of fresh leaves [Song et al. 2011].
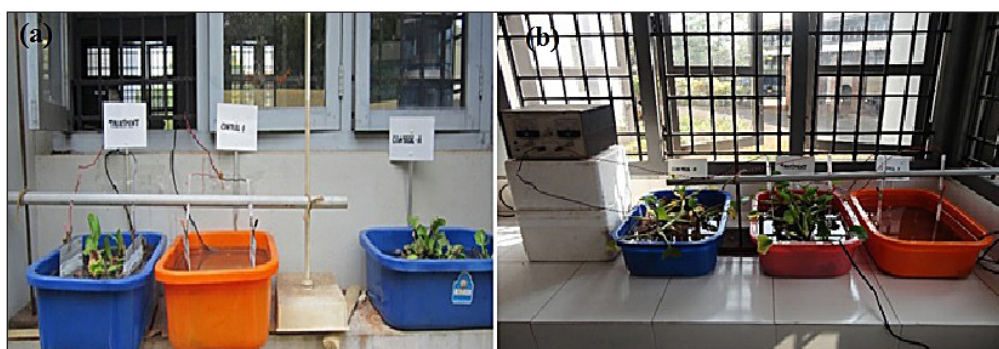

Figure 1. Experimental setup: (a) outdoor experiment and (b) indoor experiment

DATA ANALYSIS

The bioconcentration factor (BCF) and translocation ability (TA) are the factors used to evaluate the mobility of the heavy metals from the polluted substrate into the roots of the plants and their ability to translocate the metals from roots to the harvestable aerial part. The translocation ability indicates the efficiency of the plant in translocating the accumulated metal from its roots to the upper part of the plant. Translocation ability (TA) was calculated by dividing the concentration of a trace element accumulated in the root tissues by that accumulated in shoot/leaf tissues [Liao and Chang, 2004]. TA is given by,

$$TA = (A_r / A_s) \quad (1)$$

where TA is the translocation ability and is dimensionless. A_r represents the amount of trace element accumulated in the roots (mg kg^{-1} dry wt), and A_s represents the amount of trace element accumulated in the shoot/leaf (mg kg^{-1} dry wt). A larger TA ratio implies poor translocation capability. The bioconcentration factor (BCF) was calculated as the ratio of the trace element concentration in the plant tissues to the concentration of the element in the external environment [Liao and Chang, 2004]. BCF is given by,

$$BCF = (P / E) \quad (2)$$

where BCF denotes the bioconcentration factor and is dimensionless. P represents the trace element concentration in plant tissues (mg kg^{-1} dry wt); E represents the trace element concentration in the water (mg/L) or in the sediment (mg kg^{-1} dry wt). A larger ratio implies better phytoaccumulation capability. All the tests were conducted in triplicates and the data were statistically analyzed.

RESULTS AND DISCUSSION

Removal of lead, cadmium and copper from synthetic solution using electro-phytoremediation system

The initial values of the pH, EC and TDS of the synthetic solution were found to be 6.29 ± 0.01, 274 ± 1.2μS/cm and 193 ± 0.78 mg/L respectively. The initial heavy metal concentra-

tions of simulated water are summarized in Table 1. The metals like Fe^{2+}, Mn^{2+}, Ni^{2+} and Zn^{2+} were found to be within the permissible limit.

Four different voltages 2V, 3V, 4V and 5V were applied for 2h/day for 10 days. We did not continue the experiment in which 5V was applied due to the formation of bubbles and heat generation. Maximum removal of Cd, Pb and Cu was observed in phytoremediation system operated at 4V for 10 days. So 4V was applied for further experiments. The plants used in outdoor experiment had grown better than the plants in indoor experiment due to the presence of sunlight. So after one week, the indoor experiment was discontinued. Treatment of lead, cadmium and copper from synthetic solution using electrically enhanced phytoremediation system was conducted using Al rod and Al sheet as electrodes and the results were compared.

Variation of pH

pH changes were recorded during every 5 days and the variations were depicted in Figure 2. No significant change in pH was observed in control A (phytoremediation system) during study. In both experimental sets (i.e., in experiments using Al rod and Al sheet as electrodes), control A presented a lower pH than control B (electro-remediation system) and treatment (electrically stimulated phytoremediation). With electrical exposure, an increase in pH was observed in control B and treatment. The OH$^-$ concentration in solution increases while electrolysis is taking place, which resulted in an increase in pH [Song et al. 2011].

Removal performance of heavy metal by electrically stimulated phytoremediation system

The residual concentrations of Cd, Pb and Cu in water collected from control A, control B and treatment are summarized in Table 2. In the experiment, where aluminum sheets were used as electrodes, the electro assisted phytoremediation system (i.e. treatment) reduced 100% of cadmium within 15 days, while in control A and control B, 48.21 ± 1.8 and 84.24 ± 1.7% of cadmium reduc-

Table 1. Initial concentration of heavy metals in synthetic solution

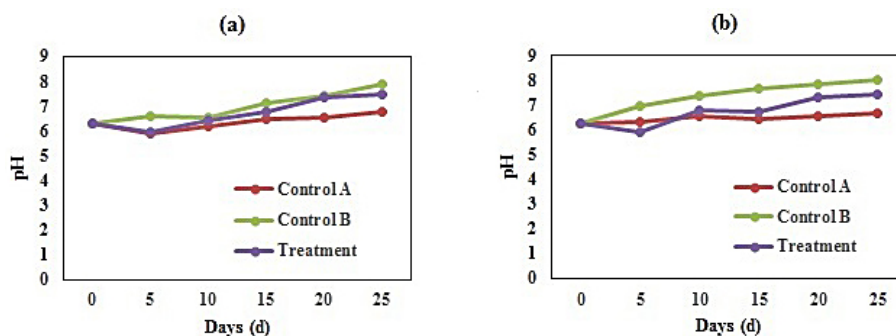| Heavy metal	Cd	Pb	Cu	Fe	Mn	Ni	Zn
(mg/L)	18.86 ± 0.4	20.34 ± 0.23	19.77 ± 0.54	0.26 ± 0.05	0.02 ± 0.003	0.04 ± 0.001	0.16 ± 0.021

Figure 2. Variation of pH during the study (a) Aluminum rods as electrodes (b) Aluminum sheets as electrodes

tion was observed after 25 days of experiment. Maximum Cd was removed within a short period in electro assisted phytoremediation system. The order of removal efficiency of Cd is Treatment > Control B > Control A. Maximum removal of lead was attained by electrically stimulated phytoremediation system within 15 days. After 25 days, it was observed that 66.67 ± 1.2 and 81.51 ± 0.7% of lead was removed in control A and control B respectively. The result indicated that, electrically coupled phytoremediation system exhibited better efficiency than phytoremediation system and electrolysis system in lead removal. The electrically stimulated phytoremediation system attained 100% of copper removal within 10 days and took only 5 days to attain a reduction of 99.94 ± 0.004 %. The results indicated that, in

control A and control B, removal of copper was found to be 89.93 ± 1.6 % and 99.98 ± 0.003% respectively after 25 days. This result also showed that electrically stimulated *Eichhornia crassipes* can exhibit maximum removal efficiency for copper from water.

In the experiment where aluminum rod was used as electrode, maximum concentration of lead was removed in electro assisted phytoremediation system compared to control A and control B within 20 days. 96.96 ± 0.22 % of cadmium and 99.97 ± 0.01% copper was eliminated by electro assisted phytoremediation system from water within 15 days. The electro assisted phytoremediation experiment where aluminum sheet was used as electrodes exhibited fast and better removal efficiency compared to the elec-

Table 2. The residual Cd, Pb and Cu concentrations in water

Metal	Days	Concentration of metals, mg/L					
		Aluminum sheet used as electrodes			Aluminum rod used as electrodes		
		Control A	Control B	Treatment	Control A	Control B	Treatment
Cd	0	18.86 ± 0.4	18.86 ± 0.4	18.86 ± 0.4	20.41 ± 0.45	20.41 ± 0.45	20.41 ± 0.45
	5	14.57 ± 0.1	11.23 ± 0.21	2.31 ± 0.12	15.34 ± 0.67	14.56 ± 0.21	6.22 ± 0.42
	10	12.56 ± 0.3	8.74 ± 0.15	0.56 ± 0.14	13.42 ± 0.39	11.87 ± 0.71	2.54 ± 0.34
	15	11.98 ± 0.45	6.41 ± 0.34	ND*	12.17 ± 0.47	9.13 ± 0.18	0.62 ± 0.05
	20	10.21 ± 0.23	5.32 ± 0.24	ND*	11 ± 0.19	7.20 ± 0.24	ND*
	25	9.77 ± 0.34	2.97 ± 0.33	ND*	9.36 ± 1.01	4.72 ± 0.37	ND*
Pb	0	20.34 ±0.23	20.34 ± 0.23	20.34 ± 0.23	19.18 ± 0.56	19.18 ± 0.56	19.18 ± 0.56
	5	15.54 ± 0.43	14.98 ± 0.28	7.45 ± 0.23	14.99 ± 0.29	14.35 ± 0.64	13.11 ± 0.74
	10	13.99 ± 0.25	11.97 ± 0.13	0.99 ± 0.12	13.69 ± 0.54	12.97 ± 0.64	9.35 ± 0.36
	15	12.98 ± 0.41	9.87 ± 0.17	ND*	11.52 ± 0.24	8.68 ± 0.35	3.14 ± 0.37
	20	8.01 ± 0.23	6.23 ± 0.53	ND*	9.55 ± 0.06	7.35 ± 0.25	ND*
	25	6.78 ± 0.25	3.76 ± 0.14	ND*	8.18 ± 0.30	4.39 ± 0.28	ND*
Cu	0	19.77 ± 0.54	19.77 ± 0.54	19.77 ± 0.54	19.34 ± 0.42	19.34 ± 0.42	19.34 ± 0.42
	5	11.06 ± 0.24	7.03 ± 0.31	0.01 ± 0.001	12.35 ± 0.81	11.25 ± 0.21	4.93 ± 0.24
	10	8.05 ± 0.32	2.01 ± 0.12	ND*	10.27 ± 0.38	9.08 ± 0.29	0.64 ± 0.34
	15	5.03 ± 0.45	1.62 ± 0.23	ND*	7.27 ± 0.62	5.60 ± 0.28	0.01 ± 0.002
	20	2.90 ± 0.27	0.09 ± 0.09	ND*	4.92 ± 0.38	3.52 ± 0.41	ND*
	25	1.99 ± 0.31	0.004±0.001	ND*	2.94 ± 0.20	1.78 ± 0.24	ND*

* Not detected

tro assisted phytoremediation system where aluminum rods were used as electrodes. In the case of cadmium, within 10 days, 97.05 ± 0.7% was reduced in electro assisted phytoremediation experiment where aluminum sheets were used as electrodes while only 87.56 ± 1.66% reduction was noticed in aluminum rod used in the experiment. Within 10 days, 95.13 ± 0.6% of lead was eliminated from water in the experiment where aluminum sheets were used, while Al rod removed only 51.25 ± 1.86% of lead. 99.94 ± 0.004% of copper was reduced by electro assisted phytoremediation experiment where aluminum sheet used as electrodes within 5 days but only a 74.49 ± 1.25% of reduction in copper was observed in aluminum rod used in the experiment. In control B also i.e., the system where only electrolysis is taking place, maximum removal of heavy metals was noticed when aluminum sheets were used as electrodes. The results indicate that the treatment of Cd, Pb and Cu using electrically enhanced phytoremediation using aluminum sheet electrodes is more effective than aluminum rod electrode. The treatment system (electrically enhanced phytoremediation using aluminum sheet electrodes) had more favorable conditions to accumulate heavy metals than did the control A (phytoremediation system), such as the higher pH, and the presence of aluminum ions, which caused chemical precipitation, physical adsorption and flocculation of metal. So, we had carried our further study using electrically enhanced phytoremediation using aluminum sheet electrodes.

Accumulation of cadmium, lead and copper in *Eichhornia crassipes*

For the detailed study, heavy metal accumulation in plants collected from control A and electrically enhanced phytoremediation system using aluminum sheet electrodes was analyzed. The segmentation of *Eichhornia crassipes* into root, stem and leaves was carried out. The accumulation of Cd, Pb and Cu in plant parts is shown in Figure. 3. The results indicated that maximum concentration of Cd, Pb and Cu were accumulated in *Eichhornia crassipes* collected from treatment (electrically enhanced phytoremediation) than in control A (phytoremediation). Cadmium is a toxic non-essential heavy metal and it can cause inhibitory effects on plant growth. Lu et al. 2004 reported that Cd can suppress the development of new roots and reduce the relative growth rates and substantially reduce the growth of *Eichhornia crassipes*. The control plant accumulated maximum level of Cd in its root but in treatment plant maximum accumulation was observed in leaf. This result indicates that *Eichhornia crassipes* can translocate maximum Cd to plants' aerial parts under electrified condition. Maximum concentration of Pb was attained by roots in both control A (5653.51 mg/Kg) and treatment (7532.4 mg/Kg) plant. Under electrified condition, more Pb content was translocated to its aerial part by the treatment plant compared to control A.

Copper (Cu) is one of the micronutrient, essential for plants at very low concentrations. However, excessive concentrations of this metal
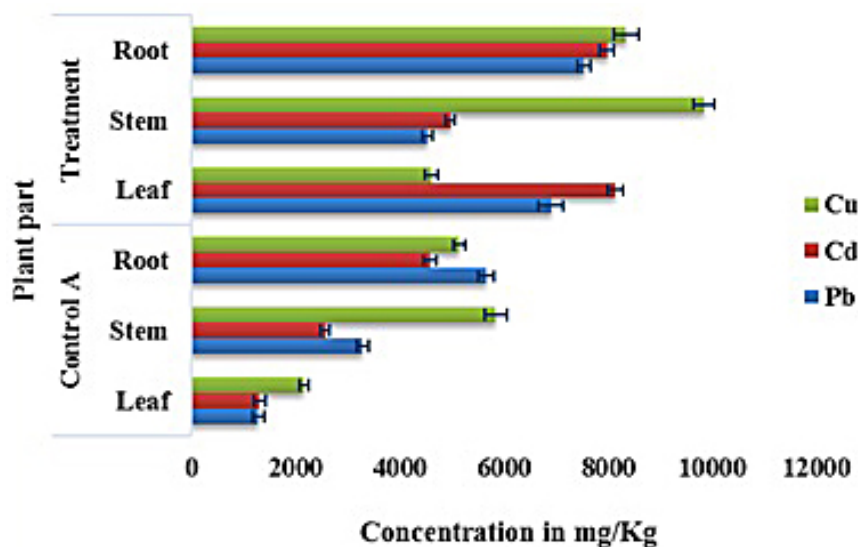

Figure 3. Accumulation of Cd, Pb and Cu in plant

are highly toxic. In both treatment (9842.76 mg/Kg) and control A (5845.68 mg/Kg), the highest value of Cu concentration was recorded in stem. Compared to control A, treatment plant accumulated more amount of Cu in its aerial part under electrified condition. Many studies revealed that *Eichhornia crassipes* accumulated more amount of heavy metals like Cd, Co, Cr, Cu, Mn, Ni, Pb and Zn in its roots than in the aerial parts [Soltan and Rashed, 2003]. But our results indicated that, metals like Pb, Cd and Cu are translocated to its areal parts under electrified condition. Many researchers reported the mechanisms of heavy metal removal in aquatic plants and mentioned that the main way of heavy metal uptake in emergent and surface-floating plants like *Eichhornia crassipes* was through the roots system. The heavy metal uptake in plants takes place by exchange of cations which occurred in the cell wall. The plants take up metals by absorption and translocation. The accumulation of heavy metals by plant tissue is by absorption to anionic sites in the cell walls. This is the reason why wetland plants can accumulate high magnitude of heavy metals in their pant parts compared to their surrounding environment [Lu et al. 2004].

Bioconcentration factor and translocation ability of electrically stimulated *Eichhornia crassipes*

The potential of plants for accumulating heavy metals was assessed by bioconcentration factor (BCF). The ratio between metal concentration in plant and that of the growth media expresses the bioconcentration factor (BCF), which indicates the affinity of aquatic macrophytes to a specific heavy metal or pollutant [Kabeer et al. 2014]. Bioconcentration factors of plant for Cd, Pb and Cu in the present study are graphically depicted in Figure 4. Higher BCF values reflect the higher phytoaccumulation ca-

pacity. Accumulation of metals by macrophytes can be affected by metal concentrations in water and the ambient metal concentration in water was the major factor influencing metal uptake efficiency. When metal concentration in water increases, the amount of metal accumulation in plants increases, but the BCF values decrease. The maximum BCF value for Cd under electrified condition was 1118.18, indicating that electrically stimulated *Eichhornia crassipes* is good hyper accumulator of Cd.

If the BCF value is more than or equal to 1000 then that plant species is considered as a hyper accumulator. The plant having the abilities to grow in very high concentration of metal and concentrating high heavy metals in their tissues are known as hyperaccumulators [Wahab et al. 2014]. The BCFs of control A for Pb, Cd and Cu were 502.65, 448.12 and 664.90 respectively. The BCFs for all the three metals were lower than 1,000 for control plant, i.e. plant grown under normal condition. The highest level of BCFs observed for Pb and Cu was 932.26 and 1152.47 respectively for treatment. In this study, with the BCF values of treatment plant was a little under 1000 for lead (BCF = 932.26), this suggests that electrically stimulated plant can be considered as a moderate accumulator for Pb. For copper this value exceeds 1000, so electrically stimulated *Eichhornia crassipes* is considered as a good hyper accumulator. From Figure 3, Pb accumulated by treatment plants were largely retained in roots. This indicates that *Eichhornia crassipes* used in the electrically stimulated phytoremediation system bioconcentrated more amounts of Pb in its roots than the aerial parts. Accumulation pattern of Cd can be elaborated as follows:

Control A: Root system >Stem system > Leaf system
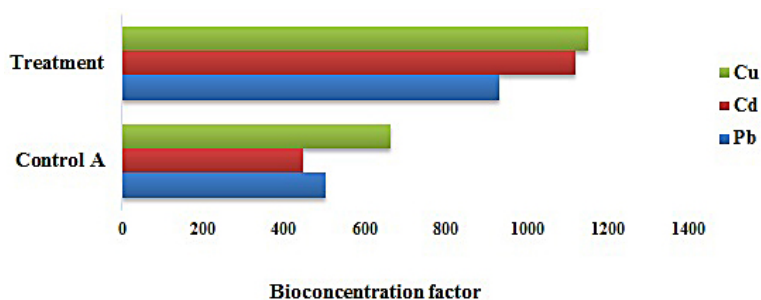
Treatment: Leaf system >Root system > Stem system

Figure 4. Bioaccumulation factors (BCF) of Pb, Cd and Cu in *Eichhornia crassipes*

This result indicates that under electrified condition, leaf can effectively bioconcentrate more amount of Cd than roots. Copper, a component of an electron carrier called plastocyanin is active during photosynthesis. It is also a constituent of ascorbic acid oxidase, tyrosinase, and phenoloxidase [Yapoga et al. 2013]. For both phytoremediation system and electrically stimulated phytoremediation system, maximum copper was bioconcentrated in stems of *Eichhornia crassipes*. Under electrified condition, more amount of copper accumulation was observed. Accumulation pattern of Cu can be observed as follows:

Control A: Stem system >Root system > Leaf system

Treatment: Stem system >Root system > Leaf system

The root pressure and leaf transpiration are the two processes mainly controlling the translocation of metals from root to shoot/leaf. Some metals are accumulated in roots, probably due to some physiological barriers against metal transport to the aerial parts, while others are easily transported in plants. Translocation of trace elements from roots to shoots could be a limiting factor for the bioconcentration of elements in shoots [Lasat, 2000 and Lu et al. 2004]. The translocation ability (TA) is the ratio between the concentrations of a trace element accumulated in the root tissues by that accumulated in stem/leaf tissues; a larger ratio implies poorer translocation capability [Hammad, 2011]. For all the three metals, low value of TA was found in treatment system, i.e., in electrically stimulated phytoremediation system (Table 3). This result indicates *Eichhornia crassipes* have the ability to translocate more amounts of Pb, Cd and Cu under electrified condition. Copper reported minimum value for translocation ability (TA (r/s) =0.85) compared to other metals. This shows that *Eichhornia crassipes* had translocated more amount of Cu from root to stem under electrified condition.

Variation in the production of chlorophyll

The first and most obvious reactions of plants under heavy metal stress are often growth changes [Lu et al. 2004]. Chlorophyll content is often measured in plants in order to assess the impact of environmental stress, as changes in pigment content are linked to visual symptoms of plant illness and photosynthetic productivity. Decrease in chlorophyll in several plant species under the impact of heavy metals have reported by many researchers [Zengin and Munzuroglu, 2005]. In this study, we emphasized exploring, whether or not an electrical exposure can stimulate *Eichhornia crassipes* growth. In green plants' life activity, chlorophyll plays the role of absorbing, transferring and transforming energy. Leaves were collected from the control plant, treatment plant and plant from fresh water and the chlorophyll content in leaves of *Eichhornia crassipes* was determined using UV-Visible spectrophotometer [Song et al. 2011].

Chlorophyll content in *Eichhornia crassipes* leaves decreased at the beginning in all the three the plant. From the 10th day of the study, the chlorophyll content of plant in electrically stimulated phytoremediation system was found to be gradually increasing with electrical exposure (Figure 5). The result shows an increase in the production chlorophyll with electrical stimulation. When the heavy metal exposure time increases, the production of chlorophyll content in control A decreased. Heavy metals hinder metabolic processes by inhibiting the action of enzymes, and this may be the main cause of inhibition. Heavy metal stress can cause inhibition of the enzymes responsible for chlorophyll biosynthesis which associated with decreased chlorophyll content. Cadmium was reported to affect chlorophyll biosynthesis and inhibit protochlorophyll reductase and aminolevulinic acid (ALA) synthesis [Zengin and Munzuroglu, 2005]. Cadmium strongly binds proteins, thereby decreasing the accumulation of pigment–lipoprotein complexes, including photosystem I (PSI) and PSII [Kupper et al. 2007]. The Cd induced inhibition of chlorophyll synthesis and interference with photosystems causes chlorosis of leaves of

Table 3. Translocation Ability of *Eichhornia crassipes*

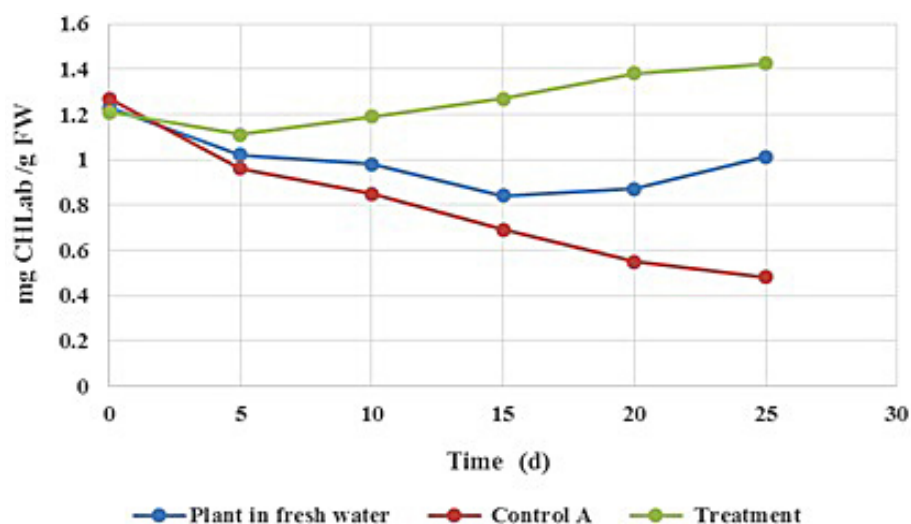| Metals	Control A		Treatment	
	TA(r/s)	TA(r/l)	TA(r/s)	TA(r/l)
Pb	1.72	4.40	1.66	1.09
Cd	1.79	3.52	1.61	0.98
Cu	0.88	2.38	0.85	1.81

Figure 5. Variation in the production of chlorophyll

E. crassipes. Cd also reduces the contents of large and small subunits of ribulose-1, 5-bisphosphate carboxylase/oxygenase (RuBisCO) along with other enzymes of photosynthesis and chlorophyll biosynthesis. Wilting, which followed chlorosis was reported in the presence of high dose of Cd by researchers [Das et al. 2016]. This reduction in chlorophyll of *E. crassipes* in control A under heavy metal stress can be regarded as a specific response of the plants to metal stress, which resulted in chlorophyll degradation and inhibition of photosynthesis. The chlorophyll content might be reduced due to increased cell or tissue damage or lipid peroxidation [Das et al. 2016].

From the experimental results, it can be postulated that 4V voltage is probably suitable to stimulate the *Eichhornia crassipes* to synthesize more chlorophyll. The longer the unit was electrified, the more obvious the stimulating effect was observed. It was in accordance with Knorr's report [Knorr, 2003]. The voltage can stimulate the plants to increase the palisade cells, chloroplast grana and thylakoid lamellas, which enhance the synthesis of chlorophyll. *Eichhornia crassipes* was stimulated by electric field to grow better so it can assimilate more metal.

CONCLUSION

The main goal of the present study was the assessment of the performance of electrically stimulated phytoremediation in the removal of heavy metal. Treatment of lead, cadmium and copper from synthetic solution using phytoremediation system coupled with electric field was conducted. In that experiment, the *Eichhornia crassipes,* an efficient phyto-remediator exhibited efficient and fast removal of heavy metals in electro assisted phytoremediation system. Both aluminum rods and sheets were used as electrodes and both indoor and outdoor experiments were also conducted. Based on the results and plants condition, outdoor experiment using aluminum sheets as electrodes was preferred for further study. The results indicate that the treatment of Cd, Pb and Cu using electrically enhanced phytoremediation using aluminum sheet electrodes is more effective than aluminum rod electrode. When the electrical exposure time increases, the pH of the synthetic solution increased in electrolysis system, but a more favorable, moderate increase was shown by the electrically stimulated phytoremediation system. From the results, it can be postulated that 4V voltage is probably suitable to stimulate the *Eichhornia crassipes* to synthesize more chlorophyll. *Eichhornia crassipes* stimulated by an electric field grown better and assimilated more metal. Heavy metal accumulation in plants collected from control A and electrically enhanced phytoremediation system using aluminum sheet electrodes indicates that maximum amount of Cd, Pb and Cu were accumulated in *Eichhornia crassipes* collected from treatment. *Eichhornia crassipes* translocated maximum Cd and Cu to plants' aerial parts under electrified condition but more amount of Pb was bioconcentrated in roots. Electrically stimulated plant translocated more amount of Pb content to its aerial part compared to plant in control A. The BCFs of control A for Pb, Cd and Cu were 502.65, 448.12 and 664.90 respectively. BCF an index of hyperaccumulation, indicates that electrically stimulated *Eichhornia crassipes* is a good hyper

accumulator of Cd (BCF = 1118.18) and Cu (BCF = 1152.47) and a moderate accumulator of Pb (BCF = 932.26). Translocation ability (TA) ratio indicates that *Eichhornia crassipes* have the ability to translocate more amounts of Pb, Cd and Cu to its upper portion under electrified condition. Taking into account the overall results, we can state that the electro-phytoremediation technique seems to be promising in the treatment of heavy metals contaminated wastewater.

REFERENCES

1. Andrew E.A. 2007. Phytoremediation: an environmentally sound technology for pollution prevention, control and remediation in developing countries. Educational Research and Review, 2 (7), 151–156.

2. Ashraf M.A., Maah M.J. and Yusoff I. 2011. Heavy metals accumulation in plants growing in ex tin mining catchment. Int. J. Environ. Sci. Technol., 8(2), 401–416.

3. Baziar M., Mehrasebi M.R., Assadi A., Fazil M.M., Maroosi M. and Rahimi F. 2013. Efficiency of non-ionic surfactants – EDTA for treating TPH and heavy metals from contaminated soil. J Environ Health Sci Eng., 11,41.

4. Das S., Goswami S. and Talukdar A.D. 2016. Physiological responses of water hyacinth, Eichhornia crassipes (Mart.) Solms, to cadmium and its phytoremediation potential. Turk J Biol., 40, 84–94.

5. Hammad D.M. 2011. Cu, Ni and Zn Phytoremediation and Translocation by Water Hyacinth Plant at Different Aquatic Environments. Aust. J. Basic & Appl. Sci., 5(11), 11–22.

6. Hooda V. 2007. Phytoremediation of toxic metals from soil and waste water. J. Env. Bio., 28(2), 367–376.

7. Kabeer R., Varghese R., Kochu J.K., George J., Sasi P.C. and Poulose S.V. 2014. Removal of Copper by Eichhornia crassipes and the Characterization of Associated Bacteria of the Rhizosphere System. EnvironmentAsia, 7(2), 19–29.

8. Knorr D. 2003. Impact of non-thermal processing on plant metabolite. J. Food Eng., 56 (2–3), 131–134.

9. Kupper H., Parameswaran A., Leitenmaier B., Trtilek M. and Setlik I. 2007. Cadmium induced inhibition of photosynthesis and long-term acclimation of cadmium stress in the hyperaccumulator Thlapsicaerulescens. New Phytol., 175, 655–674.

10. Lasat M.M. 2000. Phytoextraction of metals from contaminated soil: a review of plant/soil/metal interaction and assessment of pertinent agronomic issues. J. Hazard Sub. Res., 2(5), 1–25.

11. Li S., Liu W., Gu S., Cheng X., Xu Z. and Zhang Q. 2009. Spatio-temporal dynamics of nutrients in the upper Han River basin, China. J. Hazard. Mater., 162, 1340–1346.

12. Liao S.W. and Chang W.L. 2004. Heavy Metal Phytoremediation by Water Hyacinth at Constructed Wetlands in Taiwan. J. Aquat. Plant Manage, 42, 60–68.

13. Lu X., Kruatrachue M., Pokethitiyookb P. and Homyokb K. 2004. Removal of Cadmium and Zinc by Water Hyacinth, Eichhornia crassipes. Scienceasia, 30, 93–103.

14. Mahmood Q., Zheng P., Islam E., Hayat Y., Hassan M.J., Jilani G. and Jin R.C. 2005. Lab scale studies on Water hyacinth (Eichhornia crassipes marts solms) for biotreatment of textile wastewater. Caspian J. Env. Sci. 3(2): 83–88.

15. Shah B., Mistry C. and Shah A. 2012. Seizure modeling of Pb(II) and Cd(II) from aqueous solution by chemically modified sugarcane bagasse fly ash: isotherms, kinetics, and column study. Environ. Sci. Pollut. Res., 20(4), 2193–2209.

16. Soltan M.E. and Rashed M.N. 2003. Laboratory study on the survival of water hyacinth under several conditions of heavy metal concentrations. Adv Environ Res., 7, 321–34.

17. Song X., Yan D., Liu Z., Chen Y., Lu S. and Wang D. 2011. Performance of laboratory-scale constructed wetlands coupled with micro-electric field for heavy metal-contaminating wastewater treatment. Ecol. Eng., 37, 2061–2065.

18. Swain G., Adhikari S. and Mohanty P. 2014. Phytoremediation of Copper and Cadmium from Water Using Water Hyacinth, Eichhornia crassipes. International Journal of Agricultural Science and Technology, 2 (1), 1–7.

19. Ullah A., Mushtaq H., Ali H., Munis M.F.H., Javed M.T. and Chaudhary H.J. 2014. Diazotrophs-assisted phytoremediation of heavy metals: a novel approach. Environ. Sci. Pollut. Res., 22, 2505–2514.

20. UNEP. 2010. Final review of scientific information on lead, United Nations Environment Programme, Chemicals Branch, DTIE.

21. Wahab A.S.A., Ismail S.N.S., Praveena S.M. and Awang S. 2014. Heavy metals uptake of Water mimosa (Neptuniaoleracea) and its safety for human consumption. Iranian J. Publ. Health, 43(3), 103–111.

22. Weiliao S. and Chang W.L. 2004. Heavy metal phytoremediation by water hyacinth at constructed wetlands in Taiwan. J. Aquat. Plant Manage, 42, 60–68.

23. Yapoga S., Ossey Y.B. and Kouame V. 2003. Phytoremediation of zinc, cadmium, copper and chrome from industrial wastewater by Eichhornia crassipes. Int. J. Conserv. Sci., 4(1), 81–86.

24. Zengin F.K. and Munzuroglu O. 2005. Effects of some heavy metals on content of chlorophyll, proline and some antioxidant chemicals in bean (Phaseolus vulgaris L.) Seedlings. Acta. Boil. Cracoviensia Ser. Bot., 47(2), 157–164.

TREATMENT OF CADMIUM, LEAD AND COPPER USING PHYTOREMEDIATION ENHANCED BY TITANIUM DIOXIDE NANOPARTICLES.

Harikumar, P.S. and Megha, T.

Water Quality Division, Centre for Water Resources Development and Management, Kozhikode, Kerala, India.
Corresponding author: hps@cwrdm.org; meg8tee@gmail.com

ABSTRACT

Presently, phytoremediation is a beneficial and affordable technique used to extract or remove inactive metals and metal pollutants from contaminated water. Remediation of heavy metal from water and soil is extreme necessary. Phytoremediation ability of two aquatic plants *Eichhornia crassipes* and *Salvinia molesta* for the removal of toxic heavy metals like Pb, Cd and Cu were attempted in the present study under three different conditions. Maximum removal of Pb, Cd and Cu was observed in TiO_2 nanoparticles applied plants used phytoremediation system (C). Results obtained from heavy metal accumulation in plants parts, bioconcentration factor, translocation factor indicates that phytoremediation systems enhanced by TiO_2 nanoparticles showed more tendency to translocate metals to its areal parts. The results showed that, plants applied with TiO_2 nanoparticles exhibited significant increase in physiological response like relative growth and the production of chlorophyll content compared to others. Compared to control (A) and the phytoremediation system in which TiO_2 nanoparticles entrapped calcium alginate beads were applied to plants (B), fast and efficient removal of lead, cadmium and copper was observed in phytoremediation system enhanced by TiO_2 nanoparticles i.e., in C. Phytoremediation technique enhanced by TiO_2 nanoparticles seems to be promising in the treatment of heavy metals from water.

Key words: *Eichhornia crassipes*, *Salvinia molesta*, bioconcentration factor and translocation factor

INTRODUCTION

Heavy metal contamination is a widespread issue that disrupts the environment as a consequence of several anthropogenic activities and their invariably persisting nature in the environment. The ecological balance of the environment and diversity of aquatic organisms have devastatingly affected by heavy metal pollution (Nilantika et al. 2014). Some heavy metals like cadmium, lead and chromium etc. are phytotoxic at both low concentrations as well as very high concentration (Amin, 2012). The prevailing technologies on purification that are used to eradicate these toxic contaminants are costly and sometimes non-ecofriendly also. For the beneficial of community, the research on water purification is focused towards low cost and eco-friendly technologies (Dhote and Dixit, 2009). Phytoremediation is energy efficient, cost-effective, aesthetically pleasing technique of remediation sites with low to moderate levels of contamination.

The excessive concentration of heavy metals in plants can cause oxidative stress and stomatal resistance and can also affect photosynthesis and chlorophyll florescence processes. Copper can inhibit photosynthesis and reproductive processes; lead reduces chlorophyll production; arsenic interferes with metabolic processes, while zinc and tin stimulate the growth of leaves and shoots; ultimately plant growth becomes limited or impossible (Ashraf et al. 2011). The results of some of the experiments indicated that accumulation of some heavy metals such as Cd and Pb may damage chloroplasts in young leaves and the first impact of Cd on plants is the reduction of photosynthetic activity (Ali et al. 2014). Moreover, it has been proved that a decrease in the growth of plants under some stress is due to the restriction of photosynthetic process (Ackerson and Herbert, 1981).

Nanoparticles can be used to increase the supply of elements to plant shoots and foliage and its application can also increase seed germination and seedling growth (Morteza et al. 2013). Furthermore, nanoparticles can facilitate enhanced ability of water and fertilizer absorption by roots, and increase antioxidant enzyme activity such as superoxide dismutase and catalase. Thus, nanoparticles can increase plant resistance against different stresses. Titanium dioxide nanoparticles are used

in agriculture to increase growth and can improve yield; improve the rate of photosynthesis and reduce diseases (Morteza et al. 2013). Titanium dioxide (TiO_2) nanoparticles (NPs) are known for its photocatalytic activity, environmental friendly nature, high stability and are found to be safe for human. These particles have been used in pathogen treatments as well as decomposition of phytotoxic compounds (Raskar and Laware, 2013).

The effects of nano-TiO_2 on the germination and growth of spinach seeds were studied by many researchers. These nanoparticles improved light absorbance and promote the activity of rubisco activase thus accelerated spinach growth (Remya et al. 2010). Nano-TiO_2 improved the plant growth by enhanced nitrogen metabolism (Yang et al. 2006) that promotes the absorption of nitrate in spinach and accelerating conversion of inorganic nitrogen into organic nitrogen, thereby increasing the fresh weight and dry weight. It has also been found that nano-anatase TiO_2 promoted antioxidant stress by decreasing the accumulation of superoxide radicals, hydrogen peroxide, malonyldialdehyde content and enhance the activities of superoxide dismutase, catalase, ascorbate peroxidase, guaiacol peroxidase and thereby increase the evolution oxygen rate in spinach chloroplasts under UV-B radiation (Lei et al. 2008). In this perspective, we tried to enhance efficiency of phytoremediation capacity of *Eichhornia crassipes* and *Salvinia molesta* using titanium dioxide nanoparticles in this study. The aim of our study was to offer an effective approach to enhance the efficiency of the phytoremediation system for the treatment of heavy metals like Pb, Cd and Cu from water.

MATERIALS AND METHODS
Experimental setup

Two free-floating aquatic plants, *Eichhornia crassipes* and *Salvinia molesta* (plate 1) were collected from a natural wetland area, viz. Kottooli wetland in Kozhikode City. In order to simulate the natural environment, plants were placed under natural sun light for one month and the second generations of the plants with similar size were utilized for this study. Before starting the phytoremediation experiment, the epiphytes and insect larvae grown on plants were removed by rinsing with distilled water. The present study was conducted in two stages. During the Stage I, three different conditions (A, B and C) were applied to *Eichhornia crassipes* and *Salvinia molesta* for 10 days. Tanks were setup with different operating conditions and each contained plants and distilled water. Condition A was the control, in which the plants were kept in water under natural conditions. In condition B, TiO_2 nanoparticles entrapped calcium alginate beads (2gm) was applied to the plants and in condition C, TiO_2 powder (2gm) was applied. TiO_2 photocatalyst does not require ultraviolet rays that have an energy level as high as 254nm and are hazardous to humans. It also allows reaction to be initiated by the near – ultraviolet rays with relatively long wavelength contained in sunlight. So, all the experimental setup was placed in the outdoor for maximum sunlight exposure and was conducted during the summer season. Before and after stage I, the chlorophyll content and fresh weight of *Eichhornia crassipes* and *Salvinia molesta* in A, B and C were determined.

In stage II, plants exposed to different conditions were used for the treatment of heavy metals like lead, cadmium and copper from water. Before that, plants were washed and rinsed with distilled water. Thirteen liters of mixed heavy metal (Cd, Pb and Cu) solution was taken in each tank (45 × 30 × 15cm) and the tanks were named A, B and C for both experiments using *Eichhornia crassipes* and *Salvinia molesta*. Thirteen liters of simulated contaminated water was prepared for each tank by dissolving 0.416g of Pb ($NO_3)_2$, 1.022g of $CuSO_4.5H_2O$,

Plate 1: (A) *Eichhornia crassipes* and (B) *Salvinia molesta*

and 0.593g of $(3CdSO_4).8H_2O$ in distilled water. All chemicals used were of the highest purity available and of analytical grade procured from Merck. The heavy metal concentrations were determined by Atomic Absorption Spectrophotometer AAS (Thermo Series) with GF 95. The phytoremediation experiments using *Eichhornia crassipes* was conducted with water having initial concentration of Cd, Pb and Cu were 20.32 ± 0.44 mg/L, 21.45 ± 0.18 mg/L and 21.34 ± 0.22mg/L respectively. The water with initial concentration of Cd, Pb and Cu were 20.99 ± 0.37mg/L, 20.78 ± 0.45 mg/L and 20.56 ± 0.46mg/L respectively, was used in phytoremediation experiments using *Salvinia molesta*. Tank A was the control which comprised of only plants (phytoremediation system). In tank B and tank C, the plants exposed to TiO_2 nanoparticles entrapped calcium alginate beads and TiO_2 nanoparticles powder respectively were used in the treatment of Cd, Pb and Cu.

Experiment was continued for 24 days and water samples were taken in every 3 days. When the experiment was completed, stem, roots and leaves of the plants were separated and dried in a hot air oven. The residual Pb, Cd and Cu concentrations in water and the accumulated metals in different parts of the plants at the conclusion of the experiment were analyzed using Atomic Absorption Spectrophotometer. The effect of the applied conditions on the growth of *Eichhornia crassipes* and *Salvinia molesta* was examined by using relative growth and chlorophyll content. Phytoremediation potential of these native aquatic macrophytes under different applied conditions was also evaluated by metal accumulation, translocation factor and bioconcentration factor.

Plate 2:
TiO_2 nanoparticles entrapped calcium alginate beads

Synthesis of TiO_2 nanoparticles and the encapsulation method for immobilization of nanoparticles in semipermeable alginates beads

TiO_2 nanoparticles were synthesized by simple precipitation method. TiO_2 (Fluka 15%) solution in HCl (10-15%) was stirred in deionized water ([Ti^{3+}] = 0.15 mol L^{-1}). A blue-violet solution was obtained at room temperature. The pH was adjusted between 0.5 and 6.5 with sodium hydroxide (NaOH) solution. The solution was then heated at 60°C in an oven for 24h. The solid obtained was centrifuged, washed with dilute acid (pH=1) and distilled water in order to remove salts (Sophie et al. 2007). A solution containing TiO_2 nanoparticles (0.5wt %) and sodium alginate (0.5wt %) was prepared with 25ml distilled water and stirred for 30 min at 85°C. Afterwards, the solution was extruded as small drops by means of syringe into a stirred solution of calcium chloride (4.0wt %), where spherical gel beads were formed (plate 2). The gel beads were retained in the calcium chloride solution for 12 h for hardening and then washed with distilled water. Stability of beads depends on pH values of the aqueous solution and the initial physical states of the beads (Harikumar et al. 2013).

Analytical procedures

The plant samples were rinsed with tap water twice and deionized water three times. Rinsed samples were cut into pieces and oven-dried at 70°C till constant weight was obtained for the dried samples. The oven-dried samples were ground to pass through a 100-mesh sieve and were digested with HNO_3–$HClO_4$ (4:1) mixture and filtered. The filtrates were analyzed for heavy metals using AAS with GF 95 (Xinshan et al. 2011). Chlorophyll (chl.a + chl.b, CHLab) was determined by OD (optical density) values (663 nm and 645 nm using UV-Visible spectrophotometer, Thermo Evolution 201) of extracting solution, which was made by adding 80% acetone into grinding solution of 0.5 g of fresh leaves (Xinshan et al. 2011).

Relative Growth

The relative growth of plants was calculated to assess the effects of applied conditions on the growth of *Eichhornia crassipes* and *Salvinia molesta*.

RG = FFW/IFW
Where RG denotes relative growth of plants during experimental period, dimensionless; FFW denotes final fresh weight in grams of plants taken at the end of each experiment, and IFW denotes the initial fresh weight in grams of plants taken before starting experiment (Gakwavu et al. 2012).

Bioconcentration Factor and Translocation factor

The bioconcentration factor (BCF) was calculated as the ratio of the trace element concentration in the plant tissues at harvest to the concentration of the element in the external environment (Zayed et al. 1998). BCF is given by BCF = (P/E)

P represents the trace element concentration in plant tissues (mg kg^{-1} dry wt); E represents the trace element concentration in the water (mg/L). BCF is dimensionless. A larger ratio implies better phytoaccumulation capability. The translocation of heavy metal from roots to aerial part and the internal metal transportation of the plant are generally indicated by Translocation Factor (TF). The translocation factor is determined as a ratio of metal accumulated in the shoot to metal accumulated in the root (Deng et al. 2004).

TF = (A_s /A_r)

Where, TF>1 indicates that the plant is capable of effectively translocating the accumulated metals from the root to its aerial part. TF is the translocation factor and is dimensionless. A_r represents the amount of trace element accumulated in the roots (mg kg^{-1} dw), and A_s represents the amount of trace element accumulated in the shoot/leaf (mg kg^{-1} dw). All the tests were conducted in triplicates and the data were statistically analyzed.

RESULTS AND DISCUSSION

The *Eichhornia crassipes* and *Salvinia molesta* grown under different conditions were used for the treatment of heavy metals. TiO_2 nanoparticles that applied to plants were synthesized by chemical precipitation method. The materials were characterized by scanning electron microscopy (Figure 1) and energy dispersive X-ray spectroscopy (Figure 2) spectra. While synthesizing TiO_2 NPs by precipitation method, a mixture of anatase and rutile was precipitated at pH 3. By increasing the pH of the solution, the formation of anatase was favored and at pH 5, only anatase TiO_2 could be formed (Cheng et al.1995). SEM micrograph indicates the presence of nanoparticles below 50nm. The energy dispersive X-ray spectra confirm the presence of TiO_2 and showed no significant levels of impurities.

Phytoremediation of heavy metals

The ability of *Eichhornia crassipes* and *Salvinia molesta* to uptake more than one metal was analyzed by the phytoremediation of the simulated multi metal contaminated water. The residual concentration of Cd, Pb, and Cu were analyzed for each phytoremediation system (A, B and C) during the study, at an interval of 3 days using AAS and the results are summarized in table 1. The

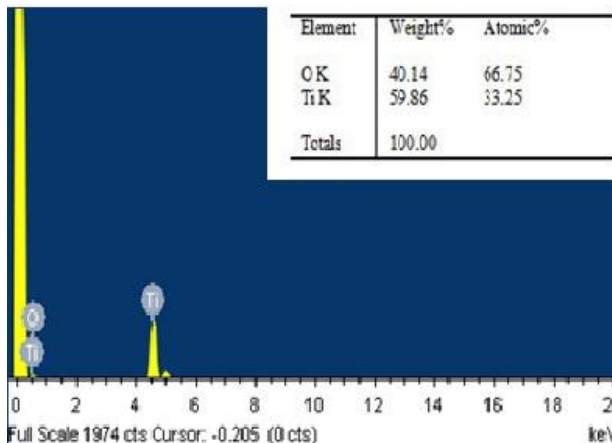metals other than Cu, Cd and Pb were found to be within the permissible limit.

a) Removal of lead from synthetic heavy metal solution

In the case of phytoremediation by *Eichhornia crassipes*, the maximum amount of lead reduction was observed in C with minimum time. Within 3 days, it attained 95.53% reduction, whereas control showed only 10.77% reduction. The TiO_2 nanoparticles applied *Eichhornia crassipes* used phytoremediation system (i.e. C) attained faster removal of Pb compared to control (A) and TiO_2 nanoparticles entrapped calcium alginate beads applied *Eichhornia crassipes* used phytoremediation system (B). Lead was reduced to 50.72% by TiO_2 nanoparticles entrapped calcium alginate beads applied *Eichhornia crassipes* used phytoremediation experiment (B) within 3 days. *Salvinia molesta* also exhibited a similar trend. All the systems attained a reduction of lead ranged from 85.61 to 100% within 24 days. But fast reduction in lead concentration

Figure 1.
SEM micrographs of titanium dioxide nanoparticles

Figure 2.
EDS spectra of titanium dioxide nanoparticles

Element	Weight%	Atomic%
O K	40.14	66.75
Ti K	59.86	33.25
Totals	100.00	

Full Scale 1974 cts Cursor: -0.205 (0 cts)

was observed in C. It showed 77.37% of lead reduction on 3rd day and 100% of reduction on 15th day. The results suggest that the plants exposed to TiO$_2$ nanoparticles showed efficient phytoremediation ability to remove lead from water.

b) Removal of cadmium from synthetic heavy metal solution

When titanium dioxide nanoparticles applied *Eichhornia crassipes* (C) was used in the phytoremediation of heavy metals, 99.06% reduction of cadmium was observed within 3 days. Only, 10.78% of cadmium was removed in the control experiment after 3 days. Cadmium was completely removed in C within 9 days, while in A and B, the efficiency of cadmium removal was found to be 88.78 and 97.64% respectively after 24 days. Maximum cadmium removal with minimum time period was observed in C; that is the phytoremediation system enhanced by titanium dioxide nanoparticles. Compared to A, better cadmium removal was exhibited by B. B is phytoremediation system, where

TiO$_2$ nanoparticles entrapped calcium alginate beads were applied *Eichhornia crassipes* was used. Titanium dioxide exposed *Salvinia molesta* (C) attained 89.57% cadmium removal within 3 days and 100% of cadmium removal within 12 days. The cadmium removal efficiency was found to be 81.99 and 96.81% after 24 days in A and B respectively. The phytoremediation of cadmium by TiO$_2$ nanoparticles applied *Eichhornia crassipes* and *Salvinia molesta* showed better performance than control plants. In *Eichhornia crassipes*, 100% of cadmium was removed in C within 9 days, while in *Salvinia molesta* the same reduction was observed only after 12 days. Results from this experiment indicate that, one of the main limitations of phytoremediation of heavy metals, i.e. the long retention period required for remediation by plants can be overcome by, phytoremediation with TiO$_2$ nanoparticles.

c) Removal of copper from synthetic heavy metal solution

Maximum removal of copper was observed in C within 18 days of exposure to contaminant water by

Table 1. Residual concentration of lead, cadmium and copper in water

Metal	DAY	Residual concentration of heavy metals, mg/L					
		Eichhornia crassipes			*Salvinia molesta*		
		A	B	C	A	B	C
Pb	3	19.14 ± 0.25	10.57 ± 0.07	0.95 ± 0.03	19.64 ± 0.01	12.55 ± 0.11	4.70 ± 0.01
	6	15.48 ± 0.23	7.96 ± 0.03	0.46 ± 0.02	15.89 ± 0.02	9.37 ± 0.06	1.42 ± 0.004
	9	11.57 ± 0.13	5.89 ± 0.12	0.35 ± 0.01	12.41 ± 0.05	7.52 ± 0.02	0.86 ± 0.01
	12	9.75 ± 0.09	3.55 ± 0.05	ND	8.21 ± 0.01	5.72 ± 0.04	0.01 ± 0.0002
	15	6.95 ± 0.04	1.51 ± 0.01	ND	7.04 ± 0.01	3.30 ± 0.04	ND
	18	5.12 ± 0.02	0.82 ± 0.01	ND	5.18 ± 0.23	2.15 ± 0.02	ND
	21	3.01 ± 0.01	0.32 ± 0.01	ND	4.53 ± 0.01	1.48 ± 0.002	ND
	24	2.08 ± 0.01	0.14 ± 0.001	ND	2.99 ± 0.003	0.97 ± 0.001	ND
Cd	3	18.13 ±0.12	14.25 ±0.28	0.19 ± 0.01	18.08 ± 0.05	16.11 ± 0.01	2.19 ± 0.005
	6	14.18 ±0.03	11.24 ±0.05	0.08 ± 0.01	16.13 ± 0.02	14.18 ± 0.08	0.51 ± 0.01
	9	12.11 ±0.11	8.16 ± 0.16	ND	14.16 ± 0.07	10.13 ± 0.01	0.05 ± 0.001
	12	9.88 ± 0.21	4.98 ± 0.21	ND	11.06 ± 0.04	7.96 ± 0.04	ND
	15	5.19 ± 0.11	2.15 ± 0.04	ND	8.11 ± 0.02	5.04 ± 0.05	ND
	18	4.05 ± 0.06	1.01 ± 0.01	ND	6.01 ± 0.05	2.81 ± 0.01	ND
	21	3.59 ± 0.03	0.89 ± 0.04	ND	5.13 ± 0.06	1.02 ± 0.001	ND
	24	2.28 ± 0.03	0.48 ± 0.01	ND	3.78 ± 0.01	0.67 ± 0.03	ND
Cu	3	14.87 ± 0.13	11.59 ± 0.03	4.07 ± 0.02	18.03 ± 0.02	14.45± 0.11	8.05 ± 0.13
	6	11.92 ± 0.06	8.37 ± 0.17	2.67 ± 0.05	14.79 ± 0.04	11.64 ± 0.03	2.51 ± 0.01
	9	8.29 ± 0.02	5.48 ± 0.05	1.41 ± 0.04	11.87 ± 0.03	7.81 ± 0.03	2.51 ± 0.03
	12	7.01 ± 0.09	5.02 ± 0.08	0.36 ± 0.03	7.37 ± 0.13	4.66 ± 0.01	1.21 ± 0.01
	15	4.62 ± 0.05	3.98 ± 0.05	0.26 ± 0.01	5.20 ± 0.03	2.64 ± 0.01	0.90 ± 0.01
	18	3.18 ± 0.05	2.32 ± 0.04	ND	4.91 ± 0.07	1.94 ± 0.02	ND
	21	2.47 ± 0.01	1.14 ± 0.01	ND	3.89 ± 0.04	0.69 ± 0.01	ND
	24	1.64 ± 0.01	0.89± 0.001	ND	2.42 ± 0.01	ND	ND

(Values represent Mean ± SD of three replicates)

ND- not detected

phytoremediation using *Eichhornia crassipes.* In control (A), compared to other metals, more amount of copper was removed by *Eichhornia crassipes* within 3 days. This may be due to the fact that; copper is one of the micronutrient. In the phytoremediation system using *Salvinia molesta*, 95.62% reduction was observed in C within 15 days. On 3rd day, the percentage removal of copper was 60.85% in C and in control (A) it was 12.31%. The residual concentration of copper observed in control (A) during the final stage was 2.42 ± 0.01 mg/L. The effectiveness of two aquatic macrophytes *Eichhornia crassipes* and *Salvinia molesta* grown under three different conditions were tested for their phytoremediation capacity of three metals (Pb, Cd and Cu) and the results indicated that *Eichhornia crassipes* exposed to nanoparticles reported the maximum and fast removal of these heavy metals.

Heavy metal accumulation in plants

The heavy metal analysis of plant segments of both the aquatic native plants, *Eichhornia crassipes* and *Salvinia molesta* were carried out. Distribution of Cd, Pb and Cu in the organs of *Eichhornia crassipes* and *Salvinia molesta* are presented in figure 3 and 4. In A (control), maximum accumulation of metals was observed in root and accumulation of Cd, Pb and Cu in roots of *Eichhornia crassipes* was 6285.04, 5786.30 and 6628.83mg/kg respectively. Many studies revealed that *Eichhornia crassipes* accumulated higher concentrations of heavy metals in the roots than that in the aerial parts. But in C, maximum accumulation of Cd was observed in leaf. More amount of metal accumulation was observed in leaf and stem of C compared to A and B. C was the phyto-remediation systems in which *Eichhornia crassipes* was directly exposed to titanium dioxide nanoparticles. But the present study showed that in C, Cu accumulation is in the order of leaves>roots >stem, Cd accumulation is in the order of leaves> stem > roots and Pb accumulation is in the order of leaves >stem > roots. The results show that, phytoremediation systems enhanced by titanium dioxide nanoparticles showed more tendency to translocate metals to its areal parts.

Salvinia also exhibited the capacity to accumulate high levels of heavy metals. Compared to all phytoremediation systems, a maximum concentration of 8928.74 mg/Kg of Cd was accumulated in leaves of *Salvinia molesta* grown under condition C. Sune et al. 2007 reported that heavy metal uptake in *Salvinia* occurs through a physical process (fast), which involves adsorption, ionic exchange, chelation, while biological processes such as intracellular uptake (transported through plasmalemma into cells) is slow and help in subsequent translocation of metals (Cd) from roots to leaves. The highest amount of lead and copper accumulated in C was 9192.63 and 9888.82mg/Kg

respectively. In control plant (A), all the three metals were accumulated at highest level in roots. Roots remain in direct contact with the medium and hence this might result in increased metal concentration in the roots. More amount of metal accumulation was observed in leaf of B compared to A. The results indicate that titanium dioxide nanoparticles applied plants were efficient to translocate the metals from root to its aerial parts.

Bioconcentration factor and translocation factor

The mobility of the heavy metals from the polluted medium to the roots of the plants and the ability to translocate the metals from roots to the harvestable aerial part were evaluated respectively by means of the bioconcentration factor (BCF) and the translocation factor (TF). Bioconcentration factor is a useful parameter to evaluate the potential of the plants in accumulating metals. The BCF values for Cd, Pb and Cu in *Eichhornia crassipes* and *Salvinia molesta* at 24 days' exposure to heavy metals are shown in figure 5 and 6, respectively. Higher BCF values indicates the higher phytoaccumulation capacity. Maximum bioconcentration factors of Cd, Pb and Cu in *Eichhornia crassipes* was observed in C. In C, the highest BCF values found for Cd, Pb and Cu were 852.49, 848.20 and 1047.99 respectively. If the BCF value is more than or equal to 1000 then that plant species is considered as a hyper accumulator. The plant having the abilities to grow in very high concentration of metal and concentrating high heavy metals in their tissues are known as hyperaccumulators (Wahab et al. 2014). The higher BCF value of *Eichhornia crassipes* for Cu (BCF >1000) in C indicates that TiO_2 nanoparticles applied *Eichhornia crassipes* is considered as a good hyper accumulator. The BCFs of control (A) for Cd, Pb and Cu were 615.67, 516.14 and 698.53 respectively. BCF of B for all the metals were higher than control but less than 1000. Phytoremediation experiments using *Salvinia molesta,* a highest BCF values was observed for Cd, Pb and Cu were 750.12, 777.90 and 896.29 respectively in (C). In experiment B of *Salvinia molesta*, BCFs of all the three metals were found higher than that of A. The results indicated that, plants exposed to TiO_2 nanoparticles were accumulated more amount of heavy metals in its upper portions compared to control plants.

The translocation factor for Cd, Pb and Cu in phyto-remediation systems using *Eichhornia crassipes* and *Salvinia molesta* are shown in table 2 and 3 respectively. The value TF > 1 indicated that there is a transport of metal from root to leaf probably through an efficient metal transporter system and the metals sequestration in the leaf vacuoles and apoplast. TF value more than 1 of plant species indicates their hyperaccumulation potential and is identified as hyperaccumulator plants (Marbaniang and Chaturvedi, 2014). For *Eichhornia crassipes,* maximum TF for cadmium was

Figure 3. Accumulation of cadmium, lead and copper in
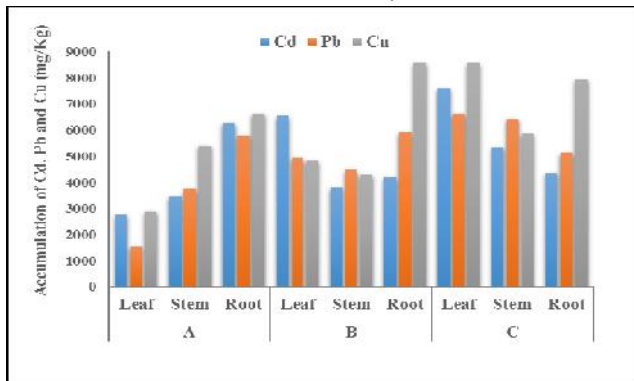*Eichhornia crassipes*

Figure 4. Accumulation of cadmium, lead and copper in
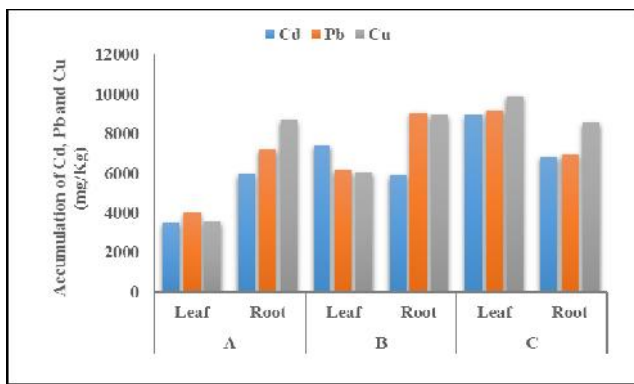*Salvinia molesta*

Figure 5: Bioconcentration factors (BCF) of Pb, Cd and Cu in
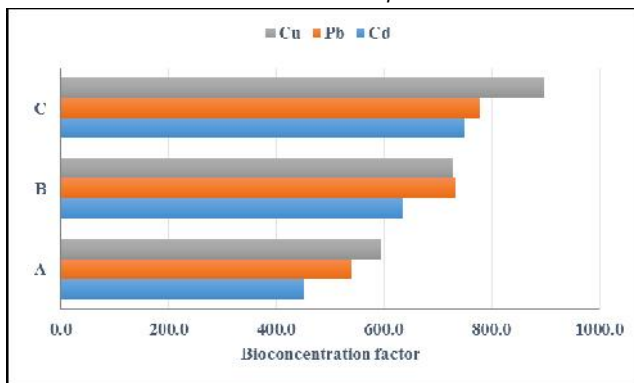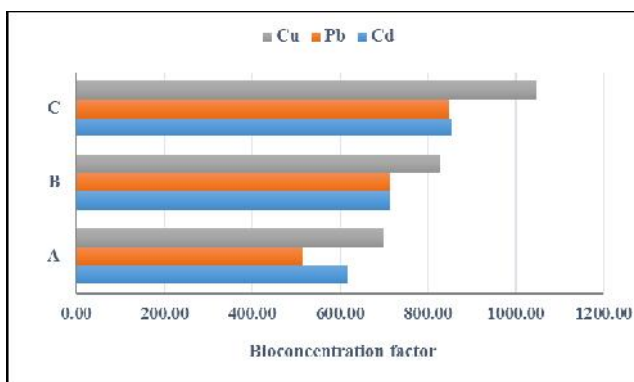*Eichhornia crassipes*

Figure 6: Bioconcentration factors (BCF) of Pb, Cd and Cu in
Salvinia molesta

observed in C (TF(s/r) = 1.22 and TF(l/r) = 1.74) compared to A and B, which indicates the translocation of high Cd content from roots to its aerial part. Similar trend was observed for Pb also and for Cu, maximum TF observed was TF(l/r) =1.08 in C. These results imply that *Eichhornia crassipes* exposed to nanoparticles accrued an ability to transfer higher metal concentrations from root to its areal part. The lowest translocation factor was observed in the A (control) for Cd and Pb. Similar results were found in phytoremediation systems using *Salvinia molesta* and the translocation factor observed in the C was TF(l/r) = 1.31, TF(l/r) = 1.32 and TF(l/r) = 1.16 for Cd, Pb and Cu respectively. TiO_2 nanoparticles applied plants (C) exhibited better potential to translocate Cd, Pb and Cu to its aerial parts.

Translocation is the movement of metal containing sap from the root to the shoot which was primarily controlled by two processes, root pressure and leaf transpiration. Some metals are accumulated in roots, probably due to some physiological barriers against metal transport to the aerial parts, while the others are easily transported in plants. Translocation of trace elements from roots to shoots could be a limiting factor for the bioconcentration of elements in shoots. It can be proposed that there has mechanism in roots that could detoxify heavy metals or transfer them to aerial parts (Gomati et al. 2014).

Physiological response of plants to the applied conditions
Variation in the production of chlorophyll

In the life activity of green plants, chlorophyll plays the role of absorbing, transferring and transforming energy. The chlorophyll content of plant after experiment was determined using UV-Visible spectrophotometer. Variation in the production of chlorophyll of both the plants is depicted in figure 7. The result shows that, plants from B and C exhibited an increase in the production of chlorophyll compared to A (control) for both *Eichhornia crassipes* and *Salvinia molesta*. Maximum chlorophyll production was observed in C for both the plants.

This may be due to the effects of nano-TiO_2 on the content of light harvesting complex II (LHC II) on thylakoid membranes of plants and nano-TiO_2 has ability to increase LHC II content (Lei et al. 2007 and Hong et al. 2005). These have the ability to promote energy transfer and oxygen evolution in photosystem II (PS II) of plants (Mingyu, 2007). It has also been reported that nano-anatase TiO_2 promoted antioxidant stress by decreasing the accumulation of superoxide radicals, hydrogen peroxide, malonyldialdehyde content and enhance the activities of superoxide dismutase,
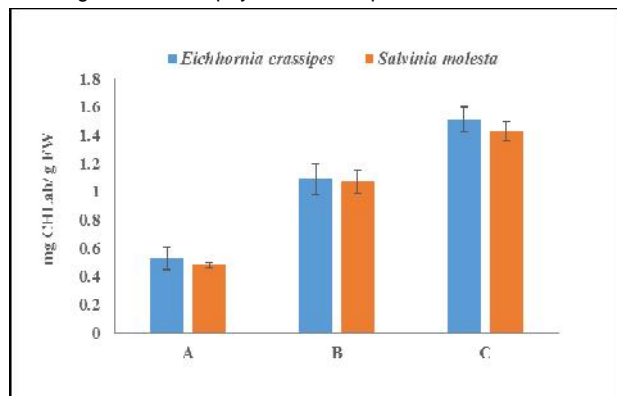
Table 2. Translocation factor of *Eichhornia crassipes*

Metals	TF	A	B	C
Cd	TF(s/r)	0.55	0.91	1.22
	TF(l/r)	0.44	1.57	1.74
Pb	TF(s/r)	0.65	0.76	1.26
	TF(l/r)	0.27	0.83	1.29
Cu	TF(s/r)	0.81	0.50	0.74
	TF(l/r)	0.43	0.56	1.08

Table 3. Translocation factor of *Salvinia molesta*

Metals	TF	A	B	C
Cd	TF(l/r)	0.59	1.26	1.31
Pb	TF(l/r)	0.55	0.68	1.32
Cu	TF(l/r)	0.41	0.67	1.16

Figure 7: Chlorophyll content of plants after treatment

Figure 8. Variations in the relative growth of *Eichhornia crassipes* and *Salvinia molesta*
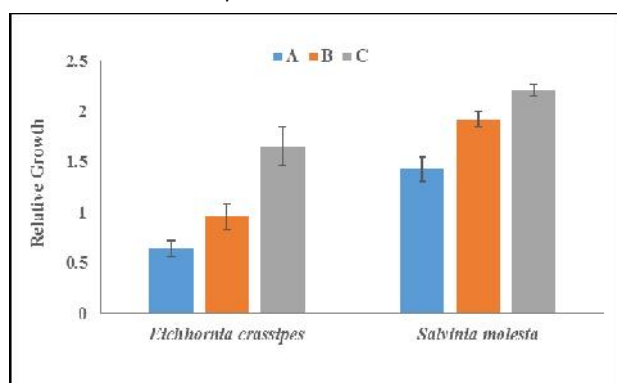
catalase, ascorbate peroxidase, guaiacol peroxidase and thereby increase the evolution of oxygen rate in plants chloroplasts (Lei et al. 2008). It helps to increase solar energy trapping that might improve the photo synthetic efficiency of plants.

Variations in the relative growth of plants under different conditions

Variations in the relative growth of *Eichhornia crassipes* and *Salvinia molesta* grown under three different conditions are graphically represented in figure 8. The relative growth of control plants showed a significant decrease for both the plants. The plants exposed to TiO_2 nanoparticles (C) exhibited significant increase in relative growth. The plants in C showed high relative growth compared to plants from A and B. In the case of *Salvinia molesta* an increasing trend was observed in all the conditions but maximum increase in weight after treatment was observed in plant from C. Plant in C was the plant exposed to nano - TiO_2. TiO_2 nanoparticles has the ability to improve light absorbance and promote the activity of rubisco activase thus accelerate the growth of plants (Zheng et al. 2005 and Hong et al. 2005).

CONCLUSION

A study was carried out to assess the enhancement of phytoremediation capacity of heavy metals (Cd, Pb and Cu) by *Eichhornia crassipes* and *Salvinia molesta* in the presence of titanium dioxide nanoparticles. TiO2 nanoparticles exposed *Eichhornia crassipes* and *Salvinia molesta* showed 99.06% and 89.57% of phytoremediation efficiency respectively for cadmium removal within 3 days. Maximum phytoremediation efficiency for lead and copper was also observed in TiO_2 nanoparticles exposed plants. It was observed that, in the nano - TiO_2 applied phytoremediation system, more efficient and faster removal of heavy metals was taking place. Results of the study on heavy metal accumulation indicates that titanium dioxide nanoparticles applied plants showed more tendency to translocate metals to its areal parts. Control plant accumulated more metals in their root portion in both the plants. Nano - TiO_2 applied plants exhibited an increase in the production of chlorophyll compared to A (control) and B. TiO_2 nanoparticles exposed plants exhibited significant increase in relative growth compared to others. This may be due to the fact that, the plant exposed to nano –TiO_2 has the ability to improve light absorbance and promote the activity of rubisco activase thus accelerating the growth of plants. The determination of bioconcentration factor indicated that, the uptake potential of metals by plants was increased under nano - TiO_2 applied conditions. Plants exposed to TiO_2 nanoparticles achieved ability to transfer higher metal concentrations from root to its areal part. TiO_2 nanoparticles applied plants (C) showed better performance than TiO_2 nanoparticles entrapped calcium alginate beads applied plants (B). Taking into account

the overall results, we can state that TiO_2 nanoparticles applied *Eichhornia crassipes* and *Salvinia molesta* seems to be promising candidate for the phytoremediation of heavy metals from water and exhibited an enhanced phytoremediation ability.

REFERENCES

Ackerson, R.C and Herbert, R.R., 1981. Osmoregulation in cotton in response to water stress. I. Alterations in photosynthesis, leaf conductance, translocation, and ultra-structure, Plant Physiology, 67, pp:484-488.

Ali, A.K.S., Matinizadeh, M., Shirvany, A., Madani, M.E., Talebi, K.T., Monemian, S.M and Abdi, E., 2014. Evaluation of Pollution Intensity in Different Districts of Tehran Based on Measuring Chlorophyll, Plumb and Cadmium Heavy Metal Contents in Trees, International Journal of Environmental Research, 8(4), pp:1105-1114.

Amin, M., 2012. Phytoremediation of heavy metals from municipal wastewater by *Typhadomingensis,* African Journal of Microbiology Research, 6(3), pp: 643-647.

Ashraf, M.A., Maah, M.J and Yusoff, I., 2011. Heavy metals accumulation in plants growing in ex tin mining catchment, International Journal of Environmental Science and Technology, 8(2), pp: 401-416.

Cheng, H., Ma, J., Zhao, Z and Qi, L., 1995. Hydrothermal preparation of uniform nanosize rutile and anatase particles, Chemistry of Materials, 7, pp:663-671.

Deng, H., Ye, Z.H and Wong, M.H., 2004. Accumulation of lead, zinc, copper and cadmium by 12 wetland plant species thriving in metal-contaminated sites in China, Environmental Pollution, 132, pp:29-40.

Dhote, S and Dixit, S., 2009. Water quality improvement through macrophytes - a review, Environmental Monitoring and Assessment, 152, pp: 149-153.

Gakwavu, R.J., Sekomo, B.C and Nhapi, I., 2012. Zinc and Chromium removal mechanisms from industrial wastewater by Water hyacinth, *Eichhornia crassipes,* Applied Ecology and Environmental Science, 10(4), pp: 493-502.

Gomati, S., Adhikari, S and Mohanty P. 2014. Phytoremediation of Copper and Cadmium from Water Using Water Hyacinth, *Eichhornia Crassipes*, International Journal of Agricultural Science and Technology, 2(1), pp: 1-7.

Harikumar, P.S., Joseph, L and Dhanya, A., 2013. Photocatalytic degradation of textile dyes by hydrogel supported titanium dioxide nanoparticles, Journal of Environmental Engineering and Ecological Science, 2(2), pp: 1-9.

Hong, F., Zhou, J., Liu, C., Yang, F., Wu, C., Zheng, L and Yang, P., 2005. Effect of nano –TiO_2 on photochemical reaction of chloroplasts of spinach, Biological Trace Element Research, 105, pp:269-280.

Lei, Z., Mingyu, S., Xiao, W., Chao, L., Chunxiang, Q., Liang, C., Hao, H., Xiaqing, L and Fashui H., 2008. Antioxidant stress is promoted by nano-anatase in spinach chloroplasts under UV-B radiation, Biological Trace Element Research, 121, pp:69–79.

Lei, Z., Zheng, L and Su, M., 2007. Effects of nano-anatase on spectral characteristics and distribution of LHCII on the thylakoid membranes of spinach, Biological Trace Element Research, 120, pp: 273-283.

Marbaniang, D and Chaturvedi, S. S., 2014. Assessment of Cr^{+6} Accumulation and Phytoremediation Potential of Three Aquatic Macrophytes of Meghalaya, India, International Journal of Science and Research, 3(6), pp: 36-42.

Morteza, E., Moaveni, P., Aliabadi, F.H and Kiyani, M., 2013. Study of photosynthetic pigments changes of maize (Zea mays L.) under nano TiO_2 spraying at various growth stages, *SpringerPlus,* 2, pp: 247.

Nilantika, P., Samujjwal, C and Mahuya, S., 2014. Lead toxicity on non-specific immune mechanisms of freshwater fish Channa punctatus, Aquatic Toxicology, 152, pp:105–112.

Raskar, S and Laware, S.L., 2013. Effect of titanium dioxide nano particles on seed germination and germination indices in onion, Plant sciences feed, 3 (9), pp: 103-107.

Remya, N., Saino, H.V., Baiju, G.N., Maekawa, T., Yoshida, Y and Sakthi, K. D., 2010. Nanoparticulate material delivery to plants, Plant Science, 179, pp:154-163.

Sune, N., Sanchez, G., Caffaratti, S and Maine, M.A., 2007. Cadmium and chromium removal kinetics from solution by two aquatic macrophytes, Environmental Pollution, 145, pp: 467-473.

Wahab, A.S.A., Ismail, S.N.S., Praveena, S.M and Awang, S., 2014. Heavy metals uptake of Water mimosa (*Neptuniaoleracea*) and its safety for human consumption, Iranian Journal of Public Health, 43(3), pp:103-111.

Xinshan, S., Denghua, Y., Zhenhong, L., Yan, C., Shoubo, L and Daoyuan, W., 2011. Performance of laboratory-scale

constructed wetlands coupled with micro-electric field for heavy metal-contaminating wastewater treatment, Ecological Engineering, 37, pp: 2061- 2065.

Yang, F., Hong, F., You, W., Liu, C., Gao, F., Wu, C and Yang, P., 2006. Influences of nano-anatase TiO_2 on the nitrogen metabolism of growing spinach, Biological Trace Element Research, 110 (2), pp:179-190.

Zayed, A., Gowthaman, S and Terry, N., 1998. Phytoaccumulation of trace elements by wetland plants: I. Duckweed, Journal of Environmental Quality, 27, pp: 715-721.

Zheng, L., Hong, F., Lu, S and Liu, C., 2005. Effect of nano-TiO_2 on strength of naturally aged seeds and growth of spinach, Biological Trace Element Research, 104, pp: 83-91.

***

Immobilization and mobilization effect of ammonium molybdate on phytoremediation of toxic heavy metals in soil

Megha Tharayil, Harikumar Puthenveedu Sadasivan Pillai

Water Quality Division, Centre for Water Resources Development and Management, Kozhikode, Kerala, 673571, India, Email: meg8tee@gmail.com

ABSTRACT

Rapid industrialization and urbanization have resulted in elevated emission of toxic heavy metals to the environment. Many of the current remediation techniques available for heavy metal removal from contaminated sources are expensive, time consuming and environmentally not sound. Unlike organic compounds, metals will not degrade, and therefore requires effective cleanup techniques to reduce or remove toxicity. Phytoremediation, an emerging cleanup technology for contaminated area is both low-tech and cost effective. The objective of this study was to investigate the effect of ammonium molybdate on phytoremediation of toxic heavy metals (Cd, Pb, Cu, Ni and Zn) from soil by *Amaranthus retroflexus*. Five concentrations of ammonium molybdate solutions having Mo contents 0.05, 0.10, 0.30, 0.50, 1.00 g/L respectively were added to pots containing *Amaranthus retroflexus*. Ammonium molybdate shows immobilization and mobilization effect on phytoremediation of toxic heavy metals in soil. It was found that ammonium molybdate has the potential ability to precipitate with Pb and Zn and it decreases the biotoxicity of these metals to plant. Ammonium molybdate also has the ability to chelate and form more soluble fractions with Cd, Cu and Ni and it increases the bioavailability of these metals to plant. From the bioconcentration factor and translocation factor, it was found that application of ammonium molybdate to soil is a promising technology in phytoremediation.

Keywords: Ammonium molybdate, phytoremediation, bioconcentration factor, translocation factor.

INTRODUCTION

Pollution of the biosphere with toxic metals has accelerated dramatically since the beginning of the industrial revolution. The primary sources of this pollution are the burning of fossil fuels, mining and smelting of metalliferous ores, metallurgical industries, municipal wastes, fertilizers, pesticides and sewage [1]. Environmental pollution by heavy metals is now a global issue that requires considerable attention. This is due to the fact that unlike many substances, metals are not biodegradable and hence accumulate in the environment. Trace amount of some heavy metals such as Cu, Zn, Fe and Co are required by living organisms, however, any excess amount of these metals can be detrimental [2]. Non-essential heavy metals include arsenic, antimony, cadmium, chromium, mercury, lead; these metals are of particular concern because they cause air, soil and water pollution [3]. Decontamination of such soils has therefore, become imperative for the safety of animals and humans. A number of techniques have been developed to remove metals from the contaminated soils. However, many sites remain contaminated because of economical problem of the available technologies. Techniques such as excavation and disposal of contaminated soils in landfills are not

environment friendly and may serve as secondary pollution sources [4]. Therefore, new environmental friendly and less expensive techniques are required. With current trends moving towards greener technologies, the focus is shifting to phytoremediation, where plants are used for the uptake of metals or pollutants from the environment or transform them into harmless compounds [5]. Phytoremediation presents a cheap, noninvasive, and safe alternative to conventional cleanup techniques and can be accomplished by phytoextraction, phytodegradation, phytostabilization, phytovolatilization and rhizofiltration [6].

Green plants are not only the lungs of nature with an ability of purifying impure air by photosynthesis, but some species also have the unique ability to uptake, tolerate and even hyperaccumulate heavy metals and other toxic substances from soils and water through roots and concentrate them in roots, stem and leaves[7]. The high bioconcentration factor, which is the ability of the plant to extract metals from the soil and the efficient root to-shoot transport system endowed with enhanced metal tolerance provide hyper accumulators with a high potential detoxification capacity. The heavy metal accumulation capacity of plants belonging to the Amaranthaceae family was reported earlier. *Amaranthus retroflexus* is a good metal accumulator and it has been used for the uptake of cadmium, mercury, zinc and copper [8].

Plants that accumulate metals can extract metals from soils (phytoextraction) or, on the other hand, are used in combination with soil amendments to improve soil conditions (phytostabilization) [9]. Chelate-enhanced phytoremediation has been proposed as an effective tool for the extraction of heavy metals from soils by plants. The most frequently used solutions for extraction also have deficiencies: ethylene diamine tetraacetic acid (EDTA) is expensive and toxic, and presents a low level of biodegradability [10,11]; nitrilotriacetic acid (NTA) is also the toxicant as a class II carcinogen [12]; nitric acid (HNO3) is lethal to soil micro-flora and destructive to the physical and chemical properties of soil; hydrochloric acid (HCl) can alter soil properties [13]; citric acid is a nontoxic acid that forms relatively strong complexes. It is easily biodegradable, but it presents of lower effectiveness in the removal of metal ions [14]. EDGA enhanced metal solubility but plant uptake did not increase accordingly [15].

The addition of chelators effectively increased the mobility of target heavy metals in soils, and significantly enhanced the accumulation of these heavy metals in aerial parts of the plants but the application of chelators had inhibitory effects on the growth of the plants [16]. The ammonium molybdate (containing nitrogen and molybdenum) is fertilizer to plants, which can produce more biomass [17]. In this study, we assessed phytoextraction potential of the *Amaranthus retroflexus* with ammonium molybdate, to evaluate the ability of the *Amaranthus retroflexus* to remediate soils contaminated with multiple heavy metals. Heavy metals selected for study include two essential (copper (Cu) and zincZn)) and three toxic (cadmium (Cd), lead (Pb) and nickel (Ni)) elements.

MATERIALS AND METHODS
Physicochemical characteristics of soil samples

Soil used for the experiment was spiked with heavy metals (Cd, Pb, Cu, Ni and Zn) solutions. The contaminated soil received the metals Cd as $CdSO_4$; Pb as $Pb(NO_3)_2$; Cu as $CuSO_4$; Ni as $NiSO_4$ and Zn as $ZnSO_4$. Physicochemical factors of soil such as pH, electrical conductivity (EC), texture, calcium, magnesium, organic carbon, inorganic phosphorous, sodium, potassium were analyzed.

Plant culture and experimental design

Each plastic pot was filled with 5Kg of soil. *Amaranthus retroflexus* seeds were germinated in pots containing soil to a depth of 1cm under normal condition. After seedlings grew for 10 days, 18 seedlings were transplanted to pots containing heavy metal contaminated soil at a rate of one

seedling per pot. The experiment consists of 5 treatments (No.1, No.2, No.3, No.4 and No.5) and control with replicates for each. Experiments were exposed to natural day and night temperatures. The plants were watered daily with 300 ml of distilled water per pot. In the case of 5 treatments, 50 ml of ammonium molybdate solutions (having Mo contents 0.05, 0.10, 0.30, 0.50 and 1.00 g/L respectively) were added to pots containing *Amaranthus retroflexus*. Ammonium molybdate solution was not applied in control [17].

Analysis of heavy metals in soil and plant

After 45 days the plants were harvested and heavy metal concentrations in plants and soil were determined. The extraction of heavy metals from soil was done by using perchloric acid-nitric acid mixture. The powerful oxidizing and dehydrating properties of hot, concentrated perchloric acid were extremely effective in decomposing organic matter and sulphides. Nitric acid dissolves the majority of the metals occurring in nature, with the exception of gold and platinum. 0.2g of soil was digested with 20ml of concentrated HNO_3, 5ml distilled water and 10 ml of $HClO_4$ and heated on a hot plate for 2 hrs. The mixture was heated until the white fumes come and the soil become white. Then the solution was filtered and made up to 50 ml. The filtrate was analyzed for heavy metals using Atomic Absorption Spectrophotometer (AAS) (Thermo Series). Replicates were carried out as part of the measurement.

The plants were harvested after 45days. The lengths of the roots and shoots were measured. The roots and shoots were separated and washed with distilled water to remove soil and dust. The plant parts were dried in an oven at 70°C for 72 hr and the dry weight were recorded by electronic balance. 0.2 g of plant parts were digested at 150°C for 200 min with 10 ml mixtures of $HNO_3/HClO_4$ (4:1) [18]. After complete digestion, the volume of digested samples was adjusted to 50 ml with distilled water. Subsequently, the amount of heavy metals was determined by Atomic Absorption Spectrophotometer (AAS) (Thermo Series). In this experiment, three replicates were maintained.

Bioconcentration and translocation factor

The bioconcentration factor (BCF) was used to determine the quantity of heavy metals absorbed by the plant from the soil. This is an index of the ability of the plant to accumulate a particular metal with respect to its concentration in the soil and is calculated using the below given formula [19]. The higher BCF value the more suitable for phytoextraction (BCF Values>2 were regarded as high values) [20, 21].

$$\text{Bioconcentration factor} = \frac{\text{Metal concentration in the plant tissue}}{\text{Metal concentration in the soil}}$$

To evaluate the potential of *A. retroflexus* for phytoextraction, the translocation factor (TF) was calculated. This ratio is an indication of the ability of the plant to translocate metals from the roots to the aerial parts of the plant [22]. Metals that are accumulated by plants and largely stored in the roots of plants are indicated by TF values<1, with values greater indicating translocation to the aerial part of the plant [21].

$$\text{Translocation factor} = \frac{\text{Metal concentration in aerial parts}}{\text{Metal concentration in roots}}$$

RESULTS AND DISCUSSION

Physicochemical characteristics and heavy metal concentration of the soil samples were given in table 1. As compared with controls, the concentration of Ni, Cd and Cu in treated soil were lower but the concentrations of Pb and Zn in treated soil were higher (Table 2).
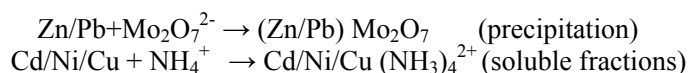
Table 1. Physico-chemical characteristics and heavy metal concentration of contaminated soil.

Parameters	Value
pH	6.71±0.05
EC µS/m	24.6± 0.05
Alkalinity (mg/kg)	644±0.07
Chloride (mg/kg)	320.8± 0.61
Sulphate (mg/kg)	304.8±0. 82
Inorganic phosphorous (mg/kg)	8± 1.00
Sodium (mg/kg)	250± 0.6
Potassium (mg/kg)	75±0.5
Organic carbon %	0.279± 1.22
Exchangable Calcium`(mg/kg)	1280±1.14
Exchangable Magnesium (mg/kg)	583.2±1.38
Nickel mg/kg	155.87±1.46
Cadmium mg/kg	6.98±1.5
Cupper mg/kg	86.11±2.77
Lead mg/kg	74.79±2.32
Zinc mg/kg	109.27±1.25

Table 2. Heavy metal concentration in soil after treatment.

Treatment	Ni (mg/Kg)	Cd(mg/Kg)	Cu(mg/Kg)	Pb (mg/Kg)	Zn (mg/Kg)
Control	122.95±2.47	3.73±0.36	45.7±2.18	33.11±1.54	41.81±1.80
No.1	97.37±1.25	2.87±0.73	38.53±2.33	41.09±1.58	46.15±2.12
No.2	83.93±2.89	0.87±0.25	35.52±1.24	47.93±1.82	53.28±1.70
No.3	66.83±4.06	0.075±0.07	33.53±1.32	53.51±2.94	58.45±4.31
No.4	55.79±3.62	0.05±0.02	26.32±1.22	56.02±1.00	65.82±2.23
No.5	21.56±1.74	0.025±0.02	6.48±1.39	63.59±1.75	67.61±1.64

Amaranthus retroflexus uptakes more amount of Ni, Cd and Cu than Pb and Zn in the presence of ammonium molybdate. It may be due to that Ni, Cd and Cu were chelated and form more soluble fractions with ammonium molybdate and Pb and Zn were precipitated with ammonium molybdate. The mechanism of the reaction of ammonium molybdate with toxic metals can be reported as follows [17]:

$$Zn/Pb + Mo_2O_7^{2-} \rightarrow (Zn/Pb)\ Mo_2O_7 \quad \text{(precipitation)}$$
$$Cd/Ni/Cu + NH_4^{+} \rightarrow Cd/Ni/Cu\ (NH_3)_4^{2+} \text{(soluble fractions)}$$

The heavy metal concentrations in the root of *A. retroflexus* are indicated in Table 3. Compared to control, the concentrations of Ni, Cd and Cu in root were higher but the concentrations of Pb and

Zn were lower. A similar trend was also observed in the shoot of *A. retroflexus* (Table 4). Ammonium molybdate has the potential ability to precipitate with Pb and Zn so it stabilizes these metals in soil and decreases the bioavailability of these metals to plant. It also has the ability to chelate and form more soluble fractions with Cd, Cu and Ni, thus it increases the bio-availability of these metals to plant. Maximum reduction of heavy metal in soil was observed in treatment No.5 (with maximum concentration of ammonium molybdate). After treatment 86.16% of Ni, 99.64% of Cd and 92.47% of Cu were reduced in soil. The result indicated that, *A. retroflexus* can remove heavy metal (Cd, Cu and Ni) efficiently with ammonium molybdate. The ammonium molybdate has the potential to enhance metal mobility in soil profiles by forming complexes with toxic metals [17]. It acts as stabilization agent for Pb and Zn and as extracting agent for Cd, Cu and Ni.

Table 3. Heavy metal concentration in the root of *Amaranthus retroflexus*.

Treatment	Ni (mg/Kg)	Cd(mg/Kg)	Cu(mg/Kg)	Pb (mg/Kg)	Zn (mg/Kg)
Control	16.92±1.6	0.91±0.03	16.6±1.23	26.41±0.68	32.49±1.28
No.1	36.44±3.46	1.53±0.3	21.87±1.7	17.74±0.72	26.74±0.84
No.2	47.14±1.36	2.15±0.26	23.83±0.36	12.56±1.00	22.7±1.38
No.3	57.39±3.27	2.80±0.17	26.81±1.14	9.63±0.61	18.39±2.48
No.4	68.81±1.81	3.07±0.14	31.37±0.78	7.73±0.94	11.75±1.24
No.5	92.66±3.39	3.45±0.11	41.18±1.69	4.51±1.38	7.72±1.03

Table 4. Heavy metal concentration in the shoot of *Amaranthus retroflexus*.

Treatment	Ni (mg/Kg)	Cd(mg/Kg)	Cu(mg/Kg)	Pb (mg/Kg)	Zn (mg/Kg)
Control	7.41±1.28	0.78±0.06	7.86±0.91	11.46±0.80	21.23±0.49
No.1	18.11±2.58	0.89±0.07	8.02±0.09	9.59±0.53	19.73±0.96
No.2	23.58±5.49	1.43±0.08	9.66±0.60	8.73±0.35	15.8±0.65
No.3	24.34±4.39	2.24±0.25	10.58±0.68	6.15±0.28	13.8±0.42
No.4	23.20±3.89	2.28±0.31	11.82±0.34	4.91±0.28	8.6±0.83
No.5	26.91±3.98	2.44±0.12	17.49±2.00	2.06±0.57	5.99±0.87

Accumulation of nickel in the plant parts increased with increasing ammonium molybdate concentration. Concentrations of Ni accumulated ranged from 16.92 mg/Kg to 92.66 mg/Kg with highest concentration being stored in the roots. Much higher Ni levels were found in the roots rather than in the shoots or leaves. Bioaccumulation of cadmium in the roots (0.91 to 3.45 mg/kg) was higher than the shoot (0.78 to 2.44 mg/kg) and leaf (0 to 0.98 mg/kg). The cadmium content in the leaf of control plants was below detectable levels. A steady increase was noticed in the accumulation of the cadmium in the plant parts with increasing ammonium molybdate. The bioaccumulation of copper by *A. retroflexus* exhibited variation among plant parts and bioaccumulation of copper in plant increases with the application ammonium molybdate. Among the plant parts, the roots accumulated more copper than the shoot and leaf.

The control plant species accumulated more amounts of lead and zinc than the treated plant species. With increase in the concentration of ammonium molybdate, the bioaccumulation of Pb and Zn decreases. The metals like Pb and Zn in soil can precipitate with $Mo_2O_7^{2-}$ and the toxicities of these metals to plant will be decreased [23]. The content of toxic metals in the root were higher than shoots, which may be related to plant uptake of toxic metals and xylem translocation from roots to shoots. Restriction of upward movement from roots into shoots can be considered as one of the

tolerance mechanism [24]. The NH_4^+ ion present in ammonium molybdate chelate with toxic metals (such as Cd, Ni and Cu) and form soluble chelating complexes [25]. Ammonium molybdate increases the bioavailability of Ni, Cd and Cu in soils and the *A. retroflexus* uptakes more amount of these toxic metals with ammonium molybdate. It also increases the toxicities of these metals to plant.

After 45 days, length of shoot and root of *A. retroflexus* were measured and shoot lengths were shown in figure 1. *A. retroflexus* plant had exhibited high biomass production with the application of ammonium molybdate. The results show that ammonium molybdate could promote *A. retroflexus* plants to produce more biomass, because nitrogen and molybdenum are fertilizer, which can promote *A. retroflexus* plant to improve tillering and biomass gain. Biomass can express the tolerance of plants to toxic metals indirectly [26]. The average shoot lengths of treatment plants were longer than the control plants, but the shoot lengths of No.4 and No.5 were shorter than controls. It may be due to the reason that with addition of ammonium molybdate into soils, Cd, Ni and Cu formed more soluble fractions and the toxicities of Cd, Ni and Cu have reduced the chlorophyll content [27]. Figure 2 shows the phytotoxicity symptoms exhibited by *A. retroflexus*. Wilting and leaf necrosis have been described as typical visible symptoms of Ni^{2+} toxicity [28].
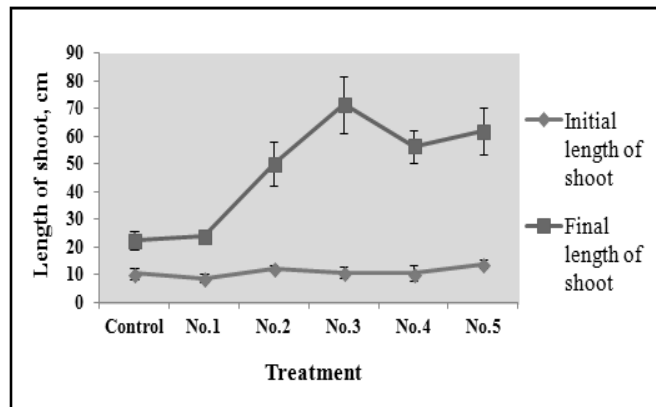
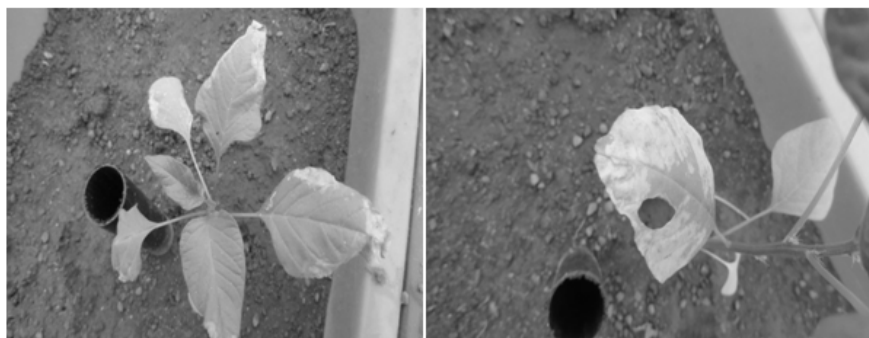Figure 1. Shoot lengths of *A. retroflexus*.

Figure 2. Toxicity symptoms exhibited by *A. retroflexus*.

BCF is the ratio of the metal concentration found within the tissues over the metal concentration found in the soil. The greater is the coefficient, the greater will be the uptake of heavy metal. It was

observed that for Cd, Ni and Cu the average BCF values (Table 5) of *A. retroflexus* plant treated with ammonium molybdate were higher than control but for Pb and Zn it was lower than control.

Table 5. The average bioconcnetration factor and translocation factor value of *Amaranthus retroflexus*.

Bioconcentration factor of shoot					
Treatment	Ni	Cd	Cu	Pb	Zn
Control	0.06	0.21	0.17	0.35	0.51
No.1	0.19	0.31	0.21	0.23	0.43
No.2	0.28	1.64	0.27	0.18	0.3
No.3	0.36	29.87	0.32	0.11	0.24
No.4	0.42	45.6	0.45	0.09	0.13
No.5	1.25	97.6	2.7	0.03	0.09
Bioconcentration factor of root					
Control	0.14	0.24	0.36	0.8	0.78
No.1	0.37	0.53	0.57	0.43	0.58
No.2	0.56	2.47	0.67	0.26	0.43
No.3	0.86	37.33	0.8	0.18	0.31
No.4	1.23	61.4	1.19	0.14	0.18
No.5	4.3	138	6.35	0.07	0.11
Translocation factor					
Control	0.44	0.86	0.47	0.43	0.65
No.1	0.5	0.58	0.37	0.54	0.74
No.2	0.5	0.67	0.41	0.7	0.7
No.3	0.42	0.80	0.39	0.64	0.75
No.4	0.34	0.74	0.38	0.64	0.73
No.5	0.29	0.71	0.42	0.46	0.78

Maximum BCF value of *A. retroflexus* was found for Cd in treatment No.5. It was 97.6 and 138 for shoots and root respectively. The maximum BCF value of Ni and Cu was also found in treatment No.5. Low BCF value of *A. retroflexus* for Pb and Zn indicates that low amount of metal uptake. This indicates that *A. retroflexus* plant had higher ability to uptake Cd, Ni and Cu with ammonium molybdate. This may be due to that complexation of ammonium molybdate increased the mobility of these metals [29]. TF is a measure of the ability of plants to transfer accumulated metals from the roots to the shoots. It is given by the ratio of concentration of metal in the shoot to that in the roots [30, 31]. A TF value greater than 1 is indicative of metal accumulation and transport into the different plant parts, and less than 1 is suggestive of storage of metal in roots. In this experiment, TF values of *A. retroflexus* were lower than 1, which indicates that maximum amount of heavy metals were stored in roots.

This study therefore has proved the possibility of using ammonium molybdate with phytoremediation for phytostabilization of Pb and Zn and for phytoextraction of Cd, Ni, and Cu by *A. retroflexus*. Ammonium molybdate shows immobilization and mobilization effect on phytoremediation of the toxic heavy metals in soil. Ni, Cd and Cu were chelated and form more soluble fractions with ammonium molybdate and Pb and Zn were precipitated with ammonium molybdate. Mobilization effect of ammonium molybdate on Ni, Cd and Cu increases the bioavailability of these metals to plant. Immobilization effect of ammonium molybdate on Pb and Zn decreases the biotoxicity of these metals to plant by decreasing the bioavailability of these

metals to plant. It was found that application of ammonium molybdate to soil is a promising technology in phytoremediation; it acts as a stabilization agent and as an extracting agent.

REFERENCES

[1] Marques APGC, Rangel ANOSS, Castro PML. Critical Reviews in Environmental Science and Technology. 2009, 39:622-654.
[2] Berti WR, Jacobs LW. J. Environ. Qual. 1996, 25:1025-32.
[3] Kennish MJ. Ecology of Estuaries: Anthropogenic Effects, CRC Press, Inc., Boca Raton, FL, 1992, p. 494.
[4] Garba ST, Osemeahon AS, Maina HM et al. Journal of Environmental Chemistry and Ecotoxicology. 2012, 4(5):103-109.
[5] Berti W, Cunningham S. Phytostabilization of metals. In: Phytoremediation of toxic metals: using plants to clean-up the environment. John Wiley & Sons, New York, 2000, 71-88.
[6] Glick B. Biot. Adv. 2003, 21:383-393.
[7] Sharma PD. Ecology and environment. Meerut: Rastogi Publications, 2007, 501-502.
[8] Mellem JJ, Himansu B, Bharti O. African Journal of Agricultural Research. 2012, 7(4):591-596.
[9] Vangronsveld J, van Assche F, Clijsters H. Environmental Pollution. 1995, 87:51-59.
[10] Dirilgen N. Chemosphere. 1998, 37:771-783.
[11] Finzgar N, Zumer A, Lestan D. J. Hazard Mater. 2006, 135:418-422.
[12] Peters RW. J. Hazard Mater. 1999, 66:151-210
[13] Neilson JW, Artiola JF, Maier RM. J. Environ Qual. 2003, 32:899-908.
[14] Di PL, Mecozzi RJ. Hazard Mater. 2007, 147:768-775.
[15] Paul R, Lucas B, Jan J, et al. Environmental Pollution. 2002, 116:109-121.
[16] Yue-bing S, Qi-xing Z, Jing A, et al. Geoderma. 2009, 150:106-112.
[17] Jiao Q, Le W, Xing Y, et al. Environ Earth Sci. 2011, 64:2175-2182.
[18] Qu J, Yuan X, Cong Q, et al. Spectrosc Spect Anal. 2008, 28:2674-2678.
[19] Ghosh M, Singh SP. Environ. Poll. 2005, 133: 365-371.
[20] Blaylock M, Salt D, Dushenkov S, et al. Environ. Sci. Technol. 1997, 31: 860-865.
[21] Mellem J, Baijanth H, Odhav B. J. Environ. Sci. Health. 2009, 44: 568-575.
[22] Marchiol L, Assolari S, Sacco P, et al. Environ. Poll. 2004, 132: 21-27.
[23] Xu L, Xiao LS, Zhang QX. Rare metals and cemented carbides. 2002, 38:6-8.
[24] Verkleij JAC, Schat H. Heavy metal tolerance in plants-evolutionary aspects, Boca Raton: CRC Press, 1990, 179-193.
[25] Rubin J, Bartolome J, Tomkinson JJ. Phys Condensed Matter. 1995, 46: 8723-8740.
[26] Lasat MM. J Environ Qual. 2002, 31:109-120.
[27] Peralta Videa JR, Gardea- Torresdey JL, de la Rosa G, et al. Adv Environ Res. 2004, 8:679-685.
[28] Llamas A, Ullrich CI, Sanz A, et al. Physiology and Biochemistry. 2008, 46: 905-910.
[29] Pushenreiter M, Stoger G, Lombi E, et al. J Plant Nutr Soil Sci. 2001, 164:615-621.
[30] Cui S, Zhou Q, Chao L. Environ. Geol. 2007, 51: 1043-1048.
[31] Li MS, Luo YP, Su ZY. Environ. Pollut. 2007, 147: 168-175.

Defluoridation of water using biosorbents

Puthenveedu Sadasivan Pillai Harikumar[*], Chonattu Jaseela, Tharayil Megha

Centre for Water Resources Development and Management, Water Quality Division, Kozhikode, India;
[*]Corresponding Author: drpshari@yahoo.co.in

ABSTRACT

Contamination of drinking water due to fluoride is a severe health hazard problem. Excess of fluoride (>1.5 mg/l) in drinking water is harmful to human health. Various treatment technologies for removing fluoride from groundwater have been investigated. The present study showed that Vetiveria zizanioides, a herbal plant of Kerala—commonly known as Vetiver is an effective adsorbent for the removal of fluoride from aqueous solution. Phosphoric acid activated Vetiver root showed good adsorption capacity than the fresh powdered Vetiver root. Batch sorptive defluoridation was conducted under variable experimental conditions such as pH, agitation time, dose of adsorbent and particle size. Maximum defluoridation was achieved at pH 6; there is a greater possibility of columbic interaction between fluoride ion and adsorbent surface at this pH. The percentage of fluoride removal increases with adsorbent dose and time at a given initial solute concentration. The surface and sorption characteristics were analyzed using SEM techniques. Freundlich as well as Langmuir isotherm were plotted and kinetic constants were determined.

Keywords: Defluoridation; Fluorosis; Batch Adsorption; Vetiver; Phytoremediation

1. INTRODUCTION

Water is most abundant and is an essential component of our life supporting system. But today most of the countries are facing drinking water problems. In India, drinking water is contaminated at many places by various pollutants such as fluorides, nitrates, iron etc.

Fluoride is often considered as a "two edged sword" because deficiency of fluoride intake leads to dental caries while excess consumption leads to dental and skeletal fluorosis. Symptoms affecting the soft tissues such as muscles and ligaments are also reported [1]. Fluorosis is an important clinical and public health problem in several parts of the world. Global prevalence of fluorosis is reported to be about 32% [2].

Due to high toxicity of fluoride to mankind, there is an urgent need to treat fluoride-contaminated drinking water to make it safe for human consumption. According to World Health Organization (WHO), the maximum acceptable fluoride concentration in drinking water is 1.5 mg/L. From the literature surveys, the groundwater of the two districts in Kerala, India (Palakkad and Alleppy) shows high fluoride content [3].

The use of plant materials is a traditional technology for purifying potable water that is still in widespread use in rural areas of Latin America. The use of natural products has recently been rediscovered by water-supply technologists and is being further developed with more scientific rigour [4,5].

The conventional method of fluoride removal includes: ion-exchange, reverse osmosis and adsorption [4,6,7]. The ion-exchange, reverse osmosis are relatively expensive. Therefore, still adsorption is the viable method for the removal of fluoride. Adsorption is the process considered to be efficient to defluoridate the water. Adsorption involves the passage of contaminated water through an adsorbent bed, where fluoride removed by physical, ion-exchange or surface chemical reaction with adsorbent. Because of its ease of operation and cost-effectiveness, adsorption is still widely accepted pollution removal technique. Plant materials are reported to accumulate fluoride and hence application as defluoridating agents has been suggested. The use of medicinal plant materials for the fluoride removal was investigated.

Several publications are available on the effective removal of fluoride using low cost materials. The tested materials include activated alumina, amorphous alumina, activated carbon, calcite, zeolite clay, charcoal, bleaching earth, red mud etc [1,8-12]. The materials like kaolinite, bentonite, charfines, lignite and nirmali seeds were also investigated for the removal of fluoride [13].

Kerala is one of the states in southern India, which has a rich biodiversity of medicinal plants. In the present

study, the efficiency of removal of fluoride by using various locally available medicinal plants from Kerala was investigated. The study assesses the suitability of inexpensive adsorbents to effectively remediate fluoride contaminated water. The study investigated defluoridation capacities of the following plant materials-Ramacham (*Vetiveria zizanioides*), Tamarind seed (*Tamarindus indica*), Clove (*Eugenia carryophyllata*), Neem (*Azadirachta indica*), Acacia (*Acacia catechu willd*), Nutmeg (*Myristica fragarns*), and coffee husk (*Coffea arabica*) which are grown indigenously Kerala [2].

Effect of important controlling factors, viz pH, dose of adsorbent, contact time, particle size and initial fluoride ion concentration on the fluoride removal efficiency was studied. The kinetics of removal was studied and the mechanism of removal suggested is controlled by adsorption and inter particle bridging.

2. MATERIALS AND METHODS

All the reagents used for the present study were of GR grade from E. Merck Ltd. India. A standard solution of 1000 ppm fluoride was prepared by dissolving 2.21 g of anhydrous sodium fluoride in 1000 ml of double distilled water. The fluoride solution of required concentration was prepared by diluting this standard solution. SPADNS spectrophotometric method was used to determine the fluoride concentration [14]. The instrument was calibrated and a curve was prepared using standard solutions.

The batch adsorption study was carried out in three stages-in the first stage; locally medicinal plants were selected as the study materials. Initial studies indicated that plants like Vetiver root, Tamarind seed and Clove were comparatively more efficient in the removal of fluoride. Activated form of Vetiver root has high degree of micro porosity and high surface area. The surface modification of activated Vetiver root as shown in Scanning Electron Microscope image. So in the third stage detailed studies on activated Vetiver root was carried out.

All the adsorbents used in this study were collected locally, washed well with tap water and then with distilled water, dried in an air oven at 110°C for 5 hour, micronized in a flour mill and sieved to get particles of sizes 0.1, 0.2 0.3, 0.5 mm. A synthetic solution of fluoride was prepared from analytical reagent sodium fluoride and stored in polythene bottles. The pH of the solution was adjusted to the required level, using HCl (0.1 mol/l) and NaOH (0.1 mol/l) solutions [15].

Activation of Vetiver root was carried out by giving heat treatment (at 600°C - 800°C) and with the use of phosphoric acid in the ratio 1:4. The activated product is washed with water and dried. Activity was controlled by altering the proportion of raw material to activating agent, between the limits of 1:05 to 1:4.

2.1. Batch Studies

The batch experiments were carried out in 250 mL stoppered bottles by agitating a pre-weighed amount of the adsorbent with 50 mL of the fluoride solutions [15]. The adsorbent was separated with filter paper. The concentration of fluoride remaining in the filtrate was analyzed spectrophotometrically, using SPADNS reagent at 570 nm [14].

2.2. Adsorption Isotherms

Freundlich and Langmuir equations were used to find the patterns of adsorption by adsorbent activated Vetiver root for fluoride removal. The sorption isotherm studies are conducted by varying the initial concentration of fluoride from 1 to 5 mg/L and maintaining the adsorbent dosage of 0.5 g.

2.2.1. Freundlich Adsorption Isotherm

The non-linear form of Freundlich equation is:

$$X/m = KCe^{1/n}$$

where,

X/m = Amount adsorbed per unit weight of adsorbent (mg/g) or adsorption capacity and is calculated as follows.

$X/m = (Ci - Ce) \times V \times eq.wt./1000 \times m$.

Ci = Initial concentration of solution in mg/L.

Ce = Equilibrium concentration of the solution in mg/L.

V = volume of the solution in mL.

K = Constant of the system depending on temperature and is known as Freundlich adsorption coefficient. It represents the adsorption capacity.

n = Freundlich constant, which should be between 1 and 10 for favorable adsorption. Values of "n" greater than unity suggest that adsorption is relatively more efficient at low concentration.

This equation is conveniently used in the linear form by taking the log on both sides as,

$$Log(X/m) = \log K + (1/n)\log Ce$$

A plot of $\log(X/m)$ against log p or log Ce, yield a straight line. The constants K and n are determined from the intercept and slope respectively.

2.2.2. Langmuir Adsorption Isotherm

Langmuir equation is based on the assumption of a monolayer of adsorbate molecules. It is of the form,

$$(X/m) = (aV_m Ce)/(1 + aCe)$$

where,

a = adsorption bond energy

V_m = maximum adsorption density (corresponding to

monolayer formation on the adsorbent)

Linear form of the equation is,

$$Ce/(X/m) = 1/(aV_m) + (1/V_m)Ce$$

A plot of $Ce/(X/m)$ against Ce, yield a straight line. The Langmuir constants a and V_m were calculated from intercept and slope respectively

3. RESULTS AND DISCUSSION

3.1. Stage 1

The first stage of the study provided the order of removal efficiency of different adsorbents from a solution contaminated with 2 mg/L fluoride. The order of removal of fluoride is: Vetiver root (*Vetiveria zizanioides*, 80%), Tamarind seed (*Tamarindus indica*, 75%), Clove (*Eugenia carryophyllata*, 70%), Neem (*Azadirachta indica* 52%), Acacia (*Acacia catechu willd*, 47%), Nutmeg (*Myristica fragarns*, 45%), and Cofee husk (*Coffea arabica*, 38%) as shown in **Figure 1**. Effect of important controlling factors, viz, pH, dose of adsorbent, contact time and initial fluoride ion concentration on the fluoride removal efficiency was studied. The kinetics of removal was studied and the mechanism of removal is due to adsorption and inter particle bridging.

3.2. Stage 2

The results of Batch sorptive defluoridation of Tamarind seed, Vetiver root and Clove was conducted under variable experimental conditions are discussed in the following section.

3.2.1. Effect of Agitation Time

The effect of agitation time was found to be increased up to a certain period of time after which the rate of sorption was found to be constant. In **Figure 2** it was found that the percentage removal of fluoride for tama-
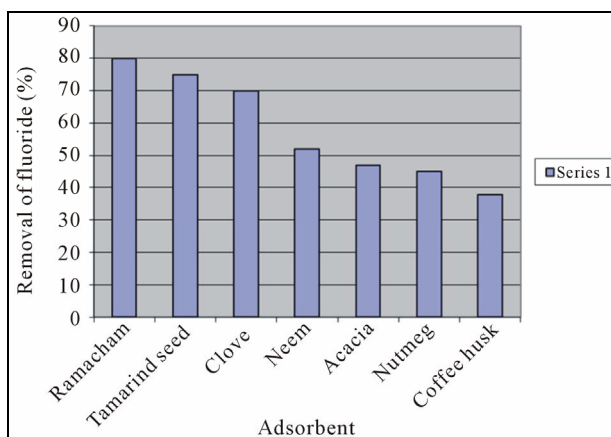
Figure 1. Comparison of fluoride removal efficiencies of different plant materials.

rind seed, Vetiver root and clove was 51, 54, and 51 respectively.

3.2.2. Effect of Sorbent Dosage

As the weight of adsorbent dose increased the sorption percentage also increased. The response of adsorbent dose on the removal of fluoride is presented in **Figure 3**. This might be due to the fact that at higher doses of adsorbent, more sorbent surface and pore volume would be available for the adsorption interaction and this result in higher removal. It was also observed that, initially, the removal of fluoride increases with the dose but beyond certain dose range, there is no significant increase in removal. This perhaps is due to non-adsorbability of fluoride ion as result of sorbent-sorbate interaction. Results shows that the biosorbents, viz, Vetiver root removes 80% of fluoride at a dose of 1g in 50ml of fluoridated water and tamarind seed and clove removes 75 and 70% at the same dose.

3.2.3. Effect of Particle Size

The effect of particle size on fluoride sorption is given in **Figure 4**. Increase in particle size reduces the sorption rate. Increase in particle size from 100 to 500 micron reduces the sorption level from 75 to 45 per cent. The breaking of larger particles tends to open tiny cracks and
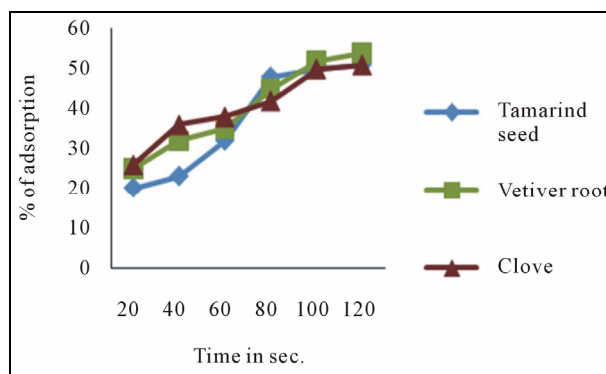

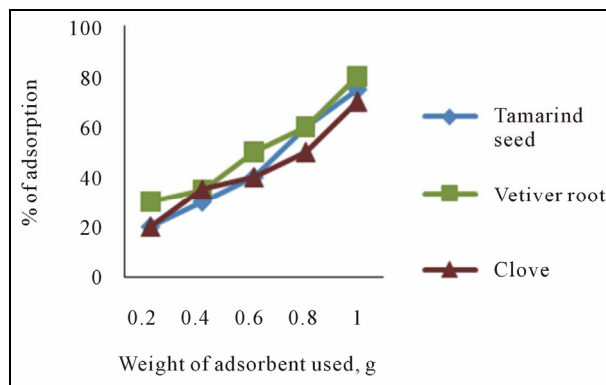**Figure 2.** Effect of agitation time on defluoridation.

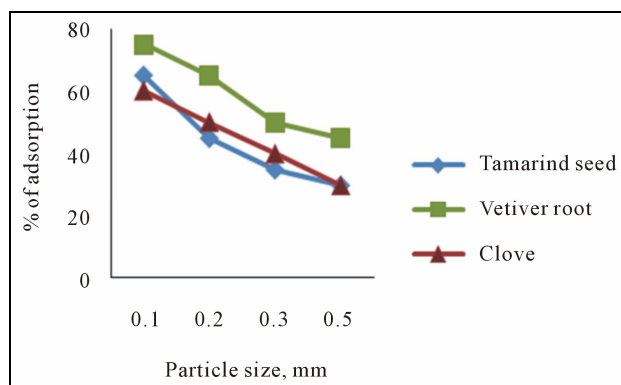**Figure 3.** Effect of sorbent dosage on defluoridation.

Figure 4. Effect of particle size on sorption of fluoride.

channels on the particle surface of the sorbent. The smaller particle provides more sorption sites and surface area leading to greater sorption.

The study indicates that the three biosorbents are suitable for the removal of fluoride ions. The percentage of fluoride removal increases with adsorbent dose and time at a given initial solute concentration. The fluoride removal efficiency decreases with increasing initial fluoride ion concentration.

3.3. Stage 3

From the adsorption study, it is clear that Vetiver root has the potential to be an efficient defluoridating agent (80% removal), so further study was carried out using activated Vetiver root. Powdered activated Vetiver showed higher efficiency (90%) than the other. The batch sorptive defluoridation of powdered activated vetiver was conducted under variable experimental conditions such as pH, agitation time, dose of adsorbent and particle size.

3.3.1. Effect of pH

The adsorption was found to be sufficiently influenced by the pH of the medium. The effect of pH change on the defluoridation was carried out within a range of pH 2 - 10. Maximum removal was observed around neutral pH (around neutral pH, the surface will be positively charged-columbic interaction between fluoride ion and adsorbent surface was higher) is shown in **Figure 5**.

In the acidic pH range, the amount of fluoride adsorbed slightly decreased and this can be attributed to the formation of weak hydrofluoric acid. In alkaline pH range, there was sharp drop in adsorption which may be due to the competition of the hydroxyl ions with the fluoride for adsorption [16].

3.3.2. Effect of Agitation Time on Defluoridation

The effect of agitation time was found to be increasing up to a certain period of time after which the rate of

sorption was found to be constant as shown in **Figure 6**.

3.3.3. Effect of Sorbent Dosage on Defluoridation

The response of adsorbent dose on the removal of fluoride is presented in **Figure 7**. The fluoride uptake increases with the corresponding increase in the amount of adsorbent. Initially, the removal of fluoride increases with the dose but beyond certain dose range, there is no significant increase in removal.
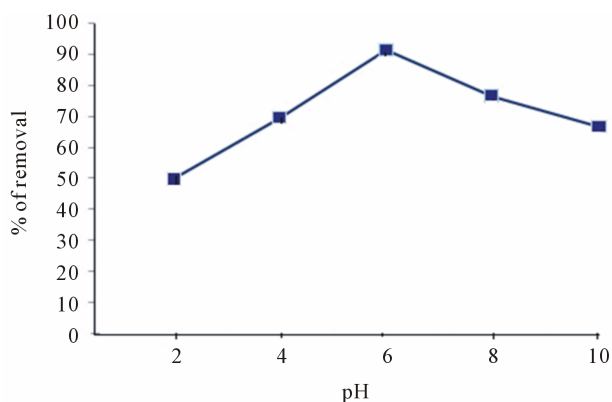

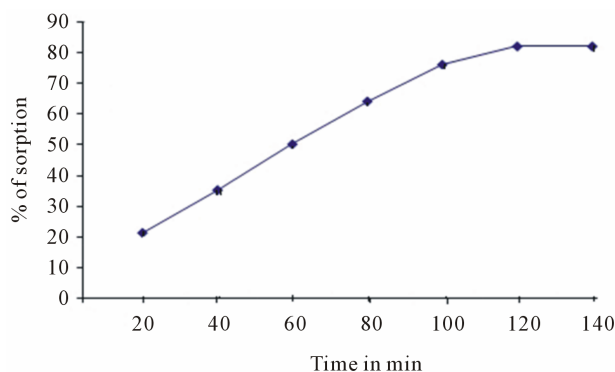**Figure 5.** Effect of pH on sorption of fluoride.

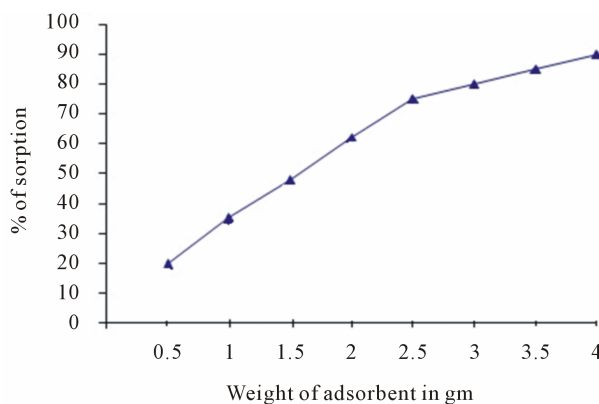**Figure 6.** Effect of agitation time on defluoridation.

Figure 7. Effect of sorbent dosage on defluoridation.

3.3.4. Effect of Particle Size on Sorption of Fluoride

The effect of particle size on fluoride sorption is given in **Figure 8**. Increase in particle size from 100 to 500 micron reduces the sorption level. The smaller particles provide more sorption sites and surface area leading to greater sorption.

3.3.5. Effect of Temperature on Defluoridation

There is no significant effect of sorption of fluoride observed with varying temperature.

The study indicates that the powdered activated Vetiver root is suitable for the removal of fluoride ions. The percentage of fluoride removal increases with adsorbent dose and time at a given initial solute concentration. The fluoride removal efficiency decreases with increasing initial fluoride ion concentration.

3.4. Adsorption Isotherm

The sorption isotherm studies are conducted by varying the initial concentration of fluoride from 1 to 5 mg/L and maintaining the adsorbent dosage of 0.5 g. Adsorption isotherm of activated Vetiver root mare discussed in **Table 1**.

3.4.1. Freundlich Adsorption Isotherm for the Adsorption of Fluoride

From **Figure 9**, the observation from the kinetic study are given below
- The value of k and 1/n are 3.467 mg/g and 0.357 respectively.
- Since the value of the constant 1/n (adsorption intensity) is less than unity, it indicates favorable adsorption.
- The higher value of k indicates rate of adsorbate removal is high.

3.4.2. Langmuir Adsorption Isotherm for the Adsorption of Fluoride

The observation from **Figure 10** are given below
- The values of Langmuir parameters, V_m and a are 4.2918 and 0.231 respectively.

- The linear plot obtained indicates the applicability of Langmuir adsorption isotherm for the adsorption of fluoride.

The surface modification of the fluoride adsorbed material was further confirmed through Scanning Electron Microscope image.

SEM micrograph of activated Vetiver adsorbent before fluoride loading was somewhat smooth (as shown in **Figure 11**), after fluoride adsorption the surface became much rockier in appearance (as shown in **Figure 12**).
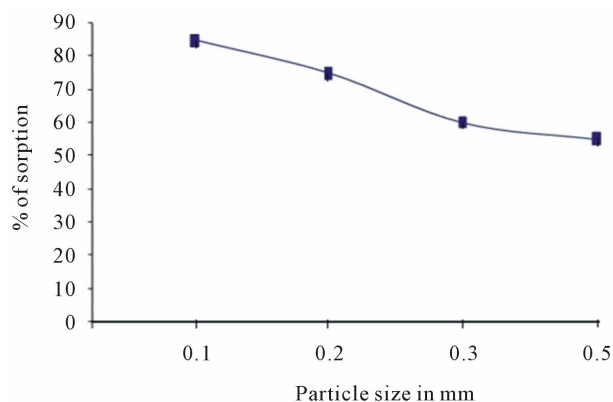

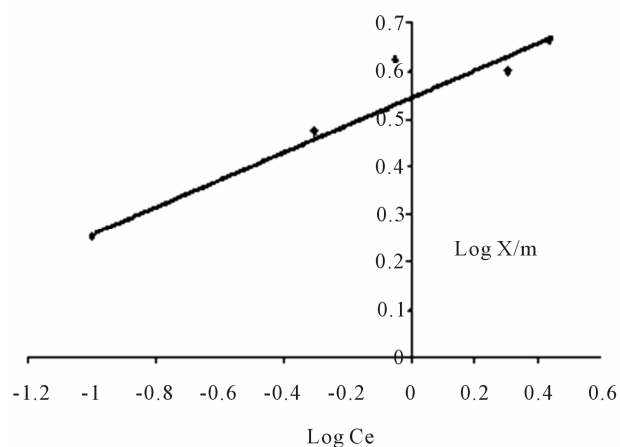**Figure 8.** Effect of particle size on sorption of fluoride.

Figure 9. Freundlich adsorption isotherm.

Table 1. Adsorption isotherm of activated vetiver.

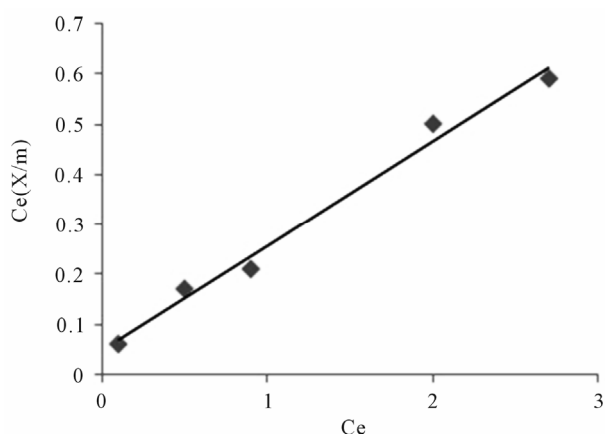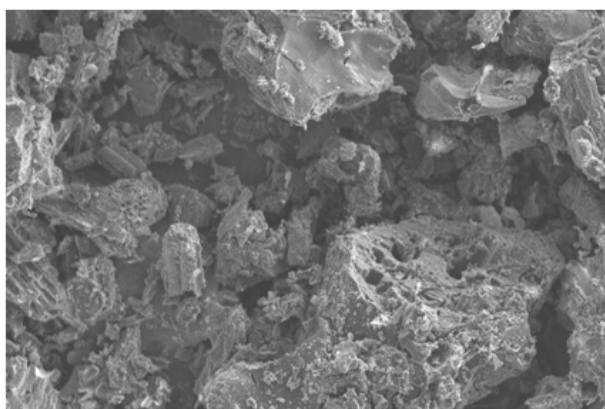| Ci (mg/l)	Ce (mg/l)	X (mg)	m (g)	X/m (mg/g)	Ce/(X/m)	log Ce	log X/m
1	0.1	0.9	0.5	1.8	0.056	−1.000	0.255
2	0.5	1.5	0.5	3	0.167	−0.301	0.477
3	0.9	2.1	0.5	4.2	0.214	−0.046	0.623
4	2	2	0.5	4	0.500	0.301	0.602
5	2.7	2.3	0.5	4.6	0.587	0.431	0.663

Figure 10. Langmuir adsorption isotherm.

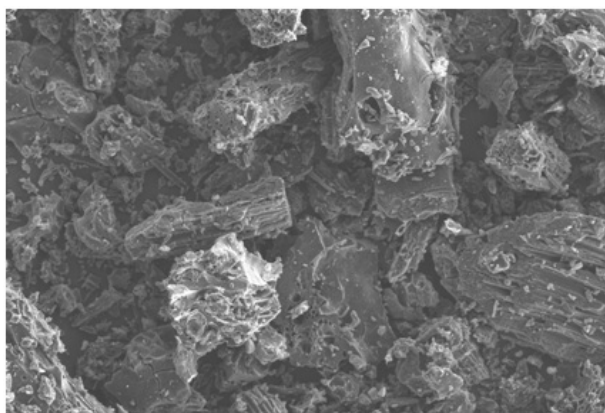**Figure 11.** SEM images of free activated vetiver root (×500 magnification).

Figure 12. SEM images of fluoride loaded activated vetiver root (×500 magnification).

3.5. Fabrication of Domestic Filter Using Tested Material

Based on the adsorption study of activated Vetiveria zizanioides, a water treatment unit for defluoridation was developed.

The column of an ordinary household water filter (7.5

cm height and 8 cm diameter) was packed with four materials in five layers-sand, activated Vetiver root, activated carbon and pebbles are in a ratio of 1:2:4:6. Different weights of Vetiver adsorbent were used for fluoride filtration. The resultant filtrate was measured for fluoride by spectrophotometer using SPADNS method. The efficiency of the column was evaluated through the elution of a solution of known concentration of fluoride. The fluoride removal efficiency of the filter system was found low when the filtrate was collected immediately, that is the time of contact between the sample and Vetiver was small. As the time of contact increased, the efficiency of removal of fluoride also increased and maximum efficiency of fluoride removal was 90% when the time of contact was increased to 20 minutes. Removal efficiency depends on the amount of activated Vetiver root powder, time of contact and volume of the sample taken. This filter system has a removal efficiency of 90 % fluoride solution with adsorbent regeneration capacity.

4. CONCLUSION

Different plant species were studied for testing the efficiency of fluoride removal. Vetiver root was found to be promising for the removal of fluoride. In its activated powdered form, Vetiver root has the potential to be an efficient defluoridating agent. The sorption process of fluoride ion on activated Vetiver root was influenced by many experimenttal conditions. The equilibrium data obtained fitted well with Langmuir and Freundlich isotherms. SEM micrographs of activated Vetiver adsorbent after fluoride loading confirmed the adsorption of fluoride.

5. ACKNOWLEDGEMENTS

REFERENCES

[1] Kharb, P. and Susheela, A.K. (1994) Fluoride ingestion in excess and its effect on organic and certain inorganic constituents of soft tissues. *Medical Science Research*, **22**, 43-44.

[2] Varier, P.S. (1996) Indian medicinal plants: A compendium of 500 species, Vol. 1-5. Orient Longman Ltd., Madras

[3] Antu, C.D. and Harikumar, P.S. (2007) Genesis of fluoride in the shallow unconfined aquifer of muthalmada area in Bharatapuzha Basin. *Proceedings of XIX Kerala Science Congress*, 29-31 January 2007, Kannur.

[4] Hichour, M., Persin, F., Sandeaux, J. and Gavach, C. (2000) Fluoride removal from waters by Donnan dialysis. *Separation and Purification Technology*, **18**, 1-11.

doi:10.1016/S1383-5866(99)00042-8

[5] Folkard, G.K., Grant, W.D. and Sutherland, J.P. (1990) Natural coagulants for small scale water treatment: Potential applications. *Experiences in the Development of Small-Scale Water Resources in Rural Areas*: *Proceedings of the International Symposium on Development of Small-Scale Water Resources in Rural Areas*. Carl Duisberg Gesellschaft, South East Asia Program Office, Bangkok, 115-123.

[6] Amor, Z., Malki, S., Taky, M., Bariou, B., Mameri, N. and Elmidaoui, A. (1998) Optimization of fluoride removal from brackish water by electrodialysis. *Desalination*, **120**, 263-271. doi:10.1016/S0011-9164(98)00223-9

[7] Hichour, M., Persin, F., Molenat, J., Sandeaux, J. and Gavach, C. (1999), Fluoride removal from diluted solutions by Donnan dialysis with anion-exchange membranes. *Desalination*, **122**, 53-62. doi:10.1016/S0011-9164(99)00027-2

[8] Rubel, J.F. (1983) The removal of excess fluoride from drinking water by the activated alumina method. In: Shupe, J.L., Peterson, H.P. and Leone, N.C. Eds., Fluoride effects on vegetation animals and humans. Paragon Press, Salt Lake City, 345-349

[9] Yang, M., Hashimoto, T., Hoshi, N. and Myoga, H. (1999) Fluoride removal in a fixed bed packed with granular calcite. *Water Research*, **33**, 3395-3402. doi:10.1016/S0043-1354(99)00052-4

[10] Li, Y.H., Wang, S., Cao, A., Zhao, D., Zhang, X., Xu, C., Luan, Z., Ruan, D., Liang, J., Wu, D. & Wei, B. (2001) Adsorption of fluoride from water by amorphous alumina supported on carbon nanotubes. *Chemical Physics Letters*, **350**, 412-416. doi:10.1016/S0009-2614(01)01351-3

[11] Wang, Y. and Reardon, E.J. (2001) Activation and regeneration of a soil sorbent for defluoridation of drinking water. *Applied Geochemistry*, **16**, 531-539. doi:10.1016/S0883-2927(00)00050-0

[12] Christopher, J., Kenneth, G., Ishida, P. and Richard, M. (2004) Bold testing of drinking water treatment: Copolymers for compatibility with polyamide reverse osmosis membranes. *9th World Filtration Congress*, 18-22 April 2004, New Orleans, 1-10.

[13] Srimurali, M., Pragathi, A. and Karthikeyan, J. (1998) A study on removal of fluorides from drinking water by adsorption onto low-cost materials. *Environmental Pollution*, **99**, 285-289. doi:10.1016/S0269-7491(97)00129-2

[14] APHA. (2005) Standard method for the examination of water and waste water. 21st Edition, American Public Health Association, Washington DC, 85-86.

[15] Murugan, M. and Subramanian, E. (2006) Studies on defluoridation of water by Tamarind seed, an unconventional biosorbent. *Journal of Water and Health*, **4**, 453-461.

[16] Kumar, S., Gupta, A. and Yadav, J.P. (2008) Removal of fluoride by thermally activated carbon prepared from neem (*Azadirachta indica*) and kikar (*Acacia arabica*) leaves. *Journal of Environmental Biology*, **29**, 227-232.